Digitized by the Internet Archive
in 2023 with funding from
Kahle/Austin Foundation

https://archive.org/details/contributionsfro0013unse

Carnegie Institution of Washington

UNIVERSITY OF ARIZONA
STEWARD OBSERVATORY
TUCSON, ARIZONA

CONTRIBUTIONS

FROM THE

MOUNT WILSON OBSERVATORY

VOLUME XIII

NOS. 283-303

WITH TWENTY PLATES

AUGUST, 1924—SEPTEMBER, 1925

CF

UNIVERSITY OF ARIZONA
LIBRARY

C28
v.13

CONTENTS

NO. PAGE

283. THE ELECTRIC FURNACE SPECTRA OF VANADIUM AND CHROMIUM IN THE ULTRA-VIOLET. *Arthur S. King* 1

284. INVESTIGATIONS ON PROPER MOTION. ELEVENTH PAPER: THE PROPER MOTION OF MESSIER 13 AND ITS INTERNAL MOTION. *Adriaan van Maanen* 21

285. A STUDY OF ELECTRICALLY EXPLODED WIRES. *Sinclair Smith* . 29

286. A LIST OF ULTIMATE AND PENULTIMATE LINES OF ASTROPHYSICAL INTEREST. *Henry Norris Russell* 47

287. THE MEAN COLOR-INDEX OF STARS OF DIFFERENT APPARENT MAGNITUDES. *Frederick H. Seares* 109

288. SOME RELATIONS BETWEEN MAGNITUDE SCALES. *Frederick H. Seares* 125

289. REDUCTION OF THE HARVARD-GRONINGEN *Durchmusterung* TO THE INTERNATIONAL SYSTEM OF MAGNITUDE AND COLOR. *Frederick H. Seares, Mary C. Joyner, and Myrtle L. Richmond* . . 145

290. THE PHOTOGRAPHIC DETERMINATION OF STELLAR PARALLAXES WITH THE 60- AND 100-INCH REFLECTORS. EIGHTH SERIES. *Adriaan van Maanen* 163

291. THE ORBITS OF FOUR SPECTROSCOPIC BINARIES. *Roscoe F. Sanford* 181

292. ANALYSIS OF RADIAL VELOCITIES OF GLOBULAR CLUSTERS AND NON-GALACTIC NEBULAE. *Gustaf Strömberg* 195

293. THE ASYMMETRY IN STELLAR MOTIONS AS DETERMINED FROM RADIAL VELOCITIES. *Gustaf Strömberg* 205

294. DISCOVERY AND OBSERVATIONS OF STARS OF CLASS BE. *Paul W. Merrill, Milton L. Humason, and Cora G. Burwell* . . . 231

295. TWO STELLAR SPECTRA OF THE P CYGNI TYPE. *Paul W. Merrill* . 261

296. THE THEORY OF THE STELLAR ABSORPTION COEFFICIENT. *S. Rosseland* 267

297. NOTE ON THE DISTRIBUTION AND NUMBER OF NEBULAE. *Frederick H. Seares* 287

298. SPECTROSCOPIC PHENOMENA OF THE HIGH-CURRENT ARC. *Arthur S. King* 299

299. RADIATION MEASUREMENTS OF THE SOLAR CORONA, JANUARY 24, 1925. *Edison Pettit and Seth B. Nicholson* 327

CONTENTS

NO. PAGE

300. THE LAW OF SUN-SPOT POLARITY. *George E. Hale and Seth B. Nicholson* 351

301. MEAN DISTRIBUTION OF STARS ACCORDING TO APPARENT MAGNITUDE AND GALACTIC LATITUDE. *Frederick H. Seares, P. J. van Rhijn, Mary C. Joyner, and Myrtle L. Richmond* . . . 383

302. ON THE STRUCTURE AND ORIGIN OF SOLAR MAGNETIC FIELDS. *Svein Rosseland* 439

303. PHOTOGRAPHIC STUDIES OF NEBULAE. FOURTH PAPER. *John Charles Duncan* 461

LIST OF PLATES

NO.		FACING PAGE
I.	SPARK, ARC, AND FURNACE SPECTRA OF VANADIUM	19
II.	INTERNAL MOTIONS IN THE GLOBULAR CLUSTER M 13 . .	25
III.	SPECTROGRAMS WITH ROTATING-MIRROR SPECTROGRAPH; (*a*) MAGNESIUM; (*b*) CADMIUM; (*c*) TIN	33
IV.	SPECTROGRAMS OF LEAD WITH ROTATING-MIRROR SPECTROGRAPH	34
V.	SPECTROGRAMS WITH ROTATING-MIRROR SPECTROGRAPH: (*a*), (*b*), (*c*) ALUMINUM; (*d*) LEAD	41
VI.	(*a*) PORTION OF AN OBJECTIVE-PRISM SPECTROGRAM TAKEN WITH THE TEN-INCH COOKE TELESCOPE; (*b*) OBJECTIVE-PRISM SPECTROGRAM OF β PISCIUM	236
VII.	(*a*) H.D. 51480; (*b*) DM. $-27°11944$	261
VIII.	ARC SPECTRUM OF IRON: (*a*), (*d*) LOW-CURRENT ARC; (*b*) HIGH-CURRENT ARC; (*c*) HIGH-CURRENT ARC, IRON-CARBON, LARGE ELECTRODES	307
IX.	ARC SPECTRUM OF IRON: (*a*), (*c*) LOW-CURRENT ARC; (*b*), (*d*) HIGH-CURRENT ARC	324
X.	ARC SPECTRUM OF IRON: (*a*), (*c*) LOW-CURRENT ARC; (*b*), (*d*) HIGH-CURRENT ARC	324
XI.	HIGH-CURRENT ARC SPECTRUM OF MAGNESIUM (*b*, *c*, *d*) AND COPPER (*g*); LOW-CURRENT ARC SPECTRUM (*a*, *e*, and *f*) .	324
XII.	REFLECTING TELESCOPE AND THERMOCOUPLE AS USED FOR OBSERVATIONS OF CORONAL RADIATION	328
XIII.	SOLAR CORONA OF JANUARY 24, 1925: EXPOSURE OF 2 SECONDS	336
XIV.	SOLAR CORONA OF JANUARY 24, 1925: EXPOSURE OF 15 SECONDS	336
XV.	SOLAR CORONA OF JANUARY 24, 1925: EXPOSURE OF 73 SECONDS	336
XVI.	SOLAR CORONA OF JANUARY 24, 1925	336
XVII.	THE DARK NEBULA BARNARD 86	461
XVIII.	NEBULOSITY PRECEDING THE AMERICA NEBULA IN CYGNUS .	463
XIX.	NEBULOSITY FOLLOWING γ CYGNI	464
XX.	NEBULOSITY NORTH—PRECEDING γ CYGNI	465

Contributions from the Mount Wilson Observatory, No. 283
Reprinted from the *Astrophysical Journal*, Vol. LX, pp. 282–300, 1924

THE ELECTRIC FURNACE SPECTRA OF VANADIUM AND CHROMIUM IN THE ULTRA-VIOLET

By ARTHUR S. KING

ABSTRACT

Furnace spectra of vanadium, λ *2340*–λ *3185, and of chromium,* λ *2362*–λ *3575.*—This paper supplements *Mount Wilson Contribution*, No. 94, which covered these spectra from the foregoing limits into the red. Temperature stages of 2000°, 2300°, and 2600° C. were employed to observe the initial appearance and rate of increase in intensity of the ultra-violet lines to about λ 2700, while for shorter wave-lengths the absorption furnace was compared with the arc. The tables give the temperature classification of 515 vanadium and 640 chromium lines and their relative intensities in arc and furnace. New wave-lengths are given for 133 vanadium and 94 chromium lines which have not been measured in the arc spectrum or for which, owing to diffuseness or blends, the previous wave-lengths are poor. Comparison photographs of the spark spectrum were made for the selection of enhanced lines. Many enhanced lines of vanadium are emitted by the furnace, while those of chromium require, for the most part, the higher excitation of the arc for their initial appearance. In the discussion, mention is made of notable groups of low-temperature and high-temperature lines, also of the phenomena of reversal and dissymmetry in the condensed spark.

This paper supplements a previous one on the spectra of vanadium and chromium,[1] which covered the visible spectrum and reached ultra-violet limits for the two spectra at λ 3165 and λ 3550, respectively. The present tables of furnace lines extend to about λ 2340. As far as possible, emission spectra for three temperature stages of approximately 2000°, 2300°, 2600° C. have been used, and the intensities have been listed for these furnace temperatures and for the arc spectrum. A comparison with the spark spectrum served to select the enhanced lines. As in previous papers on furnace spectra, a classification has been made according to the temperature at which a line appears and its rate of growth with increase of temperature.

The emission spectra, extending to about λ 2700 for vanadium and λ 2800 for chromium, were made in the second order of a 15-foot concave grating, the scale of which is 1.86 A per millimeter. For shorter wave-lengths, the furnace material consists of absorption spectra of the two elements, obtained by placing a graphite plug in the furnace tube behind the powdered metal to be vaporized. The temperature of this plug was held at 3000° C. According to former observations,[1] the temperature of the absorbing vapor should then be near 2600°, and the resulting spectrum is to be rated as one of high temperature. By comparing the absorption lines in this region with those above λ 2800, where data for the emission spectra at three temperatures were also available, the classification was made to correspond as closely as the material permitted. For chromium, a low-temperature absorption spectrum beginning at λ 2726 was also obtained by the use of a tungsten lamp, with quartz window behind the furnace when the latter, with unobstructed tube, contained chromium vapor at 2000°. Absorption lines appearing in this spectrum may safely be placed in Classes I and II, and lines of shorter wave-length have been judged on the same basis, the degree to which they maintain their strength indicating their probable class.

---

[1] *Mt. Wilson Contr.*, No. 94; *Astrophysical Journal*, 41, 86, 1915.

Wave-lengths, either new or better than those thus far available for the arc spectrum, are given as measured by the writer for 133 lines of vanadium and 94 of chromium. Some of these measurements resulted from the resolution of close lines, some are for faint lines which are strengthened in the furnace, while others are for diffuse lines not previously measured in the arc, which are usually much sharpened in the vacuum furnace.

EXPLANATION OF THE TABLES

Tables I and II contain vanadium lines which appear with fair strength in the arc spectrum, Table I being for the region where only the arc and absorption furnace are available for comparison, while Table II gives intensities for the arc and for three temperatures of the emission furnace. Tables III and IV treat the chromium spectrum in the same way.

Wave-lengths.—International wave-lengths to two decimal places are given in the first column of each table. These are reduced from the values of Exner and Haschek except for lines marked with a dagger, which were measured by the writer. An asterisk after the wave-length refers to a note at the end of the table, explaining some peculiarity of the line.

---

[1] *Mt. Wilson Contr.*, No. 174; *Astrophysical Journal*, 51, 13, 1920.

Arc and furnace intensities.—Intensity estimates for lines in the arc and at three furnace temperatures are given in the four succeeding

TABLE I

VANADIUM LINES IN ARC AND ABSORPTION FURNACE

λ (I.A.)	Arc	Absorption Furnace	Class	λ (I.A.)	Arc	Absorption Furnace	Class
2340.49	15	1	IV	2554.87	4	1	III
2399.97	10	1	IV	2556.01	2	tr	III
2401.89	10	1	IV	2556.79†	1	tr	III
2406.7*†	15	2	III	2558.92	3	1	III
2407.94	8	1	III	2562.16	15	3	III
2412.72	10	2	III	2564.29	6	1	III
2413.06	8	1	III	2564.84	10	2	III
2415.35	10	2	III	2574.05	20	4	III
2416.75	15	3	III	2577.28	5	1	III
2417.36	10	2	III	2602.7†	1	tr	III
2420.16	12	2	III	2607.75†	2	1	III
2421.08	12	2	III	2611.75†	1	tr	III
2422.01	12	2	III	2614.90†	2	1	III
2428.31	12	2	III	2620.28	4	tr	III
2432.01	10	2	III	2632.15†	2	1	III
2435.52	12	2	III	2637.15*	5	2	III
2439.12	6	1	III	2640.4†	2	1	III
2441.36	2	1	III	2642.24	12	3	III
2441.91	4	1	III	2643.13	10	3	III
2480.64	3	1	III	2645.23	10	3	III
2482.14	4	2	III	2647.70	15	5	III
2482.75	2	1	III	2651.86	15	5	III
2483.65†	2	1	III	2652.86	4	tr	IV
2498.08	3	1	III	2653.79	4	tr	IV
2498.24	3	1	III	2656.16	20	6	III
2499.24	2	1	III	2661.39	20	6	III
2501.66	8	2	III	2665.94	6	2	III
2503.34	5	2	III	2670.94	2	1	III
2505.57†	2	1	III	2671.65	8	2	III
2507.85*	15	3	III	2671.99	20	tr	V E
2510.28	2	1	III	2675.73	3	1	III
2511.65	8	2	III	2677.10	1	tr	III
2511.97	8	2	III	2677.77	25	tr	V E
2515.16	5	1	III	2678.55*	25	4	III
2517.14	8	2	III	2679.30	25	tr	V E
2519.60	15	3	III	2682.89	20	....	V E
2521.56*	4	1	III	2683.10	20	tr	V E
2526.21	12	4	III	2685.12	4	1	III
2530.18	15	3	III	2686.51	8	3	III
2543.73	4	1	III	2687.95	35	1	V E
2545.93	20	3	III	2688.70	20	tr	V E
2549.26	8	1	III	2689.89	20	tr	V E
2549.62†	3	1	III	2690.27	25	tr	V E
2552.63	10	2	III	2690.80	25	tr	V E

TABLE II

Temperature Classification of Vanadium Lines

λ (I.A.)	Arc Int.	Furnace Intensities			Class
		High Temp.	Medium Temp.	Low Temp.	
2696.21....	1	.....	.....	.....	V
2696.76....	2	1	.....	.....	IV
2696.99....	15	3	tr	.....	IV
2697.71....	15	3	tr	.....	IV
2698.70....	12	2	tr	.....	IV
2699.07....	8	1	.....	.....	IV
2700.91....	20	1	.....	.....	V Eru
2701.25....	3	1	.....	.....	IV
2701.51....	1	.....	.....	.....	V
2702.14....	15	.....	.....	.....	V E
2705.16....	2	.....	.....	.....	V E
2706.11....	20	tr	.....	.....	V Eru
2706.63....	8	.....	.....	.....	V E
2707.82....	5	.....	.....	.....	V E
2711.73....	6	.....	.....	.....	V E
2713.04....	4	.....	.....	.....	V E
2714.15....	6	.....	.....	.....	V E
2714.99....	4	.....	.....	.....	V
2715.65....	8	.....	.....	.....	V E
2721.11....	6	1	.....	.....	IV
2722.54....	15	3	tr	.....	IV
2723.20....	2	.....	.....	.....	V E
2728.59....	10	.....	.....	.....	V E
2731.33....	40	5	1	.....	IV
2731.49....	15n	1	.....	.....	IV
2733.34....	3	3	tr	.....	IV
2733.90....	2	.....	.....	.....	V E
2739.70....	5	.....	.....	.....	V E
2742.41....	3	.....	.....	.....	V E
2742.67....	3	.....	.....	.....	V E
2743.77....	1	.....	.....	.....	V
2747.50*...	5	4	1	.....	III
2753.08....	3	.....	.....	.....	V
2753.41....	2	.....	.....	.....	V E
2755.64*...	5	tr	.....	.....	V
2757.75....	2	.....	.....	.....	V
2760.13....	2	.....	.....	.....	V E
2760.69....	2	.....	.....	.....	V E
2765.66....	5	.....	.....	.....	V E
2766.10....	1	.....	.....	.....	V
2766.45....	4	1	.....	.....	IV E
2768.30....	3	tr	.....	.....	IV
2768.55....	3	.....	.....	.....	V E
2768.93....	6	2	tr	.....	IV
2770.94*...	2	tr	.....	.....	IV
2773.66....	8	3	.....	.....	IV
2774.01....	3	1	.....	.....	IV
2774.27....	2	.....	.....	.....	V E
2775.75....	1	.....	.....	.....	V
2776.47....	6n	1	.....	.....	IV
2776.67†...	2n	.....	.....	.....	V
2777.70*...	8n	2	.....	.....	IV
2778.03....	4	3	.....	.....	IV
2783.76....	7	1	.....	.....	IV
2785.52....	8	2	.....	.....	IV
2785.66....	10	3	.....	.....	IV
2788.16....	2	.....	.....	.....	V
2797.02....	1	.....	.....	.....	V E
2798.75....	1	.....	.....	.....	V E
2799.45....	2	.....	.....	.....	V E
2802.77....	1	.....	.....	.....	V E
2803.45....	3	.....	.....	.....	V E
2810.24....	2	.....	.....	.....	V E
2815.97....	5n	.....	.....	.....	V
2817.49....	2	.....	.....	.....	V E
2834.88....	3	.....	.....	.....	V
2835.64....	5	tr	.....	.....	V
2836.49....	2	.....	.....	.....	V E
2836.65....	3	5	1	.....	IV
2838.06....	5	5	2	.....	III
2839.43....	4	tr	.....	.....	IV
2841.04....	2	.....	.....	.....	V E
2844.92....	2	tr	.....	.....	IV
2845.22....	1	.....	.....	.....	V
2846.55....	20	5	tr	.....	IV
2847.59....	1	.....	.....	.....	V
2848.74....	15	6	4	2	II
2849.14....	15	6	4	2	II
2850.74....	1	.....	.....	.....	V
2851.79*...	20	10	12	4	II
2852.88....	25	5	tr	.....	IV
2853.54....	2	.....	.....	.....	V
2853.82....	3n	2	.....	.....	IV
2854.01....	4n	2	.....	.....	IV
2854.32....	2	.....	.....	.....	V E
2855.21....	20	10	6	2	II
2855.48....	6	4	tr	.....	IV
2855.64....	2	1	.....	.....	IV
2857.98....	20	8	1	.....	IV
2858.79....	10	5	.....	.....	IV
2859.00....	4n	2	.....	.....	IV
2859.99....	25	10r	4	2	II
2861.67*†..	1	tr	.....	.....	IV
2862.45....	10	5	tr	.....	IV
2863.06....	12	6	tr	.....	IV
2864.38....	30r	12r	5	3	II
2866.41....	20	10	2	.....	IV
2866.60....	15	8	1	.....	IV

TABLE II—*Continued*

λ (I.A.)	Arc Int.	Furnace Intensities			Class	λ (I.A.)	Arc Int.	Furnace Intensities			Class
		High Temp.	Medium Temp.	Low Temp.				High Temp.	Medium Temp.	Low Temp.	
2866.95....	10	5	1	.....	IV	2920.07†...	6	.....	.....	.....	V E
2868.12....	20	10	1	.....	IV	2920.40....	8	1	.....	.....	IV E
2869.15....	1	.....	.....	.....	V	2921.18†...	6n	1	.....	.....	IV
2869.49....	3	2	.....	.....	IV	2922.64....	4	10	8	.....	III A
2870.04....	5	3	.....	.....	IV	2922.76†...	5n	1	.....	.....	IV
2870.57....	35r	15r	8	5	II	2923.41†...	2n	.....	.....	.....	V
2875.68....	2	.....	.....	.....	V E	2923.60....	70R	35r	15r	8	II
2877.68....	2	.....	.....	.....	V	2924.01....	30	12	tr	.....	IV Er
2879.15*...	5	.....	.....	.....	V E	2924.61....	25	8	tr	.....	IV Er
2880.04....	10	tr	.....	.....	V E	2924.92†...	5n	2	.....	.....	IV
2882.51....	12	1	.....	.....	V E	2925.32....	1	.....	.....	.....	V E
2884.79....	12	1	.....	.....	V E	2925.86....	4	10	5	.....	III A
2887.69....	2	5	2	.....	III A	2926.23....	12	12	12	10	I
2888.23....	3	.....	.....	.....	V E	2927.62†...	10n	3	.....	.....	IV
2888.50....	2	5	2	.....	III A	2928.62....	2	1	.....	.....	IV
2889.62....	12	1	.....	.....	V E	2928.74†...	1n	tr	.....	.....	IV
2890.56†...	5N	1	.....	.....	IV	2930.14....	1	.....	.....	.....	V E
2891.37†...	2n	1	.....	.....	IV	2930.78†...	15	3	.....	.....	IV Er
2891.65....	15	2	.....	.....	IV Er	2930.89†...	15n	5	.....	.....	IV
2891.94†...	2n	2	.....	.....	IV	2932.34....	1	.....	.....	.....	V E
2892.44....	15	1	.....	.....	V Er	2933.20†...	3n	1	.....	.....	IV
2892.67....	20	3	.....	.....	IV Er	2933.82....	1	.....	.....	.....	V E
2893.34....	20	3	.....	.....	IV Er	2934.39....	8	tr	.....	.....	V E
2893.47†...	4n	2	.....	.....	IV	2934.62†...	2	6	4	.....	III A
2894.59....	8	12	10	2	III	2934.72†...	20n	4	.....	.....	IV
2895.16†...	4n	tr	.....	.....	V	2935.87†...	15	10	10	8	I
2896.22....	10	tr	.....	.....	V E	2937.73....	15	15	15	10	I
2898.84....	5	10	3	.....	III A	2938.30†...	5n	1	.....	.....	IV
2899.19....	20	15	8	4	II	2938.67†...	6	8	8	3	II
2899.60....	30	20r	10	6	II	2939.26†...	2n	.....	.....	.....	V
2900.86*†..	5N	1	.....	.....	IV	2941.11†...	1	3	1	.....	III A
2903.09....	10	tr	.....	.....	V E	2941.39†...	10	1	.....	.....	IV E
2903.70....	12	12	12	5	II	2941.50†...	5	tr	.....	.....	IV E
2904.14....	20	15	8	5	II	2942.02....	tr	3	1	.....	III A
2905.62....	1	.....	.....	.....	V E	2942.33*†..	10	8?	8	6	I
2906.14....	40r	20r	10	6	II	2942.39*†..	10	8?	8	6	I
2906.48....	20	2	.....	.....	IV Er	2943.19†...	30r	15r	8	5	II
2907.47....	15	1	.....	.....	IV E	2943.84†...	12n	8	1	.....	IV
2908.83*...	30	6	tr	.....	IV Er	2944.59....	20	3	.....	.....	IV Er
2910.03....	10	2	.....	.....	IV Er	2944.76....	10n	8	1	.....	IV
2910.41*...	5?	12	12	6	II A	2946.54....	15	12	10	5	II
2911.09....	10	2	.....	.....	IV Er	2949.09†...	1	2	.....	.....	IV A
2914.30†...	2n	1	.....	.....	IV	2949.15....	1	.....	.....	.....	V E
2914.43†...	2n	1	.....	.....	IV	2949.62....	25	15r	8	6	II
2914.94*...	50R	25r	15r	6	II	2949.91†...	2n	tr	.....	.....	IV
2915.33*...	10	12	12	6	II	2950.35....	10	1	.....	.....	V E
2916.00....	8	5	1	.....	IV	2951.84†...	2n	3	.....	.....	IV
2917.34....	4	.....	.....	.....	V E	2952.09....	20	3	.....	.....	IV Er
2917.52....	4	3	.....	.....	IV	2954.33....	20	15	10	6	II
2917.94....	8	5	1	.....	IV	2955.79....	15	12	10	5	II
2919.98....	6	12	10	2	III A	2956.12....	1	5	1	.....	IV A

TABLE II—*Continued*

λ (I.A.)	Arc Int.	Furnace Intensities			Class
		High Temp.	Medium Temp.	Low Temp.	
2956.57†	1n	.....	.....	.....	V
2957.12	8n	6	tr	.....	IV
2957.30*	10?	10?	8?	3	II
2957.50	10	tr	.....	.....	V E
2959.99†	2	2	.....	.....	IV
2961.14	10	8	2	.....	III
2962.07	1	.....	.....	.....	V
2962.78	30r	20r	15	10	II
2963.83	6	5	1	.....	IV
2968.29†	5	10	1	.....	IV A
2968.38	8	.....	.....	.....	V E
2968.98	3	3	.....	.....	IV
2972.27	3	.....	.....	.....	V E
2974.23	8	5	tr	.....	IV
2975.04	8	5	tr	.....	IV
2975.64	3	.....	.....	.....	V E
2976.17	5	.....	.....	.....	V E
2976.51	8	4	tr	.....	IV E
2977.50	25r	15r	20	15	I
2978.88	4	3	.....	.....	IV
2979.21†	2	tr	.....	.....	IV
2981.20	1	.....	.....	.....	V E
2982.18	2	2	.....	.....	IV
2982.74*	1	1	.....	.....	IV
2988.01	3	.....	.....	.....	V E
2989.58	2	.....	.....	.....	V E
2990.31†	1	1	.....	.....	IV
2990.93	8	8	2	.....	III
2991.14†	2	2	.....	.....	IV
2992.79†	?N	tr	.....	.....	IV
2994.01†	1	2	.....	.....	IV A
2994.50†	1	1	.....	.....	IV
2994.61*†	2n	1	.....	.....	IV
2995.58	4	5	1	.....	IV
2995.99	3	tr	.....	.....	IV E
2996.48	6	6	1	.....	IV
2997.08†	3N	1	.....	.....	IV
2997.87†	5N	2	.....	.....	IV
2998.62	4	4	tr	.....	IV
2999.20	12	15	4	.....	III
3000.59†	tr	1	.....	.....	IV A
3001.05†	1n	1	.....	.....	IV
3001.18	7	.....	.....	.....	V E
3001.90†	10N	3	.....	.....	IV
3002.44	6	4	1	.....	IV
3002.65	8	8	3	.....	III
3003.25	5	6	.....	.....	IV
3003.44	2	.....	.....	.....	V E
3004.33	4	8	1	.....	IV A
3004.82	10	12	2	.....	IV
3006.24†	5N	3	.....	.....	IV
3006.34	6	5	tr	.....	IV
3006.90*†	5N	2	.....	.....	IV
3008.61	2	.....	.....	.....	V E
3009.66†	?N	1	.....	.....	IV
3010.84†	?N	1	.....	.....	IV
3011.40†	?N	2	.....	.....	IV
3011.58†	1	tr	.....	.....	IV
3013.09	4	.....	.....	.....	V E
3014.19†	?	4	.....	.....	IV A
3014.33	15N	5	.....	.....	IV
3014.82	5	.....	.....	.....	V E
3014.92†	1	6	1	.....	IV A
3016.17	20	15	8	.....	III
3016.36†	1	2	.....	.....	IV A
3016.74	5	.....	.....	.....	V E
3021.78	6	6	1	.....	IV
3022.77†	10N	4	.....	.....	IV
3027.07	2	tr	.....	.....	IV
3030.93*†	5?	10?	6?	1	III A
3031.00*†	10?	8?	3?	.....	III
3033.43	6	.....	.....	.....	V E
3033.75*†	?	1	.....	.....	IV
3033.80	10	.....	.....	.....	V E
3038.06†	?N	1	.....	.....	IV
3038.76	10	6	1	.....	IV
3039.46†	?N	1	.....	.....	IV
3040.13†	1	1	.....	.....	IV
3041.40	2	.....	.....	.....	V E
3041.83	8	6	tr	.....	IV
3042.23	3	tr	.....	.....	IV E
3043.08*	50r	25r	20	15	II
3043.51*	50r	25r	20	15	II
3044.93	50r	25r	20	15	II
3047.21†	?N	1	.....	.....	IV
3048.17	6	.....	.....	.....	V E
3048.83	3	.....	.....	.....	V E
3050.33†	1	1	.....	.....	IV
3050.38	25	12	2	.....	IV
3050.88	35r	20r	20	12	II
3051.39†	tr	1	.....	.....	IV A
3052.19*	20	20	20	12	II
3053.37	4	.....	.....	.....	V E
3053.65†	80R	40R	30r	25	II
3053.84	2	.....	.....	.....	V E
3054.89†	1	2	tr	.....	IV A
3056.36*	100R	50R	35r	25	II
3056.59*†	?	1	.....	.....	IV
3060.45	125R	60R	40r	25	II
3060.93*	2	6	6	2	III A
3062.71	1	.....	.....	.....	V E
3063.25	4	.....	.....	.....	V E

TABLE II—*Continued*

λ (I.A.)	Arc Int.	Furnace Intensities			Class	λ (I.A.)	Arc Int.	Furnace Intensities			Class
		High Temp.	Medium Temp.	Low Temp.				High Temp.	Medium Temp.	Low Temp.	
3063.72	12	10	12	8	II	3102.29	40	15	5	.....	III Er
3065.62	1N	.....	.....	.....	V	3103.60†	1	1	.....	.....	IV
3066.38*	125R	60R	50r	35r	II	3103.99	6	6	1	.....	IV
3066.51*†	20	?	15	15	I	3104.92	1	.....	.....	.....	V E
3067.11	6	3	tr	.....	IV E	3106.12	5	5	1	.....	IV
3069.75	30r	20r	15	15	I	3107.12	5	5	1	.....	IV
3070.88†	2	5	2	.....	III A	3108.56†	N	1	.....	.....	IV
3072.73†	2n	2	.....	.....	IV	3108.68	2	.....	.....	.....	V E
3073.80*	60r	30r	20	20	II	3109.42†	1	1	.....	.....	IV
3074.06†	10n	3	.....	.....	IV	3110.71	30	10	4	.....	III Er
3074.83†	8n	2	.....	.....	IV	3110.9†	1	tr	.....	.....	IV
3075.28	10	8	2	.....	III	3112.13†	3	1	.....	.....	IV
3075.93	8	8	4	.....	III	3112.93	8	10	3	.....	III
3076.63†	4	3	1	.....	III	3113.56	2	.....	.....	.....	V E
3076.69†	5n	1	.....	.....	IV	3116.35†	1	tr	.....	.....	IV
3077.73	6	2	.....	.....	IV	3118.39	30	10	4	.....	III Er
3077.86†	5n	1	.....	.....	IV	3120.75	3	.....	.....	.....	V E
3079.35	4	8	4	.....	III A	3121.17	20	4	tr	.....	IV E
3080.16	6	10	6	2	III	3121.78	4	8	2	.....	III A
3080.34	12	6	2	.....	III	3122.92	2	.....	.....	.....	V E
3081.28	1	.....	.....	.....	V E	3123.25†	1	.....	.....	.....	V
3081.31†	1	1	.....	.....	IV	3125.29	40	15	3	.....	III Er
3081.96†	6	6	1	.....	IV	3126.19	25	6	1	.....	III Er
3082.08	50r	25r	20	15	II	3130.26	25	6	1	.....	III Er
3082.56	1	.....	.....	.....	V E	3131.3†	1	tr	.....	.....	IV
3083.21	1	.....	.....	.....	V E	3131.9†	1N	tr	.....	.....	IV
3083.50	30	15	6	1	III	3133.0†	1N	tr	.....	.....	IV
3084.38	20	10	5	1	III	3133.31	20	5	1	.....	III E
3085.84†	1n	1	.....	.....	IV	3134.54†	1	tr	.....	.....	IV
3086.50	1	.....	.....	.....	V E	3134.91	4	.....	.....	.....	V E
3087.07	15	10	3	tr	III	3135.17†	2	2	.....	.....	IV
3087.49	2n	1	.....	.....	IV	3136.48	4	tr	.....	.....	V E
3088.10	30	15	6	1	III	3138.50	3	2	.....	.....	IV
3089.12	25	12	4	tr	III	3139.04	3	1	.....	.....	IV
3090.40*†	?	1	.....	.....	IV	3139.70	4	.....	.....	.....	V E
3090.54†	3n	2	tr	.....	III	3139.97	4	3	tr	.....	IV
3090.81	4	10	5	1	III A	3141.44	1	.....	.....	.....	V E
3091.42†	20	15	15	10	II	3142.45	8	.....	.....	.....	V E
3091.52†	15	10	10	5	II	3143.2†	1	tr	.....	.....	IV
3092.72*	8	3	3	1	III	3145.32*	10	1?	.....	.....	IV E
3092.85†	1	1	.....	.....	IV	3145.65†	?N	1	.....	.....	IV
3093.14	50	20	12	.....	III Er	3145.95	5	tr	.....	.....	V E
3093.24*†	6?	10	7	1	III	3146.29*	4	2	tr	.....	IV
3093.79	25	12	7	tr	III	3146.8†	1N	tr	.....	.....	IV
3094.21	6	.....	.....	.....	V E	3147.26	8	5	tr	.....	IV
3094.70	20	10	5	tr	III	3147.97†	3N	1	.....	.....	IV
3095.90	5	5	1	.....	III	3150.03†	2N	1	.....	.....	IV
3096.04†	2	tr	.....	.....	IV	3150.59	5	4	tr	.....	IV
3099.59†	2n	1	.....	.....	IV	3151.32	2	.....	.....	.....	V E
3100.93	5	.....	.....	.....	V E	3152.75†	2N	1	.....	.....	IV
3101.4†	1	1	.....	.....	IV	3153.54†	5N	3	tr	.....	IV

TABLE II—*Continued*

λ (I.A.)	Arc Int.	Furnace Intensities			Class
		High Temp.	Medium Temp.	Low Temp.	
3155.37....	2	.....	.....	.....	V E
3156.19....	10	5	1	.....	IV
3156.89†...	2n	2	.....	.....	IV
3158.77†...	?n	1	.....	.....	IV
3159.87....	2	.....	.....	.....	V
3161.9†....	3N	1	.....	.....	IV
3162.73....	1	.....	.....	.....	V E
3163.02....	1	.....	.....	.....	V E
3163.89....	4	2	tr	.....	IV
3164.5†....	1	tr	.....	.....	IV
3164.83....	5	.....	.....	.....	V E
3165.59....	3	2	.....	.....	IV
3168.12....	5	.....	.....	.....	V E
3169.6†....	1	1	.....	.....	IV
3177.83†...	1	1	.....	.....	IV
3180.09....	1	1	.....	.....	IV
3180.56....	1	1	.....	.....	IV
3181.63†...	1	1	.....	.....	IV
3182.76†...	1	1	.....	.....	IV
3183.40....	150R	75R	75r	40r	II
3183.96*†.	300R	150R	150R	40r	II
3184.00*†.				50r	II
3185.38....	200R	100R	100r	60r	II

λ	
2406.7	Blend *Fe* in arc.
2507.85	Double.
2521.56	Probably double.
2637.15	Probably double.
2678.55	Blend in arc with enhanced line.
2747.50	Blend in arc with enhanced line.
2755.64	Enhanced line on red side.
2770.94	Probably double.
2777.70	Coincides with enhanced line.
2851.79	Blend *Fe*. Furnace line probably all *V*.
2879.15	Double. Red component strongest.
2900.86	Furnace line at violet edge of diffuse arc line.
2908.83	Double. Violet component strongest.
2910.41	Coincides with enhanced line of same intensity in spark as λ 2911.09.
2914.94	Enhanced line on violet side.
2915.33	Similar to λ 2910.41
2942.33 2942.39	Not resolved at high temperature. Measured in low-temperature furnace.
2957.30	Blend *Fe*. Probable intensity *Fe* line subtracted.
2982.74	Blend in arc with enhanced line.
2994.61	Blend in arc with enhanced line.
3006.90	Furnace line at violet edge of arc line.
3030.93 3031.00	Not fully resolved.
3033.75	Blend in arc with following line.
3043.08	Measures λ 3043.12 in low-temperature furnace.
3043.51	Measures λ 3043.55 in low-temperature furnace. Strength in spark indicates blend with enhanced line.
3052.19	Probably unresolved doublet. Components of about equal intensity.
3056.36	Measures λ 3056.32 in low-temperature furnace.

λ	
3056.59	Blend in arc with preceding line.
3060.93	Measures λ 3060.91 in low-temperature furnace.
3066.38	Measures λ 3066.36 in low-temperature furnace.
3066.51	Blend with preceding line at high temperature.
3073.80	Red side of reversal strongest, as if double. Sharp line in low-temperature furnace, measures λ 3073.82.
3090.40	Very faint in arc. Close to following line.
3092.72	Measures λ 3092.70 in low-temperature furnace.
3093.24	Blend in arc with preceding line.
3145.32	Faint furnace line to violet of enhanced line.
3146.29	Faint enhanced line to violet in arc.
3183.96	Measured with incomplete resolution as sharp impurity lines in low-temperature spectrum of titanium.
3184.00	

columns. A line distinctly outlined in the negative is given the intensity "1," a fainter appearance being indicated as "trace" ("tr"); "n" and "N" denote degrees of diffuseness in the structure of arc lines, while "r" and "R" indicate partial and complete self-reversal, respectively. Cases of extreme diffuseness, difficult blends, or disturbance by the cyanogen bands have their intensities questioned, and are usually noted in the remarks after Tables II and IV.

Classes.—In the final column, the classes are assigned according to the usual method. Lines in Classes I and II appear at low temperature and are conspicuous in the absorption spectrum. In the ultra-violet, the distinction between these two classes is difficult and may not always be significant. The Class I lines are usually not strong at high temperature or in the arc and maintain their strength at low temperature to a greater degree than those of Class II. Lines are not usually placed in Class I unless a low-temperature spectrum is available, but exception is made for a group of chromium lines, λ 2678–λ 2703, whose strength in the absorption furnace as compared with the arc is noteworthy. Lines of Class III are usually well developed at medium temperature, while lines belonging distinctly to high temperature are placed in Classes IV and V, those of Class V being absent or very faint in the furnace spectrum.

The letter "A" after the class number designates lines relatively stronger in the furnace than in the arc. Enhanced lines, selected from spark spectra having the same scale as those of arc and furnace, are distinguished by "E" following the class number. If the

TABLE III

Chromium Lines in Arc and Absorption Furnace

λ (I.A.)	Arc	Absorption Furnace	Class	λ (I.A.)	Arc	Absorption Furnace	Class
2362.22....	6	1	III	2549.51....	12	10	II
2364.74....	20n	15	II	2553.06....	6	3	II
2365.96....	12n	10	II	2557.15....	10	7	II
2366.85....	15n	10	II	2560.71....	12	8	II
2370.41....	10	2	III	2566.56....	4	3	II
2373.72....	15	3	III	2568.09*...	4	3	II
2378.02*...	10	1	III	2568.53*...	3	2	II
2379.92*...	10	1	III	2571.76....	15	6	II
2383.29....	20	5	III	2572.14....	7	3	II
2385.72†...	4n	1	III	2577.66....	10	5	II
2386.17†...	4	1	III	2578.27....	2	....	V
2389.42....	5	1	III	2579.16....	6	2	II
2392.88....	8	1	III	2583.04....	2	....	V
2395.78....	5	1	III	2584.64....	5	2	II
2396.37....	10	1	III	2588.21....	6	3	II
2399.06....	8	1	III	2591.87....	15	8	II
2399.57....	7	1	III	2603.57....	5	2	II
2408.66....	15	10	III	2608.41....	2	1	II
2408.75....	10		III	2610.31....	2	1	II
2474.08....	8	1	III	2612.04....	3	1	II
2479.16....	6	....	V	2612.21....	3	1	II
2491.34....	10	4	II	2613.32....	3	1	II
2492.55....	15	5	II	2618.28*...	10	2	III
2495.06....	7	3	II	2619.49....	3	tr	III
2496.31....	20	8	II	2620.00....	4	tr	III
2499.86....	5	3	II	2620.47....	6	1	III
2500.66....	3	1	II	2620.85....	3	tr	III
2502.55....	15	3	III	2622.87....	8	2	III
2504.31....	15	8	II	2625.35....	6	1	III
2507.34....	4	....	V	2626.58....	6	1	III
2508.12....	8	3	II	2629.82....	5	tr	III
2508.99....	8	3	II	2638.88....	3	....	V
2510.61*...	5	3?	II	2639.45*...	2	....	V
	5	3?	II	2642.13....	6	....	V
2511.98....	5	....	V	2653.57....	15	....	V E
2513.62....	7	2	II	2658.60....	15	....	V E
2516.90....	10	4	II	2661.74....	5	....	V E
2517.56....	5	2	II	2663.41....	15	....	V E
2517.87....	5	2	II	2663.68....	6	....	V E
2518.06....	3	1	II	2666.02....	15	....	V E
2518.71....	8	3	II	2668.71....	15	....	V E
2519.52....	15	10	II	2669.39....	4	1	III
2527.11....	10	4	II	2671.80....	15	....	V E
2528.02....	6	3	II	2672.00....	5	3	II
2528.23....	4	2	II	2672.83....	12	....	V E
2529.14....	3	2	II	2673.65....	3	2	II
2530.45....	7	4	II	2677.14....	25	....	V E
2534.32....	4	....	V	2678.14....	6	5	I
2541.37....	12	5	II	2678.75....	15	....	V E
2541.66....	4	2	II	2680.29....	4	3	I
2545.21....	3	1	II	2681.41....	3	1	II
2545.64....	6	2	II	2687.07....	10	....	V E

TABLE III—*Continued*

λ (I.A.)	Arc	Absorption Furnace	Class	λ (I.A.)	Arc	Absorption Furnace	Class
2688.03....	8	6	I	2742.02....	12	....	V E
2690.26....	5	4	I	2742.15....	10	....	V
2691.06....	12	....	V E	2743.11....	12	....	V E
2696.55....	3	3	I	2748.26....	50	30	II
2697.90....	1	....	V E	2748.99....	15	....	V E
2698.40....	10	....	V E	2750.75....	15	....	V E
2698.67....	10	....	V E	2751.60....	6	6	I
2700.58....	4	3	I	2751.89....	12	....	V E
2701.95....	12	6	II	2752.87....	60	25	II
2702.50....	3	....	V	2754.90....	3	....	V
2703.47*...	5	4	I	2755.28....	4	....	V
2703.75....	3	....	V E	2756.76....	3	....	V
2704.73....	3	....	V	2757.12....	60	20	II
2705.40....	4	....	V	2757.73....	12	....	V E
2705.70....	3	2	II	2759.40....	2	....	V
2710.2.....	10n	....	V	2761.75....	50	20	II
2712.30....	12	....	V E	2762.61....	25	....	V E
2716.15....	6	4	II	2763.07....	6	....	V
2717.45....	4	....	V E	2764.39....	50	25	II
2722.75....	10	....	V E	2766.56....	30	....	V E
2726.49....	80	40	II	2767.54....	5	....	V
2727.26....	2	....	V E	2769.91....	100	50	II
2731.90....	60	30	II	2771.46....	4	....	V
2736.43....	60	20	II	2775.70....	4	....	V
2737.27*...	3	5?	II?	2777.68....	5	....	V
2739.37....	10	....	V	2778.10....	6	....	V E
2740.10....	7	....	V E	2780.73....	150	60	II
2741.07....	10	....	V				

enhanced line reverses in the condensed spark, this is denoted by "Er," while "u" is added if the reversal is unsymmetrical.

In the use of this material, as close regard as possible should be paid to the intensities themselves, in addition to the class assigned. Faint lines may in some cases be placed in too high a class owing to their failure to appear in the lower-temperature spectrograms, which usually have less general intensity.

DISCUSSION

Low-temperature lines.—On account of their importance in the search for regularities in the spectrum, it may be worth while to call attention to certain groups of lines which are prominent in the absorption furnace. As a rule they are strong arc lines, and belong usually in Class II.

TABLE IV

TEMPERATURE CLASSIFICATION OF CHROMIUM LINES

λ (I.A.)	Arc Int.	Furnace Intensities			Class	λ (I.A.)	Arc Int.	Furnace Intensities			Class
		High Temp.	Medium Temp.	Low Temp.				High Temp.	Medium Temp.	Low Temp.	
2835.64	40	2	.....	.....	V Er	2921.81	3	.....	.....	.....	V E
2843.24	35	2	.....	.....	V Er	2925.58†	8n	1n	.....	.....	IV
2845.99	5	tr	.....	.....	V	2928.14	3	.....	.....	.....	V E
2849.29	4	tr	.....	.....	V	2928.25	3	.....	.....	.....	V E
2849.83	30	1	.....	.....	V Er	2929.59	12n	2	tr	.....	IV
2855.68	25	1	.....	.....	V Er	2932.5†	4n	.....	.....	.....	IV
2858.90	20	1	.....	.....	V E	2933.43†	8n	2	tr	.....	IV
2860.94	15	1	.....	.....	V E	2933.96	2	.....	.....	.....	V E
2862.59	20	1	.....	.....	V E	2934.49	15n	2	.....	.....	IV
2865.10	20	tr	.....	.....	V E	2935.13	3	.....	.....	.....	V E
2866.76	15	tr	.....	.....	V E	2935.54	3	.....	.....	.....	V
2867.64	15	tr	.....	.....	V E	2938.85†	15n	4n	1n	.....	III
2870.04†	8n	1	.....	.....	IV	2940.33†	12n	2	tr	.....	IV
2870.17†	4	1	.....	.....	IV	2941.89*	3	6	3	1	II A
2870.43	6	.....	.....	.....	V E	2946.82	1	.....	.....	.....	V E
2871.64	12	6	3	2	II	2948.85	12n	3n	1n	.....	III
2873.21	7	2	.....	.....	IV	2956.29	8	8	4	3	II
2873.49	12	.....	.....	.....	V E	2957.2*†	10n	?	.....	.....	V
2873.82	4	.....	.....	.....	V E	2959.04	2	.....	.....	.....	V
2875.98	10	.....	.....	.....	V E	2962.38	2	.....	.....	.....	V
2876.24	10	.....	.....	.....	V E	2963.68	8n	2	1	.....	III
2877.97	7	.....	.....	.....	V E	2967.67	20r	15r	10r	10	I
2879.28	15	8	3	2	II	2968.18†	5n	1n	.....	.....	IV
2880.89	5	.....	.....	.....	V E	2968.98	1	5	3	2	II A
2881.15	5	2	.....	.....	IV	2971.10	30r	20r	15r	12	II
2886.99	15	12	3	2	II	2971.90	6	.....	.....	.....	V E
2888.38	2	5	2	.....	III A	2975.43	25r	18R	12r	12	II
2889.22*†	15	6?	2?	1?	II	2979.73	5	.....	.....	.....	V E
2889.29*†	8	5?	2?	1?	II	2980.80	20r	15r	10r	8	II
2890.19	4	1	.....	.....	IV	2984.03	4	1	.....	.....	IV
2890.76	4	1	.....	.....	IV	2984.84*†	6?	6?	4?	4?	I?
2891.42	8	2	.....	.....	IV	2985.32	4	.....	.....	.....	V E
2893.26	20r	15r	4	2	II	2985.85	30R	20r	15r	12	II
2894.09	12	8	3	2	II	2985.98	60R	50R	30R	25r	II
2896.75	15	10	4	2	II	2986.10*	10	8	8	8	I?
2899.23	10	7	4	2	II	2986.49	100R	80R	60R	30r	II
2900.27	2	4	2	1	II A	2988.60	75r	40R	20r	15	II
2902.46	1	2	1	.....	III A	2989.16	4	.....	.....	.....	V E
2904.70	5	1	tr	.....	IV	2991.89	25r	15r	12r	10	II
2905.50	15	10	3	2	II	2994.03	15	12	10	7	II
2909.05	20	12	5	3	II	2995.09	30r	20r	15r	12	II
2910.91	20	12	5	3	II	2996.58	40r	30R	20r	15	II
2911.18	15	10	5	3	II	2998.10	4	.....	.....	.....	V
2913.73	10	2	tr	.....	IV	2998.79	30r	20r	15r	10	II
2916.16	4	6	2	1	II	3000.89*	40r	30R	25R	20r	II
2917.09†	6n	.....	.....	.....	V	3003.73	3	.....	.....	.....	V
2917.50†	3n	.....	.....	.....	V	3005.07	35r	25R	20r	12	II
2919.42†	2n	.....	.....	.....	V	3011.08	3	.....	.....	.....	V
2921.36*	4	.....	.....	.....	V	3013.00	15	12	10	10	I

TABLE IV—*Continued*

λ (I.A.)	Arc Int.	Furnace Intensities			Class	λ (I.A.)	Arc Int.	Furnace Intensities			Class
		High Temp.	Medium Temp.	Low Temp.				High Temp.	Medium Temp.	Low Temp.	
3013.68....	40R	30R	20r	15	II	3110.78†...	3n	.....	.....	.....	V
3014.78....	50R	40R	30R	25r	II	3110.89....	8	3	1	.....	III
3014.92....	75R	60R	40R	30r	II	3110.99†...	4n	.....	.....	.....	V
3015.17....	30r	25R	20r	15	II	3111.34....	2n	.....	.....	.....	V
3017.50....	100R	80R	60R	40R	II	3111.94†...	1n	.....	.....	.....	V
3018.45....	40R	30R	20r	15	II	3112.98....	2	.....	.....	.....	V
3018.80....	25r	20r	15r	12	II	3113.72†...	2n	.....	.....	.....	V
3020.64*...	50R	40R	30R	20r	II	3114.10†...	4n	.....	.....	.....	V
3021.56....	100R	80R	60R	40R	II	3114.44....	2	.....	.....	.....	V
3024.35....	70R	50R	35R	25r	II	3114.85....	4	.....	.....	.....	V
3024.64....	4	1	tr	.....	IV	3118.65....	15	.....	.....	.....	V E
3029.18....	20	15	12	10	II	3119.19....	10	5	2	.....	III
3030.26....	60R	40R	30R	20r	II	3119.68....	8	4	1	.....	III
3031.34....	12	10	10	10	I	3120.38....	15	.....	.....	.....	V E
3031.43....	5	1	.....	.....	IV	3120.70....	5	2	tr	.....	IV
3032.87....	2	.....	.....	.....	V E	3121.63....	6n	1	.....	.....	IV
3034.15....	40r	20r	15r	12	II	3124.98....	20	.....	.....	.....	V
3037.00*...	40r	30R	20r	15	II	3125.85....	3	1	.....	.....	IV
3039.75....	15	12	10	10	I	3127.53....	3n	tr	.....	.....	IV
3040.87*...	50r	35R	25r	15	II	3128.60....	8	.....	.....	.....	V E
3047.44....	6	1	tr	.....	IV	3131.17....	6	4	2	.....	III
3049.80....	4	5	4	2	II	3132.06....	20	.....	.....	.....	V E
3050.11....	5	.....	.....	.....	V E	3132.82....	6	3	1	.....	III
3052.18....	8	1	tr	.....	IV	3134.92....	4	1	.....	.....	IV
3053.88....	125R	50R	30R	20r	II	3135.87....	4	1	.....	.....	IV
3061.68....	6	2	1	.....	III	3136.64....	8	.....	.....	.....	V E
3061.81....	3	tr	.....	.....	IV	3138.18....	4	1	.....	.....	IV
3065.05....	10	3	1	.....	III	3141.83....	4	1	.....	.....	IV
3071.30....	4	2	tr	.....	IV	3143.67....	3n	1	.....	.....	IV
3073.68....	12	4	2	.....	III	3144.39....	15n	5n	3n	.....	III
3076.17....	2	tr	.....	.....	IV	3145.57....	5	.....	.....	.....	V
3076.54....	2	1	.....	.....	IV	3147.18....	12	.....	.....	.....	V E
3077.79....	10	3	1	.....	III	3148.40....	15	8	5	1	III
3080.72....	2	.....	.....	.....	V	3152.88....	6	2	1	.....	III
3084.53....	2	tr	.....	.....	IV	3153.52....	5	1	.....	.....	IV
3086.74....	2	1	.....	.....	IV	3154.7†....	5n	tr	.....	.....	IV
3087.49....	3	1	tr	.....	IV	3155.14....	15	10	7	1	III
3094.28....	1n	.....	.....	.....	V	3159.57....	20n	8n	5n	tr	III
3095.34....	6	1	tr	.....	IV	3163.74....	20	12	8	1	III
3095.81....	12n	5	3	.....	III	3169.54....	3	tr	.....	.....	IV
3096.03....	1	.....	.....	.....	V E	3179.22....	10n	4n	2n	.....	III
3096.48....	6n	3	1	.....	III	3180.69*...	20	2	1	.....	III
3096.65....	2	tr	.....	.....	IV	3181.41....	4	.....	.....	.....	V E
3099.44....	1	tr	.....	.....	IV	3187.98....	25n	8n	5n	tr	III
3104.68....	3	tr	.....	.....	IV	3192.10....	5	10	10	5	II A
3105.54....	2	.....	.....	.....	V	3197.07....	10	.....	.....	.....	V E
3105.83....	1n	.....	.....	.....	V	3198.06....	8	3	1	.....	III
3107.23....	2n	.....	.....	.....	V	3208.51....	3	.....	.....	.....	V E
3108.9†....	2n	.....	.....	.....	V	3209.16....	12	.....	.....	.....	V E
3109.29....	10	4	1	.....	III	3211.25....	6	2	1	.....	III
3109.7†....	4n	.....	.....	.....	V	3217.35....	8	.....	.....	.....	V E

TABLE IV—*Continued*

λ (I.A.)	Arc Int.	Furnace Intensities			Class
		High Temp.	Medium Temp.	Low Temp.	
3218.13	1n	.....	.....	.....	V
3218.67	10n	3n	1n	.....	III
3219.57	8	2	1	.....	III
3226.54	3	10	10	6	II A
3229.18	8	2	tr	.....	IV
3233.26	5	15	15	8	II A
3235.12	1	.....	.....	.....	V
3237.25	1	.....	.....	.....	V
3237.69	10	5	4	tr	III
3238.08	5	2	1	.....	III
3238.48	2	tr	.....	.....	IV
3240.93	6	15	12	8	II A
3244.10†	7	15	12	10	I A
3245.46†	5	10	10	12	I A
3245.53†	8	3	2	.....	III
3247.27	5	12	12	10	I A
3251.56	4	tr	.....	.....	IV
3251.84	15	8	5	2	II
3253.26	2	1	.....	.....	IV
3254.91	8n	.....	.....	.....	V
3257.81	20	8	5	2	II
3259.69	2	6	5	3	II A
3259.96	20	8	4	2	II
3262.81	1	.....	.....	.....	V
3266.59	5	15	15	8	II A
3267.02	1	.....	.....	.....	V
3270.08	1	.....	.....	.....	V E
3270.67	2	.....	.....	.....	V
3271.91	3n	.....	.....	.....	V
3275.73	1	.....	.....	.....	V
3277.81	3	.....	.....	.....	V
3284.81	1n	.....	.....	.....	V
3286.29	4	2	1	.....	III
3287.7	8N	.....	.....	.....	V
3291.0†	3N	.....	.....	.....	V
3293.77*	10N	.....	.....	.....	V
3295.38	2	.....	.....	.....	V E
3296.81	1n	.....	.....	.....	V
3297.28	3n	.....	.....	.....	V
3298.26	5	2	1	.....	III
3300.76	1	.....	.....	.....	V
3302.16	6n	1n	.....	.....	IV
3302.82	4	2	1	.....	III
3304.33	1	.....	.....	.....	V
3305.16	1	.....	.....	.....	V
3307.69	8	4	3	1	II
3309.80	2	1	tr	.....	III
3311.27	1	.....	.....	.....	V
3312.06	2	1	tr	.....	III
3312.69	1	.....	.....	.....	V
3313.01*	2	1	?	.....	III ?
3313.70	2	1	tr	.....	III
3314.16	1	tr	.....	.....	IV
3314.48	1	.....	.....	.....	V
3315.16	1	.....	.....	.....	V
3316.16	1	.....	.....	.....	V
3316.47	3	.....	.....	.....	V
3318.1	8N	.....	.....	.....	V
3321.19	2	1	tr	.....	III
3323.24	1	3	tr	.....	III A
3324.06	3	.....	.....	.....	V
3324.36	1	.....	.....	.....	V
3326.59	10	5	3	tr	III
3327.23	2n	tr	.....	.....	IV
3328.36	2	.....	.....	.....	V E
3329.07	8	4	2	tr	III
3330.61	3n	1n	.....	.....	IV
3332.89	6	3	1	.....	III
3333.61	20n	8	5	1	III
3334.71	30n	12	8	2	III
3334.91	4	2	1	.....	III
3336.34	4	.....	.....	.....	V E
3336.95	2	.....	.....	.....	V
3337.21	1	.....	.....	.....	V
3339.76	7	.....	.....	.....	V E
3341.41	3n	.....	.....	.....	V
3342.56	3	.....	.....	.....	V E
3343.20†	3	1	1	.....	III
3343.30†	6	3	2	tr	III
3343.72*†	5n	3	2	.....	III
3344.47	3	1	tr	.....	III
3345.10	3	1	tr	.....	III
3345.32	2	tr	.....	.....	IV
3345.96†	8	5	4	1	III
3346.09†	8n	3	2	tr	III
3346.66†	8	4	4	1	III
3346.74	6	3	3	1	III
3347.42	2	tr	.....	.....	IV
3347.77	6	.....	.....	.....	V E
3348.99	15n	6	5	1	III
3349.27	6	3	2	tr	III
3351.51†	5n	1	tr	.....	III
3351.61†	5	2	1	.....	III
3351.96*	10	20	20	20	I A
3353.05	3	1	tr	.....	III
3353.60	2	tr	.....	.....	IV
3356.39	4n	.....	.....	.....	V
3356.73	4n	.....	.....	.....	V
3357.41	1	.....	.....	.....	V
3358.54	8	.....	.....	.....	V E
3359.20	1	tr	.....	.....	IV
3360.15†	1	tr	.....	.....	IV

TABLE IV—*Continued*

λ (I.A.)	Arc Int.	Furnace Intensities			Class	λ (I.A.)	Arc Int.	Furnace Intensities			Class
		High Temp.	Medium Temp.	Low Temp.				High Temp.	Medium Temp.	Low Temp.	
3360.31....	6	.....	.....	.....	V E	3431.27....	6	6	4	1	III
3361.75....	1	.....	.....	.....	V	3431.57†...	2	2	2	.....	III
3362.26*...	20n	8	8	3	II	3431.67†...	4	3	2	.....	III
3362.73....	5n	4	3	1	II	3431.96....	5	5	3	tr	III
3365.55....	2	1	tr	.....	III	3432.30....	5	5	3	tr	III
3367.56*...	20n	12	8	3	II	3432.82....	2	.....	.....	.....	V
3368.07....	20	.....	.....	.....	V E	3433.29....	7	.....	.....	.....	V E
3370.26....	10n	2	.....	.....	IV	3433.60....	25	25	20	15	II
3374.61....	3	3	1	.....	III	3433.85†...	2n	1	.....	.....	IV
3374.96....	2	1	tr	.....	III	3434.09....	7	8	6	3	II
3375.63†...	2n	.....	.....	.....	V	3435.46....	2	1	1	.....	III
3376.18†...	6n	.....	.....	.....	V	3435.67....	6	5	5	2	II
3376.42....	6	1	.....	.....	IV	3435.81*...	6	5	4	2	II
3378.36....	2	.....	.....	.....	V E	3436.17....	20	20	15	8	II
3379.18*...	10	20	20	20	I A	3439.35....	2	tr	.....	.....	IV
3379.36....	2	.....	.....	.....	V E	3441.11....	6	8	5	3	II
3379.55*†..	5n	4	2	tr	III	3441.45....	20	20	15	8	II
3379.85*...	10n	6	4	1	III	3443.83†...	5	2	1	.....	III
3382.07....	2	1	.....	.....	IV	3445.61....	20	20	15	8	II
3382.68....	8	.....	.....	.....	V E	3447.01....	8	8	5	2	II
3384.26....	4	3	1	tr	III	3447.43....	20	15	12	8	II
3384.66....	8	5	3	1	III	3447.75....	12	10	8	3	II
3385.32....	6	1	tr	.....	III	3448.19....	2	1	1	.....	III
3386.51....	5	1	tr	.....	III	3450.85....	2	.....	.....	.....	V
3388.68....	8	6	4	1	III	3453.35....	20	15	15	8	II
3390.79....	5	1	.....	.....	IV	3453.75....	8	6	5	2	II
3391.11†...	1	1	tr	.....	III	3454.79†...	1	1	tr	.....	III
3391.41*...	6	1	.....	.....	IV	3455.26....	6	5	4	2	II
3393.03....	3	.....	.....	.....	V E	3455.60....	20	20	15	7	II
3393.84....	4	.....	.....	.....	V E	3456.60†...	1	1	tr	.....	III
3394.31....	4	.....	.....	.....	V E	3457.90†...	1	tr	.....	.....	IV
3402.39....	3	.....	.....	.....	V E	3458.07....	5	1	.....	.....	IV
3403.31....	15	.....	.....	.....	V E	3460.41....	12	5	4	1	III
3403.62....	10	1	tr	.....	IV	3463.70....	2	.....	.....	.....	V
3404.03†...	1	tr	.....	.....	IV	3464.84....	4	3	2	1	II
3406.92†...	2n	.....	.....	.....	V	3465.07†...	1	tr	.....	.....	IV
3407.26....	12n	2n	tr	.....	IV	3465.22....	12	8	8	3	II
3408.04....	8n	1n	tr	.....	IV	3465.58....	4	3	2	1	II
3408.76....	15	.....	.....	.....	V E	3467.00....	10	2	1	.....	III
3409.36....	10n	2n	tr	.....	IV	3467.69....	12	6	4	2	II
3411.04....	12n	2n	tr	.....	IV	3468.73....	4	tr	.....	.....	IV
3414.29*†..	1n	.....	.....	.....	V	3469.57....	10	4	2	tr	III
3415.58†...	2n	.....	.....	.....	V	3470.40....	8	5	4	tr	III
3418.00†...	1n	.....	.....	.....	V	3470.50....	5	3	2	tr	III
3419.67†...	1n	.....	.....	.....	V	3471.50....	4	3	2	.....	III
3419.89†...	2n	tr	.....	.....	IV	3472.77....	8	6	4	tr	III
3421.21....	10	.....	.....	.....	V E	3472.87....	7	4	2	tr	III
3421.72....	1	.....	.....	.....	V	3473.61....	8	8	4	1	III
3422.74....	15	.....	.....	.....	V E	3474.38....	7	5	2	tr	III
3425.99....	2	2	1	.....	III	3474.85....	5	2	1	.....	III
3427.66....	2n	tr	.....	.....	IV	3475.11....	2	tr	.....	.....	IV

TABLE IV—*Continued*

λ (I.A.)	Arc Int.	Furnace Intensities			Class	λ (I.A.)	Arc Int.	Furnace Intensities			Class
		High Temp.	Medium Temp.	Low Temp.				High Temp.	Medium Temp.	Low Temp.	
3476.17†...	2	.....	.....	.....	V	3536.49*†..	3n	?	?	.....	IV ?
3477.16....	4	2	1	.....	III	3536.77*†..	6n	?	?	.....	IV ?
3477.24†...	2	tr	.....	.....	IV	3537.23*...	5	1 ?	tr ?	.....	IV ?
3478.76....	5	3	1	.....	III	3545.8*†...	1n	?	.....	.....	IV ?
3479.10....	3	1	tr	.....	III	3546.4†....	1n	.....	.....	.....	V
3479.30....	5n	.....	.....	.....	V	3547.98†...	8n	5	2	.....	III
3480.30....	3	2	1	.....	III	3548.73†...	1n	.....	.....	.....	V
3481.31....	20	10	8	4	II	3548.97†...	2n	1	.....	.....	IV
3481.56....	15	6	4	1	III	3549.29†...	6n	4	1	.....	III
3483.51....	2	tr	.....	.....	IV	3550.66....	15	.....	.....	.....	V
3484.16....	3	.....	.....	.....	V E	3552.97*†..	8n	2	.....	.....	IV
3486.48....	3	.....	.....	.....	V	3553.97†...	2	.....	.....	.....	V
3488.41....	8	3	1	.....	III	3555.75....	3	.....	.....	.....	V
3494.96....	12	5	2	.....	III	3556.12....	3	.....	.....	.....	V
3495.37....	6	.....	.....	.....	V E	3558.51....	30	10	2	.....	III
3495.96†...	5	1	.....	.....	IV	3559.22*†..	5n	?	.....	.....	IV ?
3501.45....	2	tr	.....	.....	IV	3559.80*...	3	?	.....	.....	IV ?
3501.75....	1	.....	.....	.....	V	3560.6*†...	2n	?	.....	.....	IV ?
3502.30....	5	4	2	.....	III	3560.9†....	2n	.....	.....	.....	V
3503.88†...	1n	tr	.....	.....	IV	3562.26....	2	.....	.....	.....	V
3507.21†...	4n	1n	.....	.....	IV	3562.48....	1	.....	.....	.....	V
3508.10....	5	2	tr	.....	III	3562.91....	2	.....	.....	.....	V
3508.85....	8n	4	1	.....	III	3563.79†...	1n	.....	.....	.....	V
3510.34*†..	10N	4	2	.....	III	3564.27....	1	.....	.....	.....	V
3510.53....	12	6	3	.....	III	3564.72....	3	2	.....	.....	IV
3511.81....	6	.....	.....	.....	V E	3564.96†...	2	1	.....	.....	IV
3512.67†...	3n	3	1	.....	III	3565.16†...	2	1	.....	.....	IV
3517.18....	1	1	.....	.....	IV	3566.13....	40	8	2	.....	III
3518.38....	2	tr	.....	.....	IV	3568.42*†..	2n	1 ?	.....	.....	IV ?
3519.5.....	1n	.....	.....	.....	V	3568.99*†..	2n	?	.....	.....	IV ?
3519.7.....	4n	4	1	.....	III	3569.30†...	2n	.....	.....	.....	V
3522.8*†...	3n	1	.....	.....	IV	3571.65†...	1n	.....	.....	.....	V
3522.95†...	3	1	.....	.....	IV	3572.44†...	1n	.....	.....	.....	V
3523.60....	3	1	.....	.....	IV	3572.75....	5	3	tr	.....	IV
3525.5†....	8N	1	.....	.....	IV	3573.65....	10	4	2	.....	III
3527.07....	8n	4	2	.....	III	3574.04....	7	4	2	.....	III
3531.08....	2	.....	.....	.....	V	3574.40†...	15n	4	2	.....	III
3532.5†....	5N	1	.....	.....	IV	3574.80†...	8	3	2	.....	III
3532.90†...	5	.....	.....	.....	V	3574.94†...	4	2	1	.....	III

λ	
2378.02	Double.
2379.92	Double.
2510.61	Double, partially resolved.
2568.09	Double, red component strongest.
2568.53	Double, violet component strongest.
2618.28	Double.
2639.45	Double, violet component strongest.

λ	
2703.47	Enhanced line on red side.
2737.27	Furnace line probably largely *Fe*.
2889.22	Not resolved in furnace.
2889.29	
2921.36	Close to enhanced line.
2941.89	Close to enhanced line.
2957.2	*Fe* line on red side.
2984.84	Coincides with *Fe* λ 2984.83.
2986.10	Close to preceding strong line and difficult.
3000.89	*Fe* line on red side.
3020.64	Blend *Fe*.
3037.00	More widely reversed in arc than λ 3034.15.
3040.87	Enhanced line on red side.
3180.69	Probable blend with enhanced line in arc.
3293.77	Sharp line of class V superposed.
3313.01	Superposed on diffuse arc line which shows faintly in furnace.
3343.72	Line has strong center, possibly a superposed sharp line.
3351.96	Very strong in absorption. Compare λ 3379.18.
3362.26	Unusual type of diffuse line.
3367.56	Compare λ 3362.26.
3379.18	Very strong in absorption. Compare λ 3351.96.
3379.55	Furnace line may be due to impurity.
3379.85	Blend in arc with enhanced line.
3391.41	Enhanced line on red side.
3414.29	Probably double.
3435.81	Probably double.
3510.34	Arc line made up of three unresolved lines, central line sharp in furnace.
3522.8	Structure resembles λ 3510.34.
3536.49	Disturbed by band lines.
3536.77	
3537.23	Furnace line may be band line.
3545.8	Coincides with band line.
3552.97	Arc line superposed on hazy patch, probably made up of three nebulous lines. Furnace line may be band line.
3559.22	Disturbed by band lines.
3559.80	
3560.6	
3568.42	
3568.99	

For vanadium, the first of these groups extends from λ 2400 to λ 2442. This region is very difficult for the furnace, and the intensities are low, resulting in the lines being placed in Class III. Succeeding groups are contained between the limiting lines λ 2502 and λ 2577, λ 2642 and λ 2671, λ 2849 and λ 2871, λ 2895 and λ 2978, λ 3043 and λ 3091. The sources which bring out these groups most distinctly are the absorption furnace and the low-temperature emission spectrum, the former giving lines of shorter wave-length. In the high-temperature furnace, lines of higher classes are often comparable in strength with the pronounced low-temperature lines.

In the chromium spectrum, similar groups occur between λ 2365 and λ 2408, λ 2491 and λ 2592, λ 2726 and λ 2781, λ 2872 and λ 2911, λ 2968 and λ 3054. A long stretch of spectrum then contains only scattered low-temperature lines and the powerful triplet λλ 3579, 3594, 3605, until the group of Class I lines between λ 3883 and λ 3941 is reached. In this region, λ 3351.96 and λ 3379.18 are notable on account of their decided I A type, there being no other lines of comparable strength at low temperature in the neighborhood.

High-temperature lines.—The most interesting of these are the diffuse lines. They are numerous in both spectra, and occur in groups as distinct as those of any other type. In the vanadium spectrum, lines diffuse in the arc can usually be obtained sharp in the furnace and thus give improved wave-length values. This is true also for lines which in the arc are merely hazy patches. The diffuse lines of chromium are for the most part difficult to obtain in the furnace, and many of the new measurements of these lines were made in arc spectra exposed to make lines of this kind as sharp as possible. Some of the chromium lines are of an unusual type. They are moderately diffuse in the arc and retain about the same degree of diffuseness in the furnace, persisting thus sometimes at the medium-temperature stage. Three groups are noted in Table IV, near λ 2940, λ 3180, and λ 3410. In view of the exceptional behavior of these lines, it seems probable that they are of complex structure, and retain their satellites at the furnace temperatures.

Enhanced lines.—Both vanadium and chromium are very rich in ultra-violet enhanced lines, and the degrees of excitation required to produce them are similar to those required for the enhanced lines of titanium and iron, respectively. Vanadium enhanced lines frequently show self-reversal in the condensed spark; the stronger ones are prominent in the arc and persist as sharp lines in the furnace, in some cases at medium temperature. A comparison of the arc and high-temperature furnace serves to separate the enhanced lines by their relative weakness in the furnace, though

PLATE I

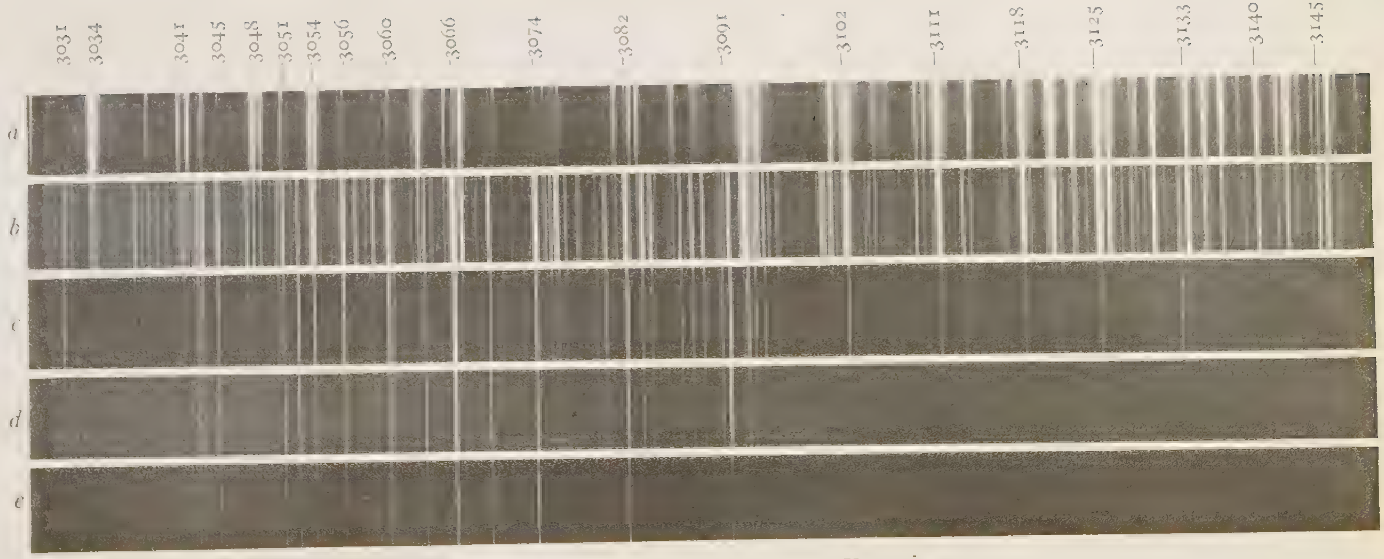

Spark, Arc, and Furnace Spectra of Vanadium

a, Spark spectrum *b*, Arc spectrum
c, *d*, *e*, Furnace spectra at 2600°, 2300°, 2000° C., respectively

the lines designated as enhanced in the tables were selected by a direct comparison of arc and spark spectra photographed during this investigation. A group of enhanced lines near λ 2710, probably forming a multiplet, has its lines reversed unsymmetrically. A very strong group of reversible lines lies near λ 3100, its first member, λ 3093.14, being the strongest spark line in this region. Another set of reversible enhanced lines is near λ 2900, while near λ 3040 occur some very strong spark lines which do not reverse, are faint in the arc, and absent in the furnace. Such lines as these latter may be regarded as the "high-temperature" lines of the ionized spectrum.

The enhanced lines of chromium require stronger excitation than those of vanadium, and only some of the strongest of chromium near λ 2850, which reverse in the spark, show faintly in the high-temperature furnace. As a result, the enhanced lines of chromium, many of which have considerable strength in the arc, go as a whole into Class V. The available data indicate that 2200° for vanadium and 2600° for chromium are approximately the initial temperatures for the appearance of enhanced lines.

Description of the plate.—Plate I reproduces a section of the vanadium spectrum for the spark, arc, and three furnace temperatures. It shows a group of prominent low-temperature lines, together with enhanced lines which persist to varying degrees in the arc and furnace spectra.

MOUNT WILSON OBSERVATORY
August 1924

Contributions from the Mount Wilson Observatory, No. 284
Reprinted from the *Astrophysical Journal*, LXI, pp. 130–136, 1925

INVESTIGATIONS ON PROPER MOTION

ELEVENTH PAPER: THE PROPER MOTION OF MESSIER 13 AND ITS INTERNAL MOTION

By ADRIAAN VAN MAANEN

ABSTRACT

Proper motions and internal motion of M 13.—Two pairs of photographs taken with the 80-foot focus arrangement of the 60-inch Mount Wilson reflector, with intervals of eleven and nine years, respectively, were measured for proper motion. The results indicate motions of the cluster as a whole amounting to 0.″001 in each co-ordinate, while the internal motions are less than 0.″001 annually.

The results are therefore negative, but they afford a good confirmation of Shapley's estimate of the distance of this object, and, furthermore, show that the internal motions found in several spiral nebulae cannot be due to the 60-inch reflector or to the measuring instrument used.

The unexpected discovery of internal motions in spiral nebulae by the writer made it seem desirable to try measures of a globular cluster as soon as the interval of time between old and new plates had become such as to make measurable displacements a possibility. Before the measurement of M 101 it was generally supposed that the spirals were located at enormous distances. The evidence for this belief, however, was principally the appearance of the many novae in these objects; and its inconclusiveness was pointed out in *Mount Wilson Contribution*, No. 243 (pp. 6 and 7).

Although the enormous distances of the globular clusters as derived by Shapley are based on considerably more substantial data than were those for the spiral nebulae, it seemed worth while to attempt to discover whether measurable motions, either internal or of the clusters as a whole, could be detected.

Several photographs of the great cluster in Hercules, M 13, were obtained soon after the 80-foot focus arrangement of the 60-inch Mount Wilson reflector had been made available for direct photography, and many other photographs of this and other clusters were taken later. Those listed in Table I were selected for measurement. The plates were combined into two pairs, 3878–5 and 3728–119, and measured in four positions each with the new stereocomparator in the manner used for the later measures of the spirals.

Dr. Shapley had indicated which stars might be members of the cluster and which not, the latter to be used for comparison purposes. With his help fifty comparison stars were selected, while sixty-two other stars were measured, which, with considerable probability, might be accepted as members of the cluster. His selection was based on the distance from the center, the magnitude, and the color-index of the individual stars.

The results of the measures are collected in Table II. When available, Ludendorff's number has been used; otherwise the stars are designated by the letters *a* . . . *v*. The first fifty in the list are the comparison stars. The magnitudes in the second column are the photographic magnitudes derived by Dr. Shapley; the co-ordinates in the third and fourth columns are given in seconds of arc and are taken from Ludendorff's catalogue,[1] except for 1120 and the stars *a* . . . *v*, which do not appear in that source. For these the co-ordinates were derived from one of the 80-foot focus plates and are accurate within 2 or 3 seconds of arc, which is sufficient for identification purposes. The origin of the co-ordinates is the same as that used by Ludendorff, viz., $\alpha=16^{h}38^{m}6^{s}$, $\delta=+36^{\circ}19'19''$ (1900).

TABLE I

Plate No.	Date	Exp.	Plate	H.A. at Middle of Exp.	Quality
5..............	1913, May 26	30^{m}	Seed 27	− 1°.2	g
119..............	1914, April 18	30	Seed 27	−11.7	g
3728..............	1923, June 8	30	Seed 23	−10.5	g
3878..............	1924, May 30	31¼	Seed 30	+18.5	fg

For the reduction, the two sets of measures of each pair of plates in the two positions in right ascension and declination were combined into single sets. The displacements were then reduced to thousandths of a second of arc per year by multiplying the measured quantities by 0.229 in the case of 3878–5 and 0.276 in the case of 3728–119. The resulting quantities were used as the first members of equations of condition of the form:

$$m_{\alpha}=a+bx+cy+dx^{2}+exy+fy^{2}+\mu_{\alpha}\,.$$

$$m_{\delta}=a'+b'x+c'y+d'x^{2}+c'xy+f'y^{2}+\mu_{\delta}\,.$$

---

[1] *Publikationen des Astrophysikalischen Observatoriums zu Potsdam*, No. 50, 1905.

TABLE II

Co-ordinates and Annual Displacements

(The motions are given in 0″.001 as a unit)

No.	Pg. Mag.	x	y	$\mu_{1\alpha}$	$\mu_{2\alpha}$	$\mu_{1\delta}$	$\mu_{2\delta}$	μ_{α}	μ_{δ}
a..........	14.50	−583″	−288″	−9	−6	+4	+12	−8	+8
c..........	14.52	491	−400	+4	+4	−6	3	+4	−2
b..........	13.06	483	+182	17	7	+5	+9	12	+7
e..........	13.40	415	−144	2	1	+3	−7	2	−2
d..........	14.52	411	+346	10	8	−14	−12	9	13
1..........	14.85	389	+150	6	11	1	+2	8	0
f..........	13.30	364	−371	+3	3	−2	−2	+3	−2
10..........	15.14	339	+78	−1	1	+6	2	0	+2
13..........	15.50	322	165	0	+3	9	−4	+2	2
15..........	13.06	310	333	−25	−19	+21	+22	−22	+22
19..........	15.91	298	194	1	+5	−3	−5	+2	−4
36..........	16.13	259	+113	10	−6	+1	−18	−8	8
g..........	14.95	256	−394	−7	4	−4	+5	6	0
43..........	14.52	250	191	+5	6	6	−3	0	4
47..........	15.89	237	228	+3	4	2	+3	0	0
h..........	14.95	176	510	0	4	0	−2	−2	1
90..........	16.22	168	110	−26	13	−18	−25	20	−22
99..........	16.03	156	−89	2	7	+13	+11	4	+12
1120..........	16.17	138	+36	13	−7	−24	−8	−10	−16
234..........	16.16	77	222	−4	+4	−13	+4	0	−4
i..........	15.00	51	+505	+3	+5	+8	+8	+4	+8
331..........	16.13	45	−249	11	0	11	−11	6	0
j..........	15.17	6	+478	7	0	2	+2	4	2
505..........	16.16	−2	264	5	−6	+8	−2	0	+3
557..........	15.11	+10	379	0	+7	−3	−3	+4	−3
599..........	16.17	19	+264	3	−3	−12	+4	0	−4
k..........	13.82	24	−485	+10	+15	+10	3	+12	+6
687..........	13.76	40	−319	−3	1	+1	+5	−1	+3
762..........	15.95	60	+238	−3	1	−1	−7	−1	−4
814..........	16.20	73	+147	+3	4	7	+2	+4	2
831..........	16.06	77	−173	7	0	−4	−7	4	−6
1015..........	16.14	160	253	4	8	+5	+7	6	+6
1019..........	12.98	163	84	3	6	−15	−8	4	−12
l..........	14.34	205	368	+8	+7	+11	+6	+8	+8
1057..........	15.86	212	136	−2	−5	14	4	−4	9
1075..........	15.79	247	−234	+6	+2	5	12	+4	8
1087..........	13.14	264	+234	−5	−11	13	+15	−8	+14
m..........	14.88	318	456	+6	+1	+3	−8	+4	−2
1111..........	16.10	342	+183	−7	−5	−19	−10	−6	−14
1114..........	14.63	351	−330	+8	+12	+5	+10	+10	+8
1115..........	15.70	354	+363	−2	4	6	3	1	4
n..........	13.90	434	−182	+11	+7	10	9	+9	10
p..........	13.14	437	−479	−29	−25	51	57	−27	54
o..........	14.88	461	+75	−4	−7	2	0	−6	1
r..........	14.09	482	−58	+3	+5	+22	+14	+4	+18
q..........	14.33	493	+369	+5	+3	−25	−22	+4	−24
s..........	14.88	503	−402	−3	−2	−110	−111	−2	−110
t..........	15.77	553	+392	−6	3	+8	+3	−4	+6
u..........	15.50	557	−21	+1	−1	16	24	0	20
v..........	15.28	+590	−181	+4	+5	+16	+13	+4	+14

TABLE II—*Continued*

No.	Pg. Mag.	x	y	$\mu_{1\alpha}$	$\mu_{2\alpha}$	$\mu_{1\delta}$	$\mu_{2\delta}$	μ_{α}	μ_{δ}
2	14.96	−389″	+138″	+7	+12	−4	0	+10	−2
7	15.04	364	+382	9	+12	3	+12	10	+4
17	14.86	307	−273	1	−2	−1	−5	0	−3
25	15.06	285	+107	+6	4	+5	−5	+1	0
46	15.57	240	−114	−14	−10	−3	+1	−12	1
49	14.83	235	−10	+4	0	4	−6	+2	5
59	15.08	221	+195	+7	+6	13	+2	+6	6
70	13.45	202	+147	−9	−5	0	−2	−7	1
72	13.74	198	−139	7	9	3	3	8	3
96	13.70	161	+10	−4	7	3	5	−6	4
118	15.03	143	−56	+6	2	10	2	+2	6
158	13.86	118	+113	−3	5	0	11	−4	6
222	12.54	82	−103	2	11	−2	0	6	−1
246	15.49	74	−98	−6	4	+8	3	5	+2
252	13.84	71	+142	+1	1	0	4	0	−2
299	15.31	56	+23	+4	7	0	2	2	1
306	var.	54	−3	−4	8	+6	−9	6	2
310	15.30	53	−114	+3	2	−2	+3	0	0
311	15.50	52	+29	−15	7	7	−4	11	6
313	15.42	51	+96	1	4	−1	0	2	0
323	15.42	47	−60	10	5	+1	1	8	0
325	15.31	46	−21	−4	−5	−7	4	−4	6
326	13.76	46	+180	+1	+3	+4	−8	+2	−2
363	15.18	34	−237	0	0	6	+1	0	+4
406	15.20	24	87	5	−4	1	−8	0	−4
418	15.46	21	−169	0	−9	+7	5	−4	+1
500	15.44	−3	+129	2	+3	−2	4	+2	−3
523	15.31	+2	42	+3	−5	10	2	−1	6
559	15.20	10	54	−7	1	6	1	4	4
641	15.14	29	217	+5	5	1	−2	0	−2
653	15.18	32	+189	−2	3	0	+4	2	+2
686	15.42	40	−135	+2	4	−6	+8	1	+1
690	15.26	41	+56	−5	0	+2	−7	2	−2
712	15.36	46	−69	+1	9	−2	4	−4	3
737	15.20	54	72	9	6	1	3	+2	2
775	14.91	63	−159	5	−3	0	2	1	1
784	15.31	65	+41	0	+1	−15	0	0	8
796	14.93	68	−127	+4	+3	+2	−3	+4	0
804	15.20	70	+24	−2	−4	−7	+2	−3	−2
808	15.30	72	+251	+5	+6	+4	−5	+6	0
816	var.	73	−25	−5	−5	4	+3	−5	+4
822	15.09	75	+321	0	+2	6	−4	+1	1
829	15.20	77	+4	+2	−6	8	0	−2	4
835	13.23	79	−115	−5	5	2	+3	−5	2
837	15.42	80	80	+11	−1	+9	0	+5	+4
840	15.50	80	38	3	+1	−1	−4	+2	−2
851	15.30	84	20	0	−6	+2	4	−3	1
852	15.17	85	129	+1	+1	−2	7	+1	−4
861	14.86	88	−145	−2	−1	+2	0	−2	+1
873	15.09	93	+115	+2	+1	−5	3	+2	−4
899	15.14	100	+106	0	+1	−4	4	0	−4
925	15.07	108	−120	+8	−1	+4	−5	+4	0
935	14.50	+112	+70	+3	+2	+2	0	+2	+1

PLATE II

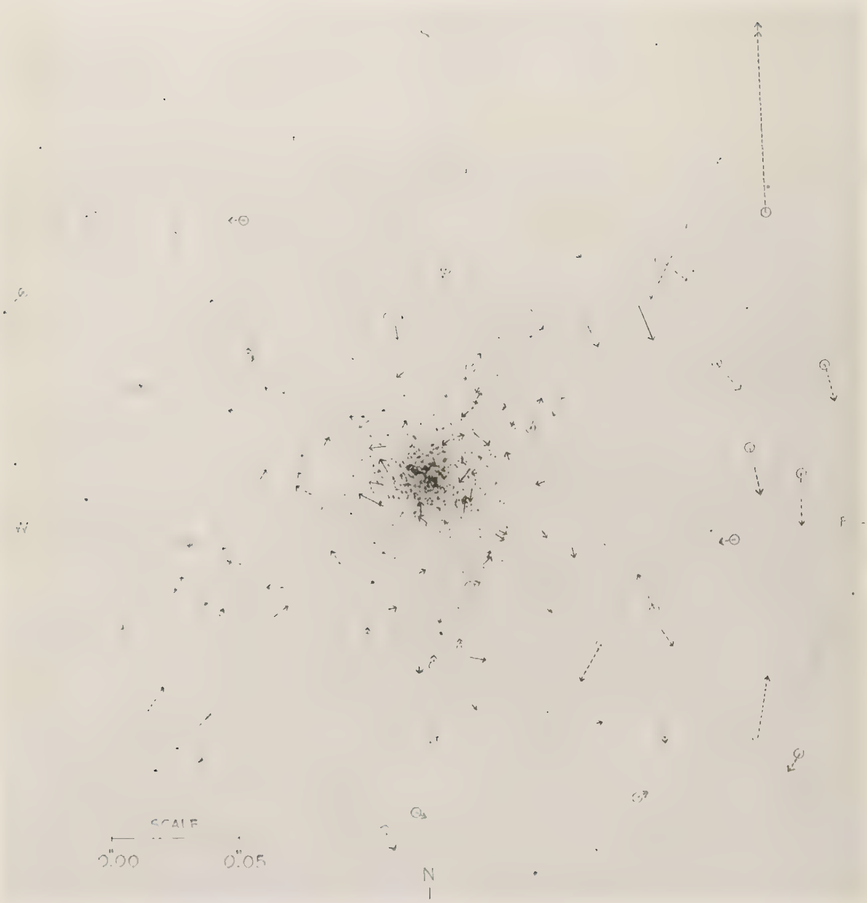

Internal Motions in the Globular Cluster M 13

Star images inclosed in circles represent comparison stars. Images with full-line arrows attached are of stars probably belonging to the cluster, whose motions are relative to the system of comparison stars.

TABLE II—*Continued*

No.	Pg. Mag.	x	y	$\mu_{1\alpha}$	$\mu_{2\alpha}$	$\mu_{1\delta}$	$\mu_{2\delta}$	μ_α	μ_δ
953..........	15.20	+117″	+ 65″	+ 5	− 2	+ 2	− 1	+ 2	0
978..........	15.04	132	− 39	− 2	3	− 2	− 5	− 2	− 4
989..........	15.60	139	− 95	+ 2	6	+ 1	+ 1	− 2	+ 1
1038β	15.07	180	+ 67	+ 7	5	6	− 2	+ 1	2
1042..........	15.09	182	− 6	− 6	2	4	4	− 4	0
1063..........	15.08	223	+ 90	+ 2	− 2	6	0	0	+ 3
1079..........	15.14	255	+350	2	+ 3	5	− 9	+ 2	− 2
1106..........	15.18	321	−263	4	+ 4	14	+11	4	+12
1113..........	15.26	+350	+208	+10	− 1	+11	+ 1	+ 4	+ 6

The plate constants a . . . . f and a' . . . . f' were computed in each case from the fifty equations of condition for the fifty comparison stars. These were subsequently substituted in all 112 equations in order to derive $\mu_{1\alpha}$, $\mu_{2\alpha}$, $\mu_{1\delta}$, and $\mu_{2\delta}$. These quantities are therefore proper motions of individual stars with respect to the group of comparison stars. The last two columns of Table II give the mean μ_α and μ_δ for the two pairs of plates.

The accuracy of the measures is highly satisfactory, the probable error of the motion in each co-ordinate as derived from a comparison of the measures of each pair of plates being only 0″.0023.

The next step is to derive the mean proper motion of the cluster as a whole. Since the distribution of the stars is nearly symmetrical with respect to the center, the straight mean was taken, giving

$$\mu_\alpha = -0''.001 \pm 0''.0004, \qquad \mu_\delta = -0''.001 \pm 0''.0003\,,$$

as the motion of the cluster with respect to the comparison stars. Subtracting these quantities from the last two columns in Table II, we derive the values in the second and third columns of Table III. These differences represent the internal motions and have been plotted in Plate II. For the comparison stars, which are surrounded by circles, the motions are taken from Table II and are plotted as broken lines. The scale of the motions is given in the lower left-hand corner. The length of the arrows represents the motions in about four thousand years.

For the star s the motion is 50 per cent larger than indicated on the plate. Since its motion is over a tenth of a second, it might better have been omitted, but as it did not show any motion in right ascension the normal equations in this co-ordinate had already been formed and solved before the displacement in declination was found. Furthermore, as the number of comparison stars is considerable, its influence is small, contributing only a positive displacement in declination to the stars in the southeastern quadrant.

TABLE III

INTERNAL MOTIONS IN M 13

(Given in 0″.001 as a unit)

No.	μ_α	μ_δ	$\mu_{rad.}$	$\mu_{rot.}$	No.	μ_α	μ_δ	$\mu_{rad.}$	$\mu_{rot.}$
2	+11	−1	−11	+3	686	0	+2	−2	0
7	11	+5	4	+11	690	−1	−1	1	−1
17	1	−2	0	−2	712	−3	2	−3	+2
25	+2	+1	−1	+2	737	+3	1	+3	−2
46	−11	0	+10	+4	775	2	0	+1	−2
49	+3	−4	−3	−4	784	1	−7	−5	+5
59	+7	5	−9	+1	796	+5	+1	+1	−5
70	−6	0	+4	−4	804	−2	−1	−2	−1
72	7	2	7	+2	808	+7	+1	+3	+6
96	−5	3	+4	−4	816	−4	5	−5	−4
118	+3	5	−2	5	822	+2	2	+2	+2
158	−3	−5	−1	−6	829	−1	5	+1	−5
222	5	0	+3	+4	835	−4	3	−5	+2
246	−4	+3	+1	5	837	+6	+5	+1	−8
252	+1	−1	−1	+1	840	+3	−1	+3	0
299	−1	0	+1	0	851	−2	0	−2	0
306	−5	−1	+4	−3	852	+2	−3	+3	1
310	+1	+1	−1	1	861	−1	+2	−2	−1
311	−10	−5	+4	−10	873	+3	−3	1	+4
313	1	+1	1	0	899	1	−3	−2	+2
323	7	+1	5	+5	925	5	+1	+3	−4
325	−3	−5	+3	−5	935	3	2	4	0
326	+3	−1	−1	+3	953	+3	+1	+3	+1
363	1	+5	−5	0	978	−1	−3	0	+3
406	+1	−3	+3	−2	989	−1	+2	−2	−1
418	−3	+2	−2	+3	1038β	+2	3	+3	2
500	+3	−2	2	+3	1042	−3	1	−3	1
523	0	5	5	−1	1063	+1	+4	+2	−3
559	−3	3	3	−3	1079	3	−1	+1	+3
641	+1	−1	−1	+1	1106	5	+13	−5	−13
653	−1	+3	+3	−1	1113	+5	+7	+8	−3

A glance at the plate shows that the internal motions must be very small, and a discussion of the data corroborates this fact. If we accept for a moment that the motions of the cluster stars are due to accidental errors only, we find a probable error in each co-ordinate of 0″.0026. It is true that this is slightly larger than the value stated above, but it is well known that the internal probable error is always somewhat, and sometimes considerably, smaller than the external probable error. The difference between the two values given indicates that the internal motions of the members of the cluster can scarcely exceed 0″.001 in each co-ordinate.

For completeness the motions were further resolved into two components, one radial and one perpendicular thereto. These are given in the last two columns of Table III. The first component is one that might a priori be expected from a contraction or dispersion of the cluster; the result, however, is that the mean radial component is exactly zero.

There is little reason to anticipate a component at right angles to the radius, except that such a component has been shown to exist in the measures of the spiral nebulae. In M 13 this component comes out 0″.0005±0″.0004, in the direction N-W-S-E.

We may thus conclude that the internal motions in the cluster are of the order of 0″.001 or less. A considerably longer interval will therefore be required to detect any possible motion.

Although these results are negative, they are, nevertheless, of importance for two reasons. First, they are a beautiful confirmation of Shapley's distances, because with the parallax derived by him, 0″.00009, even a fairly large velocity would still give an extremely small proper motion; and second, because the results obtained for M 13 show again that the internal motions found in several spirals cannot be due either to the 60-inch reflector or to the measuring instrument. The only possibility that the displacements found in the spirals are not real motions would seem to lie in a systematic difference along the spiral arms between the old and the new plates. This possibility is extremely doubtful, because in that case the effect would hardly be proportional to the time interval, as was found in several of the spirals for which pairs of plates with different time intervals were available. Moreover, such displacements would be considerably less in the case of an object with starlike points, such as M 33, than in some of the others. Finally, we should expect such a systematic error to be larger near the center than near the edge of a spiral, while the measures show just the reverse in all cases.

Mount Wilson Observatory
August 20, 1924

Contributions from the Mount Wilson Observatory, No. 285
Reprinted from the *Astrophysical Journal*, Vol. LXI, pp. 186–203, 1925

A STUDY OF ELECTRICALLY EXPLODED WIRES

By SINCLAIR SMITH

ABSTRACT

A new type of spectrograph.—The converging beam of light from a grating is reflected from one of the faces of a rotating mirror to the focal plane of the instrument. The rotation of the mirror causes the spectrum to move along a photographic film, and changes that take place in the spectrum of the light-source under investigation are recorded upon this film.

Time-resolving power.—The term "time-resolving power," analogous to optical-resolving power, is defined, and, for the instrument described, is shown to be about one one-millionth of a second.

Spectra.—The spectra of electrically exploded wires of various elements have been studied with the rotating-mirror spectrograph in the interval λλ 3000–5000, and results for *Pb*, *Sn*, *Al*, *Cu*, *Cd*, and *Mg* are described.

A new absorption phenomenon.—In the case of certain elements, small areas on the surface of the mass of vapor produced by an explosion proved to be very opaque for wave-lengths in the region studied. This absorption was not perfectly uniform, but showed irregularities in regions close to strong arc lines, which suggests that anomalous dispersion may explain the phenomenon.

The resistance of metallic vapors at high temperatures.—A method is described for determining the relative resistances of metallic vapors, and results are given for *Cu*, *Ag*, *Au*, *Ni*, *W*, *Zn*, *Al*, *Pb*, *Sn*, *Li*, and *Fe*.

Anderson[1] has shown that electrically exploded wires furnish spectroscopists with a source of metallic vapor at an exceedingly high temperature, and further that this vapor retains a high intrinsic brilliancy for a relatively long time after the excitation has ceased. As the spectrum shows a great variety of lines, the question naturally arises, Do all the lines appear simultaneously, or do different lines appear at different times? In order to answer this question, a new type of spectrograph was built which made possible the study of the variations of the spectrum with time.

METHODS AND APPARATUS

The spectrograph.—The essentially new feature of this spectrograph is a rotating mirror so mounted that the beam, after having passed through the slit and suffered dispersion, is reflected from one of the faces of the rotating mirror to the focal plane of the instrument. Two of these instruments were built, one with a prism and the other a concave grating. The arrangement of the optical parts of the prismatic instrument is shown diagrammatically in Figure 1. Figure 2 shows the position of the photographic film relative to the rotating mirror. This kind of instrument should be faster than the one to be described, but though a number of good camera lenses were tried, no lens combination having the desired characteristics was available. What is needed is a combination which will accurately focus the desired range of spectrum on a plane perpendicular to the axis of projection. Since a range of about 100 A was the best that could be done with the lenses available, this form of instrument was abandoned and the concave grating-type was adopted.

---

[1] *Mt. Wilson Contr.*, No. 178; *Astrophysical Journal*, 51, 37, 1920.

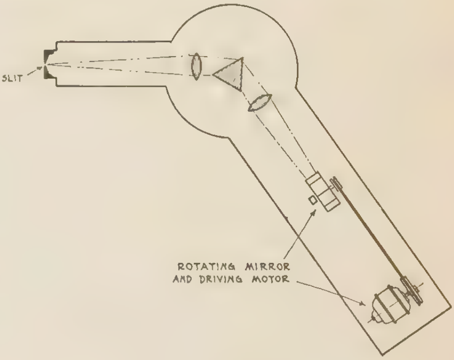

FIG. 1

The arrangement of the slit, grating, and rotating mirror is shown in Figure 3, while the position of the film relative to the rotating mirror is as before (see Fig. 2). A 4-inch, concave grating of 1-meter radius, having 15,000 lines per inch, was used. The slit was placed 2 meters from the grating, which fixed the distance from the grating to the focal plane at 66 cm, and gave in the first order a scale of 25 A per mm. The film was held in a circular holder having a 25-cm radius. The actual focal curve is not a circle, but a circle was found to be a sufficient approximation. The octagonal mirror was used to insure a record of every exposure. Since the film subtended an angle of slightly more than 90° as seen from the rotating mirror, the light from the grating always fell somewhere on the film, regardless of the position of the mirror.

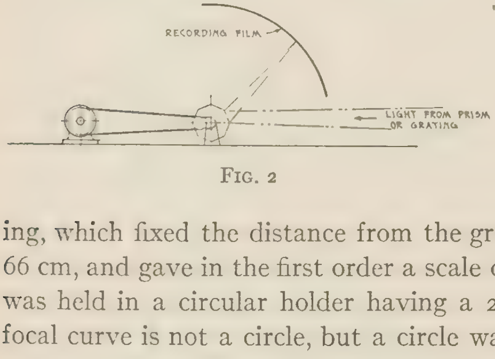

FIG. 2

When the instrument is in adjustment, the spectrum must of course be in focus; further, the rulings of the grating must be parallel to the slit and, at the same time, the projected slit images, i.e., the spectral lines, must be parallel to the direction in which they move when the mirror is rotated. The focusing can be done visually with a high-power lens, but the other conditions cannot be met so easily. The procedure adopted was as follows: The grating was first rotated to a position such that the central image would fall on the film. A film was then placed in the holder and exposed to a series of slit images with the mirror in different positions, and, finally, a reference line was put on the film by making a short exposure with the mirror slowly rotating. An arc was used for illumination. The parallel position was determined by measuring the inclination of the slit images to the reference line. This operation so oriented the slit that its projected image on the photographic film moved accurately along its own length when the mirror was rotated. The grating was then rotated back to its original position, and the normal adjusted. The rulings were made parallel to the slit by watching the spectral lines with a high-power lens and slowly rotating the grating about its normal.

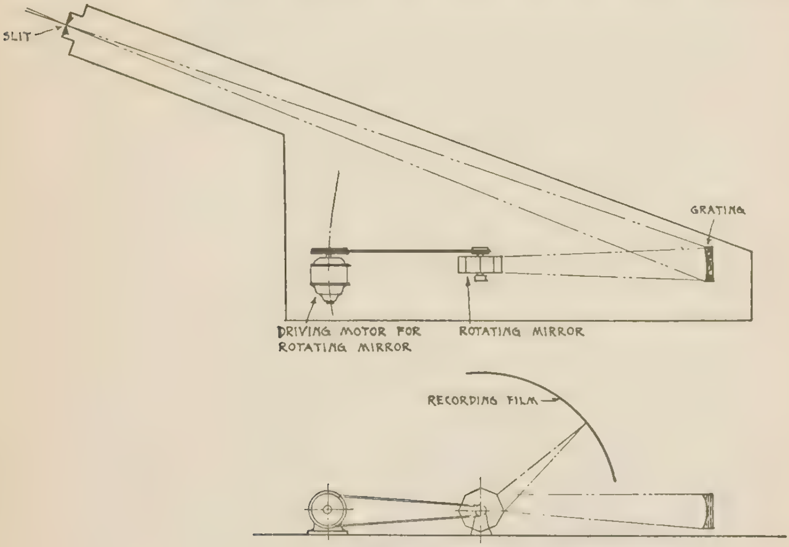

FIG. 3

Time-resolving power.—Since we shall be interested in determining differences in time as well as in wave-length, let us call the smallest time difference that can be measured the "time-resolving power" of the instrument. Since time differences are determined by measuring the distances along the time axis of the film from some arbitrary zero line to the two points in question, and multiplying the difference between these two distances by a factor (the time required for the image to move unit distance along the film), it might appear that the accuracy with which linear distances can be measured is the only limit to the determination of small time intervals. This, however, would be crediting the instrument with powers it does not possess. A consideration of optical-resolving power makes this clear. It is quite true that, regardless of the optical-resolving power of the spectrograph, the difference in wave-length of two spectral lines which are widely separated can be determined to the degree of accuracy with which we can measure the linear distance between them on the plate. If the two lines are very close together, however, the determination no longer depends on our ability to make close settings but on the resolving power of the instrument. For this reason we shall mean by time-resolving power, not the smallest measurable interval between the appearance of two different spectral lines, but rather the smallest measurable interval between changes that take place in some particular line. For example, suppose that a line disappears for a very short time and then reappears. If the interval of disappearance is less than the time-resolving power of the instrument, we shall not be able to detect the change, but, if greater, we shall be well aware of it. It appears, then, that the time-resolving power will be the interval required for the image on the photographic film to move its own width. Thus the time-resolving power depends both on the speed of the rotating mirror and on the width of the spectrum in the focal plane.

In order to limit the width of the spectrum, a horizontal slit was used, as well as the slit proper. Since the concave grating is not used in parallel light, the system is astigmatic. The conjugate focus of a line in the focal plane perpendicular to the spectral lines is farther from the grating than the conjugate focus of the lines themselves. The spectrograph slit is of course at the conjugate

PLATE III

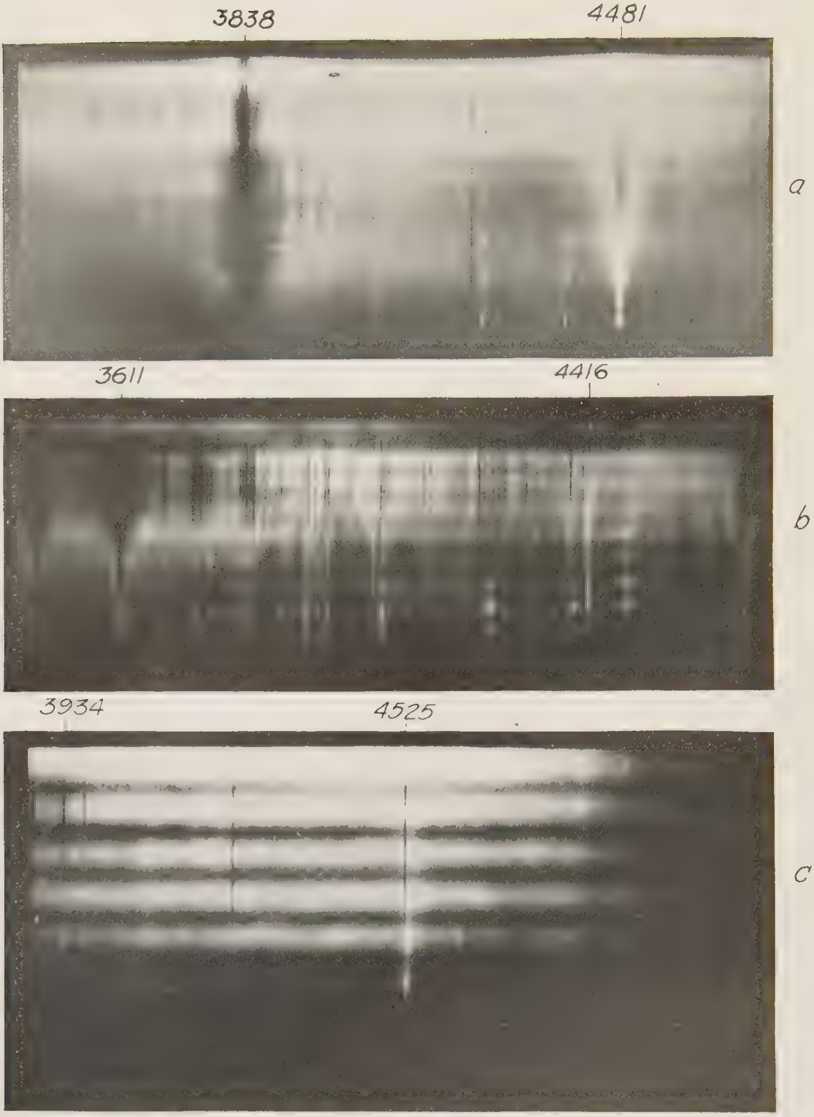

Spectrograms with Rotating-Mirror Spectrograph

a, Magnesium, 55,000-volt condenser. Note reversal of λ 4481
b, Cadmium, 55,000-volt condenser
c, Tin, 20,000-volt condenser

focus of the spectral lines, but the horizontal slit must be placed at the conjugate focus of the line in the focal plane perpendicular to the spectral lines. The width of the second slit is governed by the intensity of the light-source. In the present work, the width used was such that the spectrum was 0.5 mm wide in the focal plane.

In most of the work to be described, the speed of the mirror was about 150 rev. per sec., corresponding to a motion of the spectrum along the film at the rate of about 450 m per sec. Assuming that uncertainties of measurement along the axis of the film arising from the finite width of the spectrum and a possible lack of critical focus do not exceed 0.5 mm, we find the time-resolving power to be of the order of one one-millionth of a second.

The condensers.—The spectra studied were produced in the manner described by Anderson. Two different condensers were used. One of them, which has already been described by Anderson,[1] consists of 200 single-strength window-glass plates, 20×24 inches, having tin-foil coatings 17×21 inches. Its capacity is about 1 microfarad, and in use was charged to 20,000 volts. The second condenser was also built under Anderson's direction. The plates, furnished by the Mississippi Glass Company, are 36×36 inches and $\frac{7}{16}$ inch thick. A closely woven wire gauze 32×32 inches was imbedded in the center of the plates during the manufacture, and a single wire was brought out on one side to serve as a lead. The plates are stacked in holders with the leads of alternate plates on opposite sides. All the leads on the same side are joined to a common terminal. This type of condenser can be charged to a much higher voltage than the ordinary form, and in the present work a voltage of 55,000 was used. During the assembly, the condenser plates were tested in pairs at 85,000 volts, but on account of surge difficulties it was not thought safe to use the whole condenser at this voltage. The complete condenser consists of 150 plates, which give a capacity of 0.6 microfarad.

As the intensity of the light varies with the oscillations present in the explosions, the oscillations themselves furnished a time scale very convenient for practical purposes. After having once determined the period of each of the electrical circuits, time differences on the spectrograms were determined by comparison with the separation of the oscillations. The frequency of the 20,000-volt circuit was 87,000, and that of the 55,000-volt circuit, owing to much less inductance, was 185,000. This makes the maximum current in the 20,000-volt circuit about 10,700 amperes, and in the 55,000-volt circuit, about 40,000 amperes.

---

[1] *Mt. Wilson Contr.*, No. 269; *Astrophysical Journal*, **59**, 76, 1924.

Some of the explosions studied were produced in air, while others were confined within a slotted block of wood. These blocks were of oak, $2 \times 2 \times 2\frac{1}{2}$ inches, with a $\frac{1}{8}$-inch slot, $\frac{3}{4}$ inch deep, cut the long way in each block. Holes were drilled in the sides and electrodes, 2 inches apart, inserted in such a manner that their tops were just above the bottom of the slot.

DISCUSSION OF SPECTROGRAMS

The spectra of a number of elements were examined in the region from λ 3000 to λ 5000. Very great differences were found in the behavior of different lines. The details for *Pb*, *Sn*, *Al*, *Cu*, *Cd*, and *Mg* are shown in the tables. In general, the arc lines were found to be completely reversed, while the spark lines frequently appeared in emission. The latter were generally strongest at the peaks of the oscillations, and some of them appeared only on the peaks. Ordinarily these lines disappeared when the oscillations ceased; but, as may be seen from the reproductions, there were large variations in behavior.

The lines were also found to behave differently with the two condensers. For example, when the explosions were produced with the 20,000-volt condenser, the two spark lines of *Pb*, λ 4245 and λ 4387, appeared as sharp lines and showed no tendency to reverse. With the 55,000-volt condenser, they became very broad and diffuse and showed definite reversal (see Plate IV). As a rule, the spectra obtained with the second condenser were almost wholly absorption spectra.

The spectra also behaved differently when the explosions were confined in a slot and when produced in the open air. The difference was very marked when the 20,000-volt condenser was used, but less noticeable in the case of the 55,000-volt condenser. With the lower-voltage condenser, confining the explosions increased

PLATE IV

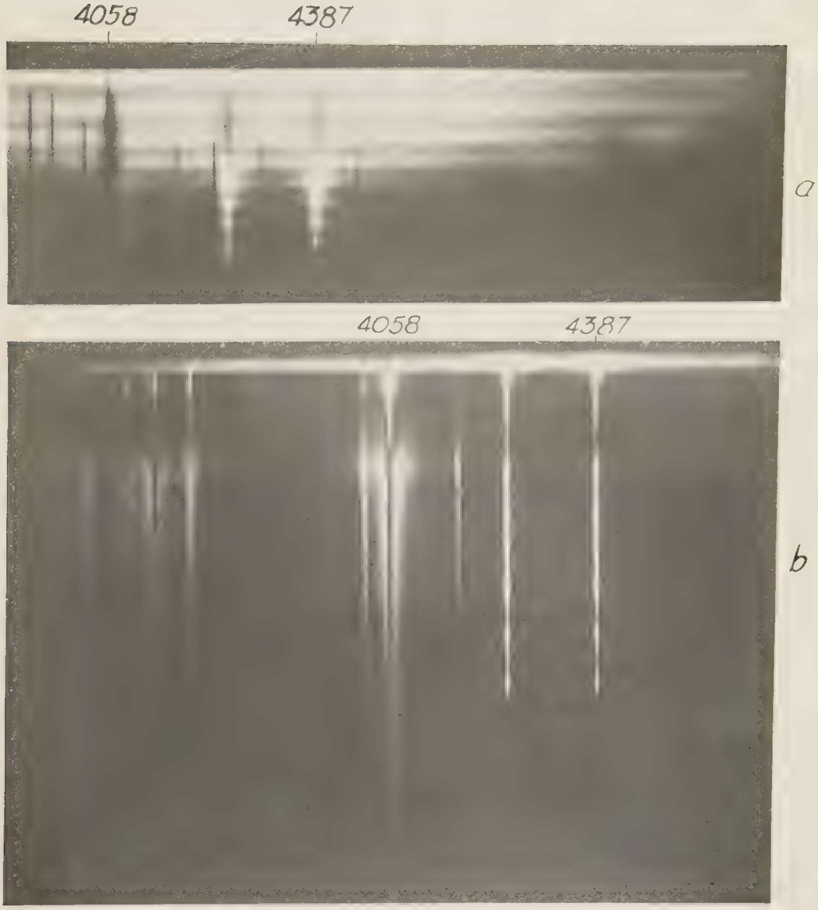

Spectrograms of Lead with Rotating-Mirror Spectrograph

a, 55,000-volt condenser; *b*, 20,000-volt condenser

the strength of the continuous spectrum and also the tendency for lines to reverse. When the higher-voltage condenser was used, the difference was not so marked, for in this case the continuous spectrum was already quite strong in the unconfined explosions, and confining them added little to its strength.

The presence of the continuous spectrum is interesting in itself. In the case of most of the elements studied it is fairly strong throughout the third half-oscillation, and in some cases it persists as late as the fifth. Direct rotating-mirror photographs of the explosions show that by the time the third half-oscillation occurs, the vapor is expanding relatively slowly, from which it may be inferred that the pressure is not much above 1 atmosphere. This is significant in that it shows that we have a mass of vapor, certainly not much above atmospheric pressure, in which the excitation is sufficiently high to produce radiation almost entirely continuous. Just how much of this excitation is electrical, and how much is due to temperature, is of course not known. But the strongly marked increase in the continuous spectrum with the development of the electrical oscillations does not necessarily preclude a pure temperature excitation, since the effect of the current during the peaks of the oscillations may be only to increase the temperature of the vapor.

The fact that the enhanced lines appear most prominently when the continuous spectrum is strongest lends weight to the hypothesis that the quanta contributing to continuous radiation are produced when ionized atoms recombine. When recombination occurs, we should expect the sum total of the change in potential energy of the system, plus the kinetic energy of the electron relative to the atom, to be radiated in a single quantum. But no two of these quanta need have anything like the same value. The kinetic energy of the electron may have almost any value, and in recombining the electron may stop in any one of many orbits, so that the potential energy contributed to the quantum radiated can have a wide range of values. However true or false this picture may be, it is at least in qualitative agreement with the foregoing, and, furthermore, it explains the existence of the continuous background found in spark spectra.

Another interesting feature is the behavior of impurity lines. In general, for the first six or eight millionths of a second, the spectrum is that of the element under observation, and practically no impurity lines appear. Those that do appear, air lines in the case of unconfined explosions and calcium lines when the explosions are confined, apparently arise from neighboring materials rather than from the material under observation. The source of the air lines is obvious, while the calcium lines probably originate in the wooden blocks. This effect is noticeable in the reproduction of the cadmium spectrogram.

In one of the aluminum spectrograms the following impurity lines were identified in the region λ 3510–λ 4500:

Lead:
λ 3572.95
3639.72
3683.62
3740.20
3835.15
λ 3842.2
3854.11
4058.00
4245.42
4387.11

No trace of λ 4019.20 or λ 4168.19

Calcium:
λ 3933.81
3968.62
λ 4226.90
4307.90

Iron:
λ 3553.87
3557.02 (D ?)
3565.54
3570.29
3581.38
3585.88 (D ?)
3618.91
3621.61
3631.60
3648.00
λ 3720.09
3727.79
3735.02
3737.30
3745.70
3749.62
3758.39
3763.99
3765.69
3767.35
λ 3786.81
3795.12
3816.00
3820.61
3826.07
3828.00
3834.40
3840.61
3860.03
3872.70
λ 3878.19
4045.99
4063.77
4071.92
4118.70
4132.25
4143.59
4144.08
4181.94
4199.25
λ 4202.20
4260.68
4271.95
4325.97
4383.71
4404.95

EXPLANATION OF TABLES

For convenience the lines were classified as follows:

I. Pure absorption lines which remain sharp throughout their existence.

II. Pure absorption lines which are somewhat diffuse.

III. Pure absorption lines which widen very greatly during certain phases of the explosions.

IV. Strongly reversed lines showing emission edges and only a slight tendency to vary with the oscillations.

V. Diffuse lines showing faint reversal and pronounced variation with the oscillations.

VI. Diffuse lines showing no trace of reversal but pronounced variation with the oscillations.

VII. Sharp lines showing no trace of reversal, but definite variation with oscillations.

VIII. Diffuse lines showing no trace of reversal and appearing only on the peaks of the oscillations.

IX. Sharp lines showing no trace of reversal and appearing only on the peaks of the oscillations.

This classification is purely arbitrary, and in many cases not sufficient, but a detailed discussion of the behavior of each line is out of the question. Intensities are given merely as *w*, *m*, or *s*, meaning weak, medium, or strong. A more elaborate system seems unnecessary. In a few cases, the series classification is given after the wave-length. In the column headed "Remarks" is listed the time of first appearance in terms of the half-oscillations. For example, "late in 3rd" means that the line first appeared on the spectrogram during the latter part of the third half-oscillation. Any extraordinary behavior of the line is also noted in that column.

TABLE I

TIN

50,000-Volt Condenser, Explosions Confined in Block

Wave-Length	Int.	Class	Remarks
4525	*s*	I	Appears at beginning
			Impurities
3934 *Ca*	*m*	I	Appears in 2nd
3969 *Ca*	*m*	I	Appears in 2nd
4227 *Ca*	*m*	I	Appears in 2nd
4737 *C*	*w*	Band	Four heads show faintly in 4th, 5th, and 6th

TABLE II

MAGNESIUM

50,000 Volt Condenser, Explosions Unconfined

Wave-Length	Int.	Class	Remarks
3829	*s*	III	Appears at beginning
3832	*s*	III	Appears at beginning
3838	*s*	III	Appears at beginning
4481	*s*	V	Appears at beginning; very wide at first (possibly 50 A)

TABLE III

CADMIUM

WAVE-LENGTH	55,000-VOLT CONDENSER, EXPLOSIONS CONFINED IN BLOCK			20,000-VOLT CONDENSER, EXPLOSIONS UNCONFINED		
	Int.	Class	Remarks	Int.	Class	Remarks
3081 $1p-2s$	*m*	II	Begins late in 1st	......	......	
3081 $1p-2s$	*m*	II	Begins late in 1st	......	......	
3253 $1p-2s$	*m*	II	Begins late in 1st	......	......	
3261 $1S-1p_2$	*m*	I	Appears at beginning; very sharp throughout	......	......	
3404 $1p-2d$	*s*	III	Appears at beginning	*s*	IV	Appears at beginning
3466 $1p-2d$	*s*	III	Appears at beginning	*s*	IV	Appears at beginning
3536	......	......	Not present	*m*	IX	Appears at 1st and 2nd only
3611 $1p-2d$	*s*	III	Appears at beginning	*s*	IV	Appears at beginning
4416	*s*	V	Appears late in 1st	*m*	VII	Very strong in 1st
4678 $1p-1s$	*s*	II	Appears late in 1st	......	......	
4800 $1p-1s$	*s*	II	Appears late in 1st	......	......	
5086 $1p-1s$	*s*	II	Appears late in 1st	......	......	
	Impurities					
3159 *Ca*	*w*	I	Begins late in 2nd	......	......	
3179 *Ca*	*w*	I	Begins late in 2nd	......	......	
3934 *Ca*	*m*	I	Begins late in 1st	*m*	VII	Begins late in 1st
3969 *Ca*	*m*	I	Begins late in 1st	*m*	VII	Begins late in 1st
4227 *Ca*	*m*	I	Begins late in 1st	*m*	VII	Begins late in 1st

A NEW ABSORPTION PHENOMENON

In the case of a number of explosion spectrograms of *Al*, *Pb*, *Cd*, *Ca*, and *Mg*, a new absorption phenomenon presented itself. For a very short interval, usually not more than about three-millionths of a second, that part of the explosion which was projected on the

TABLE IV

ALUMINUM

Wave-Length	55,000-Volt Condenser, Explosions Unconfined*			20,000-Volt Condenser, Explosions Unconfined		
	Int.	Class	Remarks	Int.	Class	Remarks
3587	*s*	V	Very wide in first gradually narrowing to a class IX line in the 5th or 6th	*s*	VI	In some cases this line appears in the 1st as a broad diffuse line and continues until about the 4th when it disappears. In other cases it appears very faintly in the 1st and then disappears until the 3rd when it appears quite strong and persists until the 8th or 10th
3602	*m*	IX	Appears on peaks of 2nd, 3rd, and 4th	......	......	
3613	*m*	IX	Appears on peaks of 2nd, 3rd, and 4th	......	......	
3944	*s*	I	Appears at beginning	*s*	IV	These lines appear throughout and show a marked widening about the time 3587 disappears
3962	*s*	I	Appears at beginning	*s*	IV	
4480	*w*	VII	Appears on peaks of 2nd to 5th	......	......	
4513	*m*	IX	Appears on peaks of 2nd to 5th	......	......	
4530	*m*	IX	Appears on peaks of 2nd to 5th	......	......	
4664	*s*	VI	Appears first in 3rd	*s*	VI	Behaves like 3587
	Impurities					
3995 *N*	*m*	IX	Appears on peaks of 1st, 2nd, 3rd, and 4th	*w*	IX	Appears in 1st only
4447 *N*	*m*	IX	Appears on peaks of 1st, 2nd, 3rd, and 4th	......	......	
4631 *N*	*m*	IX	Appears on peaks of 1st, 2nd, 3rd, and 4th	......	......	

* Explosions confined in block:

The *N* lines do not appear and *Ca* lines come up in the usual manner.

The two strong lines λλ 3944 and 3961 develop very wide wings in the beginning; the central portion, however, remains quite sharp.

The spark lines λλ 4480, 4513, and 4529 disappear almost entirely, showing only as mere traces on a few spectrograms.

λ 4664 appears later than before, beginning with the 5th. It is rather diffuse and shows more pronounced variation with the oscillations.

The *Al* band λ 4842.40 shows faintly in the 1st.

slit of the spectrograph became highly absorbing and produced no photographic effect. As may be seen from the reproductions, the light appears to be completely cut off. In the regions very close to strong arc lines this cutting off occurs a little later than in more remote regions, so that the general appearance is that of an infin-

TABLE V

Lead

Wave-Length	55,000-Volt Condenser, Explosions Confined in Block			20,000-Volt Condenser, Explosions Unconfined		
	Int.	Class	Remarks	Int.	Class	Remarks
3574...........	*s*	III	Begins in 2nd, widens during 3rd	*s*	V	These lines become class IV lines after the 3rd
3640...........	*s*	III	Begins in 2nd, widens during 3rd	*s*	V	
3672...........	*s*	II	Begins in third	*s*	V	
3684...........	*s*	III	Begins in 2nd, widens during 3rd	*s*	V	
3740...........	*s*	III	Begins in 2nd, widens during 3rd	*s*	V	
3786...........	......	......	No trace	*m*	VII	Appears late in 1st
3854...........	......	......	No trace	*m*	IX	Appears at very beginning of 1st again in 3rd to 8th
3833...........	......	......	No trace	*w*	IX	On peaks of 3rd to 8th
3842...........	......	......	No trace	*w*	IX	On peaks of 3rd to 8th
4020...........	*m*	I	Begins in 2nd	......	VII	Begins at end of 1st. Trace of reversal on some exposures
4058...........	*s*	II	Appears throughout	*s*	V	Changes to class IV after the 3rd
4168...........	*w*	I	Begins in 2nd	......	VII	Behaves like 4019.76
4245...........	*s*	V	Almost entirely reversed in 1st	*s*	VII	Diffuse in 1st
4387...........	*s*	V	Almost entirely reversed in 1st	*s*	VII	Diffuse in 1st
4437...........	*m*	I	Begins in 3rd	......	......	
4455...........	*m*	I	Begins in 3rd	......	......	
5006...........	*m*	I	Begins late in 1st	......	......	
	Impurities					
3248 *Cu*.......	*w*	I	Begins in 3rd	......	......	
3274 *Cu*.......	*w*	I	Begins in 3rd	......	......	
3934 *Ca*.......	*m*	I	Begins late in 1st	*m*	VII	Begins late in 1st
3944 *Al*.......	*w*	I	Begins in 3rd	*w*	VII	Begins in 3rd
3962 *Al*.......	*w*	I	Begins in 3rd	*w*	VII	Begins in 3rd
3969 *Ca*.......	*m*	I	Begins late in 1st	*m*	VII	Begins late in 1st
4227 *Ca*.......	*m*	I	Begins in 2nd	*w*	VII	Begins in 3rd
4283 *Ca*.......	*w*	I	Begins in 3rd	......	......	
4289 *Ca*.......	*w*	I	Begins in 3rd	......	......	
4299 *Ca*.......	*w*	I	Begins in 3rd	......	......	
4303 *Ca*.......	*w*	I	Begins in 3rd	......	......	
4308 *Ca*.......	*w*	I	Begins in 3rd	......	......	
4319 *Ca*.......	*w*	I	Begins in 3rd	......	......	

PLATE V

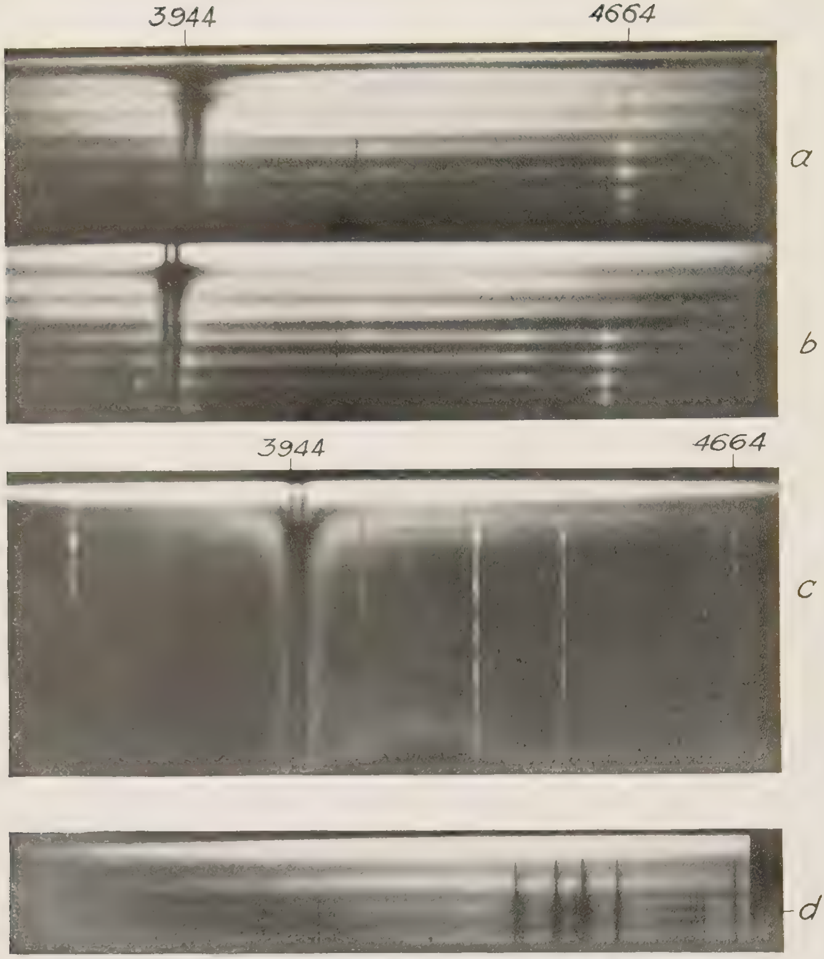

SPECTROGRAMS WITH ROTATING-MIRROR SPECTROGRAPH

a, *b*, *c*, Aluminum, showing behavior of absorption band near two strong arc lines
d, Lead, showing an absorption band on the peak of the third half-oscillation

itely wide absorption line rapidly becoming narrow. This delayed absorption is best illustrated by the aluminum spectrogram (Plate V), in which the light from the explosion first appears to be

TABLE VI

Copper

Wave-Length	55,000-Volt Condenser, Explosions Confined in Block			20,000-Volt Condenser, Explosions Unconfined		
	Int.	Class	Remarks	Int.	Class	Remarks
2824	*w*	II	Appears at beginning	......	......	
2863	*w*	II	Appears at beginning	......	......	
2961	*m*	I	Appears at beginning	......	......	
2998	*w*	I	Appears at beginning	......	......	
3011	*m*	I	Appears at beginning	......	......	
3036	*m*	I	Appears at beginning	......	......	
3064	*m*	I	Appears at beginning	......	......	
3094	*m*	II	Begins late in 1st	......	......	
3100	*m*	II	Begins late in 1st	......	......	
3109	*m*	II	Begins late in 1st	......	......	
3126	*m*	II	Begins late in 1st	......	......	
3143	*m*	II	Begins late in 1st	......	......	
3194	*w*	I	Appears at beginning	......	......	
3208	*w*	I	Appears at beginning	......	......	
3248	*s*	III	Very wide throughout	......	......	
3274	*s*	III	Very wide throughout	......	......	
3291	*m*	I	Appears at beginning, slightly diffuse	......	......	
3308	*m*	I	Appears at beginning, slightly diffuse	......	......	
3317	*w*	II	Appears at beginning, slightly diffuse	......	......	
3338	*w*	I	Appears at beginning, very sharp	......	......	
3355	*w*	I	Begins in 2nd	......	......	
3450	*w*	I	Begins late in 1st	......	......	
3476	*w*	I	Begins late in 1st	......	......	
3484	*w*	I	Begins late in 1st	......	......	
3512	*w*	I	Begins late in 1st	......	......	
3599	*m*	I	Appears at beginning	......	......	
3602	*m*	I	Appears at beginning	......	......	
4023	......	......	A mere trace appearing in the 5th and 6th only	*s*	VI	Appears throughout; no variation with oscil's
4063	......	......	A mere trace appearing in the 5th and 5th only	*s*	VI	Appears throughout; no variation with oscil's
4076	......	......	......	*w*	VII	Appears throughout; no variation with oscil's
4081	......	......	......	*w*	VII	Appears throughout; no variation with oscil's
4104	......	......	......	*w*	VII	Appears throughout; no variation with oscil's
4123	......	......	......	*m*	VII	Appears throughout; no variation with oscil's
4178	......	......	......	*m*	VII	Appears throughout; no variation with oscil's
4249	......	......	......	*m*	VII	Appears throughout; no variation with oscil's
4259	......	......	......	*m*	VII	Appears throughout; no variation with oscil's

TABLE VI—*Continued*

Wave-Length	55,000 Volt Condenser, Explosions Confined in Block			20,000 Volt Condenser, Explosions Unconfined		
	Int.	Class	Remarks	Int.	Class	Remarks
4275	*m*	IV	Appears at beginning	*s*	VII	Appears throughout; no variation with oscil's
4378	*m*	IV	Appears at beginning	*s*	VII	Appears throughout; no variation with oscil's
4416	*m*	IV	Appears at beginning	*w*	VII	Appears throughout; no variation with oscil's
4510	*m*	IV	Appears at beginning	*m*	VII	Appears throughout; no variation with oscil's
4540	*m*	IV	Appears at beginning	*m*	VII	Appears throughout; no variation with oscil's
4587	*m*	IV	Appears at beginning	*m*	VII	Appears throughout; no variation with oscil's
4651	*m*	IV	Appears at beginning	*m*	VII	Appears throughout; no variation with oscil's
4675	*w*	IV	Appears at beginning	......	......	
4705	*w*	IV	Appears at beginning	......	......	

completely cut off, except in the region within a few angstroms from the two strong arc lines λ 3944 and λ 3961. Then as time progresses, the vapor becomes transparent to wave-lengths remote from these two lines, but opaque to wave-lengths within a few angstroms from them. Immediately after the absorption sets in, the appearance is of an infinitely wide absorption line having an emission center some 50 A wide, with the emission core itself showing two sharp absorption lines upon its central region. In the lead spectrogram (Plate IV*b*) the same effect is seen, except that in this case the lack of a continuous background makes it less prominent. Here the arc lines λλ 3574, 3640, 3684, 3740, and the very strong arc line λ 4058, play the prominent part. The phenomenon shows considerable variation, both as regards duration, as can be seen from the series of aluminum spectrograms, and as to time of occurrence. In one of the lead explosions, it occurred about twenty-five millionths of a second after the beginning of the explosion. Ordinarily it coincides with a minimum of one of the oscillations, but not always. Thus on the lead spectrogram (Plate V*d*), one of these "absorption bands" was found on the peak of the third half-oscillation. This particular one was of very short duration, somewhat less than two millionths of a second.

It is very probable that this absorption occurs only over a very small area of the explosion. Direct rotating-mirror photographs show that the explosions of elements which exhibit the effect have a mottled appearance. Small areas apparently give off no light, or at least not enough to affect the photographic film. The area of these spots is only a few square millimeters, and it seems very probable that they are the regions in which the absorption described above is occurring. It would be very strange, indeed, if the whole mass of vapor stopped emitting light for a short time, and if this ever occurs the direct rotating-mirror photographs should show it; but no such effect was found, and it seems reasonable to conclude that the absorption occurs only in small areas at any one time.

No explanation of the phenomenon is offered. Possibly it may be a type of photo-electric absorption; but while this might explain the general absorption, it is difficult on this basis to see why the absorption should be delayed in the vicinity of strong arc lines. The fact that it seems to occur only in small regions at any instant might be explained as follows: Suppose that for some reason a large percentage of the atoms in some small region are in the same state of excitation, such that they can be ionized by the absorption of a quantum of visible light. We might then expect the vapor in this small region to be opaque to all wave-lengths below that having just the ionizing energy; in other words, to all wave-lengths below some long wave-length limit. In the case of aluminum, such a limit was looked for. By using a wide slit and red sensitized films, the spectrum was photographed out to λ 7500, but no long wave-length limit was found. This, of course, has very little bearing on the explanation, for even though the absorption were of a photo-electric nature, it might be produced by a mixture of atoms in various states of excitation. In this case the atoms in different states would have different long wave-lengths as limits, and we should not expect any very definite red limit to the absorption. But even if we grant that photo-electric absorption may play a part, the delayed action in the neighborhood of strong arc lines remains to be explained. To the writer at least, photo-electric absorption is therefore very unsatisfactory as an explanation of the phenomenon.

Dr. Anderson has suggested that anomalous dispersion may furnish the real explanation. In case the surface of the incandescent mass takes the proper shape, the vapor may behave very much as described by Julius.[1] The fact that the phenomenon is associated with strong absorption lines is very much in line with this suggestion, but further work will be necessary before the question can be settled.

THE RESISTANCE OF METALLIC VAPORS

During the study of the explosions, it developed that some metals were more difficult to explode than others. Anderson[2] has reported that when wires of copper, silver, or gold were exploded, a spark would pass across the space between the leads to the electrodes which supported the wires, unless they were well separated, a part of the discharge thus being shunted around the explosion. It was found, however, that by keeping the leads well separated, all the discharge could be made to go through the explosion.

In order to investigate this phenomenon, a sphere gap was placed in parallel with the wire to be exploded, so that maximum voltage built up across the vapors of the explosion could be measured. The electrodes supporting the wires were arranged so that their separation could be varied, and measurements were made with separations of from 1 to 10 cm. The observations consisted in determining the minimum separation of the sphere gap which would force all the discharge through the vapors of the explosion. The 55,000-volt condenser was used.

Curves showing the electrode separation, i.e., the length of wire exploded, against the voltage built up across the vapors of the explosion, were plotted for a number of elements. A few of these curves are shown in Figure 4. They appear to depart only slightly from straight lines through the origin. As a basis for comparison, the minimum voltage in kilo-volts corresponding to a 5-cm length of wire is listed for all the elements studied:

Cu	79 k.v.	*Au*	75–85	*W*	58	*Al*	51	*Li*	42
Ag	81	*Ni*	72	*Zn*	58	*Pb*	49	*Fe*	39
						Sn	51		

As the supply of gold wire gave out before sufficient data were obtained, a definite value for this element cannot be given. The evidence on hand indicates, however, that its value is very close to those of copper and silver.

---

[1] *Astrophysical Journal*, **12**, 185, 1900.

[2] *Mt. Wilson Comm.*, No. 82; *Proceedings of the National Academy of Sciences*, **8**, 231, 1922.

The fact that these three "high" elements belong to the same group in the periodic system suggests that elements in any one group should behave alike in the explosions, but a glance at the results for the elements just listed shows that the agreement is rather haphazard.

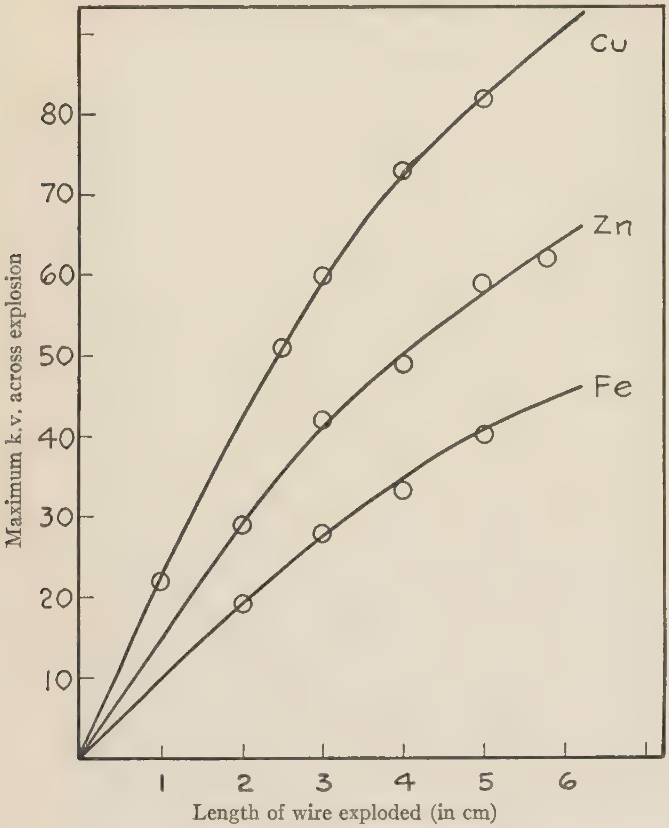

FIG. 4

Two 1.5-inch spheres were used for the gap, and the voltages listed on the curves were computed in the usual way. That some of the voltages are much higher than that used on the condenser is not surprising when one remembers that we are dealing with rapidly changing currents.

In order to determine just when the voltage across the explosion reached a maximum, the apparatus was so arranged that light from both the gap and the explosion fell on the slit of the rotating-mirror spectrograph. As far as could be determined by means of the spectrograph, the beginning of the spark and the beginning of the explosion seemed to be simultaneous. Probably the wire first vaporized and then developed a high resistance, but did not become sufficiently luminous to photograph until the high-resistance stage was reached.

When the sphere gap was set near the critical position for the wire in question, only part of the current of the first half-oscillation passed through the gap. The balance and that of all subsequent oscillations passed through the vapors of the explosion. If the gap was made sufficiently short, practically all the discharge could be made to pass across the gap.

The mass of the wire exploded seems to have very little effect on the determinations of voltage as wires of various sizes of the same metal gave similar sphere-gap settings. Screening the gap from the light of the explosion made no noticeable difference. It is thought that the measured voltages are proportional to the resistance of the various metallic vapors.

In conclusion, the author wishes to express his deepest appreciation to Dr. J. A. Anderson, under whose direction this work was done.

Mount Wilson Observatory
September 1924

Contributions from the Mount Wilson Observatory, No. 286
Reprinted from the *Astrophysical Journal*, Vol. LXI, pp. 223–283, 1925

A LIST OF ULTIMATE AND PENULTIMATE LINES OF ASTROPHYSICAL INTEREST

By HENRY NORRIS RUSSELL

ABSTRACT

Spectral lines of astrophysical interest.—The very rapid development of the analysis of complex line-spectra makes it desirable to prepare a preliminary list of lines of astrophysical interest for which the spectroscopic and energy-relations are known. *A brief summary of the theory is given*, followed by a list of lines, the elements being arranged in order of the successive groups of the periodic table, and the individual lines in order of the energy-level of origin within the atom. *A bibliography* of the more important recent papers is appended.

Terminology.—The name *ultimate lines* is suggested for those lines which originate in the lowest energy-level (or normal state) of an atom (whether neutral or ionized) or in another state very close to this. Lines originating in neighboring but higher energy-levels may be called *penultimate lines;* those originating in still higher levels, *antepenultimate lines*. Ultimate lines, as here defined, are nearly, but not quite, synonymous with the *raies ultimes* of De Gramont. The difference is discussed in the text. The meaning of the terms "flame," "arc," and "spark lines" is also discussed. An index to the table has been made in which the elements are arranged in the alphabetical order of their chemical symbols.

The great advances which have recently been made in the interpretation of line-spectra, and the astrophysical importance of the results, appear to justify a collection from the widely scattered sources of the material of most importance in astrophysical work.

1. *Summary of the theory.*—It is now generally accepted that the emission of a given spectral line depends upon a transition of the emitting atom between two definite states (fixed by quantum conditions) in which its internal energy is different, and that the number of waves per second (or per centimeter) in the resulting radiation is exactly proportional to the energy released by the atom. In absorption this process is reversed.

The familiar spectroscopic terms, whose differences give the wave-numbers of the various lines, therefore indicate the *energy-levels* of the corresponding atomic states, which may thus be mapped out with extreme accuracy. According to Bohr, each term corresponds to a different arrangement of electron orbits within the atom, and for terms belonging to the same series the orbital angular momentum of the outermost electron is the same. Series for which this differs by a unit may be called "adjacent." Most terms are multiple and represent several closely neighboring energy-levels, differing probably in the arrangement of inner orbits. They may thus be grouped into systems, each containing several series, characterized by a certain multiplicity or maximum number of components (which, however, is not attained in all terms).[1] Three or more systems of different multiplicity may occur in the same spectrum. In such cases they are all of odd or all of even multiplicity, according as the atomic number is even or odd (the only known exception occurring in helium).

The spectrum of an ionized atom (enhanced lines) is in these respects similar to that of the element of the next preceding atomic number: that of a doubly ionized atom, to the element preceding this, and so on.

Transitions accompanied by radiations or "combinations" occur normally between terms belonging to adjacent series in the same system. Which components combine with one another is determined by the "inner-quantum" rules.[2] Such a combination forms a "multiplet," or group of lines, which may number from 1 to 16.

In the more complex spectra, combinations between terms belonging to the same series occur, and a few between terms of non-adjacent series, and also between terms of different systems. The last two classes usually give faint lines.

2. *Levels of origin. Ultimate, penultimate, and antepenultimate lines.*—In astrophysical applications, these somewhat complex series relations are less important than the simpler matter of the energy-level of origin of the lines, by which is meant the lower of the two levels involved in the corresponding transition. An atom cannot absorb the line unless it is in this state.

The relative numbers of atoms which, under equilibrium conditions, will be in the various energy-levels, are determined by general thermodynamic considerations.[3] At low temperatures, practically all the atoms will be in the state of least internal energy, and capable of absorbing only lines which correspond to transitions from this state to others. These lines alone will be found in the absorption spectrum of the cool gas, or its emission spectrum at a slightly higher temperature. As the temperature is raised, a small but ever increasing proportion of the atoms will, at any given instant, be in states of higher energy-content, and the lines originating in these will appear in the order of their levels of origin, and increase in relative intensity with rising temperature. Comparison of the spectroscopic data with King's temperature classification shows, in all cases which have been investigated, a beautifully perfect correlation, which puts the correctness of this interpretation beyond doubt.

---

[1] For details see Landé, *Zeitschrift für Physik*, **15**, 189, 1923.

[2] Sommerfeld, *Atombau und Spektrallinien*, 1922.

[3] Fowler and Milne, *Monthly Notices*, **83**, 403, 1923.

Lines originating in the lowest level are, for obvious reasons, prone to reversal, and are usually the last lines to disappear when only traces of the element are present. The latter are De Gramont's *raies ultimes*. Following his lead, we may call all lines originating in the lowest energy-level "ultimate lines." For those originating in the next lowest level, we may borrow a good word from the grammarians and call them "penultimate lines"; while lines arising from still higher levels may be termed "antepenultimate."

If the two lowest levels are very near together (as in Ti^+), lines arising from both may be called ultimate, and two or more nearby levels may similarly be included as origins for penultimate lines.

Enhanced lines may be classified in the same way. Ultimate lines, arising from the lowest energy-level in the ionized atom, will be absorbed as soon as the gas begins to be ionized, and will therefore appear even in the furnace, and be strong in the arc, like H and K. Antepenultimate enhanced lines, like $Mg^+\lambda\,4481$, which require that the ionized atom shall receive a large additional input of energy before it can absorb them, and still more before it can emit them, may not appear in the arc at all.

It should be added that ultimate lines, in the sense here defined, are not always identical with De Gramont's *raies ultimes*. The latter denote the most persistent lines in the region of the spectrum which is easily observable, and, if this includes no lines originating in the lowest level, lines arising from the lowest available level will be chosen, so that the *raies ultimes* may be penultimate lines (for example, the green magnesium triplet for visual observations).

Conversely, ultimate lines, though originating in the lowest level, are sometimes faint, and disappear when the concentration is small, so that they are not recorded as *raies ultimes*. For example, the calcium line λ 4226.7 ($1S-1P$) is a typical *raie ultime*, while λ 6572.7 ($1S-1p^3$), an intersystem combination, is of moderate intensity; and λ 4575.4 ($1S-1D$), a combination between non-adjacent series, is a very faint line. All these are true ultimate lines, greatly strengthened in the furnace at low temperatures, in sun-spots, and in dwarf stars.

There would appear to be no reason why the French phrase should not be retained in use, as at present, with the significance attached to it by its author, while a somewhat different meaning is given to the English words.

In the spectra first investigated (the alkalis and alkaline earths), the lowest energy-level (or normal state) of the atom is 1S, and the ultimate lines belong to the principal series $1S-mp$; but this is not always the case. In aluminum, for example, the normal state is $1p^2$; in iron, $1d^5$; and in titanium, $1f^3$. The principal series in these spectra, when they have been detected at all, are inconspicuous, and the ultimate lines belong, in different cases, to very different series, many of which have no specific names.

3. *Ionization and excitation potentials.*—As the vapor of a given element is heated, the ultimate arc lines appear first, followed by the penultimate and antepenultimate. In due time ionization begins; the ultimate enhanced lines appear, and later the penultimate, while the arc lines fade, disappearing in the inverse order of their appearance, since, even at high temperatures, many more neutral atoms are in the normal state than in any other. Still farther on, the enhanced lines give place to lines corresponding to a higher degree of ionization, or often apparently to nothing at all, if the latter lie far in the ultra-violet.

In a normal atmosphere, however, various elements will go through this process at very different rates, determined by the ionization and excitation potentials, which measure the energy required to ionize an atom, starting from its normal state, or to raise it from this state to the various energy-levels from which penultimate and antepenultimate lines originate. This energy is usually expressed in volts, one "volt" being the energy acquired by an electron which has fallen through this potential difference, and equaling 8100 of the frequency units used to express the spectroscopic terms.

These data bid fair to furnish the basis for a quantitative theory of stellar spectra, permitting the calculation of pressures and temperatures in the atmosphere.[1] Qualitatively, the order of appearance and disappearance of the lines of various elements in the stellar sequence may be understood by mere inspection of the data.

In Table I data are collected for those elements for which information is at present available, or can be readily derived from published data. Fowler's memoir[2] is the principal source, supplemented as indicated in the references. The lines of each element are grouped according to their excitation potentials (E.P.), the ultimate lines coming first. The wave-lengths are given in I.A.; the intensities and temperature classes are taken from King when possible. Intensities from other sources are placed in parentheses. Following this, in the fifth column, is the series notation showing between what terms the transition occurs (the lower coming first). The successive series of terms are denoted, as usual, by the letters "s," "p," "d," "f," "g," "h," "i," and the system to which they belong by an exponent representing the multiplicity—singlet terms being represented, as usual, by capitals. The successive terms of a series are numbered consecutively, starting with the lowest, which is usually numbered 1. Fowler's notation has been followed for lines given by him.

Terms for which the combining properties are peculiar, and which do not belong to the regular series, are denoted by accents as "p′," "p″." Lines of different systems are listed separately. Distinctions between the components of multiple terms, which are unimportant for the present purpose, are ignored, and but a single-series designation given for a whole multiplet (except in one or two cases, such as *Tl*, where the separations are very wide). The ionization potentials, I.P., and the excitation potentials, E.P., for penultimate and other lines, are given when known.

---

[1] Fowler and Milne, *loc. cit.*

[2] *Report on Series in Line Spectra.* London: Fleetway Press, 1922.

The spectra of ionized atoms are listed independently, as are those of multiply ionized atoms in the few cases that have been investigated. As the list has been prepared for astrophysical purposes, only lines between λ 3000 and λ 8500 are listed except for important ultimate and penultimate lines. Only the strongest lines are given for elements like *Hg*, which do not appear in the solar spectrum; while the lists for astrophysically important elements like *Ca* and *Ti* are extended. The fainter components of multiplet groups are given only in the region where they may be observed in the sun-spot spectrum. Cases where lines are omitted are denoted by an asterisk under the series notation. Intersystem combinations, and those between non-adjacent series, are placed in parentheses.

As an illustration of the notation, the calcium line λ 6572.78 ($1S-1p^3$) is seen to be an intersystem combination line between a singlet level, 1S, and a triplet level, 1p. Since it is an ultimate line, 1S must be the normal state of the atom, and since the excitation potential is less for the lines arising from 1p than for any others, this is the next lowest energy-state, and the lowest in the triplet system.

4. *Flame, arc, and spark lines.*—The data which are summarized in Table I throw a flood of light on many spectroscopic problems.

Consider, for example, the relation of flame (or furnace), arc, and spark spectra. In the first of these, when the temperature is low, only ultimate lines appear (as in the Bunsen-flame spectra of the alkalis and alkaline earths (neglecting band-spectra due to compounds). For refractory elements, such as iron or titanium, the temperature of volatilization is usually high enough to bring out the penultimate lines in addition; though, when the spectrum is obtained at the very lowest practicable temperature, the ultimate lines may appear alone, as King has shown in the case of the emission spectrum of iron[1] and Grotrian for several absorption spectra.[2] When the ultimate lines of the neutral atom lie far in the ultraviolet, and the excitation potential for the penultimate lines is high (as in hydrogen or oxygen), no observable flame or furnace spectrum is found.

---

[1] *Mt. Wilson Contr.*, No. 247; *Astrophysical Journal*, **56**, 370, 1922.

[2] *Zeitschrift für Physik*, **18**, 169, 1923.

Under the strong excitation of the arc all the lines of the neutral atom appear, and, since ionization is necessary for the passage of the current, lines of the ionized atom are also present. The ultimate lines of this second spectrum are always strong in the arc (unless, indeed, they lie in regions inaccessible to observation, as is presumably the case with the alkalis), and, if the ionization potential is low, they may appear in the furnace, even at moderate temperatures (as in *Ca*, *Sc*, *Ti*, etc.). Penultimate enhanced lines of low excitation potential appear faintly in the furnace, and are fairly strong in the arc. With increasing E.P. such lines become harder to get, and antepenultimate lines, such as Mg^+ λ 4481, cannot be produced in the ordinary arc at all, though the corresponding ultimate lines are strong.

In the spark, the lines of the ionized atom are conspicuous (and those of the multiply ionized atom also, if they are accessible), while the lines of the neutral atom also appear, since the atoms ionized by the discharge must return to normal. Enhancement, and not mere presence, in the spark is therefore the practical test.

If, however, the ionization and excitation potentials for a line of the neutral atom are both high (as in the case of the red triplet of oxygen), these lines may actually appear stronger in the spark than the arc, the excitation in the former being too weak for them.[1] The degree of enhancement for the lines of the ionized atom is, however, so much greater that there is usually little difficulty in deciding which are the true enhanced lines.

The use of the familiar and convenient terms "flame" or "furnace" lines for the ultimate lines of the neutral atom (or penultimate lines of low E.P.), "arc" lines for those of the neutral atom in general, and "spark" or "enhanced" lines for those of the ionized atom meets with no real difficulties, so long as it is remembered that the visible arc lines of one element may demand a higher degree of excitation than the enhanced lines of another.

The table also explains the great astrophysical importance of the elements in the first half of the first long period of the periodic table—from *Ca* to *Fe*. Ultimate lines of all these elements lie in

[1] Merrill, *Mt. Wilson Contr.*, No. 183, p. 7; *Astrophysical Journal*, 51, 242, 1920.

the easily observable region, and are usually numerous, while penultimate lines, usually of low excitation potential, abound. Their ionization potentials are also moderately low, and fairly similar, so that their enhanced lines are fairly prominent in the sun and conspicuous in stars of class F, but disappear above class A, owing to double ionization.

For the lighter elements of the two short periods, the ultimate lines are in the far ultra-violet (except for six lines belonging to *Li*, *Na*, *Al*, and *Mg*), and the excitation potentials of the penultimate lines are, in general, high. For this very reason, as well as their high ionization potentials, elements of this group furnish the characteristic lines in the spectra of classes A and B.

The prominence of scandium, titanium, and vanadium in the sun-spot spectrum follows at once from their low ionization potentials, and the great number of their ultimate and penultimate lines in the region which is best observable.

The analysis of the more complex spectra is at present advancing very rapidly. Among those not yet interpreted, the most important astrophysically are *Si*, *Co*, *Ni*, *Nb*, *La*, *Ce*, and among spark spectra C^{++}, N^{+}, O^{+}, Si^{+}, Si^{++}, V^{+}, Cr^{+}, Mn^{+}. Almost all of these are known to be already under investigation, and some of the others (notably Fe^{+}) are being studied at this observatory. The present list will therefore require considerable extension in a year or two. It is planned to use it here in studies of solar, sun-spot, and stellar spectra, and it is published in its present incomplete form in the hope that it may be of use to other workers in astrophysics.

The writer takes pleasure in expressing his obligation to Drs. Meggers, Kiess, and Walters for their generous communication of valuable data in advance of publication and to Miss Charlotte E. Moore for much help in tabulating and checking the data.

TABLE I

E.P.	λ	Int.	Class	Type	Notes
	Hydrogen, *H*, I.P. 13.54				
0.0	1215.68	....	....	1S−2P	
	1025.83	....	....	1S−3P	
10.15	6562.79	(10)	....	2P−3D (Hα)	
	4861.33	(9)	....	2P−4D (Hβ)	
	4340.46	(8)	....	2P−5D (Hγ)	
	4101.74	(7)	....	2P−6D (Hδ)	
	3970.08	(6)	....	2P−7D (Hε)	
	3889.05	(5)	....	2P−8D (Hζ)	
	3835.39	(4)	....	2P−9D (Hη)	
	3797.90	(3)	....	2P−10D (Hθ)	
	3770.63	(2)	....	2P−11D (Hι)	
	3750.15	(1)	....	2P−12D (Hκ)	
12.63	18751.05	(10)	....	3D−4F	
	12818.11	(5)	....	3D−5F	
	Helium, *He*, I.P. 24.41				(1)
0.0	591.5	....	....	$(0S-1p^2)$	
	584.4	....	....	0S−1P	
	557.1	....	....	0S−2P	
19.68	10830.30 10829.09	(200)	....	$1s^2-1p^2$	
	3888.65	(10)	....	$1s^2-2p^2$	
	3187.74	(8)	....	$1s^2-3p^2$	
20.49	20582.04	(20)	....	1S−1P	
	5015.68	(6)	....	1S−2P	
	3964.72	(4)	....	1S−3P	
	3613.64	(3)	....	1S−4P	
	3447.59	(2)	....	1S−5P	
20.81	7065.68 7065.19	(1) (5)	....	$1p^2-2s^2$	
	5875.96 5875.61	(1) (10)	....	$1p^2-2d^2$ (D_3)	
	4713.37 4713.14	(1) (3)	....	$1p^2-3s^2$	
	4471.69 4471.48	(1) (6)	....	$1p^2-3d^2$	
	4120.98 4120.81	(1) (3)	....	$1p^2-4s^2$	
	4026.36 4026.19	(1) (5)	....	$1p^2-4d^2$	
	3867.62 3867.46	(1) (2)	....	$1p^2-5s^2$	
	3819.75 3819.61	(1) (4)	....	$1p^2-5d^2$	
	3705.13 3705.00	(1) (3)	....	$1p^2-6d^2$	

TABLE I—*Continued*

E.P.	λ	Int.	Class	Type	Notes
	Helium—*Continued*				
21.12......	7281.35	(3)	....	1P−2S	
	6678.15	(6)	....	1P−2D	
	5047.74	(2)	....	1P−3S	
	4921.93	(4)	....	1P−3D	
	4437.55	(1)	....	1P−4S	
	4387.93	(3)	....	1P−4D	
	4143.77	(2)	....	1P−5D	
	4009.27	(1)	....	1P−6D	
	Ionized Helium, He^+, I.P. 54.18				
0.0.......	303.8	....	....	1S−2P	
40.63......	1640.49	....	....	2P−3D	
	1215.18	....	....	2P−4D	
48.16......	4685.81	....	....	3D−4F	
	3203.16	....	....	3D−5F	
50.79......	6560.16	....	....	4F−6G	
	5411.57	....	....	4F−7G	
	4859.36	....	....	4F−8G	
	4541.63	....	....	4F−9G	
	4338.71	....	....	4F−10G	
	4199.87	....	....	4F−11G	
	4100.08	....	....	4F−12G	
	4025.64	....	....	4F−13G	
	3968.47	....	....	4F−14G	
	3923.51	....	....	4F−15G	
	Neon, *Ne*, I.P. 21.5				(2)
16.56(s_5) to 16.78 (s_2)..	6598.95	(15)	....	$1s_2-2p_2$	
	6506.53	(15)	....	$1s_4-2p_8$	
	6402.25	(20)	....	$1s_5-2p_9$	
	6382.99	(12)	....	$1s_4-2p_7$	
	6266.49	(15)	....	$1s_3-2p_5$	
	6217.28	(15)	....	$1s_5-2p_7$	
	6163.59	(12)	....	$1s_3-2p_2$	
	6143.06	(12)	....	$1s_5-2p_6$	
	5975.53	(12)	....	$1s_5-2p_5$	
	5881.90	(20)	....	$1s_5-2p_2$	
	5852.49	(50)	....	$1s_2-2p_1$	
	5400.56	(50)	....	$1s_4-2p_1$	
	3593.52	(10)	....	$1s_2-3p_4$	
	3520.47	(20)	....	$1s_2-3p_1$	
	3472.57	(10)	....	$1s_5-3p_9$	
	3417.90	(10)	....	$1s_4-3p_4$	
	3369.91	(15)	....	$1s_5-3p_2$	
	3369.81	(10)	....	$1s_5-3p_4$	

TABLE I—*Continued*

E.P.	λ	Int.	Class	Type	Notes
	Neon—*Continued*				
18.3 to 18.5	5764.43	(15)	....	$2p_9-4d'_4$	
	5343.30	(12)	....	$2p_{10}-4d_6$	
	5341.10	(20)	....	$2p_{10}-4d_5$	
	5330.79	(12)	....	$2p_{10}-4d_3$	
	4788.93	(12)	....	$2p_9-5s_5$	
	4715.34	(15)	....	$2p_9-6d'_4$	
	4708.86	(12)	....	$2p_{10}-5d_5$	
	4704.39	(15)	....	$2p_{10}-5d_3$	
	Lithium, *Li*, I.P. 5.37				
0.0.......	6707.85	(10R)	....	$1s^2-1p^2$	
	3232.61	(8R)	....	$1s^2-2p^2$	
1.84......	8126.52	(10)	....	$1p^2-2s^2$	
	6103.53	(10R)	....	$1p^2-2d^2$	
	4971.93	(7r)	....	$1p^2-3s^2$	
	4602.99	(9R)	....	$1p^2-3d^2$	
	4273.28	(5r)	....	$1p^2-4s^2$	
	4132.29	(8)	....	$1p^2-4d^2$	
	Sodium, *Na*, I.P. 5.12				
0.0.......	5895.93	(10R)	....	$1s^2-1p^2$ (D_1)	
	5889.96	(8R)	....	(D_2)	
	3427.1	(1)	....	($1s^2-2d^2$)	
	3302.94	(8R)	....	$1s^2-2p^2$	
	3302.34	(7R)			
2.09......	8194.82	(10R)	....	$1p^2-2d^2$	
	8183.30	(8R)			
	6160.72	(8r)	....	$1p^2-3s^2$	
	6154.21	(8r)			
	5688.22	(10)	....	$1p^2-3d^2$	
	5682.67	(8)			
	5153.64	(6n)	....	$1p^2-4s^2$	
	5149.09	(5n)			
	4982.87	(6r)	....	$1p^2-4d^2$	
	4978.61	(5r)			
	Potassium, *K*, I.P. 4.32				
0.0.......	7699.01	(10R)	....	$1s^2-1p^2$	
	7664.94	(10R)			
	4642.17	(2)	....	($1s^2-2d^2$)	
	4641.58	(1)			
	4047.20	(6R)	....	$1s^2-2p^2$	
	4044.14	(8R)			

TABLE I—*Continued*

E.P.	λ	Int.	Class	Type	Notes
	Potassium—*Continued*				
1.61......	6938.98	(8)	....	$1p^2-3s^2$	
	6911.30	(7)			
	5832.31	(7R)	....	$1p^2-4d^2$	
	5812.71	(6R)			
	5802.16	(6R)	....	$1p^2-4s^2$	
	5782.77	(5R)			
	Rubidium, *Rb*, I.P. 4.16				
0.0.......	7947.64	(8R)	....	$1s^2-1p^2$	
	7800.29	(10R)			
	4215.56	(7R)	....	$1s^2-2p^2$	
	4201.82	(8R)			
1.58......	7757.83	(8)	....	$1p^2_*-3d^2$	
	7619.12	(8)			
	7408.37	(10)	....	$1p^2-3s^2$	
	7280.22	(10)			
	Caesium, *Cs*, I.P. 3.88				
0.0.......	8943.46	(10R)	....	$1s^2-1p^2$	
	8521.12	(10R)			
	4593.16	(6)	....	$1s^2-2p^2$	
	4555.26	(8)			
1.45......	9172.23	(2)	....	$1p^2_*-3d^2$	
	8761.25	(5)			
	7944.11	(6)	....	$1p^2-3s^2$	
	7609.13	(5)			
1.71......	8079.24	(8r)	....	$2d^2-4f^2$	
	8015.90	(8r)			
	Copper, *Cu*, I.P. 7.69				
0.0.......	3273.97	(10R)	....	$1s^2-1p^2$	
	3247.55	(10R)			
1.64......	5782.16	(8)	....	$x-1p^2$	
	5700.25	(6)			
3.80......	8092.76	(10)	....	$1p^2-2s^2$	
	7933.19	(10)			
	5220.04	(6)	....	$1p^2-2d^2$	
	5218.17	(10)			
	5153.23	(8n)			
	4530.84	(6r)	....	$1p^2-3s^2$	
	4480.38	(6r)			
	4063.30	(4n)	....	$1p^2-3d^2$	
	4062.69	(6n)			
	4022.67	(6n)			

TABLE I—*Continued*

E.P.	λ	Int.	Class	Type	Notes
	Silver, *Ag*, I.P. 7.54				
0.0.......	3382.86	(10R)	....	$1s^2-1p^2$	
	3280.66	(10R)			
3.86......	8273.73	(10)	....	$1p^2-2s^2$	
	7688.12	(10)			
	5471.51	(6)	....	$1p^2-2d^2$	
	5465.45	(10R)			
	5209.08	(10R)			
	4668.52	(8r)	....	$1p^2-3s^2$	
	4476.12	(6r)			
	4210.71	(8R)	....	$1\underset{*}{p}^2-3d^2$	
	4055.31	(6R)			
	Gold, *Au*, I.P. 9.20				(3)
0.0.......	2675.95	(10R)	....	$1s^2-2p^2$	
	2427.98	(10R)			
4.60.....	7510.74	(6)	....	$2p^2-2s^2$	
5.08	5837.43	(6)			
	4811.63	(5)	....	$2p^2-2d^2$	
	4792.60	(8)			
	4065.07	(6)			
	Beryllium, *Be*, I.P. 7.5:				(4) (5)
0.0.......	2348.63	(10)	....	$1S-1P$	
?........	3321.35	(8)	....	$1p^3-1s^3$	
	3321.09	(8)			
	3321.01				
5.21......	4572.69	(9)	....	$1P-1D$	
	Ionized Beryllium, *Be*$^+$, I.P.?				
0.0.......	3131.07	(12)	....	$1s^2-1p^2$	
	3130.42	(12)			
	Magnesium, *Mg*, I.P. 7.61				
0.0.......	4571.15	5	I A	$(1S-1p^3)$	
	2852.11	300R	III	$1S-1P$	
2.67......	5183.67	125	II	$1p^3-1s^3$	
	5172.70	80	II		
	5167.38	40	II		

TABLE I—*Continued*

E.P.	λ	Int.	Class	Type	Notes
	Magnesium—*Continued*				
2.67—*Cont.*	3838.29	100r	II	$1p^3-2d^3$	
	3832.31	80r	II		
	3829.36	40	II		
	3336.69	20	III	$1p^3-2s^3$	
	3332.14	15	III		
	3329.93	10	III		
4.33......	8806.75	(8)	....	$1P-2D$	
	5711.13	1	V	$1P-3S$	
	5528.42	10	V	$1P-3D$	
	4703.00	40	V	$1P-4D$	
	4351.91	30	IV	$1P-5D$	
	4167.39	10n	III ?	$1P-6D$	
	4057.63	5n	III	$1P-7D$	
	Ionized Magnesium, *Mg*+, I.P. 14.97				
0.0.......	2802.70	(50)	IV	$1s^2-1p^2$	
	2795.52	(50)	IV		
4.41......	2936.50	(35)	IV	$1p^2-2s^2$	
	2928.63	(35)			
	2797.99	(40)	....	$1p^2-2d^2$	
	2790.77	(40)			
8.42......	3615.64	(3)	....	$2s^2-3p^2$	
	3613.80	(4)			
8.83......	4481.33	(100)	....	$2d^2-3f^2$	
	4481.13	....			
	3104.81	(30)	....	$2d^2-4f^2$	
	3104.71	....			
9.95......	4433.99	(8)	....	$2p^2-4s^2$	
	4427.99	(7)			
	4390.58	(10)	....	$2p^2-4d^2$	
	4384.64	(8)			
	Calcium, *Ca*, I.P. 6.09				(6)
0.0.......	6572.78	8	I A	$(1S-1p^3)$	
	4575.43	0	....	$(1S-1D)$	
	4226.73	500R	I	$1S-1P$	
1.88......	6162.18	150	II	$1p^3-1s^3$	
	6122.22	100	II		
	6102.72	80	II		
	4456.61	10	II	$1p^3-2d^3$	
	4455.88	40	I		
	4454.77	80	I		
	4435.67	40	I		
	4434.95	60r	I		
	4425.43	50	I		

TABLE I—*Continued*

E.P.	λ	Int.	Class	Type	Notes
	Calcium—*Continued*				
1.88—*Cont.*	4318.65	45	I	$1p^3-1p'^3$	
	4307.74	45	I		
	4302.52	60r	I		
	4298.99	30	I		
	4289.38	40	I		
	4283.01	40	I		
	3973.72	12	III	$1p^3-2s^3$	
	3957.05	10	III		
	3948.90	6	III		
	3644.40	40	III	$1p^3-3d^3$	
	3630.75	30	III		
	3624.11	20	III	*	
2.53.......	6508.84	(1)	..	$1d^3-1f''^3$	
	6499.65	30	II		
	6493.79	80	II		
	6471.66	40	II		
	6462.58	125	II		
	6439.09	150	II		
	6464.70	(1)	..	$(1d^3-1D')$	
	6455.61	10	II		
	6449.81	50	II		
	6169.58	40	III	$1d^3-2p^3$	
	6169.03	25	III		
	6166.44	15	III		
	6163.75	10	III		
	6161.31	10	III		
	6156.08	(0)			
	5602.83	20	III	$1d^3-1d'^3$	
	5601.28	30	III		
	5598.48	50	III		
	5594.46	60	III		
	5590.11	20	III		
	5588.75	80	III		
	5581.97	25	III		
	5270.27	60	III	$1d^3-1p''^3$	
	5265.56	40	III		
	5264.24	20	III		
	5262.23	25	III		
	5261.70	20	III		
	5260.38	2	III		
	4585.87	50	II	$1d^3-3f^3$	
	4581.41	40	II		
	4578.57	30	II		
	4098.55	15	III	$1d^3-4f^3$	
	4094.94	12	III		
	4092.65	8	III		
2.70.......	7202.16	3	II	$(1D-1f'^3)$	
	7148.12	10	II	$1D-1D'$	
	6717.69	30	III	$1D-2P$	

TABLE I—*Continued*

E.P.	λ	Int.	Class	Type	Notes
	Calcium—*Continued*				
2.70—*Cont.*	5349.47	25	III	1D−1F′	
	5041.61	40	III	1D−3P	
	4878.13	50	III	1D−3F	
	4526.94	30	III	1D−4P	
	4355.10	25	III	1D−4F	
	4240.46	6	III	1D−5P	
	4108.55	10N	III	1D−5F	
	3972.58	3	III	1D−6F	
2.92.......	7326.10	2	III	1P−2D	
	5857.48	100	III	1P−1P′	
	5512.98	20n	III	1P−3s	
	5188.85	50	III	1P−3D	
	4847.29	2	III A	1P−4s	
	4685.26	12	III	1P−4D	
	Ionized Calcium, *Ca*+, I.P. 11.82				
0.0........	3968.47	350R	II	$1s^2-1p^2$ (H)	
	3933.66	400R	II	(K)	
1.71.......	8662.11	(9)	V	$1d^2-1p^2$	
	8542.15	(10)	V		
	8498.00	(8)	V		
3.14.......	3736.90	12	V	$1p^2-2s^2$	
	3706.02	10	V		
	3181.28	4	V	$1p^2-2d^2$	
	3179.34	15	V		
	3158.88	10	V		
	Strontium, *Sr*, I.P. 5.67				(6)
0.0........	6892.62	50r	I	$(1S-1p^3)$	
	4607.34	600R	I	1S−1P	
1.79.......	7070.10	400	II	$1p^3-1s^3$	
	6878.35	300	II		
	6791.05	100	II		
	4962.24	40	I	$1p^3-2d^3$ *	
	4872.49	40	I		
	4832.08	50r	I		
	4811.87	40r	I	$1p^3-1p'^3$ *	
	4784.32	30	I		
	4741.92	30	I		
	4722.27	30	I		
2.27.......	6617.27	50	III	$1d^3-1f''^3$ *	
	6503.99	80	II		
	6408.47	100	II		

TABLE I—*Continued*

E.P.	λ	Int.	Class	Type	Notes
	Strontium—*Continued*				
2.27—*Cont.*	5521.75	25	II	$1d^3-1d'^3$ *	
	5504.17	30	II		
	5480.84	40	II		
	5256.90	50	II	$1d^3-1p''^3$ *	
	5238.54	30	II		
	5225.11	20	II		
	Ionized Strontium, Sr^+, I.P. 10.98				
0.0........	4215.52	300r	II	$1s^2-1p^2$	
	4077.71	400r	II		
1.82.......	10915.4	....	....	$1d^2-1p^2$ *	
	10328.0	....			
3.03.......	4305.46	40	III	$1p^2-2s^2$	
	4161.81	30	IV ?		
	3474.90	10	V	$1p^2-2d^2$	
	3464.47	50	V		
	3380.72	50	V		
	Barium, *Ba*, I.P. 5.19				(6)
0.0........	7911.36	3	I A	$(1S-1p^3)$	
	5535.53	1000R	I	$1S-1P$	
	3501.11	200R	II	$1S-1P''$	
1.18.......	7672.12	25r	I	$1d^3-1f''^3$ *	
	7280.31	150r	II		
	7060.00	400r	II		
	6595.35	200	I	$1d^3-1d'^3$ *	
	6527.32	250	I		
	6498.78	300r	II		
	6110.81	300r	II	$1d^3-1p''^3$ *	
	6063.15	200	II		
	6019.50	100	II		
	3993.40	80	II	$1d^3-3f^3$ *	
	3935.72	50	II		
	3909.92	40	II		
	3579.67	80n	III	$1d^3-4f^3$ *	
	3544.66	80n	III		
	3524.97	80n	III		
1.41.......	5826.29	150	II	$1D-1P''$	
1.56.......	7905.80	6	III	$1p^3-1s^3$	
	7392.44	30	II		
	7195.26	80	III		
	5777.70	400r	II	$1p^3-2d^3$ *	
	5519.12	200	II		
	5424.62	100	II		

TABLE I—*Continued*

E.P.	λ	Int.	Class	Type	Notes
	Ionized Barium, *Ba*+, I.P. 9.96				
0.0.......	4934.10	700R	II	$1s^2-1p^2$	
	4554.04	1000R	II		
0.65......	6496.90	600r	III	$1d^2-1p^2$	
	6141.76	600r	III		
	5853.70	200	III		
2.71......	4899.97	35	IV ?	$1p^2-2s^2$	
	4524.95	35	V		
	4166.02	20	V	$1p^2-2d^2$	
	4130.68	80	V		
	3891.79	50	V		
	Zinc, *Zn*, I.P. 9.35				
0.0.......	3075.88	(8R)	....	$(1S-1p^3)$	
	2138.61	(8R)	....	$1S-1P$	
4.01......	4810.53	(10R)	....	$1p^3-1s^3$	
	4722.16	(10R)			
	4680.20	(10R)			
	3344.91	(10R)	....	$1p^3-2d^3$ *	
	3302.56	(8R)			
	3282.28	(8R)			
5.77......	6362.37	(10)	....	$1P-2D$	
	4629.88	(8r)	....	$1P-3D$	
	Ionized Zinc, *Zn*+, I.P. 18.2				
0.0.......	2061.96	(7)	....	$1s^2-2p^2$	
	2025.49	(8)			
6.10......	6214.65	(5)	....	$2p^2-md^2$?	
	5894.43	(6)			
	Cadmium, *Cd*, I.P. 8.95				
0.0.......	3261.04	(10)	....	$(1S-1p^3)$	
	2288.02	(10R)	....	$1S-1P$	
3.78......	5085.88	(10R)	....	$1p^3-1s^3$	
	4799.91	(10R)			
	4678.19	(10R)			
	3610.51	(10R)	....	$1p^3-2d^3$ *	
	3466.18	(10R)			
	3403.60	(10R)			
5.39......	6438.47	(10)	....	$1P-2D$	

TABLE I—*Continued*

E.P.	λ	Int.	Class	Type	Notes
	Ionized Cadmium, Cd^+, I.P. 17.3				
0.0	2265.04	(8R)	....	$1s^2-1p^2$	
	2144.39	(8R)			
	Mercury, *Hg*, I.P. 10.39				
0.0	2536.52	(10n)	....	$(1S-1p^3)$	
	1849.57	....	....	$1S-1P$	
5.44	5460.74	(10)	....	$1p^3-1s^3$	
4.87	4358.34	(10)			
4.65	4046.56	(10)			
6.67	5790.66	(10r)	....	$1P-2D$	
	5769.60	(10r)	....	$(1P-2d^3)$	
	Boron, *B*, I.P. 7:				(5)
0.0	2497.7	(10)	....	$1p^2-1s^2$	
	2496.8	(10)			
	Aluminium, *Al*, I.P. 5.96				
0.0	3961.54	(10R)	....	$1p^2-1s^2$	
	3944.03	(10R)			
	3092.84	(6R)	....	$1p^2-2d^2$	
	3092.72	(10R)			
	3082.16	(10R)			
3.13	6698.73	(3)	....	$1s^2-3p^2$	
	6696.06	(3)			
	Ionized Aluminium, Al^+, I.P. 18.18				(7)
0.0	3057.16	(10)	....	$(1S-1p^3)$	
	1670.98	(20)	....	$1S-1P$	
4.04	1862.48	(10)	....	$1p^3-2s^3$	
	1858.13	(7)			
	1856.00	(3)			
10.69	7063.62	(3)	....	$2s^3-2p^3$	
	7056.56	(4)			
	7042.06	(5)			
11.09	3587.44	(7)	....	$1d^3-2f^3$	
	3587.06	(8)			
	3586.55	(9)		*	

TABLE I—*Continued*

E.P.	λ	Int.	Class	Type	Notes
	Doubly Ionized Aluminium, Al^{++}, I.P. 28.32				(8)
0.0	1854.67	(10)	....	$1s^2-1p^2$	
	1862.90	(10)			
6.64	1611.94	(8)	....	$1p^2-1d^2$	
	1605.72	(8)			
14.32	3612.35	(15)	....	$1d^2-1p^2$	
	3601.62	(20)			
	Gallium, *Ga*, I.P. 5.97				
0.0	4172.06	(30R)	....	$1p^2-1s^2$	
	4033.03	(30R)			
	2944.18	(5R)	....	$1p^2-2d^2$	
	2943.66	(10R)			
	2874.24	(10R)			
	Indium, *In*, I.P. 5.76				
0.0	4511.27	(10R)	....	$1p^2-1s^2$	
	4101.72	(8R)			
	3258.52	(6R)	....	$1p^2-2d^2$	
	3256.03	(10R)			
	3039.34	(10R)			
	Thallium, *Tl*, I.P. 6.08				
0.0	3775.72	(10R)	....	$1p^2_2-1s^2$	
	2767.67	(10R)	....	$1p^2_2-1d^2$	
0.96	5350.46	(10R)	....	$1p^2_1-1s^2$	
	3529.43	(8R)	....	$1p^2_1-2d^2$	
	3519.24	(10R)			
	Ionized Carbon, C^+, I.P. 24.28				(9)
0.0	1036.84	(5)	....	$1p^2-x$	
	1036.22	(5)			
	858.2	(7)	....	$1p^2-2s^2$	
11.90	2837.60	(8)	....	$x-2p^2$	
	2836.71	(10)			
14.37	6582.85	(8)	....	$2s^2-2p^2$	
	6578.03	(10)			
16.24	7236.19	(8n)	....	$2p^2-2d^2$	
	7231.12	(6n)			
	3920.77	(8)	....	$2p^2-3s^2$	
	3919.06	(6)			

TABLE I—*Continued*

E.P.	λ	Int.	Class	Type	Notes
	Ionized Carbon—*Continued*				
17.94......	4267.27	(10n)	....	$2d^2-3f^2$	
	4267.02	(8n)			
	5891.65	(2)	....	$2d^2-3p^2$	
	5889.97	(3)			
	Trebly Ionized Silicon, *Si*+++, I.P. 44.95				(10)
0.0.......	1393.9	(10)	....	$1s^2-1p^2$	
	1402.9	(8)			
23.98......	4088.86	(10)	....	$2s^2-2p^2$	
	4116.10	(8)			
	Lead, *Pb*, I.P. 7.38				(11)
0.0.......	2833.07	(6R)	....	$2p_4-2s$	
	2170.00	(6R)	....	$2p_4-3d$	
0.96......	3639.58	(6R)	....	$2p_3-2s$	
	2657.10	(2)	....	$2p_3-3d$ *	
1.32......	4057.83	(5R)	....	$2p_2-2s$	
	2873.32	(4R)	....	$2p_2-3d$ *	
2.64......	7228.97	(4)	....	$2p_1-2s$	
	4168.04	(3)	....	$2p_1-3d$	
	4062.15	(3)			
	4019.64	(3)			
	3671.50	(3R)	....	$2p_1-3s$	
	3572.74	(5R)	....	$2p_1-x$	
3.64......	5201.47	(3)	....	$y-3s$	
	5005.44	(4)	....	$y-x$	
	Oxygen, *O*, I.P. 13.56				(12)
0.0.......	1355.67	....	....	(op^3-1s^5)	
	1358.60				
	1306.09	....	....	op^3-1s^3	
	1304.95				
	1302.25				
9.11......	7775.68	(6)	....	$1s^5-1p^5$	
	7774.01	(8)			
	7771.97	(10)			
	3947.61	(4)	....	$1s^5-2p^5$	
	3947.51	(7)			
	3947.33	(10)			
9.48......	8446.38	(10)	....	$1s^3-1p^3$	
	4638.30	(10)	....	$1s^3-2p^3$	

TABLE I—*Continued*

E.P.	λ	Int.	Class	Type	Notes
	Oxygen—*Continued*				
10.69	6456.07	(9)	....	$1p^5-3s^5$	
	6454.55	(7)			
	6453.69	(6)			
	6158.20	(10)	....	$1p^5-3d^5$	
	6156.78	(8)			
	6155.99	(7)			
10.94	7254.05	(2)	....	$1p^3-3s^3$	
	7002.22	(4)	....	$1p^3-3d^3$	
	6046.34	(7d)	....	$1p^3-4s^3$	
	5958.53	(6d)	....	$1p^3-4d^3$	
	Sulphur, *S*, I.P. 10.31				(13)
0.0	1914.96	....	....	$(0p^3-1s^5)$	
	1900.47				
	1826.35	....	....	$0p^3-1s^3$	
	1820.53				
	1807.42				
6.50	9237.71	....	....	$1s^5-1p^5$	
	9228.17				
	9212.80				
	4696.31	(6)	....	$1s^5-2p^5$	
	4695.51	(8)			
	4694.18	(10)			
7.84	6757.16	(7)	....	$1p^5-4d^5$	
	6748.83	(6)			
	6743.69	(5)			
	Selenium, *Se*, I.P. ?				
?	4742.58	(8)	....	$1s^5-2p^5$	
	4739.28	(9)			
	4731.04	(10)			
	Scandium, *Sc*, I.P. 5.4:				(14)
0.0	6448.10	1	II A	$1d^2-1d'^2$	(28)
	6413.37	50	I A		
	6378.83	40	I A		(15)
	6344.84	5	II A		
	6305.99	20	I A	$1d^2-2d'^2$	
	6305.69	400	I A		
	6239.78	100	I A		
	6239.40	20	II A		
	6276.30	15	II A	$1d^2-3d'^2$	
	6258.97	100	I A		
	6210.68	200	I A		
	6193.66	(3)	II A		

TABLE I—*Continued*

E.P.	λ	Int.	Class	Type	Notes
	Scandium—*Continued*				
0.0—*Cont.*	5349.71	15	II A	$1d^2-1p'^2$	
	5342.96	10	II A		
	5301.94	2	II A		
	4791.51	4	I A	$1d^2-1f'^2$	
	4779.35	20	I A		
	4753.16	15	I A		
	4082.40	40	I	$1d^2-4d'^2$	
	4054.54	35	I		
	4047.79	25	I	$1d^2-5d'^2$	
	4023.69	100	II		
	4020.40	75	II		
	3996.61	30	I		
	3933.37	20	II	$1d^2-2f'^2$	
	3911.81	100	II		
	3907.49	75	II		
	3273.64	20	II A	$1d^2-2p'^2$	
	3269.91	15	II A		
	3255.69	6	I A		
?..........	5724.09	15	III A	$1f^4-1g'^4$ *	
	5717.30	15	III A		
	5711.75	100	III A		
	5708.62	15	III A		
	5700.14	100	II		
	5686.84	150	II		
	5671.80	200	II		
	5086.95	40	II	$1f^4-1f'^4$ *	
	5085.54	40	II		
	5083.72	80	II		
	5081.56	125	II		
	4743.81	40	III	$1f^4-1d'^4$ *	
	4741.02	30	III		
	4737.65	20	III		
	4734.10	15	III		
	4729.23	30	III		
	4728.76	5	III		
2.10......	6198.44	(2)	IV A	$1f^2-3f'^2$	
	6146.25	(3)	IV A		
	6026.18	15	IV	$1f^2-6d'^2$ *	
	5988.42	20	IV		
	Ionized Scandium, Sc^+, I.P.?				(14)
0.0	3666.54	2	III	$1d^3-1f'^3$	
	3651.80	7	III		
	3645.31	10	III		
	3642.79	25	II		
	3630.76	12	II		
	3613.84	30	II		

TABLE I—*Continued*

E.P.	λ	Int.	Class	Type	Notes
	Ionized Scandium—*Continued*				
0.0—*Cont.*	3590.48	6	II	$1d^3-1d'^3$	
	3589.64	6	II		
	3580.94	7	II		
	3576.35	8	II		
	3572.53	20	II		
	3567.70	6	II		
	3558.55	7	II		
	3372.14	12	III	$1d^3-1p'^3$	
	3368.94	8	III		
	3361.94	6	III		
	3361.26	6	III		
	3359.68	6	III		
	3352.05	2	II		
?	4246.83	75	III	?	(16)
0.60	4431.35	4	V	$1f^3-1f'^3$	
	4420.66	(1)	...		
	4415.55	40	III		
	4400.38	50	III		
	4384.80	8	IV		
	4374.46	60	III		
	4354.60	8	V		
	4325.00	50	III	$1f^3-1d'^3$	
	4320.73	75	III		
	4314.09	100	III		
	4305.71	10	IV	*	
	4294.77	10	IV		
1.50	6320.86	(2)	...	$1p^3-1d'^3$	
	6309.90	(2)	...		
	6300.70	(1)	...		
	6279.74	(3)	...	*	
	6245.64	(4)	V		
	5684.21	8	V	$1p^3-1p'^3$	
	5669.05	2	IV		
	5667.16	2	V		
	5658.35	2	V		
	5657.89	15	V		
	5640.99	2	V		
	Yttrium, *Y*, I.P. 5?				(26)
0.0	6435.02	(5)	....	$1d^2-md'^2$	
	6402.02	(3)			
	6222.58	(4)			
	6191.71	(1)			
	6138.43	(4)	....	$1d^2-mp'^2$	
	6023.41	(3)			
	5944.86	(1)			

TABLE I—*Continued*

E.P.	λ	Int.	Class	Type	Notes
	Yttrium—*Continued*				
0.0—*Cont.*	4760.99	(5)	....	$1d^2-mf'^2$	(29)
	4674.84	(10)			
	4643.70	(10)			
	4174.14	(8)	....	$1d^2-np'^2$	
	4142.87	(20)			
	4083.71	(8)			
	4128.32	(30)	....	$1d^2-n'p'^2$	
	4102.38	(20)			
	4039.83	(5)			
	Ionized Yttrium, *Y*+, I.P. ?				
0.0.......	4422.60	(10)	....	$1d^3-1p'^3$	
	4398.03	(15)			
	4358.72	(8)			
	4309.61	(20)			
	4235.71	(6)			
	4199.28	(3)			
	3788.69	(30)	....	$1d^3-1f'^3$ *	
	3774.33	(50)			
	3710.30	(50)			
	3611.05	(30)	....	$1d^3-1d'^3$ *	
	3601.91	(20)			
	3600.72	(50)			
0.93......	4900.11	(30)	....	$1f^3-1d'^3$	
	4883.69	(50)			
	4854.88	(30)			
	4823.32	(10)			
	4786.57	(5)			
	5320.79	(1)	....	$1f^3-1f'^3$	
	5289.82	(2)			
	5205.72	(10)			
	5200.41	(10)			
	5119.10	(3)			
	5087.43	(10)			
	4982.12	(3)			
	Titanium, *Ti*, I.P. 6.5				(17)
0.0.......	6413.30	....	II A	($1f^3-1g'^5$)	
	6359.90	0	II A		
	6325.17	1	II A		
	6296.68	2	II A		
	6295.27	1	II A		
	6273.42	....	II A		
	6257.80	....	II A		
	6031.71	0	II A	($1f^3-1f'^5$)	
	5984.59	....	II A		
	5944.65	1	II A		
	5940.66	1	II A		
	5913.71	0	II A		

TABLE I—*Continued*

E.P.	λ	Int.	Class	Type	Notes
			Titanium—*Continued*		
0.0—*Cont.*	5490.82	1	I A	($1f^3-1d'^5$)	
	5460.51	4	I A		
	5446.67	2	II A		
	5426.27	3	I A		
	5408.93	(1)	I A		
	5396.57	1	I A		
	5376.58	(0)	. . .		
	5252.11	8	I A	$1f^3-1f'^3$	
	5219.72	8	I A		
	5210.39	40	I		
	5192.98	35	I		
	5173.74	30	I		
	5152.18	10	I A		
	5147.48	10	I A		
	5064.66	25	I	$1f^3-1d'^3$	
	5039.96	22	I		
	5014.19	(25)	I		
	5009.65	7	I A	*	
	4997.10	8	I A		
	4715.31	4	II A	$1f^3-1g'^3$	
	4693.68	5	II A		
	4681.91	30	I		
	4667.59	25	I		
	4656.47	25	I		
	4562.63	6	II A	($1f^3-1D'$)	
	4527.46	(4)	III A		
	4496.24	2	III A	($1f^3-1F'$)	
	4462.08	2	III A	*	
	4112.73	20	II	($1f^3-1G'$)	
	4076.38	4	III A		
	4024.57	35	II	$1f^3-2f'^3$	
	4008.94	35	II		
	3998.65	100R	II		
	3989.77	80R	II		
	3981.77	70R	II		
	3964.27	35	II		
	3962.85	35	II		
	3958.21	80	II	$1f^3-2d'^3$	
	3956.28	60	II		
	3948.66	60	II		
	3929.87	40	II		
	3924.51	50	II		
	3898.49	8	III		
	3771.64	25	I	$1f^3-4f'^3$	
	3753.63	25	I		
	3752.87	80r	I		
	3741.06	60r	I		
	3729.77	50r	I		
	3722.58	15	II		
	3717.39	20	I		

TABLE I—*Continued*

E.P.	λ	Int.	Class	Type	Notes
	Titanium—*Continued*				
0.0—*Cont.*	3689.89	15	I	$1f^3-3d'^3$	
	3668.95	15	I		
	3660.62	12	I		
	3654.58	15	I		
	3646.19	12	I		
	3637.97	10	II		
	3671.66	20	I	$1f^3-2g'^3$	
	3658.14	20	I		
	3653.49	100r	I		
	3642.68	80r	I		
	3635.47	80r	I		
	3385.93	40r	II	$1f^3-5d'^3$ *	
	3377.57	30r	I		
	3370.42	40r	II		
	3371.44	80R	II	$1f^3-3g'^3$ *	
	3354.64	60r	II		
	3341.87	50r	II		
	3199.91	100R	II	$1f^3-4g'^3$ *	
	3192.00	80R	II		
	3186.45	60r	II		
0.82......	8435.64	(5)	....	$1f^5-1d'^5$ *	
	8434.89	(4)			
	8426.46	(4)			
	8412.34	(3)			
	8396.85	(2)			
	5045.43	5	III A	$1f^5-2g'^5$	
	5043.59	7	III A		
	5040.63	6	III A		
	5024.85	20	II		
	5022.87	25	II		
	5020.04	25	II		
	5016.17	20	II		
	5014.28	(25)	I		
	5007.22	40	II		
	4999.51	45	II		
	4991.08	50	II		
	4981.75	60	II		
	4555.50	30	II	$1f^5-2f'^5$	
	4552.56	35	II		
	4548.77	35	II		
	4544.70	30	II		
	4536.00	40	II		
	4535.92	40	II		
	4535.58	50	II		
	4534.78	60	II		
	4533.25	80	II		
	4527.32	35	II		
	4522.80	40	II		
	4518.03	50	II		
	4512.74	40	II		

TABLE I—*Continued*

E.P.	λ	Int.	Class	Type	Notes
	Titanium—*Continued*				
0.82—*Cont.*	4305.91	60	II	$1f^5-2d'^5$	
	4301.08	50	II		
	4300.55	50	II		
	4298.67	40	II		
	4295.75	22	II		
	4290.93	22	II		
	4289.08	25	II		
	4287.41	22	II		
	4286.01	25	II		
	4281.40	10	III		
	4274.60	15	III		
	4272.44	8	III A		
	4326.35	9	II	$(1f^5-5d'^3)$ *	
	4314.80	25	II		
	4299.64	15	III		
	4288.18	3	III A		
0.90......	6743.14	10	III A	$1D-1D'$	
	6599.12	12	III A	$1D-1F'$	
	4958.25	2	III A	$(1D-3d'^3)$ *	
	4840.88	25	I	$1D-2D'$	
	3904.77	40n	II	$1D-2F'$	
	3786.03	20	II	$1D-1P'$	
1.05......	8692.29	(1)	....	$1p^3-1d'^3$ *	
	8682.93	(2)			
	8675.33	(2)			
	6126.21	20	II	$1p^3-1s'^3$	
	6085.22	20	II		
	6064.64	9	II A		
	5941.73	12	II A	$1p^3-2d'^3$	
	5937.79	6	III A		
	5922.11	18	II		
	5899.29	25	II		
	5866.45	35	II		
	5295.78	4	III	$1p^3-3d'^3$ *	
	5284.39	2	III A		
	5282.38	3	III A		
	4723.18	10	III	$1p^3-5d'^3$	
	4722.63	10	III		
	4710.19	18	III		
	4698.79	20	II		
	4691.34	20	II		
	4082.46	20	III	$1p^3-3p'^3$	
	4078.47	30	III		
	4065.11	15	III		
	4064.22	15	III		
	4060.27	20	III		
	4055.02	20	III		

TABLE I—*Continued*

E.P.	λ	Int.	Class	Type	Notes
	Titanium—*Continued*				
1.05—*Cont.*	3725.12	20	III	$1p^3-2s'^3$	
	3709.95	20	III		
	3702.29	10	III		
1.44.......	7364.11	2	IV	$2f^3-2f'^3$ *	
	7357.73	3	IV		
	7344.69	4	IV		
	7299.67	(2)	...		
	7271.47	(0)	...		
	7251.74	8	III	$2f^3-2d'^3$	
	7244.82	10	III		
	7209.44	20	III		
	7188.59	(1)	...		
	7138.92	(1)	...		
	6556.08	25	III	$2f^3-4f'^3$	
	6554.23	20	III		
	6546.26	20	III		
	6508.15	3	III A		
	6497.71	3	III A		
	6366.38	8	III	$2f^3-3d'^3$	
	6336.10	8	III		
	6318.00	5	III A		
	6312.23	10	III	$2f^3-2g'^3$	
	6303.76	10	III		
	6261.10	35	II		
	6258.70	50	II		
	6258.10	40	II		
	5514.54	25	II	$2f^3-5d'^3$	
	5514.36	20	II		
	5512.54	25	II		
	5481.90	5	I A		
	5471.19	5	III		
	5474.28	6	II	$2f^3-3g'^3$	
	5453.67	3	III A		
	5438.33	1	III A		
	5145.47	12	II	$2f^3-6d'^3$ *	
	5113.45	10	III		
	5087.07	8	III		
	5038.41	25	II	$2f^3-4g'^3$ *	
	5036.47	25	II		
	5035.92	25	II		
	4457.42	40	II	$2f^3-6f'^3$ *	
	4455.32	30	II		
	4453.32	30	II		
1.50.......	7949.11	(3)	....	$1G-1G'$	
	4820.42	20	II	$1G-2F'$	
	4427.10	40	III	$1G-2G'$	
	4186.12	25	III	$1G-3G'$	

TABLE I—*Continued*

E.P.	λ	Int.	Class	Type	Notes
	Titanium—*Continued*				
1.73......	4656.06	6	III	$1p^5-3d'^5$	
	4650.02	10	III		
	4645.19	12	III		
	4639.94	15	III		
	4639.66	15	III		
	4639.36	18	III		
	4629.34	15	III		
	4623.10	25	III		
	4617.27	30	II		
	4496.15	20	III	$1p^5-1p'^5$	
	4489.10	20	III		
	4481.27	30	III		
	4480.61	5	III A		
	4479.70	9	III		
	4471.24	20	III		
	4465.80	20	III		
1.87......	8548.06	(2)	....	$1g^3-4f'^3$	
	8518.20	(4)			
	8468.45	(3)			
	8068.21	(2)	....	$1g^3-2g'^3$	
	8024.83	(2)			
	7978.87	(4)			
	6146.22	3	III	$1g^3-4g'^3$	
	6121.03	3	III		
	6092.79	4	III		
	5996.01	2	III	$1g^3-1h'^3$	
	5988.58	2	III		
	5978.54	25	II		
	5965.83	30	II		
	5953.16	30	II		
	5297.29	6	III	$1g^3-6f'^3$ *	
	5283.45	8	III		
	5265.97	10	III		
	4925.42	5	IV	$1g^3-2h'^3$	
	4915.24	5	III		
	4913.63	20	III		
	4899.93	20	III		
	4885.09	20	II		
	4453.70	20	III	$1g^3-5g'^3$ *	
	4450.90	25	III		
	4449.13	30	III		
1.98......	5025.58	18	III	$1g'^5-2f^5$ *	
	5013.30	18	III		
	5001.01	10	III A		
	4989.16	10	III		
	4978.21	10	III		

TABLE I—*Continued*

E.P.	λ	Int.	Class	Type	Notes
	Titanium—*Continued*				
2.08......	5224.96	8	III	$1f'^{5}-2f^{5}$ *	
	5224.57	6	III		
	5224.32	15	III		
	5223.64	6	III		
	5222.68	6	III		
2.16......	6186.15	3	III	$1d^{3}-5f'^{3}$ *	
	6149.81	2	III		
	6138.38	1	IV		
	4948.21	3	IV	$1d^{3}-7f'^{3}$	
	4941.58	3	IV		
	4928.36	12	III		
	4921.79	12	III		
	4919.88	10	III		
2.24......	5999.66	8	III	$(1h^{3}-2G')$	
	5565.48	9	III	$(1h^{3}-3G')$	
	4778.27	10	III	$(1h^{3}-4G')$	
	7496.12	(2)	....	$1h^{3}-4g'^{3}$	
	7489.61	(2)			
	7440.58	(3)			
	5740.04	4	IV	$1h^{3}-2h'^{3}$	
	5739.50	9	III		
	5715.13	9	III		
	4893.06	2	IV	$1h^{3}-1i'^{3}$	
	4882.34	2	IV		
	4870.14	20	III		
	4868.28	18	III		
	4856.01	20	III		
	4769.78	4	III	$1h^{3}-3h'^{3}$	
	4766.33	4	III		
	4759.28	25	III		
	4758.13	25	III		
	4747.69	3	III		
	4742.80	20	III		
	4734.68	3	IV		
2.26......	6861.47	6	III	$2G-2F'$	
	6091.17	20	III	$2G-2G'$	
	5644.14	18	III	$2G-3G'$	
	4799.81	12	III	$(2G-3h'^{3})$	
2.28......	5720.49	3	III	$1d'^{5}-2f^{5}$	
	5716.48	4	III		
	5713.93	3	IV		
	5711.94	4	IV		
	5708.27	3	IV		
	5702.69	6	III		
	5689.47	10	III		
	5675.41	9	III A		
	5662.16	12	III		

TABLE I—*Continued*

E.P.	λ	Int.	Class	Type	Notes
	Titanium—*Continued*				
2.33......	4812.25	5	III	$3p^3-9d'^3$	
	4805.43	12	III		
	4797.99	5	III		
	4796.22	6	III		
	4792.50	10	III		
2.39......	5488.24	5	III	$1f'^3-3f^3$	
	5481.45	6	III		
	5477.70	8	III		
2.47......	5679.95	2	III	$1d'^3-3f^3$	
	5662.91	4	III		
	5648.63	5	IV		
2.56......	7189.92	2	IV?	$1H-2G'$	
	6575.19	3	V	$1H-3G'$	
	5503.89	8	III	$1H-4G'$	
	4938.31	8	IV	$1H-6G'$	
2.67......	6221.42	8	III	$1g'^3-3f^3$ *	
	6220.45	12	III		
	6215.24	20	III		
	Ionized Titanium, *Ti*+, I.P.??				(18)
0.0.......	3409.80	5	IV	$1f^4-1g'^4$	
	3407.20	4	IV		
	3394.57	15r	III		
	3387.83	15r	III		
	3383.76	40r	III		
	3380.28	15r	III		
	3372.80	30r	II		
	3361.22	40r	III		
	3349.41	40r	II		
	3254.23	20r	III	$1f^4-1f'^4$	
	3252.85	25r	III		
	3251.89	20r	III		
	3241.97	40r	III		
	3239.03	40r	III		
	3236.57	50r	III		
	3234.52	60r	III		
	3229.18	15r	III		
	3222.82	15r	III		
	3217.04	15r	III		
	3088.03	60r	III	$1f^4-1d'^4$ *	
	3078.64	45r	III		
	3075.22	40r	III		
	3072.97	40r	III		
	3072.10	30r	III		
	3066.36	20r	IV		
	3066.20	30r	IV		

TABLE I—*Continued*

E.P.	λ	Int.	Class	Type	Notes
	Ionized Titanium—*Continued*				
0.13......	3500.47	4	IV	$2f^4-1g'^4$	
	3491.05	8ru	III		
	3489.74	4	IV		
	3477.18	15ru	III		
	3476.99	2	V		
	3461.50	20ru	III		
	3444.31	15ru	III		
	3348.82	5	III	$2f^4-1f'^4$	
	3346.72	7	III		
	3343.76	6	III		
	3340.33	15ru	III		
	3335.19	20ru	III		
	3329.45	20ru	III		
	3326.76	5ru	III		
	3322.93	20ru	III		
	3318.01	8ru	III		
	3308.79	8ru	III		
	3168.52	30ru	III	$2f^4-1d'^4$	
	3162.56	25ru	III		
	3161.76	20ru	III		
	3161.19	20ru	III		
	3155.65	10ru	IV		
	3154.18	10ru	IV		
	3152.24	12ru	IV		
0.59......	4025.13	4	V	$(1f^2-1g'^4)$	
	4012.40	10	V	*	
	3761.33	40r	IV	$1f^2-1f'^2$	
	3759.30	40r	IV		
	3721.64	8	V		
	3685.19	40r	IV	$1f^2-1d'^2$	
	3372.20	5	V	$1f^2-1g'^2$	
	3349.02	20r	III		
	3341.87	50r	II		
1.08......	4450.49	4	V	$1d^2-1f'^2$	
	4443.80	25	V		
	4395.04	25	V		
	4344.31	3	V	$1d^2-1d'^2$	
	4337.92	10	V		
	4294.10	8	V		
	4287.88	2	V		
1.12......	4501.27	25	V	$1g^2-1f'^2$	
	4468.49	25	V	*	
	4341.39	2	V	$(1g^2-1d'^2)$	
	3913.45	40	V	$1g^2-1g'^2$	
	3900.53	50	V	*	
	3232.26	8ru	IV	$1g^2-2f'^2$	
	3229.40	10ru	V		

TABLE I—*Continued*

E.P.	λ	Int.	Class	Type	Notes
	Ionized Titanium—*Continued*				
1.16......	4417.71	8	V	$(1p^4-1d^2)$ *	
	4330.71	1	V	$1p^4-1d'^4$	
	4320.95	1	V		
	4314.98	5	V		
	4312.88	7	V		
	4307.89	12	V		
	4301.93	5	V		
	4300.05	12	V		
	4290.23	8	V		
1.22......	4708.65	(2)	....	$(1p^2-1f'^2)$	
	4589.96	3	V	$1p^2-1d'^2$	
	4563.77	15	V		
	4533.97	20	V		
	4399.77	6	V	$(1p^2-1d'^4)$ *	
	4394.06	2	V		
	3641.33	10	V	$1p^2-1s'^2$	
	3624.84	8	V		
1.56......	5418.77	1	V	$2d^2-1f'^2$	
	5381.02	(4)	...		
	5336.78	2	V		
	5262.14	(1)	...	$2d^2-1d'^2$	
	5226.56	3	V		
	5188.70	4	V		
	5154.07	(1)	...		
	3757.68	8	V	$2d^2-2d'^2$ *	
	3741.63	8ru	V		
1.57......	4571.98	15	V	$1h^2-1g'^2$	
	4549.64	25	V		
	4529.46	1	V		
	3224.23	8ru	V	$1h^2-2g'^2$ *	
	3218.25	8ru	IV		
1.88......	5185.90	(5)	....	$2g^2-1g'^2$ *	
	5129.17	(8)			
	4053.84	4	V	$2g^2-2f'^2$	
	4028.35	5	V		
	3510.84	10r	V	$2g^2-2g'^2$ *	
	3504.89	8r	V		
2.05......	6559.58	(1)	....	$2p^2-1d'^2$	
	6491.68	(2)			
	4805.11	4	V	$2p^2-1s'^2$	
	4779.99	2	V		
2.58......	4386.84	(5)	...	$2f^2-2g'^2$	
	4367.67	1	V		

TABLE I—*Continued*

E.P.	λ	Int.	Class	Type	Notes
	Ionized Titanium—*Continued*				
3.10......	5072.30	(3)	....	$3d^2-3d'^2$	
	5069.12	(1)			
	5010.21	(1)			
	4911.19	(1)	....	$3d^2-2p'^2$	
	4873.95	(3)			
	Zirconium, *Zr*, I.P. 6?				(27)
0.0.......	6143.23	(6)	....	$1f^3-md'^3$	
	6134.58	(5)			
	6127.49	(6)			
	5935.24	(3)			
	5885.61	(2)			
	3891.39	(6)	....	$1f^3-mf''^3$ *	
	3863.57	(7)			
	3835.96	(4)			
?.........	7169.15	(8)	....	$1f^5-md'^5$ *	
	7103.77	(6)			
	7102.96	(6)			
	7097.78	(7)			
	7087.36	(6)			
	4851.36	(6)	....	$1f^5-mg'^5$ *	
	4824.30	(7)			
	4815.62	(7)			
	4805.89	(7)			
	4788.70	(7)			
	4772.33	(8)			
	4739.49	(8)			
	4710.08	(8)			
	4687.81	(8)			
?.........	5797.77	(7)	....	$1p^3-ms'^3$	
	5680.94	(7)			
	5623.57	(5)			
	4539.97	(7)	....	$1p^3-nd'^3$ *	
	4535.75	(6)			
	4553.02	(6)			
	Ionized Zirconium, Zr^+, I.P.?				
0.0.......	3572.46	(8)	....	$1f^4-1g'^4$ *	
	3496.17	(9)			
	3438.23	(9)			
	3391.96	(8)			
	3357.27	(7)	....	$1f^4-1f'^4$ *	
	3306.28	(7)			
	3279.26	(7)			
	3273.05	(7)			
	3165.98	(7)	....	$1f^4-1d'^4$ *	
	3138.66	(7)			
	3129.70	(6)			
	3125.92	(6)			

TABLE I—*Continued*

E.P.	λ	Int.	Class	Type	Notes
	Ionized Zirconium—*Continued*				
0.40......	3934.14	(6)	....	$2f^4-1g'^4$ *	
	3843.01	(5)			
	3766.72	(5)			
	3697.46	(5)			
	3674.72	(8)	....	$2f^4-1f'^4$ *	
	3614.78	(7)			
	3576.85	(7)			
	3556.59	(7)			
	3430.54	(7)	....	$2f^4-1d'^4$ *	
	3410.25	(7)			
	3404.84	(6)			
	3399.35	(6)			
	Vanadium, *V*, I.P.?				(19)
0.0.......	5632.47	1	II A	$(1f^4-1d'^6)$ *	
	5592.96	1	II A		
	4881.55	50	I	$1f^4-1d'^4$	
	4875.46	40	I		
	4864.74	40	I		
	4851.48	40	I		
	4832.43	30	I		
	4831.64	35	I		
	4827.45	30	I		
	4799.78	5	II A		
	4784.48	5	II A		
	4635.18	15	I	$1f^4-1g'^4$ *	
	4619.77	25	I		
	4606.15	15	I		
	4594.10	60	I		
	4586.36	50	I		
	4580.39	40	I		
	4577.17	40	I		
	4368.05	10	I	$1f^4-1f'^4$	
	4355.95	10	I		
	4352.89	50	I		
	4341.02	40	I		
	4332.83	30	I		
	4330.03	30	I		
	4309.80	20	I		
	4307.18	12	I		
	4306.22	15	I		
	3902.26	50r	I	$1f^4-2f'^4$ *	
	3875.08	35	I		
	3864.86	35	I		
	3855.37	30	I		
	3855.86	60r	I	$1f^4-2d'^4$ *	
	3840.76	60r	II		
	3828.56	60r	II		
	3822.01	30	I		
	3818.24	60	II		
	3813.49	60	II		
	3808.52	40	II		

TABLE I—*Continued*

E.P.	λ	Int.	Class	Type	Notes
	Vanadium—*Continued*				
0.0—*Cont.*.	3185.40	40r	II	$1f^4-2g'^4$ *	
	3184.02	25r	II		
	3183.96	35r	II		
	3183.41	30r	II		
0.28.......	6296.52	15	I	$1d^6-1d'^6$	
	6292.86	20	I		
	6285.19	20	I		
	6274.67	15	I		
	6258.80	....	......		
	6258.60	8	II A		
	6256.91	8	II A		
	6251.83	30	I		
	6243.11	30	I		
	6242.80	15	I		
	6230.73	30	I		
	6216.37	30	I		
	6199.20	30	I		
	6268.84	8	II A	$1d^6-1f'^6$	
	6266.32	7	II A		
	6261.24	5	II A		
	6245.21	2	II A		
	6240.14	6	II A		
	6233.19	12	I A		
	6224.50	15	I		
	6213.87	15	I		
	6189.35	3	II A		
	6170.34	8	I A		
	6150.13	15	I		
	4460.30	50	I	$1d^6-1p'^6$	
	4459.77	30	I		
	4457.48	15	I		
	4444.22	20	I		
	4441.69	25	I		
	4437.84	20	I		
	4436.14	15	I		
	4428.52	15	I		
	4419.94	12	I		
	4429.80	15	I	$1d^6-2f'^6$	
	4426.01	15	I		
	4421.58	20	I		
	4416.48	20	I		
	4408.51	45	I		
	4408.21	70	I		
	4407.65	70	I		
	4406.65	80	I		
	4400.59	60	II		
	4395.24	80	II		
	4389.99	100	II		
	4384.73	125r	II		
	4379.24	150r	II		

TABLE I—*Continued*

E.P.	λ	Int.	Class	Type	Notes
	Vanadium—*Continued*				
0.28—*Cont.*	4209.86	20	I	$(1d^6-2f'^4)$ *	
	4191.55	10	II		
	4189.85	12	I		
	4182.60	10	I		
	4134.50	60	I	$1d^6-2d'^6$	
	4132.02	60	I		
	4128.08	60	I		
	4123.56	60	I		
	4116.70	4	I A		
	4116.48	50	I		
	4115.18	60	I		
	4111.79	100R	I		
	4109.78	50	I		
	4105.17	60	I		
	4099.80	60	I		
	4092.69	50	I		
	3705.03	30	I	$1d^6-2p'^6$	
	3704.70	60	II		
	3703.57	100	II		
	3695.87	40	II		
	3692.22	50	II		
	3690.27	40	II		
	3688.07	50	II		
	3683.11	30	I		
	3675.70	20	I		
1.05......	8198.85	(3)	....	$1d^4-1d'^4$ *	
	8186.71	(3)			
	8161.06	(4)			
	8116.78	(5)			
	6812.42	2	III A	$1d^4-1f'^4$ *	
	6785.02	3	III A		
	6766.53	4	III A		
	6753.03	5	III A		
	6135.36	15	II	$1d^4-1p'^4$	
	6119.51	40	I		
	6111.62	25	II		
	6090.18	50	I		
	6081.42	25	I		
	6058.11	5	II A		
	6039.69	25	I		
	6002.60	4	II A		
	5782.60	2	III A	$1d^4-2f'^4$	
	5761.41	2	III A		
	5743.44	18	II		
	5737.04	25	II		
	5727.66	20	II		
	5727.02	60	I		
	5706.97	30	I		
	5703.56	40	I		
	5698.51	60	I		

TABLE I—*Continued*

E.P.	λ	Int.	Class	Type	Notes
	Vanadium—*Continued*				
1.05—*Cont.*	5668.37	12	II	$1d^4-2d'^4$	
	5657.45	12	II		
	5646.11	10	II		
	5627.63	30	I		
	5626.01	8	II		
	5624.90	10	II		
	5624.61	20	I		
	5604.94	8	II		
	5592.41	12	I		
	5584.49	10	I		
	4670.48	25	III	$1d^4-2p'^4$ *	
	4646.40	15	III		
	4640.74	7	III		
	4640.06	8	III		
	4104.78	15	III	$1d^4-3f'^4$ *	
	4102.16	20	II		
	4095.49	25	II		
	4090.59	25	I		
1.20.......	6624.86	5	III A	$1p^4-1p'^4$	
	6605.98	5	III A		
	6565.88	2	III A		
	6543.51	3	III A		
	6531.44	20	II		
	6504.16	8	II A		
	6452.35	8	II A		
	6017.90	1	III A	$1p^4-2d'^4$ *	
	6008.65	1	III A		
	6002.27	2	II A		
	5984.60	1	III A		
	5980.74	2	III A		
2.05.......	4807.54	25	III	$1g'^6-mf^6$ *	
	4796.93	20	III		
	4786.51	20	III		
	4776.36	15	III		
	4766.63	12	III		
	4757.50	8	III		
	Chromium, *Cr*, I.P. 6.72				(20)
0.0........	4289.72	350R	II	$1s^7-1p^7$	
	4274.80	400R	II		
	4254.34	500R	II		
	3732.05	12	I	$(1s^7-1p^5)$	
	3730.84	10	I		
	3605.34	140R	II	$1s^7-2p^7$	
	3593.50	160R	II		
	3578.70	200R	II		
	3379.36	(1)	....	$(1s^7-1p'^5)$	
	3351.96	(2)			

TABLE I—*Continued*

E.P.	λ	Int.	Class	Type	Notes
	Chromium—*Continued*				
0.94......	6362.83	15	I A	$(1s^5-1p^7)$	
	6330.10	25	I A		
	5208.42	300r	II	$1s^5-1p^5$	
	5206.05	200r	II		
	5204.51	150r	II		
	4964.93	6	II A	$(1s^5-2p^7)$	
	4942.48	8	II A		
	4580.05	20	I	$1s^5-1p'^5$	
	4545.96	20	I		
	4496.85	25	I		
0.98......	6630.01	4	I A	$(1d^5-1p^7)$	(21)
	6580.91	....	.....		
	6572.90	2	I A		
	6537.90	3	I A		
	6501.21	2	I A		
	6467.18	....	.....		
	6452.58	....	.....		
	5409.83	100	I	$1d^5-1p^5$	
	5348.33	50	I		
	5345.81	70	I		
	5300.72	25	I		
	5298.26	60	I		
	5296.70	50	I		
	5265.72	25	I		
	5264.16	50	I		
	5247.57	40	I		
	5123.46	6	I	$(\underset{*}{1}d^5-2p^7)$	
	5091.86	3	II A		
	5068.28	2	II A		
	5048.78	2	II A		
	4652.20	30	I	$1d^5-1p'^5$	
	4651.31	20	I		
	4646.17	40	I		
	4626.18	20	I		
	4616.11	25	I		
	4613.36	15	I		
	4600.73	20	I		
	4591.44	20	I		
	4565.53	12	I		
	4412.28	6	I A	$1d^5-1f^5$	
	4391.77	8	I		
	4384.99	20	I		
	4373.26	8	I		
	4371.32	20	I		
	4359.66	20	I		
	4351.82	60	I		
	4351.06	20	I		
	4344.52	40	I		
	4339.74	20	I		
	4339.46	40	I		
	4337.58	30	I		

TABLE I—*Continued*

E.P.	λ	Int.	Class	Type	Notes
	Chromium—*Continued*				
0.98—*Cont.*	3941.53	20	I	$1d^5-1d'^5$	
	3928.68	25	I		
	3921.07	20	I		
	3919.18	35r	II		
	3916.27	12	I		
	3908.77	25	II		
	3903.15	8	I		
	3902.91	12	II		
	3894.06	15	I		
	3886.78	15	I		
	3885.22	15	I		
	3883.34	15	I		
2.88......	7462.34	(10)	....	$1p^7-2s^7$	
	7400.22	(10)			
	7355.93	(10)			
	5329.80	5n	II	$1p^7-1d^7$	
	5329.15	20n	II		
	5328.34	50n	II		
	5297.96	15n	II		
	5297.33	20n	II		
	5276.07	20n	II		
	5275.66	15n	II		
	5275.17	20n	II		
	4514.50	8	III	$1p^7-3s^7$	
	4491.68	3n	III		
	4475.36	8n	III		
	4129.21	20n	III	$1p^7-2d^7$	
	4111.67	20n	III		
	4111.46				
	4110.87				
	4098.18	20n	III		
	4097.96				
	4097.65				
3.30......	9021.69	(4)	....	$1p^5-2s^5$	
	9017.10	(5)			
	9009.95	(6)			
3.42......	6981.04	(3)	....	$2p^7-1d^7$	
	6980.81	(2)			
	6979.79	(10)			
	6925.99	(1)			
	6925.20	(9)			
	6924.14	(10)			
	6883.03	(9)			
	6882.38	(9)			
	6881.62	(9)			

TABLE I—*Continued*

E.P.	λ	Int.	Class	Type	Notes
	Molybdenum, *Mo*, I.P. 7.35				(22)
0.0.......	3902.97	(50R)	....	$1s^7-1p^7$	
	3864.12	(50R)			
	3798.26	(50R)			
	3466.83	(8)	....	$(1s^7-1p^5)$	
	3456.39	(10)			
1.32......	5570.46	(25R)	....	$1s^5-1p^5$	
	5533.01	(30R)			
	5506.51	(40R)			
	Manganese, *Mn*, I.P. 7.41				(23)
0.0.......	5432.55	4	I A	$(1s^6-1p^8)$	
	5394.68	10	I A		
	4034.49	100R	I	$1s^6-1p^6$	
	4033.07	150R	I		
	4030.76	200R	I		
	2801.06	(8R)	....	$1s^6-2p^6$	
	2798.27	(9R)			
	2794.82	(10R)			
2.16......	5537.75	5	III	$1d^6-2p^6$	
	5516.77	7	III A		
	5505.88	2	III		
	5481.40	4	II A		
	5470.64	8	II A		
	5457.47	1	II A		
	5420.37	10	III A		
	5407.43	5	III A		
	5341.07	20	III A		
	4083.64	12	I	$1d^6-1d'^6$ *	
	4082.95	12	I		
	4079.43	10	I		
	4079.24	12	I		
	4058.94	10	I		
	4055.55	20	I		
	4048.76	15	I		
	4041.37	50r	I		
	4035.73	15	I		
	4018.11	20	I		
	3841.08	10	II	$1d^6-1f^6$ *	
	3834.36	12	II		
	3823.90	10	II		
	3823.51	20r	II		
	3809.60	10	II		
	3806.87	20r	I		

TABLE I—*Continued*

E.P.	λ	Int.	Class	Type	Notes
	Manganese—*Continued*				
2.16—*Cont.*	3629.74	12	III	$1d^6-3p^6$	
	3623.79	15	III		
	3619.40	15	III		
	3610.30	20	III		
	3608.48	20	II		
	3607.53	20	II		
	3595.11	20	III		
	3586.54	30	II		
	3577.88	40	II		
2.29.......	4823.52	50	I	$1p^8-1s^8$	
	4783.43	50	I		
	4754.04	50	I		
	3570.03	20	III	$1p^8-1d^8$	
	3569.80	40	III		
	3569.50	60	III		
	3548.18	30	III		
	3548.02	40	III		
	3547.79	50	III		
	3532.11	50	III		
	3531.99	50	III		
	3531.83	30	III		
3.07.......	6021.78	50	III	$1p^6-2s^6$	
	6016.64	40	III		
	6013.49	30	III		
	4061.74	5	V	$1p^6-3d^6$	
	4059.40	5	IV		
	4057.96	4	V		
4.41.......	7326.55	(7)	....	$2p^6-3s^6$	
	7302.92	(6)			
	7283.80	(6)			
?..........	4766.43	20	III	$1d^4-1f'^4$	(24)
	4765.86	10	III		
	4762.37	30	III		
	4761.53	10	III		
	4739.00	8	III		
	4727.46	10	III		
	4709.70	10	III		
	4701.16	3	V		
	4671.69	3	V		
	4502.22	7	III	$1d^4-1d'^4$	
	4498.90	7	III		
	4490.08	5	III		
	4472.79	5	III		
	4470.14	6	III		
	4464.68	8	II		
	4453.01	6	III		
	4451.58	15	II		
	4436.36	8	III		
	4414.89	10	II		

TABLE I—*Continued*

E.P.	λ	Int.	Class	Type	Notes
	Manganese—*Continued*				
?—*Cont.*....	4312.55	3	II	$1d^4-1p'^4$	
	4284.08	(5)	...		
	4281.10	6	II		
	4265.92	6	II		
	4257.66	5	II		
	4239.73	5	II		
	4235.30	8	I		
	4235.14	6	II		
	Iron, *Fe*, I.P.?				(25)
0.0.......	5254.96	1	I A	$(1d^5-1d'^7)$	
	5250.21	1	I A		
	5247.05	1	I A		
	5225.53	1	I A		
	5204.59	2	I A		
	5168.90	4	I A		
	5166.29	4	I A		
	5110.41	10	I		
	4489.74	3	I A	$(1d^5-1f'^7)$	
	4482.18	4	I		
	4461.65	8	I		
	4445.43	(1)	I A		
	4427.31	10	I		
	4375.93	9	I		
	4347.24	(1)	.....		
	4291.47	4	I A	$(1d^5-1p'^7)$	
	4258.38	2	I A		
	4232.72	1	I A		
	4216.18	8	I		
	4206.70	3	I A		
	4199.98	1	I A		
	4134.34	(1)	.....		
	3930.30	25R	I	$1d^5-1d'^5$	
	3927.92	30R	I		
	3922.92	25R	I		
	3920.26	20r	I		
	3906.48	8	I		
	3899.71	30R	I		
	3895.66	25r	I		
	3886.29	40R	I		
	3878.58	100r	II		
	3859.91	300R	I		
	3856.37	50r	I A		
	3824.44	50r	I A		

TABLE I—*Continued*

E.P.	λ	Int.	Class	Type	Notes
	Iron—*Continued*				
0.0—*Cont.*	3748.26	60R	I A	$1d^5-1f'^5$	
	3745.90	40r	I A		
	3745.56	100R	I		
	3737.14	150R	I		
	3733.32	40r	I A		
	3722.57	50r	I A		
	3719.94	250R	I		
	3707.83	20	I		
	3705.57	100r	I		
	3683.06	10	I A		
	3679.92	40r	I A		
	3649.31	5	I A		
	3526.07	20	I	$1d^5-1p'^5$	
	3497.84	40	I		
	3490.58	100r	I		
	3476.71	40	I		
	3475.45	70r	I		
	3465.86	60r	I		
	3443.88	50r	I		
	3440.99	75R	I		
	3440.61	150R	I		
0.94......	8075.16	(1)	....	$(1f^5-1d'^7)$	
	8047.63	(1)			
	7912.89	(1)			
	6625.04	(1)	.....	$(1f^5-1f'^7)$	
	6574.24	(2)	.....		
	6498.95	(2)	.....		
	6462.74	(4)	.....		
	6400.33	(2)	.....		
	6358.68	3	I A		
	6280.62	2	I A		
	6221.70	(0)	.....		
	6120.25	(0)	....	$(1f^5-1p'^7)$	
	5958.20	(2)			
	5956.70	(3)			
	5949.35	(2)			
	5506.78	18	I	$1f^5-1d'^5$	
	5501.47	12	I		
	5497.52	15	I		
	5455.62	40	I		
	5446.92	40	I		
	5434.53	30	I		
	5429.70	40	I		
	5405.78	40	I		
	5397.14	40	I		
	5371.50	50	I		
	5328.04	50	I		
	5269.54	60	I		

TABLE I—*Continued*

E.P.	λ	Int.	Class	Type	Notes
	Iron—*Continued*				
0.94—*Cont.*	5151.92	4	I	$1f^5-1f'^5$	
	5150.84	6	I		
	5142.93	6	I		
	5127.36	5	I		
	5123.72	6	I		
	5107.45	6	I		
	5083.34	7	I		
	5079.74	4	I		
	5051.64	10	I		
	5041.08	7	I		
	5012.07	12	I		
	4994.13	8	I		
	4939.69	4	I		
	4239.85	2	III	$(1f^5-1f'^3)$	
	4177.60	4	II A		
	4152.18	4	II A		
	4139.93	2	II A		
	4100.75	3	II A		
	4092.51	(1)	.....		
	3940.89	5	II	$1f^5-2d'^5$	
	3917.19	8	II		
	3898.01	10	II		
	3887.05	15	I		
	3878.02	60	II		
	3872.50	60	II		
	3865.53	30	II		
	3849.97	40	II		
	3840.44	80r	II		
	3834.23	100r	II		
	3825.89	200R	II		
	3820.43	250R	II		
	3876.04	4	III	$(1f^5-1p'^3)$	
	3850.82	12	II		
	3814.53	5	III A		
	3812.97	40	II		
	3790.09	12	II		
	3786.68	8	III		
	3799.55	50	II	$1f^5-2f'^5$	
	3798.51	40	II		
	3795.00	60	II		
	3787.88	50	II		
	3767.19	80r	II		
	3763.79	100r	II		
	3758.23	150R	II		
	3749.49	200R	II		
	3743.36	20	II A		
	3734.87	300r	II		
	3727.62	50r	II		
	3709.25	75r	II		
	3687.46	40r	I		

TABLE I—*Continued*

E.P.	λ	Int.	Class	Type	Notes
	Iron—*Continued*				
0.94—*Cont.*	3647.84	100R	I	$1f^5-1g'^5$ *	
	3631.46	125R	I		
	3618.77	125R	I		
	3608.87	100r	I		
	3581.20	250R	I		
	3570.10	100R	I	$(1f^5-1g'^3)$	
	3565.38	60r	II		
	3558.52	30	II		
1.54......	7362.32	(0)	....	$(1f^3-1d'^5)$	
	7180.02	(1)			
	6739.54	(1)	....	$(1f^3-1f'^5)$	
	6710.31	(1)			
	6581.22	(2)			
	5853.18	(1)	....	$(1f^3-1p'^5)$	
	5341.03	20	II	$1f^3-1d'^3$	
	5328.53	15	II		
	5270.36	30	II		
	5227.19	40	II		
	5167.49	40	II		
	5332.91	4	I	$1f^3-1f'^3$	
	5307.36	2	III		
	5216.28	10	II		
	5194.95	10	I		
	5171.60	20	II		
	5107.65	8	II		
	5041.76	10	III		
	4798.74	(1)	...	$(1f^3-2d'^5)$	
	4772.82	3	III		
	4733.59	4	I		
	4765.48	(1)	....	$(1f^3-1p'^3)$	
	4680.30	(2)	.....	$(1f^3-2f'^5)$	
	4654.50	5	II		
	4632.92	2	III ?		
	4602.94	9	I		
	4602.01	(2)	.....		
	4592.66	5	I		
	4547.02	(2)	.....		
	4531.15	8	II		
	4415.13	20	II	$(1f^3-1g'^5)$	
	4404.75	30	II		
	4383.55	45r	II		
	4367.91	2	III A		
	4337.05	10	II		
	4294.13	15	II		
	4291.47	4	I A		
	4229.75	(1)	III		

TABLE I—*Continued*

E.P.	λ	Int.	Class	Type	Notes
	Iron—*Continued*				
1.54—*Cont.*	4325.77	35	II	$1f^3-1g'^3$	
	4307.91	35	II		
	4271.76	35	II		
	4250.79	25	II		
	4202.03	30	I		
	4147.68	10	III		
	4143.87	30	I	$1f^3-2f'^3$	
	4132.06	25	II		
	4071.75	40	II		
	4063.60	45	II		
	4045.82	60r	II		
	4005.25	25	II		
	3969.26	30	II		
	3966.07	10	III	$1f^3-2d'^3$	
	3902.95	20	II		
	3888.52	20	II		
	3841.05	80r	II		
	3827.83	75r	II		
	3815.84	100r	II		
2.19.......	8824.18	(6)	....	$1p^5-1p'^5$	
	8688.58	(7)			
	8661.85	(6)			
	8514.01	(3)			
	8468.35	(7)			
	8387.74	(8)			
	8327.04	(8)			
	6430.86	10	III	$1p^5-2d'^5$	
	6335.34	10	III		
	6297.80	5	III		
	6265.14	6	III		
	6219.29	6	III		
	6213.44	5	III		
	6173.35	3	III		
	6151.63	(2)	...		
	6137.00	(2)	...		
	6240.65	(2)	...	$(1p^5-1p'^3)$	
	6163.56	(1)	...		
	6082.71	(1)	...		
	5250.65	6	IV	$1p^5-2p'^5$	
	5202.34	8	IV		
	5198.72	4	IV		
	5142.54	(3)	...		
	5131.48	(2)	...		
	5098.71	8	IV		
	5079.23	6	IV		
	4889.02	(1)	....	$(1p^5-2d'^3)$	
	4817.78	(1)			
	4771.70	(1)			
	4745.12	(1)			

TABLE I—*Continued*

E.P.	λ	Int.	Class	Type	Notes
	Iron—*Continued*				
2.19—*Cont.*	4528.62	18	II	$1p^5$—$3d'^5$	
	4494.57	12	II		
	4482.26	6	I		
	4459.13	10	III		
	4447.73	9	III		
	4442.35	12	III		
	4430.62	6	III		
	4408.42	6	III		
	4407.72	5	III		
	4352.74	9	III	$1p^5$—$1s'^5$	
	4315.09	10	III		
	4282.41	12	III		
2.46.......	4299.25	18	III	$1d'^7$—md^7	
	4271.17	20	III		
	4260.49	35	III		
	4250.13	25	III		
	4235.95	25	III		
	4233.61	18	III		
	4222.23	12	III		
	4210.36	15	III		
	4198.31	20	III		
	4191.45	15	III		
	4187.81	20	III		
	4187.05	20	III		
2.84.......	5044.24	(2)	...	$1f'^7$—md^7	
	5006.13	20	III		
	4985.56	7	V		
	4957.61	60	III		
	4957.31	20	III		
	4938.82	10	IV		
	4920.52	60	III		
	4919.01	30	III		
	4903.32	12	III		
	4891.51	50	III		
	4890.77	25	III		
	4878.23	12	III		
	4872.15	20	III		
	4871.33	25	III		
	4859.76	15	III		
	4579.34	(1h)	....	($1f'^7$—md^5)	
	4554.47	(1)			
	4525.88	(1)			
	4495.39	(1h)			
2.96.......	5281.80	10	IV	$1p'^7$—md^7	
	5266.57	30	IV		
	5232.96	40	III		
	5226.88	15	IV		
	5192.36	30	IV		
	5191.47	20	IV		
	5139.48	20	IV		
	5139.27	10	IV		
	5068.78	10	V		

TABLE I—*Continued*

E.P.	λ	Int.	Class	Type	Notes
	Iron—*Continued*				
2.96—*Cont.*	4800.14	(1)	V	$(1p'^7-md^5)$	
	4787.84	(1)			
	4768.40	3n			
	4759.98	(1h)			
	4726.17	(1h)			
3.25…….	5393.19	10	IV	$1d'^5-md^5$	
	5339.95	12	V		
	5324.20	30	IV		
	5302.31	10	V		
	5283.63	18	IV		
	5273.18	(3)	...		
	5263.32	8	V		
	5253.48	(2)	...		
	5229.84	5n	V		
	5217.40	5	V		
	5215.20	6	IV		
	5208.61	7	IV		
	4736.79	12	II?	$1d'^5-mf^5$	
	4707.29	8	IV		
	4668.15	6	IV		
	4654.64	5	V		
	4637.52	3	IV		
	4625.06	3	IV		
	4613.22	2n	V		
	4607.66	3n	V		
	4598.14	(2)	...		
	4568.79	(1)	...		
	4565.68	(2)	...		
3.38…….	5784.69	(1)	...	$1f'^5-md^5$	
	5712.15	(2)	...		
	5709.40	10	IV		
	5658.84	10	IV		
	5658.54	(1)	...		
	5624.56	10	IV		
	5615.66	50	IV		
	5602.96	10	IV		
	5586.77	40	IV		
	5576.10	10	IV		
	5572.86	30	IV		
	5569.63	20	IV		
	5039.27	(2)	...	$1f'^5-mf^5$ *	
	5002.82	(2)	...		
	4966.10	8	V		
	4950.12	(1)	...		
	4946.40	4	IV		
	4910.03	(2)	...		
	4907.74	(1)	...		
	4882.17	(2)	...		
	4863.65	(2)	...		
	4855.69	(2)	...		
	4843.16	(2)	...		
	4838.52	(2)	...		

TABLE I—*Continued*

E.P.	λ	Int.	Class	Type	Notes
	Iron—*Continued*				
3.64......	6411.67	12	IV	$1p'^5-md^5$	
	6408.04	8	V		
	6400.02	25	III		
	6336.84	12	V		
	6302.51	6	V		
	6301.52	15	IV		
	6246.34	15	V		
	6232.67	5	V		
	6141.74	4	V		
4.13......	7207.41	3	V	$2d'^5-mf^5$	
	7187.35	5	V		
	7164.49	(9)	...		
	7130.96	(10)	...		
	7090.41	(6)	...		
	7038.23	(4)	...		
	7022.98	(5)	...		
	7016.30	(9)	...		
	6999.92	(4)	...		
4.23......	7710.40	(3)	....	$2f'^5-mf^5$	
	7661.24	(3)			
	7568.94	(4)			
	7511.06	(9)			
	7495.12	(8)			
	7491.68	(2)			
	7445.80	(9)			
	7411.21	(8)			
	7389.43	(7)			
	7311.13	(4)			
	7306.60	(2)			
	7293.01	(6)			
	7288.79	(4)			
4.35......	8497.00	(2)	....	$1g'^5-mf^5$	
	8401.42	(1)			
	8248.09	(3)			
	8232.33	(2)			
	8220.42	(7)			
	8207.85	(1)			
	8179.03	(1)			
	8085.22	(5)			
	8046.08	(5)			
	7999.00	(6)			
	7937.19	(9)			
4.40......	8360.79	(2)	....	$(1g'^3-mf^5)$	
	8339.41	(4)			
	8331.94	(6)			

TABLE I—*Continued*

E.P.	λ	Int.	Class	Type	Notes
	Ionized Iron, Fe^+, I.P.?				(18)
0.0	2625.68	(9)	...	$1d^6-1d'^6$ *	
	2611.89	(9)	...		
	2599.40	(10)	...		
	2585.89	(10)	IV		
	2410.53	(8)	...	$1d^6-1f'^6$ *	
	2404.89	(8)	...		
	2395.63	(8)	...		
	2382.04	(10)	II		
	2373.73	(7)	II		
	2343.49	(7)	....	$1d^6-1p'^6$ *	
	2332.80	(6)			
	2327.39	(6)			
0.33	2519.09	(6)	....	$(1f^4-1f'^6)$ *	
	2493.29	(10)			
	2366.59	(4)	...	$1f^4-1f'^4$ *	
	2362.04	(4)	...		
	2360.00	(5)	...		
	2354.88	3	II		
	2375.19	(6)	...	$1f^4-1d'^4$ *	
	2368.60	(6)	III		
	2360.31	(5)	...		
	2348.12	(6)	...		
1.04	3281.30	(2)	....	$(1d^4-1d'^6)$ *	
	3277.36	(3)			
	3255.89	(2)			
	2979.36	(3)	...	$(1d^4-1f'^6)$ *	
	2970.52	(3)	V		
	2953.78	5	V		
	2926.58	(6)	V		
	2755.74	(9)	....	$1d^4-1f'^4$ *	
	2749.33	(10)			
	2746.49	(8)			
	2743.20	(8)			
	2746.99	(7)	III	$1d^4-1d'^4$ *	
	2739.55	(10)	...		
	2736.97	(7)	...		
	2714.42	(8)	...		
	2591.55	(7)	....	$1d^4-1p'^4$ *	
	2582.59	(8)			
	2562.54	(9)			
1.69	3227.76	(7)	....	$1p^4-1d'^4$ *	
	3213.32	(5)			
	3210.46	(4)			

TABLE I—*Continued*

E.P.	λ	Int.	Class	Type	Notes
	Ionized Iron—*Continued*				
1.69—*Cont.*	3002.65	(7)	V	$1p^4-1p'^4$ *	
	2985.55	(6)	V		
	2984.83	(8)	IV		
2.68.......	4369.41	..	....	$2p^4-1f'^4$ *	
	4296.56	(6)			
	4258.16	..			
	4178.87	(6)			
	4416.81	(4)	....	$2p^4-1d'^4$ *	
	4385.39	..			
	4351.77	(6)			
	4303.18	(4)			
	4233.16	(8)			
	4173.48	(6)			
	4128.74	..			
2.82.......	4666.75	..	....	$2f^4-1f'^4$	
	4629.33	(4)			
	4582.84	..			
	4555.90	(6)			
	4534.17	..			
	4520.24	(6)			
	4515.33	(6)			
	4491.41	(4)			
	4489.21	(4)			
	4472.93	..			
	4620.52	..	....	$2f^4-1d'^4$ *	
	4583.84	(8)			
	4576.31	(4)			
	4549.48	(4)			
	4541.52	..			
	4522.64	(6)			
	4508.29	(8)			
2.88.......	6516.08	(4)	....	$1s^6-1d'^6$	
	6432.69	..			
	6369.48	..			
	5284.11	..	....	$1s^6-1f'^6$	
	5256.94	..			
	5169.03	(8)	....	$1s^6-1p'^6$	
	5018.44	(8)			
	4923.92	(10)			
	4731.49	(1)	....	$(1s^6-1d'^4)$	
	4656.98	..			

TABLE I—*Continued*

E.P.	λ	Int.	Class	Type	Notes
	Ionized Iron—*Continued*				
3.18	5425.26	..	....	$1g^4-1f'^4$ *	
	5325.56	(4)			
	5316.62	(8)			
	5276.01	(6)			
	5234.62	(4)			
	5197.56	(4)			
	5362.87	..	....	$1g^4-1d'^4$	
	5316.78	..			
	5264.81	(1)			
3.88	7711.76	(1)	....	$2d^4-1d'^4$	
	7655.47	..			
	7515.89	..			
	7449.36	..			
	7310.23	..			
	7308.09	..			
	7224.48	..			
	7222.42	..			
	6456.39	(6)	....	$2d^4-1p'^4$	
	6416.92	(2)			
	6407.30	..			
	6247.56	(4)			
	6239.95	..			
	6238.39	(4)			
	6149.25	(4)			
	6147.85	(6?)			
	Cobalt, *Co*, I.P. ?				(32)
0.0	3602.08	40 R	II	$1f^4-1f''^4$ *	
	3594.87	50 R	II		
	3575.36	60 r	II		
	3526.86	100 R	II		
	3474.02	100 R	II		
	3533.36	25 r	I	$1f^4-1g^4$ *	
	3529.04	30 r	I		
	3513.48	50 R	II		
	3465.80	100 R	II		
	3510.42	30 r	I	$1f^4-1d^4$ *	
	3502.63	20 r	I		
	3455.24	25 r	I		
	3442.92	20 r	II		
	3431.58	50 r	II		
	3412.64	80 R	II		
	3159.66	10	II	$1f^4-1d'^4$ *	
	3149.30	10	II		
	3139.94	12	II		
	3121.41	10	II		

TABLE I—*Continued*

E.P.	λ	Int.	Class	Type	Notes
	Cobalt—*Continued*				
0.41.......	4076.13	4	I A		
	4058.19	8	I		
	4020.90	20	I	$1f'^{4}-1f''^{4}$	
	4019.30	5	I	*	
	3987.12	6	I		
	3952.33	8	I		
	3978.66	10	I		
	3941.74	20	II		
	3906.30	10	I	$1f'^{4}-1g^{4}$	
	3876.84	20	I	*	
	3808.11	10	I		
	3957.94	15	II		
	3894.98	60	II		
	3881.91	25	I	$1f'^{4}-1d^{4}$	
	3873.91	40	II	*	
	3873.12	60	II		
	3585.16	25 R	I		
	3574.96	25 r	I		
	3560.90	20 r	I		
	3523.44	25 r	I	$1f'^{4}-1d'^{4}$	
	3512.64	60 R	II	*	
	3506.32	80 R	II		
	3502.28	100 R	II		
1.61.......	6450.23	80	I		
	6282.64	40	I	$1p^{4}-1d^{4}$	
	6188.98	10	II A	*	
	6093.14	10	I		
	5483.34	40	I		
	5369.58	20	I		
	5331.45	15	II	$1p^{4}-1d'^{4}$	
	5301.04	15	II	*	
	5237.91	15	II		
	5230.20	25	II		
1.81.......	7084.97	15	I		
	7052.85	8	I		
	6872.38	10	I	$1p'^{4}-1d^{4}$	
	6814.95	15	I	*	
	6771.05	20	I		
	5935.37	5	III	$1p'^{4}-1d'^{4}$	
	5922.35	(1u)	...		

TABLE I—*Continued*

E.P.	λ	Int.	Class	Type	Notes
	Ionized Lanthanum, La^+, I.P.?				(33)
0.0	4141.71	(10)	....	$1d^3-1d'^3$	
	4031.70	(20)			
	3988.53	(30)			
	3921.54	(10)			
	3886.34	(15)			
	3380.88	(10)	....	$1d^3-1p'^3$	
	3344.55	(7)			
	3337.50	(15)			
	3303.10	(5)			
	3265.66	(4)			
0.39	4724.39	(5)	....	$1p^3-1d'^3$	
	4613.39	(4)			
	4526.12	(5)			
	3854.96	(3)	....	$1p^3-1p'^3$	
	3835.12	(5)			
	3780.70	(3)			
	3714.88	(3)			
	3705.80	(5)			
	3637.16	(3)			
	Ionized Nitrogen, N^+, I.P. 24:				(34)
15.0	5730.64	(0)	....	mp^3-md^3	
	5710.64	(5)			
	5686.20	(6)			
	5679.49	(10)			
	5675.96	(6)			
	5666.54	(8)			
	5045.02	(5)	....	mp^3-ms^3	
	5010.54	(4)			
	5002.66	(2)			
	4643.11	(8)	....	$mp^3-mp'^3$	
	4630.55	(10)			
	4621.41	(7)			
	4613.88	(6)			
	4607.17	(7)			
	4601.49	(8)			
	3955.85	(5)	....	(mp^3-mS)	
	3408.14	(3)	....	(mp^3-nS)	
15.2	5767.47	(2)	....	$(mP-md^3)$	
	5747.32	(3)			
	5073.55	(1)	....	$(mP-ms^3)$	

TABLE I—*Continued*

E.P.	λ	Int.	Class	Type	Notes
	Ionized Nitrogen—*Continued*				(34)
15.2—*Cont.*	4674.98	(2)	....	$(mP-mp'^3)$	
	4667.28	(2)			
	4654.57	(2)			
	3995.00	(10)	....	$mP-mS$	
	3437.16	(6)	....	$mP-nS$	
17.2.......	4810.27	(2)	....	$md^3-md'^3$	
	4803.30	(6)			
	4793.66	(2)			
	4788.13	(5)			
	4781.21	(2)			
	4779.72	(4)			
	4774.24	(2)			
	3331.32	(3)	....	md^3-np^3	
	3330.30	(2)			
	3328.79	(4)		*	
17.7.......	5961.25	(0)	....	$mp'^3-md'^3$	
	5952.57	(3)			
	5941.90	(8)			
	5940.42	(2)			
	5931.96	(7)			
	5928.02	(4)			
	3856.07	(3)	....	mp'^3-np^3	
	3855.08	(3)			
	3847.38	(2)			
	3842.20	(2)			
	3838.39	(4)			
	3829.80	(3)			
	Phosphorus, *P*, I.P. 13.3				(30)
0.0........	2034.02	(7)	....	$1d-1d'$?	
	2032.98	(6)			
	2024.98	(6)			
	2023.98	(7)			
0.38.......	2154.77	(7)	....	$1S-1d'$?	
	2153.63	(6)			
1.25.......	2555.68	(8)	....	$1D-1d'$?	
	2554.02	(9)			
	2536.38	(10)			
	2534.75	(8)			
	2149.81	(8)	....	$1D-1P'$?	
	2136.79	(8)			
	2136.10	(6)			

TABLE I—*Continued*

E.P.	λ	Int.	Class	Type	Notes
	Arsenic, *As*, I.P. 11.7				(31)
0.0	2898.72	(4R)	....	$1d-1d'$	
	2860.43	(6R)			
	2780.20	(8R)			
	2744.99	(6R)			
	2349.84	(10R)	....	$1d-1p'$	
	2288.12	(10R)			
0.21	2381.20	(4R)	....	$1S-1p'$	
	2363.04	(2)			
0.41	3119.57	(4)	....	$1D-1d'$	
	3075.32	(2)			
	3032.84	(4)			
	2990.99	(2)			
	Antimony, *Sb*, I.P. 8.7				(31)
0.0	6097.60	(2)	....	$(1d_2-1D_2)$	
	2311.50	(6R)	....	$1d_2-\alpha$	
	2175.88	(5R)	....	$1d_2-\beta$	
	2127.46	(3)	....	$1d_2-\gamma$	
	2023.86	(4)	....	$1d_2-\epsilon$	
1.05	2877.92	(5R)	....	$1d_1-\alpha$	
	2670.66	(5R)	....	$1d_1-\beta$	
	2598.08	(6R)	....	$1d_1-\gamma$	
	2445.53	(4R)	....	$1d_1-\epsilon$	
1.22	2769.94	(5R)	....	$1s-\beta$	
	2528.54	(6R)	....	$1s-\epsilon$	
1.98	3722.79	(3)	....	$1D_2-\alpha$	
	3383.15	(3)	....	$1D_2-\beta$	
	3267.50	(4R)	....	$1D_2-\gamma$	
	3029.82	(4R)	....	$1D_2-\epsilon$	
2.24	4033.56	(3)	....	$1D_1-\alpha$	
	3637.83	(3)	....	$1D_1-\beta$	
	3504.45	(2)	....	$1D_1-\gamma$	
	3232.54	(4R)	....	$1D_1-\epsilon$	
	Bismuth, *Bi*, I.P. 7.7				(31)
0.0	8754.88	(2)	....	$(1d_2-1d_1)$	
	6476.24	(3)	....	$(1d_2-1D_2)$	
	4615.53	(1)	....	$(1d_2-1D_1)$	
	4615.09	(1)			

TABLE I—*Continued*

E.P.	λ	Int.	Class	Type	Notes
	Bismuth—*Continued*				
0.0—*Cont.*	3067.69	(10R)	....	$1d_2-\alpha$	
	2276.57	(8R)	....	$1d_2-\delta$	
	2230.63	(10R)	....	$1d_2-\epsilon$	
1.41	4722.54	(10R)	....	$1d_1-\alpha$	
	3076.61	(2)	....	$1d_1-\delta$	
	2993.34	(8R)	....	$1d_1-\epsilon$	
	2989.03	(8R)	....	$1d_1-\zeta$	
	2897.97	(10R)	....	$1d_1-\eta$	
1.92	3510.88	(4R)	....	$1D_2-\delta$	
	3397.17	(4R)	....	$1D_2-\zeta$	
2.68	4492.99	(2)	....	$1D_1-\delta$	
	4492.62	(2)			
	4308.54	(4)	....	$1D_1-\zeta$	
	4308.18	(4)			
	4121.86	(6)	....	$1D_1-\eta$	
	4121.54	(6)			

INDEX TO TABLE I*

Symbol	Element	Page	Symbol	Element	Page
Ag	Silver	13	*Fe*	Iron	44
Al	Aluminum	19	*Fe+*	Ionized iron	52
Al+	Ionized aluminum	19	*Ga*	Gallium	20
Al++	Doubly ionized aluminum	20	*H*	Hydrogen	9
			He	Helium	9
As	Arsenic	58	*He+*	Ionized helium	10
Au	Gold	13	*Hg*	Mercury	19
B	Boron	19	*In*	Indium	20
Ba	Barium	17	*K*	Potassium	11
Ba+	Ionized barium	18	*La+*	Ionized lanthanum	56
Be	Beryllium	13	*Li*	Lithium	11
Be+	Ionized beryllium	13	*Mg*	Magnesium	13
Bi	Bismuth	58	*Mg+*	Ionized magnesium	14
C+	Ionized carbon	20	*Mn*	Manganese	42
Ca	Calcium	14	*Mo*	Molybdenum	42
Ca+	Ionized calcium	16	*N+*	Ionized nitrogen	56
Cd	Cadmium	18	*Na*	Sodium	11
Cd+	Ionized cadmium	19	*Ne*	Neon	10
Co	Cobalt	54	*O*	Oxygen	21
Cr	Chromium	39	*P*	Phosphorus	57
Cs	Caesium	12	*Pb*	Lead	21
Cu	Copper	12	*Rb*	Rubidium	12

*In this table the elements have been arranged in the alphabetical order of their chemical symbols.

INDEX TO TABLE I—*Continued*

Symbol	Element	Page	Symbol	Element	Page
S........	Sulphur	22	*Ti*+	Ionized titanium	32
Sb.......	Antimony	58	*Tl*.......	Thallium	20
Sc.......	Scandium	22	*V*.......	Vanadium	36
Sc+	Ionized scandium	23	*Y*.......	Yttrium	24
Se.......	Selenium	22	*Y*+.....	Ionized yttrium	25
Si+++ ..	Trebly ionized silicon	21	*Zn*.......	Zinc	18
Sr.......	Strontium	16	*Zn*+.....	Ionized zinc	18
Sr+	Ionized strontium	17	*Zr*.......	Zirconium	35
Ti.......	Titanium	25	*Zr*+	Ionized zirconium	35

NOTES TO TABLE I

1. Lyman, *Physical Review*, **21**, 202, 1923; *Science*, **59**, 422, 1924.

2. Paschen, *Annalen der Physik*, **60**, 405, 1919. Only lines of intensity greater than 10 (or equal to 10 in the ultra-violet) are listed. The ultimate lines are unknown, and the ionization potential is taken from the electrical determination by G. Hertz (*Zeitschrift für Physik*, **18**, 307, 1923). Lines originating in the four 1s-levels, which have an extreme range of 0.22 volts, are listed together for convenience, and similarly for the 2p-terms.

3. V. Thorsen, *Die Naturwissenschaften*, **11**, 501, 1923.

4. Back, *Annalen der Physik*, **70**, 347, 1923. The E.P. for the triplets is probably less than for the singlets, by analogy with other elements in the group.

5. I.P. estimated by Saunders, *Science*, **59**, 51, 1924.

6. The lines not belonging to the ordinary series are as classified by Russell and Saunders (in press).

7. Paschen, *op. cit.*, **71**, 538, 1923. Russell, *Nature*, **113**, 163, 1924.

8. Paschen, *op. cit.*, **71**, 151, 1923.

9. Fowler, *Proceedings of the Royal Society*, A, **105**, 299, 1924.

10. Fowler, *ibid.*, **103**, 413, 1923.

11. Thorsen, *Die Naturwissenschaften*, **11**, 78, 1923; Grotrian, *Zeitschrift für Physik*, **18**, 169, 1923.

12. Hopfield, *Astrophysical Journal*, **59**, 114, 1924.

13. Hopfield, *Nature*, **112**, 437, 1923.

14. Catalan, *Anales Soc. Españ. Fis. y Quim.* **20**, 606, 1922, and **21**, 464, 1923. Supplemented by the writer (unpublished).

15. The lowest term cannot be a p^2-term, as Catalan supposes, for it combines with doublet terms in adjacent series on both sides. It may be a d- or f-term. The Zeeman separations in sun-spots (the only ones available) favor the former, and the terms have been provisionally classified accordingly.

16. The important enhanced line λ 4247 probably belongs to the singlet system. From its behavior in the furnace it is probable that it originates from a higher level than the ultra-violet triplets.

17. C. C. and H. H. Kiess, *Proceedings of the Washington Academy of Sciences*, **13**, 270, 1923, and unpublished investigations by the writer.

18. Unpublished investigations by the writer.

19. W. F. Meggers, *Journal of the Washington Academy of Sciences*, **13**, 317, 1923. Supplemented by unpublished investigations communicated by Dr. Meggers.

20. H. Gieseler, *Zeitschrift für Physik*, **22**, 228, 1924.

21. The three faint lines appear in the sun-spot spectrum, and agree exactly with the predicted positions of members of this group.

22. C. C. Kiess, *Scientific Papers of the Bureau of Standards*, **19**, 113 (No. 474), 1923.

23. M. A. Catalan, *Philosophical Transactions*, A, **223**, 127, 1922.

24. Back, *Zeitschrift für Physik*, **15**, 234, 1923. The excitation potential for these groups is shown by their temperature behavior to be fairly high.

25. F. M. Walters, Jr., *Journal of the Optical Society of America*, **8**, 245, 1924. Supplemented by unpublished work of Dr. Walters and of the writer.

26. From unpublished data communicated by Dr. Meggers.

27. From unpublished data communicated by Dr. Kiess.

28. The wave-lengths here given are from unpublished measures made at the Bureau of Standards by Dr. Meggers, and kindly communicated by him.

29. Unpublished Zeeman observations by Moore confirm the classification of the lowest level as a D-term.

30. Miss Saltmarsh, *Philosophical Magazine*, **47**, 874, 1924. Energy-levels and designation of terms added by the writer in analogy with those for *As*, *Sb*, and *Bi*.

31. Ruark, Mohler, Foote, and Chenault, *Scientific Papers*, *Bureau of Standards*, No. 490, 1924. I.P.'s from critical potentials and uncertain by 0.5 volt.

32. Walters, *Journal of the Washington Academy of Sciences*, **14**, 407, 1924.

33. Gouschmidt, *Die Naturwissenschaften*, **41**, 851, 1924. The d^3-term is assumed to be the lowest, by analogy with $Sc+$ and $Y+$. Many other terms are present, with peculiar Zeeman effects.

34. Fowler, *Proceedings of the Royal Society*, A, **107**, 31, 1925. I.P. estimated by Miss Payne, *Harvard College Observatory Circular*, No. 256, 1924.

MOUNT WILSON OBSERVATORY
May 12, 1924

Additions have been made to date.

PRINCETON UNIVERSITY OBSERVATORY
January 27, 1925

Contributions from the Mount Wilson Observatory, No. 287
Reprinted from the *Astrophysical Journal*, Vol. LXI, pp. 114–129, 1925

THE MEAN COLOR-INDEX OF STARS OF DIFFERENT APPARENT MAGNITUDES

By FREDERICK H. SEARES

ABSTRACT

Variation of mean color-index with magnitude.—The increase in mean color with magnitude for stars of all galactic latitudes together has been determined from the data in the *Revised Harvard Photometry*, the *Draper Catalogue*, the *Göttingen Aktinometrie*, the *Yerkes Actinometry*, and the magnitudes and colors of stars near the North Pole. The results to the seventeenth magnitude are expressed by the linear relations

(Stars grouped according to visual magnitude) $C_v = +0.50 + 0.029 m_v$ (6)

(Stars grouped according to photographic magnitude) $C_p = -0.18 + 0.071 m_p$. (7)

Kreiken's measures of effective wave-lengths of stars in the Milky Way (mean lat. = 5°) also show an increase in mean color with increasing magnitude, but the absolute values and the rate of change are smaller than those defined by (6) and (7).

Variation in mean color with galactic latitude.—Data from the *Revised Harvard Photometry*, the *Draper Catalogue*, and the *Göttingen Aktinometrie* give values for mean magnitude 7.4, which are illustrated by the curves in Figure 2. The pronounced galactic concentration of blue stars is plainly seen in the relatively small mean color-indices of the stars in low latitudes. A few fragmentary results for latitudes less than 30° are also available for stars of the fourteenth magnitude.

Transformation of star counts for a grouping according to visual magnitude into a grouping according to photographic magnitude, and vice versa.—This transformation is of much importance in combining data derived by visual (or photovisual) and photographic methods for a study of the distribution of stars over the face of the sky. It can be effected by applying a color-correction to the magnitudes, that required being approximately the mean of the values of C_v and C_p. For all latitudes together, the result from (6) and (7) is

$$C = +0.16 + 0.050 m. \tag{10}$$

This is to be added in transforming from a visual to a photographic grouping, and subtracted for the reverse transformation.

The average color of the stars of different apparent magnitudes is an item of importance in statistical discussions of stellar distribution. Thus star counts have been based on both photographic and photovisual scales of magnitude. To combine these results, as must be done in deriving the surface distribution of stars over the sky, the use of mean colors is necessary, since the colors of individual stars are mostly unknown. Further, the time is approaching when the determination of luminosity curves for the different spectral types can be undertaken. A knowledge of mean color will give a valuable control on the results of this difficult investigation, for naturally the adopted frequency curves must provide a mixture of spectral types which will reproduce the observed colors.

It should be emphasized at the outset that the relative frequency of different colors, and hence the mean color, depends upon the grouping of the stars, whether according to photographic or visual magnitude. It is also important to note that the means for neither method of grouping can be used directly to transform the data for one grouping into those of the other. This question will be considered in detail later.

The material now available is sufficient for the derivation of the mean color-index over a considerable range in brightness for all galactic latitudes together, and for a general indication of the variation of mean color with distance from the Milky Way.

The results are affected by several uncertainties, but none of these is of serious consequence. For example, some of the magnitude scales to which the counts are referred require small corrections to reduce them to a homogeneous system; but since the change in mean color with magnitude is slow, the influence of scale error is very small. Further, the colors in many instances must be inferred from the spectral types; but color, for the later types at least, depends on absolute magnitude as well as spectrum. The mean absolute magnitude of each apparent magnitude is known and could have been used in deriving the color-indices, but for simplicity it has been assumed that stars brighter than about 6.5 are all of zero absolute magnitude, while the fainter stars are supposed to have the mean intrinsic brightness of the giants and dwarfs. Again, the results suffer somewhat from systematic errors of spectral classification and from incompleteness of the counts of stars near the limiting magnitudes of the various series. Finally, the stars of faint apparent magnitudes are much restricted in their range in galactic latitude.

For the discussion of the brighter stars the Harvard data are fundamental. These have been collected in spectral groups for which the median spectral types are as shown in Table I:

TABLE I

SPECTRAL GROUPS AND COLOR-INDEX

Harvard group	B	A	F	G	K	M
Median spectral class	B2	A0	F0	F8	K0	M
Color-index, $m<6.5$	−0.26	0.00	+0.38	+0.83	+1.48	+1.88
Color-index, $m>6.5$	−0.26	0.00	+0.38	+0.76	+1.25	+1.80

The color-indices in the last two lines are on the international system, and were taken from *Mount Wilson Contribution* No. 226, Table XII,[1] in accordance with the convention mentioned above. The details for the various sources of data are as follows:

Revised Harvard Photometry.—Tables XVII and XVIII of *Harvard Annals*, 64, IV, show in detail the distribution of nearly 9000 stars according to visual magnitude and spectral type. Results are given separately for four regions of the sky, designated by N,S,P,M, respectively. The first two are outside the Milky Way, to the north and the south; the third is partly, and the fourth mainly, in the Milky Way. These data are condensed into the totals shown in the upper half of Table II and in Table III, the former of which refers to half-magnitude intervals for the whole sky, the latter to the totals in the separate regions for all magnitudes together. The column heading indicates the median magnitude, except that the second column refers to stars brighter than $m=2.25$, with a mean of about 1.6.

The mean color-indices, C_v, for a grouping according to visual magnitude, are found at once with the aid of the data in Table I. The mean values in Table III, for all magnitudes together, correspond to a mean magnitude of 5.7.

To obtain the results for a grouping according to photographic magnitude, it is to be noted that the counts for any line and column in the upper part of Table II refer to the photographic magnitude $m+C$, where m is the column heading and C the color-index for the spectral group in question. Thus for group G, the numbers 2, 12, 12, etc., beginning with the third column, correspond to median photographic magnitudes 3.33, 3.83, 4.33, etc., respectively. By plotting numbers, or better, the logarithms of the numbers, against photographic magnitudes, the totals in each spectral group for the median photographic magnitudes 2.5, 3.0, 3.5, etc., are readily found. These are collected in the lower half of Table II; the mean color-indices, C_p, for the photographic grouping, appear in the last line.

For the late spectral types the limits of photographic magnitude for the different groups are shifted from one to two magnitudes below the visual limits, while for the B stars there is a small shift in the opposite direction. The full utilization of the material, therefore, requires some extrapolation of the curves; but this can be done with little uncertainty, for when plotted in logarithmic form the curves are very smooth and nearly linear. This extrapolation accounts for the extension of the limit for the photographic data to 7.5. The weight for the last two values of C_p is naturally low, and there is probably a small systematic error arising from the fact that the numbers for the B stars are obviously incomplete, since they decrease from about 5.5 on.

---

[1] *Astrophysical Journal*, **55**, 198, 1922.

TABLE II

Mean Color-Index from *Revised Harvard Photometry*
(All Galactic Latitudes Together)

Sp.	1.6	2.5	3.0	3.5	4.0	4.5	5.0	5.5	6.0	6.5	7.0	7.5
B	18	9	28	27	51	103	164	170	146	105	......	......
A	12	10	10	25	41	94	141	541	959	872	......	......
F	4	4	8	10	17	46	101	186	345	376	......	......
G	6	2	12	12	32	47	94	127	277	323	......	......
K	8	6	21	44	91	129	239	419	762	821	......	......
M	7	5	9	12	17	39	87	120	169	172	......	......
Totals	55	36	88	130	249	458	876	1563	2658	2669	......	......
C_v	0.49	0.53	0.61	0.73	0.75	0.64	0.68	0.63	0.66	0.72	......	......
Res	+0.06	+0.04	−0.02	−0.13	−0.13	−0.01	−0.04	+0.03	+0.01	−0.03	......	......
B	......	13	23	42	74	129	166	158	126	87	58	40
A	......	7	13	25	50	100	195	398	724	1259	1778	2399
F	......	1	4	7	14	27	55	112	209	372	575	794
G	......	1	2	4	9	19	35	62	102	182	295	427
K	......	1	2.2	4.5	9.3	20	41	81	155	269	468	776
M	......	0.3	0.5	10	2.2	4	8	15	28	48	79	126
Totals	......	23.3	44.7	83.5	148.5	299	500	826	1344	2217	3253	4562
C_p	......	0.00	0.03	0.04	0.08	0.09	0.17	0.24	0.31	0.34	0.40	0.45
Res	......	0.00	0.00	+0.03	+0.02	+0.05	+0.01	−0.03	−0.06	−0.06	−0.08	−0.10

TABLE III

Color-Index and Galactic Latitude from *Revised Harvard Photometry*

Sp.	N	S	P	M	All
B	44	97	197	483	821
A	525	381	787	1062	2755
F	210	254	292	341	1097
G	207	199	224	302	932
K	533	594	616	797	2540
M	137	147	149	204	637
Totals	1656	1672	2265	3189	8782
C_v	0.78	0.83	0.63	0.57	0.67^5 ($\overline{m}=5.7$)
Lat	+51°.2	−50°.2	21°.9	8°.8	....
C_p	0.38		0.29	0.22	.... ($\overline{m}=5.5$)

The values of C_p in the last line of Table III were found by a transformation similar to that just described.

Henry Draper Catalogue.—In Table III of *Harvard Circular* 226, Shapley has given the relative frequencies of 98,675 stars brighter than visual magnitude 8.75 as derived from counts based on the *Henry Draper Catalogue.* The form of the table is similar to Table II above, except that frequencies instead of numbers are given. The mean values of C_v found from these data with the aid of the last line of Table I are in the last line but one of Table IV.

To find the values of C_p the data of Table II of *Harvard Circular* 226 were referred to the photographic scale by the method used in the case of the *Revised Harvard Photometry.* The results represent the total numbers of stars for each spectral group to successive limits of photographic magnitude. The numbers in each half-magnitude interval found by differencing the totals were reduced to relative frequencies with the results shown in Table IV. The values of C_p, calculated as before, are in the fourth line from the bottom of the table.

TABLE IV

MEAN COLOR-INDEX FROM *Henry Draper Catalogue*

(All Galactic Latitudes Together)

Sp.	5.4	6.5	7.0	7.5	8.0	8.5	9.0	9.5	10.0
B	20.8	10.5	7.1	5.3	3.3	2.5	1.5	1.0	0.6
A	50.3	52.7	53.2	48.5	52.0	49.8	41.8	39.5	37.7
F	10.4	13.0	13.3	15.2	13.6	13.9	14.2	11.1	7.8
G	5.5	7.8	9.5	11.2	11.9	13.6	18.4	22.0	27.1
K	11.1	13.9	15.0	17.6	17.0	18.2	21.8	23.5	23.7
M	2.0	2.0	2.0	2.1	2.1	2.1	2.3	2.9	3.0
C_p	0.20	0.29	0.33	0.39	0.38	0.42	0.50	0.58	0.61
Res.	.00	− .01	− .01	− .04	+ .03	.00	− .04	−0.08	−0.08
C_v	.61	.66	.68	.75	.78	.76	.74	....	....
Res.	+0.05	+0.03	+0.02	−0.03	−0.05	−0.01	+0.02	....	....

The limiting magnitude to which the *Henry Draper Catalogue* is complete is stated by Shapley to be about 8.25 for the northern sky and 8.75 for the southern. For the present purpose incompleteness in the fainter magnitudes given in Table IV is of no consequence, provided the selection of spectral types is representative. Of this we cannot be sure, but in any case the effect on the mean color is probably not serious.

The frequencies of the spectral classes in different galactic latitudes are not yet available for the *Draper Catalogue* in numerical form, but Shapley has given them diagrammatically,[1] for all magnitudes together, to the visual limit 8.25. Frequencies scaled from this diagram and combined with the values of the color from the last line of Table I lead to the following mean colors:

Gal. lat.	0°	10°	30°	45°	60°	75°	90°
C_v	0.51	0.62	0.79	0.86	0.94	0.94	0.93
Smoothed	0.51	0.62	0.78	0.86	0.91	0.94	0.94

(1)

The number of stars involved is 58,508,[2] and their mean magnitude is 7.4.

Göttingen Aktinometrie.—Counts of the stars in this catalogue for half-magnitude intervals of Potsdam visual magnitude and various intervals of the color-index J_p were made for another purpose some years ago. These are collected in Table V, for which the magnitude headings, as usual, are median values. The mean values of J_p within the intervals used were found from the data in Table 29*a* of the *Aktinometrie* (Part B, p. 34), and reduced to the international system by adding +0.29. This reduction constant was found by comparing the data in the first two columns of Table 23 of the *Aktinometrie* with the Mount Wilson color-indices for stars of absolute magnitude zero.

The resulting values of C_v, in the fourth line from the bottom of Table V, are seriously influenced by selection. The general increase in mean color with increasing magnitude is masked, if not actually reversed. The values for the bright stars are too large because the photographic images of early-type stars were oftentimes too dense for measurement, while late-type stars of the same visual magnitude were easily measurable. For faint stars, on the other hand, the selection operates in the opposite direction. The value for the middle of the series, $C_v = 0.71$ for $m = 6.25$, is probably the only one that can be trusted.

The difficulty should disappear, however, when the counts are reduced to a photographic grouping by the method already used. The values of C_p thus found are in the last line but one of Table V. As usual, the first and last values are less reliable because of extrapolation of the transformation curves.

---

[1] *Proceedings of the American Academy of Arts and Sciences*, **59**, 227, 1924.

[2] *Harvard Circular* 226, Table II.

TABLE V

MEAN COLOR-INDEX FROM *Göttingen Aktinometrie*
(All Galactic Latitudes Together)

Limits J_p	Mean Color Int. System	4.25	4.75	5.25	5.75	6.25	6.75	7.25	7.75	8.25
<-0.32	-0.15	......	15	18	43	80	126	129	60	......
-0.32 to 0.00	$+.13$	4	16	29	41	84	145	217	159	......
$.00$ to $+.34$	.41	8	8	19	41	54	109	182	148	......
$+0.35$ to $+0.99$	0.96	10	21	28	55	117	215	264	129	......
$+1.00$ to $+1.90$	1.57	10	21	42	68	117	207	189	54	......
$>+1.90$	$+2.30$	......	2	1	2	3	2	2	......	......
Totals	....	32	83	137	250	455	804	983	550	......
C_v	....	0.91	0.73	0.76	0.72	0.71	0.72	0.65	0.51	......
Res	....	$-.29$	$-.09$	$-.11$	$-.05$	$-.03$	$-.02$	$+.06$	$+.21$	......
C_p	....	.29	.27	.27	.30	.31	.33	.35	.41	0.46
Res	....	-0.17	-0.11	-0.08	-0.07	-0.05	-0.03	-0.02	-0.04	-0.05

Although the *Aktinometrie* includes only the zone 0°–20° in declination, it gives valuable information as to the variation of color with galactic latitude. Tables 29*a*, 29*b*, and 30 contain data bearing on the question, which, it is stated, refer to the stars between 4.50 and 6.99 of *photographic* magnitude. This, however, seems to be an error. The mean values of the color are in agreement with those found from other sources for a grouping according to visual magnitude, and a recount for the data given in Table 30, based on a grouping according to Göttingen photographic magnitude, shows clearly that this is the case.

TABLE VI

COLOR AND GALACTIC LATITUDE, *Göttingen Aktinometrie*, $m=6.3$

R.A.	Gal. Lat.	C_v	C_p	R.A.	Gal. Lat.	C_v	C_p
$0^{h}.5$	$-52°$	0.84	0.40	$12^{h}.5$	$+72°$	0.85	0.38
2.5	44	.64	.30	14.5	59	.88	.42
4.5	-23	.56	.22	16.5	34	.85	.43
6.5	$+2$	.62	.17	18.5	$+7$	.72	.25
8.5	28	.78	.31	20.5	-18	.93	.36
10.5	$+54$	0.81	0.37	22.5	-40	0.79	0.41

The third and seventh columns of Table VI show the results from Table 30 of the *Aktinometrie*, which are here given their correct designation C_v. The fourth and eighth columns give the values of C_p based on the recount for intervals of photographic magnitude. Both series have been reduced to the international system of color and refer to the mean magnitude 6.3. The galactic latitudes are for the centers of the areas over which the colors have been averaged. The smoothed results are

$$\left.\begin{array}{lccccccc} \text{Gal. lat.}\dots\dots\dots & 0^\circ & 10^\circ & 30^\circ & 45^\circ & 60^\circ & 75^\circ & 90^\circ \\ C_v\dots\dots\dots\dots & (0.66) & (0.70) & (0.76) & 0.80 & 0.85 & 0.88 & 0.90 \\ C_p\dots\dots\dots\dots & 0.19 & 0.24 & 0.32 & 0.37 & 0.40 & 0.42 & 0.44 \end{array}\right\} \qquad (2)$$

The values of C_v, like those in Table V, are affected by the selection in the data described above. The exclusion of the bright early-type stars increases the mean color in low galactic latitudes. In high latitudes, on the other hand, early-type stars occur but rarely. The compensating influence arising from the omission of faint late-type stars probably does not enter to any appreciable degree, because the lower limit is visual magnitude 6.99 and the totals in Table V show that to this limit they are nearly if not quite complete. A comparison of the second line of (2) with the last line of (1) supports this view. From 45° to 90° the differences are practically constant, with a mean value of 0.055. The difference to be expected because of the fact that the data from the *Draper Catalogue* are for mean magnitude 7.4 while those of the *Aktinometrie* are for 6.3 is 0.032 mag. The agreement for the higher latitudes is therefore within the uncertainty, but for low latitudes the results for C_v in (2) are certainly too large. The values of C_p, on the other hand, should be reliable for all latitudes.

Yerkes Actinometry.—The number of stars in the catalogue is not large, and the range in galactic latitude is small. It will be sufficient to quote here the result derived by Kapteyn,[1] who found for the stars of visual magnitude 6–7

$$C_v = +0.66 \qquad (m = 6.6). \qquad (3)$$

North polar stars.—Well-determined color-indices are available[2] to photovisual magnitude 17.4. Mean values are given in Table VII.

[1] *Mt. Wilson Contr.*, No. 83; *Astrophysical Journal*, **40,** 187, 1914. eq. (16).

[2] *Transactions International Astronomical Union*, **1,** 69, 1922.

Stars brighter than about the twelfth magnitude are omitted; they are few in number and many of them are selected because of small color-index. The galactic latitude is 28°.

Since the photographic magnitudes extend to about magnitude 20, a grouping according to photovisual magnitude should be free from the influence of selection. This is not true, however, when the data are grouped according to photographic magnitude. For example, color-indices are available for stars as faint as photographic magnitude 19.1, but these stars are all very red. Stars of this photographic brightness having moderate color-indices do not occur among the data because their photovisual magnitudes are below the limit 17.4. The last value of C_p in Table VII is certainly too large; but there is no reason to suspect any disturbance of the last C_v beyond that arising from the small number of stars.

TABLE VII

MEAN COLOR-INDICES FOR NORTH POLAR STARS

Pv. Mag.	C_v	Res.	No. Stars	Pg. Mag.	C_p	Res.	No. Stars
12.2	0.86	−0.04	18	12.8	0.77	−0.04	25
13.7	.90	.00	28	14.6	.81	+ .05	27
14.5	.83	+ .09	25	15.4	.98	− .07	26
15.4	0.94	+ .01	16	16.3	0.93	+ .05	12
17.1	1.30	−0.30	17	18.3	(1.29)	(−0.17)	19

Field of S Cygni.—The colors of about 400 stars between photovisual magnitudes 12 and 17 have been measured at Mount Wilson. The increase in the minimum color-index appears, as it did in the case of provisional values for about 200 stars in this region which were illustrated in *Contribution* No. 81;[1] but the customary increase in mean color is masked by a large percentage of red stars between the twelfth and fourteenth magnitudes. Moreover, the magnitude scales are not wholly satisfactory. It seems best, therefore, to use only mean values for the entire series. The results are

$$\left.\begin{array}{l} C_v=0.70\ (m=13.9) \\ C_p=0.70\ (m=14.3) \\ \text{Gal. lat.}=13^\circ \end{array}\right\} \qquad (4)$$

---

[1] *Astrophysical Journal*, **39**, 361, 1914.

Colors of faint stars in the Milky Way.[1]—The color-indices of about 3350 stars in eight different regions of the Milky Way were determined by Kreiken from objective grating photographs made by Hertzsprung with the 60-inch reflector at Mount Wilson in 1912. The galactic latitudes for the separate regions range from −8° to +12°, with a mean of 5°. The colors are on the international system, and were grouped by Kreiken according to intervals of photographic magnitude. Table 38 of his paper shows that the systematic differences in the mean colors from region to region are not large. The counts have therefore been combined, and, in a somewhat abbreviated form (3098 stars), are given in Table VIII. With the exception of the first value of C_p, which depends on a small number of stars, the mean color-index shows the characteristic increase. The results for C_v were obtained by the usual transformation.

TABLE VIII

NUMBERS AND MEAN COLORS OF STARS IN MILKY WAY (KREIKEN)

C. I.	10	11	12	13	14	15
−0.6	....	....	....	....	2	5
.4	1	2	....	1	2	12
− .2	3	12	4	14	12	22
.0	3	14	16	60	58	48
+ .2	9	29	53	185	197	161
.4	6	20	41	121	222	210
.6	3	8	17	51	156	235
0.8	1	5	11	35	65	180
1.0	2	8	10	43	82	141
1.2	3	7	9	37	76	119
1.4	2	3	3	32	32	70
1.6	1	2	1	11	21	36
1.8	....	....	....	1	3	20
+2.0	....	....	....	....	1	10
Totals...	34	110	165	591	929	1269
C_p	0.46	0.39	0.43	0.49	0.57	0.70
C_v	0.67	0.68	0.69	0.70	0.72	0.78

Harvard Standard Regions.—A discussion of about 800 stars in these regions by Miss Leavitt has been given in *Harvard Circular* 230. The counts according to photographic magnitude in Table I of that publication have been combined and appear in Table IX below. The spectral types are the mean values given by Miss Leavitt. The corresponding color-indices in the second column of the table are Mount Wilson values and represent the mean for giant and dwarf stars. The increase in the resulting values of C_p is abnormal, and a comparison with the other data shows that the entire series is systematically too large by about 0.3 mag. The counts are obviously incomplete, and apparently the selection has been such as to favor the stars of high color. When grouped according to the four sections of the sky designated by N, S, P, and M, the means for all magnitudes together ($\overline{m}=8.7$) are

---

[1] E. A. Kreiken, *On the Colour of the Faint Stars in the Milky Way and the Distance of the Scutum Group.* This publication bears neither date nor imprint, but seems to have been issued from Groningen.

TABLE IX

MEAN COLOR-INDEX FOR HARVARD STANDARD REGIONS

Sp.	C. I.	7	8	9	10	11
B5..........	−0.18	7	11	2	1	....
A1..........	+ .04	41	63	59	27	3
A9..........	.34	21	29	33	9	....
F9..........	.75	22	60	50	48	9
G9..........	1.20	26	66	68	80	30
K6..........	+1.60	2	6	14	10	5
Totals...	....	119	235	226	175	47
C_p......	....	0.49	0.61	0.68	0.87	1.08
Res.....	....	−0.17	−0.22	−0.22	−0.34	−0.40

$$\left.\begin{array}{lrrrr} & \text{N} & \text{S} & \text{P} & \text{M} \\ \text{Gal. lat}\ldots\ldots\ldots\ldots\ldots & +51.2 & -50.2 & 21.9 & 8.8 \\ C_p\ldots\ldots\ldots\ldots\ldots\ldots & 0.85 & 0.79 & 0.73 & 0.42 \end{array}\right\} \qquad (5)$$

COMBINATION OF DATA

Change in mean color-index with magnitude.—The results for all galactic latitudes together derived from the *Revised Harvard Photometry*, the *Draper Catalogue*, and the *Göttingen Aktinometrie* (Tables II, IV, V) are shown graphically in Figure 1. The Mount Wilson values for stars near the North Pole (Table VII) are also included. The galactic latitude of 28° is not far from the mean for all the stars of moderate brightness,[1] and at present these data

---

[1] Because of the change in galactic concentration with increasing magnitude, the mean latitude also varies with the magnitude of the stars considered.

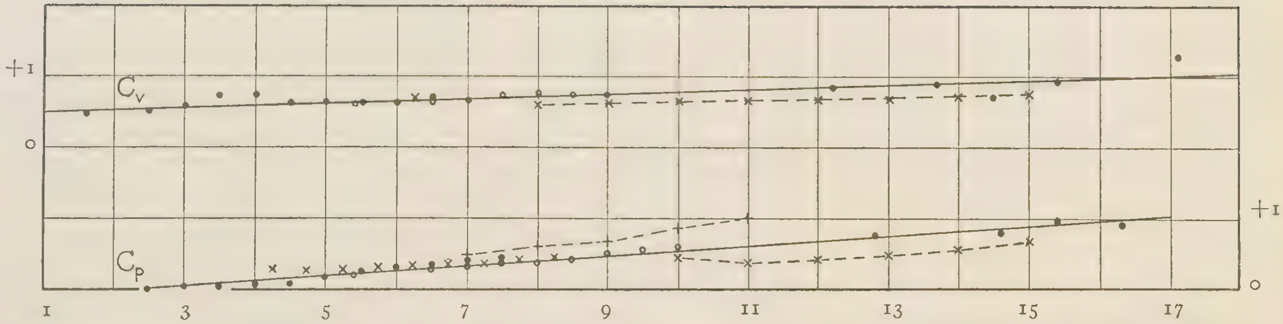

FIG. 1.—Mean color-index and apparent magnitude, all galactic latitudes together. C_v, stars grouped according to visual or photovisual magnitudes; C_p, according to photographic magnitude. Points: data from *Revised Harvard Photometry*, and, for faint stars, Mount Wilson measures at the Pole; circles: *Henry Draper Catalogue;* crosses on full-line curve: *Göttingen Aktinometrie.* The dotted curves for faint stars are results from Kreiken's measures in the Milky Way (mean lat.$=5°$), and show the influence of the concentration of blue stars in this region. The discordant values for C_p between $m=7$ and 11 are from the Harvard Standard Regions and show the effect of selection in the data.

provide the only means available for extending the mean results for all latitudes to the faint stars. Kreiken's measures of fields in mean latitude 5° are so close to the galactic circle that they supply only a rough control on the general accuracy of the results.

An inspection of Figure 1 shows that the values of both C_v and C_p as functions of the magnitude are well represented by simple linear relations. Those adopted are

$$\text{All latitudes together}\begin{cases} C_v=+0.50+0.029m_v & (6)\\ C_p=-0.18+0.071m_p. & (7)\end{cases}$$

The corrections to the tabular values necessary to reduce them to those defined by (6) and (7) are given in the various tables opposite the designation "Res." The influence of selection upon the values of C_v for the *Göttingen Aktinometrie* (Table V) is clearly evident, and the large systematic discordance for the Harvard Standard Regions is shown in the last line of Table IX. Otherwise, the residuals are well within the inherent uncertainties.

Variation of mean color with galactic latitude.—Most of the data bearing on the change in color with latitude refer to stars between mean magnitudes 5.7 and 7.4. It cannot be supposed that the coefficients of m in (6) and (7) are valid for all galactic latitudes; but no serious error will be introduced by using them to calculate the changes in C for an interval of one or two magnitudes. In this way the values of C_v for the *Harvard Photometry* in Table III ($m=5.7$) and for the *Göttingen Aktinometrie* in (2) ($m=6.3$) can be reduced to $m=7.4$ for comparison with the results from the *Draper Catalogue* given in (1). The corrections are +0.05 and +0.03, respectively. The agreement of the three series of results is shown graphically in the upper part of Figure 2. With the exception of the first two points for the *Göttingen Aktinometrie*, which have been discussed above, the deviations from the curve for the *Draper Catalogue* are small, and for the present it will be sufficient to accept this curve as a reasonably good approximation.

The lower part of Figure 2 shows the agreement of the values of C_p from the *Harvard Photometry* (last line of Table III) with those from the *Aktinometrie*, given in (2). The systematic difference is 0.02 mag., which again is well within the uncertainty of the data.

Reduced to $m=14.0$, the results for S Cygni given in (4) are shown in the third column of Table X. The values for the same magnitude found from Kreiken's data (Table VIII) and from the polar stars by (6) and (7) are in the second and fourth columns of this table. C_v for S Cygni is the only discordant value. By comparing Kreiken's values for $m=14$ with $C_v=0.56$ and $C_p=0.20$, read from the curves in Figure 2 for latitude 5°, and assuming a linear increase in color with m, we find

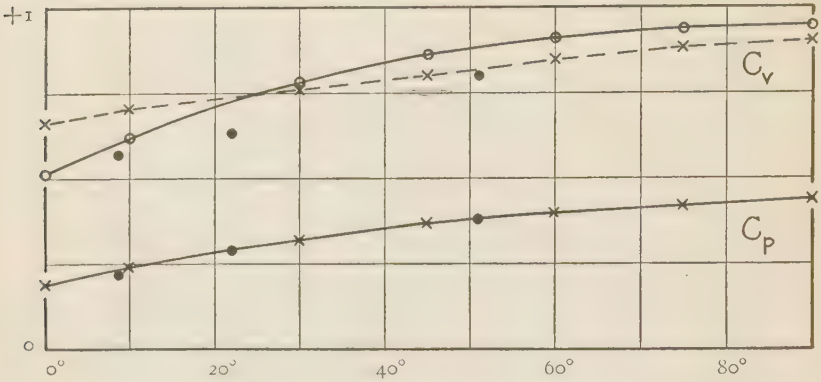

FIG. 2.—Mean color-index and galactic latitude for stars grouped according to visual (C_v, $m=7.4$) and photographic (C_p, $m=6.3$) magnitude. Points: *Revised Harvard Photometry;* circles: *Henry Draper Catalogue;* crosses: *Göttingen Aktinometrie.*

TABLE X

MEAN COLORS FOR $m=14.0$

	Kreiken, Milky Way	S Cygni	N. Polar Stars
Lat.	5°	13°	28°
C_v	0.72	0.70	0.91
C_p	0.57	0.68	0.81

$$\text{Gal. lat.}=5^\circ \begin{cases} C_v=+0.38+0.024m_v & (8) \\ C_p=-0.10+0.048m_p. & (9) \end{cases}$$

The coefficients in these relations are in general agreement with the variation in color shown by Kreiken's measures in the interval $m=10$ to 15. The relatively slow increase in the mean color in the Milky Way indicated by a comparison of (8) and (9) with (6) and (7) is in accordance with what we know of the distribution of colors among bright and faint stars in different parts of the sky.

Transformation of star counts for a grouping according to visual magnitude into a grouping according to photographic magnitude, and vice versa.—A simple illustration shows that the values of C_v and C_p found above cannot be used directly for this transformation. The increase with magnitude in the number of stars in a constant interval of magnitude is nearly that of a geometrical progression. Suppose this to be strictly the case, and, further, suppose that we have only two classes of stars, I and II, with color-indices of 0 and 1 mag., respectively. Let the numbers for a grouping according to visual magnitudes be as shown in the second, third, and fourth lines of Table XI. With the adopted color-indices, the numbers for a photographic grouping will then be those given in the last three lines of the table.

TABLE XI

Median mag.	4	5	6	7	8
No. I_v	....	2	4	8	16
No. II_v	2	4	8	16	32
Total $= N_v$	....	6	12	24	48
No. I_p	....	2	4	8	16
No. II_p	....	2	4	8	16
Total $= N_p$	....	4	8	16	32

The mean color-indices C_v and C_p are in both cases constant and equal, respectively, to 0.67 and 0.50. The mean photographic magnitudes of the groups N_v are therefore

$$p' = \ldots .\ 5.67,\ 6.67,\ 7.67\ \ldots .,$$

while the mean visual magnitudes of the groups N_p are

$$v' = \ldots .\ 4.50,\ 5.50,\ 6.50\ \ldots .$$

We cannot, however, take the sequences p' and N_v and by interpolation arrive at the true values of N_p for photographic magnitude = 5, 6, and 7. The result of such an interpolation is 3.77, 7.55, and 15.10, whereas the correct values, as shown in the last line of Table XI, are 4, 8, and 16. Nor can we use the sequences v' and N_p and by interpolation obtain correct values of N_v, that is, of the totals for a grouping according to visual magnitude. In each case a statistical error enters; these errors are opposite in sign, and, for the data of the illustration, equal in percentage amount.

In the absence of definite knowledge of the frequencies of the various spectral types for different magnitudes the statistical errors are difficult to determine, and it is simpler to approach the question by comparing the values of N_v and N_p and ask what photographic magnitudes, in a grouping according to this magnitude, will correspond to the totals N_v (or vice versa). This comparison of totals, or better, a comparison of the values of log N_v and log N_p, leads to the following sequences of corresponding magnitudes:

Visual...............	5	6	7
Photographic.........	5.585	6.585	7.585

The meaning of the sequences is that if, in a grouping according to visual magnitude, a total of N stars corresponds to the median magnitude m, then, in a grouping according to photographic magnitude, the total N will correspond to median magnitude $m+0.585$. Hence, the color-index which must be applied to the magnitudes in order to transform the totals grouped according to visual magnitude into the corresponding grouping according to photographic magnitude is 0.585. The result for the reverse transformation is the same. From conditions of symmetry we should expect this value to be sensibly equal to the mean of $C_v=0.67$ and $C_p=0.50$, which, in fact, is the case.

This suggests a practical method of procedure. The relations between the actual counts are not as simple as those of the illustration. Nevertheless, only small errors of the second order will be introduced by using the mean values of C_p and C_v found above, which for the case of all galactic latitudes together are defined by equations (6) and (7). For this general case the mean color-index for the transformation of star counts referred to visual scale into counts referred to the photographic scale, or vice versa, is therefore

$$C=+0.16+0.050\,m. \qquad (10)$$

This relation is approximate, but within the limits of error of the existing data.

MOUNT WILSON OBSERVATORY
September 1924

Contributions from the Mount Wilson Observatory, No. 288
Reprinted from the *Astrophysical Journal*, Vol. XLI, pp. 284–302, 1925

SOME RELATIONS BETWEEN MAGNITUDE SCALES

BY FREDERICK H. SEARES

ABSTRACT

Systematic corrections to various systems of magnitudes.—The *principal purpose* is the *reduction of the Harvard visual scale* to the Mount Wilson *photovisual system.* Incidentally, it is necessary to discuss the relation of this system to the photographic and photovisual magnitudes of King and the visual results of the *Potsdam Durchmusterung.* A direct comparison of Polar Sequence measures gives the values of the *color equation,* which seems to depend on the magnitude, and the scale correction *for the Harvard scale between* $m=4$ and 13 (Table II and [2]). King's extra-focal measures define scales which are sensibly parallel to *MW* and *H* results for $m<4$ (Tables III–V) and extend the series of color coefficients, but leave the zero-point correction to the Harvard visual magnitudes of bright stars rather uncertain. The result, however, is confirmed by comparing, in the critical region, the *PD* and *HR* and the *PD* and *MW* systems. The *scale corrections for Harvard* are approximately -0.08 to $m=5$; $+0.07\ (m-6)$ for $m=5$ to 9.5; and $-0.08\ (m-12.5)$ for $m=9.5$ to 13. The changes in the run in the differences correspond to the division-points between measures made with the 2-inch, 4-inch, and 12-inch meridian photometers. The comparison of *Harvard* and *Potsdam* is based mainly on the data of Müller and Kempf and leads finally to the scale and color corrections for the *PD* (Table VI), confirmed in part by direct comparison of *PD* and *MW* magnitudes for Polar Sequence stars.

The problem of reducing existing photometric data to a homogeneous system is very complicated and cannot be satisfactorily accomplished at present because of lack of information as to scale errors and color equations. The difficulties in the case of visual magnitudes are especially troublesome, since the color equation frequently varies with the brightness of the stars.[1] The following pages discuss the relations between certain photometric systems, chiefly Harvard, Potsdam, and Mount Wilson, for which details can now be traced with some definiteness.

Satisfactory photographic standards are now available in the magnitudes of stars near the Pole, collected and combined by the Commission on Stellar Photometry.[2] The state of affairs with respect to visual standards is less satisfactory. Because of certain definite advantages, the photovisual scale is much to be preferred as an ultimate standard to which all other systems of visual and photovisual magnitudes shall be reduced. Briefly, these advantages are, first, the general advantages of a photographic method over that of visual photometry. Second, the freedom, at least comparatively speaking, of the color equation from changes depending on the brightness of the stars. And third, the slight dependence of the color equation on the instrument. As an illustration of the last point, photovisual magnitudes determined at Mount Wilson with the 10-inch Cooke refractor and the 60-inch reflector are sensibly identical in color value, although measures of photographic brightness with these instruments show a relative equation amounting to one-fifth the color-index.[1] Even large differences in the photographic plate and the filter make surprisingly little difference. Thus Parkhurst, for the photovisual magnitudes of the Yerkes actinometry, used a trichromatic plate and a visual-luminosity filter covering the interval λ 4000–λ 6200. At Mount Wilson we have used an isochromatic plate and a filter which limit the region of spectral sensibility to λ 5000–λ 5900, and yet the two color systems are practically the same.

---

[1] See, for example, *Harvard Annals*, **64**, 116 ff.; *Potsdam Publikationen*, **17**, Introduction, 1917; *Göttingen Aktinometrie*, B, p. 24, 1912.

[2] *Trans. Internat. Astron. Union*, **1**, 69, 1922. For brevity this report of the Commission is referred to in the text simply as the *Report.*

I. THE MOUNT WILSON PHOTOVISUAL SYSTEM

The only photovisual scale covering a wide interval in brightness is that defined by the Mount Wilson magnitudes of stars near the Pole. These were determined with the 10-inch Cooke refractor and the 60-inch reflector and are given in final form in the *Report.* The results have not been confirmed by published data obtained elsewhere, but for the following reasons there can be little doubt of their substantial accuracy. (1) The methods used were those employed in establishing the photographic scale, which is known to be free from sensible systematic error. (2) Measures with the Cooke refractor between $m = 6.5$ and 12.5 agree with those made with the reflector.[2] (3) Reduced to photovisual values by means of color-indices determined by the method of exposure ratios, the photographic magnitudes define a photovisual scale which agrees closely with that established directly. The differences from $m=3.0$ to 17.4 are the same as those shown in Table III of the *Report*. The maxi-

---

[1] Seares and Humason, *Mt. Wilson Contr.*, No. 234; *Astrophysical Journal*, **56**, 84, 1922.

[2] See columns 17 and 18, Table I, of the *Report.*

TABLE I

PHOTOVISUAL AND HARVARD VISUAL SCALES, POLAR SEQUENCE

Group	No.	*MW Pv*	*Harv. Vis.*	*C*	*MW−HV* Corr. for Sc.	Final Color Corr.	Scale Diff. *Pv−HV*	Residuals
	1*s*	2.08	2.12	0.49	+0.01	−0.06	+0.02	....
I......	1	4.37	4.44	0.01	− .02	.00	− .07	0.00
	1*r*	5.09	5.26	1.57	.14	− .19	+ .02	+ .07
	2	5.28	5.38	−0.11	.08	+ .01	− .11	− .07
	3	5.56	5.62	0.18	.04	− .02	− .04	.00
	4	5.84	5.86	0.14	.01	.02	.00	+ .02
II.....	2*s*	6.30	6.28	0.17	.00	.02	+ .04	+ .04
	3*s*	6.35	6.33	0.26	.00	.03	+ .05	+ .04
	2*r*	6.32	6.55	1.58	.27	− .20	− .03	− .05
	5	6.45	6.43	0.01	.01	.00	+ .02	.00
III.....	6	7.06	7.01	0.06	− .02	− .01	.06	.00
	7	7.55	7.44	−0.17	+ .01	+ .02	.09	− .01
	3*r*	7.57	7.57	1.41	− .12	− .18	.18	+ .07
	8	8.13	7.97	0.25	+ .01	.03	.19	+ .05
	4*r*	8.27	8.26	1.00	− .16	.14	.15	− .01
IV.....	5*r*	8.63	8.67	1.53	− .24	.22	.18	− .02
	9	8.83	8.61	0.17	+ .03	.02	.24	+ .04
	10	9.06	8.94	0.12	− .09	.02	.14	− .09
	6*r*	9.24	9.25	1.26	− .23	.19	.18	− .07
V......	11	9.56	9.30	0.24	+ .03	.04	.30	+ .04
	12	9.77	9.54	0.31	.00	.05	.28	.00
	4*s*	9.83	9.58	0.50	+ .02	.08	.33	+ .05
	7*r*	9.87	9.84	1.11	− .19	.19	.22	− .05
	5*s*	10.06	9.86	1.06	.02	.18	.38	+ .11
VI.....	13	10.37	10.25	0.22	.08	.04	.16	− .07
	8*r*	10.46	10.39	0.98	.11	.17	.24	.00
	14	10.56	10.44	0.42	.06	.08	.20	− .01
	6*s*	10.72	10.75	0.68	.18	.13	.10	− .08
	15	10.88	10.78	0.38	− .05	.07	.17	− .01
VII....	16	11.22	11.07	0.36	+ .02	.07	.22	+ .07
	17	11.30	11.18	0.54	+ .01	.11	.22	+ .08
	18	11.90	11.93	0.39	− .08	.08	.05	− .03
	11*r*	12.07	12.24	1.12	.20	.27	.00	− .04
	19	12.24	12.22	0.44	.01	.11	+ .13	+ .09
	20	12.52	12.65	0.50	.09	− .12	− .01	−0.01
	23	13.00	13.34	0.56	.24	− .16	− .18	....
	9*s*	13.74	13.94	1.04	−0.03	−0.31	+0.11	....

mum difference is, direct observation *minus* calculation $= +0.08$ mag., at $m = 8.6$. (4) Unpublished photovisual data obtained at the Harvard Observatory and communicated some years ago by Miss Leavitt agree well, in general, with the Mount Wilson results. The comparison extends from 6.5 to 14.5. A small divergence enters at the eighth magnitude; at the tenth magnitude it attains a maximum of $+0.10$ mag., in the sense $MW - H$, and thereafter remains nearly constant.

The Mount Wilson photovisual magnitudes of the *Report* are accordingly adopted as provisional standards, and for brevity the scale defined by them is frequently referred to in what follows simply as the "photovisual scale."

2. HARVARD VISUAL MAGNITUDES OF THE POLAR SEQUENCE

The differences in column 16, Table I, of the *Report* show that these magnitudes differ systematically from the photovisual scale. A color equation of approximately $-0.14\,C$ is also indicated.[1] A detailed examination of these differences follows.

The numbers, the Mount Wilson photovisual, and the Harvard visual magnitudes of the thirty-seven stars available for discussion are in the second, third, and fourth columns of Table I. The color-indices in the fifth column are the means of those found from magnitudes and by the method of exposure ratios, and given in the *Report* under the designation C_m and C_e, respectively.

The differences $Pv - HV$ were provisionally corrected for color by applying $-0.14\,C$. This led to an approximate scale correction which was then applied to the original values of $Pv - HV$, the results being in the sixth column of Table I. For the final determination of the color equation these corrected differences were grouped as indicated in the first column, the first star and the last three stars being omitted because of uncertainty in the scales for the extremes of brightness.

Each of the seven groups includes one or two red stars and several having small or moderate color-indices. Graphical solutions for the separate groups gave the following values of the color coefficient:

---

[1] The sign, here as elsewhere in this discussion, is such that the algebraic addition of the correction reduces the data in question to the adopted standard system. Unless otherwise stated, the color-index C is that referred to the standard system.

Group........	I	II	III	IV	V	VI	VII	
Mean vis. mag.	5.26	6.55	7.90	8.96	9.85	10.57	12.24	(1)
Color coeff.....	−0.08	−0.18	−0.14	−0.15	−0.18	−0.17	−0.24	

These results indicate an increase in color equation with increasing magnitude. The smoothed values (that for $m=3$ is from section 3) are

COLOR EQUATION, HARVARD VISUAL MAGNITUDES

Vis. mag............	3	5	6	7	8	
Color coeff..........	−0.09	−0.11	−0.12	−0.13	−0.14	(2)
Vis. mag....................		9	10	11	12	
Color coeff..................		−0.15	−0.17	−0.20	−0.23	

These were used to correct once more the original differences $Pv-HV$, the corrections themselves being in the seventh column of Table I. The results in the eighth column define the adopted correction to the Harvard visual scale of the Polar Sequence. A plot of the differences is shown in Figure 1; the smoothed values are given in Table II, and, finally, the last column of Table I shows the residual differences $Pv-HV$ found with the aid of (2) and the smoothed scale correction in Table II.

TABLE II

North Polar Sequence, Scale Difference $Pv-HV$*

HV	$Pv-HV$	HV	$Pv-HV$	HV	$Pv-HV$
4.0.........	−0.08	7.5.......	+0.10	11.0.......	+0.16
4.5.........	.07	8.0.......	.14	11.5.......	.11
5.0.........	.06	8.5.......	.19	12.0.......	.06
5.5.........	.04	9.0.......	.24	12.5.......	+ .02
6.0.........	− .01	9.5.......	.28	13.0.......	− .03
6.5.........	+ .02	10.0.......	.25	13.5.......	−0.07
7.0.........	+0.06	10.5.......	+0.20	....	....

---

* The correction to the magnitudes of the *Revised Harvard Photometry* for $m<4.0$ is −0.08. This, together with the tabular values, represents the provisionally adopted scale correction for reduction of the Harvard visual to the Mount Wilson photovisual scale. The corrections have been freed from color equation by means of the data under (2).

The corrected difference for Polaris in the first line of Table I is +0.02, which suggests that for the interval $m=2$ to 6 the scales are

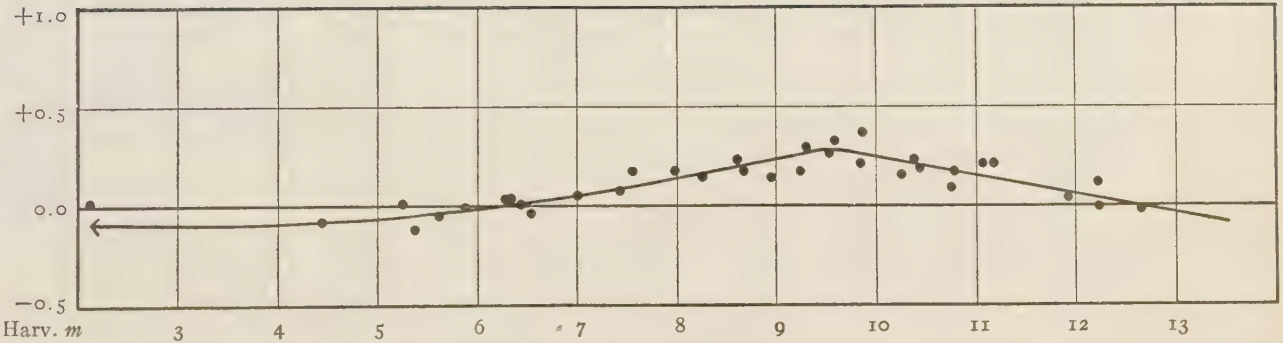

FIG. 1—Reduction of the Harvard visual scale to the Mount Wilson photovisual system. The ordinates represent the differences *Pv*−*HV*, reduced to the photovisual color system.

nearly parallel. Between $m=6$ and $m=9.5$ the divergence is approximately represented by $+0.07\,(m-6)$, while below 9.5 it has the form $-0.08\,(m-12.5)$. This peculiar behavior probably represents the characteristics of the instruments commonly used for the Harvard visual measures—the 2-inch, 4-inch, and 12-inch meridian photometers. Generally speaking, measures with the 2-inch photometer extend to the sixth magnitude, and with the 4-inch to the tenth magnitude. With allowance for overlapping, these limits agree with the division-points of the run in the differences between the two scales.

3. COMPARISON OF THE HARVARD VISUAL SCALE WITH THE EXTRA-FOCAL MEASURES OF KING

The visual scale for the bright stars—practically that of the 2-inch meridian photometer—can be checked by comparison with the photographic and photovisual magnitudes of King.[1] The conclusions assume the substantial accuracy of King's scales, but there is reason to believe that this assumption is justified. It is based partly on the character of the method and the care with which it was applied, and partly on the good agreement of King's photographic magnitudes of the Polar Sequence with the international photographic scale.[2]

Consider first the color relations. The color-indices based on King's photographic magnitudes (*KPg*) and the visual magnitudes of the *Revised Harvard Photometry* (*HR*) which are given in *Harvard Annals*, **76**, No. 6, Table IX, appear in the second column of Table III below.[3] The third column of the table gives the color-indices derived from his extra-focal photographic and photovisual measures, taken from *ibid.*, **85**, No. 3, Table VI. The differences between the two series, $KPv-HR$, are in the fourth column of Table III. Similar differences found by comparing the photovisual magnitudes directly with the *HR* magnitudes and thus based on somewhat different data are in the fifth column. These are from Table V (*ibid.*), after correction by −0.13 mag. to make the differences for A0 stars equal to zero. The means for the fourth and fifth columns of Table III are in the sixth column, and define the color equation of the Harvard visual magnitudes of bright stars relative to King's photovisual system. These mean differences are represented by

---

[1] *Harvard Annals*, **76**, No. 6; **85**, No. 3.

[2] These magnitudes constitute Group 1 in Miss Leavitt's memoir in *Harvard Annals*, **71**, No. 3.

[3] These are also given in *ibid.*, **85**, No. 3, Table VI.

$$KPv-HR=-0.05-0.09\,C. \tag{3}$$

This relation is based on stars brighter than $m=5$, and refers to a mean magnitude of approximately 3. Since the various spectral groups in Table III include stars of all magnitudes within the interval covered, (3) may be regarded as unaffected by differential errors in the magnitude scales.

TABLE III

Comparison of Color-Indices

Harv. Sp.	*KPg−HR*	King *Pg−Pv*	*KPv−HR*	*Pv−Ptm*	*Pv−Vis*	*MWC* *M*=0	*KC* Smoothed	*MWC* −*KC*
B0.....	−0.29	−0.23	−0.06	−0.05	−0.06	−0.32	−0.23	−0.09
B1.....	.28	.17	.11	+ .06	.03	.29	.22	.07
B2.....	.34	.26	.08	− .08	.08	.26	.20	.06
B3.....	.25	.20	.05	+ .02	.02	.23	.19	.04
B5.....	.17	.10	.07	− .01	.04	.17	.15	− .02
B8.....	− .12	.08	− .04	.07	− .05	− .07	− .08	+ .01
A0.....	.00	− .02	+ .02	.00	+ .01	.00	.00	.00
A2.....	+ .12	+ .13	− .01	.06	− .03	+ .07	+ .06	.01
A3.....	.20	.18	+ .02	.05	.01	.11	.10	.01
A5.....	.20	.21	− .01	− .04	− .02	.19	.17	.02
F0.....	.33	.25	+ .08	+ .03	+ .06	.38	.35	.03
F5.....	.45	.59	− .14	− .09	− .12	.62	.59	+ .03
F8.....	.56	.80	.24	.14	.19	.77	.78	− .01
G0.....	.70	0.88	.18	.15	.17	0.86	0.85	+ .01
G5.....	0.98	1.16	.18	.21	.19	1.15	1.13	.02
K0.....	1.12	1.28	.16	.16	.16	1.48	1.43	.05
K2.....	1.50	1.61	.11	.18	.14	1.63	1.59	.04
K5.....	1.62	1.73	.11	.16	.13	1.84	1.73	.11
M.....	+1.66	+1.87	−0.21	−0.19	−0.20	+1.88	+1.87	+0.01

It is probably safe to assume that the color equation of King's photovisual system relative to the Mount Wilson system is zero. The similarity in color value of photovisual magnitudes derived with different instruments and plates has been mentioned. In the present case, the same kind of plate and the same type of filter were employed at both observatories. The only difference is in the telescopes—the 8- and 11-inch Draper, and the 13-inch Boyden refractors, as against the 60-inch reflector. Since the instruments used by King are intermediate in color sensibility to the reflector and the Mount Wilson Cooke refractor, which give identical photovisual results, it is unlikely that his measures will show any systematic deviation in color from the Mount Wilson series.

The matter can be tested by comparing King's color-indices in the third column of Table III (the smoothed values in the eighth column are used) with the Mount Wilson indices in the seventh column, for which, since the stars are bright, values corresponding to absolute magnitude zero are used. The differences in the two series given in the last column of the table are represented by

$$\text{Color-index, } MW-\text{King}=+0.05\,C. \tag{4}$$

If it be assumed, as suggested above, that the two photovisual systems are identical in color value, relation (4) will then represent the color equation of King's photographic system relative to the Mount Wilson system. As a matter of fact, the coefficient of (4) is very nearly that to be expected. In discussing[1] the photographic magnitudes in Miss Leavitt's memoir (*H.A.*, **71**, No. 3), the following color equations were found

$$\left.\begin{aligned} MW-I&=+0.06\,C \text{ (8-inch Draper telescope)}\\ MW-C&=+0.08\,C \text{ (11-inch Draper telescope)}\end{aligned}\right\} \tag{5}$$

Further, King (*ibid.*, **76**, 116) finds that the color sensibility of all three of the telescopes used by him is practically the same. A mean coefficient of +0.07 is therefore probably near the truth, and this, within the limit of uncertainty, agrees with +0.05 given in (4).

This seems to justify the conclusion that the color values of the two photovisual systems are the same; but it should be remarked that King's measures are extra-focal, while the results under (5) depend on focal images. The color value of such images may depend to some extent upon the aberrations of the objective, but the glass absorption is probably the more important factor.

In spite of this uncertainty, the general argument as to the agreement of the photovisual system holds, so that the term —0.09 C in (3) is probably a good approximation for the color equation of the Harvard visual measures of the bright stars. This result (for $m=3$) is in good agreement with what might be expected from an extrapolation of the smoothed values under (2).

---

[1] *Mt. Wilson Contr.*, No. 98; *Astrophysical Journal*, **41**, 259, 1915.

The relation between the magnitude scales can now be considered. This is best done by transforming King's photographic magnitudes into photovisual values with the aid of the color-indices for the various spectral types and comparing them with the *HR* magnitudes corrected for color equation.

The photographic magnitudes were taken from King's list in *Harvard Annals*, **76**, 117, Table VIII, which contains 229 stars. Doubles and a few O stars, for which no color-indices are available, were rejected, thus leaving a total of 198 stars suitable for discussion. The difference, $KPg-HR$, was formed for each star, from which was derived $KPg-RHR$, where RHR indicates the *HR* magnitude reduced to the photovisual system by applying the appropriate correction from the sixth column of Table III. The remaining step involves the subtraction of the color-index $KPg-KPv$ taken from the third column of this table. The result is $KPv'-RHR$.[1] No smoothing was employed, and the corrections from Table III were used as they stand, except that allowance was made for the dependence of color-index upon absolute magnitude. This variation in color is clearly shown by the differences $KPg-RHR$ for the late F's and the G and K stars, in agreement with earlier results for these classes.[2] The changes range from $-0.025\,M$ for F8 to $-0.044\,M$ for types G5–K0.

Eight of the 198 corrected differences $KPv'-RHR$ exceed 0.3 mag.; seven of these are positive, which suggests, for some at least, an excess of color over the normal for the spectral type in question. Four differences exceeding 0.4 mag. are clearly abnormal and were rejected. The remaining values were grouped according to the *HR* magnitude and formed into means, with the results shown in Table IV. These represent the systematic difference between the scale of the brighter stars of the *Revised Harvard Photometry* (essentially that of the 2-inch meridian photometer) and King's photographic scale after correction for color.

---

[1] The notation Pv' denotes photovisual magnitudes calculated from photographic values, as distinguished from those directly measured.

[2] Seares, *Mt. Wilson Comm.*, No. 59; *Proc. Nat. Acad. of Sciences*, **5**, 232, 1919. The variation for the A stars given in this *Communication* is probably illusory, and to be explained by a systematic error in the spectral classification whose existence was then unknown. The behavior of the B stars is still in doubt.

To about the fourth magnitude the scales are very accordant. Since 20 of the 25 differences included in the last two means are positive, the small systematic divergence at the end is probably real, although it is difficult to say which of the two scales is in error. The mean of the 194 differences without regard to sign is ±0.085 mag. This represents the mean difference between the *Pv′* and *HR* magnitudes of the same star, including all sources of error, and indicates a probable error of about ±0.05 mag. in the magnitudes. The zero-point of King's magnitude depends upon an assumed photographic magnitude of 2.69 for Polaris.

TABLE IV

SCALE DIFFERENCE—KING PHOTOVISUAL (CALCULATED FROM *KPg*) AND *Revised Harvard Photometry*, REDUCED TO PHOTOVISUAL COLOR SYSTEM*

HR Mag.	*KPv′−RHR*	No. Stars	*HR* Mag.	*KPv′−RHR*	No. Stars
0.0–0.5	+0.006	5	3.0–3.5	−0.006	42
0.5–1.0	− .070	4	3.5–4.0	− .004	22
1.0–1.5	+ .011	7	4.0–4.5	+ .086	19
1.5–2.0	+ .032	16	4.5–5.0	+0.077	6
2.0–2.5	− .033	28			
2.5–3.0	+0.002	45	Total......	....	194

* Zero-point for King corresponds to 2.69 as photographic magnitude for Polaris.

There remains the comparison of King's photovisual magnitudes with those of the *HR*—more direct, but less satisfactory than that just given, because of the smaller number of stars and the shorter interval of brightness covered. The eighth column of Table IV, *Harvard Annals*, 85, No. 3, gives directly the differences *Pv*−*HR*. Rejecting doubles, correcting for the color equation of *HR* as before, and grouping the differences according to *HR* magnitude, we find the means given in Table V. The differences show a slight tendency to increase with magnitude, but in the well-determined region the scales are practically parallel.

The mean zero-point difference of +0.12 mag. depends upon an assumed visual magnitude of 2.12 for Polaris. The difference found by King, without correcting the *HR* for color equation, is +0.13. To bring the zero-point of his *Pv* magnitudes into agreement with that of the *HR*, and thus obtain his "completed" magnitudes, he subtracts this difference and finds accordingly for Polaris a photovisual magnitude of 1.99 and a color-index of 0.70. Part of this difference is accounted for by color equation. With allowance for this, the *HR* value for Polaris becomes 2.07. The Mount Wilson value is 2.08, so that the agreement seems to be very good. But another point remains still to be considered.

The international zero-point for the stars at the Pole was determined by the condition that the mean magnitude of the A0 stars between $m = 5.5$ and 6.5 should equal the Harvard value; but owing to the small number of stars this condition may not have been exactly satisfied. Here we are adopting the polar stars as standards, and attempting to find the relation of the Harvard magnitudes to this system. The evidence indicates that for $m < 4$ the correction to the *HR* magnitudes is a constant. If we were to accept the Mount Wilson *Pv* magnitude of Polaris, 2.08, as exact, King's photovisual measures, all of which are referred to Polaris, would indicate that the *HR* requires (for the bright stars) a zero-point correction of +0.08 mag. to reduce it to the photovisual system. On the other hand, King's photographic measures combined with the international photographic magnitude of Polaris (2.55 as against 2.69 used by King) would lead to a zero-point correction of −0.14 mag. for the *HR*. These more or less hypothetical corrections include the full amount of the accidental errors in the magnitudes adopted for Polaris and any systematic divergence in King's scales. The internal evidence and the small run in the differences in Table V

TABLE V

SCALE DIFFERENCE—KING PHOTOVISUAL AND *Revised Harvard Photometry*, REDUCED TO PHOTOVISUAL COLOR SYSTEM*

HR Mag.	*KPv−RHR*	No.	*HR* Mag.	*KPv−RHR*	No.
0.0–0.5	+0.07	4	2.5–3.0	+0.11	35
0.5–1.0	.09	4	3.0–3.5	.19	12
1.0–1.5	.12	4	3.5–4.0	+0.13	1
1.5–2.0	.14	13			
2.0–2.5	+0.11	20	Total	....	93

* Zero-point for King corresponds to 2.12 as photographic magnitude for Polaris. To obtain agreement with *HR*, King has subtracted 0.13 from the magnitudes used here. His "completed" magnitudes are the differences thus found.

suggest that King's measured differences in photovisual magnitudes are slightly too large. A reasonable allowance would reduce the zero-point correction of +0.08 mag. to zero.

If it were certain that King's photographic scale is accurate at the lower end, the corrections to the *HR* magnitudes of the bright stars could be found by using the condition that the corrected values of the last two differences in Table IV must agree with the initial values in Table II. The correction thus indicated would be −0.16 mag., which agrees well with −0.14 mag., based on King's photographic measures and the international photographic magnitude of Polaris. But as shown in section 5, King's photographic magnitudes for the fainter stars observed by him deviate from the *PD* values in the same way that they do from the *HR*. The positive differences at the end of the series in Table IV perhaps indicate, therefore, a small divergence in his scale for $m<4$.

It is probably safer, therefore, to accept the mean of the corrections indicated by the magnitudes of Polaris, namely, −0.14 and 0.00 mag., respectively. Although uncertain, a correction of −0.07 mag. for $m<4.0$ is consistent with results in Table II and is satisfactorily confirmed by the more reliable discussion in section 6.

4. COMPARISON OF THE HARVARD VISUAL SCALE WITH THAT OF THE *Potsdam Durchmusterung*

The complicated character of the relation between these scales is well known from the comparisons of Pickering,[1] Müller and Kempf,[2] and Schwarzschild.[3] Consider first the comparison of Müller and Kempf, who have formed the mean differences for four color classes and each half-magnitude interval between the *Potsdam Durchmusterung* and *Harvard Annals*, 44 and 45. The latter catalogues deviate slightly from the *Revised Harvard Photometry*, but are easily reduced to the *HR* system by the corrections given in *Harvard Annals*, 64, 117, 118, supplemented by the following color equivalents:

Potsdam color class	W	GW	WG	G	(6)
Mt. Wilson color-index.......	+0.02	+0.30	+1.04	+1.66	

---

[1] *Harvard Annals*, 64, 119.

[2] *Pub. des Astrophys. Observatoriums zu Potsdam*, 17, xxxiii, 1907.

[3] *Göttingen Aktinometrie*, B, p. 23, Table 20.

Harvard spectral group........	B	A	F	G	K	M	(7)
Mt. Wilson color-index.........	−0.26	0.00	+0.38	+0.83	+1.48	+1.88	

Those under (6) were found from the data in Table 25 of the *Göttingen Aktinometrie*, B, p. 29, combined with the following relation between the Mount Wilson and Göttingen color-indices:

$$C = J_p + 0.29. \tag{8}$$

The values in (7) are the Mount Wilson colors for giant stars corresponding to the median spectral types of the various groups.[1]

TABLE VI

MEAN DIFFERENCES, *PD−HR*

MED. *HR* MAG.	POTSDAM COLOR CLASS				REL. COL. EQ. *C*	COLOR EQ.		*PD−HR* CORR. FOR *C*	*Pv−PD*	*Pv−HR*	*Pv−HR* TABLE II	DIFF.
	W	*GW*	*WG*	*G*		*HR* *C*	*PD* *C*					
2.25.........	+0.27	+0.24	+0.15	+0.09	+0.10	−0.08	+0.02	+0.26	−0.26	0.00	......	......
2.75.........	.26	.23	.14	.08	.10	.09	.01	.25	.26	− .01	......	......
3.25.........	.25	.22	.12	.07	.11	.09	.02	.24	.26	.02	......	......
3.75.........	.24	.21	.11	.06	.11	.10	.01	.24	.26	.02	−0.08	−0.06
4.25.........	.24	.20	.10	.04	.12	.10	.02	.24	.26	.02	.08	.06
4.75.........	.25	.20	.09	.02	.14	.10	.04	.24	.26	− .02	.06	.04
5.25.........	.26	.21	.08	+ .01	.16	.11	.05	.26	.25	+ .01	.05	.06
5.75.........	.28	.23	.08	− .02	.18	.12	.06	.28	.23	.05	− .03	.08
6.25.........	.30	.24	.06	.02	.20	.12	.08	.30	.22	.08	.00	.08
6.75.........	.32	.27	.09	.02	.21	.13	.08	.32	.20	.12	+ .04	.08
7.25.........	.33	.27	.08	.04	.22	.13	.09	.33	.19	.14	.08	.06
7.75.........	.34	.28	.08	.05	.24	.14	.10	.34	.17	.17	.12	.05
8.25.........	+0.35	+0.28	+0.07	−0.06	+0.25	−0.14	+0.11	+0.35	−0.16	+0.19	+0.16	−0.03
C........	0.02	0.30	1.04	1.66	......	......	......	......	......	......	Mean	−0.06

The reduction to the *HR* system thus outlined leads finally to the mean differences given in the first five columns of Table VI. Within the magnitude interval for which a comparison is possible, the results are in almost exact agreement with those found by Pickering. The differences include both relative scale error and color equation. The coefficients for the color equations appear in the sixth column of the table. These were found graphically by plotting the differences in each line of the four columns immediately preceding against the values of *C* given at the bottom of the table.

The color equation of the *HR* relative to the photovisual system has already been found, and is given under (2). The values corresponding to the magnitudes listed in the first column of Table VI appear in the seventh column. Combining these with the data in the sixth column, we find the values of the color equation of the *PD* referred to the photovisual system given in the eighth column of Table VI. For the bright stars the correction is sensibly zero and increases slowly to about $+0.10\,C$ at $m=8$. The *HR* and *PD* systems therefore deviate from the photovisual systems in opposite directions, and the combination of the two equations, differing in sign, is responsible for the large relative equation shown in the sixth column of the table.

---

[1] *Mt. Wilson Contr.*, No. 287, Table I; *Astrophysical Journal*, **61**, 114, 1925.

The differences in the second to the fifth columns of Table VI, corrected for relative color equation as given in the sixth column, give the mean differences in the ninth column. These represent the scale divergence of the two systems in the sense $PD-HR$. The scales are sensibly parallel to about $m=5$; thereafter the difference is represented by

$$PD-HR=+0.25+0.03\,(HR-5.0). \qquad (9)$$

The remaining columns of Table VI are considered in section 6.

A characteristic feature of the comparisons between the *HR* and *PD* systems made by Pickering and by Müller and Kempf is the dependence of color equation upon magnitude. In one case the magnitudes were grouped according to Harvard spectra taken from the original *Draper Catalogue*, in the other, according to Potsdam color estimates. As already mentioned, the results are sensibly identical. In contrast to these are the two comparisons by Schwarzschild,[1] one, based on a grouping according to the spectral types of Miss Cannon in *Harvard Annals*, **56**, No. 4, the other depending on the Göttingen color-indices. His formulae are, respectively:

$$PD-HR=+0.45+0.046\,(HR-6.5)-0.14\,Sp \quad \text{(Sch. 5)}$$
$$PD-HR=+0.52+0.086\,(HR-6.5)-0.13\,Sp \quad \text{(Sch. 11)}$$

where *Sp* indicates the spectral type, as defined on page 19 of the *Aktinometrie*.

Here, as Schwarzschild notes, the color terms do not involve the magnitude. His suggested explanation is that the *Draper Catalogue* spectra and the Potsdam color estimates are affected by systematic errors. Whether this is the case or not would be immaterial were the various formulae always used in connection with the data upon which they are based, but it does raise some question as to the reduction in Table VI, for which color-indices have been used on the assumption that the same value of the index always corresponds to a given color estimate.

---

[1] *Göttingen Aktinometrie*, B, eq. 5, p. 26, and eq. 11, p. 25.

For comparison with the earlier results of this section, Schwarzschild's formulae may be expressed in terms of the standard color-index with the aid of equation (4) of the *Aktinometrie*,

$$J_p=G-P=-1.03-0.09\,(PD-6.5)+0.63\,Sp \tag{10}$$

combined with (8) above, from which

$$Sp=1.59\,C+1.18+0.143\,(PD-6.5). \tag{11}$$

This formula does not refer to the general catalogue of the *PD*, but to one of the earlier volumes; and the final expression for *Sp* in terms of *C* requires the substitution of equation (9) of the *Aktinometrie*. This gives

$$Sp=1.59\,C+0.140\,PD+0.264, \tag{12}$$

whence Schwarzschild's comparison formulae become

$$PD-HR=+0.27+0.025\,(HR-6.5)-0.22\,C \tag{13}$$
$$PD-HR=+0.36+0.067\,(HR-6.5)-0.20\,C. \tag{14}$$

The magnitude intervals covered are about 4.5 to 7.5 and 5.0 to 8+, respectively, while the mean magnitudes are 5.6 and 7.0. The relative color equations corresponding to these means, given in the sixth column of Table VI, are 0.18 *C* and 0.21 *C*, respectively, which are in satisfactory agreement with the color terms in (13) and (14).

The scale differences expressed by the first two terms of (13) and (14) are discordant, but that corresponding to (13), which is directly comparable with (9), reproduces the differences in the ninth column of Table VI, for the interval in question, within the uncertainty of the comparison. The outstanding difference is in the zero-point and amounts to only 0.03 mag. As far as scale difference is concerned, Schwarzschild's comparison based on Miss Cannon's spectra in *Harvard Annals*, **56**, No. 4, is therefore in agreement with the results of Pickering and Müller and Kempf. The larger divergence which appears when the data are grouped according to Göttingen color-indices and the apparent constancy of the color equation shown by both Schwarzschild's comparisons remain obscure.

5. COMPARISON OF KING'S EXTRA-FOCAL MEASURES WITH THE *Potsdam Durchmusterung*

Some further light is thrown on the relation of scales and color equations by comparing King's magnitudes with the visual magnitudes of the *PD.* Because of their greater number, the photographic series was used, after reduction to the photovisual system by the color-indices in the third column of Table III. The differences $KPv'-PD$ for the 115 stars common to the two lists were grouped according to spectral type and plotted. The stars are all brighter than the fifth magnitude, and most of them fall between $m=2.0$ and 4.5. Within this interval the differences are well represented by

$$KPv'-PD=-0.14+0.04\,(PD-6). \qquad (15)$$

The systematic deviations from this formula for the different spectral types are only 0.01 or 0.02 mag. To $m=4.5$ or 5.0, therefore, the color equation of the *PD* magnitudes relative to the photovisual system is sensibly zero. This confirms the very small values of the color coefficient for the *PD* system shown in the upper part of the eighth column of Table VI.

As for scale difference, the coefficient of 0.04 in (15) does not accurately represent the relations. If the stars fainter than $m=3.0$ be disregarded, the differences can be represented satisfactorily by a constant. Except for a zero-point correction, the scale divergence is therefore very similar to that shown by the differences $KPv'-RHR$ in Table IV. And this, indeed, is to be expected, for the mean differences given in the ninth column of Table VI show that to the fifth magnitude the Harvard and Potsdam scales are sensibly parallel. This suggests that the small scale-divergence shown by the last two differences in Table IV is in King's scale rather than in that of the *HR.*

6. COMPARISON OF THE POTSDAM MAGNITUDES OF THE POLAR SEQUENCE STARS WITH THE MOUNT WILSON PHOTOVISUAL VALUES

The number of stars available for this comparison is only twelve, but their magnitudes are well determined and cover the critical interval from $m=4.7$ to 7.7 in such a way as to give, in connection with the *PD* and *HR* comparison, a fairly reliable indication as to the characteristics of the Harvard scale in this region. Because of the importance of the comparison, the details are shown (Table VII).

TABLE VII

Polar Sequence Stars—Potsdam and Mount Wilson

Star	*MW Pv*	*C*	*PD Vis.*	*Pv−PD*	*O−C*
1*s*..........	2.08	+0.49	2.31	−0.23	0.00
1..........	4.37	0.01	4.69	.32	− .06
1*r*..........	5.09	+1.57	5.18	.09	+ .05
2..........	5.28	−0.11	5.37	.09	(+.17)
3..........	5.56	+0.18	5.82	.26	− .03
4..........	5.84	0.14	6.10	.26	− .04
2*s*..........	6.30	0.18	6.50	.20	+ .01
2*r*..........	6.32	1.58	6.47	.15	− .04
3*s*..........	6.35	0.26	6.48	.13	+ .07
5..........	6.45	0.02	6.70	.25	− .04
6..........	7.06	+0.06	7.28	.22	− .03
7..........	7.55	−0.16	7.70	−0.15	+0.04

The uncorrected differences in the fifth column are represented by the formula

$$Pv-PD=-0.26+0.03\,(PD-5.0)+0.07\,C, \tag{16}$$

in which the second term is to be disregarded for stars brighter than 5.0. The residuals in the last column of Table VII show only one discordant value. The mean magnitude of the stars is about six. The color equation of $+0.07\,C$ is therefore in agreement with the results given in the eighth column of Table VI.

The ninth column of Table VI gives the values of $PD-HR$, reduced to the photovisual system of color. If now the *PD* scale correction defined by the first two terms of (16) be applied to these differences, the result will be the scale differences $Pv-HR$. These are given in the eleventh column of Table VI. Because of the indirect nature of the comparison and the small number of polar stars, the zero-point may require correction; but the characteristics of the *HR* scale in the critical region between $m=4$ and 7 should be reasonably well defined. For comparison, the results from Table II, found by a direct comparison of magnitudes of Polar Sequence stars, are given in the twelfth column of Table VI. The differences in the last column indicate a mean zero-point correction of -0.06 mag. for stars involved in the comparison of Table VII; but what is important is the fact that these differences are sensibly constant. This shows that the relative values of the corrections to the *HR* scale found by the two methods are sensibly the same and that the initial values of the correction to the Harvard scale given in Table II are therefore probably near the truth. Further, since the *HR* and *Pv* scales for $m<4.0$ seem to be parallel, the constant correction required to reduce these stars to the photovisual system may be taken as -0.08 mag. This agrees well with the rather uncertain result found in section 3, and is the value given in the note to Table II.

Mount Wilson Observatory
October 1924

Contributions from the Mount Wilson Observatory, No. 289
Reprinted from the *Astrophysical Journal*, Vol. LXI, pp. 303–319, 1925

REDUCTION OF THE HARVARD-GRONINGEN *DURCHMUSTERUNG* TO THE INTERNATIONAL SYSTEM OF MAGNITUDE AND COLOR

By FREDERICK H. SEARES, MARY C. JOYNER, AND
MYRTLE L. RICHMOND

ABSTRACT

The data.—The *Durchmusterung* in *HA*, **101**, **102**, **103**, gives the brightness of stars in Selected Areas 1–206, to a limiting magnitude of about 16.0. Many of these appear in the Mount Wilson *Catalogue of Selected Areas*, which includes Areas 1–139. It is shown that the *Catalogue* is on the international photographic scale. The *Durchmusterung* can therefore be reduced to the latter scale by direct comparison of magnitudes for stars observed in common.

Color equation and scale correction for bright stars.—The *Durchmusterung* magnitudes for the northern hemisphere, measured with the Metcalf 16-inch telescope, are affected by a large color equation. This was determined from the central stars of the areas, whose color-indices are known. The complete reduction thus found from eighty stars for the Metcalf telescope before the objective was reground is

$$MW-DM=+0.06\ (DM-6)+0.21\,C\quad (m \lesseqgtr 10). \tag{9}$$

The scale-divergence is the same as that of *HA*, **71**, No. 3, as it should be.

Scale and color correction for faint stars.—Corrections for each area, for scale and color combined, were derived from the stars common to the two catalogues (Table III). With allowance for color equation based on the mean color-index of stars of different magnitudes, it is found that to $m=13$ the scale correction of the *DM* is the same as that of *HA*, **71**, No. 3 (Table IV), but for fainter stars there is an appreciable divergence. The fluctuations in the corrections from area to area are large, and obscure the systematic difference for stars of high and low galactic latitude, which depends on the fact that the former are redder than the latter. For statistical purposes the separate areas should be reduced to the international system with the aid of Table III.

The following discussion relates to the stars of the Harvard-Groningen *Durchmusterung of the Selected Areas*[1] included in the 139 regions on and north of declination −15°. The fields measured were 40′×40′, 60′×60′, or 80′×80′, according to galactic latitude. The *Durchmusterung* includes the stars in these fields to a limiting photographic magnitude of about 16.0.

These data form an important contribution to the study of stellar distribution, but, as they stand, cannot be combined with other results, since they are referred to the scale of *Harvard Annals*, **71**, No. 3, which deviates appreciably from the international scale.

---

[1] *Harvard Annals*, **101**, 1918; **102**, **103**, 1924.

Moreover, there is a difficulty in that about half of the photographs were made with the 16-inch Metcalf telescope, which is known to have a large color equation relative to most other instruments.[1] Referred to the international system,[2] the color equation is 20 or 25 per cent of the color-index; and since the mean color of the stars, grouped according to photographic magnitude for all galactic latitudes together, is represented by the linear relation[3]

$$C_p = -0.18 + 0.071 m_p \, , \qquad (1)$$

it follows that the effect of the color equation on star counts will be considerable and will enter as an additional disturbance of scale, which for the faint stars is of considerable importance. The remaining photographs for the *Durchmusterung* were made with the Bruce telescope whose color equation is still to be investigated.

The simplest method of determining the total systematic deviation from the international scale is to compare the magnitudes of the *Durchmusterung* with those of the Mount Wilson *Catalogue of the Selected Areas*.[4] The latter catalogue gives the photographic magnitudes, on the international scale, of all the stars in fields 23′ in diameter, centered on the central stars of Areas 1–139.

For stars fainter than the tenth or eleventh magnitude, the data are sufficient for a comparison of scales in individual areas. For the brighter objects, including chiefly the central stars, only the mean scale-divergence can be determined. As a matter of fact, the discussion can be carried somewhat farther, for the visual magnitudes of the central stars were measured by Professor Pickering with the 4-inch and 12-inch meridian photometers. Combined with the photographic magnitudes, these results give the colors of the individual stars, and hence permit a good determination of the color equation of the Metcalf telescope. With the aid of (1), the expression for mean color, it then becomes possible to separate the influence of color equation from the true scale-divergence and thus obtain a comparison of the scales of the *Durchmusterung* and *Harvard Annals*, **71**, No. 3, which are supposed to be identical.

---

[1] See Table II, *Mt. Wilson Contr.*, No. 98; *Astrophysical Journal*, **41**, 259, 1915. In this tabulation *MC* indicates the Metcalf telescope.

[2] As defined by the adopted photographic magnitudes of stars near the Pole given in *Trans. Internat. Astron. Union*, **1**, 69, 1922.

[3] *Mt. Wilson Contr.*, No. 287; *Astrophysical Journal*, **61**, 114, 1925.

[4] For an account of this catalogue, which is complete but not yet in print, see P. J. van Rhijn, *Third Report on the Progress of the Plan of Selected Areas*, Groningen, 1923; particularly, the Second Appendix, by F. H. Seares.

Because of the manner in which they were derived,[1] the magnitudes of the *Durchmusterung* are necessarily approximate; but, as far as probable error goes, they are of ample precision for statistical purposes. Nevertheless, their approximate character is disadvantageous for the determination of the color equation, and the uncertainty is increased by the fact that this calculation is based on stars brighter than the tenth magnitude, for which the photographic magnitudes, whether Harvard, Groningen, or Mount Wilson values, are much less reliable than those of the fainter stars. The large differences affecting many of the stars are therefore not unexpected.

I. AGREEMENT OF THE MOUNT WILSON *Catalogue of Selected Areas* WITH THE INTERNATIONAL SCALE

Since the reduction of the *Durchmusterung* to the international scale depends upon its relation to the Mount Wilson *Catalogue*, it is important to show that this catalogue is really in agreement with the international system. Such agreement is to be expected, since the scale for the *Catalogue* was established in each area independently by the methods used in deriving the Mount Wilson magnitudes at the Pole,[2] which are known to be on the international scale.[3] The matter can be tested by means of the polar comparison photographs which were used to determine the zero-points of the scales in the individual areas. Thirty-seven of the fields, uniformly distributed over the northern heavens, were directly connected with the Pole by duplicate plates. These have been used to transfer the scale of the polar stars to the areas themselves for comparison with the scales adopted for the *Catalogue*. The magnitude interval thus covered is less than that of the *Catalogue*, because the comparison exposures were short, but sufficient for the present purpose. The mean result of this comparison for the thirty-seven fields is as follows:

---

[1] *Harvard Annals*, **101**, ix, 1918.

[2] *Mt. Wilson Contr.*, No. 97; *Astrophysical Journal*, **41**, 206, 1915.

[3] *Trans. Internat. Astron. Union*, **1**, 69, 1922.

Med. mag.	10.5	11.5	12.5	13.5	14.5	15.5	16.5
Int. Sc.–MW Cat.	+0.09	−0.05	−0.01	+0.01	0.00	0.00	+0.05
No. diff.	16	75	181	381	519	401	70

With the exception of the first difference, for which the images on the comparison photographs are too large for reliable measurement, the corrections to the *Catalogue* necessary for reduction to the international system are negligible. This applies to zero-point as well as to scale errors.

2. COLOR EQUATION AND SCALE ERROR FOR THE BRIGHT STARS OF THE *Durchmusterung*

Forty of the 139 areas were photographed with the Bruce telescope; sixteen others were photographed with the Metcalf instrument after the regrinding of the objective. For the central stars of two others (Nos. 42, 48) there are no Mount Wilson magnitudes, while for a third (No. 30), the central star was measured as a double at Mount Wilson and a single star at Groningen. This leaves a total of eighty regions for the determination of the color equation of the Metcalf telescope and the scale error for the bright stars. Central stars in 39 of the areas photographed with the Bruce telescope (that in No. 126 was not measured at Mount Wilson) are also available for the discussion of the color equation, but these lead to no definite result. The magnitudes of about half of these stars are Harvard standards, supplied by Professor Pickering apparently on the basis of measures with the Metcalf telescope, while the others must also be influenced by the color equation affecting the standards.

The data for the central stars observed with the Metcalf objective in its original state are listed in Table I, the first four columns of which give in succession the number of the area, the Mount Wilson photographic magnitude, and the Harvard photographic and visual magnitudes taken from *Harvard Annals*, **101**, xlviii; **102**, vi. The sixth column gives the value of the color-index $C_1 = MWPg - HV$, and the eighth column, the difference between

TABLE I

Central Stars—Metcalf Telescope, Original Objective

S.A.	*MWPg*	*HPg*	*HV*	V_0	C_1	*C*	*MWPg*−*HPg*
1	7.23	7.11	7.01	7.07	0.22	0.19	+0.12
3	8.51	8.64	8.62	8.84	−0.11	−0.38	− .13
4	9.94	9.37	8.41	8.60	1.53	1.55	+ .57
5	9.35	9.16	8.60	8.82	0.75	0.61	.19
6	10.49	10.10	8.91	9.15	1.58	1.55	.39
8	8.84	8.18	8.11	8.27	0.73	0.66	.66
10	8.89	8.76	8.59	8.81	0.30	0.09	.13
11	8.30	7.93	7.14	7.21	1.16	1.26	.37
12	8.64	8.48	8.17	8.33	0.47	0.36	+ .16
13	7.83	8.05	7.17	7.25	0.66	0.67	− .22
14	10.50	10.14	9.22	9.48	1.28	1.18	+ .36
15	9.98	9.55	8.35	8.53	1.63	1.68	.43
16	9.16	8.69	7.92	8.06	1.24	1.28	.47
17	9.05	8.44	7.51	7.61	1.54	1.67	.61
20	8.97	8.63	8.66	8.89	0.31	0.09	.34
21	10.03	9.50	8.53	8.74	1.50	1.50	.53
23	8.83	7.86	7.52	7.62	1.31	1.40	.97
24	10.28	9.81	8.92	9.16	1.36	1.30	.47
25	9.29	9.17	8.97	9.22	0.32	0.08	.12
26	10.47	10.15	9.35	9.61	1.12	1.00	.32
27	10.40	9.82	9.00	9.25	1.40	1.33	.58
28	10.59	9.93	9.06	9.21	1.53	1.60	.66
29	8.78	8.60	8.28	8.46	0.50	0.37	.18
31	9.49	9.24	8.72	8.95	0.77	0.63	.25
32	9.71	9.35	8.89	9.13	0.82	0.67	+ .36
33	9.40	9.42	9.02	9.27	0.38	0.15	−0.02
34	9.63	8.37	7.86	7.99	1.77	1.90	+1.26
35	10.85	9.63	8.91	9.15	1.94	1.97	1.22
36	9.34	9.00	8.75	8.98	0.59	0.42	0.34
37	10.58	9.71	9.20	9.46	1.38	1.30	.87
38	9.71	9.30	8.24	8.41	1.47	1.51	.41
39	9.16	9.02	8.06	8.21	1.10	1.10	.14
40	9.84	9.53	8.66	8.88	1.18	1.11	.31
41	10.06	9.84	9.31	9.57	0.75	0.57	.22
43	10.10	9.75	8.25	8.42	1.85	1.95	.35
44	8.96	8.78	8.70	8.93	0.26	0.03	.18
45	9.00	8.86	8.18	8.36	0.82	0.74	.14
46	9.51	9.19	8.36	8.53	1.15	1.11	+ .32
49	9.90	9.93	8.71	8.94	1.19	1.11	− .03
50	8.55	8.09	8.04	8.19	0.51	0.42	+ .46
51	10.71	10.05	9.56	9.82	1.15	1.03	.66
52	8.53	8.35	8.08	8.24	0.45	0.34	.18
54	10.23	9.53	9.26	9.52	0.97	0.82	.70
55	10.08	9.47	8.68	8.91	1.40	1.36	.61
56	10.13	9.53	8.23	8.40	1.90	2.01	.60
57	9.01	8.83	8.53	8.73	0.48	0.32	.18
58	9.72	9.35	7.68	7.80	2.04	2.23	.37
59	9.42	9.34	9.01	9.26	0.41	0.19	.08
60	9.50	9.30	8.57	8.78	0.93	0.84	.20
61	9.56	9.06	8.94	9.19	0.62	0.43	0.50
62	8.36	7.20	7.05	7.12	1.31	1.44	1.16
63	9.61	8.90	9.14	9.40	0.47	0.24	+0.71

TABLE I—*Continued*

S.A.	*MWPg*	*HPg*	*HV*	V_e	C_1	*C*	*MWPg*−*HPg*
64	8.31	8.12	7.62	7.73	0.69	0.67	+0.19
65	9.45	9.04	8.88	9.12	0.57	0.38	.41
66	10.10	9.68	9.04	9.29	1.06	0.94	.42
67	9.67	8.98	8.20	8.37	1.47	1.51	.69
68	9.08	8.13	8.27	8.45	0.81	0.73	.95
69	8.14	7.97	7.39	7.49	0.75	0.75	.17
70	8.20	7.63	7.90	8.04	0.30	0.19	.57
71	9.74	9.36	8.65	8.87	1.09	1.01	.38
72	6.89	6.82	6.22	6.24	0.67	0.75	.07
73	8.34	7.94	8.14	8.30	0.20	0.04	.40
74	8.89	8.86	9.13	9.38	−0.24	−0.57	.03
75	9.62	9.37	8.48	8.68	1.14	1.09	.25
76	9.57	9.09	9.03	9.28	0.54	0.34	.48
77	8.66	8.57	8.19	8.36	0.47	0.35	.09
78	9.58	9.43	8.40	8.59	1.18	1.15	.15
79	9.60	9.09	8.37	8.56	1.23	1.21	.51
80	8.53	8.35	8.21	8.38	0.32	0.17	.18
81	10.29	9.81	9.14	9.40	1.15	1.03	.48
82	9.74	9.44	8.26	8.44	1.48	1.51	.30
83	9.25	9.21	8.58	8.80	0.67	0.52	.04
84	8.82	8.65	8.52	8.72	0.30	0.12	.17
85	9.37	8.82	8.28	8.46	1.09	1.06	.55
86	10.49	9.69	9.18	9.44	1.31	1.22	.80
87	9.66	9.01	8.05	8.20	1.61	1.69	.65
88	8.82	8.16	8.66	8.88	0.16	−0.07	.66
89	8.70	8.22	8.11	8.27	0.59	0.50	+ .48
90	9.04	9.12	9.03	8.27	0.01	−0.28	− .08
100	9.27	9.06	8.49	8.69	0.78	0.67	+0.21

the Mount Wilson and Harvard photographic magnitudes. These differences include the influence of scale error, color equation, and the large accidental errors to which reference has been made. The fifth and seventh columns require more detailed explanation.

A reference to the sixteenth column of Table I of the *Report of the Commission on Stellar Photometry*[1] shows the existence of an appreciable difference between the Harvard visual and Mount Wilson photovisual scales and color systems. The matter is discussed in detail in *Contribution* No. 288, and there can be little doubt that the Harvard magnitudes require corrections for scale and color of the order of those given in Table II and under (2) in that paper. The scale correction has its maximum value between the ninth and tenth magnitudes, in the region where measures made with the 12-inch meridian photometer overlap those made with the 4-inch photometer. The color equation seems to increase with the magnitude.

---

[1] *Trans. Internat. Astron. Union,* 1, 71, 1922.

For the present purpose, however, which is that of freeing the color-indices of the central stars of the Selected Areas from systematic errors, a constant mean value of the color equation is ample, and the formula for reduction to the photovisual system may be written

$$Pv = HV + \text{Table II, } \mathit{Contr.}\ 288 - 0.139\,C\,, \tag{2}$$

in which C is the color-index on the international system.

It is not certain that (2) is strictly applicable to the Harvard magnitudes in Table I. Whether this is the case or not probably depends on the manner in which measures with the two meridian photometers have been combined, and possibly on other factors as well. On this account, a double reduction has been made, using both the corrected and uncorrected values of the Harvard visual magnitudes.

For the actual discussion it is the corrected color-indices and not the visual magnitudes themselves that are required. The index C_1, corresponding to the uncorrected magnitudes, has already been found. The values of C, based on the corrected visual magnitudes, were derived as follows: The values of HV corrected for scale error are given in the fifth column of Table I under the heading V_c.[1] Introducing V_c into (2), we have

$$Pv = V_c - 0.139\,C\,. \tag{3}$$

Further, for data on the international system,

$$Pg - Pv = C\,, \tag{4}$$

whence

$$C = 1.16\,(Pg - V_c)\,. \tag{5}$$

The values of C in the seventh column of Table I were calculated with this formula, using for Pg the Mount Wilson value, $MWPg$, given in the second column of the table.

The relation between the differences $MWPg - HPg = n$, given in the last column of Table I, and the coefficients of the scale and color corrections to the *Pg* scale of the *Durchmusterung* can be expressed in the form

---

[1] As a matter of fact, the scale corrections actually used were provisional values, differing in some cases by 0.02 or 0.03 mag. from those in Table II of *Contribution* No. 287. The differences are of no consequence for the present discussion.

$$x+ym+zC=n\,. \tag{6}$$

The three unknowns, x, y, z, cannot be determined simultaneously, however, because of an inherent uncertainty in the solution. A preliminary examination showed that the scale coefficient y is very nearly 0.06, in agreement with the known error of the scale of *Harvard Annals*, 71, No. 3. Since the range in m is not great, it is convenient to adopt this provisional value of y and reduce all the differences n to $m=9$. Equation 6 accordingly becomes

$$x+zC=n-0.06\,(m-9), \tag{7}$$

where x is now the difference between the two scales at the ninth magnitude, corrected for color equation.

For the application of (7) the data for the eighty stars were combined into twelve groups, arranged according to *HPg* and C (or C_1). The corrections arising from the last term in (7) do not exceed 0.05 or 0.06 mag., so that any error in the assumed value of y is unimportant.

Least-squares solutions for x and z thus gave

HV Uncorrected	*HV* Corrected	
$x=+0.154$	$x=+0.199$	(8)
$z=+0.243$	$z=+0.211$	

These results are a sufficient indication of the influence on the reduction of the difference between the Harvard visual and the Mount Wilson photovisual scales. For the further calculation the corrected *HV* series is used as the more probable of the two.

To investigate the coefficient y, which measures the scale-divergence, the original differences in the last column of Table I were corrected for color equation by subtracting from each the quantity 0.211 C, and then grouped according to Harvard photographic magnitude. The means for four groups are shown in the first two and the last two lines of Table II (first and second columns). Seven discordant differences were excluded (Areas 8, 23, 62, 68, 70, and 88) from the first group, and that for Area 63 from the second. For the first group in particular, the discordant differences are so large that there can be no question of their abnormality, which doubtless arises from the brightness of the stars. The results in parentheses in Table II are from (8), in which x is the scale difference at the ninth magnitude derived from all the stars.

TABLE II

SCALE-DIVERGENCE OF *Durchmusterung* FOR BRIGHT STARS

Mean *HPg*	*MW−HA* 101	No. Stars	*O−C*
8.00	+0.10	14	−0.02
8.74	.15	13	− .01
(9.00)	(.20)	(80)	(+ .02)
9.23	.12	26	− .07
9.78	+0.24	20	+0.01

The representation of the differences in the second column of Table II by the term $+0.06\ (HPg-6)$ is shown in the last column of the table. The residuals are satisfactorily small and show that the magnitudes of the bright stars of the *Durchmusterung*, after correction for color equation, are really in agreement with the scale of *Harvard Annals*, **71**, No. 3. This follows from the fact that the divergence of the latter from the Mount Wilson photographic scale for $m<10$ was shown in *Contribution* No. 98[1] to have the form $+0.061\ (HPg-6)$. Since the Mount Wilson results are on the international system, the complete reduction to this system of the bright stars in the areas of the *Durchmusterung* photographed with the Metcalf telescope before regrinding is therefore

$$+0.06\ (DM-6)+0.21\ C, \tag{9}$$

which applies for $m \lesseqgtr 10$.

Strictly speaking, a knowledge of this correction is not in itself of much importance because of the small number of stars to which it is applicable. The value of the discussion is in the information it gives as to the scale of the *Durchmusterung* and the color equation of the instrument. The latter, it should be repeated, refers to data obtained before the objective was reground.

---

[1] *Astrophysical Journal*, **41**, 259, 1915.

An attempt has been made to determine the effect of regrinding upon the color equation by discussing the sixteen areas photographed after this had been done. The color coefficient is perhaps a little smaller than was previously the case, but the result is very uncertain. The main conclusion is that the scale difference for these particular areas is about 0.2 mag. greater than that found above, an irregularity not easily explained.

3. CORRECTION FOR THE FAINT STARS OF THE *Durchmusterung*

As already mentioned, the faint stars are numerous enough to permit a direct comparison of scales for each area. Since the colors of individual stars are unknown, color equation cannot be allowed for, and what is obtained is the mean difference between the *Durchmusterung* scale, affected by color equation, and the international photographic scale. The corrections thus obtained will answer for a statistical treatment of the data; but used for individual stars, they may give results considerably in error.

The results for each of Areas 1–139 are in Table III, which gives the corrections, in hundredths of a magnitude, for the statistical reduction of the *Durchmusterung* values to the international system. An asterisk following the number of an area in the first column indicates regions photographed with the Metcalf telescope after regrinding; a dagger, those photographed with the Bruce telescope. All other areas were observed with the original objective of the Metcalf telescope. The arguments at the heads of the columns are *Durchmusterung* magnitudes. The numbers of stars given in the last column are the totals used in deriving the corrections. In rich regions these do not always represent the totals common to the two catalogues, although available data have not been omitted unless really superfluous. For example, all the stars brighter than the twelfth or thirteenth magnitude, which at best are none too numerous, were used. The tabular corrections themselves are the ordinates of smooth curves drawn through plots of the differences $MW-HA$ 101, which were made for each of the areas.

TABLE III

Area	Lat.	10.0	10.5	11.0	11.5	12.0	12.5	13.0	13.5	14.0	14.5	15.0	15.5	16.0	16.5	17.0	No. Stars
1	+28°	....	....	....	+29	+34	+37	+41	+44	+48	+49	+50	+50	+50	....	....	40
2*	13	....	....	+47	47	43	38	32	26	18	11	4	− 2	−11	....	....	115
3	17	....	....	49	49	48	46	45	40	37	33	27	+20	....	....	....	74
4	32	....	....	48	48	46	41	38	36	30	27	22	14	....	....	....	54
5	42	+64	+64	65	65	66	68	70	74	78	83	89	....	....	....	....	34
6	36	33	32	29	26	24	23	23	21	20	20	20	18	....	....	....	34
7*	+20	....	....	58	58	57	56	51	45	38	37	39	38	+31	+18	....	121
8	− 3	48	48	49	50	50	50	48	54	63	60	54	50	....	....	....	157
9*	+ 2	....	....	....	40	47	53	56	58	56	52	45	32	16	− 5	....	103
10	13	....	....	58	63	70	75	77	68	53	43	40	43	45	....	....	93
11	26	....	49	51	53	54	52	50	48	46	44	41	38	34	....	....	75
12	41	....	....	56	54	50	47	42	39	35	31	30	28	....	....	....	25
13	53	....	....	2	4	8	10	11	12	14	15	18	19	....	....	....	25
14	57	....	33	33	32	32	32	32	32	32	34	32	....	....	....	....	23
15	48	....	....	30	30	30	30	28	23	20	18	21	18	13	+ 4	....	49
16	33	....	74	74	74	72	70	63	47	37	24	14	4	....	....	....	35
17	19	....	74	73	71	67	58	49	45	44	42	37	30	....	....	....	89
18*	+ 6	....	....	....	39	41	41	40	37	33	26	18	11	4	− 6	....	213
19*	− 1	....	....	....	3	9	16	25	28	32	36	40	43	38	....	....	141
20	18	....	....	20	22	25	27	26	27	25	24	19	13	4	....	....	85
21	17	....	....	41	41	42	41	40	40	40	40	41	41	41	....	....	108
22*	13	....	....	....	41	44	48	52	62	64	56	49	43	35	+29	....	160
23	− 7	....	....	19	38	51	53	47	42	39	40	43	41	40	....	....	88
24	0	....	....	48	50	53	52	50	44	37	38	43	+47	+43	....	....	110
25	+ 8	....	27	31	36	40	44	41	33	24	13	3	−12	−27	....	....	81
26	18	....	....	49	48	46	40	33	25	22	21	25	+28	....	....	....	68
27	28	53	52	50	47	41	36	32	27	28	28	27	27	....	....	....	52
28	39	....	+21	31	40	46	48	50	46	44	41	35	29	....	....	....	38
29	49	....	−15	0	12	24	30	29	+28	+31	33	36	38	+40	....	....	34
30	60	....	....	....	7	9	5	2	− 1	− 3	3	15	22	+26	....	....	31
31	68	....	....	28	26	+24	20	18	+17	+16	13	10	6	− 1	....	....	26
32	72	....	....	....	....	− 6	3	8	11	12	10	6	0	−11	−23	....	32
33	68	....	....	45	43	+42	42	42	40	39	38	38	36	+30	....	....	30
34	59	....	+33	33	33	33	31	34	34	37	39	38	30	18	....	....	39
35	49	....	....	56	66	78	82	78	67	58	53	44	32	22	....	....	43
36	39	....	....	38	38	37	36	35	32	30	29	37	+40	....	....	....	49
37	28	....	85	89	88	82	68	53	37	24	15	7	− 3	....	....	....	57
38	18	....	....	27	36	44	51	52	49	42	34	25	+14	2	....	....	106
39	+ 9	....	....	23	32	37	40	38	34	29	29	34	37	+30	....	....	206
40	0	....	12	19	26	33	40	45	43	37	29	19	8	− 6	....	....	118
41	− 8	....	14	+23	29	33	33	38	40	39	34	29	24	....	....	....	144
42	13	....	....	−18	0	13	25	32	34	+31	29	26	21	+15	....	....	112
43	16	+12	+17	+24	+30	+31	+28	+17	+ 1	−10	7	+38	+52	....	....	....	72
44	−32	....	....	−30	−19	−12	− 8	− 7	− 1	+ 7	+ 6	− 6	−22	−44	....	....	51

*Observed with Metcalf Telescope after regrinding objective.

TABLE III—*Continued*

Area	Lat.	10.0	10.5	11.0	11.5	12.0	12.5	13.0	13.5	14.0	14.5	15.0	15.5	16.0	16.5	17.0	No. Stars
45	−32	....	+43	+45	+47	+47	+45	+47	+48	+49	+46	+43	+32	....	....	....	56
46	27	....	....	32	44	53	60	61	57	50	40	28	16	+ 1	....	....	55
47*	21	....	....	....	....	....	....	....	....	1	6	11	18	21	+17	....	13
48	12	....	....	....	62	63	63	61	56	51	45	41	37	32	....	....	71
49	− 2	....	10	27	41	53	58	59	60	60	60	60	60	60	....	....	234
50	+10	....	....	59	58	56	54	52	52	58	66	73	+63	47	....	....	167
51	22	....	....	38	42	44	46	43	39	33	24	12	−10	....	....	....	78
52	34	....	....	31	31	33	34	32	26	19	16	17	+20	24	....	....	58
53*	47	....	....	....	....	17	19	19	20	27	36	53	64	69	....	....	41
54	60	....	50	50	48	46	44	40	42	44	48	50	50	....	....	....	24
55	74	....	34	35	35	35	36	36	42	50	57	60	....	....	....	....	23
56	80	....	....	38	38	37	36	33	30	27	26	23	18	+14	....	....	30
57	85	....	....	....	80	77	73	65	52	37	22	11	+ 3	− 6	....	....	30
58	73	....	....	23	23	23	21	19	16	11	6	0	−10	−19	....	....	26
59	59	....	....	....	49	49	52	49	39	22	8	0	+ 7	+ 6	− 8	....	43
60	48	....	....	42	41	38	34	29	24	20	15	10	7	2	....	....	42
61	34	....	20	27	32	32	29	26	23	23	30	37	42	46	....	....	71
62	23	....	....	....	36	46	50	44	37	24	16	11	+10	4	− 7	....	111
63	+10	+33	43	49	51	50	43	32	18	6	1	0	− 4	....	....	....	142
64	− 1	....	29	41	51	55	57	58	56	51	46	40	+34	27	....	....	277
65	12	....	....	22	28	31	33	37	33	31	25	19	11	....	....	....	90
66	20	....	....	36	36	32	30	29	28	29	34	38	29	+16	....	....	88
67	28	....	69	67	63	54	45	39	31	28	28	26	....	....	....	....	47
68	47	....	30	31	32	31	29	26	22	17	15	9	0	....	....	....	36
69	47	....	57	59	60	60	65	66	64	58	44	26	....	....	....	....	22
70	42	....	....	55	55	55	56	56	56	50	37	24	+ 5	−16	....	....	27
71	34	....	....	24	27	29	26	25	20	14	10	3	− 4	−12	....	....	36
72	24	....	....	....	....	....	....	20	20	16	17	18	+17	+13	+ 2	....	31
73	−12	....	....	65	66	68	68	65	54	35	17	8	9	30	....	....	60
74	+ 1	....	15	25	36	44	49	51	50	50	50	45	41	34	....	....	81
75	14	....	....	....	63	62	56	50	45	42	42	39	+35	30	....	....	115
76	27	....	....	....	....	37	32	27	21	15	9	1	−12	....	....	....	42
77	39	....	....	12	12	10	9	6	4	4	6	11	+15	20	....	....	37
78	54	....	....	7	9	11	17	21	28	39	44	+46	+50	+50	....	....	25
79	67	....	....	37	34	32	29	22	17	9	1	− 7	−14	−22	....	....	25
80	76	....	....	....	37	38	37	36	25	15	3	−17	−28	−39	−43	....	21
81	76	....	....	34	34	36	37	38	42	43	38	+30	+17	0	....	....	26
82	66	....	....	29	29	28	28	28	28	28	28	29	30	+34	....	....	18
83	54	....	....	23	24	24	23	19	16	16	16	15	14	9	....	....	42
84	40	....	....	63	59	52	43	32	22	13	9	9	9	9	....	....	57
85	27	....	43	43	41	40	39	36	37	32	26	18	8	....	....	....	55
86	15	....	....	42	44	45	45	45	44	41	34	27	28	38	....	....	103
87	+ 1	....	....	50	50	52	50	48	44	38	34	30	27	23	+22	....	143
88	−12	....	40	39	39	37	34	29	23	25	33	33	27	18	....	....	215
89	−23	....	+23	+22	+21	+20	+18	+20	+25	+30	+34	+40	+37	+27	....	....	90

90	−34	....	....	+61	+59	+54	+46	+41	+41	+41	+44	+44	+45	+42	....	....	64
91*	43	....	....	....	....	....	29	29	28	22	18	19	24	30	+28	+20	83
92*	62	....	....	....	43	49	50	51	51	50	46	40	32	18	....	....	40
93*	58	....	....	....	54	54	51	48	41	35	32	41	46	46	41	....	51
94*	49	....	....	....	44	44	47	50	50	46	43	44	43	35	22	....	51
95*	38°	....	....	....	....	56	54	51	46	42	40	46	52	54	54	....	33
96*	25	....	....	....	22	22	29	32	34	32	33	33	34	30	+23	....	69
97*	−11	....	....	+39	39	41	37	34	37	42	47	50	45	32	....	....	48
98*	+ 1	....	....	34	36	37	40	43	40	35	28	+23	16	+ 5	−10	....	234
99†	15	+46	+46	48	50	50	45	37	26	17	8	− 4	....	....	....	....	79
100	28	....	....	....	67	66	64	59	52	44	35	+25	12	− 8	....	....	87
101†	41	....	....	....	46	45	44	43	43	39	32	24	11	− 3	....	....	40
102†	52	....	....	....	....	67	63	62	57	51	45	43	36	+32	+29	....	78
103†	60	....	....	44	44	43	42	40	38	34	26	18	26	34	44	....	50
104†	62	....	....	....	39	41	45	48	48	42	32	24	20	18	19	....	61
105†	60	....	....	....	....	17	20	20	20	19	16	12	15	22	32	....	57
106†	51	....	....	....	79	80	82	80	76	71	63	55	54	54	....	....	88
107†	41	....	....	61	61	61	59	51	45	36	+27	+29	+66	80	....	....	66
108†	28	....	70	70	69	64	54	44	32	13	− 5	−18	− 4	55	....	....	155
109†	14	....	....	....	43	43	46	47	49	47	+38	+20	+ 7	4	28	....	176
110†	+ 1	....	....	36	36	35	34	35	36	34	29	26	36	49	53	....	44
111†	−11	....	....	....	105	98	86	72	53	44	43	42	41	44	46	....	228
112†	25	....	....	....	14	21	31	40	44	42	37	30	29	30	+27	+24	178
113†	38	....	....	....	42	38	33	25	19	14	14	16	18	19	....	....	66
114†	49	....	....	....	36	38	40	41	40	38	36	34	32	30	....	....	57
115†	58	....	....	67	64	64	62	62	57	49	43	+41	+42	+45	....	....	41
116†	76	....	....	....	....	36	31	22	15	8	2	− 7	−19	−23	−24	−24	31
117†	75	....	....	....	....	....	46	46	43	40	43	+47	+50	+48	....	....	37
118†	65	....	....	....	29	32	32	29	24	19	14	10	+ 3	− 3	15	....	29
119†	53	....	....	....	....	45	43	40	33	20	12	1	− 4	− 9	14	....	39
120†	40	+33	35	35	37	41	43	45	52	54	53	49	....	....	....	....	28
121†	26	....	....	....	....	....	33	32	29	25	20	18	+17	+12	0	....	85
122†	−13	....	....	....	28	34	35	34	29	30	40	+46	+42	+29	....	....	120
123†	0	....	....	33	32	28	22	17	+15	+10	0	−18	−31	−30	....	....	260
124†	+13	....	....	16	16	14	8	1	− 4	− 6	+ 2	+18	+31	....	....	....	155
125†	24	....	+27	+27	26	24	22	19	+13	+ 4	− 6	−22	−29	−23	....	....	84
126†	35	....	....	....	11	21	33	34	30	26	+25	+25	+36	+48	....	....	57
127†	42	....	....	....	....	+30	30	25	+18	+ 3	− 7	−41	−56	−66	68	....	51
128†	47	....	....	....	....	....	6	0	−13	−26	−41	−53	−62	−65	68	71	72
129†	47	....	....	....	....	....	61	56	+47	+33	+18	+16	+24	+40	....	....	80
130†	42	....	....	....	....	− 7	4	9	15	17	11	2	−11	−20	17	....	78
131†	34	....	....	....	....	+30	33	34	30	23	16	9	+ 5	0	−11	18	109
132†	24	....	....	....	....	2	17	30	41	53	54	49	40	+24	+16	5	124
133†	+12	....	....	....	....	59	58	55	52	49	47	40	40	45	....	....	121
134†	0	....	....	....	52	55	60	67	66	57	43	31	17	4	− 4	....	383
135†	−14	....	....	....	41	43	46	48	51	52	50	44	32	17	....	....	288
136†	26	....	....	....	+38	39	39	38	35	32	30	28	26	20	+13	....	120
137†	40	....	....	....	....	30	32	34	30	27	20	14	6	2	− 2	− 5	114
138†	53	....	....	....	....	68	64	55	45	34	23	22	36	59	+64	....	81
139†	−66	....	....	....	....	+72	+70	+65	+58	+57	+57	+53	+49	+48	+45	....	40

---

†Observed with Bruce telescope.

Examination of the curves shows that the accidental errors are large, and that the correction curves differ much from area to area. The average deviation of the plotted points from the curves, which represents the combined accidental error of the two catalogues, was formed for eleven areas, Nos. 1, 11, 21 . . . . , 101, with results as follows:

±0.27, 0.20, 0.18, 0.26, 0.22, 0.19, 0.22, 0.16, 0.19, 0.16, 0.16,

or an average of about ±0.20 mag.

Since the probable error of a Mount Wilson magnitude, including scale error, ranges from 0.04 to 0.08 mag., according to the number of images measured, it follows that the larger part of the accidental error is in the *Durchmusterung* magnitude. This is to be expected, however, for the values of these magnitudes depend on one, or at most two, images measured on a single plate and reduced with standards whose values were found by a method which cannot be expected to give high precision.

The fluctuations in the correction curves from area to area represent the combined effect of scale errors in the catalogues. The Mount Wilson results are means based on six separate determinations of the scale in each area. The *Durchmusterung* depends on standard stars whose magnitudes were determined at Harvard with the aid of a relation between magnitude and scale reading of images found from three plates, taken from each box of twelve, and exposed on the Polar Sequence. The mean reduction curve for the three plates was used to determine the magnitudes of the standards on the nine remaining plates, which were exposed directly to the areas. Although the twelve plates were developed together, gradation differences from plate to plate seem to have affected the results appreciably.

In *Contribution* No. 287 it is shown that the mean color-index of the stars of the sixth photographic magnitude increases about 0.25 mag. in passing from the galaxy to the galactic pole, and that for the stars of the fourteenth magnitude or fainter the increase is probably larger. Since the color equation of the Metcalf telescope is +0.21 *C*, the total correction to the *Durchmusterung* should be systematically larger for stars in high galactic latitudes than for those near the Milky Way.

To see whether this difference, apparently of the order of 0.10 mag., can be detected, the corrections in Table III for the eighty-three areas observed with the Metcalf telescope in its original state were collected in four groups arranged according to the galactic latitude given in the second column of the table. The mean corrections for all the areas are in the second column of Table IV, while the deviations for each of the four groups, in the sense, Group *minus* Mean, are in the columns immediately following. The figures in parentheses indicate the number of areas included in each value.

The deviations for the second and third groups are small and show no important systematic effect. The first and third, however, diverge systematically, but in the direction opposite to that to be expected from the known difference in the average color of stars in high and low latitudes. Since the color equation is positive and the stars near the galactic pole are redder than those in the Milky Way, the corrections for the fourth group should be the largest, whereas this is actually the case for the first group. There is no obvious explanation of this anomaly.

Mean corrections for the areas observed with the Metcalf telescope after regrinding and with the Bruce telescope were also formed. Their deviations from the corrections in the second column of Table IV are in the seventh and eighth columns, respectively.

With the aid of (1), which gives the mean color-index for a grouping according to photographic magnitude, and the color equation $+0.211\,C$ from (8), it is possible to separate the scale-divergence from the values of the total mean correction in the second column of Table IV. The color corrections thus found, which are to be subtracted, are in the ninth column, and the resulting scale-divergence from the international system, in the tenth column. The following columns, on the other hand, give the scale reduction to the international system for the Harvard magnitudes of the Polar Sequence stars in *Harvard Annals*, **71**, No. 3, after correction for color. These quantities are smoothed values of the differences $MW - HH_w$, derived from Table III of *Contribution* No. 98.[1] The differences in the last col-

---

[1] *Astrophysical Journal*, **41**, 259, 1915.

TABLE IV

Comparison of Systematic Corrections

Harv.-Gron. *DM* Mag.	Mean Total Correction	Correction for Groups				Metcalf Reground	Bruce Telescope	Color Corrn.	Mean Scale Corrn.	*Pg* − *HA* 71	Red. to *HA* 71
		0°–15°	16°–28°	32°–49°	53°–85°						
10.0.........	+0.40(6)	0(2)	− 8(2)	+ 8(2)	....	....	0(2)	0.12	+0.28	+0.24	+0.04
10.5.........	.38(30)	−12(9)	+14(8)	− 2(9)	0(4)	....	+ 6(4)	.12	.26	.24	.02
11.0.........	.37(71)	− 2(19)	7(16)	+ 1(22)	− 7(14)	+ 7(4)	7(10)	.13	.24	.24	.00
11.5.........	.41(80)	+ 2(21)	4(19)	− 1(22)	9(18)	− 2(12)	2(24)	.14	.27	.24	.03
12.0.........	.41(82)	6(21)	4(20)	0(22)	11(19)	− 1(14)	1(36)	.15	.26	.24	.02
12.5.........	.41(82)	8(21)	+ 2(20)	1(22)	11(19)	0(15)	0(40)	.16	.25	.24	+ .01
13.0.........	.39(83)	9(21)	0(21)	1(22)	10(19)	+ 2(15)	1(40)	.16	.23	.24	− .01
13.5.........	.35(83)	9(21)	0(21)	0(22)	8(19)	5(15)	+ 1(40)	.17	.18	.24	.06
14.0.........	.32(83)	8(21)	− 1(21)	0(22)	6(19)	4(16)	− 1(40)	.18	.14	.24	.10
14.5.........	.30(83)	7(21)	1(21)	1(22)	6(19)	4(16)	5(40)	.18	.12	.24	.12
15.0.........	.27(83)	7(21)	− 1(21)	1(22)	6(19)	8(16)	8(40)	.19	.08	.23	.15
15.5.........	.21(78)	9(21)	0(20)	3(20)	6(17)	13(16)	− 3(38)	.20	+ .01	.20	.19
16.0.........	+ .16(55)	12(17)	+ 1(11)	− 4(12)	10(15)	12(16)	+ 2(37)	.20	− .04	.16	.20
16.5.........	−0.08(7)	+30(1)	+ 6(2)	+12(1)	−17(3)	+27(11)	+17(22)	0.21	−0.29	+0.13	−0.42

umn represent the mean correction for scale required to reduce the *Durchmusterung* to *Harvard Annals*, 71, No. 3. To about magnitude 13.5 the corrections are negligible, and show that the scales are dentical, as was intended. For the fainter stars, however, there is an appreciable divergence. This seems to be less pronounced for the areas observed with the Metcalf reground and the Bruce telescope, although the uncertain color equations for these instruments make quantitative estimates unreliable.

From this discussion it is clear that the corrections for individual areas given in Table III fluctuate to such an extent as to obscure the differential effect of color and make it unwise to attempt to use a mean reduction curve except in certain special cases. For general statistical purposes it is probably safer to correct the scales of the separate areas by means of the data in Table III. Finally, it should be remarked that only a small part of these fluctuations can originate in the zero-point errors of the Mount Wilson magnitudes. Great care was taken to make these results homogeneous in the matter of zero-point,[1] and the internal agreement is such as to indicate that the errors affecting the individual areas are very small.

MOUNT WILSON OBSERVATORY
October 1924

---

[1] See *Third Report on the Progress and Plan of the Selected Areas*, Second Appendix, Groningen, 1923.

Contributions from the Mount Wilson Observatory, No. 290

THE PHOTOGRAPHIC DETERMINATION OF STELLAR PARALLAXES WITH THE 60- AND 100-INCH REFLECTORS

EIGHTH SERIES

By ADRIAAN VAN MAANEN

ABSTRACT

Trigonometric parallaxes determined with the 60-inch and the 100-inch reflectors.—The detailed measurements are given for twenty-five fields, including twenty-eight stars and nebulae. The star H.D. 7307 was put on the program as an M-type object which might have an absolute magnitude between the giants and dwarfs. The parallax here derived makes its absolute magnitude +3.9. α Arietis, Lalande 26289, γ Draconis, Groombridge 2875, β Delphini, and Lalande 43492 were included on account of the discordance in the older parallax determinations. The list contains seven faint Wolf stars having large proper motions, Nos. 134, 219, 358, 629, 630, 851, 922; the photographic absolute magnitudes range from +9.9 to +14.7. The list further contains two novae, Nova Ophiuchi 1919 and Nova Cygni 1920, for which the relative parallaxes are −0″005 and +0″003, respectively, and three planetary nebulae, B.D.+30°3639, N.G.C. 7027, and N.G.C. 7635, for which the relative parallaxes found are 0″000, +0″008, and +0″016, respectively.

The present paper contains the results for twenty-five fields which have recently been measured for parallax. The work has been carried out in the same way as for the previously published series.[1]

All plates were measured with the stereocomparator described in *Mount Wilson Contribution* No. 224. The last column in Table I, which contains the results of the measures, gives the instrument used in each case. With the 60-inch reflector the plates were taken at the Cassegrain focus (80 ft.); with the 100-inch, at the Newtonian focus (42 ft.).

The necessary data for each field are collected in tables which are arranged as in the Sixth and Seventh Series.[2] The mean number of exposures is 16.0, the mean probable error ±0″0064, and the mean number of comparison stars 7.6.

The following fields require special comment:

a) *H.D. 7307.*—This star, of spectrum Ma, magnitude 8.7, and proper motion 0″035 annually, was placed on the observing list because of the possibility that its absolute magnitude might be intermediate to those of giants and dwarfs. The parallax derived, corrected for systematic error, shows it to have an absolute magnitude of +3.9; H.D. 4143, which was placed on the program for the same reason, has an absolute magnitude of +1.2.[1]

---

[1] *Mt. Wilson Contr.*, Nos. 111, 1916; 136, 1917; 158, 1918; 182, 1920; 204, 1921; 237, 1922; 270, 1923.

[2] *Ibid.*, No. 237, 1922; 270, 1923.

TABLE I

Object	α 1900	δ 1900	Vis. Mag. Harvard	Mount Wilson Spectrum	Relative Parallax	μ_α	P.E.	No. of Exp.	Instrument
H.D. 7303	$1^h\ 8^m 12^s$	+26°36′	8.7	Ma†	+0″.012	−0″.025	5 3	16	60
α Arietis	2 1 32	+22 59	2.23	K2	+ .044	+0.192	6 4	16	60
Wolf 134	3 7 35	+18 29	15.2*	....	+ .052	+1.290	7 11	14	100
Wolf 219	3 38 48	+18 9	14.3*	....	+ .069	+0.416	4 7	16	100
ξ Persei	3 52 28	+35 30	4.05	O8*n*	− .006	+ .004	4 4	16	60
Wolf 358	10 45 44	+ 7 21	13.2**	....	+ .131	− .877	11 13	16	100
Lalande 26289	14 18 8	+ 1 43	6.34	G2	+ .044	+ .236	7 3	16	60
ε Scorpii	16 43 41	−34 7	2.36	K0	− .016	− .544	9 6	14	100
Wolf 629	16 49 34	− 8 8	11.7*	M‡	+ .190	− .832	7 8	16	100
Wolf 630	16 50 8	− 8 9	9.2	M3e	+ .187	− .816	16 20	16	100
Boss 4504	17 43 43	+72 12	4.90	F3	+ .057	+ .022	9 2	16	60
Boss 4505	17 43 45	+72 12	6.07	F7	+ .068	+ .030	6 1	14	60
γ Draconis	17 54 17	+51 30	2.42	K5	+ .020	− .011	6 4	16	60
Nova Ophiuchi 1919	18 9 27	+11 35	Var.	Q	− .005	− .006	8 14	16	100
Wolf 851	18 36 31	+ 0 52	12.2*	....	+ .034	+ .013	6 3	16	100
β.G.C. 9043 A	19 2 39	+22 1	7.10	F3	+ .002	− .012	9 10	16	60
β.G.C. 9043 B	19 2 39	+22 1	8.2R	B5	− .003	+ .001	6 6	16	60
Groombridge 2875	19 29 28	+58 23	6.70	K4	+ .058	− .513	6 3	18	60
B.D.+30°3639	19 30 54	+30 18	10.02	Ocp†	.000	− .002	1 1	16	60
Nova Cygni 1920	19 55 55	+53 21	Var.	Q	+ .003	+ .011	5 7	14	60
β.G.C. 10146 A	20 17 5	+43 32	6.83	Oa†	+ .003	− .008	4 2	20	60
β Delphini	20 32 52	+14 15	3.72	F3	+ .037	+ .115	8 3	16	60
N.G.C. 7027	21 3 18	+41 50	10.9*	Pl. Neb.	+ .008	− .018	4 2	16	60
T Cephei	21 8 12	+68 5	Var.	M7e	.000	−0.041	3 4	16	60
Wolf 922	21 25 51	−10 14	13.6*	....	+ .163	+1.171	6 7	16	100
Lalande 43492	22 12 15	+12 24	6.9	G1	+ .042	+0.841	8 3	16	60
δ Cephei	22 25 27	+57 54	Var.	cG0	− .002	+ .009	5 4	16	60
N.G.C. 7635	23 16 19	+60 39	8.5*$_*$*	Pl. Neb.	+0.016	+0.001	2 2	16	60

* These magnitudes are photographic, derived from counts of the number of stars of equal and brighter magnitude, and are based on Table IV of *Groningen Publications*, No. 27.

** Photographic magnitude determined by Seares.

$_*$ Photographic magnitude determined by Hubble.

R For β.G.C. 9043 B the difference in magnitude as given by Burnham has been added to the Harvard magnitude of A.

† Spectrum from the *Henry Draper Catalogue.*

‡ Spectrum from *Lick Observatory Bulletin*, No. 344.

b) *Wolf 134, 219, 358, 629, 630, 851, 922.*—These seven faint stars having large proper motions were all observed with the 100-inch telescope. Including the three stars, Wolf 1037, 1039, and 1040, published in the Seventh Series, ten of these faint Wolf stars with large proper motions have now been observed. The absolute magnitudes are all very low, ranging from $M=+9.9$ to $M=+14.7$ photographic. Russell's diagram in Volume III of the American Astronomical Society contains only fourteen stars fainter than absolute magnitude +10. A search was made through the material now available for other absolutely faint objects. It was found that at present more than sixty objects of absolute magnitude fainter than +10 are known. The list of these has been published in *Publications of the Astronomical Society of the Pacific*, February, 1925.

---

[1] *Mt. Wilson Contr.*, No. 270, 1923.

c) *ϵ Scorpii.*—For this object only one other parallax is available, viz., that by Flint who derived $\pi_{\text{rel.}}=-0.''065\pm0.''046$. Undoubtedly the parallax is very small. Since the apparent magnitude is 2.36, it must be a very luminous giant.

d) *Nova Ophiuchi 1919 and Nova Cygni 1920.*—The relative parallaxes derived are both small, $-0.''005$ and $+0.''003$, respectively. For two others, Nova Persei No. 2 and Nova Aquilae No. 3, parallaxes have been derived with the Mount Wilson reflector, while for only three others, Nova Geminorium No. 2, Nova Lacertae, and Nova P Cygni, have trigonometric parallaxes been derived by other observers. All the values found are very small indeed, and it seems hopeless to obtain much evidence as to the absolute magnitudes of these stars in this way. On the other hand, it seems doubtful if we do well to derive the distance of a nova from its absolute magnitude, as has recently been done by some astronomers, by assuming the dispersion among these objects to be small; for from the novae thus far discovered in the Andromeda nebula, we know that the range is at least 12 magnitudes. As in the case of the planetaries, the best outlook for a determination of distances is from the proper motions, for which some very valuable material should be available before many more years have elapsed.

e) *B.D.+30°3639; N.G.C. 7027 and N.G.C. 7635.*—For the first of these three objects a parallax of $+0.''005\pm0.''009$ was formerly derived.[1] While the other two cases give absolute magnitudes for the central stars of +5.1 and +4.4, I wish to call attention to the remarks in the Sixth Series[2] about these interesting objects. The work on the proper motions of the planetaries is being continued, and for nine objects relative proper motions have now been determined by Mrs. Marsh. The results are collected in Table II.

---

[1] *Ibid.*, No. 204, 1921.

[2] *Ibid.*, No. 237, pp. 11–14, 1922.

TABLE II

RELATIVE PROPER MOTIONS OF PLANETARIES

N.G.C.	μ_α	μ_δ	P.E.	Interval
2022	+0″.004	−0″.002	4, 5	6 years
6210	+ .024	− .016	3, 9	5
6572	− .071	+ .040	3, 3	5
6720	− .006	+ .016	2, 5	6
6804	− .007	− .002	1, 1	6, 7
6905	− .002	− .007	2, 2	6
7008	+ .002	− .005	2, 2	7
7027	+ .017	+ .001	2, 2	5
7662	+0.022	−0.004	3, 3	6

Before very long we hope to have enough material to determine the parallactic motion of stars of the twelfth and thirteenth magnitudes. We shall then be able to derive the absolute motions of these and other planetaries, which undoubtedly will help materially to a better knowledge of these objects.

f) T Cephei.—The zero parallax derived for this long-period variable confirms the high luminosity of these stars at maximum which was found in the Seventh Series[1] and by other means by Merrill and Strömberg.[2]

I wish to express my acknowledgment to Messrs. W. Klemman, T. A. Nelson, and A. N. Beebe for their valuable aid in securing the plates, and to Mrs. Marsh, of the Computing Division, who has performed a large share of the necessary computations.

---

[1] *Mt. Wilson Contr.*, No. 270, p. 4, 1923.

[2] *Ibid.*, No. 267, 1923.

H.D. 7307 $\alpha=1^h8^m12^s$ $\delta=+26°36'$

Mor.	Ev.	t_1	t_2	Δp	M	v
6.663	4.879	−8°.7	+ 2°.0	+1.15	− 9	+ 3
5.639	8.928	−1.0	3.5	1.46	+35	− 5
6.657	4.879	−0.5	6.2	1.18	−19	− 7
5.639	7.879	+3.7	6.2	1.25	+46	+18
6.657	4.879	+4.2	10.5	1.18	−19	− 7
4.636	8.032	+5.0	10.7	1.65	+33	− 9
5.639	6.002	+8.5	12.5	1.62	+22	+10
4.636	8.032	+9.0	+14.7	+1.65	+38	− 4

$$+48.60\,\mu_a-13.15\,\pi=-551$$
$$-13.15\,\mu_a+15.85\,\pi=+208$$
$$\pi=+4.8=+0''.012\pm0''.005$$
$$\mu_a=-10.0\;=-0''.025\pm0''.003$$

No.	Br.	x	y	π
1.....	f	+1′.0	+1′.9	+0″.016
2.....	f	+0.5	+2.3	− .008
3.....	bf	+2.3	+5.8	− .003
4.....	bf	+7.7	−0.8	+ .002
5.....	b	+2.2	−3.3	− .013
6.....	f	−1.5	−6.5	+ .012
7.....	f	−3.8	−3.2	− .010
8.....	bf	−7.7	+2.3	+0.002

α Arietis $\alpha=2^h1^m32^s$ $\delta=+22°59'$

Mor.	Ev.	t_1	t_2	Δp	M	v
6.660	8.933	− 9°.0	− 6°.0	+1.40	−156	− 7
6.660	6.931	− 4.7	− 1.2	1.40	+ 22	+19
6.657	8.933	− 3.0	+ 0.5	1.42	−134	+15
9.675	6.931	+ 0.7	+ 3.5	1.35	+240	+ 8
6.658	8.029	+ 1.2	+ 6.0	1.71	− 89	−15
9.675	8.029	+ 4.7	+10.0	1.65	+139	−16
9.680	6.906	+ 6.2	+10.5	1.21	+239	+ 7
9.680	6.906	+12.0	+14.5	+1.21	+226	− 6

$$+37.87\,\mu_a+\;3.98\,\pi=+2951$$
$$+\;3.98\,\mu_a+16.32\,\pi=+\;586$$
$$\pi=+17.4=+0''.044\pm0''.006$$
$$\mu_a=+76.1=+0''.192\pm0''.004$$

No.	Br.	x	y	π
1.....	bf	+4′.0	+2′.7	+0″.007
2.....	bf	+4.4	−0.7	+ .008
3.....	bf	+2.1	−5.4	.000
4.....	f	−1.9	−5.5	− .008
5.....	ff	−8.2	−0.3	+ .012
6.....	f	−1.8	+5.5	− .006
7.....	f	−0.4	+2.6	−0.013

Wolf 134 $\alpha=3^h7^m35^s$ $\delta=+18°29'$

Mor.	Ev.	t_1	t_2	Δp	M	v
7.715	9.018	−16°7	− 5°7	+1.58	−321	+ 4
7.715	9.018	−13.7	− 2.5	1.58	−326	− 1
7.712	7.065	− 5.0	+ 6.2	1.71	+173	−16
7.709	7.062	− 2.2	+ 8.2	1.71	+198	+ 9
7.712	7.065	− 2.0	+ 9.2	1.71	+194	+ 5
7.709	8.043	+ 1.5	+13.2	1.67	− 72	− 3
8.772	7.062	+ 3.5	+11.2	+1.45	+467	+ 2

$$+7.67\,\mu_a+1.16\,\pi=+2031$$
$$+1.16\,\mu_a+18.65\,\pi=+502$$
$$\pi=+10.6=+0''.052\pm0''.007$$
$$\mu_a=+263.2=+1''.290\pm0''.011$$

No.	Br.	x	y	π
1.....	bf	−6′6	−3′3	−0″006
2.....	bf	−1.4	−0.5	+ .009
3.....	f	+1.6	−2.1	.000
4.....	f	+1.9	−0.5	.000
5.....	f	+1.4	+0.8	− .012
6.....	f	+0.1	+1.0	+ .019
7.....	bf	+2.7	+3.4	−0.007

Wolf 219 $\alpha=3^h38^m48^s$ $\delta=+18°9'$

Mor.	Ev.	t_1	t_2	Δp	M	v
7.715	9.016	−15°5	− 8°2	+1.57	−84	+ 4
7.715	8.043	−12.7	− 7.7	1.68	0	+ 4
7.800	9.016	− 4.2	− 3.5	1.22	−97	−10
7.712	9.018	− 3.2	− 3.2	1.59	−87	+ 2
7.712	7.065	− 0.7	+ 6.5	1.75	+82	+ 2
7.710	7.065	+ 8.2	+ 9.2	1.76	+80	+ 1
7.794	7.062	+ 9.5	+10.5	1.41	+78	− 4
7.794	7.062	+12.2	+13.2	+1.41	+80	− 2

$$+6.90\,\mu_a-1.83\,\pi=+560$$
$$-1.83\,\mu_a+19.44\,\pi=+120$$
$$\pi=+14.2=+0''.069\pm0''.004$$
$$\mu_a=+84.9=+0''.416\pm0''.007$$

No.	Br.	x	y	π
1.....	bf	−0′6	+2′5	−0″005
2.....	f	−5.6	+2.9	+ .004
3.....	f	−5.5	−1.9	− .007
4.....	b	+0.7	−8.2	+ .002
5.....	f	+2.4	−5.1	+ .013
6.....	ff	+4.0	−0.3	− .006
7.....	f	+3.9	+1.8	− .005
8.....	f	+0.8	+8.5	+0.010

ξ Persei $\alpha = 3^h52^m28^s$ $\delta = +35°30'$

Mor.	Ev.	t_1	t_2	Δp	M	v
6.737	5.048	−16°.0	− 8°.5	+1.63	− 1	0
9.675	9.086	17.2	− 8.2	1.88	− 6	− 3
9.675	9.084	13.2	− 6.5	1.87	0	+ 3
9.680	9.086	8.5	− 3.5	1.87	− 5	− 2
5.765	9.084	8.0	− 1.5	1.62	−20	−11
7.740	8.029	7.5	+ 3.5	1.55	−15	−12
5.765	8.029	4.0	+ 8.0	1.45	+ 9	+16
7.740	8.029	− 3.0	+12.5	+1.55	+ 5	+ 8

$$+20.20\,\mu_a - 3.50\,\pi = +40$$
$$-3.50\,\mu_a + 22.71\,\pi = -56$$
$$\pi = -2.2 = -0''.006 \pm 0''.004$$
$$\mu_a = +1.6 = +0''.004 \pm 0''.004$$

No.	Br.	x	y	π
1.....	f	+1′.9	+2′.9	−0″.002
2.....	bf	+7.5	−1.6	+ .006
3.....	f	+1.8	−4.5	− .015
4.....	f	+0.5	−3.8	+ .002
5.....	f	−2.2	−4.0	+ .006
6.....	bf	−2.3	+0.3	+ .008
7.....	bf	−4.0	+1.2	− .003
8.....	f	−1.6	+3.6	−0.004

Wolf 358 $\alpha = 10^h45^m44^s$ $\delta = +7°21'$

Mor.	Ev.	t_1	t_2	Δp	M	v
9.016	7.311	− 9°.0	− 4°.7	+1.49	−281	−17
9.016	8.287	− 5.7	− 4.7	1.40	− 89	+ 4
7.063	7.311	− 4.0	− 3.5	1.30	+ 74	− 6
7.063	7.314	− 2.5	− 3.0	1.31	+ 84	+ 4
7.066	8.287	− 0.2	− 2.5	1.19	+258	+ 8
7.066	7.314	+ 1.2	0.0	1.29	+ 67	−12
9.019	7.309	+ 9.5	+10.2	1.47	−258	+ 9
9.019	7.309	+13.5	+11.7	+1.47	−255	+12

$$+10.93\,\mu_a + 6.14\,\pi = -1792$$
$$+6.14\,\mu_a + 14.99\,\pi = -699$$
$$\pi = +26.7 = +0''.131 \pm 0''.011$$
$$\mu_a = -179.0 = -0''.877 \pm 0''.013$$

No.	Br.	x	y	π
1.....	bf	−7′.7	−0′.9	+0″.017
2.....	b	−2.4	−2.1	− .025
3.....	f	−1.2	−3.7	− .005
4.....	f	+1.3	−2.9	− .020
5.....	f	+5.4	−5.6	+ .032
6.....	b	+3.5	+4.2	− .046
7.....	f	+2.7	+4.8	+ .028
8.....	b	−0.6	+6.0	+0.022

Lalande 26289 $\alpha=14^h18^m8^s$ $\delta=+1°43'$

Mor.	Ev.	t_1	t_2	Δp	M	v
8.230	9.417	−14°2	− 8°7	+1.05	−100	− 7
8.230	9.417	− 9.0	− 2.2	1.05	− 87	+ 6
8.227	9.420	− 3.0	− 0.2	1.07	− 94	− 2
9.248	9.420	− 2.2	+ 7.0	0.97	+ 9	+ 8
8.227	5.445	+ 1.0	+ 7.0	1.19	+272	− 9
9.161	4.429	+ 1.2	+ 7.2	1.38	+482	+16
9.248	5.445	+ 3.2	+11.0	1.08	+367	− 7
9.161	4.429	+ 8.5	+11.5	+1.38	+458	− 8

$+71.16\,\mu_a+16.54\,\pi=+6930$

$+16.54\,\mu_a+10.67\,\pi=+1729$

$\pi=+17.3=+0''.044\pm0''.007$

$\mu_a=+93.4=+0''.236\pm0''.003$

No.	Br.	x	y	π
1.....	f	+3′7	+4′1	+0.004
2.....	bf	+0.8	−5.6	+ .001
3.....	bf	−4.5	−6.7	+ .005
4.....	f	−2.6	+1.6	+ .013
5.....	f	−0.8	+1.6	− .028
6.....	f	−0.7	+6.9	+0.005

ε Scorpii $\alpha=16^h43^m41^s$ $\delta=-34°7'$

Mor.	Ev.	t_1	t_2	Δp	M	v
9.328	7.558	−10°7	−8°0	+1.29	−196	+ 5
9.333	7.561	9.5	−6.5	1.28	−205	− 4
9.328	7.558	8.7	−5.7	1.29	−202	− 1
9.333	7.561	6.5	−4.5	1.27	−200	+ 1
7.312	9.513	4.7	−8.0	1.15	+227	−13
7.312	9.510	3.0	−6.5	1.14	+253	+13
7.309	8.528	− 2.2	+1.7	+1.24	+133	+ 1

$+23.69\,\mu_a+\ 2.53\,\pi=-2640$

$+\ 2.53\,\mu_a+10.73\,\pi=-\ 316$

$\pi=-\ \ 3.2=-0''.016\pm0''.009$

$\mu_a=-111.1=-0''.544\pm0''.006$

No.	Br.	x	y	π
1.....	f	+7′3	−3′8	−0″035
2.....	bf	+1.4	−4.3	+ .049
3.....	b	+4.3	+1.5	+ .017
4.....	f	+1.0	+4.1	− .024
5.....	bf	−0.9	+5.3	.000
6.....	f	−1.3	+1.2	+ .015
7.....	f	−4.5	+0.8	+ .018
8.....	f	−5.6	−2.6	−0.043

Wolf 629 $\alpha = 16^h 49^m 34^s$ $\delta = -8°8'$
630 16 50 8 −8 9

Mor.	Ev.	t_1	t_2	Δp	M(629)	M(630)	v(629)	v(630)
9.337	7.558	−12°.5	− 2°.2	+1.26	−252	−247	0	+ 1
8.288	7.555	− 7.0	− 1.7	1.46	− 74	− 99	−7	−33
9.329	7.561	− 3.7	− 1.5	1.32	−250	−240	−1	+ 5
9.334	7.558	− 2.5	0.0	1.27	−250	−236	+2	+11
7.312	7.555	+ 1.0	+ 0.2	1.36	+103	+ 86	+9	− 6
7.312	7.561	+ 3.5	+ 0.5	1.38	+103	+118	+8	+23
7.309	7.635	+ 5.5	+11.7	1.62	+111	+117	−8	0
7.309	7.635	+ 8.5	+14.0	+1.62	+114	+116	−5	− 1

$$\left.\begin{array}{r} +10.34\,\mu_a + 6.18\,\pi = -1516 \\ +6.18\,\mu_a + 16.07\,\pi = -427 \end{array}\right\} 629$$

$$\left.\begin{array}{r} -1485 \\ -415 \end{array}\right\} 630$$

$$\left.\begin{array}{l} \pi = +38.7 = +0''.190 \pm 0''.007 \\ \mu_a = -169.8 = -0''.832 \pm 0''.008 \end{array}\right\} 629$$

$$\left.\begin{array}{l} \pi = +38.2 = +0''.187 \pm 0''.016 \\ \mu_a = -166.4 = -0''.816 \pm 0''.020 \end{array}\right\} 630$$

No.	Br.	x	y	π
1.	bf	− 1′.6	+1′.4	+0″.016
2.	b	− 3.6	+2.3	− .014
3.	f	− 6.1	+0.2	− .010
4.	bf	− 4.8	−6.9	+ .002
5.	f	− 1.8	−4.0	+ .020
6.	f	+ 4.7	−1.8	− .030
7.	f	+10.0	−0.7	+ .008
8.	bf	+ 2.5	+7.1	+0.008

Boss 4504 $\alpha = 17^h 43^m 43^s$ $\delta = +72°12'$
4505 17 43 45 +72 12

Mor.	Ev.	t_1	t_2	Δp	M(4504)	M(4505)	v(4504)	v(4505)
7.312	7.550	− 9°.5	−12°.2	+1.32	+ 38	+ 23	+12	− 7
2.282	7.550	−10.0	− 8.0	1.41	− 1	− 24	+19	+10
7.312	0.586	− 5.2	− 6.0	1.49	+107	+124	+11	− 1
7.309	0.586	− 6.0	− 2.0	1.50	+ 95	+121	− 1	− 4
2.282	7.545	− 5.0	− 2.5	1.38	− 30	− 21	−10	+14
7.310	7.545	0.0	+ 3.2	1.30	+ 19	. . . .	− 7	. . . .
7.389	0.586	− 0.2	+ 3.5	1.12	+ 99	+125	+10	+ 8
7.389	0.586	+10.0	+ 7.5	+1.12	+ 48	+ 93	−40	−25

$$\left.\begin{array}{r} +238.49\mu_a + 20.03\pi = +2513 \\ +20.03\mu_a + 14.29\pi = +498 \end{array}\right\} 4504$$

$$\left.\begin{array}{r} +238.43\mu_a + 20.34\pi = +3354 \\ +20.34\mu_a + 12.60\pi = +576 \end{array}\right\} 4505$$

$$\left.\begin{array}{l} \pi = +22.8 = +0''.057 \pm 0''.009 \\ \mu_a = +8.6 = +0''.022 \pm 0''.002 \end{array}\right\} 4504$$

$$\left.\begin{array}{l} \pi = +26.7 = +0''.068 \pm 0''.006 \\ \mu_a = +11.8 = +0''.030 \pm 0''.001 \end{array}\right\} 4505$$

4505 was not measured on 7.310–7.545

No.	Br.	x	y	π
1.	bf	−3′.0	+0′.7	−0″.009
2.	f	−1.1	+1.9	− .008
3.	f	−0.4	−3.8	+ .019
4.	f	+1.6	0.0	− .014
5.	f	+3.7	−0.4	+ .002
6.	bf	−1.1	−4.5	+0.011

γ Draconis $\alpha=17^h54^m17^s$ $\delta=+51°30'$

Mor.	Ev.	t_1	t_2	Δp	M	v
7.391	9.597	−10°.2	−14°.5	+1.18	+17	− 2
7.391	9.597	− 5.7	− 8.7	1.18	+38	+19
7.312	9.595	− 1.2	− 4.5	1.53	+ 2	−20
7.301	9.595	− 0.2	0.0	1.56	+29	+ 6
7.312	5.641	+ 3.0	+ 8.0	1.70	+15	+ 8
9.339	5.644	+ 3.5	+ 9.0	1.61	+16	+19
7.301	5.693	+ 4.2	+11.0	1.85	− 4	−12
9.339	5.641	+10.2	+12.0	+1.60	−17	−14

$$+52.96\,\mu_a+\ 5.42\,\pi=-178$$
$$+\ 5.42\,\mu_a+19.01\,\pi=+131$$
$$\pi=+8.1=+0''.020\pm0''.006$$
$$\mu_a=-4.2=-0''.011\pm0''.004$$

No.	Br.	x	y	π
1.....	f	+0′.1	+1′.0	−0″.007
2.....	bf	+1.1	+2.1	+ .021
3.....	f	+5.6	−1.8	− .016
4.....	f	+1.9	−1.0	+ .020
5.....	f	−0.7	−7.0	− .004
6.....	f	−4.5	−0.8	+ .005
7.....	f	−3.6	+4.1	− .009
8.....	f	−0.4	+3.2	−0.011

Nova Ophiuchi 1919 $\alpha=18^h9^m27^s$ $\delta=+11°35'$

Mor.	Ev.	t_1	t_2	Δp	M	v
7.397	7.635	−12°.7	− 0°.5	+1.31	− 5	− 4
7.397	7.635	− 9.5	+ 2.2	1.31	+ 7	+ 8
7.394	7.637	− 9.2	+ 2.5	1.34	+ 5	+ 6
7.394	7.637	− 6.0	+ 6.0	1.33	0	+ 1
9.328	7.711	− 1.2	+11.2	1.80	0	+ 4
9.328	7.714	+ 2.2	+10.0	1.80	+ 3	+ 7
8.392	7.711	+ 8.5	+14.2	1.51	−12	− 9
8.392	7.714	+11.2	+15.7	+1.52	−15	−12

$$+6.37\,\mu_a+\ 6.64\,\pi=-15$$
$$+6.64\,\mu_a+18.08\,\pi=-27$$
$$\pi=-1.0=-0''.005\pm0''.008$$
$$\mu_a=-1.3=-0''.006\pm0''.014$$

No.	Br.	x	y	π
1.....	bf	−3′.2	+1′.8	+0″.001
2.....	f	−2.1	−1.1	− .004
3.....	bf	−0.6	−1.4	+ .031
4.....	f	+0.6	−3.7	− .022
5.....	bf	+2.6	−0.2	+ .028
6.....	f	+2.3	+1.0	− .024
7.....	bf	0.0	+3.1	−0.005

Wolf 851 $\alpha = 18^h36^m31^s$ $\delta = +0°52'$

Mor.	Ev.	t_1	t_2	Δp	M	v
7.312	9.589	−12°5	−10°0	+1.45	+ 4	0
7.312	9.589	−10.0	− 7.7	1.45	1	− 3
8.392	9.587	− 6.2	− 2.2	1.14	5	0
8.392	9.587	− 4.2	− 0.2	1.13	7	+ 2
9.333	6.668	− 1.5	+ 2.0	1.72	30	+11
9.328	6.668	− 0.2	+ 4.0	1.74	21	+ 2
9.333	6.586	+ 1.2	+ 5.2	1.37	12	− 5
9.328	6.586	+ 2.0	+ 7.7	+1.39	+ 7	−10

$+42.49\,\mu_a + 7.46\,\pi = +163$

$+7.46\,\mu_a + 16.58\,\pi = +136$

$\pi = +7.0 = +0''.034 \pm 0''.006$

$\mu_a = +2.6 = +0''.013 \pm 0''.003$

No.	Br.	x	y	π
1.....	bf	−8'0	+3'0	+0"013
2.....	f	−3.9	+3.9	− .016
3.....	f	−1.4	+0.2	− .012
4.....	f	+0.3	−1.1	− .004
5.....	bf	+2.8	−6.8	+ .007
6.....	f	+3.1	−6.9	.000
7.....	f	+1.2	+1.4	+ .014
8.....	f	+3.9	+4.7	+0.002

β.G.C. 9043 $\alpha = 19^h2^m39^s$ $\delta = +22°1'$

Mor.	Ev.	t_1	t_2	Δp	M	v
8.441	9.600	−14°5	−9°5	+0.95	+27	+20
8.438	9.600	−12.0	−5.0	0.96	+11	+ 4
9.341	7.621	−10.7	−3.0	1.48	+ 3	+10
8.441	7.624	−10.0	−3.0	1.06	−26	−23
8.438	7.627	− 8.0	−2.5	1.09	+ 3	+ 6
9.342	7.621	− 4.2	+1.0	1.48	+ 3	+10
7.389	7.624	− 2.5	+1.7	1.32	−25	−27
7.389	7.627	+ 3.0	+1.7	+1.33	+ 1	− 1

$+10.07\,\mu_a + 4.00\,\pi = -47$

$+4.00\,\mu_a + 12.02\,\pi = -12$

$\pi = +0.7 = +0''.002 \pm 0''.009$

$\mu_a = -4.9 = -0''.012 \pm 0''.010$

For the non-physical companion we find:

$\pi = -1.0 = -0''.003 \pm 0''.006$

$\mu_a = +0.4 = +0''.001 \pm 0''.006$

No.	Br.	x	y	π
1.....	f	+0'5	+1'5	+0"020
2.....	f	+4.1	+2.2	− .012
3.....	f	+5.8	−2.2	.000
4.....	f	+1.5	−4.0	.000
5.....	bf	−3.4	−4.1	− .001
6.....	f	−5.5	+3.6	− .009
7.....	f	−3.2	+5.5	+0.003

Groombridge 2875 $\alpha=19^h29^m28^s$ $\delta=+58°23'$

Mor.	Ev.	t_1	t_2	Δp	M	v
9.415	9.674	−12°.5	−10°.0	+1.42	+ 80	− 6
6.364	9.677	−11.0	− 6.5	1.62	+714	+ 4
9.415	9.674	− 6.7	− 5.7	1.42	+ 69	−17
6.364	3.681	− 5.5	− 4.5	1.64	−509	− 2
8.441	9.677	− 1.0	− 2.5	1.31	+298	+16
8.438	4.709	+ 2.0	− 2.5	1.42	−739	−13
8.441	3.681	+ 3.0	− 0.5	1.32	−922	+17
8.438	4.709	+ 6.0	+ 1.7	1.42	−718	+ 8
8.441	3.747	+ 8.5	+ 8.7	+1.50	−927	− 8

$$+92.30\,\mu_a+20.60\,\pi=-18307$$
$$+20.60\,\mu_a+19.10\,\pi=-3752$$
$$\pi=+23.0=+0''.058\pm0''.006$$
$$\mu_a=-203.5=-0''.513\pm0''.003$$

No.	Br.	x	y	π
1.....	bf	+0′.8	+3′.2	−0″.004
2.....	f	+1.4	+2.9	+ .009
3.....	f	+4.0	+1.0	.000
4.....	f	+3.6	−3.8	.000
5.....	f	+2.1	−4.3	.000
6.....	f	−4.9	−3.6	+ .008
7.....	bf	−3.0	−0.7	− .016
8.....	bf	−4.3	+4.1	+0.004

B.D.+30° 3639 $\alpha=19^h30^m54^s$ $\delta=+30°18'$

Mor.	Ev.	t_1	t_2	Δp	M	v
7.392	4.711	−9°.5	− 1.0	+1.64	−2	0
4.468	6.659	−5.0	+ 2.0	1.09	+4	+2
7.463	5.639	−2.0	+ 4.2	1.02	+4	+5
7.463	4.632	+2.0	+ 5.0	0.98	−4	−2
7.389	6.659	+2.5	+ 6.0	1.47	−2	−1
7.466	4.632	+5.0	+ 9.0	0.97	−3	−1
4.427	5.639	+6.5	+ 8.5	1.21	−2	−3
4.430	4.799	+8.7	+11.5	+1.58	+1	+1

$$+33.44\,\mu_a+8.42\,\pi=-25$$
$$+8.42\,\mu_a+12.94\,\pi=-5$$
$$\pi=+0.1=0''.000\pm0''.001$$
$$\mu_a=-0.8=-0''.002\pm0''.001$$

No.	Br.	x	y	π
1.....	f	+3′.6	+2′.7	−0″.003
2.....	f	+1.6	+0.3	− .003
3.....	f	+1.8	−0.5	+ .004
4.....	f	+2.3	−3.0	+ .006
5.....	f	−0.7	−2.3	+ .005
6.....	f	−2.1	−1.8	− .010
7.....	f	−1.6	−1.1	− .003
8.....	bf	−4.0	+2.1	+ .004
9.....	f	−1.9	+4.4	−0.003

Nova Cygni 1920 $\alpha=19^h55^m55^s$ $\delta=+53^{\circ}21'$

Mor.	Ev.	t_1	t_2	Δp	M	v
7.471	6.665	−10°5	− 9°0	+1.09	+11	+ 7
7.468	6.739	−10.0	− 8.5	1.37	+21	+16
7.471	6.665	− 6.5	− 4.5	1.09	+ 5	+ 1
7.468	8.763	− 6.0	− 2.2	1.43	− 3	0
8.438	6.739	+ 6.5	− 2.0	1.53	− 2	−11
8.441	8.763	+ 8.5	+ 4.7	1.57	0	− 1
8.438	8.761	+10.5	+12.5	+1.58	− 7	− 8

$$+6.63\,\mu_a+\ 2.49\,\pi=+31$$
$$+2.49\,\mu_a+13.60\,\pi=+28$$
$$\pi=+1.3=+0''.003\pm0''.005$$
$$\mu_a=+4.2=+0''.011\pm0''.007$$

No.	Br.	x	y	π
1.....	bf	+1′.4	+4′.5	+0″.006
2.....	f	+2.9	+3.7	− .007
3.....	bf	+4.8	−1.9	+ .006
4.....	bf	+0.3	−5.9	+ .003
5.....	f	0.0	−4.4	− .008
6.....	bf	−6.3	−0.3	+ .003
7.....	f	−3.8	+2.5	−0.004

β.G.C. 10146A $\alpha=20^h17^m5^s$ $\delta=+43^{\circ}32'$

Mor.	Ev.	t_1	t_2	Δp	M	v
4.471	4.711	−14°0	− 5°0	+1.30	− 5	− 8
4.468	4.709	−10.0	− 3.0	1.31	+13	+10
6.496	6.736	−10.0	−15.5	1.26	+ 2	− 1
6.496	6.736	− 6.0	−10.2	1.26	+ 2	− 1
7.463	3.679	− 3.0	− 4.0	1.21	− 9	+ 1
7.466	4.711	+ 0.5	− 1.0	1.33	−11	− 4
7.463	3.679	+ 1.5	+ 0.2	1.21	−10	0
7.466	4.709	+ 4.2	+ 1.0	1.32	−12	− 5
7.468	3.681	+ 4.2	+ 4.0	1.19	− 2	+ 9
7.468	3.682	+ 8.2	+ 8.2	+1.19	−16	− 5

$$+72.78\,\mu_a+24.25\,\pi=-207$$
$$+24.25\,\mu_a+15.86\,\pi=-\ 59$$
$$\pi=+1.3=+0''.003\pm0''.004$$
$$\mu_a=-3.3=-0''.008\pm0''.002$$

No.	Br.	x	y	π
1.....	b	+0′.7	+7′.5	+0″.001
2.....	f	+2.3	+6.2	− .008
3.....	bf	+2.6	+1.1	+ .013
4.....	f	+1.9	−5.2	+ .001
5.....	f	−0.3	−5.9	− .003
6.....	f	−2.2	−6.3	.000
7.....	ff	−0.7	−1.8	− .007
8.....	bf	−4.0	+1.8	+0.008

β Delphini $\alpha=20^h32^m52^s$ $\delta=+14°15'$

Mor.	Ev.	t_1	t_2	Δp	M	v
6.490	9.674	−16°0	−14°5	+1.04	−140	−10
6.490	9.680	−12.0	−12.2	1.07	−127	+ 2
6.493	9.674	−10.0	−10.2	1.03	−146	−16
7.479	9.680	− 8.5	− 8.2	1.13	− 72	+11
6.493	5.761	− 6.0	− 1.5	1.36	+ 73	+20
7.479	5.761	− 3.5	+ 2.7	1.43	+106	+ 7
9.505	5.696	+ 7.0	+ 8.5	1.07	+169	−21
9.505	5.696	+12.2	+12.5	+1.07	+187	− 3

$$+67.41\,\mu_a-\;0.88\,\pi=+3063$$
$$-\;0.88\,\mu_a+10.73\,\pi=+\;119$$
$$\pi=+14.8=+0''.037\pm0''.008$$
$$\mu_a=+45.4=+0''.115\pm1''.003$$

No.	Br.	x	y	π
1.	f	+1′9	+1′6	+0″008
2.	f	+6.5	−1.2	− .017
3.	b	+2.2	−3.3	+ .009
4.	f	−4.4	−0.8	− .022
5.	f	−3.7	+0.5	− .007
6.	f	−1.8	0.0	+ .020
7.	ff	−0.3	−1.8	− .020
8.	bf	−0.4	+0.5	+0.029

N.G.C. 7027 $\alpha=21^h3^m18^s$ $\delta=+41°50'$

Mor.	Ev.	t_1	t_2	Δp	M	v
6.498	7.785	−13°5	−15°7	+1.43	+20	+ 7
6.490	7.788	−12.5	−14.0	1.48	+ 7	− 6
6.498	7.785	− 9.2	−11.0	1.43	+13	0
6.490	7.740	− 8.5	− 8.0	1.33	+21	+ 8
7.463	2.815	− 4.5	− 1.5	1.64	−30	− 3
7.463	2.815	− 0.2	+ 3.0	1.64	−24	+ 3
7.471	3.744	+ 3.2	+11.2	1.44	−17	+ 5
4.468	3.747	+ 5.5	+10.5	+1.46	−15	−14

$$+64.24\,\mu_a+14.42\,\pi=-404$$
$$+14.42\,\mu_a+17.62\,\pi=-\;48$$
$$\pi=+3.0=+0''.008\pm0''.004$$
$$\mu_a=-7.0=-0''.018\pm0''.002$$

No.	Br.	x	y	π
1.	f	+0′7	+4′1	−0″001
2.	f	+0.8	+3.0	− .013
3.	f	+4.7	−0.1	− .004
4.	bf	+5.1	−1.2	+ .017
5.	f	+0.3	−3.6	− .010
6.	bf	−2.5	−4.8	+ .005
7.	bf	−4.9	+2.1	+ .016
8.	f	−2.2	+0.4	−0.011

T Cephei $\alpha=21^h8^m12^s$ $\delta=+68^\circ5'$

Mor.	Ev.	t_1	t_2	Δp	M	v
6.497	7.783	−4.°5	− 4.°5	+1.43	+28	+7
6.489	7.781	−3.2	− 0.7	1.47	+21	0
7.464	5.770	−2.0	+ 2.5	1.54	−29	−2
6.497	6.740	−0.5	+ 3.5	1.30	− 1	−5
6.489	7.781	+0.7	+ 3.5	1.47	+15	−6
6.494	5.843	+2.2	+ 5.5	1.53	− 2	+9
7.464	6.737	+2.2	+ 6.2	1.44	−18	−6
6.494	5.843	+6.5	+10.0	+1.53	− 8	+3

$+9.27\,\mu_a-0.32\,\pi=-150$

$-0.32\,\mu_a+17.17\,\pi=+6$

$\pi=+0.1=0.''000\pm0.''003$

$\mu_a=-16.2=-0.''041\pm0.''004$

No.	Br.	x	y	π
1.....	bf	+3.′6	+3.′3	+0.″002
2.....	f	+5.8	+1.9	− .001
3.....	bf	+4.4	−6.9	− .001
4.....	f	−3.3	−1.6	+ .005
5.....	bf	−5.2	+1.1	− .003
6.....	bf	−4.3	+1.9	+ .001
7.....	bf	−3.3	+2.2	−0.001

Wolf 922 $\alpha=21^h25^m51^s$ $\delta=-10^\circ14'$

Mor.	Ev.	t_1	t_2	Δp	M	v
7.474	7.714	− 3.°0	+ 4.°2	+1.28	− 13	+2
8.529	8.854	− 0.7	7.5	1.43	− 24	+5
7.474	7.712	− 0.5	6.2	1.27	− 20	−5
8.534	8.854	+ 1.7	11.7	1.40	− 34	−4
8.534	7.714	+ 5.0	7.0	1.01	+234	+4
9.514	7.709	+ 6.0	7.5	1.08	+474	+8
9.511	7.712	+ 9.2	9.0	1.11	+460	−7
9.511	7.709	+12.0	+10.2	+1.10	+463	−4

$+10.71\,\mu_a+5.23\,\pi=+2733$

$+5.23\,\mu_a+11.88\,\pi=+1644$

$\pi=+33.2=+0.''163\pm0.''006$

$\mu_a=+239.0=+1.''171\pm0.''007$

No.	Br.	x	y	π
1.....	f	−5.′6	+3.′1	0.″000
2.....	f	−1.4	+0.8	+ .009
3.....	f	−4.2	−6.5	− .002
4.....	f	+2.6	−3.4	+ .018
5.....	f	+3.4	0.0	− .024
6.....	f	+5.3	+6.4	+0.003

Lalande 43492 $\alpha=22^{\mathrm{h}}12^{\mathrm{m}}15^{\mathrm{s}}$ $\delta=+12^{\circ}24'$

Mor.	Ev.	t_1	t_2	Δp	M	v
7.553	8.761	−9°.0	− 1°.2	+1.12	− 388	− 3
7.550	3.786	−8.0	+ 0.5	1.24	+1285	+12
8.515	8.764	−6.0	+ 0.5	1.30	− 53	+ 9
7.553	3.747	−4.7	+ 1.2	1.06	+1289	+ 3
7.545	8.761	−4.7	+ 4.5	1.16	− 400	−12
7.550	3.826	−3.5	+ 5.0	1.37	+1269	+ 6
8.515	8.764	−0.2	+ 6.5	1.31	− 57	+ 4
7.545	3.745	+2.0	+11.0	+1.09	+1261	−24

$$+60.01\,\mu_a+14.51\,\pi=+20240$$
$$+14.51\,\mu_a+11.74\,\pi=+\ 5029$$
$$\pi=+16.5\ =+0''.042\pm0''.008$$
$$\mu_a=+333.3=+0''.841\pm0''.003$$

No.	Br.	x	y	π
1.....	bf	+2′.1	+6′.9	+0″.002
2.....	f	+6.3	+2.3	+ .015
3.....	f	+3.0	+0.5	− .010
4.....	f	+1.2	−5.6	− .024
5.....	f	−6.0	−4.7	+ .002
6.....	bf	−2.7	−2.7	+ .034
7.....	b	−4.0	+4.3	−0.015

δ Cephei $\alpha=22^{\mathrm{h}}25^{\mathrm{m}}27^{\mathrm{s}}$ $\delta=+57^{\circ}54'$

Mor.	Ev.	t_1	t_2	Δp	M	v
6.580	7.788	−14°.2	−11°.0	+1.10	− 4	+ 1
6.578	7.783	−12.0	− 8.7	1.10	+ 5	+10
6.580	7.788	− 9.7	− 7.0	1.10	−12	− 7
6.578	4.884	− 8.0	− 5.0	1.35	+ 8	+ 3
7.553	7.783	− 2.0	− 4.5	1.22	− 9	− 7
7.551	5.762	+ 0.5	+ 8.5	1.14	+ 7	+ 2
7.553	5.770	+ 2.0	+ 9.2	1.16	− 8	−13
7.551	5.762	+ 4.5	+12.5	+1.14	+15	+10

$$+16.84\,\mu_a+\ 4.16\,\pi=+56$$
$$+\ 4.16\,\mu_a+10.89\,\pi=+\ 5$$
$$\pi=-0.9=-0''.002\pm0''.005$$
$$\mu_a=+3.6=+0''.009\pm0''.004$$

No.	Br.	x	y	π
1....	f	+3′.2	+4′.1	−0″.002
2....	b	+7.3	−0.3	.000
3....	f	+5.1	−1.4	+ .009
4....	bf	−0.3	−6.6	− .002
5....	bf	−1.5	−4.3	− .001
6....	b	−4.1	−1.4	− .010
7....	b	−5.8	+0.8	+ .014
8....	f	−1.2	+3.2	+ .008
9....	f	−0.4	+5.6	− .010
10....	f	−2.3	+0.1	−0.003

N.G.C. 7635 $\alpha = 23^h 16^m 19^s$ $\delta = +60^\circ 39'$

Mor.	Ev.	t_1	t_2	Δp	M	v
9.598	7.791	$-8^\circ\!.2$	$-5^\circ\!.5$	+1.04	+6	−2
9.595	7.788	−4.7	−3.0	1.04	8	0
9.598	7.791	−4.0	−1.2	1.04	9	+1
6.578	6.906	−4.0	−1.0	1.50	2	−8
9.595	7.788	−0.5	+1.2	1.04	7	−1
6.578	6.906	0.0	+3.2	1.50	16	+6
6.575	7.783	+6.0	+11.0	1.10	8	+1
6.575	7.783	+10.0	+16.0	+1.10	+7	0

$$+16.26\,\mu_a + 3.87\,\pi = +30$$
$$+3.87\,\mu_a + 11.24\,\pi = +74$$
$$\pi = +6.5 = +0''\!.016 \pm 0''\!.002$$
$$\mu_a = +0.3 = +0''\!.001 \pm 0''\!.002$$

No.	Br.	x	y	π
1	bf	$+2'\!.2$	$+1'\!.0$	$-0''\!.005$
2	bf	+3.6	+2.9	− .007
3	b	+2.5	−3.4	+ .033
4	bf	+0.8	−7.3	− .022
5	bf	−3.0	−1.6	+ .007
6	f	−4.9	+5.4	+ .002
7	f	−0.8	+2.5	−0.012

MOUNT WILSON OBSERVATORY
December 1924

Contributions from the Mount Wilson Observatory, No. 291
Reprinted from the *Astrophysical Journal*, Vol. LXI, pp. 320–332, 1925

THE ORBITS OF FOUR SPECTROSCOPIC BINARIES

By R. F. SANFORD

ABSTRACT

Elements of spectroscopic binaries.—Orbital elements have been derived for the four binaries, Boss 1131, H.D. 101206, B.D. +55°2215, and βGC 9818 S (Tables IV, VI, VIII, and X).

The spectrum of B.D.+55°2215 bears a resemblance to that of some of the Cepheid variables, but has elements which differ widely from those characterizing these variables. Its light is not known to vary.

Measures of the northern component of the visual binary βGC 9818 give a radial velocity in substantial agreement with that here derived for the southern component.

Dwarf spectroscopic binaries.—The dwarf binaries H.D. 101206 and βGC 9818S have periods and eccentricities which conform with those found for the majority of dwarf spectroscopic binaries, while Boss 1131, another dwarf, has neither a short period nor a small eccentricity. The velocities of the center of mass for these dwarfs are not excessively large, although the values for Boss 1131 and βGC 9818 S are somewhat above the average.

This paper deals with the orbits of the four spectroscopic binaries whose designations, co-ordinates for 1900, apparent and absolute magnitudes, proper motions, parallaxes, and number of orbital revolutions included by their respective observations are listed in Table I. For the first three the absolute magnitudes are those determined spectroscopically by Adams and his associates, from which the parallaxes follow by the well-known formula. In the last case the parallax given is one derived by Russell from considerations of visual binaries. The absolute magnitude has been computed from this parallax. All four stars have been previously announced as

TABLE I

Name	Vis. App. Mag.	α (1900)	δ (1900)	Spectral Class	Vis. Abs. Mag.	μ	$\pi_{sp.}$	No. Rev.
Boss 1131......	6.8	4^h42^m8	+18°33′	Go	5.0	0″440	0″044	88
H.D. 101206...	8.2	11 33.7	42 52	K3	5.7	0.49	.050±	114
B.D.+55°2215..	6.5	19 29.2	55 31	cG6	−0.9±	....	.003±	12
βGC 9818 S....	7.5	19 56.6	+12 28	F3	5.5±	....	0.040	104

spectroscopic binaries.[1] Reference may be made to the introduction to *Mount Wilson Contributions*, No. 201,[2] for general remarks which are also applicable to points in this paper. The details for each binary follow.

BOSS 1131[3]

Boss 1131 has a spectrum classed as G5 at Harvard[4] and G0 by the Mount Wilson observers, which gives an absolute magnitude of +5.0, thus placing it among dwarfs. Only the lines of the primary star are present.

Eight plates secured in the interval 1913–1918 definitely established variation in its radial velocity. These plates, however, were so widely scattered as to give no clue to the period. Observations begun in 1920 showed changes in velocity that, for a time, were ascribed to a period of about a day. Following this assumption the writer has accumulated a considerably larger number of plates for this spectroscopic binary than for the others he has investigated at this observatory. This accounts for the bunching of observations at certain times.

Table II lists the data for forty-three spectrograms obtained with one-prism dispersion and an 18-inch camera in conjunction with both the 60-inch and 100-inch reflectors. Numerous trials finally led to the much longer period of 45.454 days, which affords a satisfactory assemblage of all observations at a single epoch. The possibility of a superposed short-period velocity-variation will be alluded to later. The above-stated period cannot be changed more than 0.01 day without, in certain cases, seriously disturbing the distribution of observed velocities upon the velocity-curve. The number of orbital revolutions covered by the observations, together with the possibility of a superposed short-period variation, seemed sufficient justification for not including this element for correction by least squares. $P = 45.454$ days is therefore considered determined.

---

[1] Boss 1131, *Publications of the Astronomical Society of the Pacific*, **31**, 41, 1919. The other three stars, *ibid.*, **36**, 137, 1924.

[2] *Astrophysical Journal*, **53**, 201, 1921.

[3] B.D.+18°734; A. G. Berl. A 1309; Pi 190, H.D. 30455.

[4] The *Henry Draper Catalogue* states that Hδ is unusually strong. Slit spectrograms do not bear this out.

To facilitate the least-squares solution and minimize any disturbance from a short-period variation, normal places were formed by combining, in a single mean, series of observations taken close together, due consideration being given to the nature of the veloc-

TABLE II

Observations of Boss 1131

Plate No.	Date	G.M.T.	Phase	Velocity	O−C	Wt.
				km/sec.	km/sec.	
γ 2110	1913 Feb. 13	$16^{h}33^{m}$	$9^{d}.463$	+44.9	− 3.1	....
3116	1914 Feb. 6	16 39	3.833	64.9	+ 4.9	....
3904	Nov. 25	20 52	23.288	41.2	− 6.3	....
3972	Dec. 27	20 49	9.832	51.0	+ 3.5	....
4061	1915 Feb. 25	17 33	24.241	47.8	− 0.2	....
5231	1916 Nov 8	22 28	10.089	35.0	−12.6	....
5486	1917 Jan. 31	18 15	3.005	62.3	+ 0.6	....
7621	1918 Dec. 12	21 10	1.316	69.5	+ 1.5	....
9679	1920 Oct. 27	22 08	4.547	52.8	− 4.1	1.00
9683	Oct. 28	20 25	5.478	53.7	− 0.8	1.00
C 740	Oct. 31	23 37	8.610	53.0	+ 4.0	1.00
γ 9714	Nov. 2	22 52	10.578	45.9	− 1.4	1.00
9728	Nov. 20	19 45	28.386	51.2	+ 0.8	1.00
C 806	Dec. 18	17 40	10.906	48.2	+ 1.2	1.00
γ 9806	Dec. 22	18 21	14.935	46.3	+ 0.5	1.00
9850	Dec. 30	15 17	22.808	47.6	+ 0.3	1.00
9862	1921 Jan. 21	15 25	44.822	69.6	− 3.0	1.00
9872	Jan. 24	18 55	2.505	62.0	− 1.4	0.50
9928	Feb. 20	18 04	29.470	46.2	− 5.0	1.00
9933	Feb. 21	16 02	30.385	52.8	+ 0.8	0.25
C 895	Feb. 22	15 43	31.373	51.7	− 1.2	.50
900	Feb. 23	15 25	32.358	53.7	− 0.2	0.50
903	Feb. 24	14 55	33.339	59.2	+ 4.2	1.00
γ 9996	Mar. 16	15 51	7.923	52.1	+ 2.3	1.00
10004	Mar. 17	15 40	8.916	42.8	− 6.0	1.00
C 946	Mar. 19	16 12	10.938	49.4	+ 2.4	0.50
954	Mar. 20	15 59	11.929	46.6	0.0	1.00
γ 10675	Dec. 7	17 00	1.247	68.8	+ 0.8	1.00
10680	Dec. 7	23 22	1.512	63.3	− 3.8	1.00
10751	1922 Jan. 12	17 37	37.274	60.4	− 0.4	1.00
C 1525	Jan. 13	19 37	38.357	60.8	− 2.1	0.50
1532	Jan. 14	20 23	39.388	68.6	+ 3.6	1.00
γ 10764	Jan. 15	15 29	40.184	65.0	− 1.6	1.00
10770	Jan. 15	21 17	40.384	68.0	+ 1.0	1.00
11458	Dec. 5	16 31	0.595	79.3	+ 9.3	1.00
11460	Dec. 5	20 42	0.770	61.8	− 7.7	0.50
11464	Dec. 6	0 1	0.907	78.2	+ 9.2	0.25
C 2037	1923 Jan. 1	21 35	27.806	50.8	+ 0.8	1.00
12096	Sept. 1	23 55	43.634	75.8	+ 3.0	1.00
C 2457	Sept. 27	0 35	23.207	46.6	− 0.9	1.00
γ 12260	Oct. 30	22 21	11.660	44.5	− 2.2	1.00
12300	Nov. 25	17 54	37.478	58.9	− 2.3	1.00
12403	1924 Jan. 17	17 58	45.024	+68.0	− 4.3	1.00

ity variation at the particular epoch. The observations made before 1920 were not included. The seventeen normals thus formed (Table III) gave, by Russell's method, preliminary values for the five remaining elements. Two least-squares solutions resulted in two sets of corrections to be applied to the provisional elements, and gave data for deriving the probable errors. Table IV gives the preliminary elements, the two sets of corrections, and the final ele-

TABLE III

NORMAL PLACES—BOSS 1131

No.	Phase	Limits of Phase	Velocity	O−C	Wt.
			km/sec.	km/sec.	
1	$0^{d}692$	$0^{d}60$– $0^{d}91$	+74.1	+4.3	1.75
2	1.379	1.25– 1.51	66.0	−1.6	2.00
3	2.505	....	62.0	−1.4	0.50
4	7.303	4.55–10.58	51.3	+0.6	4.00
5	9.782	7.92–11.92	47.5	−0.4	3.50
6	11.660	....	44.5	−2.2	1.00
7	12.921	10.91–14.94	47.2	+1.0	2.00
8	22.808	....	47.6	+0.3	1.00
9	23.207	....	46.6	−0.9	1.00
10	27.806	....	50.8	+0.8	1.00
11	28.386	....	51.2	+0.8	1.00
12	31.468	29.47–33.34	52.7	−0.3	3.25
13	37.478	....	58.9	−2.3	1.00
14	39.202	37.27–40.38	65.0	+0.4	4.50
15	43.634	....	75.8	+3.0	1.00
16	44.822	....	69.6	−3.0	1.00
17	45.024	....	+68.0	−4.3	1.00

TABLE IV

ELEMENTS OF BOSS 1131

	PRELIMINARY ELEMENTS	CORRECTIONS		FINAL ELEMENTS
		First. Sol.	Second Sol.	
P	$45^{d}454$	....	....	$45^{d}454$
e	0.55	− 0.160	+0.001	0.391±0.038
ω	39°	−13.96	+1.44	26°.48 ±6°.52
K	14.0	− 1.16	+0.73	13.57 ±0.45 km/sec.
T	J.D. 2423030.89	− 0.445	+0.016	3030.461±0.482
γ	+55.0	− 0.18	−0.16	+54.66 km/sec.
$a \sin i$	....	....	....	7,810,500 km
$\frac{m_1^3 \sin^3 i}{(m+m_1)^2}$	....	....	....	0.0092 ☉

ments with their probable errors, derived from a probable error ±1.9 km/sec. for a normal place of unit weight; $a \sin i$ and the mass factor have been added.

Figure 1 shows the computed radial velocity-curve with the seventeen normal places plotted as circles with radius 1.2 km/sec. Individual observations are too numerous to admit plotting in this manner.

The column headed "O − C" in Table III gives the differences between the value of the velocity of a normal place and that computed by the final elements. The corresponding quantity in Table II has been found by scaling off the difference between the individual velocities and the computed velocity-curve.

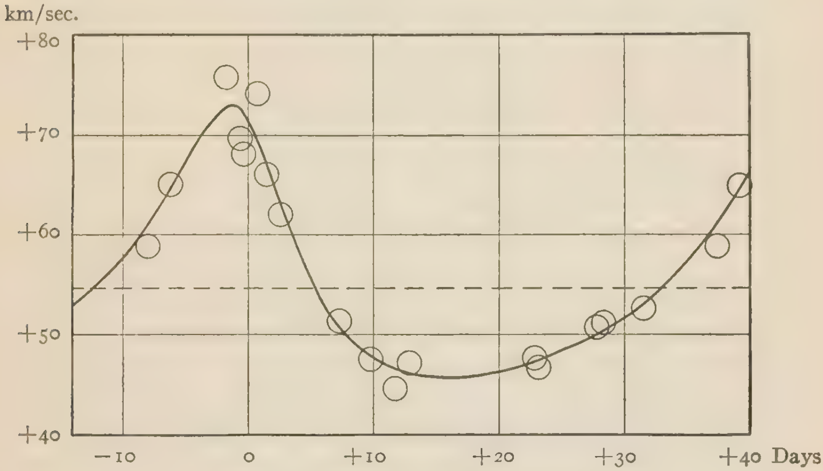

FIG. 1.—Velocity-curve of Boss 1131

The largest of the latter residuals, −12.6 km/sec., is from plate γ 5231, whose quality is decidedly poor. The others are all numerically less than 10 km/sec., and, by themselves, perhaps would not be seriously questioned, even for a spectrum as satisfactory as that of this star. The disturbing feature is best displayed by such runs of observations as those in the intervals October 27 to November 2, 1920, and December 5–6, 1922, where the range in velocity seems too great to be explained by the dispersion employed. The second set, however, involves two plates of low weight. An attempt to fit the residuals to a short period has not been successful, as is perhaps to be expected when the variations themselves are at most but slightly greater than those legitimately to be anticipated from the dispersion employed. Hence the existence of this type of variation remains unsettled.

H.D. 101206[1]

This star was observed for absolute magnitude because its known proper-motion indicated low luminosity. The discordant values for radial velocity from the first three plates led to the discovery of its binary character. The spectrum, at all times single, is of spectral class K3.

TABLE V

Observations of H.D. 101206

Plate No.	Date	G.M.T.	Phase	Velocity	O−C	Quality
				km/sec.	km/sec.	
C 420	1920 May 10	18h01m	4d332	+19.1	− 0.2	Poor
863	1921 Jan. 24	22 40	5.191	+26.2	− 2.9	Good
985	Apr. 11	19 27	4.556	+10.9	−11.3	Good−
1125	July 13	16 02	6.997	+39.5	− 1.8	Good*
1697	1922 May 12	16 46	0.026	−20.4	− 7.5	Poor
1740	June 10	17 40	3.231	+ 5.2	+ 0.3	Fair−
γ 11499	1923 Jan. 3	0 22	2.842	+11.1	+10.9	Poor
11503	Jan. 4	0 00	3.827	+21.2	+ 8.5	Poor focus
C 2101	Feb. 1	0 34	6.018	+34.2	− 2.1	Fair+
γ 11749	May 2	18 42	6.356	+40.6	+ 2.4	Fair+
C 2238	May 4	18 30	8.348	+42.8	+ 2.6	Fair−
γ 11761	May 5	17 45	9.317	+27.6	− 6.0	Fair+
11767	May 6	17 03	10.288	+18.4	− 3.8	Fair−
C 2281	May 31	17 09	9.458	+31.2	− 1.0	Good
2327	June 27	16 30	10.598	+23.0	+ 5.2	Fair−
γ 11898	June 28	16 40	11.604	+ 4.4	+ 1.7	Good*
12408	1924 Jan. 18	0 36	8.268	+35.6	− 5.0	Good
12413	Jan. 19	0 38	9.269	+35.0	+ 1.0	Fair+
C 2640	Jan. 19	21 04	10.122	+22.8	− 1.6	Fair+
2644	Jan. 20	21 28	11.138	+10.6	+ 0.9	Good
2687	Feb. 18	0 06	0.497	− 9.0	+ 6.2	Fair
γ 12507	Feb. 20	21 39	3.395	+ 0.8	− 6.3	Good*
C 2751	Apr. 18	16 36	9.519	+32.4	+ 0.8	Fair
2787	May 19	17 00	1.783	−13.8	− 2.4	Good−

* Seven-inch camera.

The apparent magnitude, spectral class, and winter observing season form a combination unfavorable to obtaining uniformly good exposures. Some plates have been made at the 60-inch reflector with a widened slit, and three were obtained with the dispersion furnished by a 7-inch camera on the one-prism spectrograph. The quality is in several cases not of the best, as is indicated in the last column of Table V, which gives the observational data for the twenty-four plates obtained. The best grouping for the velocity-curve was obtained with a period of 12.9167 days, which can hardly be in error more than 0.002 day since 114 orbital revolutions separate the first and last observations. Provisional elements obtained in the usual way and then corrected by inspection appear in Table VI. Since they reveal no points of more than ordinary interest it did not seem worth while to seek any refinement in the values of the elements because of the considerable labor involved in obtaining more and better plates. The residuals in the sixth column of Table V are quite satisfactory for the quality and number of plates involved, and do not seem to justify the extra effort necessitated by a least-squares solution.

---

[1] B.D.+43°2135; A.G. Bonn 8141; Furuhjelm 36 (*Finska Vetenskaps-Soc. Verhand.*, 59, 1917); Cin. 1435.

TABLE VI

ELEMENTS FOR H.D. 101206

P	$12\overset{d}{.}9167$	T	J.D. 2423549.34
e	0.08	γ	+15.3 km/sec.
ω	$154\overset{\circ}{.}0$	$a \sin i$	5,090,000 km
K	28.8 km/sec.	$\frac{m_1^3 \sin^3 i}{(m+m_1)^2}$	0.0316 ⊙

Figure 2 shows the velocity-curve derived from the elements in Table VI. The barred circles represent observed velocities derived from the three spectrograms of low dispersion.

B.D.+55°2215[1]

This star has been classified in the *Henry Draper Catalogue* as K2+A3, a composite spectrum, and assigned two numbers. The spectral class derived at Mount Wilson is about cG6, which not only accounts for the abnormal strength of the hydrogen lines, probably the reason for calling the spectrum composite, but is also consistent with the fact that the hydrogen lines seem to share the Doppler shift of the other lines. The spectrum resembles that of X Cygni near minimum light, and closely duplicates that of Boss 1074, which has *c*-characteristics and a radial-velocity variation in a period which, although pretty certainly long, has not yet been determined. The spectral lines of B.D. +55°2215 are at all times single, and do not change in character to any notable extent.

---

[1] A.G. Hels. 10554; H.D. 184398–9.

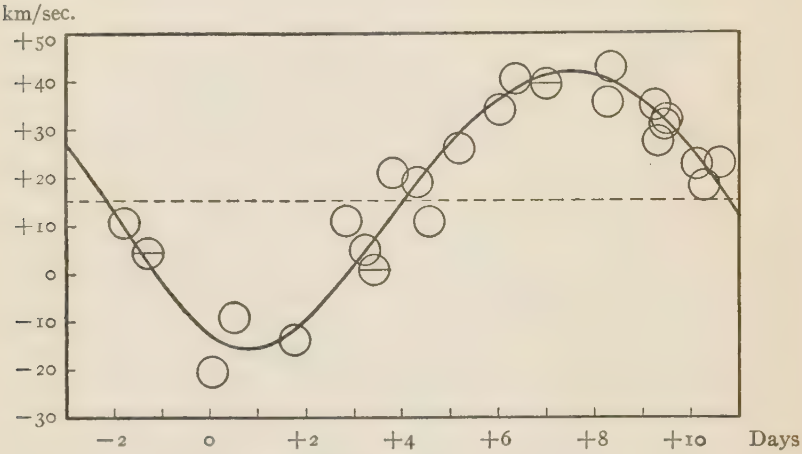

FIG. 2.—Velocity-curve of H.D. 101206

The measures of the second plate showed an undoubtedly variable radial velocity which was confirmed by the next two plates. Since May 1, 1920, the star has been under observation each season, and at present fifty spectrograms of suitable quality are available (Table VII). This number is somewhat larger than usual because of a suspected short-period variation, superposed upon the period of approximately 110 days. The shorter period was not confirmed—in fact was only suspected on the basis of some measures of weakly exposed plates. Considerable effort was expended in deriving the period (108.5707 days), which can hardly admit of a change as great as 0.05 day, and which has been adopted as final.

The points in Figure 3 represent the observed velocities collected with this period. Russell's method, with subsequent adjustment, partly by least squares and partly by trial, gave elements which define the velocity-curve shown in Figure 3. The representation is satisfactory, and these elements are adopted and given in Table VIII.

TABLE VII

OBSERVATIONS OF B.D.+55°2215

Plate No.	Date	G.M.T.	Phase	Velocity	O−C
				km/sec.	km/sec.
γ 9170	1920 May 1	$23^{\mathrm{h}}32^{\mathrm{m}}$	$24^{\mathrm{d}}.587$	−22.7	+4.6
10197	1921 June 13	21 45	106.800	− 0.2	+1.5
10300	July 20	22 56	35.279	−26.6	−2.3
10351	Aug. 13	19 36	59.140	− 1.4	−0.6
10534	Oct. 12	16 18	10.431	−17.0	+0.2
10590	Nov. 6	16 17	35.430	−25.6	−1.4
C 1570	1922 Feb. 16	0 34	28.205	−27.8	−0.7
1577	Feb. 17	1 06	29.227	−23.2	+3.8
1586	Feb. 18	1 15	30.233	−21.4	+5.2
γ 10863	Mar. 7	0 42	47.210	−17.0	−2.8
C 1644	Apr. 6	23 42	78.169	+14.2	−1.6
γ 11040	May 11	22 29	4.544	−17.4	−6.5
C 1699	May 12	22 23	5.542	− 7.8	+4.2
γ 11095	June 7	20 36	31.469	−23.6	+2.4
11099	June 8	18 08	32.367	−22.2	+3.7
C 1736	June 9	18 24	33.378	−32.2	−6.8
1741	June 10	19 42	34.432	−25.0	−0.1
γ 11120	July 2	18 43	56.391	− 4.2	−0.2
11124	July 2	23 38	56.596	− 7.8	−4.5
11126	July 3	18 17	57.373	+ 3.3	+5.9
11130	July 3	23 39	57.596	− 1.8	+0.7
11134	July 4	22 50	58.562	+ 0.6	+2.2
11200	July 16	20 42	70.473	+11.1	+0.5
11220	Aug. 5	16 04	90.280	+15.9	+0.4
11223	Aug. 5	20 40	90.472	+15.2	−0.2
11270	Aug. 30	16 51	6.742	−10.8	+2.6
C 1850	Sept. 1	15 12	8.673	−10.2	+5.8
γ 11300	Sept. 3	16 40	10.734	−20.2	−2.0
C 1864	Sept. 5	17 20	12.762	−20.2	−1.2
1872	Sept. 8	20 27	15.892	−24.4	−2.0
1919	Oct. 4	14 55	41.662	−19.2	+0.7
γ 11355	Oct. 5	15 49	42.699	−18.6	−0.1
11369	Oct. 7	17 01	44.749	−21.8	−4.8
11457	Dec. 5	15 10	103.672	+ 9.2	+6.7
C 2235	1923 May 3	22 09	35.822	−21.6	+2.5
γ 11763	May 5	20 50	37.767	−22.9	+0.1
11770	May 6	20 45	38.763	−22.3	−0.1
11874	June 23	23 19	86.871	+15.8	−1.0
C 2323	June 26	18 22	89.664	+16.8	+1.0
γ 11907	June 29	20 10	92.739	+20.5	+6.3
11930	July 4	21 53	97.811	+ 9.4	−0.5
12173	Oct. 3	15 31	79.974	+20.0	+3.7
12244	Oct. 28	16 58	105.035	+ 2.6	+1.6
12299	Nov. 25	16 00	24.424	−31.1	−3.8
C 2786	1924 May 18	23 42	91.176	+13.2	−1.8
2790	May 19	21 59	92.102	+14.0	−0.6
2835	June 17	23 31	12.594	−25.9	−6.2
γ 12784	July 13	17 06	38.329	−23.1	−0.4
12790	July 14	16 37	39.309	−24.2	−2.4
12796	July 15	17 35	40.348	−22.0	−1.0

The residuals O−C in Table VII have been scaled from the velocity-curve of Figure 3. The agreement is typical of plates of this dispersion and spectral character, and gives no indication of a superposed velocity variation of short period.

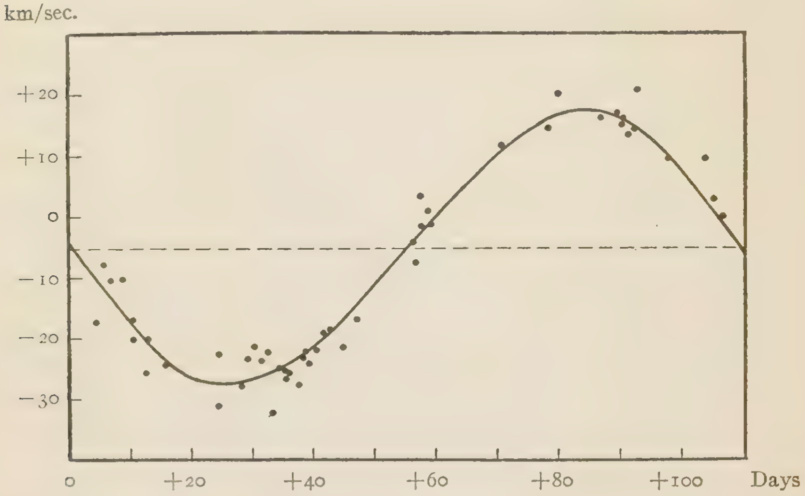

FIG. 3.—Velocity-curve of B.D.+55°2215

Aside from the spectrum, there is little to lend support to the Cepheid character of this star; for it is not known to vary in magnitude, and its orbital elements in several respects are markedly

TABLE VIII

ELEMENTS B.D.+55°2215

P	$108^{\mathrm{d}}5707$	T	J.D. 2423375.760
e	0.054	γ	−5.2 km/sec.
ω	$87^{\circ}0$	$a \sin i$	33,040,000 km.
K	22.1 km/sec.	$\frac{m_1^3 \sin^3 i}{(m+m^1)^2}$	0.1222 ⊙

different from the so-called elements of the average Cepheid variable. In addition, the period-luminosity law would demand a luminosity far greater than that consistent with the usual spectral considerations.

βGC 9818 S[1]

This star is the southern component of a visual pair whose position-angle and distance according to Burnham's *General Catalogue* remained sensibly constant at 350° and 4″.4, respectively, during the interval 1866–1905. The spectral class is F3 and is at all times that of the primary. The marked change in radial velocity revealed by the second plate was borne out by the later plates. Twenty plates obtained between June, 1923, and September, 1924, seemed to be of such quality and distribution as to define the elements of the orbit with a precision adequate for this case, which presents no particular interest. The period, 4.4698 days, found by trial, does not admit of a change greater than 0.002 day, and has been adopted. The elements derived, as in the preceding cases, are based upon the observations in Table IX. After slight modification by inspection, the comparison of the resulting curve with the observations (Fig. 4) and a consideration of the magnitude of the residuals in Table IX made it seem

TABLE IX

OBSERVATIONS OF βGC 9818 S

Plate No.	Date	G.M.T.	Phase	Velocity	O−C	Quality
				km/sec.	km/sec.	
γ11883......	1923 June 24	$23^h 21^m$	$3^d.862$	−64.2	− 0.2	f+*
11957......	July 24	23 28	2.578	−64.7	+ 7.0	f−
12114......	Sept. 23	17 55	0.770	− 2.8	− 0.5	f+
12121......	Sept. 24	16 53	1.727	−36.5	− 2.2	g
12138......	Sept. 27	16 27	0.238	−17.4	− 6.0	f+
12243......	Oct. 28	15 28	4.387	−32.5	− 2.0	g
12248......	Oct. 29	15 14	0.898	− 6.0	− 4.0	g
12256......	Oct. 30	15 30	1.910	−49.8	− 6.3	g
12571......	1924 Apr. 16	23 42	1.399	−12.3	+ 6.4	g
12576......	Apr. 17	23 10	2.377	−73.0	− 8.6	f−
C 2754......	Apr. 18	23 42	3.399	−73.5	+ 7.3	f+
12648......	May 16	22 08	0.045	−20.4	+ 0.1	f
12652......	May 17	21 45	1.024	− 5.2	0.0	f+
C 2791......	May 19	22 56	3.078	−91.8	− 9.5	vg
2834......	June 17	22 08	0.673	− 6.6	− 6.5	g
12785......	July 13	18 36	4.261	−52.0	−12.0	vg
12791......	July 14	17 52	0.760	− 0.9	− 0.8	f
12797......	July 15	18 54	1.804	−33.3	+ 5.2	g
12939......	Sept. 10	17 40	0.646	+ 7.6	+ 7.6	g
12943......	Sept. 11	17 24	1.634	−29.8	+ 0.1	g

* f = fair, g = good, vg = very good.

---

[1] Σ 2613; B.D.+10°4143; A.G. Leipz. 7630; H.D. 189783.

unlikely that a least-squares solution would afford any material gain. The adopted elements appear in Table X.

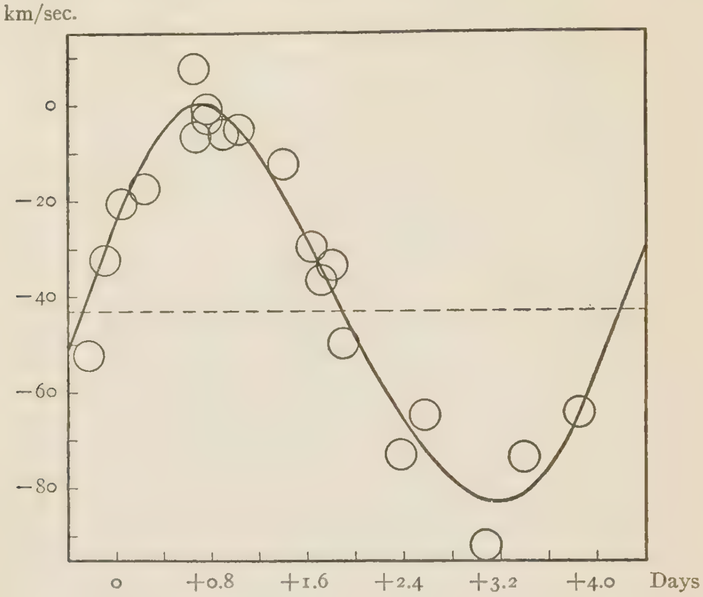

FIG. 4.—Velocity-curve of βGC 9818 S

The radius of the circles representing the observations in both Figures 2 and 4 is 3 km/sec., a quantity slightly larger than the probable error to be expected in such cases.

TABLE X

ELEMENTS βGC 9818 S

P	$4^{d}4696$	T	J.D. 2423802.192
e	0.10	γ	−43.0 km/sec.
ω	294°5	$a \sin i$	2,526,000 km
K	41.3 km/sec.	$\frac{m_1^3 \sin^3 i}{(m+m_1)^2}$	.00322 ⊙

Two plates of the northern component show its spectrum to be nearly the same as that of the southern component. Their measures agree as well as could be expected and give −39.3 km/sec. for the radial velocity, a difference of −3.7 km/sec. from γ determined above. The probable errors will account for this difference.

In conclusion, it may be noted that three of these stars may be classified as dwarfs. The second and fourth are additional examples of dwarf binaries whose periods and eccentricities are both small as compared with those of giants—a fact to which attention has been called.[1] The first star, however, is a dwarf having both a period of considerable length and a decided eccentricity. It is also perhaps worth noting that the values of γ for both Boss 1131 and βGC 9818 S are rather large.

Mount Wilson Observatory
November 1924

---

[1] *Mt. Wilson Contr.*, No. 251, 445; *Astrophysical Journal*, 56, 454, 1922; *Lick Observatory Bulletins*, 11, 132, 1924.

Contributions from the Mount Wilson Observatory, No. 292
Reprinted from the *Astrophysical Journal*, Vol. LXI, pp. 353–362, 1925

ANALYSIS OF RADIAL VELOCITIES OF GLOBULAR CLUSTERS AND NON-GALACTIC NEBULAE

By GUSTAF STRÖMBERG

ABSTRACT

List of radial velocities of globular clusters and non-galactic nebulae.—Table I contains a list of all measured radial velocities of globular clusters and non-galactic nebulae, the great majority of the determinations being by Slipher.

Solar motion.—The sun's motion relative to the two classes of objects studied is given in Table II in rectangular equatorial co-ordinates $(-\xi, -\eta, -\zeta)$ and in polar co-ordinates (A_0, D_0, V_0). The value of the sun's motion relative to the nebulae is 344 km/sec. toward $A_0=305°$, $D_0=+56°$ and, relative to the clusters, 329 km/sec. in the direction $A_0=320°$, $D_0=+65°$.

Curvature of space-time.—On the basis of De Sitter's theory of curvature of space-time, we should expect to find for very distant objects a shift of the spectral lines toward the red end of the spectrum. According to Silberstein, we may expect a shift either toward the red or the violet. The correlation-coefficients between distance and radial velocities give no clear evidence of curvature in either De Sitter's or Silberstein's sense, at least up to the limit of distance studied. The only definite correlation is one between radial velocity and position in the sky, indicating a solar motion of 300 or 400 km/sec. in about the same direction for both classes of objects.

The determination of radial velocities of globular clusters and of non-galactic nebulae is very difficult on account of the faintness of the objects and the absence, in general, of bright lines in their spectra; but through the perseverance of Professor V. M. Slipher, a fairly large number of such velocities has been derived. Two reasons prompted the writer to study these velocities. One was the large solar velocity found from these objects, which, in connection with the asymmetry of stellar motions, indicated that a fundamental reference system could be defined by them. The second reason was the desirability of ascertaining whether the velocities give any evidence of a curvature of space-time.[1] Through the courtesy of Professor Slipher it has been possible to make use of his radial-velocity determinations up to a recent date.

In Table I are collected the data on which the computations are based. Slipher's determinations are given without references; for

---

[1] After this paper was ready for printing, Lundmark's article, "The Determination of the Curvature of Space-Time in De Sitter's World," appeared in *Monthly Notices*, **84**, 747, 1924. Lundmark's conclusions as to space-curvature are about the same as those found in this study.

TABLE I

RADIAL VELOCITIES OF GLOBULAR CLUSTERS AND NON-GALACTIC NEBULAE

N.G.C.	α (1900)	δ (1900)	V		
			Slipher	Others	Mean
			km/sec.	km/sec.	km/sec.
221	$0^h37^m.2$	$+40^\circ 19'$	− 300	…	…
224	0 37	+40 43	− 300	− 320*	−315
278	0 46.4	+47 1	+ 650::	…	…
404	1 3.9	+35 11	− 25	…	…
584	1 26.3	− 7 23	+1800:	…	…
598	1 28.2	+30 9	− 260	− 70†	− 70
936	2 22.5	− 1 36	+1300	…	…
1023	2 34.1	+38 38	+ 300	…	…
1068	2 37.6	− 0 26	+1120	+ 814‡	+ 916
1700	4 52.0	− 5 1	…	+ 800§	…
2681	8 46.4	+51 41	…	+ 700‖	…
2683	8 46.5	+33 48	+ 400	…	…
2841	9 15.1	+51 24	+ 600:	…	…
3031	9 47.4	+69 32	− 30	…	…
3034	9 47.6	+70 10	+ 290	…	…
3115	10 0.3	− 7 14	+ 600	…	…
3368	10 41.5	+12 21	+ 940	…	…
3379	10 42.6	+13 7	+ 780	+ 845§	+ 812
3489	10 55.0	+14 26	+ 600::	…	…
3521	11 0.7	+ 0 30	+ 730	…	…
3623	11 13.7	+13 38	+ 800	…	…
3627	11 15.0	+13 32	+ 650	…	…
4111	12 2.0	+43 37	+ 800:	…	…
4151	12 5.5	+39 58	+ 980	+ 940¶	+ 950
4214	12 10.6	+36 53	+ 300	…	…
4258	12 14.0	+47 52	+ 500	…	…
4382	12 20.3	+18 45	+ 500:	…	…
4449	12 23.3	+44 39	+ 200	…	…
4472	12 24.7	+ 8 33	+ 850	…	…
4486	12 25.6	+12 57	+ 800::	…	…
4526	12 29.0	+ 8 15	+ 580	…	…
4565	12 31.4	+26 32	+1100:	…	…
4594	12 34.8	−11 4	+1100	+1180**	+1140
4649	12 38.6	+12 6	+1090	…	…
4736	12 46.2	+41 40	+ 290	…	…
4826	12 51.8	+22 14	+ 150	…	…
5005	13 6.3	+37 36	+ 900	…	…
5055	13 11.3	+42 34	+ 450	…	…
5194	13 25.7	+47 43	+ 270	…	…
5195	13 25.7	+47 43	+ 240:	…	…
5236	13 31.4	−29 21	+ 500:	…	…
5866	15 3.7	+56 9	+ 650	…	…
7331	22 32.5	+33 54	+ 500	…	…
Magellanic clouds	5 27	−68	…	+ 287††	…
	1 6	−73 44	…	+ 168††	…
1851	5 10.8	−40 9	+ 315	…	…
1904	5 20.1	−24 37	+ 235	…	…
5024	13 8.0	+18 42	− 170	− 200‡‡	− 180
5272	15 37.6	+28 53	− 125	− 140‡‡	130

TABLE I—*Continued*

N.G.C.	α (1900)	δ (1900)	V		
			Slipher	Others	Mean
			km/sec.	km/sec.	km/sec.
5904	$15^h13^m.5$	+2° 27′	+10	....	....
6093	16 11.1	−22 41	+70	....	....
6205	16 38.1	+36 39	−300	−230§§	−265
6218	16 42.0	−1 46	....	+160‡‡	....
6229	16 44.2	+47 42	−100:	....	....
6266	16 54.8	−29 58	+50	....	....
6273	16 56.4	−26 7	+30	....	....
6333	17 13.3	−18 25	+225	....	....
6341	17 14.1	+43 15	−160	....	....
6626	18 18.4	−24 55	0	....	....
6934	20 29.3	+7 4	−350:	....	....
7078	21 25.2	+11 44	−95	−93‡‡	−94
7089	21 28.3	−1 16	−10	....	....
7099	21 34.7	−23 38	−125	....	....

* Mean of several determinations.

† Slipher has measured a knot north following the nucleus, whereas the Mount Wilson determination is based on the spectrum of the nucleus; *A.S.P. Pubs.*, **28**, 33, 1916.

‡ Mount Wilson measures give $V=+765$; *A.S.P.*, **27**, 133, 1915; and Lick Observatory gives $V=+864$; *L.O. Pubs.*, **13**, 88, 1918.

§ Mount Wilson, *A.S.P. Pubs.*, **30**, 255, 1918.

|| *Ibid.*, **34**, 222, 1922.

¶ *L.O. Pubs.*, **13**, 122, 1918.

** *Mount Wilson Comm.*, No. 32; *Proc. Nat. Acad. of Sciences*, **2**, 517, 1916.

†† *L.O. Pubs.*, **13**, 168, 1918.

‡‡ Sanford, unpublished.

§§ Mean of 4 stars, measured by Adams, Joy, and Humason.

other observers, references are given in footnotes. In the list 43 nebulae stand first, most of which have spiral structure, although several are irregular or globular. Then follow the Magellanic clouds and 18 globular clusters. The probable error of the radial velocities for the nebulae is probably about 50 km/sec. and for the clusters about 25 km/sec. The more uncertain values are marked by one or two colons.

THE SOLAR MOTION

The elements for the solar motion were first determined. The equations of condition used were of the following form:

$$\xi \cos \alpha \cos \delta + \eta \sin \alpha \cos \delta + \zeta \sin \delta + K = V \qquad (1)$$

where ξ, η, and ζ are the rectangular equatorial components of the group-motion as referred to the sun. The co-ordinates of the sun's apex (A_0, D_0) and its velocity (V_0) relative to the groups of objects studied are determined by the equations[1]

$$\begin{aligned} V_0 \cos A_0 \cos D_0 &= -\xi \\ V_0 \sin A_0 \cos D_0 &= -\eta \\ V_0 \sin D_0 &= -\zeta\,. \end{aligned} \tag{2}$$

Several solutions were made to test the effect of omissions, especially that of the large velocity +1800 km/sec. of N.G.C. 584. Whether we ought to include the Magellanic clouds among the non-galactic nebulae is doubtful, but solutions were made including these objects, both with and without K-terms. The results of the different solutions are given in Table II. The second, fifth, and seventh solutions for the nebulae were made after the radial velocity of N.G.C. 584 had been omitted. This omission seems to be justified on account of the small number of objects used. In the last solution for nebulae and clusters, 13 and 8 groups, respectively, were formed by combining objects near each other in the sky, the different groups being given equal weights. The probable errors are given below the numbers to which they belong. The bracketed probable errors for the right ascension of the sun's apex are reduced to a great circle. The quantity σ is the mean square residual velocity.

The first solution for the nebulae is identical with Lundmark's[2] values, which are based on practically the same material. His values are:

$$\xi = -\ \ 96 \pm 48; \qquad \eta = +138 \pm 108 \text{ km/sec.}$$
$$\zeta = -629 \pm 90; \qquad K = +793 \pm\ \ 59 \text{ km/sec.}$$

By omitting N.G.C. 584, the velocity of the sun decreases from 600 to 500, or to even less than 400 km/sec. The last solution for the nebulae is probably the best and agrees closely with that derived from the globular clusters. The position of the sun's apex as determined from the nebulae and clusters can be fixed at $\alpha = 315°$, $\delta = +62°$, with an uncertainty of about 10° in each co-ordinate. The velocity as determined from nebulae and clusters is 350 and 300 km/sec., respectively, the latter having the higher weight.

---

[1] Several writers omit the negative signs of the right-hand side, and instead give V_0 a negative sign. As the direction of the sun's motion is given by A_0 and D_0, it seems to the writer that V_0 must be used without sign.

[2] *Observatory*, 47, 279, 1924.

TABLE II

SUN'S MOTION RELATIVE TO NON-GALACTIC NEBULAE AND GLOBULAR CLUSTERS

No.	ξ	η	ζ	K	$A_{\odot}$	$D_{\odot}$	$V_{\odot}$	σ	Remarks
	Non-galactic Nebulae								
	km/sec.	km/sec.	km/sec.	km/sec.			km/sec.	km/sec.	
43 . . .	− 98 ± 62	+112 ±140	−610 ±115	+785 ± 75	311° (±9)	+76° ±10	628 ±115	345	Mag. clouds omitted.
42*. . .	−196 ± 58	+162 ±127	−450 ±106	+647 ± 72	320 (±12)	+61 ±11	517 ±103	302	
45 . . .	−170 ± 66	+231 ±150	−246 ± 94	+565 ± 65	+306 (±13)	+41 ±17	378 ±121	380	Mag. clouds included with K-term.
45 . . .	−109 ± 60	+121 ±120	−506 ± 97	+737 ± 69	312 (±10)	+72 ±10	531 ± 97	344	Mag. clouds included without K-term.
44*. . .	−205 ± 56	+162 ±121	−386 ± 89	616 ± 65	321 (±12)	+56 ±11	468 ± 89	308	
45 . . .	− 65 ±102	+142 ±188	−332 ±144	+668 ± 94	295 (±19)	+65 ±26	367 ±120	. . . .	13 groups with equal weights. Mag. clouds included without K-term.
44*. . .	−111 ± 89	+160 ±160	−284 ±124	+622 ± 82	305 (±22)	+56 ±21	344 ±124	. . . .	
	Globular Clusters								
18 . . .	− 79 ± 42	+108 ± 41	−253 ± 50	+ 25 ± 30	306° (±8)	+62° ± 9	286 ± 49	113	
18 . . .	− 81 ± 41	+ 84 ± 27	−261 ± 47	0	314 (±7)	+66 ± 7	286 ± 45	114	$K=0$.
18 . . .	−104 ± 45	+108 ± 43	−288 ± 60	+ 21 ± 32	314 (±8)	+63 ± 8	325 ± 58	. . . . . .	8 groups of equal weight.
18 . . .	−106 ± 41	+ 88 ± 28	−299 ± 53	0	320 (±6)	+65 ± 7	329 ± 50	. . . . . .	8 groups of equal weight, $K=0$.

* N.G.C. 584 omitted.

The reality of this large solar motion can perhaps best be judged from the correlation diagram in Figure 1. This shows the correlation between observed radial motion and cos λ, where λ is the angular distance from the sun's antapex, which is assumed to be the same for the two classes of objects. If we omit N.G.C. 584, the correlation coefficients between V and cos λ for nebulae and clusters are $+0.54$ and $+0.73$, respectively, and the equations for the regression-lines of V on cos λ are, respectively,

$$V=452 \cos \lambda+648 \qquad \text{and} \qquad V=295 \cos \lambda+4 .$$

The Magellanic clouds are indicated by crosses in the diagram for the clusters, but are not used in the derivation of the regression-lines. All indications are that we are justified in our assumption of a vanishing value for the K-term for the clouds. The dotted horizontal line corresponds to $K = +616$ km.

The assumption of a constant K-term for the nebulae is probably only approximately correct; the K-term is probably much larger for N.G.C. 584 and smaller for the Andromeda nebula than for the rest of the objects. A variable correction to the wave-lengths would account for the fact that the dispersion in radial velocity is larger for the nebulae than for the clusters. The vanishing value of the K-term for the clusters can be seen directly from the second scatter-diagram in Figure 1.

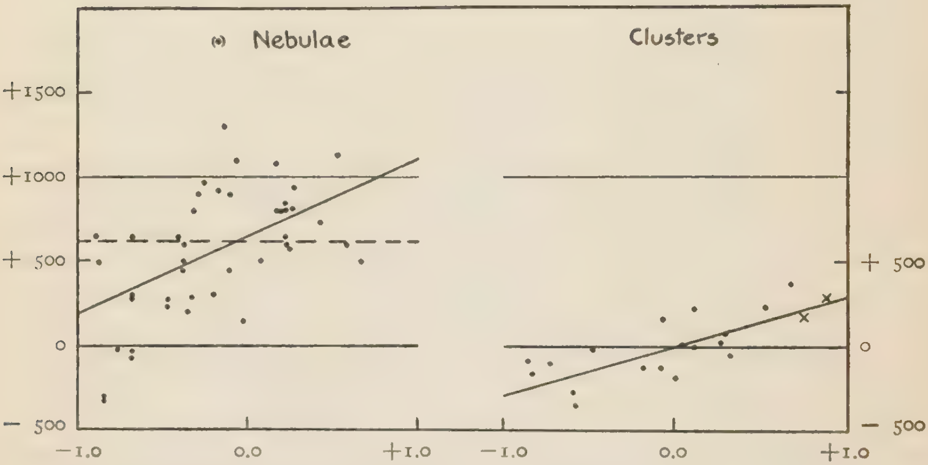

FIG. 1.—Diagram showing correlation between radial velocities (ordinates) and cos λ (abscissae) for nebulae and clusters.

The direction of the sun's motion is very nearly the same as that derived from the asymmetry in the distribution of stellar velocities on the assumption of the existence of a velocity-restriction in a fundamental reference-frame.[1] The direction of the sun's motion as derived from the asymmetrical velocity-distribution of stars in our neighborhood is $\alpha = 327°$, $\delta = +61°$, and its velocity relative to the stars of highest velocity-dispersion is about 280 km/sec.

---

[1] *Mt. Wilson Contr.*, No. 275; *Astrophysical Journal*, 59, 228, 1924.

RADIAL VELOCITIES AND CURVATURE OF SPACE

In Professor de Sitter's[1] theory of space-time of cosmical extent, a constant radius of curvature has been postulated, the expression for the line-element ds in space-time being given by the equation

$$ds^2 = -R^2[d\chi^2 + \sin^2\chi(d\theta^2 + \sin^2\theta\, d\phi^2)] + \cos^2\chi\, dt^2 . \qquad (3)$$

This expression is the equation of a hypersphere in five dimensions, the distance along a geodesic to a point being given by $\rho = R\chi$, where R is the curvature-invariant. Equation (3) differs from Einstein's expression for an elliptical (or cylindrical) space-time by the factor $\cos\chi$ for dt. In Einstein's world, the time-dimension is not curved, and the difference in curvature between space and time makes it possible to single out a fundamental space in which all the matter in the universe is at rest, and an absolute time, which is the time for an observer at rest in this absolute space. De Sitter's world, on the contrary, is perfectly isotropic.

When the distance to a star is very large, the variable $\chi = \rho/R$ may differ appreciably from zero, and when $\chi = \pi/2$, the interval ds becomes independent of dt. This is interpreted as meaning that the time appears to slow down at large distances, and we should accordingly expect an apparent slowing down of the atomic clock, i.e., a shift of the spectral lines to the red end of the spectrum. Such an effect would produce a fictitious positive radial velocity.

In Silberstein's[2] opinion, if we make the assumption that the motions are so adjusted that they are necessarily small when the object comes near the sun, we may expect a shift either to the red or to the violet.

The present collection of radial velocities can be used to ascertain whether the measured radial velocities are dependent upon the distances of the objects. The velocities of some globular clusters have been used for this purpose by Silberstein, but the result cannot be regarded as conclusive. One thing is obvious, however. If the nebulae studied are at about the same mean distance as the globular clusters, or if they are nearer, we cannot regard the large positive K-term as a De Sitter effect, as the K-term for the clusters must be very small. On the basis of De Sitter's theory, we may expect an increase of radial velocity (V) with distance; on Silberstein's theory, an increase of radial velocity, without regard to sign ($|V|$), with increasing distance from the sun.

---

[1] *Monthly Notices*, **78**, 3, 1917.

[2] *Monthly Notices*, **84**, 363, 1924; *Phil. Mag.*, **47**, 907, 1924; **48**, 619, 1924.

The writer has derived coefficients of correlation between distance, on the one hand, and radial velocity with and without sign (V and $|V|$), on the other, and similar coefficients after the velocities have been corrected for a solar motion of 300 km/sec. (V' and $|V'|$). The data for these correlations are collected in Table III. The distances for the globular clusters (ρ in kiloparsecs) are Shapley's[1] determinations. For the nebulae we do not know the distances, but we can probably get some rough indication of their relative distances by assuming that they have nearly the same total brightness. As a measure of the distance I have consequently used the quantity $\rho' = 10^{0.2m}$, where m is the total apparent brightness taken from Wirtz's[2] study. The correlation coefficients (r), together with the equations for the two regression-lines, are given in Table III. As an illustration, the scatter-diagram and the regression-lines for the correlation between $|V|$ and ρ are given in Figure 2. They may be compared with the cor-

TABLE III

CORRELATION TABLE

Objects	No.	Variates	r	Regression-Lines
Clusters..........	18......	V, ρ	-0.06	$V = -1.338\rho + 2;$ $\rho = -0.0029V + 19$
	18......	$\|V\|, \rho$	$+0.26$	$\|V\| = +3.281\rho + 77;$ $\rho = +0.0200\|V\| + 16$
	18......	V', ρ	$+0.02$	$V' = +0.326\rho + 18;$ $\rho = +0.0016V' + 19$
	18......	$\|V'\|, \rho$	$+0.33$	$\|V'\| = +2.770\rho + 43;$ $\rho = +0.0403\|V'\| + 15$
	18......	$V, \cos\lambda$	$+0.73$	$V = +295\cos\lambda + 4;$ $\cos\lambda = +0.001820V - 0.05$
Nebulae..........	29......	V, ρ'	$+0.28$	$V = +1.323\rho' + 545;$ $\rho' = +0.0596V + 53$
	29......	V', ρ'	$+0.23$	$V' = +0.960\rho' + 639;$ $\rho' = +0.0566V' + 52$
	41......	$V, \cos\lambda$	$+0.54$	$V = +452\cos\lambda + 648;$ $\cos\lambda = +0.000647V - 0.54$

---

[1] *Mt. Wilson Contr.*, No. 152; *Astrophysical Journal*, **48**, 154, 1918.

[2] *Lunds Observatorium, Meddelanden*, Serie II, No. 29, 1923.

relation data for V and $\cos\lambda$ as given in Table III and Figure 1. For the nebulae, the correlation between $|V|$ and ρ can be regarded as equivalent to the correlation between V and ρ, as nearly all the radial velocities are positive. The same holds for $|V'|$, which is nearly identical with V', as the K-term obviously must not be subtracted.

From Table III we see that the only correlation which can be accepted with any confidence is that between radial velocity and position in the sky (V and $\cos\lambda$). For the nebulae, the correlation

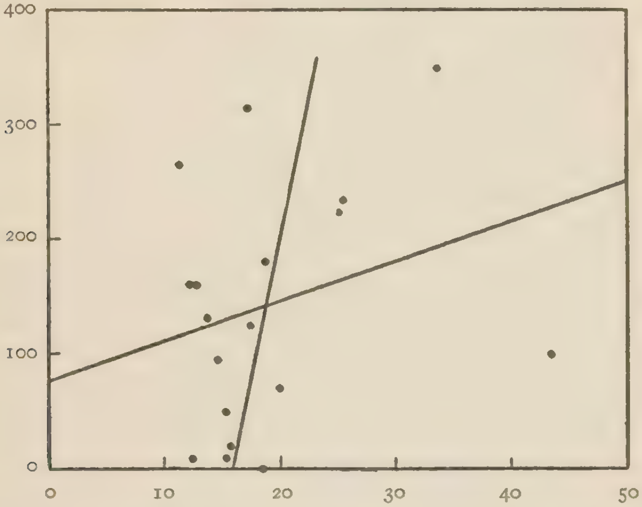

FIG. 2.—Scatter diagram showing correlation between radial velocities without regard to sign (ordinates) and distances in kiloparsecs (abscissae) for globular clusters.

coefficient is only +0.54, but the fact that the solar motion is nearly the same for the nebulae as for the clusters strengthens our belief that the correlation is real.

De Sitter's effect can be regarded as disproved by the clusters if their distances are of the same order as those of the nebulae. Silberstein's effect seems possible, but cannot be established by the data. It is significant, however, that the regression-line for the clusters, $|V| = 3.281\,\rho + 77$, does not go through the origin as expected from the theory. Silberstein's correlation is slightly improved if the radial velocities are corrected for the sun's motion.[1]

---

[1] This inclusion of the Magellanic clouds among the clusters does not materially alter the size of the correlation coefficient.

In conclusion we may say that we have found no sufficient reason to believe that there exists any dependence of radial motion upon distance from the sun. The only dependence fairly well established is one that is a function of position in the sky. This indicates a solar motion of 300 or 400 km/sec. in the direction $\alpha=315°$, $\delta=+62°$, which agrees with the solar motion as determined from the asymmetrical velocity-distribution of stars in our neighborhood.

MOUNT WILSON OBSERVATORY
November 1924

Contributions from the Mount Wilson Observatory, No. 293
Reprinted from the *Astrophysical Journal*, Vol LXI, pp. 363–388, 1925

THE ASYMMETRY IN STELLAR MOTIONS AS DETERMINED FROM RADIAL VELOCITIES

By GUSTAF STRÖMBERG

ABSTRACT

Group-motion and velocity-dispersion for different classes of objects.—From all available radial velocities the group-motion and velocity-dispersion have been determined for all classes of objects with the aid of ellipsoidal distribution-functions. For spectral classes B0–M the stars have been grouped according to the quantity $H=m+5\log\mu$. The constants of the velocity-ellipsoids for fifty groups are given in Table I. The results show a continuous change in group-motion with internal velocity-dispersion, which is expressed by a quadratic relation between group-motion along an axis in the direction $\alpha=309^{\circ}.8$, $\delta=+57^{\circ}.1$, and the dispersion along the same axis. The group-motion projected on this axis varies regularly from 9.0 km/sec. for the Cepheids of long period to 300 km/sec. for fast-moving objects, globular clusters, and spiral nebulae.

Velocity-distribution for all cosmical objects.—The velocity-distribution for the whole collection of objects studied can be expressed as a product of two symmetrical distribution-functions, S_1 and S_2, with different centers of symmetry. The center of the distribution S_1, which itself is expressed as a sum of concentric, ellipsoidal distributions, corresponds to a velocity of 14.8 km/sec. in the direction $\alpha=85^{\circ}.7$, $\delta=-22^{\circ}.0$, and the center of the second distribution, S_2, is a velocity of 300 km/sec. in the direction $\alpha=127^{\circ}$, $\delta=-56^{\circ}$. The opposite vectors are the velocities of the sun relative to these centers. The first distribution can be interpreted as the distribution-law of velocities within our local system of stars, and the second as a velocity-restriction in a universal world-frame in which the clusters and spirals are statistically at rest; but other interpretations are also possible.

1. It has been known for some time that the *general* distribution of stellar motions cannot be represented by a single ellipsoidal distribution (the ellipsoidal theory), by two or three spherical distributions (the two-stream and the three-stream theories), or by any kind of symmetrical frequency-functions. The existence of an asymmetry has been pointed out by Charlier; Boss, Raymond and Wilson; Adams and Joy; Oort, and the present writer, and is easily seen from the fact that stars of high velocity (larger than 100 km/sec.) do not move with the same frequency in opposite directions, but all move toward the region in the sky limited by galactic longitudes 134° and 343°, a region including little more than a hemisphere. This phenomenon is perfectly general, so far as we know, no exception having yet been found. The asymmetry is indicated

by an increase in group-motion in a certain direction with increase in the velocity-dispersion within the group. In *Contribution* No. 275[1] it was shown that, with the exception of the B stars, a quadratic relation between group-motion and dispersion represents the data fairly well. If this quadratic relation be accepted, it leads to the conception of a velocity-restriction in a universal world-frame in which the spiral nebulae and globular clusters are statistically at rest. As it is of importance to find to what extent and how accurately the quadratic relation between group-motion and dispersion actually represents the known stellar velocities, an analysis has been made of all available radial velocities. The results of this analysis are given in the following pages.

2. Practically all radial velocities utilized in this study have been printed in the publications of the different observatories, except those of the Cepheids of short period and some of those of long period for which data have been furnished me by Adams and Joy. The radial velocities for the non-galactic nebulae and the globular clusters have been summarized in *Contribution* No. 292.[2] The method of procedure used was to find the group-motion, relative to the sun, of a certain class of object, and determine the velocity-distribution relative to the centroid of the group with the aid of an ellipsoidal frequency-function. In many cases it was possible to use physical criteria for the grouping of the stars, such as spectral characteristics, length of period of light-variation, and nebulous appearance, which enable us to form groups of objects of different average velocity. Absolute magnitudes have not been used, since we have insufficient knowledge of this characteristic of stars in the southern hemisphere. To obtain a grouping in classes of different velocity-dispersion, the apparent magnitudes and the proper motions were used in combination with the spectral types. In order to secure sufficiently large groups all stars within certain limits of spectral subdivision were taken together and subdivided according to values of the quantity $H = m + 5 \log \mu$, where m is the apparent magnitude on the Harvard scale, and μ the annual proper motion, taken in general

---

[1] *Astrophysical Journal*, **59**, 228, 1924.

[2] *Astrophysical Journal*, **61**, 353, 1925.

from Boss's *Catalogue* or *Cincinnati Publications* No. 18. It is easily seen that

$$H = M + 5 \log T - 8.378 \,, \tag{1}$$

where M is the absolute magnitude and T the linear tangential velocity in km/sec.

As we know that the average velocity increases in general with M, and as we have strong reason to believe that a large tangential velocity is correlated with a large radial motion, we may expect that the grouping according to H will enable us to form groups of the same spectral class but with different velocity-dispersions. When H has been used as the basis for grouping, we can regard the procedure as a dissection of a velocity-distribution in several overlapping component distributions, whereas, when we use the other criteria for the grouping, we obtain the constants for a group with certain physical properties. As the proper motions, except for the "moving groups," are not used in the computation of the constants of the velocity-distribution, the main effect of selection in the list of known radial velocities is to change the proportion of objects belonging to the different groups.

3. In the following we will denote the radial velocity of a star relative to the sun by V; the right ascension and declination by α and δ (1900.0); the galactic longitude and latitude by l and b; the equatorial velocity-components by ξ, η, ζ; and the galactic velocity-components by x, y, z. The galactic system used is the standard system, the north pole of the galactic plane having the co-ordinates $\alpha = 190°$, $\delta = +28°$. The equations for converting equatorial into galactic co-ordinates are thus:

$$\left.\begin{aligned} x &= +0.1736\,\xi - 0.9848\,\eta \\ y &= +0.4624\,\xi + 0.0815\,\eta + 0.8829\,\zeta \\ z &= -0.8695\,\xi - 0.1533\,\eta + 0.4695\,\zeta \end{aligned}\right\} \tag{2}$$

From the radial velocities of the stars in the group we determine first the group-motion, which has the components ξ, $\bar{\eta}$, and ζ, from the equations of condition

$$\bar{\xi} \cos \alpha \cos \delta + \bar{\eta} \sin \alpha \cos \delta + \bar{\zeta} \sin \delta + K = V \,, \tag{3}$$

where K is Campbell's K-term. Changing the signs of $\bar{\xi}$, $\bar{\eta}$, and ζ, we obtain the components of the sun's motion relative to the objects studied. Denoting the right ascension and declination of the sun's apex by A_0 and D_0 and its velocity by v_0, we have

$$\left.\begin{aligned} v_0 \cos A_0 \cos D_0 &= -\bar{\xi} \\ v_0 \sin A_0 \cos D_0 &= -\bar{\eta} \\ v_0 \sin D_0 &= -\bar{\zeta} \end{aligned}\right\} \qquad (4)$$

In the determination of the axes of the velocity-ellipsoids the directions of the principal axes have been assumed to be the same for all the groups. This is probably not strictly correct, but facilitates the computation and is often necessary on account of the small number of objects in several of the groups. The assumed directions of the principal axes are:

	α	δ	l	b
a	271°.5	−17°.1	341°.1	− 0°.7
b	327.6	+61.2	71.0	+ 5.6
c	188.9	+22.5	259.5	+84.4

The direction of the axis denoted by b is made identical with the axis of asymmetry as determined in *Contribution* No. 275, which is in fair agreement with one of the principal axes of the velocity-ellipsoids. The letters a, b, and c represent, in the following, the dispersions (square root of the mean square of the velocity-components) along the three axes, and determine, at the same time, the axes of the velocity-ellipsoids.

To determine a, b, and c from the radial velocities, the following method was used. On a map circles were drawn around the six points where the three axes intersect the sphere. These circles had in general a radius of 45°, although in some cases, when the number of stars was small, the radius was increased to 50° or 55°. The residuals from the equations of condition (3) were computed and the arithmetic means of these residuals, disregarding their signs, were formed for the stars within the circles just mentioned, opposite areas being combined. Three values, θ_1, θ_2, and θ_3, of the average residual velocity were thus found. From these values the dispersions a, b, and c were derived by making the assumption that the velocity-distribution within each group could be represented by an ellipsoidal distribution-function. Such a function can be expressed by the formula

$$F(xyz)dx\,dy\,dz=\frac{N\,dx\,dy\,dz}{(2\pi)^{\frac{3}{2}}\,abc}\exp\left[-\frac{(x-\bar{x})^2}{2a^2}-\frac{(y-\bar{y})^2}{2b^2}-\frac{(z-\bar{z})^2}{2c^2}\right]. \quad (5)$$

The number of stars is here denoted by N; x, y, and z are the velocity-components along the principal axes, and the components of group-motion are denoted by $\bar{x}$, $\bar{y}$, and $\bar{z}$. From equation (5) we can derive the frequency-function of radial velocities for stars in $d\omega$, a small region of the sky, whose direction-cosines referred to the principal axes are γ_1, γ_2, and γ_3. We find, if we denote the residual (peculiar) radial velocities by V',

$$F(V')d\omega\,dV'=\frac{N\,d\omega\,dV'}{\sqrt{2\pi(a^2\gamma_1^2+b^2\gamma_2^2+c^2\gamma_3^2)}}\exp\left[\frac{-V'^2}{2(a^2\gamma_1^2+b^2\gamma_2^2+c^2\gamma_3^2)}\right]. \quad (6)$$

From equation (6) we derive

$$\overline{V'^2}=\sigma^2=a^2\gamma_1^2+b^2\gamma_2^2+c^2\gamma_3^2\,, \quad (7)$$

where σ is the mean square radial velocity for a small region in the sky, defined by its direction-cosines γ_1, γ_2, and γ_3.

If we form the mean square velocity for stars in circles of angular radius p, whose centers are at the intersections of the axes a, b, and c with the sphere, and denote by a'^2, b'^2, and c'^2 the means of the squares of the velocities for the three areas, we obtain, after combining opposite areas,

$$a'^2=a^2\,P+\frac{b^2+c^2}{2}\,(1-P)$$

$$b'^2=b^2\,P+\frac{a^2+c^2}{2}\,(1-P)$$

$$c'^2=c^2\,P+\frac{a^2+b^2}{2}\,(1-P)$$

$$P=\frac{1+\cos p+\cos^2 p}{3}$$

Solving these equations for a, b, and c, we find

$$\left.\begin{aligned}(3P-1)a^2&=(1+P)a'^2-(1-P)(b'^2+c'^2)\\(3P-1)b^2&=(1+P)b'^2-(1-P)(a'^2+c'^2)\\(3P-1)c^2&=(1+P)c'^2-(1-P)(a'^2+b'^2)\end{aligned}\right\} \quad (8)$$

For the particular case of $p=45°$ we have

$$a^2=1.4379\ a'^2-0.2189\ (b'^2+c'^2),$$

and similarly for b and c.

The values of a', b', and c' have been derived from the average velocities θ_1, θ_2, and θ_3 by multiplication with $\sqrt{\pi/2}=1.2533$. The effect of isolated large velocities is thus less than if the squares of the residual velocities had been used.

4. The detailed results of this analysis for fifty groups are given in Table I in the form of constants for the velocity-ellipsoids. This includes practically all known radial velocities except a few R and N stars, which are too few in number to be used as separate groups. The first twenty-nine groups include spectral types M, K, G, F, A, and B, and are all independent of one another, except group 27, which is a combination of groups 23–26. Groups 30 and 31 are the Cepheids of long and short period; group 32 contains the O stars, the elements being derived from Plaskett's radial velocities. The results from R. E. Wilson's study[1] of the space velocities of the O stars are given as group 33. Group 34 including stars with c characteristics (sharp spectral lines), is practically identical with the Pseudo-Cepheids; groups 35 and 36 are the bright-line nebulae (spectral class P). In the latter solution six objects of very high radial velocity have been omitted, the radial velocities determined by Campbell and Moore having been used.[2] Group 37 is based upon the radial velocities of the long-period variables, taken from Merrill's[3] determinations, and 38 is a group of Me stars with periods between 150 and 210 days, which in general have higher velocities than Me stars of other lengths of period.[4] Group 39 consists of the globular clusters, the solution given in *Contribution* No. 292,[5] based upon Slipher's determinations, having been used. Group 40 contains the spiral, elliptical, and irregular nebulae (by Hubble called "non-galactic nebulae") with continuous spectra, which are later referred to as "spirals." The

---

[1] *Astronomical Journal*, p. 841, 1924.

[2] *Lick Observatory Publications*, **13**, Part IV, 1918.

[3] *Mt. Wilson Contr.*, No. 264; *Astrophysical Journal*, **58**, 215, 1923.

[4] Cf. Merrill, *op. cit.*, p. 44.

[5] *Astrophysical Journal*, **61**, 353, 1925.

TABLE I

Group No.	1	2	3	4	5	6	7
Type	M0–M9	M0–M9	K4–K9	K4–K9	K4–M9	G9–K3	G9–K3
H	≤ −2.0	−1.9 to +3.0	≤ −2.0	−1.9 to +3.0	≥ +3.1	≤ −3.0	−2.9 to −2.0
No.	75	97	77	90	79	124	120
$\bar{H}$	− 3.64	− 0.66	− 3.68	− 0.33	+ 7.70	− 4.49	− 2.45
$\bar{m}$	5.09	5.30	5.04	5.51	8.12	4.88	5.12
$\underline{\mu}$	0.0179	0.0643	0.0180	0.0679	0.824	0.0134	0.0306
$\bar{\xi}$	+ 0.3	− 7.7	− 8.4	+ 4.2	−10.0	− 2.6	+ 0.3
$\bar{\eta}$	+11.8	+13.6	+19.9	+29.3	+16.4	+17.0	+12.2
$\bar{\zeta}$	− 8.7	−19.3	− 7.4	−17.5	− 4.0	−10.4	− 8.2
K	− 0.3	+ 0.8	+ 0.6	+ 4.6	....	+ 1.9	+ 2.3
v_0	14.6	24.8	22.8	34.4	19.6	20.1	14.8
A_0	269°	300°	293°	262°	301°	279°	269°
D_0	+36°	+51°	+19°	+31°	+12°	+31°	+34°
v_0'	14.6	21.4	20.9	34.1	16.2	20.0	14.7
θ'	14.0	20.8	14.0	22.9	30.1	12.0	12.9
θ	14.3	19.9	14.0	21.9	29.6	11.8	13.2
x	−11.6	−14.7	21.0	−28.1	−17.9	−17.2	−12.0
y	− 6.6	−19.4	− 8.8	−11.1	− 6.9	− 9.1	− 6.1
z	− 6.1	− 4.4	+ 0.8	−16.4	+ 4.3	− 5.2	− 6.0
a'	18.8	34.7	19.4	28.0	46.7	15.8	18.5
b'	17.4	23.1	15.2	24.5	24.8	13.8	14.9
c'	17.0	20.5	18.7	23.8	35.8	13.0	16.7
a	19.4	39.0	20.4	29.6	52.2	16.7	19.6
b	17.1	20.4	13.1	23.9	11.1	13.5	13.6
c	16.5	15.0	19.2	22.6	35.1	12.2	16.6
x'	− 7.0	− 3.6	−14.3	−19.4	−12.5	−10.8	− 7.6
y'	−12.1	−24.6	−17.4	−25.5	−13.7	−16.7	−11.9
z'	− 4.3	− 0.6	+ 3.5	−12.5	+ 6.5	− 2.6	− 4.2

Group No.	8	9	10	11	12
Type	G9–K3	G9–K3	G9–K3	G9–K3	G9–K3
H	−1.9 to −1.0	−0.9 to 0.0	+0.1 to +1.0	+1.1 to +3.0	+3.1 to +12.0
No.	102	139	109	100	104
$\bar{H}$	− 1.40	− 0.47	+ 0.49	+ 1.87	+ 5.96
$\bar{m}$	5.20	5.23	5.29	5.56	7.07
$\underline{\mu}$	0.0479	0.0724	0.1096	0.183	0.600
$\bar{\xi}$	− 4.0	− 1.4	+ 1.6	− 9.4	− 0.9
$\bar{\eta}$	+12.4	+17.4	+15.7	+36.8	+15.0
$\bar{\zeta}$	− 7.1	−15.7	−14.5	−19.7	−21.4
K	+ 0.6	− 1.2	+ 2.9	+ 3.7	+ 3.2
v_0	14.9	23.5	21.4	42.8	+26.1
A_0	288°	275°	264°	284°	273°
D_0	+28°	+42°	+43°	+27°	+55°
v_0'	14.3	23.0	20.8	41.7	23.6
θ'	17.0	18.4	23.3	24.6	23.3
θ	17.3	18.3	19.4	26.1	23.2
x	−12.9	−17.4	−15.2	−37.9	−14.9
y	− 7.1	−13.1	−10.8	−18.7	−18.1
z	− 1.7	− 8.8	−10.6	− 6.8	−11.5
a'	22.2	24.6	26.8[1]	38.9	32.2
b'	21.5	22.5	21.6	30.5	32.5
c'	18.2	18.9	20.9	31.8	23.5
a	23.2	26.0	28.9	41.9	33.7
b	22.0	22.7	20.4	28.0	34.3
c	16.3	16.5	19.2	30.4	18.3
x'	− 7.9	− 9.0	− 8.2	−24.3	− 4.5
y'	−12.5	−20.9	−18.2	−35.2	−24.5
z'	+ 0.2	− 5.6	− 7.9	− 1.2	− 7.8

TABLE I—*Continued*

Group No.	13	14	15	16	17	18
Type	Go–G8	Go–G8	Go–G8	Go–G8	Fo–F9	Fo–F9
H	≤ -2.0	−1.9 to +1.0	+1.1 to +5.0	+5.1 to +10.0	≤ -2.0	−1.9 to 0.0
No.	144	131	154	111	86	70
$\bar{H}$	− 3.37	− 0.53	+ 3.19	+ 6.51	− 4.35	− 0.74
$\bar{m}$	5.09	5.67	6.01	7.23	4.80	5.52
$\bar{\mu}$	0.0169	0.0575	0.2729	0.718	0.0148	0.0560
$\bar{\xi}$	+ 4.0	− 0.3	− 6.1	−11.9	+ 5.2	− 1.8
$\bar{\eta}$	+11.6	+17.2	+25.9	+37.4	+18.2	+14.7
$\bar{\zeta}$	−11.8	−11.4	− 8.1	−13.7	−11.5	−12.4
K	+ 2.0	+ 1.6	....	....	− 0.1	+ 0.5
v_0	17.0	20.6	27.8	41.6	22.1	19.3
A_0	251°	271°	283°	287°	254°	277°
D_0	+44°	+34°	+17°	+19°	+31°	+40°
v'_0	15.9	20.6	26.5	39.2	21.5	18.9
θ'	12.1	15.3	23.2	32.9	11.2	14.9
θ	11.5	15.0	21.9	30.4	11.1	15.4
x	−10.7	−16.9	−26.5	−38.9	−17.0	−14.8
y	− 7.6	− 8.8	− 7.8	−14.6	− 6.2	−10.6
z	−10.8	− 7.8	− 2.5	− 1.8	−12.7	− 6.5
a'	16.5	23.2[2]	38.8	42.9	18.1	22.2
b'	13.3	17.3	25.0	34.5	11.9	18.8
c'	14.1	13.8	20.9	34.4	15.[3]	15.8
a	17.6	25.8	44.0	46.2	19.7	24.0
b	12.4	16.5	21.7	32.4	9.0	18.6
c	13.6	9.4	12.7	32.1	15.	13.2
x'	− 5.8	−10.7	−19.6	−27.2	−12.0	− 7.9
y'	−13.4	−16.9	−19.7	−31.2	−15.4	−17.2
z'	− 8.8	− 5.2	+ 0.6	+ 3.1	−10.4	− 3.9

Group No.	19	20	21	22	23	24	25
Type	Fo–F9	Fo–F9[4]	Fo–F9[6]	B6–A9	B6–A9	B6–A9	B6–A9
H	+0.1 to +3.0	+3.1 to +5.0	+5.1 to +14.0	≤ -3.0	−2.9 to −2.0	−1.9 to −1.0	−0.9 to 0.0
No.	246	82	38	188	138	133	130
$\bar{H}$	+ 1.45	+ 3.84	+ 7.03	− 4.42	− 2.43	− 1.46	− 0.44
$\bar{m}$	5.53	6.09	7.61	5.15	5.15	5.14	5.12
$\bar{\mu}$	0.153	0.355	0.766	0.0122	0.0305	0.0479	0.0773
$\bar{\xi}$	+ 3.3	− 4.5	−36.6	− 1.2	+ 4.6	+ 3.2	+ 0.5
$\bar{\eta}$	+17.0	+35.8	+20.9	+13.4	+12.5	+16.5	+22.8
$\bar{\zeta}$	− 6.8	− 0.3	−99.5	−17.4	− 6.4	− 3.0	− 3.9
K	0.0	....	....	− 0.3	− 0.3	0.0	0.0
v_0	18.6	36.1	108.1	22.0	14.8	17.1	23.1
A_0	259°	277°	330°	275°	250°	259°	269°
D_0	+21°	0°	+67°	+52°	+26°	+10°	+10°
v'_0	18.1	31.2	67.9	20.3	14.0	15.8	21.6
θ'	16.2	25.0	71.1	10.1	10.2	12.7	10.9
θ	15.8	21.0	70.6	9.9	10.0	12.7	10.5
x	−16.2	−36.1	−27.0	−13.4	−11.5	−15.7	−22.3
y	− 3.1	+ 0.6	−103.1	−14.8	− 2.5	+ 0.1	− 1.4
z	− 8.6	− 1.7	−18.1	− 9.2	− 8.9	− 6.7	− 5.7
a'	26.1	41.1[5]	110[5]	13.0	12.8	17.0	14.8
b'	20.0	23.8	81	12.4	13.8	16.6	12.0
c'	15.6	25.0	70	10.6	10.0	10.9	12.1
a	28.9	48.4	122.	13.0[7]	12.5[7]	17.7[7]	15.4[7]
b	19.3	14.8	76.	12.0	14.1	17.0	10.6
c	10.7	18.1	55.	8.7	7.2	5.7	10.7
x'	−12.7	−31.9	+25.5	− 4.7	− 8.9	−13.9	−19.0
y'	−11.7	−16.8	−105.0	−20.6	− 9.0	− 8.3	−12.6
z'	− 6.9	+ 0.9	− 1.6	− 6.0	− 7.6	− 5.5	− 3.8

TABLE I—*Continued*

Group No.	26	27	28	29	30	31	32
Type	B6–A9	B6–A9	B0–B5	B0–B5	Cepheids Per. > 2.0 days	Cepheids Per. < 0.7 days	O5–O9^{18}
H	+0.1 to + 2.7	−2.9 to +2.7	≦ −4.0	−3.9 to + 0.1	....	....	....
No.	91	492	123	126	37^{13}	26^{16}	49
$\bar{H}$	+ 0.89	− 1.03	− 5.55	− 2.75	....	....	....
$\bar{m}$	5.44	5.19	4.19	4.77	....	....	....
$\underline{\mu}$	0.123	0.0570	0.0113	0.0313	....	....	....
$\bar{\xi}$	− 5.2	+ 0.9	− 5.5	− 4.0	− 2.4	−44	− 2.0
$\bar{\eta}$	+25.5	+17.7	+17.6	+15.3	+10.3	+60	+21.4
$\bar{\zeta}$	− 6.2	− 4.6	−11.0	−13.8	− 4.6	−80	−28.4
K	+ 0.5	+ 0.2	+ 6.0^{8}	+ 1.5^{11}	− 1.7	....	+11.8
v_0	26.8	18.3	21.4	21.0	11.5	109	35.7
A_0	281°	267°	287°	285°	283°	306°	275°
D_0	+13°	+15°	+31°	+41°	+24°	+47°	+53°
v'	25.2	17.7	20.7	20.2	11.2^{14}	92	32.8
θ'	13.4	12.1	7.3	9.7	11.4	57	22.2
θ	11.2	....	7.1	8.4	11.3	60	20.7
x	−26.0	−17.3	−18.3	−15.8	−10.5	−67	−21.5
y	− 5.8	− 2.2	−10.8	−12.8	− 4.3	−85	−24.3
z	− 2.2	− 5.7	− 3.1	− 5.4	− 1.7	− 8	−14.9
a'	12.8	....	8.7	9.3	15.8	73^{17}	22.0
b'	14.0	....	8.9	12.5	11.5	76	30.8
c'	11.6	....	8.9^{9}	11.0^{12}	....	88	....
a	12.1^{7}	16.4^{7}	8.1^{10}	7.4^{10}	17.3	74^{17}	19.6
b	14.1	14.6	8.4	13.0	10.0	74	33.9
c	10.0	9.1	8.4	10.6	(10)^{15}	74	(19)^{19}
x'	−20.1	−14.1	−10.9	− 7.7	− 7.2	−12	− 7.3
y'	−17.7	−10.9	−18.5	−19.4	− 9.0	−107	−33.5
z'	+ 0.5	− 4.0	− 0.2	− 2.3	− 0.2	+ 8	− 9.8

Group No.	33	34	35	36	37	38
Type	O5–O9^{18}	c stars^{21}	P	P	M1e–M6e	M2e–M5e P = 150–210 days
H	....	....	....	....	....	....
No.	41	66	107^{24}	101^{27}	86	13
$\bar{H}$	....	− 5.77	....	....	....	....
$\bar{m}$	....	4.12	....	....	....	....
$\underline{\mu}$	....	0.0105	....	....	....	....
$\bar{\xi}$	+ 2.3	+ 3.2	+ 0.5	− 7.1	−14.1	− 45
$\bar{\eta}$	+20.2	+22.1	+18.8	+20.7	+47.2	+ 75
$\bar{\zeta}$	−22.0	−13.4	−21.3	−20.8	−42.7	−136
K	....	− 0.7	+ 2.0	+ 1.8	....	....
v_0	30.0	26.1	28.4	30.2	65.2	162
A_0	263°	262°	268°	288°	287°	301°
D_0	+47°	+31°	+49°	+44°	+41°	+ 57°
v'	28.5	25.9	27.0	28.3	62.2	133
θ'	....	12.1	40.0	28.8	45.5	80
θ	....	11.9	35.2	28.6	40.1	70
x	−19.5	−21.2	−18.4	−21.6	−48.9	− 82
y	−16.7	− 8.6	−17.0	−20.0	−40.4	−134
z	−15.5	−12.5	−13.3	− 6.8	−15.0	− 36
a'	....	13.5	56.2	41.2	52^{30}	97^{31}
b'	....	16.3	31.7	31.7	55	80
c'	....	11^{22}	12^{25}	12^{28}	49	118
a	30^{20}	12.9	64.7	45.8	52	88^{32}
b	30	17.5	23.9	30.7	57	88
c	30	(12)^{23}	(15)^{26}	(15)^{29}	46	88
x'	− 9.2	−14.6	− 9.1	− 9.5	−23.7	− 7
y'	−26.1	−19.4	−25.6	−28.6	−60.5	−161
z'	−11.5	− 9.6	− 9.4	− 2.3	− 5.6	− 11

TABLE I—*Continued*

Group No.	39	40	41	42	43	44
Type	Globular clusters	Non-galactic nebulae	Stars of maximum space-velocity[37]	Stars of radial velocity > 100 km	Calcium clouds	Ursa Major group
No.	18	44[35]	22	49	64	17
$\bar{\xi}$	− 79	−111	−118	− 80	− 1.6	+ 8.7
$\bar{\eta}$	+108	+160	+ 78	+147	+16.1	−11.3
$\bar{\zeta}$	−253	−284	−243	−166	−12.4	−12.0
K	+ 25	+622	...	...	...	...
v_0	286	344	281	236	20.4	18.6
A_0	306°	305°	303°	299°	276°	127°.8
D_0	+ 62°	+ 56°	+ 60°	+ 45°	+37°	+40°.0
v_0'	220	281	189	210	20.1	...
θ'	90	239	...	100	5.6	...
θ	96	252	...	101	5.1	...
x	−120	−177	− 97	−159	−16.2	+12.6
y	−251	−289	−263	−171	−10.4	− 7.4
z	− 67	− 61	− 23	− 31	− 6.8	−11.5
a'	123[33]	...	...	(173)	5.4	...
b'	131	...	...	(93)	7.1	...
c'	112	...	...	(60)	...	...
a	117[34]	300[36]	207[38]	...	5	...
b	117	300	108	...	5	...
c	117	300	82	...	...	...
x'	+ 14	− 14	+ 40	− 58	− 9.2	+14.7
y'	−285	−344	−278	−229	−17.7	− 2.3
z'	− 22	− 8	+ 20	+ 5	− 4.2	−11.2

Group No.	45	46	47	48	49	50
Type	Taurus group	Praesepe group	Pleiades group	Perseus group	Scorpio-Centaurus group	Orion group
No.	39	10	11	29	131	17
$\bar{\xi}$	− 1.4	− 5.3	+ 1.3	− 6.3	− 1.9	+ 3.5
$\bar{\eta}$	+45.2	+40.7	+14.1	+17.0	+13.3	+17.0
$\bar{\zeta}$	+ 5.5	− 0.2	−13.4	− 9.9	−12.8	− 5.6
v_0	45.6	41.0	19.5	20.7	18.6	18.3
A_0	271°.8	277°.4	264°.8	290°.3	278°.2	258°.4
D_0	− 6°.9	+ 0°.3	+43°.3	+28°.7	+43°.6	+17°.9
x	−44.8	−41.0	−13.7	−17.9	−13.5	−16.2
y	+ 7.9	+ 0.7	−10.1	−10.2	−11.1	− 2.0
z	− 3.1	− 1.7	− 9.6	− 1.8	− 6.4	− 8.3
x'	−43.1	−36.4	− 7.2	−10.8	− 6.5	−13.3
y'	−14.7	−19.0	−16.7	−17.6	−17.0	−10.6
z'	− 0.8	+ 1.3	− 7.1	+ 1.0	− 3.8	− 6.7

NOTES

1. Group 10, one star with $V=+181$ km/sec. omitted.
2. Group 14, one star with $V=+183$ km/sec. omitted.
3. Group 17, from five stars only.
4. Group 20, four A stars included.
5. Groups 20, 21, $p=50°$.
6. Group 21, four A stars and three G stars included.
7. Groups 22, 23, 24, 25, 26, 27, dispersions are corrected for the systematic effect of a mean error in V equal to ±4.0 km/sec.
8. Group 28, probable error ±1.13 km/sec.
9. Group 28, from ten stars only.

10. Groups 28, 29, corrected for systematic effect of a mean error $= \pm 3$ km/sec.
11. Group 29, probable error ± 0.74 km/sec.
12. Group 29, from five stars only.
13. Group 30, *w* Virginis, $V = -60$ km/sec. omitted.
14. Group 30, a direct solution assuming the apex to have the value $A_0 = 270°$, $D_0 = +30°$ gives $V_0 = 12.3 \pm 1.56$, $K = -1.8 \pm 1.81$.
15. Group 30, assumed value.
16. Group 31, VX Herculis, $V = -380$ km/sec omitted.
17. Group 31, $p = 50°$, spherical distribution assumed. These values are corrected for the effect of a mean error in V of ± 15 km/sec.
18. Groups 32, 33, Plaskett's classification.
19. Group 32, assumed value.
20. Group 33, spherical distribution assumed by Wilson.
21. Group 34, this group includes Pseudo-Cepheids.
22. Group 34, from three stars only.
23. Group 34, assumed value.
24. Group 35, no omissions except Magellanic clouds.
25. Group 35, from three objects only.
26. Group 35, assumed value.
27. Group 36, six nebulae of velocities higher than 100 km/sec. omitted.
28. Group 36, from three objects only.
29. Group 36, assumed value.
30. Group 37, $p = 50°$.
31. Group 38, $p = 55°$.
32. Group 38, spherical distribution assumed.
33. Group 39, $p = 50°$.
34. Group 39, corrected for a mean error in V of ± 25 km/sec. Spherical distribution assumed.
35. Group 40, solution by groups. Magellanic clouds included without K-term.
36. Group 40, spherical distribution assumed. These values are subject to great uncertainties, particularly as the K-term is probably a variable quantity with large dispersion.
37. Group 41, determination based upon space velocities.
38. Group 41, the directions of the three principal axes are in order $L_1 = 164°$, $B_1 = +6°$; $L_2 = 73°$, $B_2 = +8°$; $L_3 = 291°$, $B_3 = +80°$.

constants given are those derived in the last-mentioned paper by a solution in groups, omitting N.G.C. 584 but including the Magellanic clouds without K-term. Group 41 is composed of stars, mostly of spectral type F, with large space velocities, which seem to form a separate group. All stars with radial velocities larger than 100 km/sec. are taken together as group 42. Since the selection of the last two groups is based directly upon the velocities of the stars in the group, they are not comparable with the other groups, but the group-motion may still be of some value. Group 43 contains the stars with stationary calcium-lines, which, according to Hartmann[1] and Plaskett,[2] are due to calcium clouds in space. This system of clouds seems to form a group with very small velocity-dispersion and can, so far as its motion is concerned, be regarded as equivalent to the other moving groups, the elements of which are given in columns 44–50. The constants for the Ursa Major group are means of Bottlinger's and Rasmuson's determinations; the elements for the Pleiades, Perseus, Scorpio-Centaurus, and Orion groups are taken from Rasmuson's study;[3] for the Taurus group, Boss's elements are given.

[1] *Astrophysical Journal*, **19**, 268, 1904.

[2] *Publications of the Dominion Astrophysical Observatory*, **2**, 287, 1924.

[3] *Lunds Observatorium, Meddelanden*, Serie II, No. 26, 1921.

For the Praesepe group, the constants are based upon a parallax of $0''.007$ and a radial velocity of $+33$ km/sec., determined by Adams and Joy.

The first line in Table I gives the current number of the group. This is followed by the types of objects studied, the limits of $H = m + 5 \log \mu$ (for those cases in which H has been used as a basis of grouping), and the number of objects in the group. Then follow the mean H, the mean apparent magnitude, and the geometric mean of the proper motions. This last quantity μ is defined by the equation

$$\mu = 10^{0.2(\bar{H} - \bar{m})} = 10^{\overline{\log \mu}} .$$

The equatorial components of the group-motion $(\bar{\xi}; \bar{\eta}, \bar{\zeta})$ and the K-term determined from the equations of condition (3) are next given. In several cases, especially for faint stars of large proper motion (large H), the observed stars are mainly in the northern hemisphere and the K-term is thus difficult of determination and is supposed to be small or zero. The sun's velocity relative to the group is next given in polar equatorial co-ordinates (v_0, A_0, D_0). The sun's velocity projected on an axis in the direction of the standard apex $(A_0 = 270°, D_0 = +30°)$ is denoted by v_0'. This may be used in computing mean parallaxes, but the mode of selection of the stars must be taken into account. θ' is defined by the equation

$$\theta' = \sqrt{2/\pi}\, \sigma = 0.7979\, \sigma ,$$

σ^2 being the mean of the squares of the residual velocities. It can be compared with θ given in the next line, which is the average residual radial velocity. These two values would be identical if the distribution could be exactly represented by an ellipsoidal distribution-function.

The velocity-components of the group-motion referred to the standard galaxy are denoted by x, y, and z. The mean square velocity in the areas of radius p around the principal vertices are denoted by a', b', and c'; a, b, and c are the dispersions along the three principal axes, and are identical with the axes of the velocity-ellipsoids. The last three lines show the components of the group-motion projected on three new axes (x', y', z'), the directions of which will be given later.

On account of the nature of the grouping, very few omissions had to be made, and these are all indicated in the notes.

5. We see immediately that the dispersion, defined by a, b, c, or by θ, increases in general with the value of H, which shows, as had been anticipated, that the velocity-components are not independent of one another. Part of this increase is due to the correlation between the absolute magnitude, which enters into H (cf. eq. [1]), and the velocity-dispersion. We see further that in general v_0 increases with H and with the dispersion, a correlation which we should expect if the distribution were asymmetrical.

The small value for the sun's velocity relative to Cepheids of long period ($v_0 = 12.3$ km/sec. Cf. note 14) is of special importance, as this affects the mean parallax of these stars and consequently the distances of the clusters, for the reason that the absolute magnitudes of the Cepheids in the clusters are assumed by Shapley to be the same as those of the Cepheids of the same period in our local system. It also affects Hubble's estimated distances of the spirals, which are based upon the same assumption. A change of solar motion from 20.0 to 12.3 km/sec. produces a change in the absolute magnitude of +1.06 and decreases the distances by 38 per cent.

The change in the declination of the sun's apex with increasing H and with increased dispersion is also of interest. In general, the declination increases with H, but this increase is counteracted by the abnormal group-motion for the dwarfs referred to later. It is possible that the observed variation in the declination of the sun's apex as determined from proper motions is almost entirely due to the asymmetrical velocity-distribution. Since apparently faint stars, which, of course, are not the same as dwarf stars, are in general intrinsically fainter than the apparently brighter stars, and presumably have a higher velocity-dispersion, we may expect an increase in the declination of the sun's apex with decreasing apparent brightness. On account of the grouping used here and the small number of faint stars with small proper motion, the rate of this shift with apparent magnitude cannot be determined.

The general result of this study is that the sun's motion is not a constant vector but changes greatly with the class of object to which the motion is referred. Our next purpose is to find if any definite laws can be established for the variation in group-motion. Figure 1 is a diagram giving the projections of the velocity-ellipsoids in the plane of the standard galaxy (xy-plane). The sun is at the origin, and a line from the origin to the center of an ellipse or circle indicates the group-motion projected on the galactic plane,

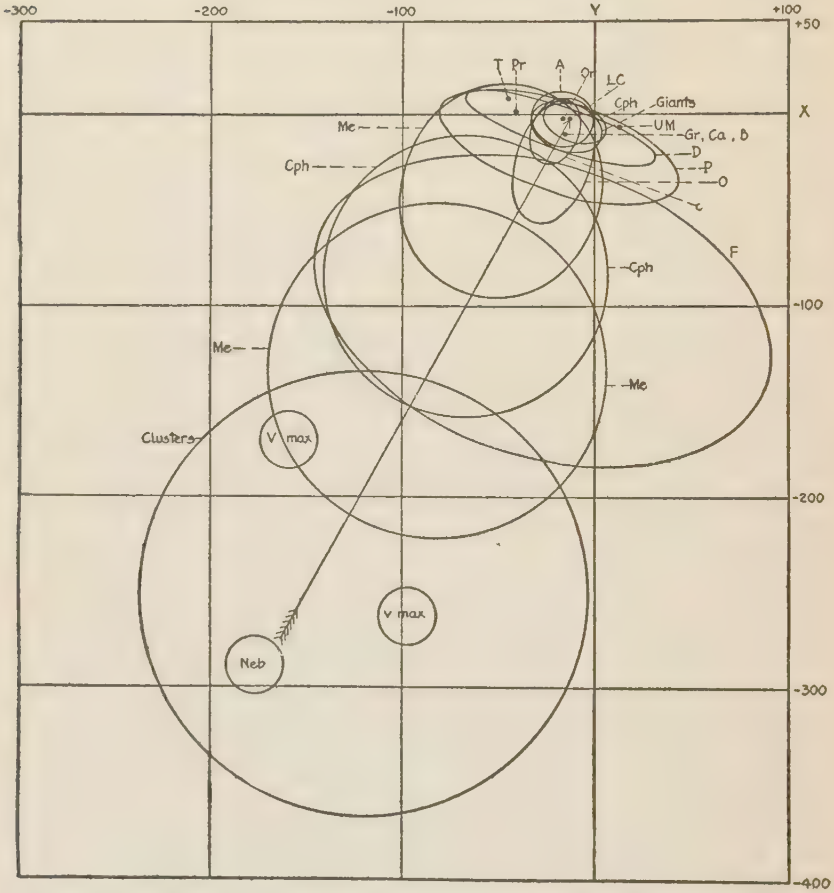

FIG. 1.—Projection of a number of velocity-ellipsoids on the galactic plane. The sun is at the origin, and a vector from the origin to the center of an ellipse or circle indicates the velocity of a certain group of objects, projected on the galactic plane. The principal axes of the ellipses are equal to the velocity-dispersion in the direction of the axes, except for the circles marked "V max," "v max," and "Neb," which indicate simply the group-motion. The points refer to moving groups with small internal velocity-dispersions.

and the size of the axes of the ellipses indicates the dispersions a and b. To avoid confusion only a few samples from the first twenty-nine groups are included in the diagram. Stars of spectral types F0–M with $H < -2.0$ have been combined in one group, the constants for which are as follows:

No.	x	y	z	a	b	c	x'	y'	z'	
626	−14.5	−7.4	−7.0	18.7	13.0	15.1	−14.4	−9.2	−4.9	km/sec.

This group is marked "Giants" in the diagram. Further, the velocity-ellipsoids for groups 5, marked *D* (dwarfs), 21 (*F*), 27 (*A*), 30 (*Cph*), 31 (*Cph*), 32 (*O*), 34 (*c*), 35 (*P*), 37 (*Me*), 38 (*Me*), and 39 (Clusters) are also shown in the figure. The group-motions for groups 40, 41, and 42 are marked by small circles with the notation *Neb*, v_{max}, and V_{max}, respectively. The velocity-vectors for the Ursa Major, Taurus, Praesepe, and Orion groups are indicated by points marked *UM*, *T*, *Pr*, and *Or*, respectively. The velocities of the Calcium Clouds, the Pleiades, Perseus, and Scorpio-Centaurus groups, and the B stars (groups 28 and 29) are very nearly alike, and have been combined into one point marked *Gr*, *Ca*, *B*, which has the co-ordinates $x = -15.9$, $y = -10.9$, $z = -5.5$ km/sec.

From the diagram we see that the centers of the velocity-ellipses show a marked shift toward the third quadrant of the xy-plane as the ellipses grow larger. This is in accordance with the results from space velocities and radial motions previously given in *Contribution* No. 275.[1] This shift determines a certain axis whose galactic longitude is now found to be $61^\circ\!.5$ with an uncertainty of about $\pm 5^\circ$. Projecting the velocity-ellipsoids on a plane through a line in galactic longitude $61^\circ\!.5$, we find the galactic latitude to be $+9^\circ\!.0$. This new projection is shown in Figure 2. The axis, of galactic longitude $61^\circ\!.5$ and latitude $+9^\circ\!.0$, is the direction of motion of objects of small velocity-dispersion relative to objects of large dispersion, and in my former investigation was estimated to have the direction $l = 71^\circ$, $b = +5^\circ$. The projections of this vector in the xy-plane and in the plane through the z-axis are indicated by arrows in Figures 1 and 2.

We will now project the velocity-ellipsoids on three new axes

---

[1] *Astrophysical Journal*, **59**, 228, 1924.

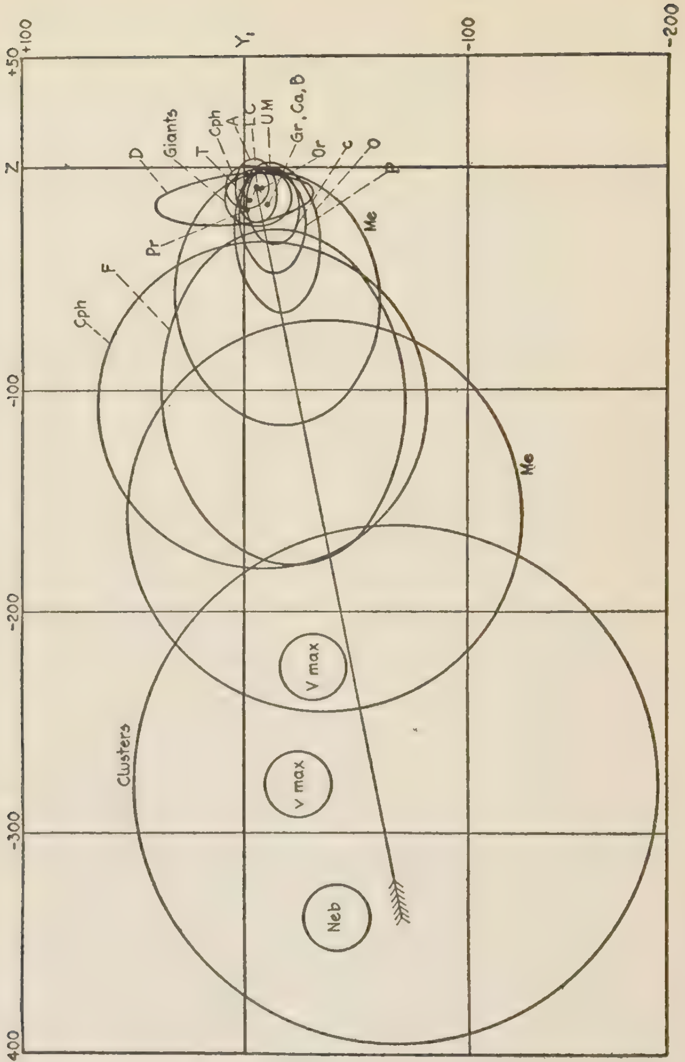

FIG. 2.—Same as Fig. 1, but the projection is here on a plane perpendicular to the galactic plane. The y_1-axis lies in galactic longitude 61°5, and the z-axis points toward the north pole of the galactic plane.

(x', y', z'), of which y' has the direction just determined and the x'-axis has zero galactic latitude. The directions of the new axes are:

	l	b	a	δ
x'	331°5	0°0	265°7	−24°9
y'	61.5	+ 9.0	309.8	+57.1
z'	241.5	+81.0	185.4	+20.0

The components of the group-motion projected on these axes appear in the last three lines of Table I. The axes coincide nearly with the directions of the principal axes assumed at the beginning.

If we study the velocity-components x', y', and z' we find that z' varies very little throughout the groups studied, the values with the largest deviations having the smallest weights. The x'-component varies somewhat more, but its variation does not seem to be systematic, except that it has an algebraically smaller value for the dwarf stars (groups 5, 11, 15, 16, 20) than for the giants. This may be due to the selection of stars of large proper motion in combination with a correlation between radial and transverse motion. The same applies to the variation of x' with H among the A stars (groups 23 to 26) where, in the absence of an asymmetry, the dispersion along the x'-axis produces a change in x' with H.

The y'-component varies enormously, from −9.0 for the Cepheids[1] of long period to −344 for the spirals. The variation in y' does not seem to be a function primarily of spectral type, absolute magnitude, or mass, but is correlated with the dispersion (b) along the same axis, and the result of the plotting is shown in Figure 3, where *all* the groups are indicated (except 23, 24, 25, and 26, which are combined in group 27). The relation between y' and b can be represented, throughout the whole range, by the parabola

$$\left.\begin{aligned} y' &= -pb^2+\beta' \\ p &= 0.0192 \text{ sec./km} \\ \beta' &= -10.0 \text{ km/sec.} \end{aligned}\right\} \qquad (9)$$

A slight ambiguity is involved here. It is, of course, possible to find a relation between y' and the dispersion along the two other

---

[1] Groups 23 and 24 (A stars) show numerically smaller values of y' than the Cepheids, but the combined group (27) has $y' = -10.9$.

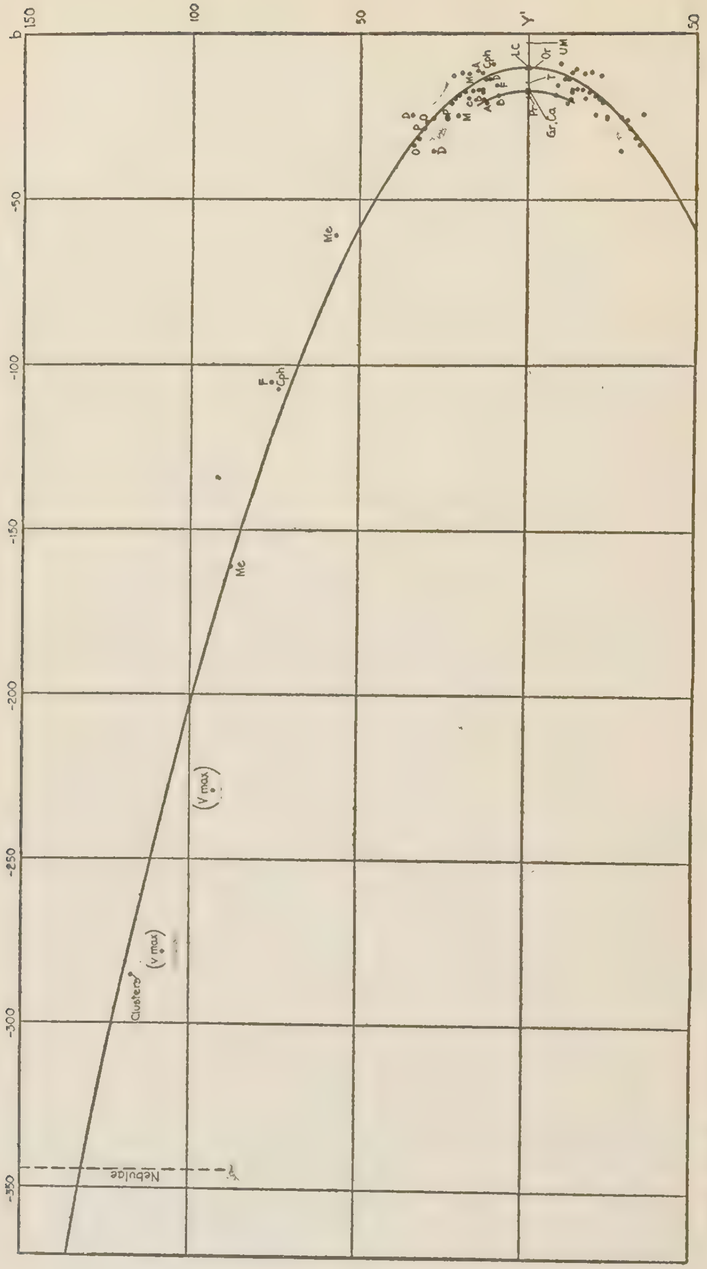

FIG. 3.—Relation between group-motion (abscissae), projected on an axis y' in galactic longitude 61°.5 and latitude +9°, and the velocity dispersion parallel to this axis (ordinates). This relation is expressed by a parabola.

axes, a and c, but this does not lead to any relation that can be simply interpreted like the one just given. Further, in the cases where a and c differ considerably from b, as in groups 5 and 21, it is the dispersion b, and not a or c, which varies regularly with y'.

The case of the dwarfs of type K4 to M (group 5) is of special interest. Here we have a group of large velocity-dispersion (average velocity $\theta = 29.6$), which gives a small value of y' (-13.7 km). But the velocity-ellipsoid is very elongated, and the axis b is of the right size for the corresponding value of y'.

As found in the previous study, the B stars (groups 28, 29) fall off the parabola in Figure 3. The same applies to the A stars for $H < -3.0$ (group 22), which have a large group-motion and a fairly small dispersion. The sudden change in group-motion among the A stars for the value $H = -3.0$, i.e., in passing from group 22 to 23, is certainly real and very illuminating. It shows that the apparently bright A stars of very small proper motion, which of course are mainly of exceedingly high luminosity, share the motions of the B stars and probably are in some way connected with the B-star system. On the other hand, we see that the moving groups, Perseus, Pleiades, Scorpio-Centaurus, and the Calcium clouds have the same group-motion as the B stars; in fact a large proportion of the B stars is included in the Scorpio-Centaurus group. We can even draw a new parabola through the points represented by groups 22, 28, and 29, parallel to the principal parabola, which cuts the y'-axis at the point represented by the four moving groups just mentioned. The c stars are represented by a point intermediate between the two parabolas and may include stars belonging to the two systems. Although the existence of the second parabola cannot be proved, there is no doubt that the B stars, the most luminous A stars, and the four moving groups mentioned have approximately the same group-motion, and do not fit so well in the general relation between group-motion and dispersion as the other objects. The scattering of the points around the parabola may be due to a mixture of two systems of objects.

The point where the principal parabola cuts the y'-axis has the co-ordinate $y' = -10.0$ km/sec. The mean of the x'- and of the z'-co-ordinates in combination with this last value of y' constitutes the apex of a parabola in a four-dimensional space (x', y', z', b) and gives us a fundamental velocity whose components we denote by α', β', and γ'. This point, which corresponds to the "limiting center" in my previous study, is marked *L.C.* in the three diagrams, and has the following co-ordinates:

$\alpha'=x'=-10.1\pm0.47$	$x=-13.3$	$\xi=+\ 1.0$	$\alpha=85\overset{\circ}{.}7$
$\beta'=y'=-10.0\pm1.0$	$y=-\ 3.3$	$\eta=+13.7$	$\delta=-22\overset{\circ}{.}0$
$\gamma'=z'=-\ 4.1\pm0.25$	$z=-\ 5.6$	$\zeta=-\ 5.5$	$v=14.8$

The velocity-vector corresponding to the limiting center is very nearly the same as the most frequent velocity found for later-type stars. The value for this velocity given in *Contribution* No. 245, page 28,[1] is $\alpha=86\overset{\circ}{.}2$, $\delta=-30\overset{\circ}{.}8$, $v=13.4$ km/sec., or $x'=-7.6$, $y'=-10.2$, $z'=-4.1$ km/sec.

The asymmetrical position in velocity-space of the most frequent velocity has also been pointed out by Boss, Raymond, and Wilson.[2] The small value for the sun's velocity when referred to the center of mass of a number of stars, as determined by Balanowsky and Samoïlova,[3] is due to the fact that in general the stars of high luminosity, which have been assigned the greater mass, have a smaller group-motion relative to the sun than those of less luminosity. The solar motion, whether we take the masses of the stars into account or not, is not a definite velocity-vector, but is greatly affected by the relative proportion of giant and dwarf stars in the system relative to which the sun's motion is determined. This phenomenon has also been found by Seares[4] by comparison of the secular parallaxes with the accepted luminosity and density functions.

The masses of the stars do not seem to enter in any simple way. Although, as has been pointed out by Halm and more thoroughly investigated by Seares,[5] there is a tendency to equipartition of kinetic energy among several classes of stars, there are several prominent exceptions. The Cepheids of short period, although less luminous and perhaps of less mass than the Cepheids of longer period, can hardly have masses considerably below those of the dwarf stars. The same applies to the Me stars and to a number of F stars of large proper motion. The O stars and the c stars, for instance, which have very large masses, show a larger dispersion b and a larger group-motion than the dwarf stars of types K4–M9.

---

[1] *Astrophysical Journal*, **56**, 292, 1922.

[2] *Astronomical Journal*, **35**, 26, 1923.

[3] *Astronomische Nachrichten*, **222**, 290, 1924.

[4] *Mt. Wilson Contr.*, No. 281; *Astrophysical Journal*, **60**, 50, 1924.

[5] *Mt. Wilson Contr.*, No. 226; *Astrophysical Journal*, **55**, 165, 1922.

6. The result of this analysis is that we have found a constant vector whose components are α', β', and γ', and a relation between group-motion and dispersion defined by the equations

$$\overline{x'}=\alpha' , \qquad \overline{y'}=-pb^2+\beta' , \qquad \overline{z'}=\gamma' ,$$

which define an axis in space[1] and a numerical relationship. If we accept this relationship, we can now write down the frequency-function for the whole collection of objects in Table I, excluding the B-star system previously defined and the Ursa Major, Taurus, Praesepe, and Orion groups, which probably must be regarded as individual objects, in the following form:

$$F(x'y'z')dx'dy'dz'$$

$$=\frac{dx'dy'dz'}{(2\pi)^{\frac{3}{2}}}\sum_{\nu}\frac{N_\nu}{a_\nu b_\nu c_\nu}\exp\left[-\frac{(x'-\alpha')^2}{2a_\nu^2}-\frac{(y'-\beta'+pb_\nu^2)^2}{2b_\nu^2}-\frac{(z'-\gamma')^2}{2c_\nu^2}\right] . \qquad (10)$$

This equation can be simplified, and we write

$$F=\exp\left[-p(y'-\beta')\right]\sum_{\nu}A_\nu\exp\left[-\frac{(x'-\alpha')^2}{2a_\nu^2}-\frac{(y'-\beta')^2}{2b_\nu^2}-\frac{(z'-\gamma')^2}{2c_\nu^2}\right] . \qquad (11)$$

There is one fact, however, which we now wish to emphasize. Besides stars and nebulae which are all within about 1000 parsecs we have in our study included the globular clusters and the spirals (non-galactic nebulae). The clusters are certainly very distant objects and, according to Hubble and Lundmark, the spirals are at even greater distances. There may still be some doubt about the distances of the spirals, especially in view of van Maanen's determinations of the internal motions, but their distances are at least above 1000 parsecs, and they may be at distances of the order of 300,000 parsecs (a million light-years). The group-motion and the dispersion for the clusters is approximately the same as that of the fastest-moving objects in our local system. The velocity-ellipsoid for the clusters seems to form the limit in the sequence of velocity-ellipsoids. Group 41 has even larger dispersion (a) along the x'-axis than the dispersion for the clusters, but this group as well as group 42 is selected on the basis of motion, and as the dispersion is in general largest along the x'-axis, we have made a selection of stars of large motion along the x'-axis. The spirals have about the same group-motion as the clusters, provided we omit the highest velocity (+1800 km/sec. for N.G.C. 584), but the dispersion for the spirals is much larger than for the clusters and the high-velocity stars, and consequently does not fit the parabola in Figure 3. It is probable that the K-term, which for the spirals has the enormous value of 600 km/sec., has a physical meaning and varies widely, being small for the Andromeda nebulae and the Magellanic clouds but very large for N.G.C. 584. If the dispersion in the K-term is very large, the actual dispersion in velocity for the spirals may be of the same order as that of the clusters.[1] As long as we do not know the cause of the large K-term or any law for its variability, we cannot correct for the extra dispersion. It does not seem to vary appreciably with distance, as would be the case if it were solely an effect of curvature of space-time.[2]

---

[1] The quantity p can be regarded as a vector, the direction of which is toward the negative y'-axis.

Equation (11) is a product of a symmetrical function and another function of the form $\exp[-p(y'-\beta')]$, which is found to be constant for all the groups. It expresses the law for the increase in dispersion with group-motion as we pass along the negative y'-axis, but it does not indicate whether there is a limit to the sequence of velocity-ellipsoids or not. The limiting velocity-ellipsoid is now found to be equal to the velocity-ellipsoid for the clusters, and we can find an explicit expression for this limit by a simple transformation of equation (11).

---

[1] A dispersion in the K-term of 275 km/sec. would bring the velocity-dispersion for the spirals down to 120 km/sec., which is about the same as that for the clusters.

[2] Cf. *Mt. Wilson Contr.*, No. 292; *Astrophysical Journal*, **61**, 353, 1925.

We write

$$\left.\begin{aligned}
F &= S_1 S_2 \\
S_1 &= \sum_{\nu} B_\nu \exp\left[-\frac{(x'-\alpha')^2}{2}\left(\frac{1}{a_\nu^2}-\frac{1}{l_1^2}\right)-\frac{(y'-\beta')^2}{2}\left(\frac{1}{b_\nu^2}-\frac{1}{l_2^2}\right)\right. \\
&\qquad\qquad\qquad\qquad\qquad\qquad\left.-\frac{(z'-\gamma')^2}{2}\left(\frac{1}{c_\nu^2}-\frac{1}{l_3^2}\right)\right] \\
S_2 &= \exp\left[-\frac{(x'+x_0')^2}{2l_1^2}-\frac{(y'+y_0')^2}{2l_2^2}-\frac{(z'+z_0')^2}{2l_3^2}\right] \\
x_0' &= -\alpha' , \qquad y_0' = -\beta' + p l_2^2 , \qquad z_0' = -\gamma'
\end{aligned}\right\} \quad (12)$$

S_1 and S_2 both represent symmetrical distributions, the center of symmetry of the first function being α', β', γ' and the center of the second function $-x_0'$, $-y_0'$, $-z_0'$. When the dispersions, represented by the quantities a, b, and c, increase up to their limits l_1, l_2, and l_3, the center of the distribution moves regularly from the center of the first distribution S_1 to that of the second distribution S_2. The name "limiting center" applied to α', β', γ' in my former study is due to this circumstance. The limits of the dispersion, l_1, l_2, and l_3, may well be equal, in which case the distribution S_2 is spherical, as seems to be the case for the clusters.

Putting the limiting value of the group-motion equal to that derived from clusters and spirals, we find this limit to be about 300 km/sec. in the direction of the negative y'-axis, and we have thus $y_0' = +300$ km/sec. If we use the known value of β' and p in combination with the dispersion for the cluster, we have $y_0' = pb^2 - \beta' = +273$. The group-motion for group 41 gives $y_0' = +278$. The velocity-vector x_0', y_0', z_0' is the velocity of the sun relative to the clusters, spirals, and fast-moving objects in general, and we can assign the following values to the components of this motion:

$$\left.\begin{aligned}
x_0' &= -\alpha' = +10.1 \text{ km/sec.} \\
y_0' &= +300 \pm 50 \quad \text{km/sec.} \\
z_0' &= -\gamma' = +4.1 \text{ km/sec.}
\end{aligned}\right\} \qquad (13)$$

In polar co-ordinates we find the velocity of the sun relative to the center of the distribution S_2 to be 300 km/sec. in the direction

$$\left.\begin{array}{ll} \alpha=307^\circ & l=60^\circ \\ \delta=+56^\circ & b=+10^\circ \end{array}\right\} \qquad (14)$$

The uncertainty in this apex is about 5° in galactic longitude and 3° in galactic latitude.

When y'_0 is known we can determine the value of l_2 from the equation $pl_2^2=y'_0+\beta'$. We have thus $l_2=123$ km/sec.

7. We will now attempt a physical interpretation of the two velocity-distributions S_1 and S_2. The function S_1 is a sum of concentric, ellipsoidal distributions, the co-ordinates of the center being α', β', γ', and can be regarded as a velocity-restriction relative to this center. This means simply that high velocities are less frequent than the smaller velocities, and that velocities of the same size are equally frequent in opposite directions, provided they are referred to this center. The same applies to the distribution S_2, which is another symmetrical distribution, its center having the co-ordinates $-x'_0$, $-y'_0$, $-z'_0$. The fundamental axis (y') is a line joining these two centers, and is represented by the arrows in Figures 1 and 2. Using the same terminology as for the distribution S_1, we may say that S_2 represents an additional velocity-restriction in a co-ordinate system in which the globular clusters and the spirals are statistically at rest. On account of its great size, and the apparent impossibility of ever observing a larger system, we will call this system the "world-frame." The distribution of velocities for almost all known cosmical objects can thus be represented by a product of two symmetrical distribution-functions. The first of these (S_1) represents probably the internal motions in our local system of stars, or rather what they would be if S_2 were not acting while S_2 represents a statistical restriction of velocities in a world-frame of enormous dimensions. This local system is probably identical with "Kapteyn's Universe," the dynamics of which has been studied by Kapteyn[1] and by Jeans.[2] The B stars studied and the A stars of high luminosity probably belong to Shapley's local star cloud, whose existence is indicated by

---

[1] *Mt. Wilson Contr.*, No. 230; *Astrophysical Journal*, **55**, 302, 1922.

[2] *Monthly Notices*, **82**, 122, 1922.

the fact that the plane of concentration for the bright B stars is inclined about 10° to the galactic plane.[1] The existence of the second distribution (S_2) indicates that the motions of the stars in the local (Kapteyn) system are determined not only by the gravitational field due to this system, but also by an outside field connected with the system of clusters and spirals.

The nature of the connection between the stars in the local system and the world-frame is not known, but there are several ways of explaining this connection.

The effect may be due to encounters between stars in the local system and stars belonging to the world-frame. This does not seem probable on account of the extremely low density of the larger system, and because, further, we should expect a strong correlation between group-motion and the masses of the stars. It can hardly be due to a system of dust at rest relative to the world-frame, as we should then expect a correlation between group-motion and the density of the stars.

The general gravitational field due to the larger system combined with the field of the local system may possibly produce a velocity-distribution similar to the one observed. On account of the low density and elongated shape of the larger system this explanation seems very improbable.

Another explanation is possible if we are allowed to regard the additional velocity-restriction as due to the action of a stationary medium in which the whole cosmical system is imbedded. The velocity vector (x'_0, y'_0, x'_0) is then the velocity of the sun relative to this medium, and l_1, l_2, and l_3 (which we will assume to be alike and equal to l) determine the effectiveness of the restrictive action, presumably dependent upon the mechanism of the interaction between the stars—or the electrons within the stars—and the medium. The dispersion in the spherical distribution S_2, whose center is at rest in the medium, is then $l = 123$ km/sec. and the most frequent velocity is $\sqrt{2}\, l = 174$ km/sec. The stars in our local system have in general a velocity of about 300 km/sec. relative to the world-frame, but they belong together and must in this connection be regarded as one unit, just as we have regarded the globular clusters as individual objects.

---

[1] *Astronomische Nachrichten*, Jubiläumsnummer, p. 25, 1921.

A popular description of the velocity-distribution and a discussion of the possible interpretations are given in *Scientific Monthly*, November, 1924.

The writer stands under great obligation to Mr. W. P. Hoge and Miss Marguerita Wiberg for the valuable help they have given in the compilation of the observational data and in the extensive computations.

Mount Wilson Observatory
January 1925

Contributions from the Mount Wilson Observatory, No. 294
Reprinted from the *Astrophysical Journal*, Vol. LXI, pp. 389–417, 1925

DISCOVERY AND OBSERVATIONS OF STARS OF CLASS Be

By PAUL W. MERRILL, MILTON L. HUMASON, and CORA G. BURWELL

ABSTRACT

Stars of class B whose spectra contain emission lines of hydrogen.—Three reasons for studying these spectra are suggested: (1) possible assistance in the interpretation of the typical nova spectrum; (2) the bright lines appear to be sensitive indicators of conditions in stellar atmospheres; (3) unusual properties of hydrogen atoms may be involved.

The *discovery* of these stars by other observers has usually been made from the Hβ line, but Hα serves better because of its greater intensity. By photographing the red portion of the spectrum we have discovered 90 early-type stars with hydrogen emission. These are listed in Table I. Eighty-four of the stars were found from objective-prism observations with the 10-inch Cooke telescope on Mount Wilson.

Data concerning the Hα line in *Be stars*, as well as in certain *nebulae*, *Wolf-Rayet stars*, and *novae*, are contained in Tables II, III, and IV. The *ultra-violet hydrogen lines* in the Be stars are usually seen in absorption even when Hα is bright. Estimates of their intensity are included in Table II.

The *blue-violet portion of the spectrum* has been observed with slit spectrographs attached to the large reflectors. Descriptions of Hβ, Hγ, and Hδ, and various other data including *radial velocities* of a few stars, are given in Table V.

The *discussion* brings out the fact that our objective-prism spectrograms have yielded *more new bright-line stars than the number previously known within the areas observed.* It is suspected that in some of these objects the bright lines have come into existence since the Harvard spectroscopic surveys. A study of the *distribution* of Be stars shows a tendency for them to fall into groups near the center line of the Milky Way. Four of these groups occupy areas which are also rich in Wolf-Rayet stars. The *frequency of bright-line stars in the various spectral subdivisions* is examined and classes B0 to B5 are found to be strongly favored.

INTRODUCTION

The sun and nearly all the stars have spectra in which the chief features are absorption lines and bands. This type of spectrum may accordingly be considered the normal one. Less than 0.5 per cent of all the stars whose spectra have been examined are known to possess well-marked emission lines, and these objects have long been regarded as stellar curiosities. It is an interesting fact that most of the bright-line spectra are associated with either the hottest or the coolest stars. More than 95 per cent of the known bright-line stars fall in Classes B and O on the one hand, or in Classes M, S, and N on the other. Among Classes A, F, G, and K, bright-line stars, while not entirely unknown, are decidedly rare. Conditions at the extremes of the stellar temperature sequence appear to be favorable either to extensive atmospheres or to relatively high spectroscopic excitation of the atmospheres. A large proportion of bright-line spectra are variable, indicating a lack of equilibrium in the outer portions of the stars concerned.

Aside from the general interest attaching to any abnormal or imperfectly understood spectrum, there are at least three specific reasons for studying bright-line stars of Class B, namely, (1) they may assist in the interpretation of novae; (2) bright lines apparently serve as sensitive indicators of conditions in atmospheres of B-type stars; (3) they may teach us new properties of the hydrogen atom.

1. It is possible to select stars of Class Be which form a fairly continuous sequence in the structure of the hydrogen lines from ordinary B stars to novae. Circumstances similar to those causing the characteristic nova spectrum, but less violent, may perhaps be responsible for the unsymmetrical bright lines in certain B-type spectra; but even if this is not the case, it seems evident that the conditions in the atmospheres of several Be stars approach in some degree those prevailing in novae, and we may thus hope to use these stars as an aid in the interpretation of nova phenomena.

2. In many instances Be stars appear to differ from ordinary B-type stars only in the presence of bright hydrogen lines. In some stars the bright hydrogen lines have disappeared without notable changes in other features of the spectrum and without appreciable variation of the total light. These facts make it possible to consider bright hydrogen lines as sensitive indicators of the density or other properties of the atmospheres of the hotter stars, and we are thus offered a method of studying variations too small to be otherwise perceptible.

3. Be stars are also of interest from the viewpoint of general physics, because in them we may observe properties of radiating hydrogen (and some other elements) which differ from the properties shown by laboratory experiments. As examples we may mention the frequent wide doubling of the lines (self-reversal?), and the structure of lines in stars of the P Cygni type, which suggests that in the atmospheres of these stars the hydrogen atoms strongly absorb light

having a wave-length somewhat shorter than each of the Balmer lines, but emit these lines in their normal positions.

I. THE Hα LINE

Historical.—The history of bright-line stars of Class B begins with the discovery by Secchi in 1866 of bright hydrogen lines in the spectra of γ Cassiopeiae and β Lyrae. No additional stars of this kind (with the exception of one or two doubtful instances) were found until the inauguration of the spectroscopic surveys of the Harvard College Observatory by Pickering in 1886. These surveys, made by the aid of the objective prism, produced rich results in this as in other fields of stellar spectroscopy. About 120 B-type spectra were found to have bright hydrogen lines. The Hβ line served most frequently for the detection of hydrogen emission, but in numerous spectra a few of the more refrangible lines were also bright. The portion of the spectrum containing Hα was not shown by these photographs, but in 1894 Campbell, observing visually at Mount Hamilton with the 36-inch refractor and attached spectroscope,[1] found that Hα also is bright. He stated the rule that the intensities of the bright hydrogen lines in B-type spectra decrease from Hα toward the violet.

Ordinary photographic plates are practically insensitive to red light, but the discovery of sensitizing dyes, particularly pinacyanol, has made it possible to prepare emulsions which are quite rapid in the region of Hα, and thus to extend to this part of the spectrum the great advantages of photography. Spectrograms obtained by Merrill[2] in 1912 with the Lick 36-inch refractor showed, in confirmation of Campbell's rule, that in B-type spectra bright Hα is much stronger than Hβ, and that, in spite of the smaller prismatic dispersion in the red, it stands out far more prominently from the background of the neighboring continuous spectrum. Comparison of the appearance of the hydrogen lines in various B-type spectra suggested that numerous stars might exist in which Hα alone is bright. Visual observations by Campbell[3] had, in fact, already shown Hα to be bright in Alcyone, a star in whose spectrum the other hydrogen lines are dark.[1] Merrill's observations of the Hα region with slit spectrographs at Mount Hamilton in 1912[2] and at Ann Arbor in 1914[3] of about forty B-type stars resulted in the discovery of six bright-line spectra. A few objective-prism spectrograms of known bright-line stars were obtained in February, 1917, by the same observer with the 2-foot reflector of the Harvard College Observatory, using red-sensitive plates.[4] Bright Hα was clearly shown in the spectra of κ Draconis, β Lyrae, and P Cygni.

---

[1] *Astrophysical Journal*, **2**, 177, 1895.

[2] *Lick Observatory Bulletins*, **7**, 162, 1913.

[3] *Loc. cit.*

The Mount Wilson observations.—It thus became evident that the use of the Hα region of the spectrum would be decidedly advantageous for the detection of hydrogen emission in B-type stars, and it was believed that objective-prism observations comparable with those made by the Harvard College Observatory at Cambridge and Arequipa for the purpose of spectral classification, but showing the Hα region, would result in the discovery of a considerable number of bright-line stars of Class B in addition to those already known. This idea was given a practical trial by Merrill during the years 1919 and 1920 with the 10-inch Cooke refractor of the Mount Wilson Observatory. The preliminary exposures showed that the Cooke telescope with a 15° objective prism was suitable for this work: in particular, that the dispersion (about 440 angstroms per mm at Hα) was sufficient for the purpose, that stars at least as faint as the ninth magnitude could readily be photographed, and that stars over an area about 18° in diameter could be obtained in good focus on a single plate. Several new bright-line stars were soon found, making it highly probable that many others having Hα sufficiently bright to observe were awaiting discovery. A general survey of the Milky Way region was then planned, and special observations of some of the brighter B stars were also included. Humason began active participation in the work at this time, and after September, 1920, made nearly all the objective-prism observations. During the past few months Miss Burwell has given the plates a very careful re-examination and has collected the data for publication.

---

[1] Later photographs have shown feeble bright portions within the broad absorption at Hβ.

[2] *Loc. cit.*

[3] *Publications of the Astronomical Observatory, University of Michigan*, 2, 181, 1916.

[4] *Scientific Papers of the Bureau of Standards*, 14, 487, 1918.

The 10-inch telescope used for the objective-prism observations is of the Cooke "Astrographic" type, having an equivalent focal length of 45.5 inches. The prism, with a circular aperture of 10 inches, has a refracting angle of 15° and causes a deviation of 8°. The linear dispersion at Hα is about 440 A per mm. The lens was so designed that it is achromatic in the blue and violet regions. The color-curve turns sharply away from the lens in the red and more gradually in the ultra-violet. The focal plane of Hα coincides with that for λ 3785 and is 4.1 mm farther from the lens than the focal plane of λ 4200. On our photographs, therefore, only the ends of the spectra are in focus. For this particular type of work a lens having the same back focus for Hα and Hβ[1] would be desirable.

An auxiliary telescope inclined 8° to the axis of the Cooke lens serves for guiding. In a few cases the guiding star has been held at exactly the same point throughout the exposure so that very narrow spectra might be obtained, but in most exposures a small east-and-west motion (parallel to the refracting edge of the prism) was purposely allowed in order to widen the spectra, which aids greatly in detecting a feeble Hα line. Several excellent plates were obtained without any guiding whatsoever. The average exposure time for the large plates is about three hours, but a few exposures have exceeded four hours.

Plates 14×17 inches in size are employed for most of the long exposures. The definition is reasonably good over practically the entire area. Very wide spectra of bright stars are obtained on smaller plates. On moonlight nights the fogging usually caused by the sky light can be avoided by the use of a red color filter; for the exposures on 4×5 plates we often use an Eastman "A" or "F" gelatine filter supported in a cardboard frame immediately in front of the plate-holder.

The emulsions employed are either Seed 23 sensitized by pinacyanol, or Ilford Special Rapid Panchromatic hypersensitized by ammonia. The pinacyanol is applied by the well-known Wallace procedure. The sensitizing bath in which the plates are immersed for four and one-half minutes is made up as follows:

---

[1] That is, having the same color correction as an ordinary visual objective.

	cc
Distilled water	260
Ethyl alcohol	200
Pinacyanol solution 1:1000	12
Concentrated ammonia	15

This is followed, before drying, by a thorough rinsing in pure ethyl alcohol. The ammoniating bath for the Ilford plates consists of

	cc
Distilled water	375
Ethyl alcohol	125
Concentrated ammonia	13

The subsequent alcohol rinse has usually been omitted. The Ilford plates are perhaps slightly faster in the sense of a lower threshold value, but the Seed 23 plates have somewhat more contrast and finer grain.

Two examples of widened spectra obtained with the ten-inch telescope and objective-prism are shown in Plate VI. (*a*) is copied from a plate taken on January 25, 1922, exposure time $2^h\ 55^m$, emulsion Ilford Special Rapid Panchromatic, hypersensitized with ammonia. The enlargement is three times. The position of the center of the illustration is R.A. $6^h\ 25^m$, Dec. $+5.^\circ 2$ (referring to the red end of the spectrum which lies toward the right). North is toward the right. The brighter stars shown are as follows:

H.D. No.	Mag.	Spect.	Distance of red end from		Remarks
46612	7.1	Mb	Top 2 mm	Left 40 mm	
46241	6.0	K0	Top 36	Left 35	
46150	6.8	B2	Top 42	Left 39	
46179	6.7	B9	Top 39	Right 0	
46105	6.8	A0	Top 46	Right 15	
45910	6.7	Be	Bottom 50	Right 9	Bright Hα
45530	7.2	B9	Bottom 15	Right 42	
45431	6.7	F0	Bottom 3	Right 48	

(*b*) β Piscium, 1900 R.A. $22^h\ 58^m.8$, Dec. $+3^\circ\ 17'$; Mag. 4.6, spectrum B5e August 4, 1919, exposure 46 minutes. Emulsion Seed 23 sensitized with pinacyanol. Enlargement five times. The Hα line is bright, while the ultra-violet hydrogen lines are dark.

Table I contains a list of stars in which we have found the Hα

PLATE VI

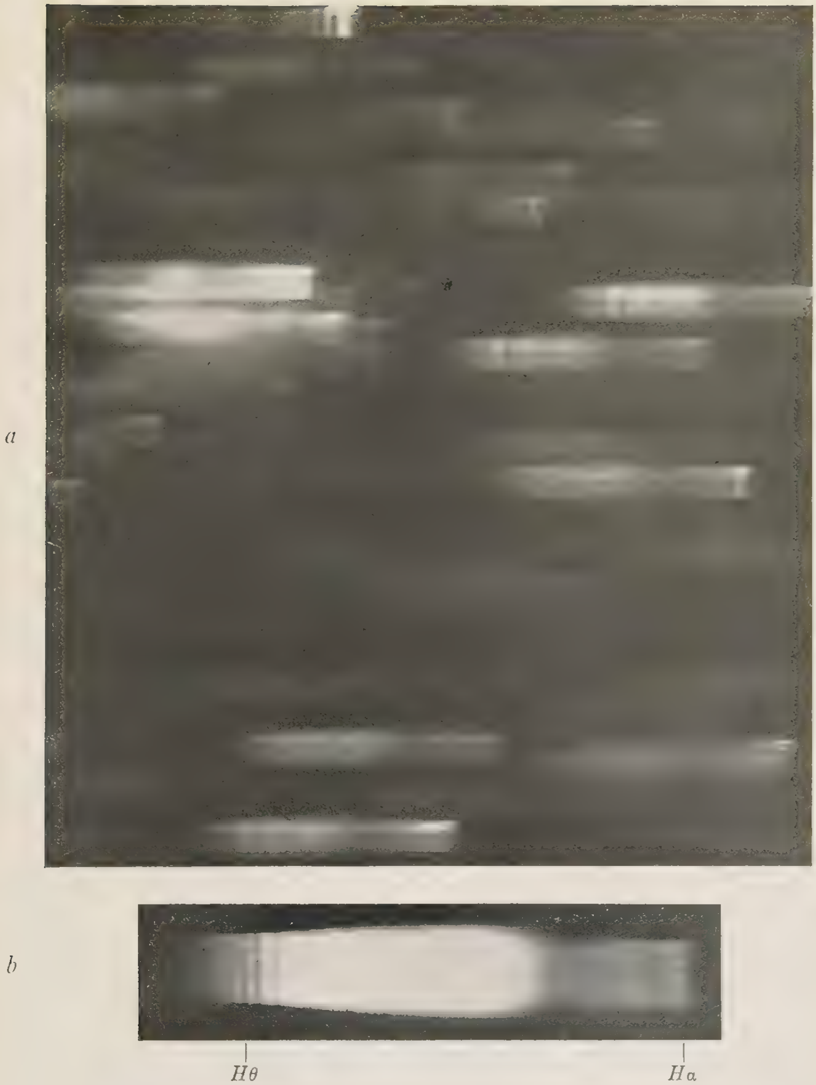

(a) Portion of an objective-prism spectrogram taken with the ten-inch Cooke telescope. See description on page 6.

(b) Objective-prism spectrogram of β Piscium. See page 6.

TABLE I

Discovery List of Stars Having the Hα Line Bright

No.	H.D.	α 1900	δ 1900	Mag.	Sp.	Ref.	Remarks
1....	108	$0^h\ 0^m9$	$+63°\ 7'$	7.4	O6e	1	
2....	698	0 6.3	+57 39	7.1	B8sea	1	
3....	2789	0 26.3	+66 36	8.2	B2ne	6	
4....	7636	1 11.2	+57 6	7.6	B2ne	1	
5....	B.D.+62°271	1 27.9	+63 7	8.2	B(8)ea	3	Near H.D. 9105
6....	B.D.+54°398	1 45.9	+54 50	8.6	B(2)e	3	
7....	12882	2 1.1	+64 33	7.5	B(2)e	1	
8....	19243	3 0.7	+62 0	6.5	B2e	1	
9....	22298	3 30.3	+54 50	8.4	B2ne	4	
10....	23302	3 39.0	+23 48	3.8	B5nea	7	Electra
11....	23480	3 40.4	+23 39	4.2	B5nea	7	Merope
12....	25348	3 56.6	+53 3	8.2	B(1)e	4	
13....	29866	4 37.3	+40 36	6.1	Bea	2	
14....	30614	4 44.1	+66 10	4.4	O9ea	1	9 Camelop.
15....	33152	5 3.2	+36 53	7.8	B2e	2	
16....	33232	5 3.7	+40 53	8.1	Bepv	2	
17....	33461	5 5.3	+41 6	8.0	B(1)e	3	
18....	33604	5 6.3	+40 5	7.3	B2e	2	
19....	37115	5 31.0	− 5 41	8.2	B(5)e	1	Brighter comp. β.G.C. 2850
20....	37490	5 33.9	+ 4 4	4.5	....	7	ω Orionis B3e
21....	37657	5 35.1	+43 0	7.0	B3ne	2	
22....	37967	5 37.2	+23 10	6.1	B3ne	2	
23....	38191	5 38.9	+21 25	9.5	Be	4	
24....	39340	5 46.9	+26 25	8.1	B3e	3	
25....	B.D.+25°1019	5 47.3	+25 43	8.5	Be	3	
26....	39478	5 47.8	+26 24	8.4	B2ne	4	
27....	41117	5 58.0	+20 8	4.7	B1sea	3	χ^2 Orionis
28....	B.D.+20°1309	6 6.3	+20 7	9.1	Be	3	
29....	43285	6 10.3	+ 6 6	6.0	B(1)e	6	
30....	44637	6 17.7	+15 9	7.7	B3e	3	
31....	45314	6 21.6	+14 57	7.1	B(0)e	3	
32....	45542	6 23.0	+20 17	4.1	....	8	ν Geminorum B5ea
33....	45910	6 25.2	+ 5 57	6.7	Beqv	2	
34....	45995	6 25.6	+11 19	5.8	B2ev	1	
35....	50138	6 46.7	− 6 51	6.6	B8ev	2	
36....	50209	6 47.1	− 0 10	8.3	B(5)e	3	
37....	51354	6 51.9	+18 2	7.1	B4e	.....	
38....	55135	7 6.6	−10 16	7.2	B3ne	2	
39....	55271	7 7.1	−21 38	6.7	Be	2	Brighter comp. β.G.C. 3887
40....	56806	7 13.4	−18 39	9.3	Be	4	

TABLE I—*Continued*

No.	H.D.	α 1900	δ 1900	Mag.	Sp.	Ref.	Remarks
41....	58715	$7^{\mathrm{h}}21^{\mathrm{m}}7$	+8°29′	3.1	B8neα	8	β Can. Min.
42....	B.D.−13°2040	7 24.5	−13 34	9.0	B(2)e	4	
43....	59497	7 25.1	−21 38	8.4	B2e	4	
44....	59773	7 26.4	−21 35	8.1	B(3)e	4	
45....	62753	7 40.4	−40 5	6.7	B(2)ne	4	
46....	154218	16 59.0	−36 36	7.7	Be	4	
47....	154243	16 59.2	−36 27	8.3	B2e	5	
48....	154450	17 0.4	−35 37	8.5	Boe	5	
49....	156468	17 12.6	−37 54	8.0	B2e	5	
50....	160095	17 32.9	−33 29	8.7	B8ep	6	
51....	160202	17 33.5	−32 9	6.9	B(1)eβ	5	
52....	161103	17 38.5	−27 12	7.9	Bne	5	
53....	161306	17 39.7	−9 46	8.3	B(0)e	5	
54....	D.M.−27°11944	17 41.9	−27 59	9.0	Beq!	5	
55....	163181	17 49.7	−32 27	6.6	B2e	6	
56....	163296	17 50.3	−21 56	6.6	A2e	.....	
57....	163454	17 51.1	−31 0	7.9	B1e	6	
58....	163868	17 53.3	−33 24	7.2	B2e	5	
59....	164906	17 58.3	−24 24	9.0	B(0)e	6	
60....	166566	18 6.1	−15 42	8.1	B2se	5	
61....	166666	18 6.6	−15 36	9.4	B2e	.....	
62....	166734	18 6.9	−10 46	8.3	Beα	.....	
63....	168229	18 13.6	−18 16	9.7	B(1)e	5	
64....	168607	18 15.5	−16 25	8.9	Aose	6	
65....	169226	18 18.6	−12 15	9.1	Be	.....	Brighter comp. β.G.C. 8523
66....	169454	18 19.6	−14 2	6.8	Boe	6	
67....	169515	18 19.9	−12 45	8.3–9.2	Pec	6	RY Scuti
68....	169805	18 21.3	−19 1	8.7	B(1)ne	6	
69....	170061	18 22.4	−14 47	10.6	Be	.....	
70....	172694	18 36.5	−15 57	8.3	Bep	.....	
71....	174105	18 43.8	+15 17	6.9	B8e	.....	
72....	175863	18 52.4	+59 53	6.9	B3e	.....	
73....	180398	19 11.3	+12 56	7.7	B(1)e	.....	
74....	B.D.+14°3887	19 17.0	+14 42	9.5	Pec	.....	
75....	B.D.+22°3687	19 20.5	+22 35	8.6	B2e	.....	Brighter comp.
76....	183143	19 23.0	+18 6	6.9	B9seα	.....	
77....	187399	19 44.7	+29 10	7.7	B9eβ	.....	
78....	187567	19 45.4	+7 39	6.4	B1e	.....	
79....	B.D.+35°3950	20 2.0	+35 37	8.8	Be	.....	
80....	192445	20 9.8	+36 1	7.1	B2e	.....	
81....	B.D.+36°3946	20 10.1	+36 18	8.5	B(0)e	.....	
82....	195407	20 26.0	+36 39	7.7	B1e	.....	
83....	198512	20 45.7	+53 32	8.0	B(2)e	.....	
84....	199218	20 50.6	+40 19	6.5	B5e	1	Brighter comp. β.G.C. 10606
85....	203025	21 14.6	+58 11	6.4	B2e	.....	

TABLE I—*Continued*

No.	H.D.	α 1900	δ 1900	Mag.	Sp.	Ref.	Remarks
86....	207232	$21^{\mathrm{h}}42^{\mathrm{m}}4$	+50° 13′	7.0	B8e	.....	
87....	209409	21 58.1	− 2 38	4.7	....	7	ο Aquarii B5e
88....	212044	22 16.5	+51 22	7.1	Be	.....	
89....	214748	22 35.1	−27 34	4.2	B8ea	1	ε Pisc. Austr.
90....	224559	23 53.7	+45 51	6.5	B3ne	.....	
	Stars of Classes F and M						
91....	B.D.+61°8	0 4.4	+62 6	9.2	Mep	.....	
92....	42474	6 5.8	+23 14	7.4	Mep	11	
93....	193182	20 13.8	+39 16	6.6	F5e	9	
94....	198287, 8	20 44.2	+38 55	7.0	cF5e	9	
95....	214369	22 32.6	+57 54	8.6–9.3	Mep	10	W Cephei

REFERENCES

1. *Publications of the Astronomical Society of the Pacific*, **32**, 336, 1920.
2. *Ibid.*, **33**, 112, 1921.
3. *Ibid.*, p. 264, 1921.
4. *Ibid.*, **34**, 223, 1922.
5. *Ibid.*, p. 294, 1922.
6. *Ibid.*, p. 351, 1922.
7. *Lick Observatory Bulletins*, **7**, 179, 1913.
8. *Publications of the Astronomical Observatory, University of Michigan*, **2**, 181, 1916.
9. *Publications of the Astronomical Society of the Pacific*, **35**, 263, 1923.
10. *Ibid.*, **34**, 59, 1922.
11. *Ibid.*, p. 133, 1922.

NOTES TO TABLE I

Electra, Merope, ω Orionis, and ο Aquarii were found with a slit spectrograph at Mount Hamilton.

ν Geminorum and β Canis Minoris were found with a slit spectrograph at Ann Arbor.

All the remaining stars were found on objective-prism spectrograms taken at Mount Wilson. For dates of observation and other data see Table II.

H.D. 25348: Remark in H.D., "The line Hβ is suspected to be bright."

H.D. 33152: Remark in H.D., "The line Hβ is not seen as a dark line and is suspected to be bright. The other lines are hazy."

H.D. 44637: Remark in H.D., "The line Hβ is not clearly seen and is suspected to be bright."

H.D. 62753: Remark in H.D., "The line Hβ is not distinctly seen and is suspected to be bright."

H.D. 198512: Remark in H.D., "The exact character of the spectrum is not well defined. On the best plates it is nearly continuous with the presence of bright lines suspected. It is apparently of a late division of Class O, or of an early Class B."

H.D. 212044: Remark in H.D., "The presence of a bright Hβ, suspected on the Harvard plate, has been found on photographs taken at Mt. Wilson."

line to be bright.[1] In the second column is given the *H.D.* number (from the *Henry Draper Catalogue*), or the Durchmusterung number in case the star does not appear in *H.D.* The spectral types given in column five are determinations from Mount Wilson slit spectrograms.[2]

The five stars placed by themselves at the end of the table are the only ones falling outside the spectral interval O6 to A2.

Details of the objective-prism observations are collected in Table II. Estimates of the intensity of the bright Hα line are given in the second column on the following scale:

1 = very weak—observable only with widened spectrum and proper exposure
2 = weakest ordinarily observable
3 = medium
4 = strong
5 = very strong—bright Hα strongly exposed even when the adjacent continuous spectrum is very weak

Estimates of the intensity of the dark hydrogen lines in the ultraviolet are given in the third column on the following scale:

0 = absent or barely visible
1 = weak
2 = medium
3 = strong (as in an A0 star)

The chief lines concerned are Hζ, Hη, Hθ, Hι, and Hκ.

In the fourth column, headed "Dates of Observation," are given the last four figures of the Julian Day numbers of representative observations. The material is more extensive than this tabulation indicates, because poor and inconclusive observations have been omitted, and of several observations of the same star made within a few days, only one has been listed in most cases.

Our objective-prism plates show a well-marked bright Hα line in the spectra of most of the "bright Hβ" stars previously announced by other observers. The comparatively few instances in which this is not the case are collected on pages 13 and 14. The spectra of the first five stars have probably changed since the previous observations.

---

[1] Six stars found at Mount Hamilton or Ann Arbor with slit spectrographs are included for completeness.

[2] See Table V and page 25.

TABLE II

Objective-Prism Observations of Stars of Class Be

H.D.	Hα	U.V. Hyd.	Dates of Observation*	Remarks
108	3	(0)	2548, 2566	
698	3	(2)	2548, 2569	
2789	3	....	2548	
5394	4	0	2139, 2232, 2580, 2893, 2957	γ Cass.
7636	4	2	2176, 2550, 2586	
B.D.+62°271	4	(0)	2586, 2624	
10516	4	1	2580	φ Persei
B.D.+54°398	(1)	....	2524, 2586	
12882	3	(0)	2586, 2623	
19243	3	....	2233, 2578	
20336	3	....	2233, 2578, 2623	
22192	4	(2)	2232, 2579, 2602, 2776	ψ Persei
22298	(3)	0	2730	
23630	1	3	2141, 2175, 2995	Alcyone
25348	3	0	2730, 2776	
25940	4	2	2586, 2776, 3103	c Persei
26906	3	2	2730, 2776	
29866	2	2	2688, 2740	
30614	1−	(1)	2602, 2605, 2624, 2969	9 Camelop.
32343	(2)	(0)	2776	11 Camelop.
33152	3	0	2688	
33232	3	....	2688	
33461	2	1	2688	
33604	3	2	2688	
34921	3	0	2688, 3104	
35345	2	0	2688	
36576	3	1	2728, 2729	
37115	3	....	2586, 2606	
37202	3	2	2362, 2728, 2995	ζ Tauri
37657	2	1	2688	
37967	2	2	2728, 3104	
38010	3	0	2728, 3104	
38191	4	0	2729	
39340	2	0	2729, 3104	
B.D.+25°1019	3	0	2729, 3104	
39478	2	0	2729, 3104	
41117	1−	(1)	2728, 2745	χ^2 Orionis
41335	3	0	2586, 2669, 3080	
B.D.+20°1309	4	0	2729	
43285	2	2	3080	
44637	2	0	2728, 3081	
45314	2	0	2728, 3081	
45725	3	1	2602, 2669	Brightest comp. β Monoc.
45910	3	1	2669, 2687	
45995	3	2	2390, 2728, 3081	
B.D.+10°1172	2	....	2729	N.G.C. 2247
50083	3	1	2669, 3080	
50138	3	2	2669, 3080	
50209	(2)	2	2669	
51354	2	2	3081	
51480	4	0	2700	

* The last four figures of the Julian Day number.

TABLE II—*Continued*

H.D.	Hα	U.V. Hyd.	Dates of Observation	Remarks
55135	3	0	2700	
55271	4	2	2700	
56014	?	1	(2410), (2700)	27 Can. Maj.
56139	2	2	2410	ω Can. Maj.
56806	3	(0)	2700	
57150	4	(0)	2763	ν' Puppis
58011	(2)	1	2700	
58343	1?	1	(2700)	
B.D.−13°2040	(3)	2	2700	
59497	3	1	2700	
59773	(2)	2	2700	
60606	4	1	2763, 2764	z Puppis
62753	3	0	2764	
68980	4	(0)	2763	r Puppis
109387	4	2	2403, 2439, 2518	κ Draconis
127972	3	2	2407, 2475	η Centauri
154218	3	....	2877, 2878	
154243	(3)	....	2877, 2878	
154450	3	....	2877, 2878	
155806	3	0	2877, 2878	
155851	4	....	2877, 2878	
156468	3	....	2877, 2878	
160095	2	....	2877, 2878	
160202	3	....	2540, 2877	
161103	4	....	2541, 2878	
161306	3	(1)	2903	
D.M.−27°11944	5!	....	2412, 2546, 2878	
163181	3	0	2539, 2877	
163296	2	3	2903	
163454	3	(0)	2541, 2878	
163868	3	1	2539, 2878	
164906	3	....	2877, 2878	
166566	3	1	2903	
166666	3	0	2903	
166734	1−	1	(2411), (2903)	
167362	4	....	2541, 2878	
168229	3	0	2903	
168607	3	....	2903	
169226	2	....	2903	
169454	3	0	2903	
169515	4	(0)	2903	RY Scuti
169805	3	1	2903	
170061	3	....	2903	
170235	4	....	2546	
172694	3	0	2903	
173219	2	0	2903	
174105	2	2	2938	
174638	4	1	2548, 2556	β Lyrae
175863	3	3	2548	
180398	4	1	2938	
B.D.+14°3887	4	....	2587, 2938	
B.D.+22°3687	5	....	2587, 2939	
183143	2	0	2587, 2938	
187399	3	1	2939	
187567	3	0	2938	

TABLE II—*Continued*

H.D.	Hα	U.V. Hyd.	Dates of Observation	Remarks
B.D.+35°3950	4	(0)	2961	
190944	3	....	2580, 2961	
191610	3	1	2579, 2961	b^2 Cygni
192445	3	(1)	2579, 2580	
B.D.+36°3946	2	0	2579, 2961	
193009	3	0	2580, 2939	
193237	4	0	2140, 2580, 2893, 2961	
195407	3	0	2579, 2961	
198512	2	....	2996	
199218	2	2	2579, 2580	
199356	3	0	2579, 2580	
200775	4	....	2487, 2518	N.G.C. 7023
202904	3	2	2580	υ Cygni
203025	2	2	2996	
203374	3	0	2996	
203467	3	0	2487	6 Cephei
206773	4	0	2996	
207232	1	2	2996	
209409	3	(1)	2602	ο Aquarii
212044	1	0	2996	
212076	1	3	2995	31 Pegasi
212571	4	1	2602	π Aquarii
214748	1	3	2141, 2175, 2578	ε Pisc. Austr.
217891	3	3	2140, 2175	β Piscium
224559	Rem	(1)	2542, 2567, 2647	
225095	4	0	2542, 2569, 2997	

NOTES TO TABLE II

H.D. 22192, ψ Persei: The ultra-violet hydrogen lines may vary in intensity.

H.D. 29866: The ultra-violet hydrogen lines may vary in intensity.

H.D. 45314: Bright Hα may have increased in intensity between J.D. 2422390 and J.D. 2423081.

H.D. 45910: The ultra-violet hydrogen lines may vary in intensity.

D.M.−27°11944: Bright Hα appears broad but is sharply bounded on the short wave-length side. It probably is of the P Cygni type. This star has an extraordinary spectrum.

H.D. 174638, β Lyrae: Bright λ 6678 He is clearly seen on plates taken on J.D. 2422548 and J.D. 2422556.

H.D. 224559: Bright Hα appears to vary in intensity.

References to bright lines in the spectra of the remaining three objects have been published by other observers, but it is not clear that the present observations constitute evidence of variability.

SPECTRA IN WHICH Hα APPEARS TO VARY

H.D. 9105: See *Publications of the Astronomical Society of the Pacific*, **34**, 180, 1922.

H.D. 58978: Bright Hα is very weak or absent on a plate taken 1921, January 10.

H.D. 181615, υ Sagittarii: The spectrum appears continuous at Hα on a plate taken 1919, July 1. This spectrum is known to be variable.

H.D. 193516: Hα is not seen as a bright line on three plates taken between 1920, September 11, and 1921, September 28.

H.D. 217050: Bright Hα is very weak or absent on a plate taken 1920, November 18. This spectrum is known to be variable.

DOUBTFUL CASES

H.D. 47129: Bright Hα is very weak or absent on several plates taken between 1920, March 6, and 1922, January 22.

H.D. 162586: Hα is not seen as a bright line on several plates taken between 1920, August 2, and 1921, July 7. On two plates it appears dark.

H.D. 193443: Hα is not seen as a bright line on three plates taken between 1920, September 11, and 1921, September 28. A slit spectrogram taken 1924, June 11, shows Hβ, Hγ, Hδ, and Hϵ as absorption lines.

Numerous bright-line spectra of various kinds, including gaseous nebulae, Wolf-Rayet stars, and novae, are shown by our objective-prism photographs, and, as the bright Hα line is an interesting feature in nearly all cases, it seems worth while to make a record of its appearance, especially as the red portion of the spectra of these objects has seldom been observed. In Table III are given the dates of observation and notes chiefly concerning the bright Hα line. For several stars having numerous observations, intermediate dates have been omitted.

The right ascension and declination for 1900 of the objects which are not in the *H.D.* are given below.

T Pyxidis: $9^{h}0^{m}.5$, $-31^\circ 57'$. See *Publications of the Astronomical Society of the Pacific*, **32**, 200, 1920.

N.G.C. 6334: $17^{h}13^{m}.7$, $-35^\circ 58'$.

N.G.C. 6357: $17^{h}18^{m}.1$, $-34^\circ 6'$. Near the Wolf-Rayet star $-34^\circ 11675$.

$-29^\circ 13988$: $17^{h}41^{m}.5$, $-29^\circ 57'$. See *Publications of the Astronomical Society of the Pacific*, **33**, 176, 1921.

Trifid nebula: $17^{h}56^{m}.6$, $-23^\circ 2'$.

Dumbbell nebula: $19^{h}55^{m}.3$, $+22^\circ 26'$.

Nova Cygni: $19^{h}55^{m}.6$, $+53^\circ 21'$. See illustration, *Publications of the Astronomical Society of the Pacific*, **32**, 321, 1920.

I.C. 1470: $23^{h}1^{m}.0$, $+59^\circ 42'$. See *ibid.*, **33**, 176, 1921.

The Hα region of a number of Be stars has been observed with single-prism slit spectrographs attached to one of the large reflectors.

TABLE III

OBJECTIVE-PRISM OBSERVATIONS OF NEBULAE, WOLF-RAYET STARS, AND NOVAE

H.D.	Object	Dates of Observation and Remarks*
37024....	Orion nebula	2605. Hα image strong.
62166....	N.G.C. 2440	2700. Hα image strong.
	T Pyxidis	2436–2441. Hα very strong.
153919....	−37°11206	2877. Hα rather weak.
155520....	N.G.C. 6302	2877. Hα image appears stronger than the combined images of N1 and N2.
	N.G.C. 6334	2877, 2878. Remarkable group of gaseous nebulae near here.
	N.G.C. 6357	2877, 2878. Hα bright.
	−29°13998	2541, 2878. Hα strong.
161944....	N.G.C. 6445	2903. Hα bright.
164270....	−36°12130	2540, 2878. Hα strong.
	Trifid nebula	2877, 2903. Hα image differs from the appearance of ordinary photographs.
164740....	N.G.C. 6523	2412, 2877. Interesting detail in Hα image.
165763....	−21°4864	2903. λ 4653 extremely strong; λ 5813 very strong.
166449....	N.G.C. 6563	2541, 2878. Hα bright.
166468....	N.G.C. 6565	2541, 2878. Hα strong.
166802....	N.G.C. 6572	2845. Hα very strong.
167276....	Nova Ophiuchi	2550. Hα very strong.
168206....	−11°4953	2903. Hα probably bright but not strong.
168520....	Omega nebula	2411, 2903. Much fine detail in Hα image.
170124....	Gaseous nebula	2877, 2878. Hα bright.
174107....	Nova Aquilae	2140, 2524, 2542, 2845. Hα very strong. On last plate continuous spectrum strong in violet and weak in red.
175353....	Ring nebula	2546. Hα strong
184738....	+30°3639	2939. The combined image of Hα and λλ 6548, 6583 is extremely strong.
186924....	N.G.C. 6826	2487. Hα bright.
	Dumb-bell nebula	2938, 2939. Interesting detail in Hα image. Fairly strong image in ultra-violet, perhaps λ 3727.
	Nova Cygni	2566, 2570, 2602, 2623. Hα very strong.
191765....	+35°4001	2579, 2961. Hα strong.
191916....	N.G.C. 6884	2961. Hα bright.
192103....	+35°4013	2579, 2961. Hα strong.
192163....	+37°3821	2579, 2961. Hα strong.
192641....	+36°3956	2579. Hα bright.
193077....	+36°3987	2579, 2961. Hα bright.
193576....	+38°4010	2579, 2961. Hα bright.
193793....	+43°3571	2487, 2579, 2961. Hα bright.
201272....	N.G.C. 7027	2580. The combined image of Hα and λλ 6548, 6583 is very strong.
	I.C. 1470	2997. Hα strong.

* The last four figures of the Julian Day numbers of the dates of observations are given. The remarks refer entirely to emission lines.

The dispersion at Hα is about 170 angstroms per millimeter. The results are collected in Table IV.

II. THE BLUE-VIOLET SPECTRAL REGION

The objective-prism spectrograms obtained with the 10-inch telescope yield little information concerning the lines Hβ, Hγ, and Hδ, as the part of the spectrum containing them is much out of focus. We have observed this spectral region, therefore, with single-prism slit spectrographs attached to one of the large reflectors. The program included all the stars found with the 10-inch telescope to have the Hα line bright, and in addition a number of previously known "bright Hβ" stars, particularly those for which there is no published record of observations with a slit spectrograph. An 18-

TABLE IV

OBSERVATIONS OF Hα WITH SLIT SPECTROGRAPHS

H.D.	Object	Date	Character of Hα
698......	....	1923 February 6	Strong bright
23302......	Electra	1919 November 8	Weak bright on absorption
23480......	Merope	1919 November 8	Very weak bright on absorption
23630......	Alcyone	1919 November 8	Strong bright
23862......	Pleione	1919 November 8	Absorption
		1921 November 12	Absorption
24534......	X Persei	1923 September 1	Strong bright
29866......	....	1923 February 5	Strong bright
30614......	9 Camelop.	1921 February 28	Very weak bright
		1924 March 12	Very weak bright
		March 13	Very weak bright
41117......	χ^2 Orionis	1921 February 28	Weak bright
		March 30	Weak bright
51354......	....	1923 January 7	Strong bright
58715......	β Can. Min.	1921 March 29	Bright
109387......	κ Draconis	1924 March 12	Strong bright
155806......	....	1923 April 30	Very strong bright
166734......	....	1922 October 8	Bright. Not sharp
183143......	....	1922 October 7	Probably bright
		October 8	Probably bright
		1923 September 1	Bright
214748......	ε Pisc. Austr.	1921 November 12	Strong bright

NOTES TO TABLE IV

H.D. 166734: The continuous spectrum is strong in the red.

H.D. 183143: The continuous spectrum is very strong in the red. The first two plates are overexposed.

inch camera was used in practically every exposure, the dispersion being as follows: at Hβ, 57 A per mm; at Hγ, 36; and at Hδ, 28. The data from these plates are collected in Table V and the accompanying notes.

In the first column is given the *H.D.* number (from the *Henry Draper Catalogue*), or the Durchmusterung number in case the star does not appear in *H.D.* The common names of a few bright objects, and, for double stars, the numbers in Burnham's *General Catalogue of Double Stars* (β.G.C.), are added in the notes. Descriptions of the hydrogen lines are found in the next three columns. The character of the lines (Ch.) is described by means of the following symbols:[1]

A = absorption
C = continuous
P = P Cygni type, i.e., a bright line with a dark line on its short wave-length edge.
S, D refer to bright components
S = single
D = double

The intensities (Int.) refer only to the bright components and are on the following basis:

0.5 = very weak
1 = weak
2 = medium
3 = strong
4 = very strong

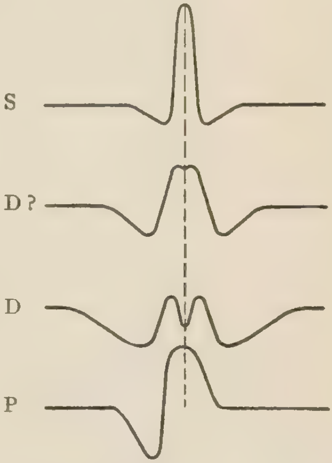

FIG. 1.—Typical intensity curves of hydrogen lines.

The bright lines are nearly all superposed on wider dark lines. Typical intensity-curves of the different types of lines are shown in Figure 1. The structure of a complex line is usually symmetrical about the normal position of the line, but there are a few exceptions. Aside from lines of the P Cygni type, which are of course decidedly unsymmetrical, there are complex lines of the ordinary type in which the two bright components are of unequal intensity. All definite instances of this kind are mentioned in the notes following Table V.

---

[1] The notation is similar to that employed by Lockyer, *Monthly Notices*, **84**, 409, 1924.

TABLE V

Data from Slit Spectrograms of the Blue and Violet Region

H.D.	Hβ		Hγ		Hδ		Type	Radial Vel.
	Ch.	Int.	Ch.	Int.	Ch.	Int.		
108	S	3	S	3	S	2	O6e	−60.
698	A	....	A	....	A	....	B8seα	Variable.
2789	C	....	A	....	A	....	B2ne	
7636	S	3	S	2	S	0.5	B2ne	−15.
9105	A	....	A	....	A	....	B4s	−43:
+62°271	S	1	A	....	A	....	B(8)eβ	
+54°398	S	1	C	....	C	....	B(2)e	
12882	D?	1	C	....	A	....	B(2)e	
15325	A	....	A	....	A	....	B1	−34.
15450	S	3	S	2	S	1	B(0)ne	
19243	S	2	S	1	C	....	B2e	−29:
22298	D?	0.5	C	....	A	....	B2ne	
23862	A	....	A	....	A	....	B8n	
24534	D?	1	C	....	C	....	B(0)e	
25348	D?	1	D	0.5	C	....	B(1)e	
29866	A	....	A	....	A	....	Beα	
30614	A	....	A	....	A	....	O9eα	
33152	S	3	S	2	S	1	B2e	−4.
33232	....	....	....	....	....	....	Bepv	
33461	D	0.5	A	....	A	....	B(1)e	
33604	S	2	S	1	S	0.5	B2e	
34921	D?	2	D?	1	C	....	B(0)e	
36576	D?	1	C	....	A	....	B1ne	
37115	D	3	D	1	A	....	B(5)e	
37657	D?	1	C	....	A	....	B3ne	
37967	S	1	A	....	A	....	B3ne	
38010	D?	2	D	1	C	....	Be	
38191	D?	2	D	1	C	....	Be	
39340	D?	2	C	....	A	....	B3e	
+25°1019	S	2	D?	0.5	C	....	Be	
39478	D?	1	D	0.5	A	....	B2ne	
41117	A	....	A	....	A	....	B1seα	
+20°1309	S	2	C	....	A	....	Be	
43285	D?	0.5	A	....	A	....	B(1)e	
44637	S	2	C	....	....	....	B3e	
45314	D?	1	C	....	C	....	B(0)e	
45677	....	....	....	....	....	....	Bep	
45910	P	....	P	....	P	....	Beqv	
45995	....	....	....	....	....	....	B2ev	
50083	D?	2	D	1	C	....	B1e	
50138	....	....	....	....	....	....	B8ev	
50209	S	1	A	....	....	....	B(5)e	
51354	C	....	A	....	A	....	B4e	
51480	P	4	P	3	P	2	B8eq	
55135	S	2	A	....	A	....	B3ne	
55271	D?	1	D	0.5	....	....	Be	
56806	D?	2	C	....	C	....	Be	
−13°2040	S	3	S	1	D	0.5	B(2)e	
59497	D?	2	D?	0.5	A	....	B2e	
59773	D?	1	A	....	....	....	B(3)e	

TABLE V—*Continued*

H.D.	Hβ		Hγ		Hδ		Type	Radial Vel.
	Ch.	Int.	Ch.	Int.	Ch.	Int.		
62753	D?	2	D	0.5	A	....	B(2)ne	
65875	S	3	D?	1	C	....	B3e	
120324	A	....	A	....	A	....	B2	
127972	A	....	A	....	A	....	B(0)n	
152236	P	1	P	1	A	....	B(2)eq	
154218	D?	2	D	0.5	....	....	Be	
154243	S	2	D?	1	....	....	B2e	
154450	S	3	S	2	....	....	B0e	See note.
155806	S	1	C	....	....	....	O8e	
156468	S	2	S	1	....	....	B2e	See note.
160095	....	....	....	....	....	....	B8ep	
160202	D?	1	A	....	....	....	B(1)eβ	
161103	D?	2	D	1	....	....	Bne	
161114	....	....	....	....	....	....	Bep!	
161306	S	3	D?	2	C	....	B(0)e	
−27°11944	P	4	P	3	....	....	Beq!	
163181	....	....	....	....	....	....	B2e	Variable.
163296	....	....	....	....	....	....	A2e	
163454	S	2	D?	1	....	....	B1e	
163868	S	2	A	....	A	....	B2e	
164906	S	1	C	....	C	....	B(0)e	
166566	S	1	A	....	....	....	B2se	
166666	D?	1	C	....	....	....	B2e	
166734	A	....	....	....	....	....	Beα	
168229	S	2	D?	0.5	....	....	B(1)e	
168607	S	3	S	1	....	....	A0se	
169226	P	2	....	....	....	....	Be	
169454	P	1	A	....	....	....	B0e	
169515	S	3	S	2	....	....	Pec	
169805	D?	2	D	1	....	....	B(1)ne	
170061	S	2	C	....	....	....	Be	
172694	....	....	....	....	....	....	Bep	
174105	D?	1	A	....	A	....	B8e	
175863	D?	1	A	....	A	....	B3e	−27.
180398	D?	1	A	....	A	....	B(1)e	
+14°3887	S	3	S	2	....	....	Pec	
+22°3687	S	3	D	2	....	....	B2e	−3.
183143	A	....	A	....	A	....	B9seα	+13.
187399	S	1	A	....	A	....	B9eβ	
187567	S	2	C	....	A	....	B1e	See note.
+35°3950	S	2	D?	1	C	....	Be	
192445	S	2	C	....	A	....	B2e	
+36°3946	S	2	D	0.5	C	....	B(0)e	
193009	S	1	D	0.5	C	....	B1ne	
195407	D	....	D	....	A	....	B1e	
198512	S	2	D?	1	C	....	B(2)e	
199218	D	1	A	....	A	....	B5e	
199356	D?	2	D	0.5	C	....	Be	
203374	S	2	S	1	C	....	Be	
206773	D	2	D	1	C	....	Be	
207232	D	0.5	A	....	A	....	B(8)e	

TABLE V—*Continued*

H.D.	Hβ		Hγ		Hδ		Type	Radial Vel.
	Ch.	Int.	Ch.	Int.	Ch.	Int.		
207757......	S	5	S	4	S	3	Bepv	
212044......	S	2	D?	1	C	....	Be	See note.
214748......	A	....	A	....	A	....	B8e*a*	
224559......	D	2	D	1	A	....	B3ne	0.
225095......	S	3	S	2	D?	1	B1e	

DATES OF OBSERVATION AND NOTES

H.D. 108: 2596, 2624, 2625, 2914, 3245, 3629. The hydrogen lines from Hβ to Hε consist of rather narrow bright lines superposed on faint dark lines. The dark components on the violet sides of the bright lines are slightly stronger than those on the red sides, and as they are near the positions of the lines which belong with the Pickering series, they are probably due in part to He+. The Pickering series appears wholly dark; the following lines are seen: λλ 4025.64?, 4199.87, 4541.63, and 5411.57. The velocity from the bright lines Hβ, Hγ, and Hδ is −58, and from the dark Pickering lines λλ4199.87 and 4541.63, −63 km/sec. These values are in substantial agreement with Plaskett's results in *Monthly Notices of the Royal Astronomical Society*, **84**, 84, 1923. λ4686 He+ is bright. D3 and λ4471 He are bright, the latter with a dark companion on the violet side. λ4552 Si is bright and there is a trace of bright λ4567 Si. There are several bright lines in the region λ 4640–50. H and K are fairly strong dark lines. This is a very interesting spectrum, well worth further study.

H.D. 698: 2626, 3244, 3245, 3809. Spectroscopic binary. Velocities from individual plates are +58, (+29), +20, and −10 km/sec., respectively.

H.D. 2789: 2916, 3339.

H.D. 7636: 2596, 3810. Sharp H and K.

H.D. 9105: 2594, 2624, 2746, 2925, 2927, 3245. This spectrum is evidently variable, as the bright hydrogen lines have disappeared since the Harvard observations. See *Publications of the Astronomical Society of the Pacific*, **34**, 180, 1922. The velocities from individual plates range from −29 to −60 km/sec., but the mean value, −43, agrees with that reported by Plaskett in *Monthly Notices of the Royal Astronomical Society*, **84**, 84, 1923.

B.D.+62°271: 2897.

B.D.+54°398: 2667, 2907. Aside from bright Hβ, the spectrum is nearly continuous.

H.D. 12882: 2719, 2917, 3988. The bright line at Hβ is stronger on the violet side.

H.D. 15325: 3307. In Praesepe cluster. Brighter component of β.G.C. 1277. The bright lines noted by Harvard seem to have disappeared.

H.D. 15450: 4018. Observed with 10-inch camera.

H.D. 19243: 2596, 2951, 3335, 3652, 3778. Sharp H and K.

H.D. 22298: 2926.

H.D. 23862, Pleione: 2271, 3006, 3339, 4046. The first two plates include Hα, which is a strong absorption line. The Balmer series, once partially bright, now consists of broad, strong, dark lines, as in 1912 (*Lick Observatory Bulletin*, **7**, 167, 1913).

H.D. 24534, X Persei: 2719, 3064, 3664. Sharp H and K. The dark lines, aside from H and K, are faint and indistinct.

H.D. 25348: 2926. H and K are probably present as weak, narrow, dark lines. The other dark lines are indistinct. Remark in H.D., "The line Hβ is suspected to be bright."

H.D. 29866: 2689, 2695, 3335. Aside from the hydrogen lines, the spectrum is nearly continuous.

H.D. 30614, 9 Camelopardalis: 2631. Sharp H and K. See description of spectrum by Lee, *Astrophysical Journal*, **37**, 1, 1913.

H.D. 33152: 2689, 3360, 3806, 3808. The bright hydrogen lines are unusually narrow. Remark in H.D., "The line Hβ is not seen as a dark line and is suspected to be bright. The other lines are hazy." On our plates the helium lines are distinct.

H.D. 33232: This variable spectrum is under observation and will be described in a future *Contribution.*

H.D. 33461: 2694, 4047. The violet component of bright Hβ is the stronger. The edges of Hγ are probably faintly bright.

H.D. 33604: 2690, 3335, 3456, 3908. The bright hydrogen lines seem to have become weaker since the first observation. On the last photograph the bright components of Hγ and Hδ are weak and indistinct.

H.D. 34921: 2973, 3692.

H.D. 36576, 120 Tauri: 2973.

H.D. 37115, brighter component of β.G.C. 2850: 2626. The measured separations of the bright components are: Hβ, 3.8 A; Hγ, 3.1 A.

H.D. 37657: 2694.

H.D. 37967: 2746.

H.D. 38010: 3653. Aside from the hydrogen lines, the spectrum is nearly continuous.

H. D. 38191: 2969. Aside from the hydrogen lines, the spectrum is nearly continuous.

H.D. 39340: 2759, 3338, 3808. The plates apparently show a slight change in the bright Hβ line: on the first plate the component of longer wave-length is the stronger, but on the other plates the two components are of nearly equal intensity. The measured separations of the bright components of Hβ on the three plates are respectively, 4.2, 3.2, and 3.1 A.

B.D.+25°1019: 2779, 2790, 2981.

H.D. 39478: 2953.

H.D. 41117, χ^2 Orionis: The orbit of this spectroscopic binary (*Lick Observatory Bulletins*, **6**, 144, 1911) is under investigation by Mr. Sanford.

B.D.+20°1309: 2779, 3782.

H.D. 43285: 3127, 3336, 3809.

H.D. 44637: 2748.

H.D. 45314: 2747, 3692. Sharp H and K. The other lines are very faint.

H.D. 45677: This peculiar spectrum is under observation and will be described in a future *Contribution.*

H.D. 45910: The remarkable variations in this spectrum have been described by Plaskett, *Publications of the Astronomical Society of the Pacific*, **35**, 145, 1923, and by Merrill, *ibid.*, p. 303, 1923.

H.D. 45995, brighter component of β.G.C. 3427: The structure of the bright hydrogen lines varies. This spectrum is under observation and will be described in a future *Contribution*.

H.D. 50083: 3725. Measured separation of the bright components of Hγ, 1.8 A.

H.D. 50138: The structure of the bright hydrogen lines varies in a period of about twelve days. This spectrum is under observation and will be described in a future *Contribution*.

H.D. 50209: 2694.

H.D. 51354: 3126, 3134, 3337. Trace of a double bright line at Hβ.

H.D. 51480: This spectrum, which is of the P Cygni type, is under observation and will be described in *Contribution* No. 295.

H.D. 55135: 2720. There is probably a very weak double bright line superposed on the broad absorption line at Hγ.

H.D. 55271, brighter component of β.G.C. 3887: 2718.

H.D. 56806: 2981.

B.D.-13°2040: 2979.

H.D. 59497: 2980.

H.D. 59773: 3038.

H.D. 62753: 3036, 3810. On the first plate the violet components of bright Hβ and Hγ are stronger than the red components. The structure of Hβ may vary, as the bright components of Hβ appear to be more nearly equal in intensity on the second plate than the first. The second plate is under-exposed at Hγ.

H.D. 65875: 3039, 3725.

H.D. 120324, μ Centauri: 3951. The recent disappearance of bright hydrogen lines from this spectrum, noted by several observers, is confirmed by our photograph.

H.D. 127972, η Centauri: 3951. This spectrum is known to vary.

H.D. 152236, ζ′ Scorpii: 3928.

H.D. 154218: 2897.

H.D. 154243: 2897. This star is very near the preceding star, H.D. 154218.

H.D. 154450: 3248, 3927, 3986. The apparent radial velocities from the bright Hβ and Hγ lines for the three plates are +24, +2, and +7 km/sec., respectively. The divergence of the first plate from the other two probably indicates a change in the structure of the lines or in the radial velocity of the star.

H.D. 155806: 3540.

H.D. 156468: 3220, 3951. The displacement of the narrow bright Hβ line corresponds to a velocity of about −50 km/sec., but it is not certain that this is the actual radial velocity of the star.

H.D. 160095: 3245. The hydrogen lines are peculiar. This spectrum will be described in a future *Contribution*, after further observation.

H.D. 160202: 2769, 3664.

H.D. 161103: 2914. The measured separation of the bright components of Hγ is 2.8 A.

H.D. 161114: The spectrum of this "iron" star is under observation and will be described in a future *Contribution*. See *Publications of the Astronomical Society of the Pacific*, **36**, 225, 1924.

H.D. 161306: 2913.

D.M.-27°11944: This P Cygni-type spectrum is under observation and will be described in *Contribution* No 295

H.D. 163181: 2914, 3247, 3605, 3960. Hβ, Hγ, and Hδ are chiefly absorption lines, but at Hβ and possibly at Hγ there appear to be indistinct bright edges. Spectroscopic binary. Approximate velocities from the last three plates are +90, +116, and −226 km/sec., respectively.

H.D. 163296: The structure of the hydrogen lines is very peculiar and appears to vary. This spectrum is under observation and will be described in a future *Contribution*.

H.D. 163454: 3190, 3928, 3987.

H.D. 163868: 2926, 3960.

H.D. 164906: 3307.

H.D. 166566: 2917.

H.D. 166666: 3221, 3976.

H.D. 166734: 3245, 3927, 3947.

H.D. 168229: 3220.

H.D. 168607: 2952, 3951.

H.D. 169226, brighter component of β.G.C. 8523: 3664, 3960, 3987. All the spectrograms are under-exposed.

H.D. 169454: The spectrum of this star, which contains strong dark lines of He, Si, and O, will be described in a future *Contribution*.

H.D. 169515, RY Scuti: This peculiar spectrum, in which a bright line is seen in the position of the nebular line λ 4658, has been described in the *Publications of the Astronomical Society of the Pacific*, **34**, 134 and 295, 1922. A more complete description will be published in a future *Contribution*.

H.D. 169805: 2979. The measured separation of the bright components of Hγ is 3.2 A.

H.D. 170061: 3244. Plate under-exposed.

H.D. 172694: This peculiar spectrum, which somewhat resembles that of H.D. 33232, is under observation and will be described in a future *Contribution*.

H.D. 174105: 2951, 3894.

H.D. 175863: 2566, 2567, 2570, 3191, 3984. The bright portions of Hβ appear weaker on the last two plates than on the others.

H.D. 180398: 2951, 3986. The bright portion of Hβ may be weaker on the second plate than on the first.

B.D.+14°3887: This spectrum, which contains some unusual bright lines, is under observation and will be described in a future *Contribution*.

B.D.+22°3687, brighter component of β.G.C. 9287: 2652, 2956, 3951, 3976. The measured separation of the bright components of Hγ is 2.3 A.

H.D. 183143: 2951, 3338, 3988. Remark in H.D., "The spectrum appears to be nearly continuous." On our plates several lines are strong and well defined, notably Hγ, λ 4471, and λ 4481. Thus it is possible that the spectrum has changed since the Harvard photographs were taken.

H.D. 187399: 3895.

H.D. 187567: 2953, 3336, 3337, 4015. Sharp H and K, measured on three plates, give a velocity of −2 km/sec. The other lines do not yield reliable results.

B.D.+35°3950: 2977, 3960. Sharp H and K.

H.D. 192445: 2834, 3984.

H.D. 193009: 2951, 3896.

H.D. 195407: 2952, 3897, 3930, 3952. The radial velocities derived from the hydrogen lines of the first, second, and fourth plates are −68, −82, and −82 km/sec. respectively, giving a mean value of −77 km/sec. The intensities of the bright portion of the hydrogen lines vary.

H.D. 198512: 3307, 3928.

H.D. 199218, brighter component of β.G.C. 10606: 2853, 2925, 3247, 3896. Measured separation of bright components of Hβ (mean value from three plates) 3.9 A.

H.D. 199356: 2973. The separation of the bright components of Hγ is not accurately measurable on this plate, but is approximately 4.2 A. Sharp H and K.

H.D. 203374: 3013. Sharp H and K.

H.D. 206773: 2955, 3947. The measured separation of the bright components of Hβ is 4.0 A; of Hγ, 4.3 A. Sharp H and K. Aside from the hydrogen and calcium lines, the spectrum is very nearly continuous.

H.D. 207232: 3039, 3926. The measured separation of the bright components of Hβ on the second plate is 4.0 A.

H.D. 207757: This spectrum, which has shown a remarkable change in the past few years (see *Harvard College Observatory Bulletin*, 762) is under observation and will be described in a future *Contribution*.

H.D. 212044: 3014, 3984. Approximate radial velocity from sharp H and K, −16 km/sec. Results from the other lines are not reliable.

H.D. 214748, ε Piscis Australis: 2179, 2576.

H.D. 224559: 2596, 2656, 2953, 3604, 3779. Measured separation of the bright components of Hβ, 3.1 A; of Hγ, 3.1 A; of Hδ, 2.8±. The bright portions of Hδ are feeble and indistinct; it is chiefly an absorption line. Sharp H and K.

H.D. 225095: 2955, 3952.

It is impossible wholly to eliminate photographic effects from the classification of the character of the hydrogen lines. Better photographs might in some instances change the description from D? to D, or even, in the case of very faint bright components, from C or A to D. In this connection, however, it must be borne in mind that the symbols C and A may include lines in which bright portions probably exist, provided the bright components exhibit a degree of distinctness less than that required for the intensity 0.5. Photographic conditions such as the width of the spectrum or the effective contrast of the emulsion might, of course, alter one's judgment on this point. In view of the fact that the bright lines of these stars are subject to change, and because it is in the weak lines that changes may first become obvious, it will perhaps be worth while to describe exactly the significance we have attached to the intensities 1 and 0.5. A line of intensity 1 is a clearly marked bright line, seen at a glance, but of the lowest intensity at which a reliable setting can be made with the measuring-microscope (magnifying-power 26). Intensity 0.5 denotes a line fainter than 1 but of whose reality one becomes convinced after careful inspection. Doubtful bright lines have been omitted from Table V.

The spectral types are those estimated from the Mount Wilson plates. For types earlier than B0 the system suggested by H. H. Plaskett[1] has been employed. When the spectral subdivision is uncertain, it is either omitted or placed in parentheses. The following additional symbols recommended at the Rome meeting of the International Astronomical Union[2] have proved convenient:

e = emission lines
n = diffuse lines
s = sharp lines
p = peculiar
v = variable
q = lines of the P Cygni type

The bright parts of the hydrogen lines grow weaker from Hα toward the violet in all cases. The letters α and β indicate which is the last line to exhibit bright components. In many stars the transition along the series from bright lines to wholly dark lines is so gradual that it is impracticable to specify the line at which it occurs.

III. DISCUSSION

Table I shows that our observations have added 90 early-type stars to the list of those known to possess hydrogen emission lines. Eighty-four of these discoveries have resulted from photographing the Hα region with the 10-inch telescope and objective prism. These observations are largely confined to the Milky Way north of declination $-40°$. The areas covered by plates having fairly good definition and about the standard effective exposure are charted in Figure 2. Within these areas 60 bright-line stars[3] were previously known, and 80 additional ones[4] have been found from our objective-prism observations. The Harvard spectrographic survey showed 49 bright-line stars in the same areas.

---

[1] *Publications of the Dominion Astrophysical Observatory*, **1**, 366, 1922.

[2] *Transactions of the International Astronomical Union*, **1**, 95, 1922.

[3] This includes two stars listed in Table I which were previously detected by Merrill from slit spectrograms.

[4] Not counting χ^2 Orionis and 9 Camelopardalis, in which the bright Hα line is too weak to show on our regular plates.

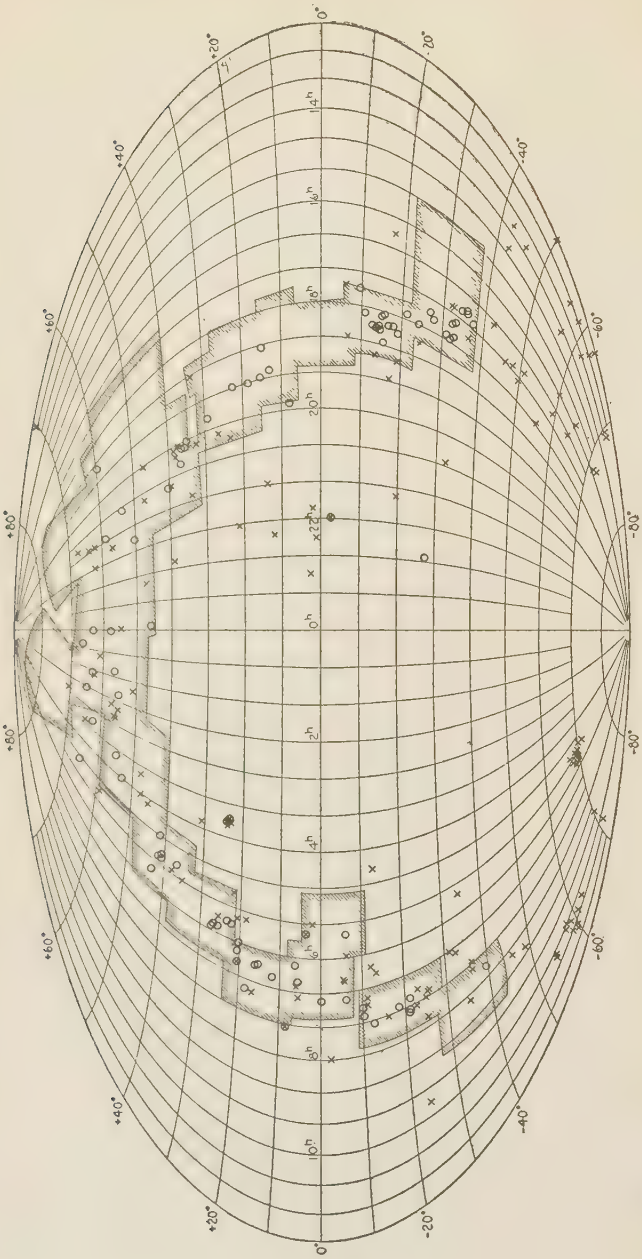

FIG. 2.—Chart of stars of class Be. Circles represent those discovered in the present investigation; crosses those previously known. Six stars found by one of the writers with slit spectrographs at Mount Hamilton or Ann Arbor are marked by crosses within circles. The areas indicated by shading were covered by the Mount Wilson objective-prism observations.

In 41 of our 84 stars, the bright Hβ line is so weak that it could scarcely have been detected on the Harvard plates. This illustrates the advantage of working with the Hα line. The average intensity of the Hβ line in the remaining 43 stars is probably nearly the same as in those discovered at Harvard, and some explanation of the non-appearance of the bright lines on the Harvard plates must be sought. Eight stars are not in the *Henry Draper Catalogue*, leaving 35 which were classified at Harvard. In a few cases the bright lines may have been missed at Harvard because of unfavorable observing circumstances, but the number appears too great to be accounted for entirely in this manner, and the question arises whether some of our additional stars are not ones in which the bright hydrogen lines have come into existence, or at least have become more intense, since the epoch of the earlier observations. Such an explanation is in harmony with the fact that variations in the intensity of the bright hydrogen lines are known to occur in numerous Be stars. A re-examination of the Harvard plates and comparison of the appearance of the hydrogen lines with the data in Table V might throw considerable light on this problem. A better attack would be the repetition of some of the Harvard observations or our own after five years or more have elapsed.

Several stars have experienced a decline in the intensity of the bright hydrogen lines in recent years, notable examples being Pleione and μ Centauri. The list on pp. 13 and 14 adds a few stars to those previously recorded.

It would be desirable to ascertain whether stars of class Be are approximately in statistical equilibrium, that is, whether in a given interval of time the B stars *entering* the bright-line stage are about as numerous as those *leaving* it. We should expect this to be true, but until recently the only known instances of progressive change were those in which the bright lines were growing weaker. This may have been caused partly by the fact that bright-line stars are more closely watched than ordinary stars and hence changes in them are more likely to be detected. A few instances of the appearance of bright lines or of an increase in their strength have, however, been announced by Miss Cannon[1] and by Perrine,[2] and the present observations may contain numerous examples of the same phenomenon. It will not be many years before this matter can be discussed much more adequately than at present, because of the increased attention being devoted to the Be stars by a number of observers. This remark also applies to a related question, namely, whether a B-type star can pass into the bright-line stage more than once.

---

[1] *Harvard Bulletin*, No. 779, 1922.

[2] *Popular Astronomy*, 27, 91, 1919.

Distribution.—Figure 2 shows the distribution of all known Be stars. There is a tendency for them to fall into groups which in nearly every instance lie near the center line of the Milky Way. The strong general condensation near the galaxy is evident from the chart. The material at hand is not suitable for an exact study of this phenomenon.

Four groups of Be stars are in regions which are also rich in Wolf-Rayet stars. The approximate centers of these regions are:

R.A.	Dec.	
5^h20^m	−68°	Greater Magellanic cloud
10 30	−58	
20 10	+36	
17 30	−35	

The last three regions are near the center line of the Milky Way.

Why should Wolf-Rayet and Be stars be concentrated in the same regions of space? Are the conditions in these regions such as to provoke emission lines in stars passing through them, or have the stars therein a common origin which favors emission lines?

The distribution of the bright-line stars in Table V among the various spectral subdivisions is as follows:

Class	No. in Table V	Class	No. in Table V
O6	1	B5	3
O8	1	B8	9
O9	1	B9	2
B0	10	A0	1
B1	16	A2	1
B2	23	B	24
B3	9	Pec.	2
B4	2		

The relatively high frequency of emission lines among Classes B0 to B3, inclusive, is evident. It becomes still more striking when compared with the total number of stars in corresponding groups. We may use for this purpose the Harvard counts of the stars brighter than 8.25 in the *Henry Draper Catalogue*.

Class	All	No. in Table V	Ratio
B0–B5	2061	63	1:N
B8	1604	9	1:5N
B9	2752	2	1:40N
A0	6320	1	1:200N

The actual values of the ratio are not of interest, because Table V contains but a small part of the total number of bright-line stars. These stars do, however, appear to represent a fair sample of the whole as far as spectral classes are concerned, and the relative proportions constitute direct evidence of the preference of bright-line stars for Classes B0 to B5.

Mount Wilson Observatory
November 1924

PLATE VII

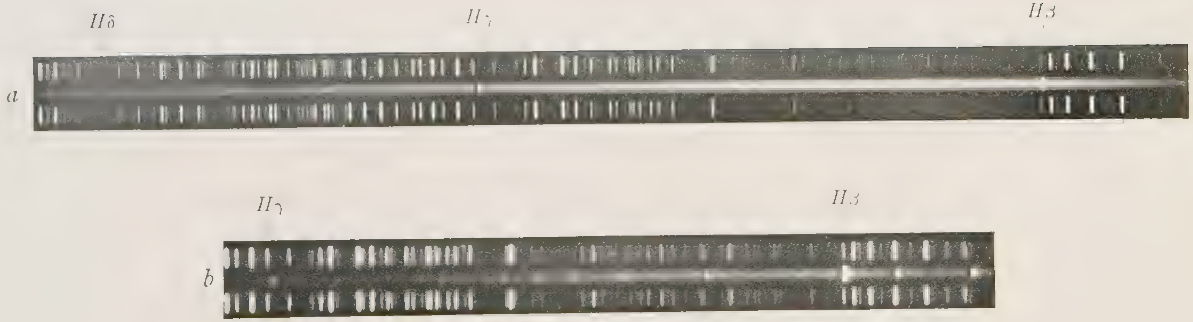

a. H.D. 51480 1921 March 28
b. DM.—27°11944 1922 May 16

Contributions from the Mount Wilson Observatory, No. 295
Reprinted from the *Astrophysical Journal*, Vol. LXI, pp. 418–423, 1925

TWO STELLAR SPECTRA OF THE P CYGNI TYPE

By PAUL W. MERRILL

ABSTRACT

H.D. 51480.—The bright lines were discovered at Harvard about 1892, and recent observations at Mount Wilson have shown them to be bordered on their violet sides by dark lines as in P Cygni. The hydrogen lines are very similar to those of P Cygni; silicon, nitrogen, and helium lines are weaker; and enhanced iron lines are stronger. The general appearance of the spectrum remained almost unaltered from 1919 to 1924, but measurements show certain changes in the positions of the lines.

DM. −27°11944.—Bright hydrogen lines were found at Mount Wilson in 1920, and subsequent observations have shown this spectrum to possess the P Cygni characteristics in a more marked degree than any star previously studied. The bright hydrogen lines are extremely intense, and all the lines are very wide. In these respects the star occupies a position intermediate between P Cygni and a typical nova.

The distinguishing features of the spectrum of P Cygni are strong bright lines bordered on their violet sides by dark lines. Detailed descriptions have been published by several observers.[1] This object appeared as a new star in 1600, and the fact that its spectrum still retains a partial resemblance to that of a typical nova is pertinent to the interpretation of the phenomena of novae. A short list of additional stars of the P Cygni type was published some years ago by Miss Cannon,[2] but thus far, aside from P Cygni itself, only one, B.D.+11°4673, has been described in detail.[3]

The two following stars have been found at Mount Wilson to possess the P Cygni characteristics:

H.D.	DM.	α 1900	δ 1900	Mag.
51480	−10°1774	$6^{h}\ 52^{m}.4$	−10° 41′	7.0
	−27°11944	17 41.9	−27 59	9.0

H.D. 51480

The discovery of bright lines in the spectrum was announced by Mrs. Fleming[4] in 1893. The following remark appears in the

---

[1] Miss Maury, *Harvard Annals*, **28**, 101 (remark 165), 1897; Belopolsky, *Astrophysical Journal*, **10**, 319, 1899; Frost, *Astrophysical Journal*, **35**, 286, 1912; Merrill, *Lick Observatory Bulletins*, **6**, 156, 1911; **7**, 24, 1913.

[2] *Harvard Annals*, **76**, 31, 1916.

[3] *Publications of the Observatory, University of Michigan*, **2**, 71, 1916.

[4] *Astronomy and Astrophysics*, **12**, 810, 1893. The identification given in this reference is incorrect.

Henry Draper Catalogue: "The line Hβ is bright, and bright lines or spaces not due to hydrogen are seen. The lines are narrow and the line K is as strong as in Class A2."

The Mount Wilson observations with slit spectrographs are listed in Table I. Several plates taken in the course of the general spectroscopic program have been available for the present investigation through the kindness of Mr. Adams.

Several lines exhibit both bright and dark components as in P Cygni, but other lines appear only in absorption (see Table II). The hydrogen lines closely resemble those of P Cygni in structure and intensity. Silicon, nitrogen, and helium lines are weaker than in P Cygni, while the enhanced iron lines and λ 4481 of magnesium are stronger. The general character of the spectrum is the same on all eight plates of the blue-violet region. The only very definite changes noticeable on inspection are, in fact, slight variations in the intensity of the absorption at Hβ. Measurements of the principal lines observed are given in Table II. As most of the lines are unsymmetrical and rather ill defined, their displacements can be determined with only moderate accuracy. The figures in Table II are the means from two independent measures of each plate. A few indistinct lines were measured but once, and the resulting displacements are in parentheses. All the values are reduced to the sun.

TABLE I

SPECTROGRAMS OF H.D. 51480

Date	Spectrograph	Camera	Region
1919 October 14	1-prism	18-inch	Blue-violet
1920 November 20	1-prism	18-inch	Blue-violet
1921 January 29	1-prism	18-inch	Blue-violet
1921 February 22	1-prism	18-inch	Blue-violet
1921 March 28	1-prism	18-inch	Blue-violet
1921 November 12	1-prism	18-inch	Blue-violet
1924 March 24	1-prism	18-inch	Blue-violet
1924 December 14	1-prism	18-inch	Blue-violet
1925 January 3	Grating	10-inch	Red

The effective displacements of the various absorption lines on individual plates, as well as in the mean, differ by many kilometers. After making allowance for the large errors of measurement,

TABLE II

MEASURED DISPLACEMENTS IN THE SPECTRUM OF H.D. 51480

LINE	1919 OCT. 14		1920 NOV. 20		1921 JAN. 29		1921 FEB. 22		1921 MAR. 28		1921 NOV. 12		1924 MAR. 24		1924 DEC. 14		MEAN			P CYGNI (FROST)
	A	E	A	E	A	E	A	E	A	E	A	E	A	E	A	E	A	E	E–A	E–A
	km	km	km	km	km	km	km	km	km	km	km	km	km	km	km	km	km	km	Ang.	Ang.
4101.74 Hδ	.....	.....	−110	+ 51	−119	+ 83	.....	.....	−101	+ 49	−119	+ 44	.....	.....	− 70	+ 82	−104	+ 62	2.28	2.28
4178.87 *Fe*	.....	.....	.....	.....	111	.....	(−66)	.....	55	.....	.....	.....	.....	.....	32	.....	66	.....	.....	....
4233.14 *Fe*	.....	.....	94	.....	107	71	70	.....	86	52	87	(59)	.....	.....	34	97	80	71	2.13	....
4340.47 Hγ	−100	+ 53	116	40	109	70	113	+ 26	112	51	134	39	−96	+ 41	77	76	107	55	2.34	2.58
4351.77 *Fe*	.....	.....	.....	.....	.....	.....	.....	.....	75	72	.....	.....	64	.....	29	77	54	74	1.84	....
4471.48 He	.....	.....	(68)	.....	139	.....	(67)	.....	50	.....	109	.....	.....	.....	105	.....	90	.....	.....	....
4481.22 *Mg*	.....	.....	62	.....	125	.....	72	.....	50	.....	124	.....	43	.....	48	.....	75	.....	.....	....
4508.29 *Fe*	.....	.....	.....	.....	.....	.....	.....	.....	(72)	.....	.....	.....	.....	.....	.....	.....	72	.....	.....	....
4549.47 *Fe*	.....	.....	.....	.....	70	(117)	96	.....	70	.....	102	.....	70	.....	28	127	72	123	2.96	....
4583.84 *Fe*	.....	.....	.....	.....	.....	(59)	100	49	58	79	106	38	(− 75)	82	.....	(110)	82	72	2.34	....
4861.33 Hβ	−143	+ 60	−162	+ 40	−186	+ 97	−146	+ 26	−138	+ 52	−139	+ 34	.....	+ 51	−100	+ 83	−145	+ 55	3.24	3.46
Mean	−122	+ 56	−102	+ 44	−121	+ 82	−91	+ 34	− 79	+ 59	−115	+ 41	−70	+ 58	− 58	+ 92	− 94	+ 58	....	....

discrepancies remain which must be inherent in the star's light. The average negative displacements of the absorption components of the hydrogen lines, especially Hβ, are greater than those of the other lines, and this is probably caused by the greater strength of the emission components. *He* λ 4471 is broad and difficult to measure. The emission lines, as in P Cygni, are in better agreement than the absorption lines. Possibly their agreement is within the errors of measurement. λ 4549 seems to be outstanding, but its measured displacement has small weight as it may be partially blended with neighboring lines.

Several plates show systematic residuals from the mean. The emission lines of the plate of February 22, 1921, for example, give an average displacement 27 km/sec. less than the mean; those of the plate of December 14, 1924, 34 km/sec. more. On the latter plate the absorption lines differ from the mean in the same sense as the emission lines. Whether the shifts are periodic or irregular cannot be determined from the plates now available. In addition to bodily displacements of the spectrum, possibly due to orbital motion, certain other changes appear to exist. The third plate, for example, gives a considerably greater mean difference between absorption and emission lines than do other plates.

The displacement of the strong emission Hα line as measured on the plate of January 3, 1925, is +72 km/sec., in approximate agreement with the mean result from the other bright lines.

DM. −27°11944

A very strong bright Hα line was found in this spectrum on an objective-prism plate taken August 4, 1920, by Mr. Milton L. Humason.[1] It appears broad even with the low dispersion employed (440 A per mm), but on the best plates is sharply bounded on the short wave-length side; it is probably of the P Cygni type. It is extremely strong compared to the adjacent continuous spectrum.

The observations of the blue-violet region photographed with a single-prism spectrograph attached to the 100-inch reflector are listed in Table III.

---

[1] *Publications Astronomical Society of the Pacific*, **34**, 294, 1922; *Mt. Wilson Contr.*, No. 294; *Astrophysical Journal*, **61**, 389, 1925.

Numerous lines exhibit the P Cygni characteristics in a marked degree. The bright portions are very broad, and in this respect the star occupies a position intermediate between P Cygni and a typical nova. Thus DM. −27°11944 supplies a missing link in the chain of bright-line objects connecting ordinary B-type stars with novae.

TABLE III

SPECTROGRAMS OF DM. −27°11944

Date	Camera	Date	Camera
1921 March 30	18-inch	1921 August 13	7-inch
1921 April 10	18-inch	1922 May 16	18-inch
1921 April 29	18-inch	1923 July 27	10-inch
1921 June 21	18-inch	1924 August 20	10-inch

The bright lines are difficult to measure on account of their diffuse, unsymmetrical character, and, except for a few of the strongest, their lack of contrast with the continuous spectrum. A few of the dark lines are fairly well defined, though unsymmetrical; but most of them are weak and, as a whole, are incapable of accurate measurement. The lines (bright and dark) which can be identified are ascribed to hydrogen, helium, or enhanced iron. About all that can be said concerning the displacements is that those of the bright lines are small and positive, those of the dark lines large and negative. Because of the southern declination of the star, we have not been able to secure well-exposed spectrograms with the 18-inch camera. Even with the shorter cameras the continuous spectrum, although strong at $H\beta$, does not extend beyond $H\gamma$. Probably the real spectral intensity-curve drops more rapidly between these two lines than for a normal B-type star as the direct image has a decidedly reddish color, although this may be due in part to the very intense $H\alpha$ line.

Measurements of line-widths are given in Table IV. They are merely rough approximations as the results depend to a considerable extent upon the judgment of the observer as well as upon the effective exposures of the plates. Frost's values for P Cygni are given for comparison.

No change has appeared in this spectrum during the three-year interval covered by our observations. Moreover, the light is sensibly constant, for "if variability now exists it probably does not exceed a tenth of a magnitude in range, as no variation is found on the Harvard photographs,"[1] fifty-one in number, extending from 1890 to 1918.

TABLE IV

APPROXIMATE LINE-WIDTHS IN ANGSTROMS

LINE	−27°11944		P CYGNI (FROST)	
	A	E	A	E
4340 Hγ	....	4.3	1.5	3.0
4471 *He*	....	4.3	1.6	2.2
4583 *Fe*	3.7	6.2	....	....
4712 *He*	....	5.0	....	....
4861 Hβ	4.8	6.8	2.0	4.3
4923 *He+Fe*	4.3	6.8	....	....
5017 *He+Fe*	6.4	7.5	....	....

MOUNT WILSON OBSERVATORY
March 1925

---

[1] *Harvard College Observatory Bulletin*, No. 807.

NOTE ADDED AUGUST, 1925

An excellent plate of DM.-27°11944 was taken with the 10-inch camera on August 13, 1925, by Professor J. C. Duncan. It closely resembles the earlier spectrograms. The observed interval during which this remarkable spectrum has remained without marked change is thus extended to four years.

Contributions from the Mount Wilson Observatory, No. 296
Reprinted from the *Astrophysical Journal*, Vol. LXI, pp. 424–442, 1925

THE THEORY OF THE STELLAR ABSORPTION COEFFICIENT[1]

By S. ROSSELAND

ABSTRACT

The stellar absorption coefficient.—A reliable theory of the absorption coefficient of strongly ionized matter is a necessary complement to any theory of the internal constitution of stars. In the present paper such a theory is developed deliberately as a generalization from X-ray absorption experiments only, and partly checked by experiments of Anderson and Harrison. On the basis of this theory the expression of the flux of radiant energy in a star is calculated, and the result compared with Eddington's theory of a star in radiative equilibrium.

The theory of the opacity of an ionized gas has acquired much interest for astrophysics through Eddington's work on "The Internal Constitution of the Stars." In fact, a reliable knowledge of the absorption coefficient of gases under all conditions would enable us to draw far-reaching conclusions about the distribution of elements throughout a star and about the localization of the sources of stellar energy, questions which are fundamental for stellar theory.

The problem of determining the absorption coefficient of stellar matter can scarcely be solved by direct comparative experiments in the laboratory as, apart from the superficial layers of a star, stellar temperatures are likely to be much higher than those accessible to terrestrial experiments. The frequencies for which the absorption of radiation in the interior of a star mainly takes place, however, can scarcely be larger than those of soft X-rays, corresponding to *L*-radiation from elements of median atomic numbers. This fact directly suggests the application of X-ray data to the stellar problem, a question which has already been discussed by Eddington,[2] whose discussion, however, was concerned with the arithmetic mean value of the absorption coefficient, whereas theory requires something like the harmonic mean value,[3] and when the absorption coefficient varies rapidly with the frequency of the incident radiation the results given by the latter procedure may differ widely from those given by the former. For this reason we shall in the following reconsider the whole problem on the new basis. Actually, the final result does not differ much from that arrived at by Eddington; but this is not due to any triviality as regards the two modes of calculating the absorption coefficient. Thus, the contribution to the stellar absorption coefficient considered by Eddington was due to absorption by atoms in the normal state, while the present theory assigns an essential rôle to atoms excited to higher quantum states. Moreover, an attempt is made to distinguish clearly between what may be taken over directly from laboratory observations and what is more or less hypothetical.

---

[1] This paper is the continuation of a paper on "Transmission of Radiation" in *Monthly Notices, R.A.S.*, **84**, 52, 1924.

[2] *Monthly Notices, R.A.S.*, **84**, 104, 1924.

[3] *Ibid.*, **84**, 525, 1924.

In considering the problem of transmission of radiation in the interior of a star, the absorption in a line spectrum is clearly of little significance, as this process can only bar the passage of the radiation confined in very small frequency intervals of the spectrum. It is therefore sufficient for such purposes to consider the continuous absorption setting in at the series limits, which is analogous to the continuous X-ray absorption. In the following we shall consider briefly the theory of absorption in general, and indicate a tentative generalization from results on X-ray absorption to absorption in other spectral regions. This theory will then be applied to the calculation of the stellar absorption coefficient, and the relation of the results to the theory of the radiative equilibrium of a star discussed.

1. *Formal theory of absorption.*—We shall in the following be concerned with absorption in the restricted sense that the energy of the absorbed radiation is converted into kinetic and potential energy of an electron which is free after the absorption process. For the general theory it is convenient to consider the absorbing atoms to be parts of a system in thermodynamic equilibrium, and the beam of incident radiation to correspond to black-body radiation for the temperature in question. In this special case the radiation absorbed within any infinitely small frequency interval will be counterbalanced by an equally large emission of radiation in the same interval. The absorption coefficient may thus be expressed in terms of a certain emission coefficient which is more easily submitted to theoretical calculations and interpretation.[1] As this latter, as well as the absorption coefficient itself, is essentially dependent upon purely atomic

---

[1] Cf. H. A. Kramers, *Philosophical Magazine*, 46, 836, 1923.

properties, the result is in itself independent of the assumption of a thermodynamic equilibrium, and susceptible of application to quite general cases. Consider, thus, an assembly of atoms and free electrons in a state of thermodynamic equilibrium at an absolute temperature T, and let there be n_e free electrons, n_i atoms with a vacant quantum state i, and n^i atoms with the i-state filled up—all figures referring to unit volume. In considering collisions between electrons and atoms the motion of the latter will be neglected. The atoms with a complete i-state will absorb the radiation of a frequency ν under expulsion of electrons with a velocity v according to the $h\nu$-relation,

$$h\nu=\tfrac{1}{2}mv^2-E_i\ , \tag{1}$$

where $-E_i$ is the energy which must be given to the electron in the i-state in order to transfer it to an infinite distance from the atom. If $B_\nu d\nu$ is the energy density of temperature radiation in the frequency interval ν to $\nu+d\nu$, the energy absorbed by the atoms in the i-state in the given frequency interval per unit volume in unit time is

$$n^i x^i_\nu c B_\nu d\nu\ , \tag{2}$$

where x^i_ν is the absorption coefficient and c the velocity of light. These absorption processes must be counterbalanced by an equal number of emission processes in which free electrons with velocity v collide with atoms with initially vacant i-states and are bound in these states in the collision. Consider collisions in which the distance from the atomic nuclei to the direction of the initial velocity of the colliding electrons is confined in the interval p to $p+dp$, the number of which is

$$n_i dn_e v 2\pi p dp \tag{3}$$

per second, where dn_e is the number of free electrons per unit volume in the velocity interval v to $v+dv$. Denoting by P_i the probability that an electron shall be bound in an i-state in the collision process, we find the total emission of radiation in the frequency interval in question by multiplying expressions (3) by $h\nu P_i$ and integrating over all possible values of p. The result thus obtained must be equal to the expression (2), or

$$n^i x^i_\nu c B_\nu d\nu=2\pi v h\nu n_i dn_e \int_0^\infty P_i p dp\ . \tag{4}$$

The function P_i must, according to the well-known theory of Einstein,[1] be independent of the energy density of radiation to the same degree of approximation that B_ν is reproduced by Wien's expression

$$B_\nu \backsim \frac{8\pi h\nu^3}{c^3} e^{-\frac{h\nu}{kT}} ,$$

and we may, therefore, without in the least committing ourselves to approximate results, assume the temperature to be so low that such conditions will obtain. Introducing the ordinary expression for $n_i dn_e/n^i d\nu$ from statistical theory

$$\frac{n_i}{n^i}\frac{dn_e}{d\nu} = \frac{4\pi h m^2}{\sigma_i} v e^{-\frac{h\nu}{kT}} , \tag{5}$$

we find, finally,

$$x^i_\nu = \frac{hm^2c^2v^2}{2\sigma_i\nu^2} 2\pi \int_0^\infty P_i p\,dp , \tag{6}$$

where σ_i is the a priori probability of the atom with the i-state filled, relative to the state with the i-electron missing. The quantity

$$y^i_\nu = 2\pi\int_0^\infty P_i p\,dp , \tag{7}$$

just as x^i_ν, has the dimensions of an area, and may be called the effective cross-section of the atom for capturing electrons of velocity v to the i-state. Conversely, when x^i_ν and y^i_ν are known, we may, by retracing the steps, obtain the value of $n_i dn_e/n^i$, and we are thus able to calculate the degree of ionization of the substance without going through all the steps of the ordinary statistical theory. This process, suitably generalized, may be susceptible of application to the problem of calculating the ionization of the material of gaseous nebulae where ordinary thermodynamic formulae very probably would break down.

For the further elucidation of the function P_i we may consider the problem from the point of view of the correspondence principle.[2]

---

[1] *Loc. cit.*

[2] Cf. H. A. Kramers, *loc. cit.*, where the discussion is carried out at length. The discussion here has a different purpose, as we wish only to obtain a method of generalizing experimental results.

Consider thus the general problem of a collision between an electron and an atomic system on the basis of ordinary electrodynamics. The total loss of energy of the electron during the collision will be given by an expression of the form

$$\delta E=\frac{2e^2}{3c^3}\int_{-\infty}^{\infty}[1-\beta^2(\lambda-1)(3\lambda-1)]\,\frac{F^2}{(1-\beta^2)^3}\,dt\;;\qquad \beta=v/c\;, \tag{8}$$

where F is the acceleration and v the velocity of the electron, while arc cos λ is the angle between these two vectors. Assume this energy to be resolved into a continuous spectrum such that $E_w dw$ is the energy falling in the frequency interval dw. For velocities of the electron which are small compared to the velocity of light, the mean value of the acceleration F at a distance r from the nucleus may be expected to have the form

$$F=\frac{N_f e^2}{mr^2}\;, \tag{9}$$

where $N_f e$ is the net electric charge contained within a sphere of radius r and having the nucleus for a center. As the emission very probably is principally stimulated during the passage close to the nucleus, we may expect that the expression of E_w will contain $(Ne^2)^2$ as an essential factor, where N is the atomic number. Denoting the initial value of the angular momentum of the electron round the nucleus by M it is possible to write

$$E_w=\frac{2}{3}\,\frac{e^2}{c^3}\left(\frac{Ne^2}{M}\right)^2 G_w\;,\qquad M=mvp \tag{10}$$

where G_w is a zero dimensional quantity which in general may be expected to be a continuous and smooth function of p, v, and w. There is no doubt that in an actual collision in nature the frequency distribution of energy in the emitted radiation will be essentially different from that predicted by a formula such as (10). In particular, it is known with certainty that the spectrum actually emitted in a collision of the foregoing type cannot extend materially toward larger frequencies than the limit $\nu=\Delta E/h$, which by the frequency relation corresponds to the total loss of energy ΔE in the collision. Moreover, the spectrum of the radiation emitted by a large number of electrons suffering collisions of identically the same type may be expected to consist of a typical line spectrum, one for each possible quantum state of the electron when bound in the atom, and a continuous spectrum corresponding to the fact that some electrons will radiate without being bound. We must, therefore, if we expect classical electrodynamics to be applicable to the case at all, postulate a general *correspondence* between the classical intensity of radiation in the interval dw and the intensity of radiation really emitted in the interval $d\nu$, such that each dw contributes an amount of energy

$$\gamma_i(\nu, w)E_w\, dw\, d\nu \tag{11}$$

to the frequency interval $d\nu$ in question. As the total amount of energy absorbed when an electron is shot out of the atom under absorption of radiation of frequency ν is $h\nu$, we have by (4) the expression

$$\frac{1}{h\nu}\int_0^\infty \gamma_i(v, w)E_w\, dw \tag{12}$$

which is by definition equal to the function which was previously denoted by P_i. By combination of (6), (10), and (12) we obtain

$$x_\nu^i = \frac{2\pi\, e^6\, N^2}{3c\, \sigma_i\, \nu^3}\int_0^\infty\int_0^\infty \gamma_i(\nu, w)G_w\, dw\, dp/p\ . \tag{13}$$

The function $\gamma_i(\nu, w)$ can have appreciable values only when w is in the vicinity of ν, otherwise the postulate of a correspondence between classical and quantum radiation would not have much sense. The integral

$$\int_0^\infty \gamma_i(\nu, w)dw \tag{14}$$

defines a frequency interval which must be roughly proportional to the energy difference between the i-state of the atom and an adjacent state, in order to comply with the requirements of the frequency relation. This energy difference is in turn approximately proportional to the square of the effective nuclear charge and inversely proportional to the third power of the effective principal quantum number n of the electronic group in question. Thus[1]

$$\int_0^\infty \gamma_i(\nu,\, w)G_w dw \backsim G_\nu \frac{\partial E_i}{\partial nh} \propto \frac{N^2}{n^3} G_\nu \qquad (15)$$

or finally

$$x_\nu^i = \frac{\nu^{-3}N^4 r}{\sigma_i n_i^3} K(\nu) \;; \qquad K(\nu) = \text{const.} \int_0^\infty G_\nu \frac{dp}{P} \,, \qquad (16)$$

where r is the number of electrons in the group in question.

One might for a moment be inclined to the belief that it would be possible to proceed in the reverse direction and from measurements of the absorption coefficient learn something about the motion of electrons in collision with atoms. The information which can be obtained in this way is, however, not very definite as it is only involved through the function G_ν, which, unfortunately, remains undetermined to a rather wide extent. In fact, the integral equation for G_ν given by theory

$$\int_0^\infty G_\nu \frac{dp}{p} = CK(\nu) \,, \qquad (17)$$

where C is some constant, has the solution

$$G_\nu = \frac{CK(\nu)Y(pU)}{\int_0^\infty Y(x)dx/x} \,, \qquad (18)$$

where $Y(x)$ is an *arbitrary* function of one argument only, and U an arbitrary function of the frequency ν. This result contains, in fact, practically all that continuous absorption experiments can teach us about the motion of electrons in collision with atoms.

2. *Generalization of the X-ray absorption coefficients.*—According to experimental results,[2] the absorption coefficient for monochromatic X-rays absorbed in a definite electronic level i of the atom is of the form

$$x_\nu^i = \nu^{-3}N^4 A_i \,, \qquad (19)$$

---

[1] This is the hypothesis which was adopted by Kramers, *loc. cit.*

[2] Cf. F. K. Richtmeyer and F. W. Warburton, *Physical Review*, **22**, 539, 1923.

where A_i is constant as long as the frequency in question is larger than $h^{-1}E_i$, E_i being the energy necessary to remove an electron from the level in question, and zero for smaller frequencies. The validity of this formula, especially for absorption of hard radiation in the K-level, has been tested for a large number of elements ranging from $N=6$ (carbon) to $N=82$ (lead). Comparing (19) with (16) we see immediately that this result demands that the function $K(\nu)$ be independent of ν for absorption in the levels in question. Experiments show further that the constant A_i decreases rapidly when passing from the K to the L-level, and so on. This fact is naturally attributed to the changes in the factor $r/n^3\sigma_i$, which are of the right order of magnitude. It would therefore seem that the function K is an absolute constant for all levels in question.

The experiments at hand are only concerned with the case of electronic groups which are located so close to the nucleus that the effective atomic number of the group is practically equal to the atomic number of the atom. When we proceed to consider absorption in electronic groups which are located so far from the nucleus that the screening effect of the intervening electrons on the motion of the electrons in the group becomes appreciable, we have no reason for expecting formula (19) to be applicable. In default of experimental evidence it may be of interest to consider the alteration in this formula which would be suggested by the formal theory given above. According to theory, the factor N^4 is a product of two factors, each of which proceeds from quite different sources. Thus one factor N^2 was introduced by the fact that a free electron colliding with an atom emits the more radiation the larger the nuclear charge of the atom. That this process alone will introduce a factor N^2 is independently evidenced by the fact that the total emission of general x-radiation from a target bombarded with electrons of given velocity is proved by experiments to be proportional to the square of the atomic number of the substance constituting the target. Therefore, on considering absorption of radiation in outer atomic groups, the foregoing factor N^2 would be expected to be carried over with little alteration, or at most with the introduction of a small screening constant α_i, thus giving $(N-\alpha_i)^2$ for N^2 in the formula. The second factor has been shown to measure the energy difference between successive quantum states. From X-ray spectroscopy this factor is known to vary considerably from level to level, and this variation we shall account for by a second screening constant, β_i. The final form of formula (16) is thus

$$\varkappa_\nu^i = \nu^{-3}(N-\alpha_i)^2(N-\beta_i)^2 \frac{K(\nu)r}{\sigma_i n_i^3} \,. \tag{20}$$

Measuring all quantities relative to the corresponding quantities in the K-level, we find the numerical values of K, according to the results of Richtmeyer, to be

$$K = 2.2 \cdot 10^{-2} c^3 \text{ c.g.s.} \,,$$

where c is the velocity of light. The foregoing formula refers to a definite level. In general, a number of levels will come into play, and, in order to obtain the mean absorption coefficient averaged over all atoms present in the system, each expression such as (20) must be multiplied by the relative probability τ that the atom shall be found in this particular level, and the sum taken over all levels which can come into consideration.

It is of particular interest to consider the case in which the distribution of atoms over the various quantum states corresponds to a state of temperature equilibrium. The numbers τ are then given by the expression

$$\tau_i = \frac{\sigma_i e^{-\frac{E_i}{kT}}}{f(T)} \,; \qquad f(T) = \sum_s \sigma_s e^{-\frac{E_s}{kT}} \,, \tag{21}$$

and the mean absorption coefficient, consequently, by

$$\varkappa_\nu = \sum_k \frac{\tau_k K r \nu^{-3}}{n_k^3 \sigma_k} (N-\alpha_k)^2 (N-\beta_k)^2 \,, \tag{22}$$

where due care must be exercised to include only those states which by the frequency relation can come into play in the absorption process. It is here assumed that the quantum states of the atom in question are sharply defined, otherwise the foregoing series of discrete terms would have to be replaced by an integral over the infinite number of possible states, and conditions would approach those contemplated in the classical statistical theory. The foregoing theory is also susceptible of application to this case, in particular, when the broadening of the states is so advanced that the distribution of atomic states in the phase space may be considered to be continuous. For this limiting case we may effect the summation involved in expression (22) by directly referring to equation (4) from which we started. In fact, integrating both sides of this expression over all possible kinds of atoms (left side) and all possible velocities of the electrons (right-hand side), we find that the resulting expression may be written in the form

$$n^0 x_\nu c B_\nu = 2\pi\, h\nu \sum_a n_a \int v\, dn_e \int_0^\infty P_i p\, dp\ , \tag{23}$$

where n^0 is the total number of atoms per unit volume, x_ν the mean value of the atomic absorption coefficient, and n_a the number of atoms in a particular state of ionization, the summation being extended to all kinds of atoms. Denote the energy emitted when a free electron with zero velocity falls to the lowest possible quantum state of the atom by $h\nu_a$, and by ν'_a, the largest frequency of the classical spectrum which corresponds to ν_a. The integration as regards v in the foregoing expression is then to be extended from the lower limit v_0 given by

$$\tfrac{1}{2} m v_0^2 = h(\nu - \nu'_a) \tag{24}$$

to infinity, provided $\nu > \nu'_a$, and from $v = 0$ for the case that $\nu \lesseqgtr \nu'_a$. Introducing the proper expressions for P_i and dn_e/dv, and remembering that

$$G_0 = \int_0^\infty G_\nu\, dp/p \tag{25}$$

is independent of v, we obtain finally by integration, the expression for x_ν,

$$x_\nu = \tfrac{4}{3} \frac{e^6}{c^4} G_0 \left(\frac{2\pi}{m^3 kT} \right)^{\frac{1}{2}} n_e B^{-1} \nu \sum_a \frac{n_a}{n^0} (N - a_a)^2 e^{-h\frac{(\nu - \nu'_a)}{kT}}\ ; \qquad n^0 = \sum_a n_a\ . \tag{26}$$

It is to be understood that an exponential factor is to be taken equal to unity in the foregoing formula in case $\nu \leqq \nu'_a$. The constant G_0 in the foregoing expression may be determined from X-ray data with some accuracy. In fact, the detailed expression for K suggested by theory is, from (15) and (16), seen to be

$$K = \frac{(2\pi)^3 e^{10} m}{3 c h^6} G_0 \tag{27}$$

Here the a priori probability is measured in units of h^3 while E_i, by atomic theory, is assumed to be given by

$$E_i = -\frac{2\pi^2 e^4 m N^2}{h^2 n_i^2} . \tag{28}$$

From the experimental value of K and from (27) it follows that

$$G_0 = 34.7 . \tag{29}$$

There can be little doubt that for large values of the quantum numbers the law suggested by (15) must be rather accurate, but for the case of the K-level, when the principal quantum number is unity, this hypothesis may be subject to some uncertainty, but probably not by more than a factor $2^{\pm 1}$. By observations of X-ray absorption in higher levels this uncertainty regarding the value of G_0 might be much reduced.

As it stands, formula (26) gives the aggregate absorption coefficient as it is caused by atoms, or possibly free electrons, which are in collision with the atoms. Putting all ν'_a equal to zero gives the absorption by free electrons alone:

$$x_\nu^e = \tfrac{4}{3} \frac{e^6}{c^4} \left(\frac{2\pi}{m^3 kT} \right)^{\frac{1}{2}} G_0 B_\nu^{-1} n_e e^{-\frac{h\nu}{kT}} \sum_a \frac{n_a}{n^0} (N - a_a)^2 . \tag{30}$$

This formula corresponds in a certain sense to that derived in the classical electron theory for the absorptive power of metals, but with the difference that it is not restricted to long wave-lengths, as was generally the case in the classical theory.[1] As one might have anticipated on general grounds, formula (30) predicts a strong increase in the absorptive power with increasing wave-lengths of the incident radiation, while for short wave-lengths it drops very rapidly to an insignificant value. To the absorptive power of the electrons due to collision with atoms,[2] must be added the scattering power of the electrons themselves when they remain perfectly free. This scattering coefficient is given by the well-known formula of J. J. Thomson

---

[1] In fact, formula (30) is not applicable to absorption of radiation of very long wave-length, which is directly evidenced by the fact that when $\nu \rightarrow 0$ it would predict an infinitely large absorption, while a revised theory would lead to an asymptotical equality of x_ν to $4\pi\sigma$, where σ is the electric conductivity of the substance, which must have a finite value.

[2] The effect of collisions between the electrons themselves will be in the sense of diminished absorption, as the electrical moment of two colliding electrons is practically zero, due to equality of masses and charges. The diverging result obtained by Eddington (*Monthly Notices, R.S.A.*, **84**, 104, 1294) arises from the fact that he neglects the systematic relation between the accelerations of two electrons in collision.

$$x=\frac{8\pi}{3}\left(\frac{e^2}{mc^2}\right)^2 \tag{31}$$

per electron for all wave-lengths longer than those of hard X-rays.

The foregoing generalization of the results from X-ray experiments is purely tentative and intended to serve only as a guide for applications to stellar theory. For this purpose it is very important to have the formulae checked in some way, in order to gain an idea of the directions in which deviations from theory are likely to take place. Unfortunately, the experimental evidence on this point is very scanty, as the only check at hand is afforded by a few absorption measurements in the optical region where we should hardly expect an extrapolation from X-ray experiments to afford any approximation at all.

Harrison[1] appears to be the first to have made quantitative measurements on the continuous absorption setting in at the series limit of the principal series of gases and vapors. He measured the absorption coefficient in the region of continuous absorption beyond the series limit of the principal series of sodium, but states that the measurements are rather uncertain, although they undoubtedly serve as a first orientation in the field. The necessary data kindly put at my disposal by Dr. Harrison himself show that the absorption coefficient per atom for a definite small frequency interval just beyond the series limit ($\lambda=2414$ A) is of the order of 10^{-19}, and that the absorbing power decreases rapidly when proceeding to shorter wavelengths. The latter circumstance is in fair-enough agreement with expectations, but the absolute value of the coefficient appears to be much smaller than can be accounted for on the basis of (22) or (19), however we twist them. In fact, even by putting $(N-\alpha_i)\times(N-\beta)=1$, which certainly is the smallest value that can possibly come into consideration, and by taking $n=1.5$ as claimed by spectroscopy, we obtain $x=7.10^{-17}$, which is several hundred times larger than the experimental value.

---

[1] *Physical Review*, **24**, 466, 1924.

Anderson[1] has investigated the opacity of electrically exploded wires. During the explosion the wires evaporate and the vapors are raised to a temperature of about 20,000°K., as a consequence of which we no longer deal with atoms in the neutral state only, as is the case in Harrison's experiments, but with atoms distributed over a variety of quantum states and partly ionized. Consequently, we should expect on theory that the absorption spectrum of the vapors would be a superposition of a variety of series-limit absorption spectra, which would be strongest in the short wave-length region where we are concerned with absorption by atoms in the lowest possible quantum state, and, because of absorption by atoms excited to higher states, would extend with diminishing intensity right up to the optical region. This, in fact, appears to be in general accordance with Anderson's results. Stewart[2] suggested that the strong absorption observed in these experiments might be due to the action of free electrons. This theory, however, does not seem calculated to account for the observed facts. On any theory (as, for instance, Stewart's own, or that given above) the effect of free electrons must be confined to long wave-lengths where the time spent by an electron on a free path is small compared to the period of a light-vibration, and for short wave-lengths it must degenerate into an ordinary Thomson scattering, which is much too small to account for the absorption in question. It would, however, be interesting to have these experiments extended to the long wave-length region where the absorption by free electrons necessarily must make itself felt. An experimental confirmation of this expectation would be all the more interesting as it would afford a case where the classical electron theory is applicable in principle.

Anderson's experiments appear thus to be in qualitative agreement with the theoretical considerations given above. Moreover, they appear also quantitatively to conform much closer to theory than was the case for Harrison's experiments. Dr. Anderson has kindly informed me that the absorption coefficient per atom of exploding iron vapor (temperature and pressure estimated as 20,000°K. and 4 atm., respectively) appears to be of the order of $2\cdot 10^{-19}$ for the spectral region λ 4000 A. This absorption must be due to atoms excited in higher quantum states, as the absorption by atoms in the normal state, whether neutral or ionized, must be confined to the ultra-violet region. The case is therefore one which suggests the application of formula (26), which just corresponds to the overlapping absorption by excited atoms. There is apparently only one stage of ionization in play in the experiments, and we may therefore write (26) in the form

---

[1] Cf. *Proceedings of the National Academy of Sciences*, **8**, 231, 1922.

[2] *Nature*, **111**, 186, 1923.

$$x_{4000}=\frac{n_e}{n^0}\left\{\frac{n_a}{n^0}(N-a_1)^2+\left(1-\frac{n_e}{n^0}\right)(N-a_2)^2\right\}10^{-20}\,, \tag{32}$$

where we have introduced experimental data given above. The ratio n_e/n^0 is of the order 1/2. The atomic number of iron is 26, and it is seen that it is necessary to introduce rather large screening constants in order to make the result coincide with experiment; but there is no indication of huge discrepancies, as in the case of Harrison's experiments. The clearing up of this puzzle seems rather to be the task of experimenters. Provisionally we must be content with the meager result that the extrapolation of the result afforded by X-ray experiments on optical absorption appears to indicate too strong an absorption; but even this result may be of some help for stellar theory, as will be apparent from the following discussion.

3. *The stellar absorption coefficient.*—It is easily proved[1] that in the interior of a star the net flux of radiation in the frequency interval ν to $\nu+d\nu$, through unit area, in an outward radial direction is to a high degree of approximation given by the expression

$$F_\nu d\nu=-\frac{c}{3x_\nu\rho}\frac{\partial A_\nu}{\partial r}d\nu\,, \tag{33}$$

where $A_\nu d\nu$ is the energy density of radiation in the frequency interval $d\nu$, ρ the density, and x_ν the mass absorption coefficient of the substance in question. This result rests on the assumption that the medium is at rest—thus excluding convection—the state stationary in time, and that the flux of radiation is very nearly the same for all directions. The net total flux of radiation in an outward direction is

$$F=\int_0^\infty F_\nu d\nu\,, \tag{34}$$

---

[1] Cf. *Monthly Notices, R.A.S.*, 84, 525, 1924.

or, introducing the auxiliary variable x defined by

$$\frac{1}{x}\frac{\partial A}{\partial r}=\int_0^\infty \frac{\partial A_\nu}{\partial r}\frac{d\nu}{x_\nu}, \tag{35}$$

we obtain

$$F=-\frac{c}{3x\rho}\frac{\partial A}{\partial r}, \tag{36}$$

where A is the total energy density of radiation. For the case of the interior of a star the deviations from thermodynamic equilibrium must be exceedingly small, and we may replace A_ν by Planck's formula.

The auxiliary quantity x is the *stellar* absorption coefficient entering Eddington's theory of radiative equilibrium of a star, and it will be the characteristic function of the medium as regards its power of transmitting radiation *en bloc*. From (35) it is seen that x may be regarded as a kind of harmonic mean value of the absorption coefficient x_ν, and because of this fact pronounced selective absorption will be of practically no importance for the total transmission of radiation.

It is not difficult to derive the general expression for x on the basis of the theory of the absorption coefficient as tentatively given above. The result, however, is very complicated, and, as there is no hope of any refined test, we shall limit the consideration to the derivation of an upper limit to x, which will also bring out its general dependence upon temperature and density of the medium. For this purpose we assume the quantum states to be so strongly broadened that the absorption coefficient may be considered as a continuous function of the frequency. This will certainly be the case as soon as we consider the long wave-length region of the spectrum (relative to the wave-length of maximum energy) where the absorption is smallest and the absorption limits in all cases would follow one another so closely as to form an almost continuous sequence. Under these circumstances the absorption coefficient is given by (26). For the transmission of radiation *en bloc* it does not matter much what expression we use for the absorption coefficient in the very long and very short wave-length region, since the absorption there is in any case so large as to cut out the essential contributions to the integral in (35). We may thus drop the exponential factors in expression (26) altogether, proceeding formally as in a *purely classical* theory of absorption. Proceeding in the manner suggested above, we obtain for the stellar absorption coefficient per atom, if we neglect the small scattering of free electrons not in collision,

$$x=\frac{n_e}{T^{\frac{7}{2}}}D\frac{e^6}{c}\frac{h^2G_0}{\sqrt{m^3k^7}}\sum_a\frac{n_a}{n^0}(N-a_a)^2\,;\qquad D=\sqrt{\frac{2}{\pi}}\frac{4\,!\,2^7}{7\,!\,3}\frac{\sum_1^\infty n^{-4}}{\sum_1^\infty (n-1)\left(\frac{2}{n}\right)^7}=0.16\,. \tag{37}$$

Here n_e is given by the approximate formula,

$$n_e=\frac{\rho}{H}\left(\frac{Z_a}{A_a}\right), \tag{38}$$

where H is the mass of a hydrogen atom, and Z_a and A_a are the numbers of positive charges and the atomic weight of any of the atoms present, the ratio being assumed to be the same for all atoms. The final expression of x referred to absorption per unit mass is

$$x=\frac{\rho}{T^{\frac{7}{2}}}\cdot\frac{Z_a}{A_a}\frac{De^6h^2G_0}{c\sqrt{m^3k^7}\sum_a\frac{n_a}{n^0}A_a}\sum_a\frac{n_a}{n^0}(N-a_a)^2\,. \tag{39}$$

This expression shows the same dependence upon temperature, density, and atomic number as the different expressions derived by Eddington, and numerically there will not be much difference either.

It is a little difficult to know exactly to what level in the stellar interior the calculation of the stellar absorption coefficient refers in Eddington's theory of radiative equilibrium, as the value entering into the mass-luminosity relation is some kind of average to be taken over a region where the mean molecular weight of stellar matter can be assumed to be constant. Since, however, the temperature does not vary much within a star on the theory in question, which, moreover, entails the constancy of ρ/T^3, the absorption coefficient will vary very slowly for the part of the star where the mean molecular weight can be considered as constant to any degree of approximation. It would therefore seem justifiable to refer the calculations to the center of the star, where the theory for the case of Capella[1] would give the following values:

$$T=9.56\cdot 10^6\,{}^\circ K.\,; \qquad \rho=0.1474\ gcm^{-3}\ ,$$

the mean molecular weight being assumed to be equal to 2.2. Introducing these values in (39), we obtain

$$x=2.4\,\frac{Z_a}{A_a}\,\frac{\sum_a \frac{n_a}{n^0}\,(N-a_a)^2}{\sum_a \frac{n_a}{n^0}\,A_a}\ cm^2\,g^{-1}\ .$$

The maximum possible value of this expression would be obtained if the star consisted of uranium only,[2] for which case the variable factor above is certainly less than 15; but for smaller atomic numbers it would be correspondingly less. The maximum possible theoretical value of x is thus 37, while the value estimated by Eddington from the mass-luminosity relation was $x=43$. These quantities are of the same order of magnitude. Taking as a sample of stellar matter an element of median atomic number, say iron ($N=26$), the theoretical value of the absorption coefficient would come out as about 10.[3] On the whole, it seems that the theory can conform with the requirements of Eddington's mass-luminosity relation only by assuming the core of a star to consist of elements of very large atomic numbers to a degree which surpasses what might be expected from the distribution of elements in the earth's crust or in meteors.

It seems to the writer that the essential weakness of the theory given above rests with the determination of the constant G_0, which perhaps may be 50 per cent off. Apart from that, effort has been made everywhere to obtain the maximum value of the stellar absorption coefficient, and when the result, in spite of precautions, comes out decidedly lower than that given by theory of radiative equilibrium it seems difficult to blame the former theory. It may therefore be of interest briefly to consider different possibilities of reconciliation between the two differing results, although a final decision will not be attempted.

---

[1] *Monthly Notices, R.A.S.*, **84**, 104, 1924.

[2] Atomic theory seems to afford strong arguments against the possible stability of atoms essentially heavier than the uranium atom, as was pointed out by the writer in a letter to *Nature*, **111**, 357, 1923. Cf., also, N. Bohr. *Annalen der Physik*, **71**, 266, 1923.

[3] On comparing this figure with that given by Eddington's discussion of this problem it must be remembered that we use a partly empirical value of G_0, while Eddington works throughout with Kramers' theory. This latter, however, gives a value of G_0 which is about one-half that used in the text.

One might for a moment think that the fact was to be explained by assuming the core of a star really to consist of very heavy elements, sorted out and concentrated at the center by the star's gravitational field. The fact that rather heavy elements are observed at the stellar surface might seem to argue in favor of this view. The arguments, however, are not conclusive, for in the interior of a star the statistical distribution of electric charges must be such as by necessity to set up an electric field which will repel positive charges, and by the fact that positive charges on an atom under those conditions must be nearly proportional to the atomic mass, the electric repulsion will be such as largely to counteract the increased attraction on heavy atoms.[1] Hydrogen forms an exception and under certain conditions will even possess a tendency to be *repelled* from the stellar core.[2] An estimate would seem to suggest that this inner core of partial mixture would extend say halfway out from the star's center. From the boundary of this core and to the stellar surface conditions are prevalent for which at present we have no detailed theory. If this outer region of a star could be shown to be in stable equilibrium as regards vertical displacements, there might be reason for expecting an appreciable concentration of heavy elements toward the core of the star. If, on the other hand, this layer is in convective equilibrium, there would be less reason for believing in such a conclusion.

Curiously enough, reconciliation would also be brought about by assuming the stars to contain an excessive amount of the *lightest* of all elements, hydrogen, as pointed out by Eddington.[3] This result is due to the fact that the mean molecular weight of ionized hydrogen is only one-half, and the absorption coefficient calculated from the mass luminosity relation would for this case be enormously diminished. There are several facts indicating that hydrogen really is present to an abnormal amount in stellar *atmospheres*,[1] but whether it is permissible to allow a sufficient amount of hydrogen to be imprisoned in the core of the star to bring about agreement with theory must provisionally remain an open question, which the calculations as regards the electrical state of the star would tend to answer in the negative.[2]

---

[1] Cf. *Monthly Notices, R.A.S.*, **84**, 720, 1924.

[2] A closer discussion of this question will be given on a later occasion.

[3] *Monthly Notices, R.A.S.*, **84**, 108, 1924.

We must finally face the possibility that the assumptions on which the theory of radiative equilibrium, in the special form preferred by Eddington, are based, may require revision. The empirical evidence in favor of this theory is mainly afforded by data on the masses and luminosities of the stars, which so far agree remarkably well with the mass-luminosity relation, which is the principal outcome of the theory.[3] Analytically, however, this result cannot be taken as unambiguous confirmation of the special assumptions on which the distribution and density in the interior of the star are based, as there are an infinite number of different possible ways of distributing sources of energy within a star so as to bring about the *same* relation between luminosity and total mass, while the distribution of density and temperature is different for each case. The freedom of choice may, however, be somewhat restricted by requirements of stability, although such considerations will scarcely be sufficient for a unique solution. A reliable theory of the absorption coefficient, on the other hand, will afford a new restriction which may be sufficient to give important information about the localization of the sources of stellar energy. This question, however, will not be discussed in this paper.

MOUNT WILSON OBSERVATORY
February 1925

---

[1] Cf. Compton and Russell, *Nature*, 114, 86, 1924. The suggestion advanced by these authors that the result might be a spurious effect due to metastable properties of the 2_1-state of the hydrogen atom seems to be negatived by (unpublished) calculations of the writer, showing that the maximum concentration generally to be expected will correspond to temperature equilibrium at the effective temperature of the star.

[2] Eddington has recently (*Observatory*, March, 1925, p. 73) shown that rotation of a star must set up convective currents which may be effective in intermixing different elements—at least within the surface region. (Added in proof).

[3] *Monthly Notices, R.A.S.*, 84, 311 (plate), 1924.

Contributions from the Mount Wilson Observatory, No. 297
Reprinted from the *Astrophysical Journal*, Vol. LXII, pp. 168–178, 1925

NOTE ON THE DISTRIBUTION AND NUMBER OF NEBULAE

By FREDERICK H. SEARES

ABSTRACT

Distribution of nebulae.—A discussion of Fath's counts of nebulae on photographs of Selected Areas 1 to 139 (limiting magnitude of stars on the optical axis = 18.6, international photographic scale) shows that non-galactic nebulae make their appearance in both hemispheres at about 20° galactic latitude. They increase rapidly in frequency to 30°, and thereafter more slowly to 70°. The concentration in the region N 70°–N 90° is pronounced; the corresponding region S 70°–S 90° is not covered by the counts. For galactic latitudes 0°–70° the average surface density in the southern hemisphere (longitudes 180°–360° unobserved) is three-fourths that in the northern. The distribution in longitude is complicated, but a band of high frequency apparently crosses the northern hemisphere in longitudes 50°–220°.

Total number of nebulae.—A grouping of the counts in 39 fields for regions $10' \times 10'$ according to distance from the center of the plate shows that at 35′ distance the loss arising from aberrations in the optical system is one-half. To reduce Fath's counts to limiting photographic magnitude 18.6 for stars at the center they must be multiplied by 1.94. The revised total number of nebulae to this limit is 210,000 for N 70°–S 70°, and about 300,000 for the whole sky.

In collecting data on the distribution of stars and nebulae I have recently had occasion to examine Fath's list of nebulae[1] compiled from photographs of the 139 Selected Areas between declinations +90° and −15°. These photographs, forming part of the observational material for the *Mount Wilson Catalogue of Magnitudes*, are on Lumière Sigma plates, exposed one hour, the limiting magnitude ranging from about 18 to 19 on the international photographic scale. The low limit of brightness and the representative character of the Selected Areas as sample regions of the sky are features of special importance for any discussion of nebular distribution. A disadvantage, on the other hand, lies in the fact that three-eighths of the sky are wholly unobserved. For the northern galactic hemisphere the defect is not serious, but in the southern hemisphere the highest latitude observed is 76°, and, practically speaking, no plates are available for any latitude between longitudes 180° and 360°. Further, the Selected Areas are rather too widely spaced for a satisfactory determination of the effect of local irregularities in distribution;

---

[1] *Astronomical Journal*, **28**, 75, 1914.

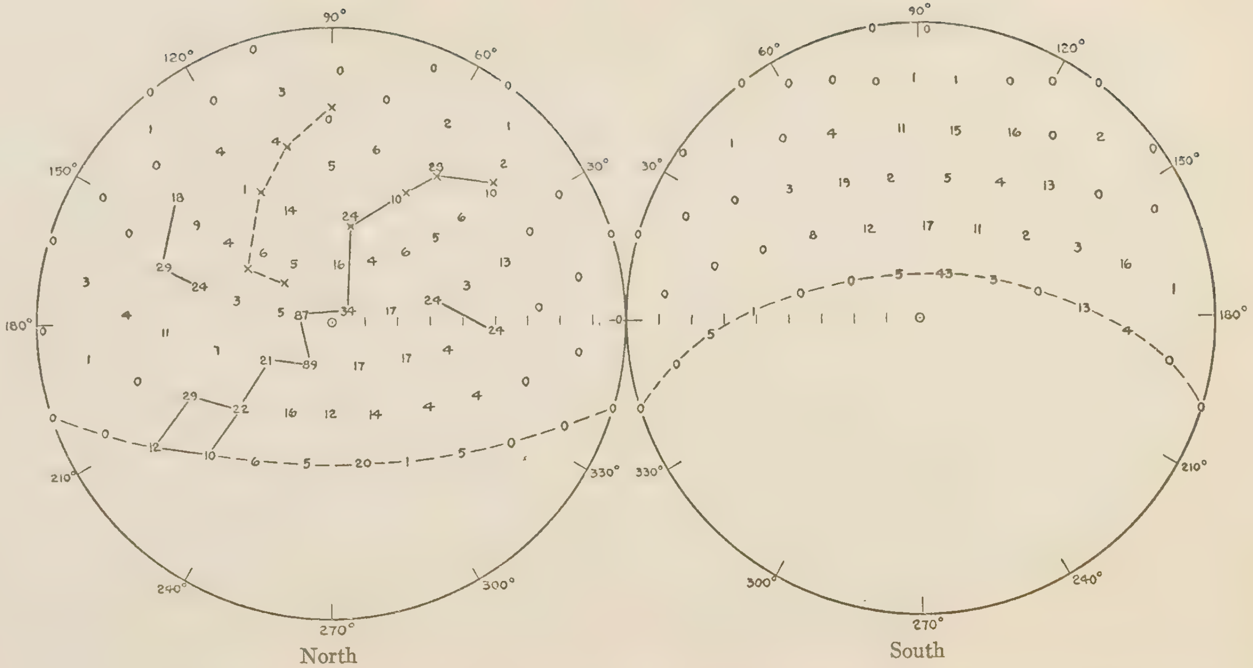

FIG. 1.—Distribution of nebulae according to Fath's counts in Selected Areas 1 to 139. The marginal numbers are galactic longitudes, the poles being at the centers of the circles.

but, in spite of these limitations, the data merit special attention because of their freedom from any selection favoring regions in which nebulae were known to exist. Sanford[1] has already discussed Fath's counts in detail from several points of view, but for the present purpose a somewhat different grouping of the material is desirable.

The numbers of nebulae counted by Fath in the 139 Selected Areas were obtained from the diagram accompanying his paper.[2] When replotted according to galactic co-ordinates[3] the distribution is that shown in Figure 1.

To illustrate the effect of local irregularities upon the mean distribution, the numbers were arranged in order of galactic latitude and divided into two series with alternate regions in each. The sums and mean latitudes for groups of five successive areas in each series are given in the first four columns of Table I and are shown graphically in Figure 2. The curves, which represent two determinations of the distribution from entirely different material, are similar, but the influence of local irregularities is obviously considerable, and a final discussion will require counts in several hundred fields. The south galactic hemisphere, and the region N 70°–N 90° in which the fluctuations in numbers are large (see Fig. 1), demand special attention.

Treated as a single series, the 139 regions in groups of five give the results in the fifth and sixth and eighth and ninth columns of Table I. These are illustrated in Figure 3, in which the curves for northern and southern galactic latitudes are shown side by side. The seventh and the last columns of the table give the average limiting photographic magnitudes to which star-counts in fields 23′ in diameter on the same series of photographs are complete.[4] Since the variation in the limit, which ranges from 17.8 to 18.6, is not closely correlated with the irregularities of the curves in Figure 3, the mean distribution cannot be seriously influenced by the lack of constancy in the limit.

---

[1] *Lick Observatory Bulletins*, **9**, 80, 1917.

[2] *Loc. cit.* The total thus found is 1032 and is that used here, although Fath's tables give a total of 1031. The difference is unimportant and is mentioned only in explanation of its origin.

[3] Taken from *Harvard Annals*, **101**, Table II, 1918; **102**, Table I, 1923.

[4] Unpublished data from the *Mount Wilson Catalogue of Selected Areas.*

Owing to the comparative rarity of diffuse nebulae and planetaries, Fath's list is practically one of non-galactic nebulae, with the small elliptical nebulae greatly predominating over the spirals. Figure 3 shows that the non-galactic nebulae appear at about lati-

TABLE I

DISTRIBUTION OF NEBULAE IN GALACTIC LATITUDE
(Observed numbers for areas of 9.4 sq. deg.)

SERIES I		SERIES II		ADOPTED GROUPING					
Lat.	No.	Lat.	No.	Lat.	No.	Mag.	Lat.	No.	Mag.
+75°...	149	+72°	146	+78°	232	18.3	+12°	0	18.4
60....	69	59	60	69	63	17.9	+ 6	2	18.2
50....	53	49	42	62	54	18.3	0	0*	18.1
42....	60	41	45	58	75	17.9	0	0	18.2
34....	99	33	25	52	48	17.9	− 6	0	18.3
26....	26	26	4	48	47	17.8	12	4	18.4
17....	8	16	3	43	33	17.8	14	1	17.8
+ 9....	1	+ 8	1	40	72	18.4	20	1	18.3
0....	0	0	0*	36	69	18.3	25	25	18.0
− 9....	1	− 9	3	31	55	17.8	31	59	18.6
16....	1	18	1	28	18	18.1	38	20	18.3
27....	24	29	60	24	12	18.0	45	32	18.2
40....	28	43	24	19	7	17.9	54	31	17.9
−60....	66	−63	33	+14	4	17.9	−69	68	18.4

* Four areas. All other groups include five each.

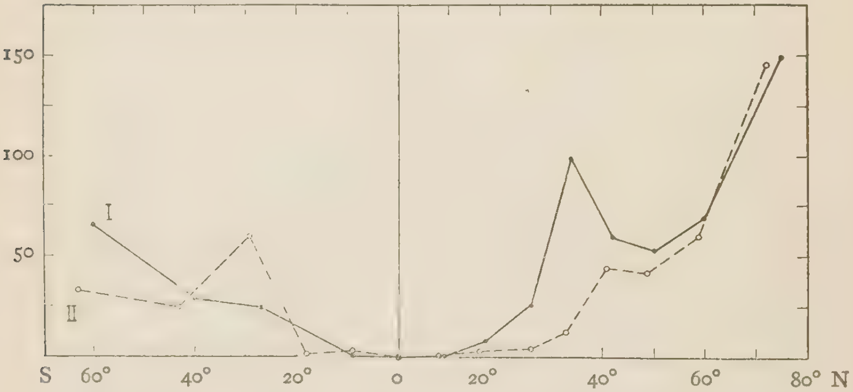

FIG. 2.—Distribution of nebulae in galactic latitude. Curves I and II represent results derived from alternate regions in the sequence of 139 Selected Areas arranged according to galactic latitude. They illustrate the influence of irregularities in distribution.

tude 20° and rapidly increase in frequency to 30°. From 30° to 70° the increase is slow, but the concentration near the north galactic pole at least is pronounced. The systematic difference between the northern and southern hemispheres seems to be real.[1]

To gain some notion of the distribution in galactic longitude, the fifty-four regions between 20° and 68° north latitude were divided into four zones: 20°–29°, 30°–39°, 40°–49°, 50°–68°. Plots of numbers of nebulae against longitude for these zones are shown in Figure 4. The series of maxima marked *A* and *B* suggest something more than local irregularities of distribution; but since Figure 1 indicates a minimum for the second curve at about 180°, the maxima *C* are perhaps of more significance than *B*. The distribution of rich fields as shown in Figure 1 seems to justify the assumption, for the most striking feature appears to be a band of high frequency crossing the northern hemisphere near the pole, in longitudes 50°–220°. The minimum starting in low latitudes at longitude 90° is clearly marked and penetrates almost to the pole itself. Figure 1 bears no close relation

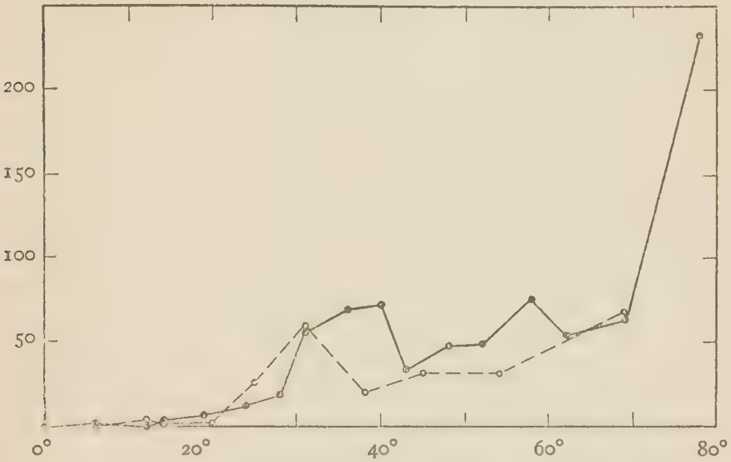

FIG. 3.—Distribution according to galactic latitude of nebulae in Selected Areas 1 to 139. Full line, northern hemisphere; dotted, southern hemisphere. Ordinates are numbers counted in areas of 9.4 sq. deg.

---

[1] In this connection see Reynolds' diagrams, *Monthly Notices, R.A.S.*, **81**, 129, 1920; **83**, 147, 1923; **84**, 76, 1923.

to the diagrams of Reynolds,[1] but it must be remembered that the great majority of the nebulae in Fath's list are much smaller than those discussed by Reynolds, nearly all of them having diameters under 30″. Apparently we have here a further illustration of what is shown by Reynolds' data, namely, that the distribution in longitude varies with the size of the nebulae.

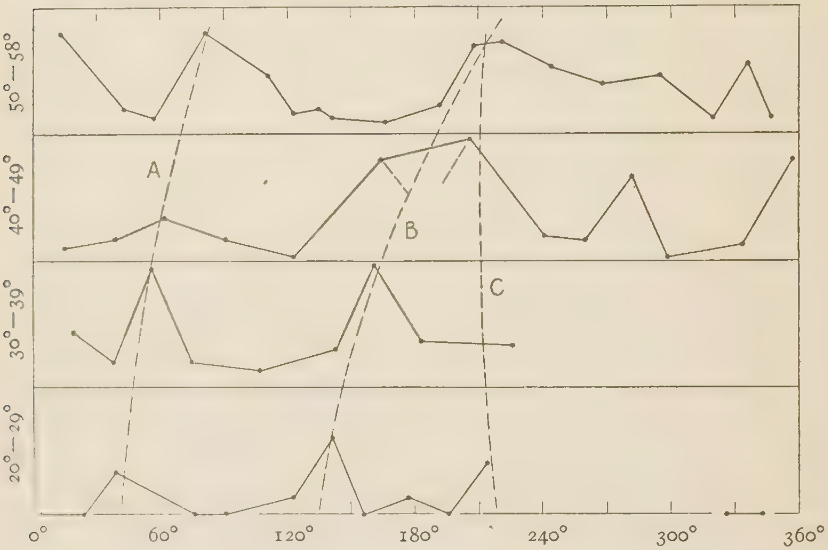

FIG. 4.—Distribution of nebulae in north galactic hemisphere according to galactic longitude (abscissae). Four curves for the latitude intervals noted in the margin. *A*, *B*, *C* are more-or-less hypothetical lines of maximum frequency. *A* and *C* correspond to the maximum in longitudes 50°–220° shown in Fig. 1.

There remains still the question of the total number of nebulae in the sky, concerning which there has been much difference of opinion. Fath's estimate of 162,000[2] differs widely from Perrine's earlier result of 500,000,[3] and still more widely from Curtis' 722,000.[4] Perrine,[5] allowing for a selection of fields favoring rich regions, subsequently reduced his estimate to 400,000; but Curtis' estimate, which like that of Perrine is based on photographs taken with the Crossley reflector, still stands. The limiting magnitude of the Crossley photographs is undetermined, but it has usually been assumed that it is nearly the same as that of the Mount Wilson plates. In fact, the circumstances of plates, telescopes, and exposure times, supplemented by direct comparisons, seem to warrant the assumption of direct comparability. To account for the discrepancy, Fath suggested that the regions photographed with the Crossley reflector are not representative. Perrine and Curtis, on the other hand, have insisted that Fath's total is too small because of losses arising from aberrations in the relatively large field used by him (about 72′×95′).

---

[1] *Loc. cit.*

[2] *Loc. cit.*

[3] *Lick Observatory Bulletins*, **3**, 47, 1904.

[4] *Publications Lick Observatory*, **13**, 15, 1918.

[5] *Astronomical Journal*, **29**, 79, 1916.

The limiting magnitude of the Mount Wilson photographs is now known. The mean for star-counts which are complete, from the data in Table I, is 18.1, photographic scale, while the mean for the faintest stars recorded, that is, the actual limiting magnitude at the center of the plate, is about 18.6. The question of aberration losses can be settled from the data themselves, and since, as far as they go, there can be no question as to the representative character of the Selected Areas, an estimate of the total number of nebulae to a specified limit of brightness, correct within a moderate percentage, should now be possible.

The first step in arriving at such an estimate is the determination of a factor for the correction of Fath's numbers for aberration losses, which do seriously affect his total. This factor has been based on counts in unit areas 10′×10′ in each of the regions showing a total of ten or more nebulae (thirty-nine Selected Areas in all). The counts, which were made by Miss Joyner from Fath's list, were in all cases between 10′ values of the declination. As a matter of convenience it was assumed that the optical axis was always located either on the edge or at the middle of a 10′ zone, the choice in any given case being determined by the declination of the central star of the area, on which the plate was centered. This choice also fixed automatically the limits in right ascension, which were so placed that the adopted center coincided either with the corner or with the center of a 10′×10′ area. In the former case the total area counted was 60′×60′; for the latter it was 70′×70′. This selection of unit areas simplified the counting, and since the average displacement of the adopted center from the true optical center is less than 2′, the precision is ample.

The results were divided into six groups (fields 60′×60′, groups I–III; 70′×70′, groups IV–VI), each group including several Selected Areas and a total of about one hundred counted nebulae. The counts within each group were summed for corresponding 10′×10′ areas, thus giving a frequency diagram showing the variation in the number of nebulae with increasing distance from the adopted center.

TABLE II

CORRECTION FACTOR FOR FATH'S COUNTS OF NEBULAE

DIST.	60′×60′, STANDARD TOTAL=100					DIST.	70′×70′, STANDARD TOTAL=123				
	I	II	III	Mean	Wt.		IV	V	VI	Mean	Wt.
7′	3.7	5.2	3.8	4.2	4	0′	4.1	5.8	1.4	3.8	1
16	2.8	2.5	3.1	2.8	8	10	4.1	2.3	4.1	3.5	4
21	2.8	3.6	4.5	3.6	4	14	3.2	2.3	3.0	2.8	4
25	2.2	2.4	2.7	2.4	8	20	2.6	5.5	3.3	3.8	4
29	2.7	2.4	1.9	2.3	8	22	3.7	3.3	1.4	2.8	8
35	3.2	1.4	1.4	2.0	4	28	2.5	2.1	3.0	2.5	4
						30	3.4	2.1	2.0	2.5	4
						32	1.1	2.1	3.0	2.1	8
						36	1.2	2.1	2.8	2.0	8
						42	1.7	0.6	0.6	1.0	4
No. S.A.	5	7	11	23	.....	....	2	6	8	16	.....
No. Fath.	150	143	140	442	.....	....	176	124	106	406	.....
No. counted.	108	105	106	319	.....	....	152	107	92	351	.....
Corr. no.	293	285	287	.....	.....	....	336	236	203	.....	.....
Corr./Fath.	1.84	1.99	2.05	.....	.....	....	1.91	1.91	1.92	.....	.....

The average densities (numbers of nebulae per 10′×10′ area) found from these diagrams for each group, reduced to standard totals for the whole area counted to make them directly comparable, are given in Table II under the headings I–VI. The standard totals used are 100 and 123; the latter, referring to regions 70′×70′, was determined by the condition that the total for the central 60′×60′ region in an area 70′×70′ should be 100. The weights in the sixth and last columns of Table II are the numbers of unit areas per field upon which the different densities are based.

All the groups show a decrease in density with increasing distance. The means for groups I–III and IV–VI, plotted in Figure 5 as points and crosses, respectively, agree well and show that the influence of irregularities and clustering have been rather thoroughly eliminated. The loss in density with increasing distance is so large that at 35′ from the center the number of nebulae recorded is only one-half that at the center.

The central density, which may be taken as 4.0, determines the true number of nebulae per square degree corresponding to an observed total of 100. The result is 4.0×36 = 144, or 271 for 1.88 square degrees, which is the field of the original photographs. The numbers of nebulae counted by Fath are given in the fourth line from the last of Table II, while the numbers counted for the present discussion are in the next line. The corrected number per 1.88 square degrees in any given case is

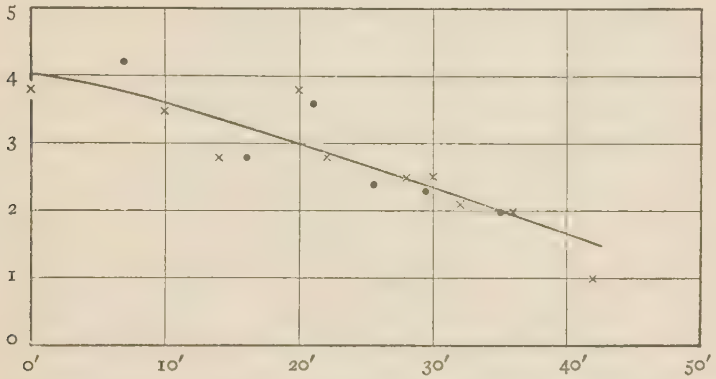

FIG. 5.—Decrease in number of nebulae counted (ordinates) with increasing distance from center of plate (abscissae). Points and crosses are mean results for groups I–III and IV–VI, respectively, including 670 nebulae in 39 Selected Areas photographed with the 60-inch reflector. Ordinates refer to a unit area of 10′×10′ and have been reduced to a standard counted total of 100 in a field 60′×60′ centered on the optical axis.

$$\text{Corr. No.} = 271 \times \text{No. Counted/Standard No.}$$

The reduction factor for Fath's counts is therefore the ratio Corr. No./Fath's No.

The close accordance of the results in the last line of Table II shows that the various groups are mutually consistent and little affected by irregularities in the distribution. The adopted mean factor is 1.94. The principal source of uncertainty affecting this result is in the density adopted for the center of the field, namely, 4.0. An inspection of Figure 5 indicates that this may be in error by as much as 5 or 10 per cent, the error being carried over into the correction factor practically unchanged, and hence also into the estimate of the total number of nebulae in the sky.

TABLE III

Mean Distribution in Galactic Latitude and Total Number of Nebulae to Phot. Mag. 18.6

Latitude	Uncorrected No. 9.4 Sq. Deg.		Corrected No. 1 Sq. Deg.		Area of Zone	Totals in Thousands	
	N.	S.	N.	S.	Sq. Deg.	N.	S.
0°–10°	1	0	0.2	0.0	3580	0.7	0.0
10–20	4	2	0.8	0.4	3474	2.8	1.4
20–30	12	26	2.5	5.4	3259	8.1	17.6
30–40	64	40	13.2	8.2	2945	38.8	24.2
40–50	50	28	10.3	5.8	2541	26.2	14.7
50–60	59	34	12.2	7.0	2063	25.2	14.4
60–70	59	58	12.2	11.9	1520	18.5	18.1
70–80	150	....	31	....	930	28.8	(21.6)
80–90	(330)	....	(68)	....	314	(21.4)	(16.0)
Totals 0°–70°						120.3	90.4
Totals 70–90						(50.2)	(37.6)
Totals 0–90						170.5	128.0

Total N 70° to S 70°, 210,000; whole sky, 300,000.

This estimate can now be made with the aid of the data in the sixth and ninth columns of Table I, which lead to the averages for 10° zones of galactic latitude given in the second and third columns of Table III. The area to which these numbers refer is $5\times1.88=9.4$ square degrees. The numbers of nebulae per square degree, corrected for aberration losses, are found by multiplying by $1.94/9.4=0.206$. The results in the fourth and fifth columns of Table III are the final values for the distribution in galactic latitude. To 70° in the northern hemisphere no great change is to be expected as a result of future counts. The values for the region about the north galactic pole, 70°–90°, are uncertain, and all the densities for the southern hemisphere are subject to considerable revision because of the unsymmetrical distribution of the photographs.

The summation for the different zones given in the last two columns of Table III indicates that the mean density for southern latitudes is about three-fourths that for northern latitudes. The numbers adopted for the region S 70°–S 90° are assigned on the basis of the rather risky assumption that this ratio holds for all latitudes. Unless the unobserved part of the southern hemisphere is quite different from the observed portion in its number of nebulae, a round total of 210,000 from N 70° to S 70° should not be seriously in error. The estimate of 300,000 for the whole sky is much less reliable; but with all reasonable allowance for deficiencies and uncertainties, this result cannot be directly reconciled with the much larger estimate of Curtis. Either the limiting magnitudes of the two series of photographs have not the equality hitherto supposed, or else the observed regions which are the basis of the larger estimate are not representative of the sky as a whole.

Mount Wilson Observatory
June 1925

Contributions from the Mount Wilson Observatory, No. 298
Reprinted from the *Astrophysical Journal*, Vol. LXII, pp. 238–264, 1925

SPECTROSCOPIC PHENOMENA OF THE HIGH-CURRENT ARC

By ARTHUR S. KING

ABSTRACT

The high-current arc.—The direct-current arc carrying 1000 amperes or more at about 100 volts, usually between rods of small diameter, gave a source of great brilliancy and somewhat explosive character, producing mainly the spectrum of the neutral atom under conditions of high excitation.

Elements studied.—The spectra studied were those of *iron* from λ 2800 to λ 8400, and selected regions of *titanium*, *magnesium*, *calcium*, *copper*, and *aluminum*. Certain lines of *sodium*, *gallium*, *oxygen*, and *nitrogen* are also described.

Spectral characteristics of high-current arc.—The distinctive features are an intensification of the high-temperature lines, and a strong development of widening phenomena, with dissymmetries toward red or violet which often result in distinct shifts of the emission lines. *Reversals* are numerous, becoming less frequent with increasing wave-length, but extending into the infra-red of the iron spectrum. *Band spectra* are absent in emission but may appear in absorption. A *continuous spectrum* appears in the ultra-violet, resembling that of the condensed spark and of exploded wires. The high temperature and explosive action of the arc produced finely divided residues of iron and iron oxide which were examined microscopically.

Widening phenomena in the iron spectrum.—The degrees of widening, usually unsymmetrical, are given for 920 iron lines from λ 4250 to λ 8400. This material permits a selection of lines which remain stable in the ordinary arc and are suitable for wave-length standards. As the members of a multiplet show similar widening in the high-current arc, the selection of series groups is facilitated. *Energy level* is indicated by the degree of dissymmetry, lines of low level being nearly symmetrical, while the lines of multiplets starting from successively higher levels show increasing susceptibility to unsymmetrical widening. The type of widening shows a close relation to the temperature classification, and for the high-temperature lines the results supplement those of electric-furnace investigations.

Phenomena for other elements.—The other spectra studied showed effects similar to those of the iron spectrum. Exceptional intensity for an enhanced line was noted in the case of λ 4481 of *magnesium*. High-temperature arc lines of *magnesium* and *copper* showed very large red displacements. The D lines of *sodium* and other lines given by minimum excitation showed distinct red dissymmetry. The *oxygen* triplet λ 7772–λ 7776 and four *nitrogen* lines in the infra-red appear in the arc between iron electrodes.

Comparison of high-current arc with other sources.—A comparison of the tendency to displacement of iron lines in the high-current arc with that observed in the *pressure arc*, polar region of the *ordinary arc*, *tube arc*, *disruptive spark*, and *exploded wires* showed similar effects as to direction and relative magnitude in all of these sources.

It is generally recognized that each of our laboratory light-sources is especially adapted to the production of a certain type of spectral line, and that in a given spectrum the response of various groups of lines to different degrees of excitation, beginning with several temperature stages of the electric furnace, can be traced through various forms of arcs and sparks, up to the most disruptive spark discharges. In the lower excitations, the spectrum of the neutral atom naturally predominates, the lines belonging to higher energy levels gradually developing, but in many metallic spectra the ionized atom begins to emit at the higher furnace temperatures, and the enhanced lines increase in strength as we pass through the scale of excitations until in the more powerful sparks the lines of the neutral atom have almost disappeared.

This paper records some observations of the spectrum of the metallic arc carrying a very large current, perhaps the most effective source thus far devised for developing the lines of the neutral atom and for showing their peculiarities of structure.

When the current of an arc that is normally operated for steady burning at about 5 amperes is increased to 20 or 30 amperes, no decided change in the spectrum results other than a general intensification and an increase in the number of reversed lines. The arc spreads over a larger area on each electrode, and there is little alteration in the character of the discharge. But if the current is increased to the order of 1000 amperes, there is no longer room on the small terminals for a normal spreading of the discharge. The electrodes are rapidly consumed, but as the arc must pass between the small areas at their ends, the current density is greatly increased and some features of the discharge, which in the low-current arc have little effect, are greatly intensified. It was with the object of observing the spectral changes brought about by such unusual arc conditions that the following experiments were carried out.

EXPERIMENTAL METHOD

Electrical power to the desired amount was available from a 500-kw direct-current generator, with voltage regulation up to 150 volts. The current leads are the same as are regularly used, with the lower voltages of the dynamo, for the electric furnace, and the connection is made with the arc holders without introduction of any extra resistance. The arc terminals are held horizontally in clamps similar to those of the tube furnace.[1] These are water-cooled bronze blocks, with graphite bushings fitting around the electrodes. The bronze pieces slide on their supporting frame, the final connection to the dynamo leads being of flexible, water-cooled copper tubing.

---

[1] *Mt. Wilson Contr.*, No. 247; *Astrophysical Journal*, **56**, 318, 1922.

The most suitable form of arc electrode for the metal in use, and also the most effective voltage, must be found by experiment. Most of the work thus far has been with iron terminals consisting of rods 4 mm in diameter inserted in the ends of 19-mm graphite rods and projecting initially about 5 cm beyond the graphite. These were used for a succession of the explosive arcs until they melted back to the graphite. Rods of magnesium, aluminum, copper, and calcium have been used in the same way. If the material is pulverized or will not make good electrical contact with the graphite, it may be held in small tubes of copper or other metal, which are inserted in the graphite rods. This method was used with powdered titanium.

The arc terminals are adjusted with the ends of the rods or tubes just touching, and the dynamo circuit is then closed. The arc is a blinding flash, and molten metal, much of it in very small droplets, is widely scattered. With a potential of 100 volts, the throw of the ammeter is usually to 1000 or 1100 amperes, but the full value of the current is evidently not recorded on account of the brief duration of the arc. It is hoped later to make detailed observations on the character of the discharge, but it is clearly a true arc and not a fusion of the rods by an overload of current, as the terminals shorten until a fairly definite gap is left, depending on the voltage, about 3 cm with 100 volts, and the arc breaks, leaving the remaining portions of the rods intact.

Iron rods having diameters larger and smaller than 4 mm have been tried with less satisfactory results. Apparently, for terminals of any given material, a size must be used that will confine the arc to a small area at the ends and still enable the rod to carry the current for the short time required, permitting the arc to pass without melting down the rods as a whole.

Carbons 19 mm in diameter loaded with the material to be vaporized were tried with several metals. The arc is started by sliding the clamps to bring the carbons into contact, and a steady-burning, though greatly overloaded, arc can be maintained for some time by pushing the carbons together as they burn away. The carbons quickly become white hot up to the clamps. The spectroscopic features of the arc when thus controlled will be described later. The explosive character is diminished, and strong vaporization of the carbon takes place. It is feasible to interrupt and re-ignite this arc by directing an air blast intermittently at the gap. The strong ionization between the terminals causes the arc to spring again when the blast is turned off.

The residues from the arc when made to discharge between 4-mm iron rods gave evidence of the high temperature prevailing through a large mass of the material. In addition to the large amount of iron turned into vapor, much more was just below the vapor state. As the arc with 100 volts normally burned to a gap of at least 32 mm before breaking, about 0.4 cc of iron was melted in the time occupied by the brief flash. The high temperature prevailing gave extreme fluidity to the portion of the iron not actually vaporized. Droplets, about 0.5 mm in diameter, caught on bits of glass, after a flight through some 2 m of air, retained sufficient heat to sink into the glass. Still more striking was the large amount of highly tenuous oxide. After the flash of the arc, a large volume of yellow smoke arose, and when this was dissipated, hundreds of filaments of iron oxide were seen floating in the air. These were usually several centimeters long, and were apparently formed in the wake of flying globules, the residue of which often remained as a black droplet at the end of the mass. My brother, L. M. King, made a microscopic examination which showed the highly divided state of the iron resulting from the high temperature and the explosive action of the arc. Magnifying powers up to 1000 diameters revealed a very beautiful structure consisting of fine yellow strands of oxide. These strands, of surprisingly uniform thickness, were more or less meshed together, and at intervals along them could be seen very tiny globules of iron, still in the black state. Micrometer measurements, under a power of 500 diameters, gave the size of the droplets and the thickness of the yellow strands. For a specimen whose total length was 2.3 mm, the droplet at the head measured 0.09 mm; the black globules along the strands were all close to 0.0018 mm diameter, while the strands themselves were only 0.0008 mm thick. The production, in a fraction of a second, of large quantities of such firmly divided matter, in addition to the larger drops of liquid iron expelled from the arc, gives some idea of the difference between this source and the quietly burning arc carrying a current of a few amperes.

PHOTOGRAPHY OF THE SPECTRUM

The spectrograms for the most part were made with the 15-ft. concave grating spectrograph, the second order, with a scale of 1.86 A per millimeter, being used for wave-lengths shorter than λ5500, while the bright first order was employed for the red end of the spectrum.

As far as the brightness of the spectra and the sensitiveness of the plates permitted, spectrograms were made with a single flash of the arc. For the first order of the grating, a single flash gave fully exposed spectra as far as λ5800, and two flashes to λ6700. The much weaker second order required ten flashes in the green, while for the infra-red of the first order, photographed on dicyanin-bathed plates, as many as twenty-three flashes were made. The terminals were usually so arranged that the light near the negative pole, as it burned backward, fell on the slit, as this radiation was found to have the maximum effect in bringing out peculiarities of the line structure.

SPECTROSCOPIC FEATURES

The high-current arc gives, in the main, the spectrum of the neutral atom, and is characterized by three distinctive features in which it supplements the spectroscopic sources regularly in use. These are, first, an intensification of the high-temperature lines; second, an absence of the band spectrum of the metal or compound, except as it may appear in absorption if a favorable background is present; third, the development in very high degree of any peculiarities of widening, especially dissymmetry toward red or violet, to which the individual lines are subject. The manner in which these effects result from the observed characteristics of the arc may now be considered.

High-temperature lines.—The physical phenomena involved in the action of the high-current arc, consisting of rapid melting of the electrodes, extreme fluidity of the molten matter, the production of a large volume of vapor, and the intense brightness of the radiation, are indications of the way in which the 100 kw or more of electrical energy are being used up. Evidently we have between the poles a considerable volume of dense vapor, subject to excitation conditions which in the ordinary arc are transient, if present at all. The low-current arc between metallic electrodes or loaded carbons is maintained in a steady state by a moderate vaporization from small areas on the electrodes; but there are moments of unusual activity during which intensely heated vapor is ejected from the poles, giving, especially in the core of the arc, a strong luminosity in which the high-temperature or "core" lines are prominent. The spectrum indicates that these conditions, transient in the ordinary arc, are the prevailing state of the high-current arc. The radiation from this central mass of vapor dominates the spectrum, and gives it the appearance of being made up of high-temperature lines. The low-temperature lines, being emitted largely by the envelope of cooler vapor, are relatively inconspicuous. The lines of Class I, the most prominent lines of the furnace spectrum, are notably narrow and weak in the high-current arc, as though practically absent from the hot central portion. Class II lines, which are the strongest group in the ordinary arc, are evidently emitted as wide lines by the central portion, but undergo very wide self-reversal, owing to their persistence in the cooler envelope. It is the strong emission of lines of Classes III, IV, and V that especially distinguishes the high-current arc. Their intensity indicates that in the scale of excitation this source is fully active at the stage where the furnace is weak and the low-current arc only moderately effective.

Band spectra.—The absence of the bands from spectrograms of the high-current arc is probably due to the short exposures required for the line spectrum emitted by the central vapor, and is a further step in the process which gives relative weakness to the low-temperature lines. With iron arc electrodes there is no question that large quantities of oxide are formed, but the envelope in which the combination takes place is apparently forced out some distance by the explosive action of the arc, and, as a result, is of relatively low density. The time required to photograph the line spectrum of the inner vapor is thus too short for the band emission to be registered. That a band spectrum is present was shown clearly in the aluminum spectrum by the band structure appearing in absorption on a background formed by broad, enhanced lines of the metal. To study the band spectrum in emission would require relatively long exposures of the arc envelope away from the region of intense line emission. The absence of bands permits an undisturbed study of the line spectrum, which, in regions such as the orange and red of iron and titanium, is highly advantageous.

Line dissymmetry.—In view of the very extensive data which have been accumulated in several lines of investigation, it seems necessary to admit that actual displacements of lines of certain types are produced in several sources of high excitation. In the ordinary arc, the unsymmetrical widening of some lines, usually toward the red, is a very familiar phenomenon; but spectroscopists have concerned themselves chiefly with the possible effect of this broadening upon wave-length measures, and the normal position of a line is established for conditions of the source in which the dissymmetry is a minimum. But when under certain conditions a line wings out strongly, say to the red, with nothing corresponding on the violet side of the normal position, it is evident that a certain proportion of the radiation is tending toward the production of a line displaced to the red. If in any source this proportion is increased, so that the radiation in question becomes dominant, the result is a line whose maximum is shifted to the red of the normal position. This happens in the high-current arc, in very different degrees for different types of lines, but so generally that lines which attain any considerable strength and show no tendency to displacement are rare. While this arc, partly because it produces high-temperature lines with great intensity, shows the displacing action more generally and with greater distinctness than any other source which has been used for spectroscopic work, other forms of electrical discharge give effects which are qualitatively similar. These will be discussed in connection with the data for the iron spectrum.

The results of a preliminary survey of high-current arc effects for several elements will now be presented. Spectrograms over an extended region were made only for iron. The effect upon individual lines will be given for part of the region, not only for direct application to problems concerning the iron spectrum, but as an example of what we may expect for the spectra of the high-current arc in general.

IRON

Continuous spectrum.—The high-current arc with iron terminals gave a continuous ground of considerable strength, beginning about λ 4300 and extending into the ultra-violet. This is noteworthy as being similar to that given by certain high-potential discharges. The spark spectra of several metals are known to show strong continuous radiation in the ultra-violet, and it is a feature especially noted by Anderson[1] and by Smith[2] in their studies of wire explosions, when these were confined in a wooden block.

Ultra-violet spectrum.—In the ultra-violet, at least as far as λ 2800, it is evident that the low-temperature iron lines, selected on the basis of the writer's investigation of the furnace spectrum,[3] are produced chiefly in an envelope outside of the region of intense excitation between the poles. They appear as absorption lines on the continuous ground noted above, with little evidence of emission wings. The continuous spectrum can be weakened by using plates of greater contrast, and then these lines are seen to have wings much narrower in proportion to the width of the reversal than those of lines of the same temperature classes in the visible spectrum. Interspersed among the low-temperature absorption lines are the higher-temperature lines in various stages of sharpness and narrow reversal, the latter usually unsymmetrical; but the outstanding emission lines in this region are the enhanced lines. These can be selected at a glance, being strong and yet not reversed. It is known that the enhanced lines of iron in the ultra-violet are relatively easy of production in the ordinary arc. The emission in the interior of the high-current arc consists mainly of these and of the high-temperature arc lines.

Visible spectrum.—The continuous spectrum holds out to about λ 4300 with sufficient strength to be disturbing when the discharge near the negative electrode is favored, and as the dissymmetry of

---

[1] *Mt. Wilson Contr.*, No. 178; *Astrophysical Journal*, **51**, 37, 1920.

[2] *Mt. Wilson Contr.*, No. 285; *Astrophysical Journal*, **61**, 186, 1925.

[3] *Mt. Wilson Contr.*, No. 247; *Astrophysical Journal*, **56**, 318, 1922.

PLATE VIII

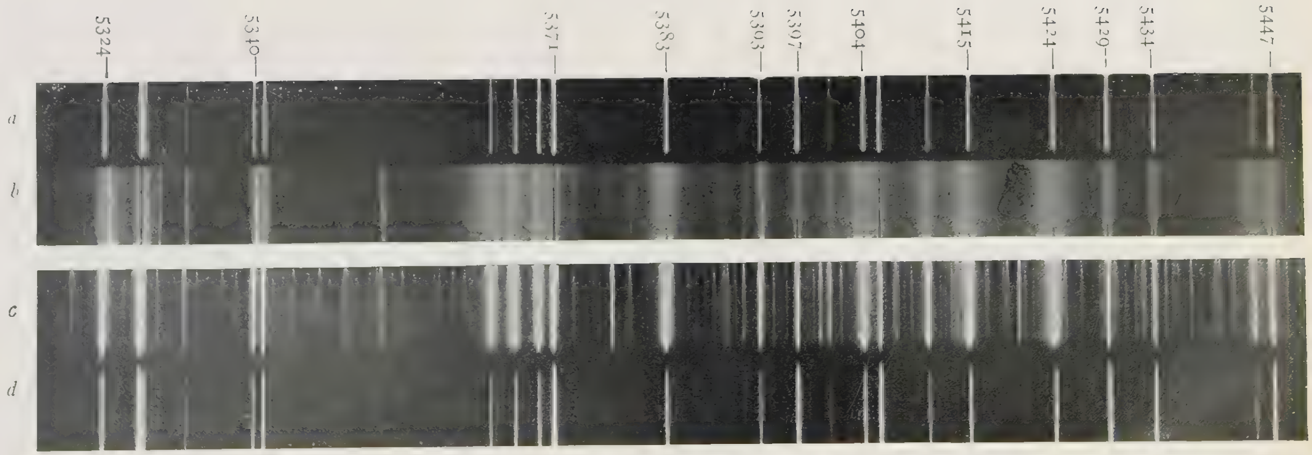

ARC SPECTRUM OF IRON

a, *d*, low-current arc
b, high-current arc
c, high-current arc, iron-carbon, large electrodes

line structure is most marked in this portion of the arc, Table I, with its description of individual lines, begins at λ 4250. From this limit into the infra-red, we have well-defined lines, and no bands; and the absorption of the cooler vapor results in self-reversal, throughout the visible spectrum, of a large proportion of the lines. The reversals, however, decrease in breadth, taking up normally but a fraction of the total width of the emission line. This lessened effectiveness of the cooler envelope corresponds with the relative scarcity of low-temperature furnace lines at the red end of the iron spectrum. In the infra-red, practically the entire radiation of the arc appears to come from the region of highest excitation.

The enhanced lines of the visible region, which can be obtained at the poles of the ordinary arc, are present in the high-current arc, but show only moderate intensity. The distinguishing feature is a very rich spectrum of the neutral atom, with an intensification of high-temperature lines which are weak in other sources.

Reversals.—In the ordinary arc, with currents below 10 amperes, seven lines to the red of λ 4250 may be expected to reverse. When higher currents within the range of the usual arc apparatus are used, the reversals increase in number and the stronger low-temperature lines up to λ 5500 may be obtained in reversal. In contrast with this condition, the high-current arc gives 176 reversals beyond λ 4250, or about one line in five. While the reversals become less common with increasing wave-length, they are frequent as far as λ 6678, and even λ 7511 was reversed. High-temperature lines, including some of those most difficult of production in the furnace, undergo reversal, if fairly strong and not extremely diffuse. Examples are the Class V lines in the green-yellow consisting of λλ 5383, 5404, 5415, 5424, and similar neighboring lines. These have a considerable degree of diffuseness, with widening toward the violet, but are clearly reversed in the high-current arc (see Plate VIII).

Intensification of high-temperature lines without notable widening.—Plate VIII also shows a phenomenon observed in the earlier work when the arc was formed between iron and carbon rods 19 mm in diameter, the former being used as a positive terminal. This arc would burn steadily for some seconds and was not nearly so bright as the explosive arc between small iron rods. The lower concentration of energy prevented any pronounced widening of the lines; at the same time the arc retained the power to give great intensity to the high-temperature lines. Comparison of its spectrum, Plate VIII*c*, with that of the ordinary iron arc in Plate VIII shows that the low-temperature lines are of equal strength in the two sources, while the high-temperature lines are strengthened in the high-current arc about in proportion to their temperature class, lines of Class V being the strongest in the region illustrated.

Widening phenomena.—Table I contains 920 lines, having widening characteristics as follows:

Unsymmetrically widened toward red	397
Unsymmetrically widened toward violet	62
Widened without clear dissymmetry	175
Sharp or symmetrically reversed	276
Uncertain on account of blends	10

About 43 per cent of the total number thus show distinct dissymmetry toward the red. These lines differ in appearance from widened lines of the ordinary arc, where we have a shading-off from the position of the normal maximum. In the high-current arc, the maximum has moved into this region of shading. Unreversed lines, when fairly narrow, appear displaced with reference to the comparison lines of the ordinary arc. The stronger lines, except in the infrared, are almost invariably reversed, the reversal being more or less on the violet edge of the line in the high-current arc, but coinciding closely with the position of the regular arc line. The displacing effect is probably very general, and under higher dispersion many lines classed as "sharp" in Table I, and some of these which appear simply widened, would probably show a slight red dissymmetry. This was indicated by photographs of two sections of the iron spectrum, one in the blue, the other in the green-yellow, taken in the second order of the 30-ft. plane-grating spectrograph, with a scale about double that of the concave grating. The freedom from astigmatism made it possible to obtain a record of the very intense radiation near the negative electrode. Under these conditions, apparently no line remained perfectly symmetrical.

Lines widened toward the violet occur in groups, notably near λλ 5100, 5400, 5700, and 6050. They are high-temperature lines, and very few have been obtained with the furnace. The outstanding exception is the Class I line, λ 5110.414, which is narrowly reversed, with the violet side clearly stronger. In the furnace spectrum[1] this line has remarkable strength at low temperature, the only comparable lines being λλ 5166.288 and 5168.904, which are disturbed by adjacent lines in the high-current arc, and may have similar dissymmetry.

Widening without dissymmetry occurs to a small degree for many lines which are sharp in the ordinary arc. Lines which become diffuse are uniformly high-temperature lines. In extreme cases of diffuse widening, the line structure disappears in the high-current arc, which probably accounts for the fact that many faint iron lines measured by Kayser[2] do not appear on my photographs.

Use in wave-length measurements.—The exaggeration in the high-current arc spectrum of any peculiarities of structure present in a more or less incipient state in the ordinary arc shows at once the lines that should not be used as wave-length standards, and also the degree in which other lines may be useful. It may be safely assumed that lines which show only slight widening or dissymmetry in the high-current arc will show very little wave-length variation in the regular laboratory arc, especially if care is taken as to what part of the arc is observed.[3] Thus lines marked S, Ro, Ru_1, u_1, or w_1 may be expected to remain fairly stable. Lines whose dissymmetry is u_3 or u_4 are totally unreliable, while u_2 lines should be discarded unless of very moderate strength. The higher degrees of symmetrical widening, denoted by w_3, w_4, w_5, belong to lines which are more or less diffuse in the regular arc and offer difficulty in setting on their centers.

There is no certain evidence that the high-current arc reveals any new iron lines. The existing tables for the iron arc were sufficient for the identification of almost all lines not to be ascribed to impurities. This would indicate that the neutral atom emits a definitely limited number of lines, that these lines are present, though often very faint, in the arc with moderate current, and that the chief characteristic of the high-current arc in this respect is an intensification of such faint lines when they arise from the higher energy levels of the atom.

---

[1] *Mt. Wilson Contr.*, No. 66; *Astrophysical Journal*, **37**, 239, 1913.

[2] *Handbuch der Spektroscopie*, **6**, 896.

[3] See St. John and Babcock, *Mt. Wilson Contr.*, No. 137; *Astrophysical Journal*, **46**, 138, 1917.

EXPLANATION OF TABLE I

Wave-lengths.—The wave-lengths are chiefly those of Burns[1] on the international system. A few faint lines are from the lists of Kayser[2] and of Meggers and Kiess.[3] These are indicated by an asterisk or a dagger, respectively.

Symbols.—The symbols used to describe the lines in the high-current arc are as follows:

Ro.	A nearly symmetrical reversal; probably never perfectly symmetrical. (See p. 10)
S.	A narrow line without distinct dissymmetry; if the line is faint, a slight one-sidedness may not show.
Ru_1.	A clear dissymmetry of reversal with the red side stronger. The dissymmetry increases up to Ru_4, in which case the absorption line is at the violet edge of the emission line. Partial reversal is indicated by r.
u_1 to u_5.	Increasing degrees of widening toward the red without reversal.
$\mathrm{u}_1\mathrm{v}$, etc.	Dissymmetry toward the violet in varying degrees. If reversed, the absorption line is to the red of the emission maximum.
w_1 to w_5.	Increasing degrees of widening without clear dissymmetry.

Remarks.—These are at the end of Table I and are referred to by numbers adjacent to the wave-lengths.

---

[1] *Lick Observatory Bulletin*, **8**, 27 (No. 247), 1913.

[2] *Handbuch der Spektroscopie*, **6**, 896.

[3] *Bulletin of the Bureau of Standards*, **14**, 637, 1919.

TABLE I

WIDENING CHARACTERISTICS OF IRON LINES IN HIGH-CURRENT ARC

λ	Type	λ	Type	λ	Type	λ	Type
4250.134	Ru$_3$	4389.251	S	4529.684	S	4687.394	w$_1$
4250.791[1]	Ru$_1$?	4390.460	u$_1$	4531.155	Ru$_1$	4688.208	w$_4$
4258.386	Ru$_1$	4390.957	u$_1$	4531.642[17]	S	4689.497	w$_1$
4258.611	u$_1$	4395.288	u$_4$	4537.684	S	4690.145	w$_2$
4258.950	u$_1$	4401.304[8]	u$_3$?	4542.422	w$_1$	4691.416	w$_1$
4259.988[2]	R	4401.447[8]	S?	4547.027	S	4700.201[28]	?
4260.135[2]	R	4404.752	Ru$_1$	4547.855	ru$_2$	4701.051	w$_3$
4260.489	Ru$_3$	4407.716	Ru$_2$	4549.477[18]	w$_1$	4704.955	u$_2$
4264.208	w$_4$	4408.420	Ru$_2$	4550.824	w$_5$	4705.460	S
4265.256	w$_4$	4409.121	S	4552.551	S	4707.287	ru$_3$
4266.968	ru$_2$	4415.127	Ru$_1$	4554.467	w$_2$	4707.485[29]	?
4267.831	Ru$_2$	4422.570	Ru$_1$	4555.904[19]	w$_2$	4708.972	w$_1$
4268.752	ru$_2$	4423.145	w$_1$	4556.128	w$_3$	4709.091	w$_4$
4271.171	Ru$_3$	4427.313	Ru$_1$	4556.941	w$_1$	4710.283	w$_1$
4271.764[3]	Ru$_1$?	4430.197	S	4558.110	S	4711.478[30]	u$_3$
4276.670	w$_4$	4430.622	Ru$_2$	4560.114	u$_3$	4712.104	w$_1$
4278.128	w$_4$	4432.575	S	4564.832	S	4714.182	w$_1$
4279.872	u$_1$	4433.222	w$_4$	4565.324	w$_1$	4721.000	S
4280.5*	w$_2$	4433.808	w$_5$	4565.684	u$_3$	4727.410	u$_2$
4282.406	Ro	4435.154	w$_1$	4566.525	S	4728.549	w$_3$
4285.448	ru$_2$	4436.931	S	4566.990	S	4729.016	S
4288.150	S	4438.355	u$_3$	4568.789	S	4731.488	w$_3$
4288.962	S	4439.886	S	4568.842[20]	u$_1$	4733.594	w$_1$
4290.384	w$_1$	4442.349	Ru$_2$	4574.240	u$_3$	4734.101	S
4290.869	w$_1$	4442.838	S	4574.730	S	4735.844	w$_1$
4291.472	Ru$_1$	4443.199	Ru$_1$	4579.344	S	4736.788	Ru$_3$
4292.293	w$_1$	4445.426	S	4579.825	S	4740.344	S
4294.132[4]	Ru$_1$	4446.853	w$_2$	4580.602	u$_2$	4741.533	w$_1$
4298.043	ru$_1$	4447.137	S	4581.529	u$_3$	4745.804[31]	w$_4$
4299.254	Ru$_4$	4447.727	Ru$_2$	4583.843[21]	w$_1$	4757.581	S
4302.191	S	4450.324	S	4584.732[22]	w$_3$	4768.334[32]	w$_3$?
4304.548	S	4454.387	Ru$_1$	4584.826[22]		4768.397[32]	w$_3$?
4305.458	ru$_1$	4456.335	S	4587.136	S	4771.703	w$_1$
4307.910	Ru$_1$	4459.128	Ru$_2$	4592.658	ru$_1$	4772.818	w$_1$
4309.041	S	4461.205	w$_1$	4595.368	S	4776.075	w$_1$
4309.382	Ru$_2$	4461.658	Ru$_1$	4596.062	u$_3$V	4779.438	S
4315.092[5]	Ru$_1$	4462.011[9]	u$_3$	4598.138	u$_3$	4785.963	w$_2$
4321.798	S	4464.773	w$_1$	4600.939	S	4786.810	w$_1$
4325.770	Ru$_1$	4466.557	Ro	4602.009	w$_1$	4788.761	S
4326.762	S	4469.390	Ru$_4$	4602.946	Ru$_1$	4789.655	ru$_1$
4327.100	ru$_1$	4472.713	w$_1$	4607.665	u$_3$	4791.250	S
4327.92*	u$_1$	4476.023[10]	Ru$_1$?	4611.290	ru$_3$	4798.269	w$_2$
4330.962	S	4476.082[10a]	u$_4$	4613.217	u$_3$	4798.736	S
4337.052	Ru$_1$	4479.608	S	4614.214	w$_2$	4799.412	S
4338.270	u$_1$	4480.143	w$_1$	4615.568[23]	u$_3$	4799.891	w$_2$
4343.278	u$_1$	4481.621	u$_2$	4618.763	S	4800.652	w$_1$
4343.704	u$_1$	4482.176[11]	Ro?	4619.295	u$_3$	4802.887	S
4346.561	u$_1$	4482.262	Ru$_2$	4625.061	u$_3$	4804.529	S
4347.239	S	4482.750	u$_2$	4629.327	w$_1$	4807.729	w$_2$
4347.854	u$_4$	4484.238	ru$_3$	4630.128	w$_1$	4808.155	S
4348.946	S	4485.674	w$_3$	4632.919	w$_1$	4809.14	S
4351.553	w$_1$	4488.134	w$_2$	4635.853	S	4809.94	S
4352.740[6]	Ru$_1$	4488.920	u$_2$	4637.522	u$_3$	4811.04	S
4358.506	u$_1$	4489.744[12]	Ru$_1$	4638.020	u$_3$	4813.11	S
4360.813	S	4490.088	S	4643.467	u$_3$V	4817.784	S
4365.902	S	4490.768	w$_4$	4647.440	ru$_1$	4824.162	S
4367.584	ru$_1$	4494.571	Ru$_2$	4654.502	w$_1$	4832.732	S
4367.910	u$_1$	4502.592	S	4654.637	u$_3$	4834.511	S
4369.777	Ru$_1$	4504.846	u$_3$	4657.598	w$_1$	4835.866	w$_4$
4372.994	S	4508.287[13]	w$_2$	4661.539[24]	w$_3$	4838.519	u$_3$
4373.568	S	4514.190	S	4661.978	S	4839.546	S
4374.495	S	4515.337[14]	w$_2$	4663.185	w$_1$	4843.156	u$_3$
4375.934	Ru$_1$	4517.530	S	4667.460[25]	rw$_3$	4844.016	S
4376.782	u$_1$	4520.238[15]	w$_1$	4668.153	ru$_3$	4845.656	S
4377.796	S	4522.530	S	4669.184	u$_3$	4848.898	w$_1$
4382.777[7]	S	4522.636[16]	w$_1$	4673.171	w$_3$	4855.688	u$_3$
4383.548	Ru$_1$	4523.399	w$_2$	4678.856[26]	rw$_3$	4859.757	Ru$_3$
4384.682	S	4525.154	Ru$_3$	4679.229[27]	?	4863.655	u$_3$
4385.260	u$_2$	4526.567	S	4680.302	S	4871.333	Ru$_3$
4387.899	u$_2$	4527.796	S	4680.475	w$_1$	4872.154	Ru$_3$
4388.422	ru$_4$	4528.624	Ru$_2$	4683.566	w$_1$	4878.226	Ru$_3$

TABLE I—*Continued*

λ	Type	λ	Type	λ	Type	λ	Type
4881.722	S	5079.228	ru_2	5283.634	Ru_4	5539.28*	S
4882.168	u_3	5079.742	ru_1	5288.533	S	5543.184	u_3V
4885.443	u_3	5080.3*	w_1	5293.973	S	5543.951	u_3
4886.342	w_5	5083.344	ru_1	5298.789	S	5546.512	u_3V
4888.651	w_2	5090.787[42]	w_4	5302.315	Ru_4	5547.00*	u_3
4889.02[33]*	S?	5096.992	u_4V	5307.362	S	5549.9*	S
4889.13*	u_2	5098.594[43]	?	5316.620[51]	w_1	5553.586[55]	w_3?
4890.770	Ru_3	5098.706	ru_2	5322.049	S	5554.879	u_3V
4891.510	Ru_3	5099.07*	u_2	5324.196	Ru_3	5557.954	w_3
4903.325	Ru_3	5107.454[44]	Ro?	5326.154	S	5560.230	w_4
4907.745	u_3	5107.645[44]	Ro?	5328.044	Ro	5562.712[56]	w_3?
4909.397	u_3	5110.414[45]	Ru_1V	5328.539	Ru_1	5563.609	u_3
4910.032	u_3	5121.646	w_4	5330.000	w_1	5565.703	u_4V
4919.008	Ru_3	5123.727	ru_1	5332.673	w_1	5567.401	S
4920.521	Ru_3	5125.137	u_4	5332.906	u_1	5569.631	Ru_4
4923.92[34]*	w_1	5127.364	ru_1	5339.949	Ru_4	5572.857	Ru_4
4924.775	w_1	5129.63*	u_3	5341.031	Ru_1	5576.106	Ru_4
4927.42*	S	5131.477	u_1	5353.386	u_3	5584.768	S
4927.875	w_4	5133.676	Ru_4V	5362.744	u_3V	5586.772	Ru_4
4930.331	u_2	5136.09*	u_3	5364.859	Ru_4V	5594.661	u_3V
4933.348	w_2	5137.394	w_4	5365.403	ro	5598.306	u_4V
4934.023	w_3	5139.269	Ru_3	5367.455	Ru_4V	5600.242	u_3
4938.183	w_3	5139.481	Ru_3	5369.960	Ru_4V	5602.965	ru_3
4938.828	Ru_3	5141.750	u_1	5371.496	Ro	5615.663	Ru_4
4939.689	u_1	5142.540	w_5	5373.704	u_3V	5618.646	u_3
4946.401	u_3	5142.934	Ru_1	5379.578	S	5624.563	ru_4
4950.121	u_3	5148.061[46]	?	5383.366	Ru_4V	5633.970	u_5
4952.646[35]	w_4	5148.260	w_5	5389.463	w_5	5636.708	S
4957.311	Ru_3	5150.845	ru_1	5391.643	u_2	5638.278	u_3
4957.612	Ru_3	5151.916	ru_1	5393.185	Ru_4	5641.464	u_3
4966.104	u_3	5159.066	w_4	5397.135	Ro	5643.99	w_1
4967.890	u_4V	5162.312	u_4	5398.285	w_5	5649.66	S
4968.709	S	5165.432	u_4	5400.504	u_4V	5652.32	u_4
4969.942	w_4	5166.288	Ro	5404.131	Ru_4V	5655.179[57]	w_2?
4970.496	S	5167.492	Ro	5405.780	Ro	5655.506	u_3
4973.112	u_3	5168.904[47]	Ro?	5410.900	Ru_4V	5658.542[58]	w_2?
4978.614	u_3	5169.029[48]	w_1	5415.189	Ru_4V	5658.836	u_4
4982.524[36]	ru_4	5171.601[49]	Ru_1	5424.057	Ru_4V	5660.79*	S
4983.274[36]	ru_4	5187.922	u_2	5429.701	Ro	5661.36*	S
4983.858[36]	ru_4	5191.475	Ru_4	5434.527	Ro	5662.533	u_3
4985.267	u_3	5192.364	Ru_4	5436.594	S	5667.533	u_4V
4985.562	u_3	5194.950	Ru_1	5445.049	u_4V	5679.023	u_4V
4988.970	u_4	5195.472	w_5	5446.922	Ro	5680.26*	S
4991.288	u_4	5198.717	ru_2	5455.435	u_4V	5686.532	u_4V
4994.133	ru_1	5202.342	Ru_2	5455.617	Ro	5691.509	u_3
5001.881	Ru_3	5204.585	w_1	5462.964[52]	u_4V	5693.638	u_3V
5002.815	u_3	5208.610	Ru_4	5463.27[52]	u_4V?	5698.05*	S
5005.729	Ru_3	5215.195	Ru_4	5464.286	w_1	5698.37*	S
5006.134[37]	Ru_3?	5216.277	Ru_1	5466.417	w_5	5700.26*	S
5007.312[37a]	w_5?	5217.405	Ru_4	5466.993	S	5701.555	S
5012.073[38]	Ru_1	5225.533	S	5472.720	u_3	5702.4*	S
5014.960	ru_3	5226.876	Ru_4	5473.913	u_3	5705.988	u_4V
5018.437[39]	S	5227.187	Ru_1	5476.296	S	5707.068	w_1
5022.255	u_3	5229.86*	Ru_4	5476.582	u_3	5709.395	u_4
5027.144	u_4	5232.954	Ru_3	5480.872	u_3	5711.867[59]	w_2?
5027.212	S	5235.392	u_2	5481.252	u_3	5712.150[59]	w_2?
5028.135	S	5236.189	w_1	5483.111	u_3	5714.155	S
5029.623	S	5242.495	ru_2	5487.78[53]	u_5	5715.107	u_4
5039.266	u_3	5243.798	w_5	5493.508	w_4	5717.848	u_4
5040.902	w_3	5247.052	S	5494.468	S	5720.8*	S
5041.079	Ru_1	5250.212	S	5497.521[54]	Ru_1	5731.775	u_4
5041.763	Ru_1	5250.650	ru_2	5501.471[54]	Ru_1	5738.3*	S
5044.24*	u_3	5251.971	S	5503.08	u_5	5741.861	u_4
5048.454	u_3	5253.479	u_3	5506.785[54]	Ru_1	5747.95	u_5V
5049.830	Ru_2	5254.956	S	5512.277	u_4	5752.035	u_5V
5051.643	Ru_1	5263.321	ru_4	5519.56*	u_4V	5753.145	u_4
5054.65*	S	5263.874	S	5521.1*	S	5754.41	S
5065.016	u_4V	5266.569	Ru_4	5522.46	u_3	5756.78[60]	w_5?
5065.201	S	5269.538	Ro	5525.552	u_3	5760.351	S
5067.162[40]	w_4	5270.357	Ru_1	5529.15*	S	5762.434	S
5068.784[41]	ru_4	5273.178[50]	u_2?	5532.752	S	5763.015	u_4
5074.750	u_4V	5273.379[50]	u_2?	5535.423	S	5775.095	u_4
5079.002	u_4V	5281.804	Ru_4	5537.71*	S	5778.47	S

TABLE I—*Continued*

λ	Type	λ	Type	λ	Type	λ	Type
5780.621[61]	S?	6082.718	S	6496.462[76]	w_5	6875.98	w_1
5780.83[61]	u_4	6085.267	w_1	6498.950	S	6880.65	u_4
5782.15	S	6089.567	S	6501.681	S	6881.6*	w_3
5784.69[62]	S?	6096.689	u_4	6509.56	w_1	6885.77	u_4
5785.29	u_4	6102.185	u_4v	6516.08	w_2	6898.31	u_4
5791.044	u_4	6103.196[72]	u_4v?	6518.380	u_2	6902.80	u_4
5793.932	u_4	6116.25	w_1	6528.53	w_1	6911.52	S
5798.194	u_4	6127.919	S	6533.97	u_5	6916.710	u_4
5804.06	u_4	6136.624	Ru$_1$	6546.251	ru$_1$	6930.64	u_2
5804.45[63]*	S?	6137.704	Ru$_1$	6569.233	u_5	6933.632	S
5806.727	u_5v	6141.74[73]*	u_4	6574.238	S	6945.215	S
5809.249	u_4	6147.85	S	6575.028	S	6947.501	u_2
5811.93	S	6151.630	S	6581.22	w_1	6951.278	u_5
5814.80	u_4	6157.733	S	6591.32	u_2	6960.334	w_1
5816.36	S	6163.560	S	6592.928	ru$_1$	6971.95	w_1
5828.48	u_5v	6165.370	S	6593.881	S	6975.46	u_5
5834.05	S	6170.499	u_4v	6597.607	u_5	6976.934	S
5835.8*	u_4v	6173.346	S	6608.03	S	6977.445	S
5837.709	S	6180.216	w_1	6609.124	S	6978.864	S
5838.4*	u_4	6188.037	u_4	6609.56	w_2	6988.541	w_1
5848.09*	u_4v	6191.568	Ru$_1$	6625.04	S	6999.928	u_4
5849.6*	S	6200.322	S	6627.563	u_4	7000.633	S
5852.19*	u_4v	6213.440	S	6633.772[77]	u_5	7008.014	u_4
5856.084	w_1	6215.151	w_1	6639.7[78]	u_2	7010.362	S
5857.134[64]	u_5?	6219.290	S	6646.98	S	7011.364	S
5859.20[65]	u_3?	6226.77	u_3	6653.88[79]	u_5	7014.99†	S
5859.612[65]	u_3?	6227.259	S	6663.26[80]	S?	7016.075	S
5862.351	u_4v	6229.234	S	6663.452[80]	S	7016.436	u_4
5864.2*	S	6230.732	Ru$_1$	6678.001	ru$_1$	7023.003	u_4
5873.211	u_3	6232.667	u_4	6699.14	u_3	7024.084	S
5883.842	u_3	6240.3*	w_2	6703.570	S	7024.649[83]	u_5v?
5891.9*	S	6240.652	S	6705.139[81]	w_5	7027.60	S
5892.71*	u_3	6246.344	u_4	6710.31	S	7038.271	u_4
5902.52	S	6252.567	ru$_1$	6713.14	u_2	7044.60[84]†	w_2
5905.677	u_4v	6254.266	S	6713.76	w_5	7067.44	S
5906.0[66]*	u_3?	6255.955	w_1	6715.410	u_4	7068.422	S
5909.99*	u_3	6256.371	S	6716.24	S	7071.88	u_4
5914.16[67]	u_3v?	6265.145	S	6717.556	u_4	7083.396[85]	u_5v
5916.250	S	6270.229	S	6725.39	u_4	7086.76	u_4
5927.798[67a]	u_5?	6280.622	S	6726.668	w_3	7090.417	u_4
5929.7[68]*	?	6283.05[74]	u_4	6732.06	S	7095.447	u_4
5930.177[69]	u_3v?	6290.968[74a]	w_4	6733.171	u_4	7107.486	S
5934.679	u_3	6297.803	S	6739.54	S	7112.182	w_1
5940.972	u_4	6301.524	u_4	6745.11	S	7130.956	u_4
5949.35	u_4	6302.512	u_4	6750.163	S	7132.999	S
5952.749	u_3	6311.506	S	6752.734	u_4	7142.522	u_5
5956.700	S	6315.317	S	6755.609	S	7145.317	u_4
5958.2*	S	6315.814	S	6777.44	w_2	7151.495	S
5959.9*	w_1	6318.027	S	6783.71	w_2	7155.64	u_5
5962.1*	u_3	6322.696	S	6786.88	u_4	7158.502	u_5
5969.8*	w_3	6330.86[75]	u_5?	6793.26	w_1	7164.480	u_4
5975.350	S	6335.341	S	6796.11	w_1	7175.937	u_5
5976.803	u_4	6336.844	u_4	6804.020[82]	S?	7180.020	S
5983.708	u_4	6344.159	S	6804.27[82]	S	7181.22	u_4
5984.809	u_3v	6355.038	u_2	6806.859	S	7187.349	u_4
5987.061	u_3v	6358.684	S	6810.28	w_4	7189.17	S
5997.808	u_4	6362.889	S	6820.43†	w_5	7207.123	w_1
6003.038	u_4	6364.717	u_3?	6828.614	u_4	7207.430	u_4
6005.15	S	6380.751	S	6833.24	w_4	7219.698	w_1
6007.965	u_4v	6393.609	ru$_1$	6837.00†	S	7221.22[86]	u_4?
6008.583	u_4	6400.021	Ru$_4$	6838.86	u_4	7223.678	w_1
6020.067[70]	w_4	6408.044	u_4	6839.828	S	7228.820	S
6020.177[70]		6411.674	u_4	6841.362	u_4	7239.904	u_4
6024.062[71]	w_4?	6419.988	u_4	6842.668	w_5	7244.86[86]	u_5v?
6027.061	S	6421.361	ru$_1$	6843.685	u_4	7254.649	S
6034.1*	u_3	6430.859	ru$_1$	6854.82	S	7261.54[87]	w_4?
6035.5*	S	6436.43	S	6855.183	u_4	7284.853	S
6042.085	u_3v	6456.39	w_1	6857.25	S	7288.782	u_4
6055.991	u_4v	6462.737	S	6858.173	u_4	7293.093	u_4
6062.89	S	6469.216	u_5	6860.29	S	7306.61	u_5
6065.496	ru$_1$	6475.635	S	6861.93	S	7307.957	S
6078.482	u_4v	6481.881	S	6862.481	w_3	7311.112	u_4
6070.02	w_4	6494.993	Ru$_1$	6875.45	w_1	7320.72	u_5

TABLE I—*Continued*

λ	Type	λ	Type	λ	Type	λ	Type
7351.56[86]......	u_5?	7454.02.......	S	7568.932......	u_4	7832.243......	u_4
7353.528[86].....	u_4?	7461.534......	S	7573.53†......	u_4	7937.182......	u_4
7375.57.......	u_4	7473.56†......	w_4	7583.803......	S	7941.09†......	S
7382.99.......	w_3	7476.30†.....	w_4	7586.060......	u_4	7945.889......	u_4
7386.402......	u_5	7482.00†.....	w_3	7617.93[90]......	S	7994.48†......	S
7389.432......	u_4	7491.678.....	u_4	7620.531......	u_4	7998.98.......	u_4
7401.707......	S	7495.099.....	u_4	7650.82[90]......	S	8028.37.......	u_4
7411.196......	u_4	7498.56.......	S	7653.80†......	u_4	8046.088......	u_4
7418.680......	S	7507.31.......	u_4	7661.24.......	u_4	8085.220......	u_4
7421.60†......	w_4	7511.059.....	ru_4	7664.303[91].....	S	8220.42.......	u_4
7430.73[88]†.....	S	7531.181......	u_4	7710.40.......	u_4	8327.080......	w_2
7440.98[89]......	w_5?	7546.173......	S	7723.20†......	S	8332.01.......	u_4
7443.022......	S	7559.68†......	w_4	7748.289......	S	8387.785......	w_3
7445.783......	u_4	7563.03†......	w_3	7780.594......	u_4		

NOTES TO TABLE I

1 Blend with λ 4250.134.
2. These lines reverse, but structure is concealed by λ 4260.489.
3. Blend with λ 4271.171.
4. Dissymmetry very small.
5. Dissymmetry very small.
6. Small dissymmetry. Cf. λλ 4282, 4315.
7. In wing of λ 4383.548, sometimes as absorption line.
8. Blend.
9. Line has sharp center, may be two lines superposed.
10. Disturbed by λ 4476.082.
10*a*. Measured by Babcock with interferometer in Pfund arc, under standard conditions. Greatly intensified in high-current arc.
11. Blend with λ 4482.262.
12. Very narrow.
13–16. Enhanced lines.
17. Shading on red side may be caused by faint adjacent line.
18, 19. Enhanced lines.
20. Blend with λ 4568.789.
21. Enhanced line.
22. Blend.
23. Very faint.
24. Enhanced line, very faint.
25. Unusual case of diffuse line symmetrically reversed.
26. Similar to λ 4667.460, but has slight red dissymmetry.
27. Blend with λ 4678.856.
28. Disappears. Diffuse in ordinary arc.
29. Concealed by λ 4707.287.
30. Very faint.
31. Diffuse shading on red side may indicate presence of another line.
32. Blend.
33. Blend with λ 4889.13.
34. Enhanced line.
35. Very faint.
36. Three lines run together.
37. Blend with λ 5005.729. Degree of widening uncertain.
37*a*. In wing of λ 5006.134. Probably very diffuse.
38. Nearly symmetrical.
39. Enhanced line.
40. Very faint.
41. Reversal at violet edge of line.
42. Slightly shaded to red.
43. Blend with λ 5098.594.
44. Blend. Structure of lines somewhat uncertain.
45. Violet side of reversal slightly stronger.
46. Blend with λ 5148.260.
47. Blend with λ 5169.029.
48. Enhanced line.
49. Dissymmetry very small.
50. Blend.
51. Enhanced line.
52. Blend.
53 Wide shading to red.
54. Slight but distinct dissymmetry.
55. In shading of λ 5554.879.
56. Close to strong line λ 5563.609.
57. Blend with λ 5655.506.

NOTES—*Continued*

58. Blend with λ 5658.836.
59. Blend.
60. May be u_5v.
61. Blend.
62. Close to λ 5785.29.
63. In shading of λ 5804.06.
64. Uniform shading to λ 5859.20.
65. Blend.
66. Blend with λ 5905.677.
67. Difficult. May be faint companion on violet side.
67*a*. Uniform shading to λ 5929.7.
68. Blend with λ 5930.177.
69. Shading affected by λ 5929.7.
70. Blend. λ 6020.177 may widen to violet.
71. May widen to violet.
72. Disturbed by λ 6102.185.
73. May be *Ba*.
74. Shades into a second very diffuse line to red.
74*a*. May widen to violet.
75. Barely visible.
76. Shades into λ 6494.993.
77. Probably double. In ordinary arc sharp line appears superposed on very hazy line.
78. May be double. Measured by writer.
79. Shading may be affected by *Ba* line.
80. Blend.
81. Some shading to red.
82. Blend.
83. Blend with λ 7024.084.
84. May be shaded to violet.
85. Extremely hazy.
86. Very faint lines.
87. Line to violet seems to come up in high-current arc.
88. Hazy line appears on red side.
89. Disappears.
90. Measured by writer.
91. Close to potassium line.

WIDENING EFFECTS AND ENERGY LEVELS

The work of Walters[1] and of Laporte[2] on regularities in the iron arc spectrum makes possible a comparison between widening effects and atomic energy levels. This is given in Table II, the notation of Walters being used, in which A is the lowest of a succession of levels. Lines of smallest dissymmetry in the high-current arc from λ 2800 to λ 8400 belong to multiplets starting from levels A, B, and C. The initial level, rather than the range of levels, is evidently the important feature. Thus a multiplet having a jump from A to M retains the Ro character of the smaller intervals which start from the A level. Jumps of B to R and C to Q have lines similar to multiplets with jumps between levels close together. An increased susceptibility to unsymmetrical widening is very distinct, however, for higher initial levels. Multiplets from level A are the most symmetrical, the A to E group consisting of sharp lines in the green in furnace Class I A, while the remaining nine multiplets include strong low-temperature lines in the ultra-violet with minimum dissymmetry. Multiplets from levels B and C are also made up of low-temperature lines, and when their structure is clearly brought out, show, in general, a slight red dissymmetry. The D multiplets are an intermediate group, some consisting of faint red lines which remain sharp, perhaps because of low intensity, but two multiplets in the blue and green have lines of pronounced ru_2 structure. The prevailing temperature class of D multiplets is III. Starting from level F and high levels, we have the high-temperature lines of Classes IV and V, showing the very general widening toward the red indicated by u_3 and u_4. It is noteworthy that none of the lines having dissymmetry toward the violet have as yet been arranged in multiplets. From their furnace behavior, it is evident that they are high-level lines, probably with unusual combinations.

---

[1] *Journal of the Optical Society of America and Review of Scientific Instruments*, **8**, 245, 1924.

[2] *Zeitschrift für Physik*, **23**, 135; **26**, 1, 1924.

TABLE II

ENERGY LEVELS OF IRON MULTIPLETS

Initial Level	Prevailing Type	Number of Multiplets
A	Ro	10
B	Ru_1	13
C	Ru_1	9
D	ru_2	5
F	u_3	2
G	u_3	1
J	u_4	1
K	u_4	1
K_1	u_4	1
L	u_4	1
M	u_4	1

Apparently the large electronic orbits giving rise to lines of high energy level are especially susceptible to disturbance by strong excitation, and the peculiarities of structure brought out by the high-current arc, especially for lines beyond the reach of the furnace, may be used to indicate energy level and thus supplement the temperature classification.

RELATION TO TEMPERATURE CLASSES

Slightly over one-third of the lines included in Table I have been classified in furnace spectra, the two most numerous types and the two next in number being given in Table III for each temperature class. The data show a sharp or symmetrical structure prevailing for lines of Class I A, small dissymmetries in Classes I and II, and an increasing proportion of strongly widened lines in the higher classes. The considerable proportion of scattered types under Classes III, IV, and V is made up chiefly of faint arc lines which have not appeared in the low-temperature furnace, perhaps partly on account of the general faintness of such furnace spectrograms. Some of these lines remain sharp in the high-current arc, which is the typical behavior of low-temperature lines when unreversed. Whether they are really low-temperature lines will be clear when their multiplet connections with other lines are worked out. Other minor variations from a close correspondence are also found. Thus a low-level multiplet given by Laporte includes the lines λλ 4376, 4427, 4461, which were shown by the writer[1] to persist at temperatures as low as 1400°C. In the high-current arc these lines, while relatively weak, show a distinctly one-sided reversal. In the same region, λλ 4282, 4315, 4352, which Laporte places by themselves in a multiplet of uncertain level, are much more nearly symmetrical, but require higher temperature. They fade rapidly below 2000°C., and are placed in Class III in the revised list. In general, however, the correspondence with temperature class is close, and an examination of the ultra-violet shows the same relation holding in that region.

COMPARISON WITH OTHER LIGHT-SOURCES

1. *Pressure arc.*—In their study of the spectrum of the iron arc under high pressure, Gale and Adams[2] arranged the lines in groups according to the amount of pressure shift and tendency to widen unsymmetrically under pressure. This grouping has been taken into account in the later wave-length measurements of the iron spectrum, as the tendency of lines from the more intense regions of the ordinary arc to give divergent wave-length values was found to correspond closely with their behavior in the pressure arc. Since the high-current arc exaggerates a displacing action which is present in some degree in the ordinary arc, we may expect to find phenomena which

---

[1] *Mt. Wilson Contr.*, No. 247; *Astrophysical Journal*, **56**, 318, 1922.

[2] *Mt. Wilson Contr.*, No. 58; *Astrophysical Journal*, **35**, 10, 1912.

follow closely those of the pressure arc. A comparison of widening effects with pressure displacements for 111 iron lines measured by Gale and Adams in the region covered by Table I is given in Table IV.

Table IV shows that the lines of groups *a* and *b*, with small or moderate pressure shift, have at most only slight dissymmetry in the high-current arc. Lines which become strongly unsymmetrical under pressure are in group *c*, and those with extreme widening toward the red in group *d*. This gradation is followed closely in the high-current arc, where lines having widening indicated by u_3 and u_4 predominate in the groups *c* and *d*, respectively. There is no case of real discordance, in which a line shows large effect for one source and small effect for the other. Evidently, by a slight adjustment of the two classification systems, lines can be assigned to the groups of Gale and Adams by examination of the high-current arc spectrograms, with the advantage that practically all the lines of the neutral atom can be treated by this method.

TABLE III

RELATIVE NUMBER OF TYPES OF IRON LINES FOUND IN EACH TEMPERATURE CLASS, λ 4250–λ 7200

	I A	I	II	III	IV	V
Most numerous types	Ro, S 9	u_1, u_2 22	u_1, u_2 19	u_1, u_2 29	u_3, u_4 39	u_3, u_4 86
Types next in number	u_1 4	Ro, S 11	Ro, S 4	u_3, u_4 20	u_1, u_2 20	w_3, w_4 11
Number of lines of other types	1	1	2	14	25	15

TABLE IV

COMPARISON OF GROUPING OF IRON LINES IN THE PRESSURE ARC AND IN THE HIGH-CURRENT ARC

TYPE IN H.C. ARC	PRESSURE GROUP			
	a	*b*	*c*	*d*
S	2	14	....	....
Ro	9	2	....	....
u_1	13	30	....	....
u_2	....	....	8	....
u_3	....	....	12	5
u_4	....	....	....	16

2. *Polar displacements in the ordinary arc.*—In their study of pole effect in the iron arc, St. John and Babcock[1] made use of the pressure groups in classifying the shifts which they measured between lines produced at the pole and in the center of the arc. The larger shifts to the red measured in this way fall into pressure groups *c* and *d*, while displacements to the violet are placed in a fifth group, *e*. In Table I of the present paper, 156 *c* and *d* lines occur, and of these 138 show large dissymmetry to the red in the high-current arc; the structure of the remaining lines is uncertain. All of the 44 lines of group *e* common to the two lists spread to the violet in the high-current arc. The one-to-one correspondence thus indicated supports the view that the polar conditions of the ordinary arc, much intensified, are the dominant conditions of the high-current arc.

3. *Tube arc.*—In this source,[2] a graphite tube containing a metal or salt is intensely heated and made to burn apart, thus forming an arc in vacuum at about 30 volts, with currents comparable with those used in the present investigation. The line dissymmetries observed correspond fully in direction and relative magnitude with those of the high-current arc in air. The tube arc, being a vacuum source, gives narrower lines than the arc in air, a feature which brings out the structure better for some strong lines, but is disadvantageous for the weaker lines, which are too narrow for classification.

4. *Disruptive spark.*—A comparison of the iron lines of a strongly condensed spark with those of the tube arc[3] has shown that the widening phenomena are of quite the same character. As the volume of vapor in the spark is small, only certain types of lines are wide enough to be satisfactorily grouped on the basis of widening, but many very strong arc lines in the ultra-violet are so reduced in intensity that the strong displacing action of the spark discharge, which was studied by microphotometer curves, shows very clearly.

5. *Exploded wires.*—The absorption spectra obtained when

---

[1] *Mt. Wilson Contr.*, No. 106; *Astrophysical Journal*, **42**, 231, 1915.

[2] *Mt. Wilson Contr.*, Nos. 73, 103; *Astrophysical Journal*, **38**, 315, 1913; **41**, 373, 1915.

[3] *Mt. Wilson Contr.*, No. 103; *Astrophysical Journal*, **41**, 373, 1915.

metal wires inclosed in a wooden block are exploded by a condenser discharge have been described by Anderson.[1] After these results were published, Anderson made a series of photographs of the iron spectrum with the same dispersion that I have used for the high-current arc spectra, and he has kindly placed this material at my disposal for comparison. The absorption lines given by the explosions show the same sort of widening or one-sided shading as appears in the high-current arc. Only the more pronounced effects are shown distinctly by the absorption lines, but evidently a displacing action is present, affecting the absorbing vapor in a way corresponding to that which in the high-current arc causes widening or displacement of the emission lines.

Six light-sources have thus been extensively investigated in this laboratory, in which the iron lines are affected in the same way. Superficially considered, these sources have little in common. The conditions vary from low arc voltages to high spark potentials, from a partial vacuum to pressures of many atmospheres, from the slight vaporization present in the spark to the large mass of vapor quickly produced in the high-current arc. Except in the case of the pressure arc, a high electrical excitation is evidently present in each source, but this is not necessary for displacements under high pressure. The tube furnace under pressure,[2] heated to moderate temperatures, has been shown to give line shifts fully as large as those of the pressure arc.

The material at disposal indicates that spectral lines possess an inherent sensitiveness to displacement toward the red or the violet (or in both directions in the case of diffuse lines), which increases for lines of high energy level. There is a possibility that agencies quite different in character may act upon the electron orbits in such a way as to produce the observed disturbances of period.

OTHER ELEMENTS

Titanium.—The spectrum was obtained best with pulverized titanium carbide contained in small copper tubes held in the ends of graphite rods. One flash of the very brilliant arc gave a strong spectrum for the region λ 4950–λ 6600. The symmetrical structure of the low-temperature lines and the varying degrees of dissymmetry toward the red for those of higher temperature showed that a grouping of lines as distinct as that for iron can be made. The band spectrum, usually very disturbing in this region, was quite absent in emission, but appeared in absorption in several places where the shading of diffuse lines furnished a background.

---

[1] *Mt. Wilson Contr.*, No. 178; *Astrophysical Journal*, **51**, 37, 1920.

[2] *Mt. Wilson Contr.*, Nos. 53, 60; *Astrophysical Journal*, **34**, 37, 1911; **35**, 183, 1912.

Calcium.—Varying amounts of the metal were used in the arc, the impurity in ordinary carbons being sufficient to show the structure of the stronger lines. Thin-walled graphite tubes of 4-mm bore containing the metal, supported in graphite rods, gave a large quantity of calcium vapor with little disturbance from the carbon. The spectrum is notable for the violet dissymmetry of many of the low-temperature lines. This was noted for H and K in the tube arc[1] and a similar reversal, with the violet side distinctly stronger, appears in the high-current arc in air. In the spectrum of the neutral atom the lines of the low-temperature sextet λλ 4283–4319 reverse with violet dissymmetry, as do the lines in the group λλ 4425–4435–4455. When λ 4227 is sufficiently weak, a slight dissymmetry with the red side stronger may be seen. Red dissymmetry, which is more or less pronounced in the ordinary arc for the triplets with violet members at λλ 3949, 4093, 4578 and for the single lines λ 4355, 4527, is intensified to such an extent that the lines almost disappear.

The pole effect as measured by Whitney[2] shows agreement with the foregoing dissymmetries as to direction and relative amount except in the case of H and K, for which the small red displacement (0.002 A) observed at the pole is perhaps within the errors of measurement for lines of this kind. The pressure displacements given by L. F. Miller[3] are also in agreement with the high-current arc data, except for a negligible pressure effect for H and K.

Aluminum.—The strong lines λλ 3944, 3962, spread to a great width in the high-current arc between metal rods, but when obtained as impurity lines in other spectra, they showed large red dissymmetry, with the reversal on the violet edge of the emission lines. A similar dissymmetry was previously observed in the tube arc. In aluminum arcs, the gallium lines λλ 4033, 4172, are frequent impurities, and in the high-current arc appeared reversed with very strong red dissymmetry.

---

[1] *Mt. Wilson Contr.*, No. 103; *Astrophysical Journal*, **41**, 373, 1915.

[2] *Astrophysical Journal*, **44**, 65, 1916.

[3] *Ibid.*, **53**, 224, 1921.

The strong aluminum bands from λ 4400 to λ 4900 showed an interesting absorption effect. The enhanced lines in this region are very strong in the high-current arc, and each of these appeared as a group of fine lines resembling a diffraction pattern. This was caused by the absorption of the outer envelope in which the bands are present. The enhanced line radiation appeared only in the spaces between the band lines.

Magnesium.—The appearance of the enhanced line λ 4481 and the structure of arc lines in the blue were observed. In the writer's study of the tube-arc spectrum,[1] λ 4481 was obtained with high intensity and its doublet structure was detected. The line was also very strong in the high-current arc in air, especially when the radiation near the negative pole fell on the slit. At the positive pole the line was weak, its width being that required by the two components, while near the negative pole, it sometimes spread to a width of 15 A.

This variation, together with the absence of λ 4481 from the arc between carbon terminals charged with magnesium, is shown in Plate XI, which also illustrates the very large displacement of the high temperature line λ 4703. This line in the ordinary arc undergoes strong widening to the red when much magnesium is present, as is shown in Plate XI*a*, but the position of the maximum is given by the point of the widened line. Plate XI*d*, taken with small vapor density, shows the line sharp. In the high-current arc, the maximum of emission was displaced into the region to the red, ordinarily merely shaded, while the reversal remained in the position of the sharp arc line. An intensity curve for λ 4703, made with the registering microphotometer by Miss Ware, is reproduced in Figure 1. On this curve the position of the emission maximum is approximately 7 A to the red of the reversal, which appears as a notch on the slope of the curve. A displacement of similar magnitude was shown by λ 4352, but was too diffuse for measurement. The low-temperature line λ 4571 is shown also in Plate XI. In the high-current arc, it was always narrow, but reversed unsymmetrically with the red side distinctly stronger.

---

[1] *Mt. Wilson Contr.*, No. 73; *Astrophysical Journal*, **38**, 315, 1913.

Copper.—The spectrum from λ 3800 to λ 4600 was photographed with the high-current arc between copper rods 6 mm in diameter. The arc was of very brief duration, with the maximum current uncertain. The effect on some of the high-temperature lines, which tend to diffuseness in the ordinary arc, is shown in Plate XI. As a rule, these lines did not reverse, but appeared as wide, fairly symmetrical lines much displaced to the red. Some showed unsymmetrical reversal, however, the best defined being λ 4275, whose reversal coincided in position with the sharp line of the ordinary arc. This showed freedom from instrumental shift and made possible a rough measurement of the displacements. These averaged 0.33 A for seven lines from λ 4100 to λ 4600. Near λ 3900 a considerable number of fainter arc lines were strongly displaced to the violet.

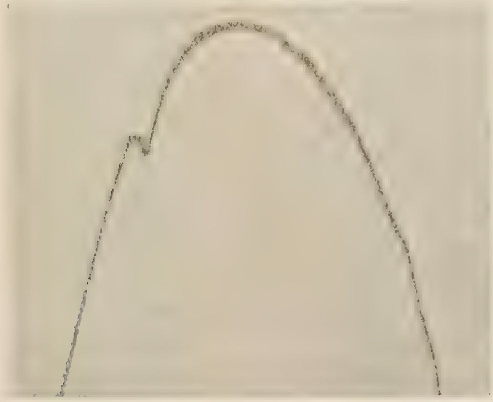

FIG. 1.—Microphotometer curve of magnesium λ 4703 in high-current arc

Sodium, D lines.—These were obtained as very weak impurity lines on several plates, and showed a reversal with the red side distinctly stronger. With the symbols used for the iron lines, they would be described as Ru_1. This is the structure most frequently found for the lowest temperature lines in the spectra thus far examined.

Oxygen and nitrogen, infra-red lines.—The oxygen triplet, λλ

7771.97, 7774.01, 7775.68, appeared in the high-current arc between iron electrodes. The lines were shaded to the red, and showed a greater increase over their strength in the ordinary iron arc than do the average iron lines.

The nitrogen lines, λλ 7423.88, 7442.56, 7468.74, in the same arc were fairly strong, with shading to the red. As a very diffuse line, λ 8216.46 also appeared. On account of the odd multiplicity found in their series regularities, these lines are assigned by Kiess[1] to the spectrum of ionized nitrogen. Their appearance in the high-current arc indicates that they belong to a lower level of the ionized atom than the powerful spark lines near λ 4600, which do not appear in this arc.

DESCRIPTION OF THE PLATES

Plate VIII was described on page 9. Three types of iron lines are illustrated in spectrum *b:* low-temperature lines with almost symmetrical reversals, such as λλ 5397, 5430, 5434; high-temperature lines with red displacement of the maximum, as λλ 5324, 5340, 5393; and the group *e* lines, λλ 5383, 5404, 5415, 5424, with strong violet dissymmetry and the very unusual self-reversal. Spectrum *c* is that of the high-current arc burning steadily with iron-carbon terminals, showing great intensification of the high-temperature lines and small dissymmetry.

Plate IX shows two sections of the iron spectrum in the green, the multiplet near λ 4900 and many other lines having strong red dissymmetry. Numerous lines remain narrow, while a group near λ 5100 is displaced to the violet. The degree to which the enhanced lines λλ 4924, 5018 are strengthened in the high-current arc represents the usual appearance of enhanced iron lines in the visible spectrum.

Plate X covers a large part of the orange and red of the iron spectrum. A comparison with the ordinary iron arc, Plate X*a*, shows many differences in relative intensity as well as numerous displacements toward red or violet. The lines which remain sharp and of nearly the same intensity in the two arcs show the usual behavior of unreversed low-temperature lines, but owing to the relatively high temperature required to produce the iron spectrum in

---

[1] *Science*, **60**, 249, 1924.

PLATE IX

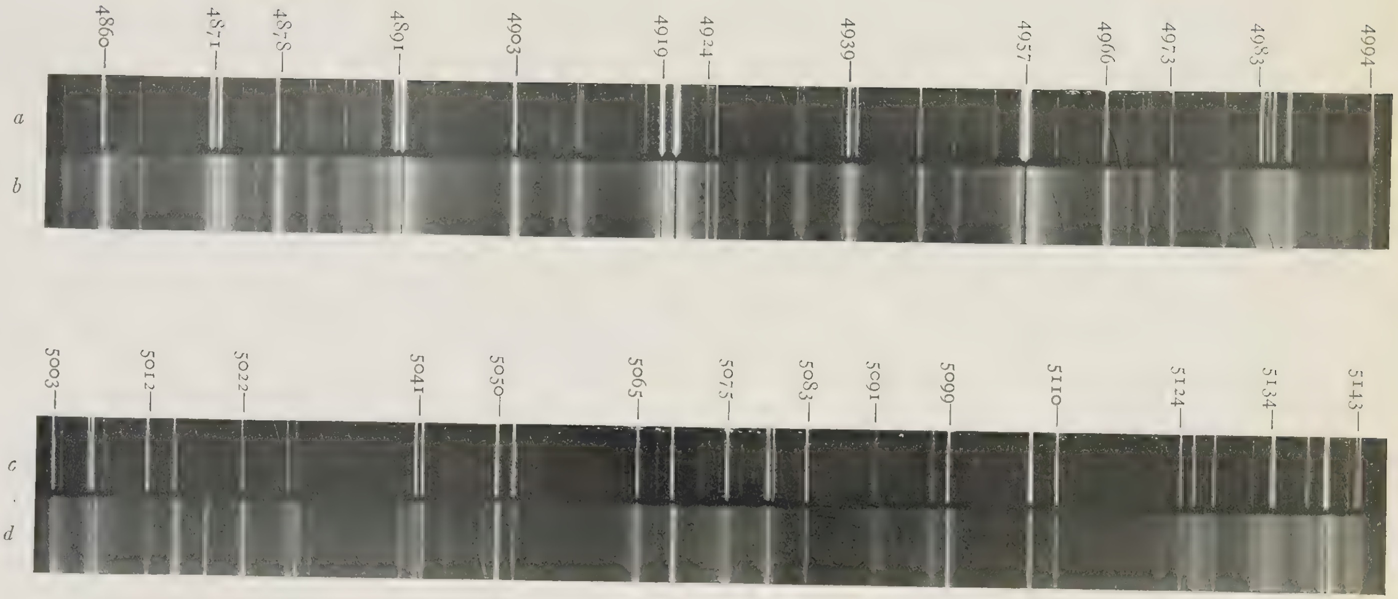

Arc Spectrum of Iron

a, *c*, low-current arc
b, *d*, high-current arc

PLATE X

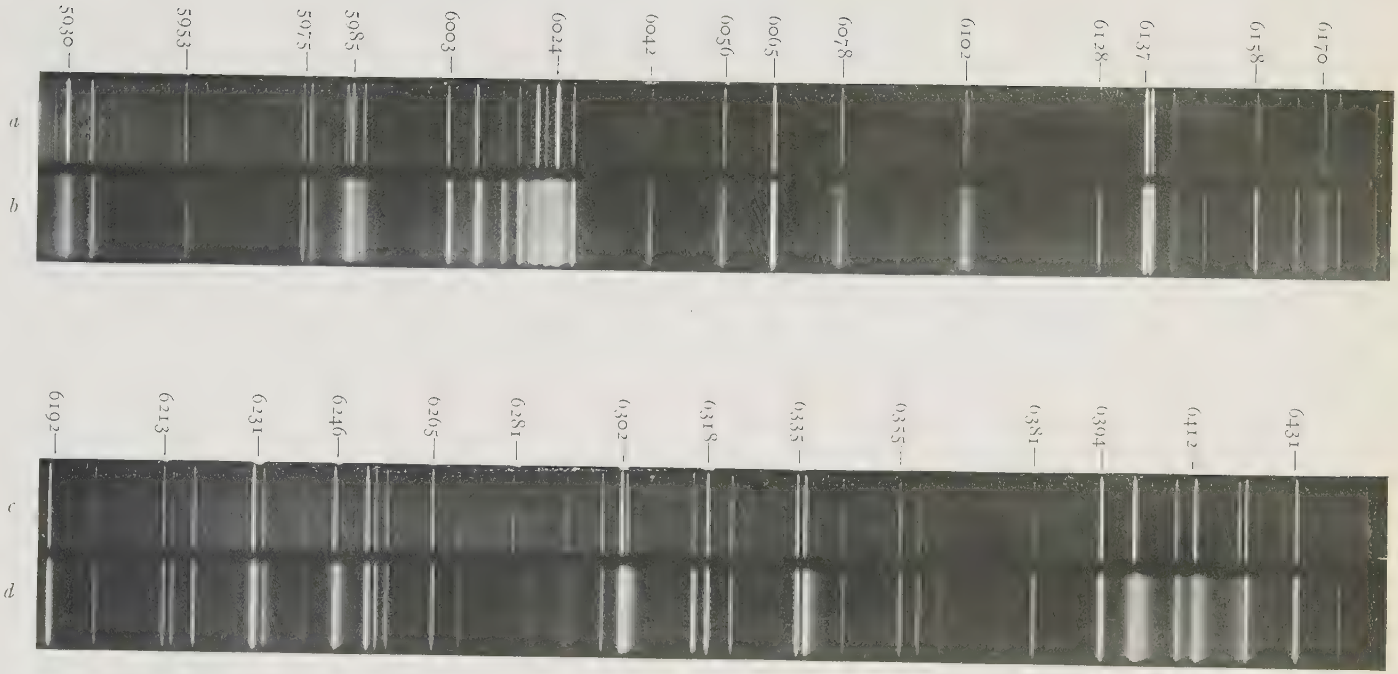

Arc Spectrum of Iron

a, *c*, low-current arc
b, *d*, high-current arc

PLATE XI

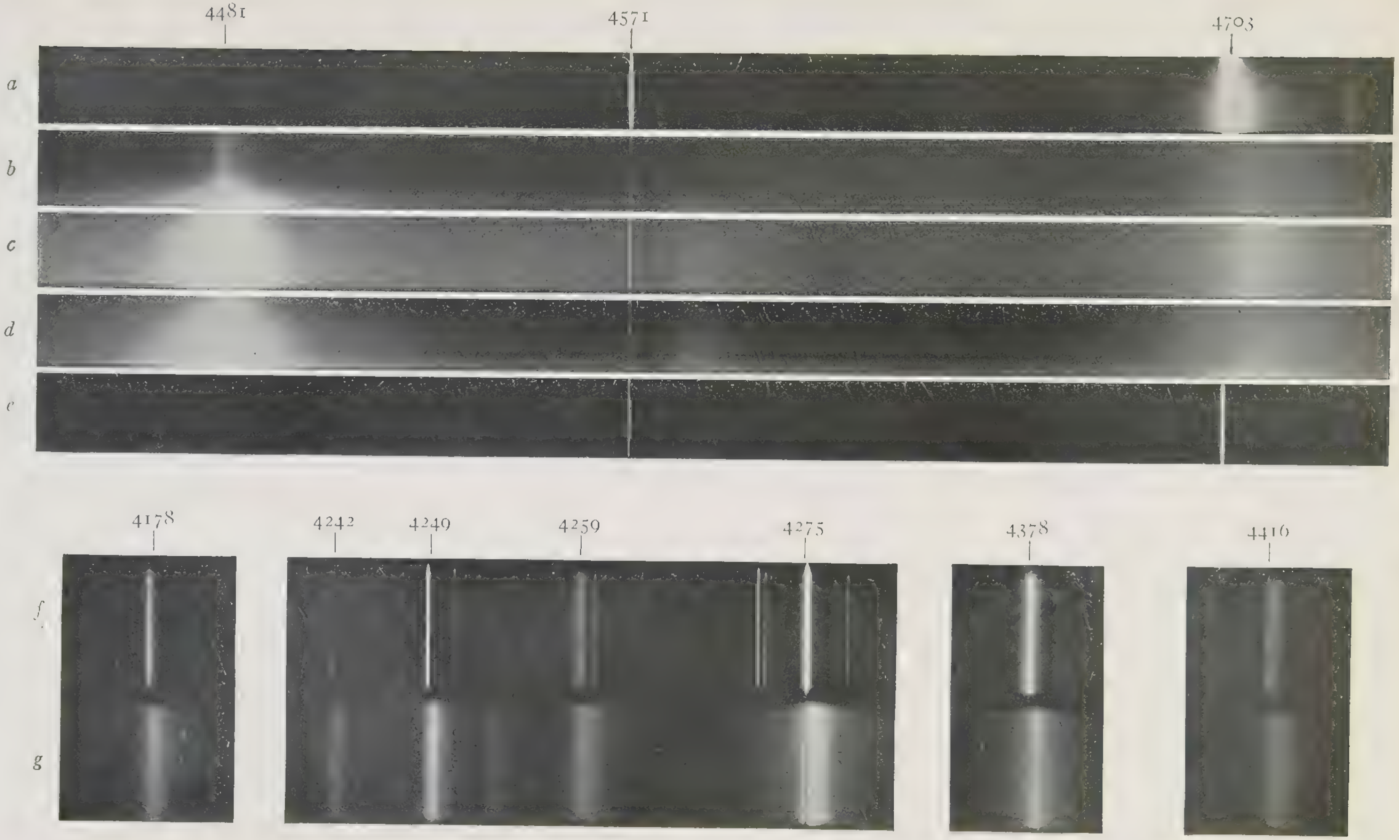

High-Current Arc Spectrum of Magnesium (*b*, *c*, *d*) and Copper (*g*)
Low-Current Arc Spectrum: *a*, *e*, and *f*

the red, they are seldom below Class III. The absence of the band spectrum from the high-current arc is notable throughout this region, especially near λ 6000.

Plate XI shows in its upper section the magnesium lines, λλ 4481, 4571, 4703, these being an enhanced line, and low- and high-temperature lines, respectively. Their features are described on page 24. The lower section gives some high-temperature lines of copper, with large displacements toward the red. The reversal of λ 4275 is in the position of the narrow arc line shown just above it.

Mount Wilson Observatory
June 1925

Contributions from the Mount Wilson Observatory, No. 299
Reprinted from the *Astrophysical Journal*, Vol. LXII, pp. 202–225, 1925

RADIATION MEASUREMENTS OF THE SOLAR CORONA JANUARY 24, 1925

By EDISON PETTIT and SETH B. NICHOLSON

ABSTRACT

Intensity and spectral distribution of the coronal radiation.—A vacuum thermocouple with a rock-salt window was placed at the focus of a 50.5-cm mirror of 101-cm focal length. Measurements were made differentially between two points in the corona 4!6 from the east and west limbs of the moon and the moon itself. The *mean intensity of the coronal radiation* at these points was found to be 5.40×10^{-7} of sunlight. By means of a water-cell and thin glass plate it was found (1) that the corona radiates slightly more energy on the violet side of 1.3 μ than the sun does, and (2) that the radiation of wave-length greater than 5.5 μ is inappreciable.

Photometry of the corona.—The corona was photographed on plates provided with standard photometric squares. Two exposures were made upon Seed 30 plates without filter, and one upon an Ilford "Special Rapid Panchromatic" plate with red filter. These plates were rotated beneath the slit of the registering microphotometer, which, beginning at the limb, recorded the transmission curves of contiguous zones about the moon. These curves gave the mean intensity for each zone in arbitrary units. A similar record of the zone through the points occupied by the thermocouple junctions of the radiation apparatus, combined with the radiometric measures at these points, furnished a calibration by means of which the mean intensity in each zone could be expressed in absolute units. The summation of the zone intensities from the Seed 30 plates gave for the intensity of the whole corona 10.1×10^{-7} times sunlight, while 10.7×10^{-7} sunlight was found from an Ilford plate with red filter. The introduction of the solar constant gave for the coronal radiation 19.3×10^{-7} cal. cm^{-2} min.$^{-1}$. The ratio of the observed coronal light to full-moon light was 0.47.

Distribution of energy in the corona.—The corrections for scattering of the coronal light and halation in the plate were found from transmission curves taken radially across the moon and the edges of the plate. These corrections were applied to the zone intensities. From the corrected intensities, it was found: (1) that the intensity in the polar region is less than half that in the equatorial region, (2) the intensity of a point in the corona as derived from Seed 30 plates varies inversely with the sixth power of its distance from the center of the sun, (3) the ratio of blue light to red light varies directly with the distance from the center of the sun, (4) the correcting factor for overlapping moon varies with the fourth power of the ratio of the apparent radius of the moon to the apparent radius of the sun.

Radiation from the whole corona.—When corrected for overlapping moon the radiation from the whole corona is 21.4×10^{-7} cal. cm^{-2} min.$^{-1}$, or 0.52 full-moon light. Comparison with photo-electric cell measures gives some evidence that the intensity of the coronal light varies with the solar constant, but with a greater amplitude.

Observation of the corona without an eclipse.—The intensity of scattered light about the image of the sun in optical instruments is at least one hundred times greater than the maximum allowable for detecting the corona without an eclipse by any radiation method.

The radiation from the corona was measured with the vacuum thermocouple at Middletown, Connecticut, during the eclipse of January 24, 1925. Briefly, the plan was (1) to determine the amount and spectral distribution of the radiation from a small area of the corona with a suitable thermocouple attached to a reflecting telescope and (2) to determine the distribution of energy in the corona by photographic photometry. The results from (1), combined with (2), would then give the total amount of radiation emitted by the corona, expressed in absolute units.

Measurements of the coronal radiation have previously been made by Abbot, during the eclipses of May 28, 1900,[1] at Wadesboro, North Carolina, and of January 8, 1908,[2] at Flint Island. Abbot used a bolometer with a glass window, attached to a telescope of 50.5-cm aperture and 100-cm focal length. Only one strip of the bolometer was exposed to the radiation, the deflections being produced by means of a shutter. A screen consisting of an asphaltum-coated glass plate was used to filter out the visual light, thus leaving only the infra-red radiation. Abbot found that the spectral distribution of radiation in the regions measured was nearly the same as, though slightly redder than, that of light from the center of the sun's image, and that the brightness of the inner corona equaled that of lunar radiation transmitted by glass.

THE APPARATUS

The telescope and auxiliary equipment employed at the eclipse of January 24, 1925, are illustrated in Plate XII. The whole apparatus was set up in the basement of the Scott Physical Laboratory of Wesleyan University, through the kind invitation of W. G. Cady, in charge of the laboratory, who placed at our disposal the many conveniences and the equipment of the institution. The telescope carried the 50.5-cm mirror used by Abbot at Flint Island in 1908, which was kindly placed at our disposal by him. The figure of the mirror in the meantime has been slightly altered, however, its focal length now being 101 cm, so that the image of the moon at the time of the eclipse was 9.79 mm in diameter.

The thermocouple and transmission cells were mounted at *A* (Plate XII), directly in the principal focus of the mirror. The thermocouple was provided with a rock-salt window to permit the measurement of all radiations reflected by the mirror of the telescope. It

---

[1] *Astrophysical Journal*, **12**, 69, 1900.

[2] *Smithsonian Miscellaneous Collections*, **52**, Part I, 31, 1908.

PLATE XII

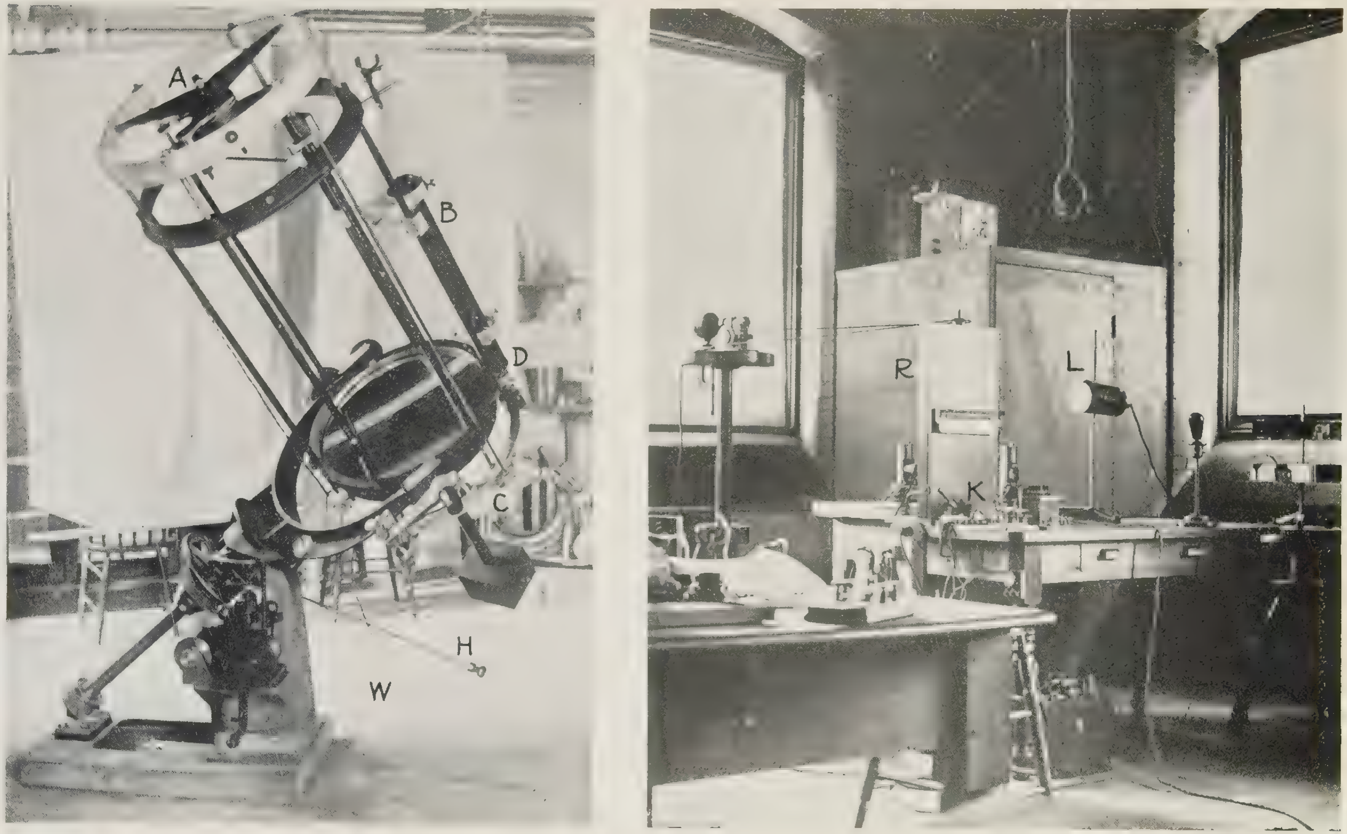

Reflecting Telescope and Thermocouple as Used for Observations of Coronal Radiation

The galvanometer and recording apparatus shown on the right were mounted in an adjoining room

had two junctions 0.76 mm square, separated 5 mm, a distance about equal to the radius of the moon's image formed by the mirror at the time of the eclipse.

The reticule in the guiding telescope *B* contained three threads, one parallel to the diurnal motion of the telescope and two others, one fixed and one movable, intersecting the first thread at right angles, and so spaced that their angular separation in the field of the finder was the same as that of the junctions of the thermocouple in the field of the reflector. The adjustment was such that when the telescope was shifted in right ascension so that a star seen in the guiding telescope moved from one intersection to the other, the image formed by the reflector moved from one thermocouple junction to the other. During the eclipse one limb of the moon was set on a speck of dust near the movable wire, and at the signal for shift the other limb was set at an equal distance from the fixed wire. This caused the junctions to be set alternately on the corona at two points $4'.6$ from the east and west points of the limb of the moon, while the opposing junction was on the moon $12'.4$ inside the limb.

Two transmission cells were provided to study the spectral distribution of the energy in the corona. One of these was a water-cell 1 cm thick, the other a microscope cover-glass 0.165 mm thick. Their transmission curves have already been given.[1] These cells could be interposed into the beam from the 50.5-cm mirror by turning the lever *C*. The insertion of the water-cell increased the effective focal length of the mirror about 2.5 mm. This was compensated by giving the lever *D* a quarter-turn, which moved the thermocouple and cells away from the mirror just the proper amount.

The telescope was set close to a window which was provided with a shutter, hinged at the lower casing. The purpose of the shutter was to prevent sunlight from striking the mirror, as the intense image would have melted the thermocouple instantly and set fire to its insulation. At the signal for totality, the shutter was thrown open, and closed again a few seconds before the end of totality. While protecting the mirror of the telescope, the shutter did not cover the guiding telescope, which was set upon the moon before the eclipse began. The tube of the telescope was covered with heavy black paper, which extended about 50 cm beyond the end of the skeleton frame in order to protect the thermocouple, as far as possible, from drafts and stray radiation. A twisted lamp-cord *W* conveyed the current produced by the thermocouple at *A* to the galvanometers set up in an adjacent room.

---

[1] *Mt. Wilson Contr.*, No. 246; *Astrophysical Journal*, **56**, 312, 1922; *Publications of the Astronomical Society of the Pacific*, **35**, 195, 1923; *Popular Astronomy*, **32**, 602, 1924.

Two Leeds and Northrup high-sensitivity D'Arsonval galvanometers were provided, having periods of five and one seconds, respectively. These were arranged on a pier so that, with the aid of fixed mirrors, an image of the filament of a 100-watt lamp *L* was cast by each upon the double slit[1] of the photographic registering device *R* at a scale distance of 7.5 m. By means of a switch, either galvanometer could be put into the thermocouple circuit in series with a resistance box.

Observations of the radiation from the moon indicated that the one-second galvanometer without additional resistance in the circuit would probably be sufficiently sensitive, and this arrangement was used during the eclipse. Had the sensitivity been too great, it could have been decreased by pulling plugs out of the resistance box, or had it been too small, the five-second galvanometer, the sensitivity of which was six times greater, could have been put into the circuit with little loss of time.

Observations of the radiation from a lamp showed that with the thermocouple used, the one-second galvanometer came to full deflection in seven seconds. A clock-driven electric contact *K* was then arranged to give signals at the telescope at intervals of seven seconds, at each of which the observer shifted the telescope by means of the right ascension slow motion handle *H*, so that the corona and the center of the moon interchanged places on the junctions of the thermocouple. A marker placed on the screw of the registering device indicated when the cells should be thrown into the beam from the telescope, and this was signaled by a buzzer.

The photometric device consisted of a 6-in. Ross doublet of 15-ft. focal length, fed by a coelostat with a 6-in. pyrex mirror.[2] Three plates were exposed, two Seed 30 without filter and an Ilford "Special Rapid Panchromatic" with Eastman "F" filter, which transmits only wave-lengths longer than 6100 A. Photometric squares were exposed along the end of each plate by the usual method of varying the distance of the plate from an electric light operated from a storage battery. The energy ratios for these squares computed from the inverse square law are represented by the numbers 1.000, 0.444, 0.250, 0.111, 0.062, 0.028, and 0.020. During the eclipse, exposures of two seconds and fifteen seconds, respectively, were given to the two Seed 30 plates, and an exposure of seventy-three seconds to the Ilford plate with red filter.

---

[1] *Journal of the Optical Society of America*, **10**, 267, 1925.

[2] *Mt. Wilson Contr.*, No. 266; *Astrophysical Journal*, **58**, 208, 1923.

ECLIPSE CONDITIONS

The mild weather prevailing during the two preceding weeks turned suddenly cold the day before the eclipse, the thermometer indicating a temperature of about −8° F., a condition which continued until after the eclipse. The water-cell froze and broke, but was repaired and refilled with saturated salt water. A series of observations on the transmission of sunlight by the cell filled first with salt water and then with distilled water revealed no measurable difference. The coelostat operating the Ross lens ran somewhat slowly, but this did not affect the short exposures, although its effect was quite noticeable on the Ilford plate. The driving clock of the 50.5-cm reflector ran very satisfactorily.

On the morning of the eclipse, the sky clouded suddenly about 6:00 A.M. and remained so until nearly 8:00 A.M., when the clouds began to break away. By 9:00 A.M. the sky was clear, save for a bank of haze in the east, and during the eclipse (9:12 A.M.) the sky was quite clear in the neighborhood of the sun.

Although excellent definition was not necessary, the windows of the laboratory-room where the telescope and coelostat were located were opened about forty minutes before totality, so that the room might come to outside temperature.

DISTRIBUTION OF ENERGY IN THE CORONAL RADIATION

During totality, five deflections were obtained for the free radiation, that is, without transmission cells, and four each for the radiation transmitted by the salt-water cell and microscope cover-glass. One deflection obtained with each of the cells was rejected, these being obviously defective, as shown by the form of the curve on the plate. The deflections were measured on a suitable comparator[1] and gave the following results:

	Millimeters	
Free	65.4	(1)
Water-cell	47.1	
Cover-glass	61.4	

On account of the shadow cast by a part of the water-cell mechanism, the deflections for the free radiation from the corona have been multiplied by a small factor which increased the observed value from 65.2 to 65.4 mm. These are the only deflections requiring this correction.

In order to compare the coronal light with integrated sunlight, a small auxiliary mirror of 47.7-mm diameter and 40.5-mm focal length was placed centrally over the 50.5-cm mirror of the telescope, the latter being covered. Under these circumstances, the sunlight intercepted by the small mirror was spread over a circle 115 cm in diameter at the thermocouple. The distribution of the radiation over the segment of the spherical surface illuminated by this mirror, its focus being at the center and the thermocouple at the surface of the sphere, was investigated and found to be essentially uniform, although this is not always true for small spherical mirrors of short focal length. The distance from the thermocouple to the focus of the mirror being 88.5 cm, it is easily shown that the reduction factor of the mirror is 22.07×10^{-4} times direct sunlight.

The measures of integrated sunlight were made when the sun had nearly the same altitude, 17°40′, that it had during the eclipse. The deflections were obtained by placing a diaphragm over the thermocouple which exposed one junction only and then rotating the mirror between fixed stops about an axis perpendicular to its optical axis. The logarithms of the deflections were plotted against air-mass, and the value for air-mass 3.29 (that for the sun at eclipse time) was read from the plot. The deflections thus obtained were as follows:

	Millimeters	
Free	57.2	(2)
Water-cell	40.8	
Cover-glass	56.2	

---

[1] *Journal of the Optical Society of America*, 10, 267, 1925.

Since double deflections were observed in the case of the corona, these values for integrated sunlight must be multiplied by 2 in computing the amount of energy radiated by the corona.

The moon was observed on January 21 at 6:15 and 6:30 A.M., the phase-angle being then 136°3. It was not possible to observe nearer full moon on account of the limits in hour-angle set by the window in the room where the telescope was placed. The deflections were made by setting the junctions each in turn upon the apparent center of the crescent. The logarithms of the deflections were plotted against air-mass, and the values corresponding to the sun's air-mass at eclipse time were obtained from these plots. The resulting deflections are:

	Millimeters	
Free	183.5	(3)
Water-cell	21.1	
Cover-glass	31.7	

The results (1), (2), and (3) give the transmissions shown in Table I. This table shows that while the spectral distribution of coronal radiation is very much like that of sunlight, the corona emits a little more radiation on the violet side of 1.3 μ than does the sun. The difference, however, is relatively small and will require data from future eclipses to determine its value accurately.

TABLE I

PERCENTAGE DISTRIBUTION OF ENERGY

	0.3 μ–1.3 μ	1.3 μ–5.5 μ	8 μ–14 μ
Corona	77.6	22.4	0.0
Sun	71.4	28.6	0.0
Moon (crescent)	12.5	6.6	80.9

Abbot,[1] at Flint Island, observed two points on either side of the sun, situated 4′ from the limb, a distance nearly the same as that of the points observed by us. One of these showed more radiation to the red of 1 μ and the other more to the violet of 1 μ than the sun. Whether these results, as compared with those obtained by us, indicate real differences in the corona or instrumental difficulties it is naturally impossible to decide.

---

[1] *Smithsonian Miscellaneous Collections*, **52**, Part I, 43, 1908.

From inspection of Table I it is patent, however, that there is no long-wave radiation beyond 5.5 μ. In future radiation measurements on the corona, glass or quartz windows can therefore be used on the measuring apparatus.

INTENSITY OF THE CORONAL RADIATION COMPARED WITH SUNLIGHT

We may compare the intensity of the coronal radiation or "surface brightness" of the corona at the points where the thermocouple junctions were placed with the intensity of direct sunlight by combining the data given under (1) and (2).

If, in making the observations on direct sunlight, the 50.5-cm mirror had been used with a diaphragm over it, having an aperture equal to the diameter of the image of the sun, and if the radiation were distributed uniformly over this image, the deflections observed would have been the same as those obtained on direct sunlight. The effect, then, of using the 50.5-cm mirror is to increase the deflections in the ratio of the exposed area of this mirror (1706 cm^2) to the area of the image of the sun (0.7156 cm^2). The ratio of the intensity of direct sunlight to the intensity of the image formed by the mirror is therefore 41.95×10^{-5}. Since the direct sunlight was weakened by spreading it over a large area by means of the small auxiliary mirror, this value must be multiplied by 22.07×10^{-4}, as has already been pointed out. This gives a total reduction factor of 9.26×10^{-7} to be used in comparing the deflections obtained from sunlight with those obtained from the corona.

The values of the deflections themselves from (1) and (2) are 65.4 mm for the free radiation from the corona and 114.5 mm for the free radiation from the sun, the latter including the factor 2 necessary to reduce to double deflections. From these data, we find that the ratio of the intensity of the coronal radiation to direct sunlight is 5.29×10^{-7}.

A correction must be applied to this quantity to allow for the fact that the cold receiver on the image of the moon received some energy from the corona scattered by our atmosphere and the telescope. The observed value is therefore too small, and from the investigation of the scattered light discussed later, it appears that the foregoing ratio should be increased by 2 per cent. The corrected value is therefore 5.40×10^{-7}.

From his observations at Flint Island in 1908, Abbot obtained the value 4×10^{-7} for the ratio of the radiation from points in the corona $4'$ from the moon's limb and in position angle 50° from the east and west points to that of sunlight. In making his comparisons, he used the 50.5-cm mirror with a small diaphragm so that the bolometer was set on an image of the sun. We determined the ratio of the intensity at the center of such an image to the mean intensity over it from drift curves made with a large image in the Pasadena Laboratory and found it to be 1.16. This must be applied as a factor to Abbot's value to make it comparable with that obtained by us. His result is therefore 4.6×10^{-7} for a point $4'$ from the moon's limb, while our value is 5.40×10^{-7} for a point $4\overset{'}{.}6$ from the moon's limb. Abbot's observations were made at the time of sun-spot maximum so that the corona was more uniformly distributed about the sun, while we observed near the east and west limbs of the sun at the time of sun-spot minimum, which will account for our somewhat greater value.

PHOTOMETRY OF THE CORONA

Plates XIII, XIV, and XV show the photographs of the corona made with the Ross lens. The first two are exposures of two seconds and fifteen seconds, respectively, on Seed 30 plates without filter, while Plate XV is an exposure of seventy-three seconds on an Ilford plate with red filter, the positive used for reproduction being shaded to bring out the detail of the inner corona. Plate XVI is from the same negative as Plate XV, but is reproduced without shading. The much greater contrast in Plates XV and XVI is striking.

These plates were placed successively on the registering microphotometer,[1] and series of deflections were recorded for each photometric square and for the unexposed strip. From these data a table was made giving the intensities corresponding to any deflection of the galvanometer of the microphotometer in terms of the intensity of the light which formed the densest square.

---

[1] *Mt. Wilson Contr.*, No. 246; *Astrophysical Journal*, **56**, 314, 1922; *Journal of the Optical Society of America*, **7**, 187, 1923.

The plates were then placed on a turntable which could be rotated beneath the photometer-microscope so that the slit, set perpendicularly to the moon's limb, described zones in the corona concentric with the image of the moon. The width of the zones was 0.16 solar radii, which was the length of a side of the square receiver of the thermocouple when projected upon the image of the sun in the field of the 50.5-cm mirror at the time of the eclipse.

Beginning at the limb, these zones were run contiguously. The upper part of Figure 1 shows a set of transmission curves obtained in this manner on the sixth, seventh, eighth, ninth, and tenth zones of the fifteen-second exposure. The scale of position-angles shown at the top of the figure was obtained with the aid of breaks made in each curve as the north point of the moon passed the photometer slit. The principal features of the corona can be traced in these curves by comparing the indicated position-angles (measured from the north toward the east) with Plates XIII, XIV, and XV. A transmission curve was also run with the photometer slit set in zone 2.33, the same as that occupied by the thermocouple junction during the eclipse. This we shall call the "standard-plate curve."

To translate the transmission curves into curves of intensity, deflections (ordinates) were read with the measuring machine for each 2 mm of abscissa. The intensities were then derived from the table of intensity against galvanometer deflection. Three such curves are shown in the lower part of Figure 1, two for the third and one for the eighth zone. The ordinates of these intensity curves are on an arbitrary scale and have had the correction for general sky-illumination subtracted from them, the constant for which was obtained from the study of the distribution of energy in the corona. It is evident that the intensity of the coronal radiation in the equatorial regions is more than twice that in the polar regions.

To find the mean intensity in each zone in terms of the intensity of the light which formed the densest square, the deflection curves were laid on co-ordinate paper, from which were read the mean ordinates for intervals of 5 mm, the corresponding intensities being taken from the table as before. The mean of these intensities for each curve is the mean intensity in the corresponding zone.

PLATE XIII

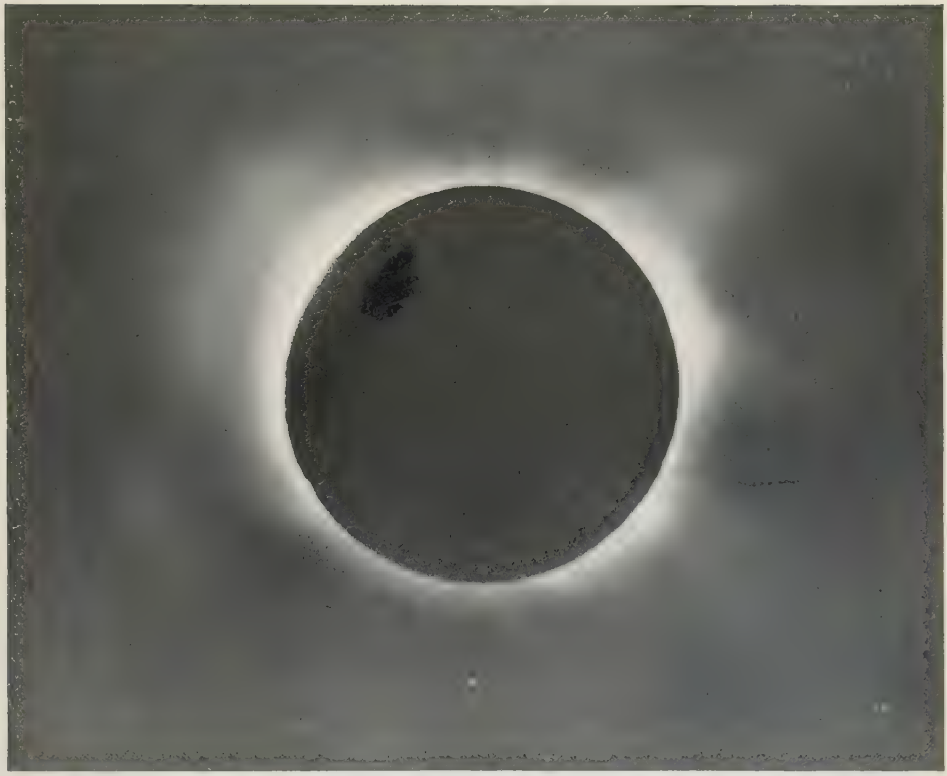

Solar Corona of January 24, 1925

Exposure of 2 seconds on a Seed 30 plate. Position of the sun's pole is 9° west of north

PLATE XIV

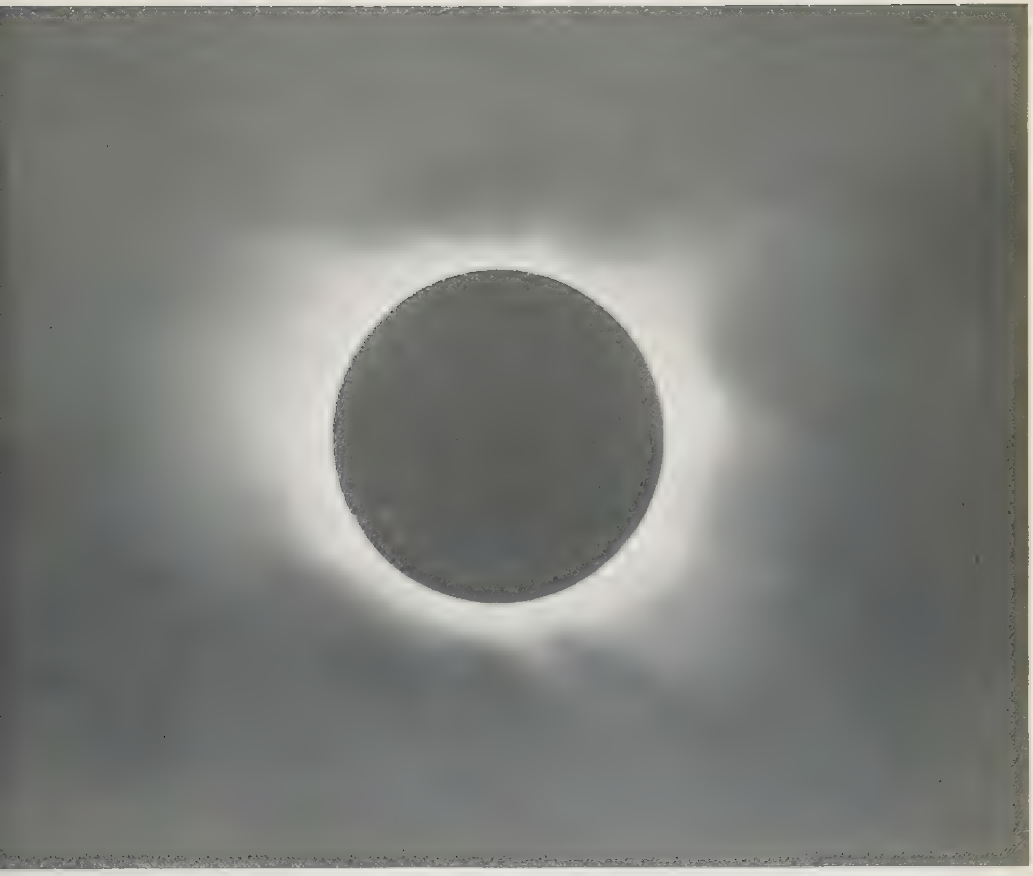

Solar Corona of January 24, 1925

Exposure of 15 seconds on a Seed 30 plate. Position of the sun's pole is 9° west of north

PLATE XV

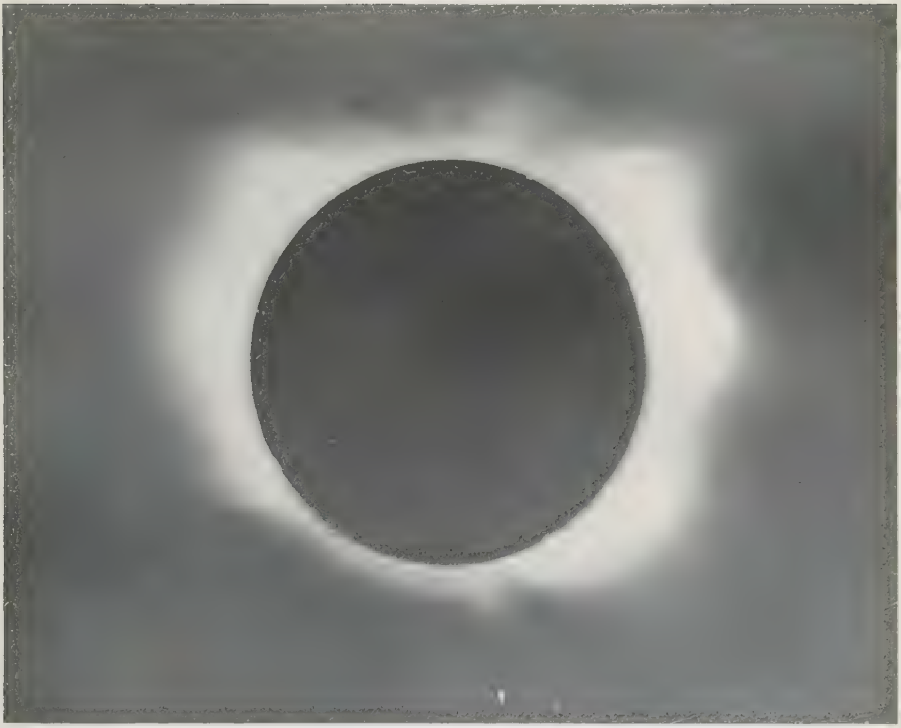

Solar Corona of January 24, 1925

Exposure of 73 seconds on an Ilford Panchromatic plate used with a red filter. The positive used for reproduction has been shaded to bring out the detail of the inner corona. The position of the sun's pole is 9° west of north.

PLATE XVI

N

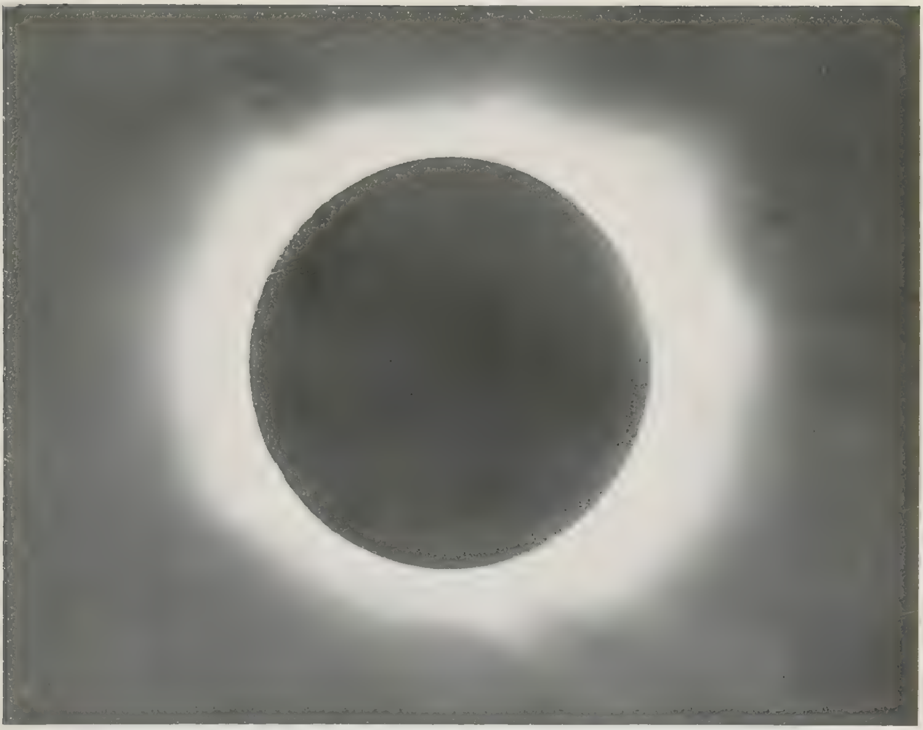

W

Solar Corona of January 24, 1925

The positive used for reproduction was made from the same negative as Plate XV, but without shading.

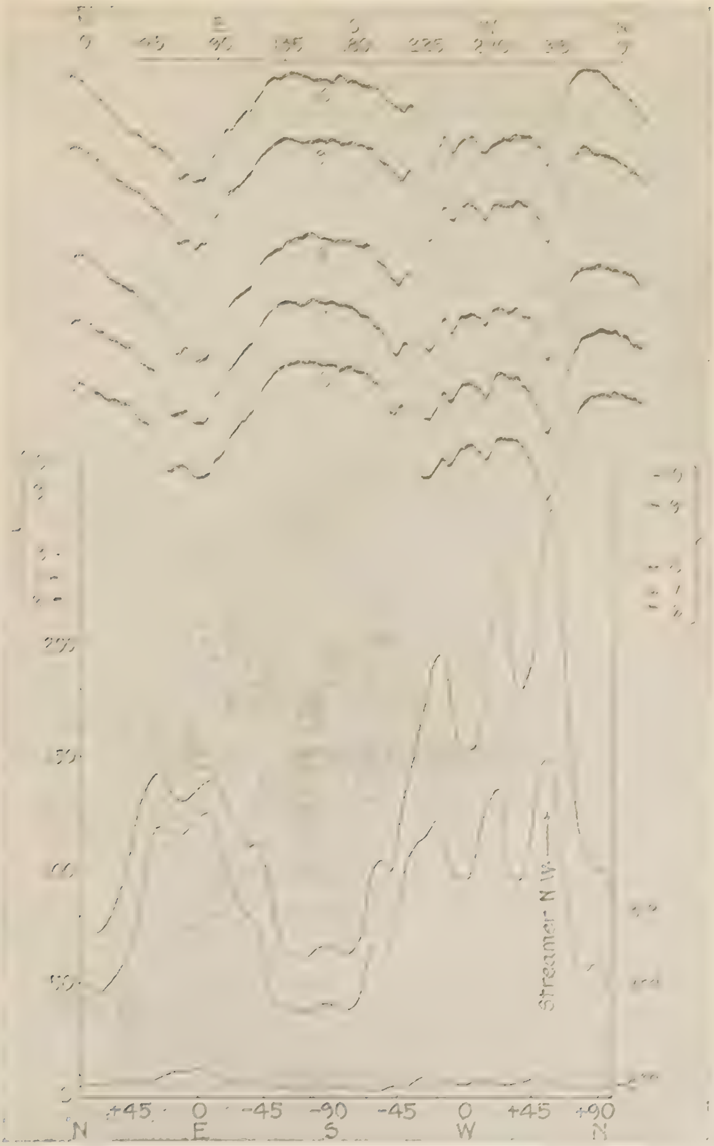

FIG. 1.—Transmission curves (above) for 15-second exposure on the corona (Plate XIV), showing variations in density with position angle for zones 6 to 10. The corresponding intensity curves for the third (75-second and 15-second exposures) and eighth (15-second) zones are shown below against a scale of latitudes.

BRIGHTNESS OF THE CORONA COMPARED WITH THE SUN AND THE FULL MOON

Before we can compare the brightness of the corona with that of the sun and moon, we must correct the measured intensities for general scattered light over the sky, most of which probably comes from sources outside the corona itself. This correction was taken to be equal to the mean intensity of the background of the plate measured at its four edges. This was found to be −0.040 on the two-second exposure, −0.020 on the fifteen-second exposure, and practically zero for the seventy-three-second plate taken through the red filter. That the correction for the two-second exposure is greater than that for the fifteen-second is probably due to the fact that it was taken immediately after second contact. The shadow had therefore just passed the observing station, and the sky was illuminated more strongly from without the shadow than during the fifteen-second exposure, which was taken later. In the case of the plate taken through the red filter, the scattering in those wave-lengths affecting the plate would naturally be very small.

TABLE II

MEAN INTENSITY FOR DIFFERENT ZONES OF THE CORONA CORRECTED FOR GENERAL SKY-ILLUMINATION AND HALATION

ZONE NUMBER	MEAN RADIUS	AREA, *A*	INTENSITY, *I*, SEED 30			*IA*	INTENSITY, *I*, ILFORD	*IA*
			2-Sec.	15-Sec.	Mean			
1	1.11	0.355	0.595	0.546	0.570	0.202	0.815	0.289
2	1.27	.406	.228	.269	.248	.100	.277	.112
3	1.43	.458	.111	.137	.124	.057	.126	.058
4	1.59	.509	.063	.068	.066	.033	.065	.033
5	1.75	.560	.039	.041	.040	.022	.031	.017
6	1.91	.611	.027	.027	.027	.016	.016	.010
7	2.07	.662	.019	.017	.018	.012	.008	.005
8	2.23	.714	.015	.012	.014	.010	.006	.004
9	2.39	.765	.010	.009	.010	.008	.004*	.003
10	2.55	.816	0.006	.007	.007	.006	.002*	.002
11	2.71	.867	....	.005	.005	.004	.001*	.001
12	2.87	.918	....	.004	.004	.004	.001*	.001
13	3.03	0.970	....	0.003	0.003	0.003	0.001*	0.001
						$\Sigma IA = 0.477$		0.536

* Computed from the seventh-power law (see Table IV).

A second correction must be applied to each zone because of halation. The values of this correction will be found in Table III, which was derived from a study of the law of scattering.

Applying these corrections to the observed intensities, we have the corrected intensities in the various zones for the three plates shown in Table II. The second and third columns give the mean radius and area of each zone in terms of the radius and area of the sun; the fourth, fifth, and sixth columns give the mean intensities in the zones obtained from the two Seed 30 plates and the mean for the two plates, while the eighth column gives similar data for the Ilford plate with red filter.

If we let I be the mean intensity in a zone, I_c the average of the two intensities at the east and west points on the standard-plate curve (the intensities at the two points in the corona occupied by the thermocouple junctions), and A the area of the zone in terms of the area of the sun, the total energy of the corona, E, in terms of sunlight is given by

$$E=\frac{5.40\times 10^{-7}\Sigma IA}{I_c}\ . \tag{4}$$

The values of IA found from the Seed 30 plates, and their sum, are given in the seventh column of Table II, while similar data for the Ilford plate are in the ninth column. For the Seed 30 plates, I_c was found to be 0.256, and for the Ilford plate, 0.271.

Substituting these values into equation (4), we find that the intensity of the coronal light in terms of the light from the sun is 10.1×10^{-7} for the Seed 30 plates, and 10.7×10^{-7} for the Ilford plate with red filter. Since these values are in good agreement, it appears that we are justified in applying the measurements of radiation with the thermocouple, which cover all wave-lengths emitted by the corona, to the photometric observations, which cover limited regions in the violet and red, respectively. Since, however, the Seed 30 plates cover a range of wave-length which is greater than that covered by the Ilford plates and is also nearer the region of maximum solar radiation, we shall adopt the value 10.1×10^{-7} in preference to the mean of the two results, as more nearly representing the energy measured by the thermocouple.

Since the radiation from the corona appears to have nearly the same spectral energy characteristics as sunlight, its absorption factors for the atmosphere will be nearly the same; hence we may apply the solar constant to the ratio of coronal light to sunlight to obtain the radiation of the corona outside the atmosphere. While no measurements of the solar constant are available for the first of the two days on which solar radiation was observed by us, its value has been inferred from results furnished by Dr. Abbot for a period of twelve days, including the eclipse day. From these data it seems very probable that the mean value of the solar constant for the two days was 1.91 cal. cm^{-2} min.^{-1} Applying this to the value of E adopted above, we have for the radiation from the corona, the sun being at mean distance,

$$E = 19.3 \times 10^{-7} \text{ cal. cm}^{-2} \text{ min.}^{-1} \tag{5}$$

According to Russell,[1] the visual light of the full moon is 21.5×10^{-7} times sunlight, both sun and moon being at mean distance. On account of the large number of observations used, which were more or less differential, this value should be free from the variability of solar radiation. Since the coronal radiation does not differ greatly from sunlight in spectral distribution, and since both corona and sun were observed at the same distance, the ratio of the coronal light to the light of the full moon at mean distance, for the visual region of the spectrum, is

$$\frac{\text{Corona}}{\text{Full moon}} = \frac{10.1 \times 10^{-7}}{21.5 \times 10^{-7}} = 0.47\ . \tag{6}$$

This agrees as well as can be expected with the provisional value 0.5 obtained visually by Professor Parkhurst[2] with an adaptation of the Hartmann microphotometer at this same eclipse.

At the eclipse of September 20, 1922, Briggs[3] determined the ratio of the brightness of the corona to the full moon, using two photo-electric cells. The values given by him are not reduced to mean distance, and since his comparisons were made at apogee, they are subject to a correcting factor of 1.11. It is also evident that the

[1] *Astrophysical Journal*, **43**, 125, 1916.

[2] *Publications of the Astronomical Society of the Pacific*, **37**, 85, 1925.

[3] *Astrophysical Journal*, **60**, 280, 1924.

first two mean intensities given in the sixth column of Table III of his paper should be reduced to full phase, and further, that the mean of the three determinations would probably give a better standard than the last value alone. Using the data given by Russell[1] to correct to full phase, and applying the factors 0.981 and 0.967 to reduce them to the distance of the sun at eclipse time, we find from Briggs's observation that the values of the brightness of the moon at "no atmosphere" are 2.19, 2.13, and 2.18 candle-meters. If we adopt the mean of these, 2.17, the value for the moon at mean distance would be 2.41 candle-meters and the mean of Briggs's six determinations for the ratio of the corona to the full moon at that eclipse becomes 0.33.

Kunz and Stebbins,[2] observing with the photo-electric cell, obtained the value 0.50 at the eclipse of June 8, 1918.

At least a portion of the differences between these results can be accounted for by the overlapping of the moon on the inner corona. In order to examine this effect it will be necessary to determine the law of radial distribution of energy within the corona.

DISTRIBUTION OF ENERGY IN THE CORONA

In studying the distribution of energy in the corona, it is necessary to correct the observed intensities for scattered light originating in the corona itself and also in the film of the plate in the form of halation. To determine these corrections, transmission curves were registered diametrically across the moon's image in position-angles 0° and 90°. Deflections were also registered for the transmission at the edge of the plate where the general sky-fog alone was effective.

The amount of scattered light on a given region of the image is evidently not constant, as Bergstrand[3] and others have assumed, but is greater over the brighter parts than over the fainter regions. To find the law of distribution of the light scattered from the corona, it was first assumed that the density at the edges of the plate is wholly due to general sky-illumination not originating in the corona. The intensity represented by this density was then subtracted from all other measured intensities. It was then assumed that the effects of halation did not extend beyond 6 mm from the image of the limb of the moon. The remaining intensities across the moon were taken to represent light scattered from the corona.

---

[1] *Ibid.*, **43**, 125, 1916.

[2] *Ibid.*, **49**, 151, 1919.

[3] *Études sur la Distribution de la Lumière dans la Couronne Solaire* (Stockholm, 1919), p. 28.

The problem which then presented itself is analogous to that arising in the study of the law of radiation along a diameter of the sun. From observations made with the 150-ft. tower telescope it was found that the light scattered from the sun upon any point outside the limb where this law can be tested is represented by assuming that the amount contributed by any small area of the disk to any other small area may be expressed by the empirical formula:

TABLE III

CORRECTIONS FOR SCATTERED CORONAL LIGHT AND HALATION

Zone Number	Seed 30		Ilford
	C	*H*	*H*
1	0.032	0.025	0.100
2	.027	.011	.015
3	.017	.004	0.000
4	.012	.002	....
5	.009	0.000	....
6	.006	....	....
7	.004	....	....
8	.004	....	....
9	.004	....	....
10	.004	....	....
11	.003	....	....
12	.003	....	....
13	0.003	....	....

$$\Delta C=\frac{kI\Delta A}{r^2+Z}\,. \tag{7}$$

As applied to the corona, ΔC is the amount of light scattered from a small area ΔA, at a distance r. The constants k and Z were varied until the amount of scattered light calculated by the integration of equation (7) agreed as well as possible with that observed over the region of the moon not affected by halation. With the intensity of the light producing the densest square as unity, the corrections for points situated in the middle of each zone arising from scattered light from the whole corona are as given in Table III. The correction H for halation, found by subtracting the intensities of the scattered light across the moon from the total intensities, is also given in Table III.

Table IV shows the resulting mean intensities in the various zones for each plate, corrected for scattered light and halation by Table III, and also for general sky-illumination as in Table II.

TABLE IV

MEAN INTENSITY FOR DIFFERENT ZONES OF THE CORONA CORRECTED FOR GENERAL SKY-ILLUMINATION, HALATION, AND SCATTERED CORONAL LIGHT

ZONE NUMBER	MEAN RADIUS	I, SEED 30 PLATES, $\lambda=4500$ A				I, ILFORD, $\lambda=6500$ A	
		2-Sec.	15-Sec.	Mean Obs.	Comp.	Obs.	Comp.
1	1.11	0.563	0.514	0.538	0.502	0.815	0.781
2	1.27	.201	.242	.221	.223	.277	.304
3	1.43	.094	.120	.107	.109	.126	.131
4	1.59	.051	.056	.054	.058	.065	.063
5	1.75	.030	.032	.031	.033	.031	.032
6	1.91	.021	.021	.021	.019	.016	.017
7	2.07	.015	.013	.014	.012	.008	.010
8	2.23	.011	.008	.010	.007	.006	.006
9	2.39	.006	.005	.006	.005	....	.004
10	2.55	0.002	.003	.003	.003	....	.002
11	2.71	....	.001	.001	.002	....	.001
12	2.87	....	.001	.001	.002	....	.001
13	3.03	....	0.000	0.000	0.001	....	0.001

As before, the mean radius of each zone is expressed in terms of the sun's radius. The fifth column gives the mean intensity as determined from the two Seed 30 plates, and the sixth column the corresponding intensities calculated from

$$I=\frac{I_0}{R^6}, \tag{8}$$

where I is the mean intensity at any point in the corona situated a distance of R solar radii from the center of the sun, and where $I_0=0.920$ is the intensity at the limb of the sun. The seventh column gives the mean intensities derived from the Ilford plate with red filter, and the eighth column, values computed from

$$I=\frac{I_0}{R^7}, \tag{9}$$

where $I_0 = 1.581$. The data from Table IV are plotted in Figure 2, the abscissae being distances from the center of the sun in solar radii, and the ordinates, the energy in units of the light which produced the densest square. The circles represent the observed intensities from the Seed 30 plates, and the full-line curve those calculated from the inverse sixth-power formula (8). The crosses indicate the observed intensities from the Ilford plate with red filter, while the dotted curve represents the inverse seventh-power formula (9).

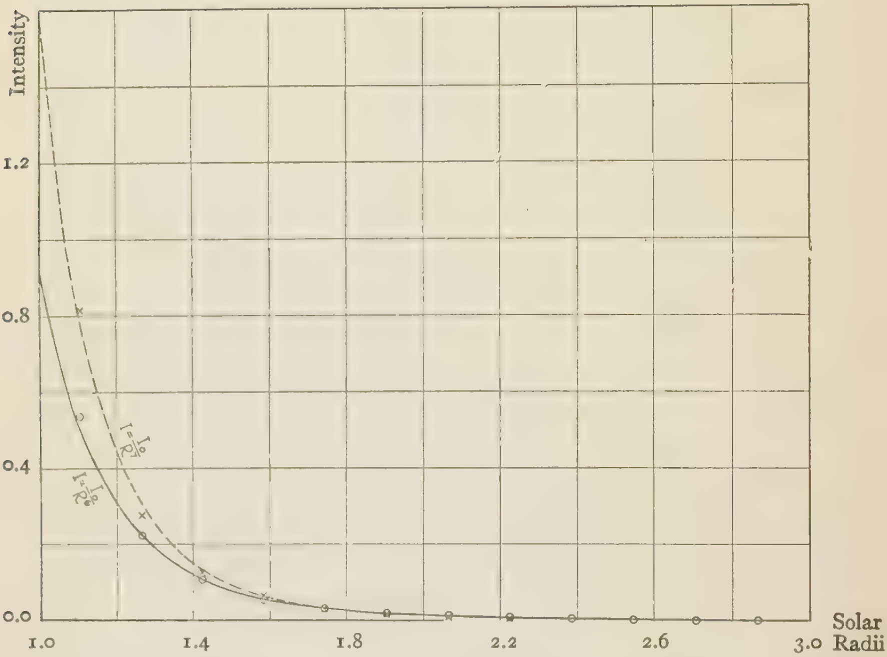

FIG. 2.—Variation of mean intensity of corona with distance from the sun's center. Circles represent measures on Seed 30 plates; crosses, measures on the Ilford panchromatic plate exposed with red filter.

If we correct the value of I_c used in equation (4) for scattered light (0.024) by Table III and use the value of the solar constant reduced to mean distance, the energy emitted from a square minute of arc of the corona at mean distance may be obtained from equation (8) by using the constant $I_0 = 0.050 \times 10^{-7}$ cal. cm^{-2} min.$^{-1}$ For equation (9), $I_0 = 0.073 \times 10^{-7}$ cal. cm^{-2} min.$^{-1}$

Since the intensity of the blue light (λ 4500) varies inversely with the sixth power of the distance from the sun's center, and of the red light (λ 6500) inversely with the seventh power, it follows that the ratio of blue light to red light varies directly with the distance from the sun's center. In other words, the corona becomes bluer as we go outward from the sun, or redder as the sun's limb is approached. This is not what we should expect from an atmosphere of incandescent particles around the sun, since the temperature of the particles should increase toward the sun, thus causing the proportion of blue radiation to increase in the opposite manner to that observed. Molecular scattering of sunlight or luminescence from electrical discharges would probably produce effects in accord with what we find.

Both Turner[1] and Schwarzchild[2] have deduced the inverse sixth-power law from photographic observations, although others[3] have obtained formulae ranging from the inverse square to the inverse eighth power, with modifications of the origin of co-ordinates. In discussion of observations with the photo-electric cell, probably the inverse sixth-power should be used; but for visual light, a slightly higher power should be applied, although the effect on the results will be small, quite beyond the accuracy of the determinations. Since the maximum of solar energy lies in the region of wave-lengths covered by the Seed 30 plates, the inverse sixth-power law is adopted for the following discussion, which relates to the measures of total radiation with the thermocouple.

We may express the energy emitted by that portion of the corona projecting beyond a disk of radius r concentric with the sun by the integral

$$E=I_0\int_0^{2\pi}\int_r^{\infty}\frac{r\,dr\,d\theta}{r^6}\,. \tag{10}$$

The value of this integral is

$$E=\frac{\pi I_0}{2r^4}\,. \tag{11}$$

At the time of eclipse, a square solar radius equaled 830 square minutes of arc. Using $I_0=0.050\times 10^{-7}$ cal. cm^{-2} min.$^{-1}$ per square minute of arc and $r=1$, we find

---

[1] *Popular Astronomy*, **14**, 548, 1906.

[2] *Astronomische Mitteilungen der Königlichen Sternwarte zu Göttingen*, **13**, 1906.

[3] Mitchell, *Eclipses of the Sun*, p. 342.

$$E=20.9\times 10^{-7} \text{ cal. cm}^{-2} \text{ min.}^{-1} \tag{12}$$

This is the radiation outside the earth's atmosphere for the whole corona at mean distance. We must correct the value of E obtained in equation (5) for the overlapping of the moon before comparing it with equation (12).

From equation (11) it follows that the factor c, which reduces the observed radiation from the corona to its total value, is given by

$$c=\left(\frac{R}{r}\right)^4 , \tag{13}$$

where r is the apparent radius of the sun, and R the apparent radius of the overlapping moon as seen from the eclipse station. For Middletown, this factor was 1.107. When this factor is applied, the value of E from equation (5) becomes

$$E=21.4\times 10^{-7} \text{ cal. cm}^{-2} \text{ min.}^{-1} , \tag{14}$$

which agrees well with equation (12).

Applying the factor 1.107 to the ratio of coronal light to full-moon light given in equation (6) we find

$$\frac{\text{Whole corona}}{\text{Full moon}}=0.52 . \tag{15}$$

It is interesting to note in this connection that the maximum correction for overlapping moon is 1.38, or 0.35 magnitude, that the surface brightness of the corona at the sun's limb on the equator is about 1.4 times as great as the visual brightness of the full moon, and that one-half the light of the corona comes from a zone extending only 3′ from the limb of the sun.

The factors which correct the observations of Kunz and Stebbins on June 8, 1918, and of Briggs on September 20, 1922, for overlapping moon are 1.100 and 1.245, respectively. Applying these factors, we obtain the results in Table V, which shows the ratios of the whole corona to full moon and the radiation emitted in cal. cm^{-2} min.$^{-1}$ The last column gives the corresponding solar constant.

Probably the material is insufficient to warrant generalizations, but Table V suggests that the total light of the corona has not varied much during the last seven years at least, and that such variation as is shown is in harmony with the variation in the solar constant, although of greater amplitude.

DETECTION OF THE CORONA WITHOUT AN ECLIPSE

The principal difficulty presented by the problem of detecting the corona without an eclipse is not that the amount of energy to be measured is itself small, but rather that it has superposed upon it the enormously greater illumination near the sun produced by scattering in our atmosphere and in the telescope. No measurements of this scattered light have been made with the apparatus used at the eclipse, but observations with the 150-ft. tower telescope under the best conditions on Mount Wilson showed that its value at the limb of the sun is about 2.5 per cent of the mean over the disk. Probably the elimination of the fixed mirror and lens might reduce this value to 1.5 per cent.

TABLE V

RADIATION FROM THE WHOLE CORONA

Eclipse	Observers	$\frac{\text{Whole Corona}}{\text{Full Moon}}$	Radiation $\text{Cal. Cm}^{-2}\text{ Min.}^{-1}$	Solar Constant $\text{Cal. Cm}^{-2}\text{ Min.}^{-}$
June 8, 1918......	Kunz and Stebbins	0.55	22.8×10^{-7}	1.94
Sept. 20, 1922.....	Briggs	.41	16.5×10^{-7}	1.89
Jan. 24, 1925......	Pettit and Nicholson	0.52	21.4×10^{-7}	1.93

Since the scattered light varies less rapidly than the coronal light with the distance from the center of the sun, it follows that the most advantageous place for measurement is near the limb of the sun. Here, the intensity of the coronal light is 1.5×10^{-6} of the mean over the disk. In other words, the scattered light is approximately ten thousand times the intensity of the coronal light.

Suppose, now, that we explore the region about the sun by revolving one junction of a thermocouple at a fixed distance from the limb, while the other remains at a fixed point in the orbit of the first junction. The variations in the corona are 50 per cent of its intensity in the equatorial regions, as may be seen from the intensity curves in Figure 1. Hence, if we assume that the scattered light is constant, the total variation in the observed radiation, scattered light plus corona, will be one-twenty thousandth (5×10^{-5}) of its value. It is probable that the changing transmission of the atmosphere, changing distance of the thermocouple junction from the limb of the sun due to mechanical difficulties, bad seeing, and other sources of error would produce, from second to second, variations in the observed radiation greater than this value.

As no measurements of the sky-radiation at the limb of the sun free from instrumental scattering are available, it is not possible to estimate how small the intensity of the scattered light near the sun can be made; hence definite judgment in the matter must be deferred until such measurements are at hand. Unless the amount of scattering can be reduced to at least 1 per cent of the value assumed here, there is little hope of detecting the corona without an eclipse by any radiometric method, for the distribution of the coronal light is, apparently, nearly like that of the sun, so that screens or dispersion apparatus will be of no avail.

CONCLUSIONS

Our observations show that:

1. At the eclipse of January 24, 1925, the intensity of the coronal radiation at points 4ʹ.6 from the east and west points of the moon's limb was 5.40×10^{-7} of the integrated solar radiation.

2. The energy to the violet of $1.3\,\mu$ is somewhat greater in coronal radiation than in sunlight, although the difference is small.

3. The long-wave radiation in the corona beyond $5.5\,\mu$ is inappreciable, so that glass or quartz windows may be used on the radiation apparatus.

4. The light from the visible corona was one-millionth (10.1×10^{-7}) as great as sunlight, and 0.47 that of the full moon at mean distance. When corrected for overlapping moon, these values become 11.2×10^{-7} and 0.52, respectively, or 21.4×10^{-7} cal. cm^{-2} min.$^{-1}$

5. There is some evidence that the amount of coronal light varies with the solar constant, but with greater amplitude. Should this prove to be true, the light from the corona cannot be reflection or radiation from solid or liquid particles, for in that case its variations

would have the same amplitude as variations in the solar radiation.

6. The intensity of the radiation emitted by a point in the corona as determined from the Seed 30 plates varies inversely as the sixth power of the distance from the center of the sun.

7. The ratio of the amount of blue light to that of red light varies directly with the distance from the center of the sun, that is, the inner corona is redder than the outer corona. This is what may be expected if the coronal light arises from luminescence, or from molecular scattering in a gaseous atmosphere, but is opposed to the theory involving solid or liquid particles.

8. The difference between the radiation of the whole corona and that observed outside the moon's limb may be as much as 0.38 magnitude.

9. The surface brightness of the corona at the limb of the sun is about 1.4 times that of the full moon, and half the light of the corona comes from a zone extending only 3′ from the limb of the sun.

10. It is not likely that the corona can be detected without an eclipse by radiometric methods unless the scattered light near the sun can be reduced to about one-hundredth that observed on Mount Wilson.

Mount Wilson Observatory
June 1925

NOTE ADDED OCTOBER 7, 1925

Measurements of the coronal radiation transmitted by one centimeter of glycerine made by Stetson and Coblentz at the eclipse of January 24, 1925, this *Journal*, September, 1925, p. 128, differ radically from our measurements of the radiation transmitted by one centimeter of salt water. Since the transmissions of salt water and glycerine are approximately the same, it seems advisable to show the original photographic record of the galvanometer deflections. Figure 3 is a reproduction of the negative taken with the photographic registering device, three-fourths the original scale. The full-line arrows indicate the deflections as measured, while the dotted arrow in *B* indicates, on the same scale, the deflection corresponding to the transmission observed by Stetson and Coblentz on the west side of the sun. Their value of the ratio of transmitted to total energy is approximately one-third that found by us.

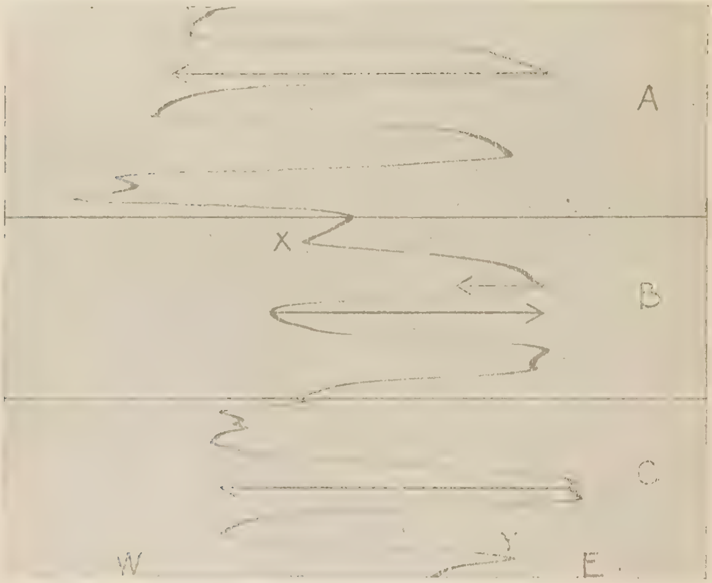

FIG. 3.—Galvanometer deflections measuring coronal radiation: *A*, total energy; *B*, water-cell transmission; *C*, cover-glass transmission. Deflections marked *X* and *Y* have been rejected as obviously defective. The letters *E* and *W* indicate that, at the time the corresponding deflections were made, the hot junction of the compensated thermocouple was on the image of the corona east and west of the moon, respectively, $4\overset{\prime}{.}6$ from the limb.

Contributions from the Mount Wilson Observatory, No. 300
Reprinted from the *Astrophysical Journal*, Vol. LXII, pp. 270–300, 1925

THE LAW OF SUN-SPOT POLARITY

By GEORGE E. HALE and SETH B. NICHOLSON

ABSTRACT

Magnetic observations of sun-spots.—The magnetic polarities of about 2200 sun-spot groups, observed on Mount Wilson between 1908 and 1925, are discussed in this paper. The polarities and approximate field-strengths are determined by daily observations of the Zeeman triplet λ 6173 in the second-order spectrum of the 75-foot spectrograph of the 150-foot tower telescope. *Invisible spots* and the method of observing them are also described. A *revised scheme of magnetic classification* of sun-spots, grouped as unipolar, bipolar, and complex, is described, and many individual cases are discussed and illustrated. Tables I, II, IV, and V give the magnetic classification of 2174 spot groups, the percentage and frequency of the groups of each class, and the magnetic classification of the groups at formation.

Law of sun-spot polarity.—Discussion of the polarities of spots belonging to the last three 11½-year cycles leads to the following law, which represents all of the observations with only 41 exceptions out of 1735 groups:

The sun-spots of a new 11½-year cycle, which appear in high latitudes after a minimum of solar activity, are of opposite magnetic polarity in the northern and southern hemispheres. As the cycle progresses the mean latitude of the spots in each hemisphere steadily decreases, but their polarity remains unchanged. The high-latitude spots of the next 11½-year cycle, which begin to develop more than a year before the last low-latitude spots of the preceding cycle have ceased to appear, are of opposite magnetic polarity.

Thus while the well-known 11½-year interval correctly represents the periodic variation in the number or total area of sun-spots, the full sun-spot period, corresponding to the interval between the successive appearances in high latitudes of spots of the same magnetic polarity, is 23 years. This may be called the "magnetic sun-spot period," to distinguish it from the 11½-year frequency period.

In a previous paper[1] we have described our methods of determining the magnetic polarity and field-strength of sun-spots and the magnetic classification of 970 spot groups observed during the years 1915–1917. We have also called attention to the remarkable reversal of magnetic polarity observed at the advent of the spots of a new 11½-year cycle in 1912, and indicated that at the conclusion of this cycle the law of sun-spot polarity should become apparent. As our observations from 1917 to 1924 have fully confirmed the earlier ones, showing at a second sun-spot minimum a general reversal of polarity corresponding to that which occurred in 1912, we are now in a position to formulate a polarity law, the validity of which can be tested in future cycles of solar activity. Brief summaries of our conclusions have already been published,[1] but without the detailed results given in the present paper. This also includes a revised outline of our scheme of classification and a discussion of various special cases which emphasizes the necessity of using a rational method of grouping sun-spots with respect to their magnetic polarities and the distribution of the accompanying flocculi.

---

[1] Hale, Ellerman, Nicholson, and Joy, "The Magnetic Polarity of Sun-Spots," *Mt. Wilson Contr.*, No. 165; *Astrophysical Journal*, **49**, 153–178, 1919.

METHOD OF OBSERVATION

The method of observation which has been used to determine the magnetic polarities and field-strengths of about 2200 spot groups during the period 1908–1925 is fully described in the article mentioned and may be briefly recapitulated here. The 150-foot tower telescope on Mount Wilson forms an image of the sun about 16.5 inches (43 cm) in diameter on the slit of a spectrograph of 75 feet (22.9 m) focal length, mounted vertically in a well beneath the tower. The iron line λ 6173.553 is observed daily in the spectra of all spots, large and small, comprised in the various groups present on the sun. In a magnetic field this line is a triplet, and the polarity of the spot in question is determined by noting visually which of the n-components, R (to the red) or V (to the violet), is transmitted by a given strip of a compound quarter-wave plate, used in connection with a Nicol prism above the slit of the spectrograph. The distance between the R- and V-components, measured with a micrometer, gives the approximate field-strength at the corresponding point in the spot. This is expressed in units of 100 gausses. Thus V_{17} means that the violet component is transmitted, and hence that the polarity of the spot is "south" (south-seeking pole) or negative, while the field-strength is approximately 1700 gausses.[2]

These observations are entered on a pencil sketch of the solar image and its spots, made by tracing their outline on a large sheet of paper supported above the slit at the focus of the tower telescope.

---

[1] For these preliminary accounts see *Nature*, **113**, 105–112, 1924, and *Proceedings of the National Academy of Sciences*, **10**, 53–55, 1924.

[2] We now give polarities as "north" and "south" instead of "positive" and "negative," because several writers have supposed the latter terms to refer to positive and negative charges in the corresponding spots, in spite of the fact that our papers have given no evidence to support such an assumption.

Drawings on wax are being made from these for reproduction on a smaller scale in a volume which will give our complete magnetic record of sun-spots for the period 1917–1925. One of these drawings is shown in Figure 1. In order that the polarity in various parts of the larger spots may be distinguished at a glance, the regions that have "south" polarity are covered with small crosses, while those of "north" polarity are dotted.[1]

In the detection of the very weak fields that betray the existence of invisible spots (see p. 10), an auxiliary half-wave plate, oscillated back and forth across the slit by means of a small electric motor, is used to cause the slight widening of the line to appear alternately toward red and violet, thus rendering the effect more readily visible.

Certain precautions necessary in the determination of polarities are mentioned in the paper cited, and need not be repeated here. In general, the angle between the lines of force and the sun's surface decreases from about 90° near the center of the umbra to about 0° near the edge of the penumbra. For this reason, polarity observations near the limb are difficult for large spots and impossible for small ones.

In the designation of spot groups it has not been possible to use the Greenwich serial numbers, partly because of the interruption in their publication during the war, and also because our magnetic scheme must frequently combine in a single group spots that would otherwise be classed separately, or vice versa. Our spot positions, however, are only roughly approximate, and serve merely for purposes of identification. The Greenwich measures should be substituted for them in all work involving accurate heliographic positions.

THE MAGNETIC CLASSIFICATION OF SUN-SPOTS

In our magnetic system, spot groups are divided into three classes, distinguished here as "unipolar," "bipolar," and "complex" (formerly called "multipolar").

Unipolar groups are single spots or groups of spots of the same magnetic polarity. The three subdivisions of this class are deter-

---

[1] Through an unfortunate error, which for some unaccountable reason was not detected until about 300 of the engravings had been completed for the printer, the crosses (which resemble plus signs) were shown in the regions of south or negative polarity, instead of in those of north or positive polarity, as originally intended.

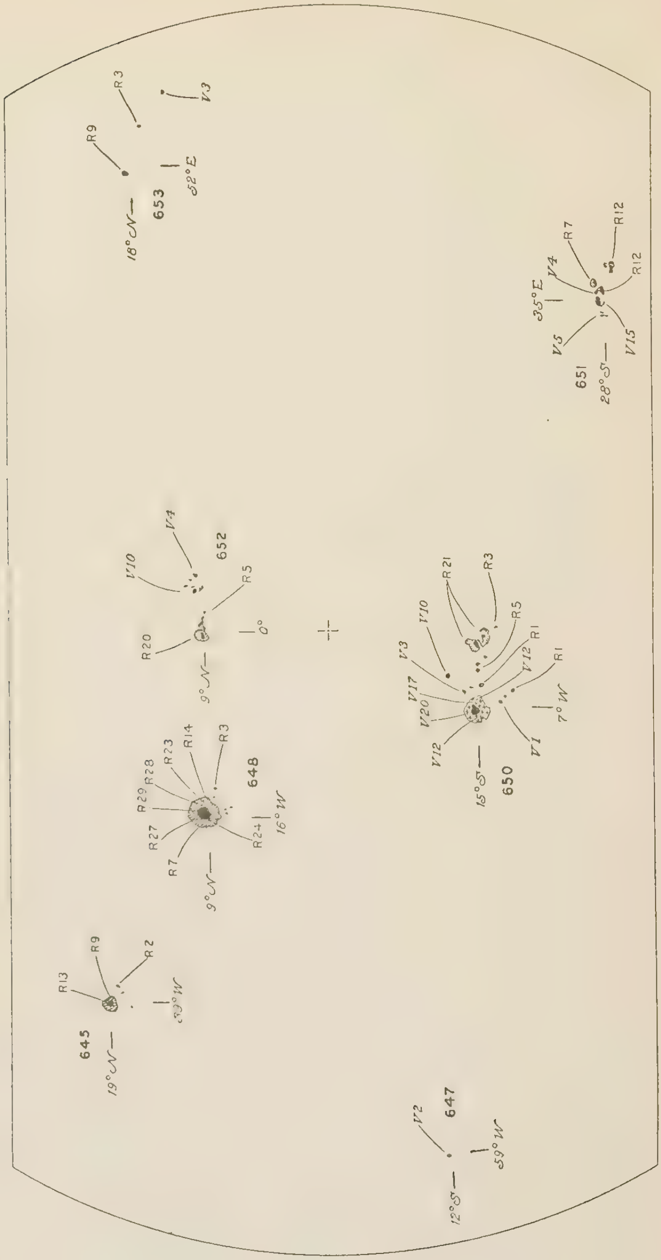

FIG. 1.—Record of sun-spot polarities, May 14, 1917

mined by the position of the group with respect to the surrounding calcium flocculi: (α) those for which the distribution of the flocculi preceding and following the group is fairly symmetrical; (αp) those which are followed by a distinctly elongated mass of flocculi; (αf) those which are preceded by a distinctly elongated mass of flocculi.

Bipolar groups consist, in their simplest form, of two spots of opposite polarity, the line joining them generally making a small angle with the solar equator. Usually, however, the bipolar group consists of a stream of spots, of opposite polarity in the preceding and following parts. The change in polarity is generally near the center of the stream, but it may be on either side of the center. Bipolar groups are subdivided as follows in accordance with the area and distribution of their constituent magnetic fields: (β) those in which the preceding and following members, whether single or multiple, are approximately equal in area; (βp) those in which the preceding member is the principal component of the group; (βf) those in which the following member is the principal component of the group; and ($\beta\gamma$) those in which the bipolar characteristics are shown, but with no clearly marked dividing-line between the groups of opposite polarity. This includes cases where the preceding or following members are accompanied by small spots of opposite polarity.

Rigorously defined, the principal component of a bipolar group, whether single or multiple, is that for which the total integrated field-strength is the greater. In daily practice it would be almost impossible to make a sufficient number of measures of field-strength and area to determine this quantity accurately. Up to a certain area, the field-strength is almost directly proportional to the diameter of the spot, with its maximum intensity near the middle of the umbra, decreasing to zero just beyond the outer edge of the penumbra. But when the spot is split into several members, the maximum field-strength in any one of them is less than that shown by an unbroken spot. Accordingly, in a bipolar group consisting of a large single spot followed by several smaller spots having the same total area, the preceding spot would be regarded as the principal component. The integrated field-strength as thus estimated, not actually measured, is sufficient for classification.

Groups αp and αf are frequently accompanied by invisible spots, or local magnetic fields, in the place of the absent component. These do not appear in the tabulated classification, however, because of the difficulty of detecting invisible spots, especially when the definition of the sun's image is poor.

Complex groups are those in which the polarities are so irregularly distributed that they cannot be classified as bipolar. Their number is small but includes some of the largest and most active spot groups. As already noted under bipolar groups, the presence of occasional small companions, which play a minor part in these or in unipolar groups, is disregarded in their classification.

In distinguishing these various classes and their subdivisions, it is thus evident that the daily observations of the Zeeman effect in spot spectra must be supplemented by photographs of the calcium flocculi. Even with both of these guides it is sometimes difficult to assign the numerous spots in crowded regions of the sun to their respective groups. To make this clear and to illustrate the danger of grouping spots without these aids, we give a number of illustrations of various deceptive cases drawn at random from our records. Because of the peculiar significance of bipolar groups, of which all spots may be regarded as variants, it will be advantageous to discuss them first.

BIPOLAR GROUPS

The fundamental importance of bipolar groups, on which our scheme of classification rests, has been greatly emphasized by the continued accumulation of observational data, the discovery of invisible spots, and the life-history of spots of various types. As we have stated, bipolar groups often consist of long streams of spots, comprising many members, and betraying no evidence in the direct telescopic image of subdivision into two distinct groups of opposite polarity. The application of the spectroscopic test instantly discloses the magnetic distinction between the constituent spots and the overwhelming tendency of those of like polarity to cluster together at opposite ends of the stream. It is quite unsafe, however, to apply the term "bipolar group" to paired spots or to binary groups of small spots, as some solar observers have done without testing the polarities. An examination of certain typical groups will make this point clear.

A simple bipolar group, with widely separate components, is No. 2091, August 18, 1924, illustrated in Figure 2. Here we see two nearly equal spots at 15° and 18° N. latitude, opposite in polarity, and with field-strengths *V* 2400 and *R* 2000 gausses, respectively. No distinct companions are present, but on August 17, and again on August 20, a small spot was observed between the principal members. It was easy to recognize these widely separated spots as the members of a single bipolar group, not merely because of their opposite polarity but also because of the distribution of the flocculi between them.

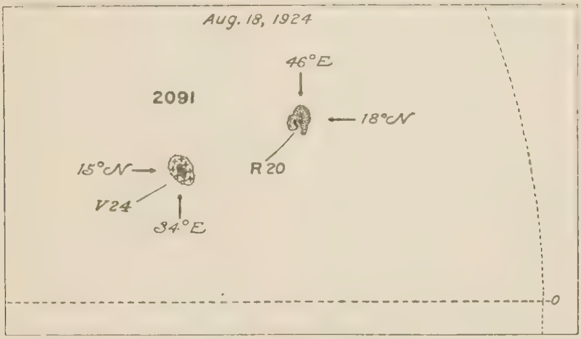

FIG. 2.—Simple bipolar group with widely separated components. No. 2091, August 18, 1924.

These spots are much more widely separated than the components of most simple bipolars, but even longer groups sometimes occur, the members of which, without spectroscopic tests, might be classified as separate spots. In most bipolar groups or streams many small spots are present, and the consistency with which the components of the eastern and western parts of the streams agree in polarity is very striking. A good example may be taken from the polarity record of June 19, 1917, which also affords several other typical instances of spot classification.

The bipolar group No. 687 stood centrally in the midst of a large aggregation of spots, easily separated into three magnetic groups (Fig. 3, No. 5). Its leading member appeared at the east limb on June 14 at 12° N. latitude, when its preceding edge was recorded as R_3 and its umbra as $(R+V)_{15}$. This appearance in the same spot of both *n*-components, as explained in our previous article, was due to the fact that the observation was made with Nicol and quarter-wave plate on the umbra near the limb, where the line of sight was nearly at right angles to the lines of force. On the following day the whole group was visible, the leading component recorded as R_{17} and

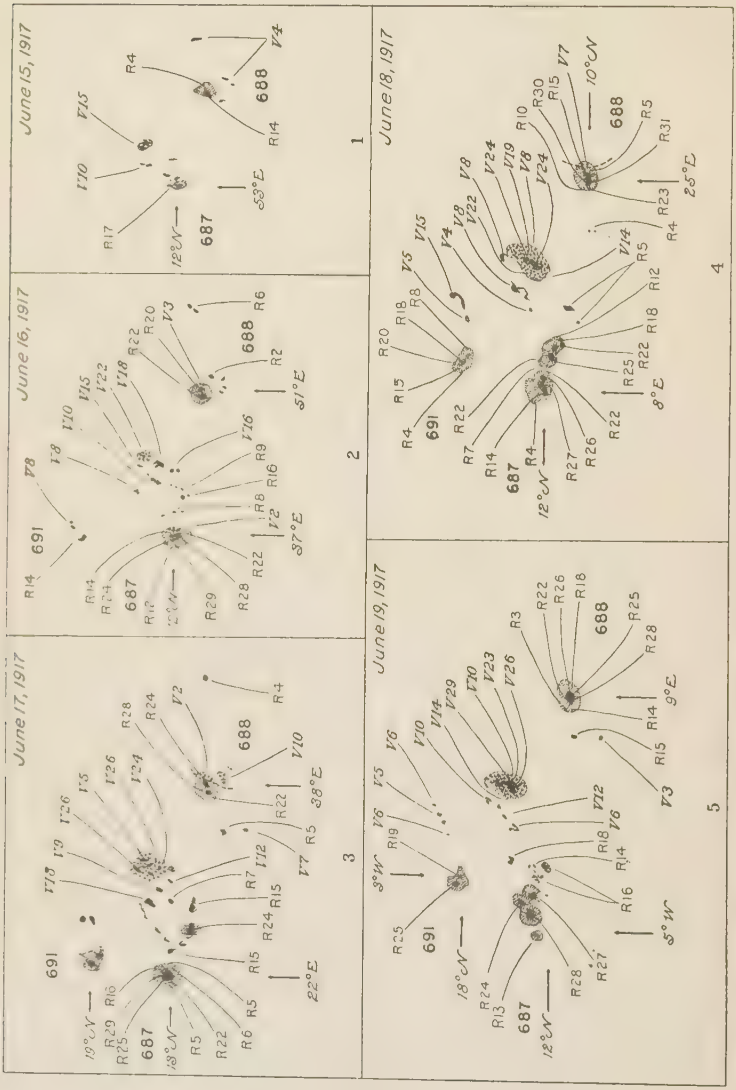

FIG. 3.—Magnetic polarities of the spot groups Nos. 687, 688, and 691, June 15–19, 1917

the two following components as V_{10} and V_{15}, respectively (Fig. 3, No. 1). A few minor companions were also present. Following this bipolar group about 2° S. and 14° E. was another group (No. 688) with a preceding member R_{14}, followed by some small V-companions. On June 16 group No. 687 contained many spots, all of the western ones recorded as R, and all of the eastern ones as V, the dividing-line being near the center of the stream. Another small bipolar group (No. 691) had appeared at 18° N. latitude, its preceding member R_{14} and its following member V_8. On June 17, as Figure 3, No. 3, shows, both Nos. 691 and 687 had many constituents, but the consistent distribution of their polarities leaves no doubt regarding their correct classification as bipolar groups. No. 688 is obviously a separate group, but its classification is less certain, as it was preceded and followed at various times in its career by small companions, both R and V. The subsequent appearance of these groups is shown in Figure 3, Nos. 4 and 5.

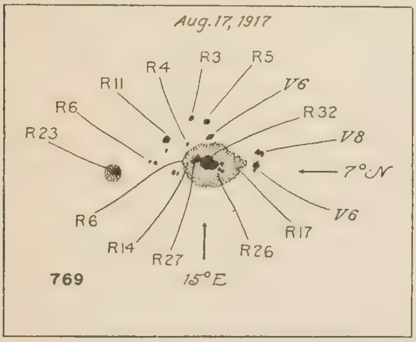

FIG. 4.—Magnetic polarities of the spots in group No. 769, August 17, 1917.

Before leaving bipolar spots, it is desirable to call attention to odd configurations, almost sure to be wrongly classified unless the polarities are known. No. 769, for example, might be called for a time a bipolar group, but not such as it appears. During several days on and after August 17, 1917 (Fig. 4), it might easily be mistaken for a βf-spot, though in fact the two principal members were on that date R_{23} and R_{32}, respectively. Several small spots at the following end of the group, which persisted until August 19, were opposite in polarity to the two large spots, and lead us to classify the whole group as βp from August 15 to 17. But after August 17 the rapid separation of the principal components and the appearance of other small V-spots, the largest (August 18) just preceding the largest umbra, seem to call for classification as two groups or as one group of mixed polarity.

As extreme cases of unusual grouping, we may mention such pseudo-bipolars as No. 796, which on September 4, 1917 (Fig. 5), would surely have been regarded as a true bipolar if classified without spectroscopic tests. The large leading spot at 16° S. latitude was recorded as V_{29}, thus corresponding to the bipolar rule for regular spots at that time. The large following spot, however, instead of being R, was actually V_{24}. Just preceding it was a very small spot R_3, presumably the following companion of V_{29}, making with it a βp-group. Behind it were several small spots, one of which was V_4, followed by two others, recorded as R_5 and R_8. This, therefore, seems to be another βp-group. On September 6 all of the small companions had disappeared, and the eastern spot was reduced to V_9. The next day it had disappeared. Another deceptive case is group No. 1744, as it appeared on September 29 and 30, 1920. The two principal spots, V_{25} and V_{26}, 12° S. (Fig. 6, No. 2), were formed by the rapid separation of the preceding and following parts of a single large spot, which on September 25 (Fig. 6, No. 1) with its many small companions of both polarities, formed a complex group.

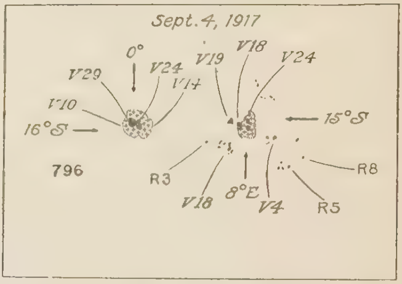

Fig. 5.—Pseudo-bipolar group No. 796, September 4, 1917.

Invisible spots.—In a large majority of bipolar groups the preceding spot is larger than the following one, which often disappears completely, leaving only the preceding spot followed by a train of flocculi. Sometimes the following spot has an intermittent existence, repeatedly appearing and disappearing. This peculiarity led us to search for local magnetic fields in the flocculi behind spots, on the hypothesis that an appreciable field might conceivably be produced by a vortex in which the cooling due to expansion is not sufficient to cause a visible darkening of the photosphere.

Such a field would be betrayed by a slight widening of λ 6173, rendered unsymmetrical by cutting off the red or violet n-component with a Nicol and quarter-wave plate. As the effect may still be so slight as to escape detection, an auxiliary half-wave plate, oscillating or rotating above the quarter-wave plate, is used to cut off in quick succession the red and violet components, thus setting the line into vibration at the point in question. This simple device has served admirably to reveal invisible spots in bipolar groups, before and after the visible stage, and in some cases where visibility was never attained.

The bearing of these local fields on the nature of sun-spots will be discussed in a subsequent paper. From the standpoint of classification, with which we are now exclusively concerned, they are seen to strengthen the evidence that some 90 per cent of all sun-spots are either bipolar or tend toward this form. Hardly 10 per cent of all spots are strictly unipolar, consisting of single spots or groups of the same polarity symmetrically surrounded by flocculi. Between these and the true bipolar groups we find single spots or unipolar groups followed (*ap*) or preceded (*af*) by flocculi, and in these flocculi invisible spots sometimes occur. If a persistent search for visible spots were made with the best of seeing and a larger solar image and higher dispersion than we employ, it is probable that great numbers of them would be found, especially in the flocculi following large unipolar spots.

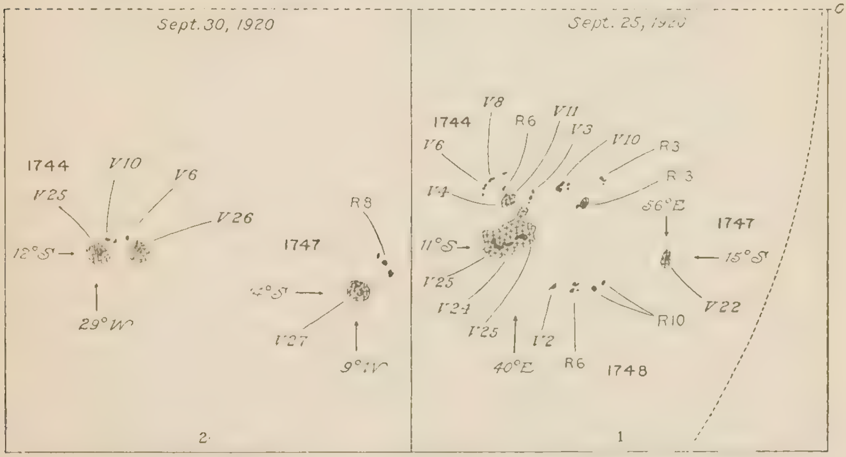

FIG. 6.—Pseudo-bipolar group No. 1744, September 25 and 30, 1920

UNIPOLAR SPOTS

Our previous paper, together with the foregoing remarks on invisible spots, perhaps describe sufficiently the characteristics of unipolar groups from the standpoint of classification. Some illustrations of scattered unipolar streams or groups may be added, however, to supplement what has already been said regarding pseudo-bipolars.

Group No. 2071, when first observed for polarity near the east limb on June 28, 1924, at 33° N. latitude, consisted of two spots, V_{15} and V_{14}. On June 30 the following spot had split in two, and the next day three small companions appeared, of undetermined polarity. On July 3 the group contained seven members, all V but two small spots, R_4 and R_2, between and slightly to the north of the two largest spots, then V_{24} and V_{20}. On July 6 Nicholson found all the widely scattered components to be of the same polarity, the small R-spots having disappeared (Fig. 7).

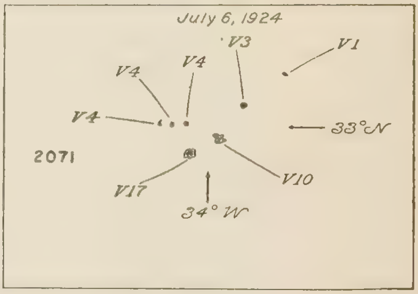

Fig. 7.—Scattered unipolar group No. 2071, July 6, 1924.

No. 697 (17° N.) is an interesting case (Fig. 8). First seen at the east limb on June 23, 1917, it had advanced far enough upon the disk on June 25 to permit of reliable polarity tests. These showed each of the three umbrae in the S-shaped preceding member to be R_{28}, and these were followed by two small spots, R_3 and R_6, followed again by three spots, V_{15}, V_6, V_8 (Fig. 8, No. 1). The next day (Fig. 8, No. 2) the preceding spot was splitting into three members, R_{26}, R_{26}, R_{22}, which on June 28 (Fig. 8, No. 3) were widely separated and followed by a faint spot without umbra V_{10}, and a small spot R_{17}. On June 30 (Fig. 8, No. 4) all the scattered members were decreasing in size, and all were R. This process of disintegration continued on July 2 (Fig. 8, No. 5), and on July 3 (Fig. 8, No. 6) the group was reduced to two small members, resembling a bipolar, but both were recorded as R_6. The small R-spot following to the south, at 10° N. latitude, was classified as a separate group.

No. 802, 18° N. (Fig. 9, No. 1), which was the return of a large γ-group observed in August, 1917, with curiously mixed polarities, also behaved in an exceptional manner in September. On September 3 (Fig. 9, No. 1) it appeared like a fairly long bipolar group, but with the exception of certain small *R*-spots south and

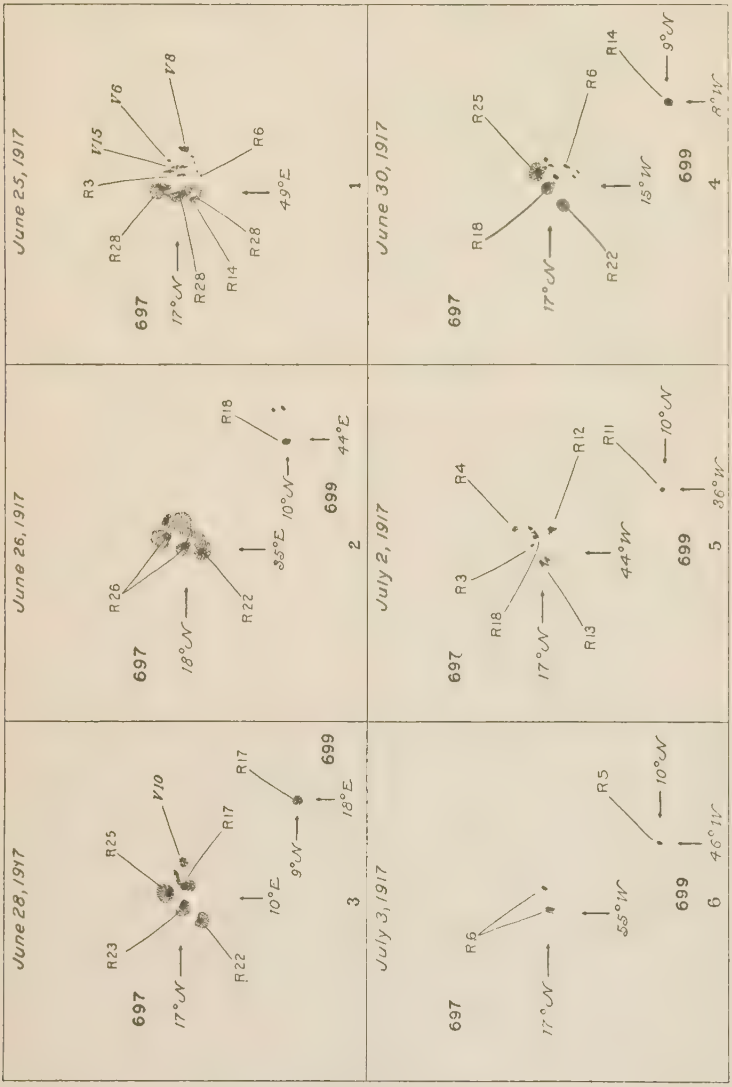

FIG. 8.—Development of groups Nos. 697 and 699, June 25—July 3, 1917

preceding, which we regard as another group (No. 805), all its members were *V*. On September 4 (Fig. 9, No. 2) No. 802 was an odd combination, the preceding member showing V_{17} on one side and R_{18} on the other, with all the other members *V* except two in their midst, R_3 and R_6. The next day (Fig. 9, No. 3), however, the group had become an orderly bipolar, with *R* preceding and *V* following members. On September 6 the *R*-members had disappeared, and all of the spots were *V*. A day later only two of these, V_{14} and V_6, were left. One of these had disappeared on September 8, and on September 9 the last spot of the group was gone.

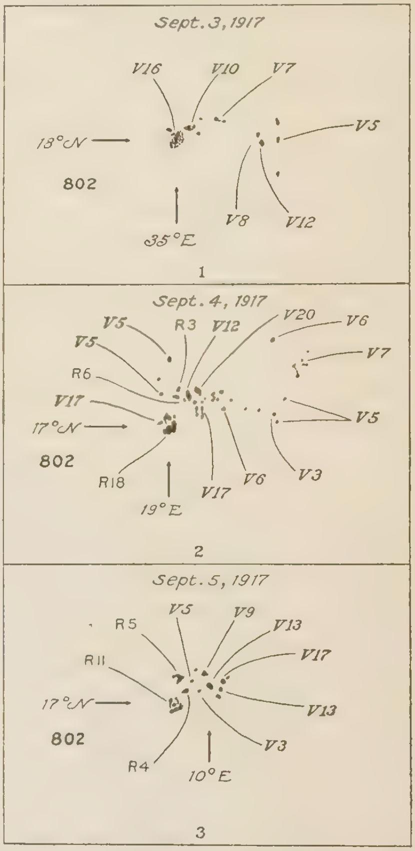

FIG. 9.—Complex group No. 802, September 3–5, 1917.

COMPLEX GROUPS

In a subsequent article on the nature of sun-spots various important characteristics of $\beta\gamma$- and γ-groups will be discussed, including their frequency in different parts of the sun-spot cycle, their area and heliographic distribution, the inclination of their axes to the solar equator, the influence of rapid development and possibly of neighboring spots, and the customary presence in them of eruptive phenomena. Here we are concerned solely with questions of classification bearing on the determination of the polarity law, and complex groups will accordingly be considered from this standpoint.

Of the 2025 spot groups observed magnetically from 1915 to date, and included in this discussion, 3.0 per cent have been classed as $\beta\gamma$-groups and 0.8 per cent as γ-groups. They are thus too few in number to hamper the certain determination of the polarity law, but it is important to observe how they may develop out of α- and β-groups.

The chief characteristic of most complex groups is the heterogeneous distribution within them of spots of opposite polarity. They thus stand in striking contrast with α-(unipolar) groups, comprising a single spot or cluster of spots of the same polarity, and β-(bipolar) groups, consisting of two such clusters, preceding and following, of spots of opposite polarity. We find occasional $\beta\gamma$-groups, with definite bipolar characteristics but including some small spots of opposite polarity associated with the preceding or following members. In general, the components of all these groups, whether large or small, are of the same polarity in all parts of each spot, but in some γ-groups spots are present which show sharply bounded regions of opposite polarity within the same penumbra.

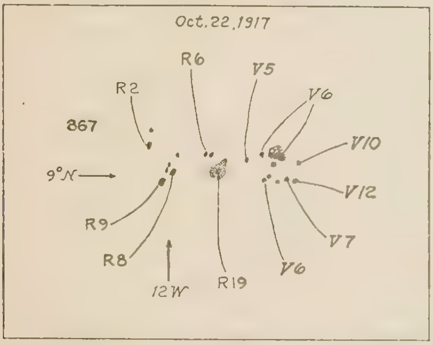

FIG. 10.—Bipolar group No. 867, October 22, 1917.

In visual or photographic observations of long trains of spots, especially those which exhibit no clustering tendency at the opposite ends of the train, we find no clue to the correct classification unless we apply the magnetic test. Take, for example, No. 867 (9° N.), as observed on October 22, 1917 (Fig. 10). The polarities show this to be a bipolar group, though it so little resembles a simple bipolar such as No. 2091, observed on August 18, 1924 (Fig. 2). Sometimes the preceding and following members of bipolar groups may actually overlap, without transformation of the group into the γ-class. No. 622, as observed by Joy on April 12, 1917, is a good illustration of this (Fig. 11, No. 1). On the previous day the spots of opposite polarity were well separated into preceding and following members, and later the bipolar nature of the group appeared even more clearly (Fig. 11, No. 2). But sometimes we observe the rapid development of a bipolar group into one of mixed polarity.

Thus No. 848 (21° N.), which suddenly broke out on the disk on October 5, 1917, was found by Ellerman to be bipolar (Fig. 12, No. 1). The next day, when additional following members had appeared, a small spot R_3 was detected to the east of another small spot, V_6. On October 7 the group had greatly increased in size, and its complex character was apparent (Fig. 12, No. 2). Great activity prevailed between the small *V*- and *R*-spots near the following end of the group (*a*, Fig. 12, No. 2), marked by a brilliant eruption showing a violet displacement of $H\alpha$, corresponding to an upward velocity of 250 km per second, and a fine "bomb" not far away (*b*, Fig. 12, No. 2). On the next two days the group was even more

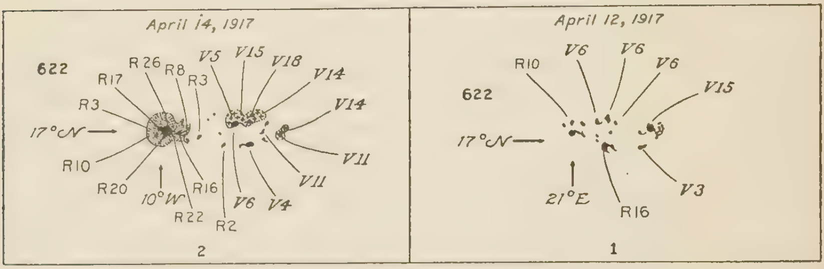

FIG. 11.—Bipolar group No. 622, April 12 and 14, 1917

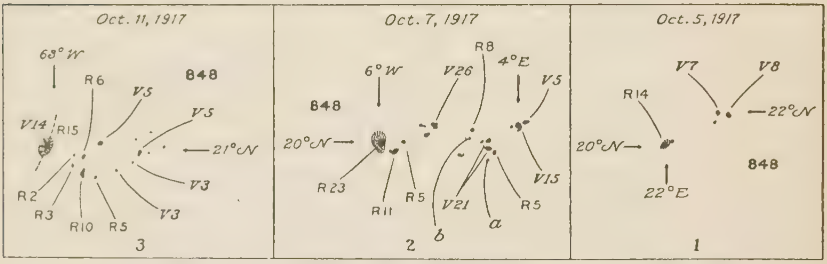

FIG. 12.—Transformation of a bipolar into a complex group, No. 848, October 5–11, 1917.

complex, and frequent bombs were seen near its center. On October 10 the polarities were still mixed, but on the following day, when nearing the west limb, the group had returned to the bipolar type (Fig. 12, No. 3).

Another case representing a change of type may also be described. No. 631 (Fig. 13), when first observed magnetically by Joy on April 19, 1917, appeared as a bipolar, with a large preceding spot, R_{18}, accompanied on the north by two small spots, R_5, and followed by two small spots, V_3. This bipolar condition persisted until April 22 (Fig. 13, No. 2), when the two following spots had disappeared and the several preceding members, the largest of which was R_{24}, were all R, scattered over a considerable area. On April 23 (Fig. 13, No. 3) the R-members were preceded by a spot recorded by Ellerman as V_{18}, while another spot, V_8, appeared north of the largest member of the group, then R_{23}. On this date the group would naturally be classified as of mixed polarity. The next day the two umbrae of the enlarged preceding spot were found by Ellerman to be V_{13} and V_{12}, respectively, while the spot to the north was

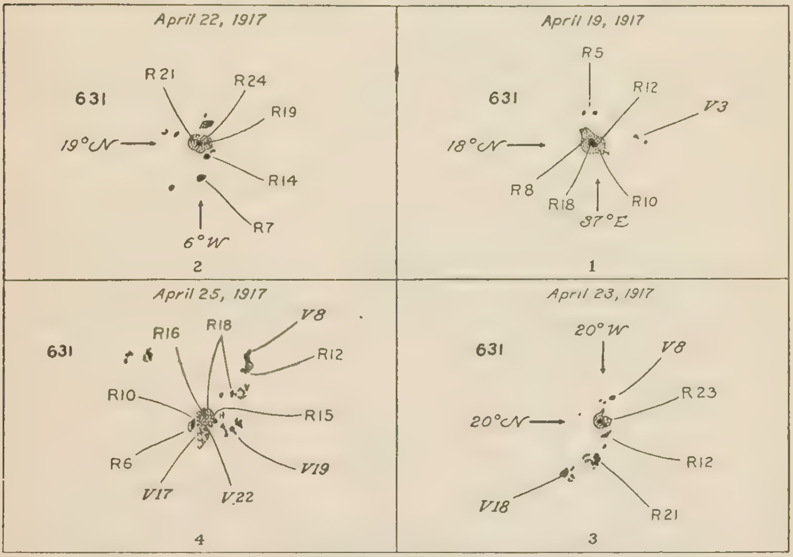

FIG. 13.—Changes in type of group No. 631, April 19–25, 1917

V_9, the group thus remaining of the γ-type, with the four other members R_{22}, R_{23}, R_5, and R_4, respectively. On April 25 (Fig. 13, No. 4),

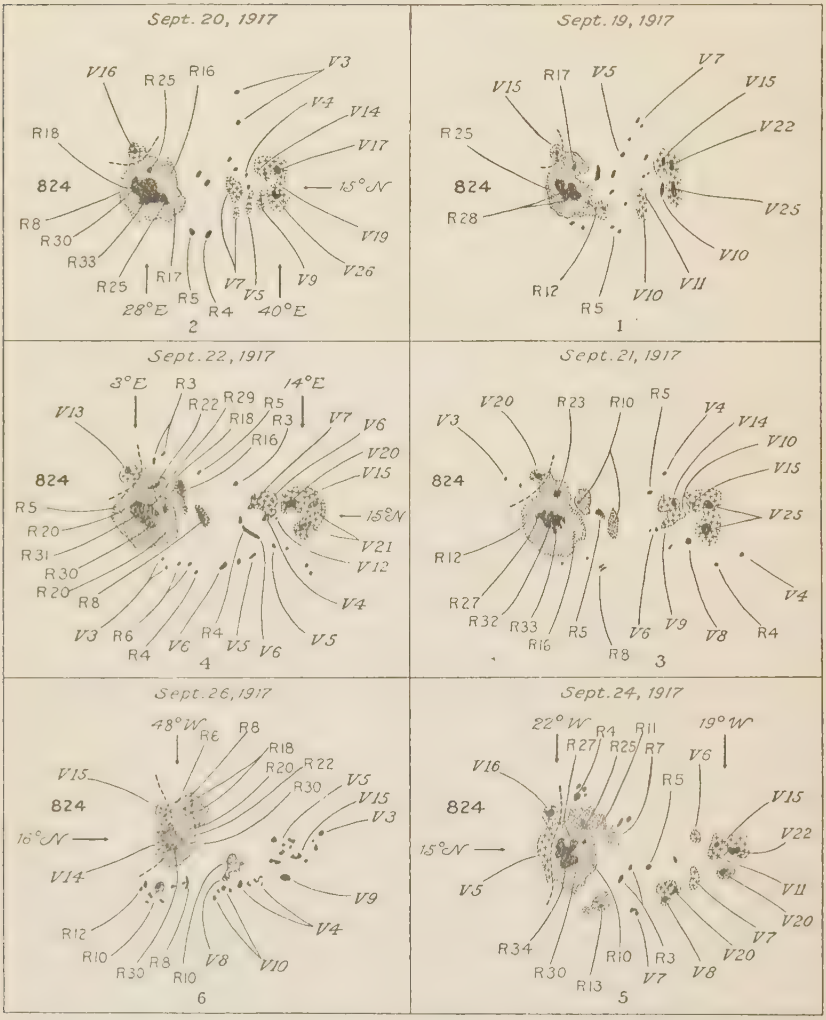

Fig. 14.—Complex group No. 824, September 19–26, 1917

the last day of observation, the polarities were similar, but the largest spot, R_{18}, had overtaken and united with the preceding spot, now V_{22}, while a similar junction had occurred to the north between

R_{12} and V_8. Thus this group, on the strength of a single day's observations, would be classified as a regular bipolar (βp) on April 19, 20, and 21; as a unipolar (αf) on April 22; and as a complex group of mixed polarity on April 22, 23, 24, and 25.

We have thus advanced by easy stages from α- and β-groups to those curious spots of the γ-type in which both polarities are sometimes found within the same penumbra. Two remarkable illustrations of this kind were given in our previous paper,[1] and many others might be added; it will suffice to mention briefly three cases.

No. 824 (16° N.) appeared at the eastern limb on September 16, 1917. If, as its position suggested, it was a return of No. 781, its previous history is unimportant, as this was a small group usually classed as α, once as β, and once as γ. Its mixed polarities, apparent on September 18, were more obvious on the following day. The large leading member, R_{31}, was accompanied on the north, on September 18, by two companions, V_{11} and V_{15}, and followed by a large spot, V_{20}. On September 19 the two northern companions had united within a single penumbra, the umbrae of which were recorded as V_{15} and R_{17} (Fig. 14, No. 1). On the following day this spot had fused with the large spot R_{33} to the south, leaving a single umbra, V_{16}, near the northern extremity of its penumbra (Fig. 14, No. 2), and this appearance persisted when the spot was nearing the west limb on September 26 (Fig. 14, No. 6). The development of the spot need not be described in detail, as it is sufficiently well shown by the cuts.

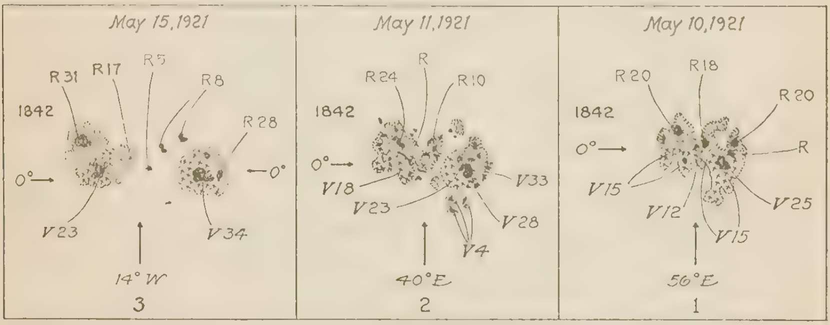

FIG. 15.—Complex group No. 1842, May 10–15, 1921

---

[1] *Mt. Wilson Contr.*, No. 165; *Astrophysical Journal*, **49**, 153–178, 1919, Fig. 2; Plate VII*a*, *b*, *c*; Plate VIII*a*, *b*, *c*, *d*.

One of the most remarkable spots we have ever observed was No. 1842, which appeared at the east limb on May 8, 1921, having formed since the previous rotation. On May 9 and 10 it was seen to consist of a very large irregular penumbra, containing a number of umbrae, of mixed polarity. The equator passed through the group, and on May 10 (Fig. 15, No. 1) Nicholson found that most of the points observed magnetically on the umbrae and various parts of the penumbra were *R* in the northern and *V* in the southern part of the group, corresponding with the polarities of the preceding spots of this cycle in the northern and southern hemispheres. On May 11 the group had split into preceding and following spots, each of which tended to be *R* in its northern and *V* in its southern parts, with the line of division near the equator, though there were some discrepancies (Fig. 15, No. 2). The *Hα*-spectroheliograms of this date showed eruptions in advance of the preceding spot, south of the small central spots, and both preceding and following the large following spot. Great activity continued in various eruptive regions in and about the group on subsequent days, and the division of each spot into two parts of opposite polarity also persisted, as illustrated in Figure 15, No. 3, from Nicholson's observations of May 15. A great terrestrial magnetic storm, accompanied by brilliant auroras, began suddenly on May 13, at 13^h 12^m G.M.T., when the leading spot was 5° east of the central meridian. The preceding edge of the bright calcium flocculi was on the meridian at this time, and the preceding bright *Hα*-flocculi had arrived there about twenty-four hours earlier. A more complete history of this remarkable group will be given elsewhere. Another interesting complex group, that of March 8, 1920, which was also accompanied by an aurora and terrestrial magnetic storm, is described by Nicholson in the *Publications of the Astronomical Society of the Pacific* for August, 1920.

MAGNETIC CLASSIFICATION OF 2174 SPOT GROUPS OBSERVED DURING THE PERIOD 1915–1925

In our previous paper we gave the magnetic classification of 970 spots observed during the period 1915–1917. Daily observations of all spots have been continued by Nicholson, Ellerman, Pettit, Joy, Benioff, Hoge, and L. Humason, and these have been classified by Nicholson and Miss Mayberry, and checked in many cases by Hale. The results, which have appeared regularly since 1920 in the *Publications of the Astronomical Society of the Pacific*, are summarized in Table I, which, for convenience of comparison, also includes our previous results.

In Table I the classification is by groups, giving all groups equal weight and counting each separately on every successive return. As the same group is often classified as unipolar on some days and as bipolar on others, the average classification is given here. Thus the successive columns give the number of groups classified under the respective heads for a majority of the days on which they were observed. There seems to be no change in the distribution of spot groups among these classes that can be associated with the changing phase of the $11\frac{1}{2}$-year cycle. This uniformity from year to year is best shown in Table II, where the percentages of the number of groups classified each year are given for each type. It should be noted that the numbers given in the "Unclassified" column are the percentages of all groups observed, while those in the other columns are the percentages of the groups actually classified.

TABLE I

MAGNETIC CLASSIFICATION OF 2174 SPOT GROUPS

Year	α	αp	αf	β	βp	βf	$\beta\gamma$	γ	Unclassified	Total
1915......	17	33	9	38	51	9	8	3	14	182
1916......	53	54	12	66	100	26	13	0	16	340
1917......	45	85	15	88	134	38	15	2	28	450
1918......	64	75	10	85	101	33	8	1	19	396
1919......	52	54	11	47	77	22	9	3	21	296
1920......	21	33	9	30	46	12	4	4	9	168
1921......	11	34	5	26	28	8	2	1	25	140
1922......	12	17	4	17	18	3	0	2	5	78
1923......	1	7	2	5	16	2	0	0	4	37
1924......	8	17	3	21	21	6	2	1	8	87
Total...	284	409	80	423	592	159	61	17	149	2174

The number of spot groups in each class was tabulated for the northern and southern hemispheres separately, and the percentage in each class was found to be the same north and south of the sun's equator. Of the 2174 groups observed, 1149, or 52.9 per cent, were north of the equator. Of the total number of spot groups in each class given in Table I, 52.9 per cent might therefore have been expected in the northern hemisphere. The numbers calculated and observed in the northern hemisphere are given in Table III.

The slight excess of *αp*- and *αf*-groups in the southern hemisphere is so small that no physical significance is attached to it.

TABLE II

PERCENTAGE OF SPOT GROUPS IN EACH CLASS

Year	α	αp	αf	β	βp	βf	βγ	γ	Unclassified
1915	10	20	5	23	30	5	5	2	8
1916	16	17	4	20	31	8	4	0	5
1917	11	20	4	21	32	9	3	0	6
1918	17	20	3	22	27	9	2	0	5
1919	19	20	4	17	28	8	3	1	7
1920	13	21	6	19	29	7	3	2	5
1921	10	30	4	23	24	7	2	1	18
1922	17	23	5	23	25	4	0	3	6
1923	3	21	6	15	49	6	0	0	11
1924	9	21	4	27	27	8	2	2	9
1915–1924	14	20	4	21	29	8	3	1	7

TABLE III

Class	α	αp	αf	β	βp	βf	βγ	γ	Unclassified
Calculated	150	216	42	224	313	84	32	9	79
Observed	151	207	37	226	313	87	36	11	81

Table IV gives as percentages the frequency with which groups of each type were observed. These numbers give the mean number of groups of each type classified daily as a percentage of the total number of groups classified daily during the year. Daily observations of the magnetic fields of all spots were not made prior to January, 1917, so that these data are not available previous to that date.

A comparison of Table IV with Table II shows marked differences in three classes—*αp*, *β*, and Unclassified. The reason for the increase from 7 per cent to 18 per cent for the total of unclassified spots is that in Table II only those spots are counted as unclassified for which no polarity observations were made. A group seen on several days may have been observed magnetically on only one or two days, because of adverse observing conditions. Its mean classification would then be given on the basis of those days for which magnetic observations were made.

The decreased percentage of β-groups and the increased percentage of αp-groups is due to the fact that the groups of long duration pass through the β-stage rather rapidly, while they exist as αp-groups for a much longer part of their life. The large groups usually begin as β- or βp-groups, but if the group is of the β-type at first, it usually changes to βp after a few days. As the following spot breaks up and decreases, the group is βp until this spot has completely disappeared. The preceding spot may still be of considerable size, and may last for many days as an αp-group. Since Table IV is based on the frequency of groups in each class, the groups are essentially weighted according to their length of life. The groups of short duration often die out before the αp-stage is reached.

TABLE IV

FREQUENCY OF SPOT GROUPS OF EACH CLASS

Year	α	αp	αf	β	βp	βf	$\beta\gamma$	γ	Unclassified
1917............	15	27	2	6	30	12	5	1	17
1918............	18	26	3	14	26	9	2	1	16
1919............	19	26	2	8	28	10	5	2	18
1920............	11	32	4	12	29	7	2	2	16
1921............	8	36	3	12	30	7	2	2	25
1922............	17	24	5	19	24	6	1	5	26
1923............	1	34	1	13	44	5	2	0	21
1924............	6	30	4	19	28	8	4	1	18
1917–1924........	15	28	3	11	29	10	3	1	18

The fact that most groups begin as bipolar groups is shown in Table V, which is based on the magnetic classification of spot groups on the day of their formation. During the interval from 1917 to 1924 inclusive, 523 groups were observed on the first day of their lives. Groups observed for the first time are not counted in this table unless observations on the day preceding the group's first appearance showed that no spots were visible in the region of the new group. Of the 523 groups mentioned above, only 426 were classified magnetically on the day of their formation. The numbers of groups thus classified which were observed on one, two, three, and on four or more days are shown in the last line of Table V under the column headings 1, 2, 3, and 4. The percentage distribution of these numbers among the various magnetic classes is shown in the columns above. The columns headed 5, 6, and 7 give similar data for groups which have lived more than five days, more than six days, and more than seven days, respectively, and thus present a segregation of the data in column 4. The last column gives the percentage in each magnetic class, irrespective of duration. The data included in columns 1, 2, and 3 usually cover the entire life of the groups in question, but many of the groups observed four or more days passed around the west limb, so that their total duration is unknown.

TABLE V

Magnetic Classification of Spot Groups at Formation

Type	1	2	3	4	5	6	7	Total
α..........	32	12	9	12	13	13	10	18
αp.........	17	13	12	7	6	7	7	12
αf.........	10	5	3	3	2	3	0	6
β..........	23	26	34	37	39	39	39	30
βp.........	10	26	33	27	26	25	29	22
βf.........	7	15	7	13	13	12	13	11
$\beta\gamma$.........	0	3	0	1	1	1	2	1
γ..........	1	0	2	0	0	0	0	1
Total....	133	85	56	152	109	76	59	426

The most striking fact brought out by all of these tables is the large preponderance of bipolar groups, and the tendency of unipolar groups, even when not lapsing intermittently into the bipolar state, to hover continually on its margin. A study of the daily history of the spots further emphasizes this tendency, as it shows the frequent passage, back and forth, from one type to the other and the development from time to time of invisible spots in unipolar groups which never visibly attain the bipolar condition.

As Table II shows, 61 per cent of all classified groups were bipolar in character during the greater part of their existence, 24 per cent were *αp* or *αf*, while only 14 per cent were *α*-spots. Another striking fact is the significance of preceding spots, which is shown by the large number of *αp*- and *βp*-groups, as compared, respectively, with those classified as *αf* and *βf*.

THE LAW OF SUN-SPOT POLARITY

We are thus amply justified, when seeking the law of sun-spot polarity, in regarding bipolar groups as the dominant type. Unipolar spots followed by flocculi (*αp*) are treated as the preceding members of incomplete bipolar groups, and those preceded by flocculi (*αf*) as the following members of such groups. In the following tables our observations for the period 1908–1925, omitting symmetrical unipolar (*α*) groups, mixed bipolars (*βγ*), and complex groups, are assembled for three different spot cycles, the first including the few polarity observations made between June, 1908, and January, 1913 (Table VI); the second those of the full period, January, 1913, to October, 1924 (Table VII); and the third those from June, 1923, to January, 1925 (Table VIII).

TABLE VI*

DISTRIBUTION OF MAGNETIC POLARITIES IN SPOT GROUPS (FIRST CYCLE)

FIRST CYCLE	REGULAR			IRREGULAR				MEAN DISTANCE FROM EQUATOR
	N. V_p–R_f	S. R_p–V_f	Total	N. R_p–V_f	S. V_p–R_f	Total	Percentage	
June, 1908–Jan., 1913..	7	17	24	0	1	1	4	9°

* The figures in these tables differ slightly from those given in our previous paper because *α*-spots were then classified with the preceding members of bipolar groups.

In Table VI, representing a period when our attention was chiefly concentrated upon the verification and detailed study of the Zeeman effect in the few spots large enough for such work on the 6.7-inch solar image of the 60-foot tower telescope, the classification of polarities as "regular" or "irregular" is determined by the transmission of the red (*R*) or violet (*V*) *n*-component of λ 6173 by the "marked strip" of the compound quarter-wave plate when set on the preceding spot. As the results show, the great majority of these spots gave the violet component (south-seeking or negative polarity) for the preceding spots of the northern hemisphere, and the red component (north-seeking or positive polarity) for the preceding spots of the southern hemisphere.

With the arrival of the high-latitude spots of the next (second) cycle, in December, 1912, we were surprised to find their polarity to be opposite to that of the spots of the first cycle. This is abundantly shown in Table VII, where the terms "regular" and "irregular" now apply to spots for which the preceding members give the red component (north-seeking or positive polarity) in the northern hemisphere, and the violet component (south-seeking or negative polarity) in the southern hemisphere. With only 2.4 per cent of exceptions, the reversal of polarities was thus complete.

TABLE VII

DISTRIBUTION OF MAGNETIC POLARITIES IN SPOT GROUPS (SECOND CYCLE)

SECOND CYCLE	REGULAR			IRREGULAR				MEAN DISTANCE FROM EQUATOR
	N. R_p–V_f	S. V_p–R_f	Total	N. V_p–R_f	S. R_p–V_f	Total	Percentage	
1913, 1914	18	13	31	1	1	2	6	22°
1915	61	60	121	1	0	1	1	19
1916	138	89	227	2	5	7	3	17
1917	188	175	363	4	3	7	2	15
1918	148	168	316	4	5	9	3	13
1919	96	122	218	0	2	2	1	12
1920	68	65	133	0	0	0	0	11
1921	54	45	99	1	2	3	3	10
1922	34	24	58	3	1	4	6	9
1923	12	5	17	0	0	0	0	7
1924	3	0	3	3	0	3	(50)	5
Jan., 1913–Oct., 1924	820	766	1586	19	19	38	2.4	....

This remarkable result led us to fear some systematic error, but scores of checks applied to our observations, which had been partly visual and partly photographic, invariably failed to shake their validity. We accordingly looked forward with the keenest anticipation to the appearance of the sporadic spots in high latitudes indicating the approach of the next cycle.

The first of these was detected by Ellerman on June 24, 1922, a small α-spot at 31° N. latitude and 10° E. longitude, found to give the violet component, and thus to be of south or negative polarity. On the assumption that this was a regular preceding spot, a general reversal of polarities, corresponding to that observed in 1912, might be expected to occur at the minimum. As Table VIII[1] and Figure 16 indicate, this reversal has since taken place.

In studying the reversal of polarity at sun-spot minimum it is natural to inquire whether it is heralded by any progressive increase in the number of irregular spots or other suggestive phenomena.

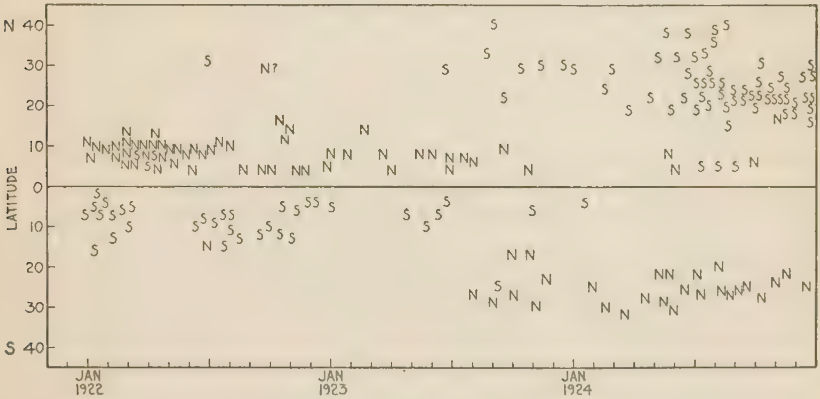

FIG. 16.—Heliocentric latitudes and magnetic polarities of sun-spot groups observed at Mount Wilson from January 1, 1922, to January 1, 1925. *N* (north-seeking) or *S* (south-seeking) represents the polarity of the preceding spot of each group.

As Table VII indicates, the percentage of irregular spots fluctuated from 0 to 6, but showed no progressive change. A test of the relative importance of preceding and following spots during various parts of the cycle can also be made by adding together all αp- and βp-spots, and comparing their number with the corresponding sum of the αf- and βf-spots, as shown in Table IX.

The results afford no clue to the impending change of polarity at the minimum. The reversal of polarity is a sudden phenomenon, just as the advent of a new cycle of spots is abrupt, beginning in high latitudes before the spots of the old cycle have completely disappeared. Thus we find that at the time of sun-spot minimum four spot zones, characterized by distinct magnetic polarities, may coexist on the sun. During the interval June 1, 1922, to January 1, 1925, the maximum latitude of the spots of the last (second) cycle was 16°. The latitude of the present (third) cycle spots, of opposite polarity, has ranged from 40° to 16°. The boundaries of these zones are not sharply defined, and in a few cases it is doubtful to which cycle the group belongs. Thus group No. 2033, which appeared on September 8, 1923, in latitude 25° S., had polarities like those of the second cycle, but because of its distance from the equator it has been considered as a spot of the third cycle with irregular polarity. A still more difficult case is No. 2079, which first appeared on July 9 in latitude 5° N. Its polarities were like those of the third cycle, but its low latitude puts it with the spots of the second cycle, as is shown in Figure 16. It has been included in Table VII, and since it was observed at two returns, as Nos. 2085 and 2094, with the same irregular polarity, it alone accounts for the irregular second-cycle

---

[1] In this table "regular" and "irregular" have the same significance as in Table VI.

TABLE VIII

DISTRIBUTION OF MAGNETIC POLARITIES IN SPOT GROUPS (THIRD CYCLE)

Third Cycle	Regular			Irregular				Mean Distance from Equator
	N. V_p–R_f	S. R_p–V_f	Total	N- R_p–V_f	S. V_p–R_f	Total	Percentage	
1923	8	7	15	0	1	1	7	27°
1924	51	18	69	1	0	1	1	25
June, 1923–Jan., 1925	59	25	84	1	1	2	2	....

TABLE IX

Year	$\alpha p+\beta p$	$\alpha f+\beta f$
1917	57	14
1918	52	12
1919	54	12
1920	61	11
1921	66	10
1922	48	11
1923	78	6
1924	58	12

groups of 1924. On its next return, as No. 2101, its polarity had changed, making it a regular group of the second cycle.[1]

The temporary existence in each hemisphere of two zones, in which the great majority of the spots are of opposite polarity, is a most striking phenomenon, which cannot fail to be of significance in its bearing on the solar constitution.

Mention should be made of the sharpness with which the equator separates spots of opposite polarity, as illustrated in Figure 17. Two bipolar groups appeared at the east limb of the sun on August 12, 1919, one 6° N., the other 3° S. During their passage across the disk the leader of the northern group moved toward the equator at the rate of 4500 miles per day, while the preceding spot of the southern group rapidly increased in diameter. By August 23 the edges of both these spots touched the equator. On their return to the east limb on September 10 the following spots of both groups had disappeared, leaving only the leaders, which remained in the same relative positions until they began to break up on September 15. Figure 17 shows them as they appeared on September 13, when the northern spot was 30,000 miles in diameter, the southern one 26,000 miles in diameter, and the distance between their centers 33,000 miles. At this time their respective maximum field-strengths were 3400 and 2900 gausses, of opposite polarity.[2] Scores of similar instances could be given, showing the almost unerring tendency of a group to exhibit the polarity characteristic of its hemisphere, even if it be within a degree or two of the equator, or actually in touch with it.[3]

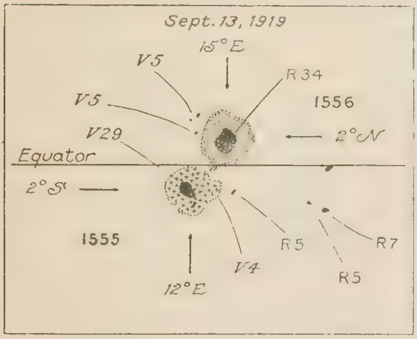

FIG. 17.—Spots of opposite polarity near the equator. Groups Nos. 1555 and 1556, September 13, 1919.

---

[1] "Summary of the Mount Wilson Observations of Sun-Spots for September and October, 1924," *Publications of the Astronomical Society of the Pacific*, **36**, 355, 1924.

[2] Nicholson, "Two Sun-Spots Close to the Sun's Equator," *ibid.*, **31**, 277, 1919.

[3] Rarely, as in the complex group No. 1842 (Fig. 15), the polarities do not correspond exactly with their respective hemispheres.

The polarity law, which represents all of our observations with only 41 exceptions out of 1735 groups, is best expressed graphically (Figs. 18 and 19), but may also be stated as follows:

The sun-spots of a new 11½-year cycle, which appear in high latitudes after a minimum of solar activity, are of opposite magnetic polarity in the northern and southern hemispheres. As the cycle progresses the mean latitude of the spots in each hemisphere steadily decreases, but their polarity remains unchanged. The high-latitude spots of the next 11½-year cycle, which begin to develop more than a year before the last low-latitude spots of the preceding cycle have ceased to appear, are of opposite magnetic polarity.

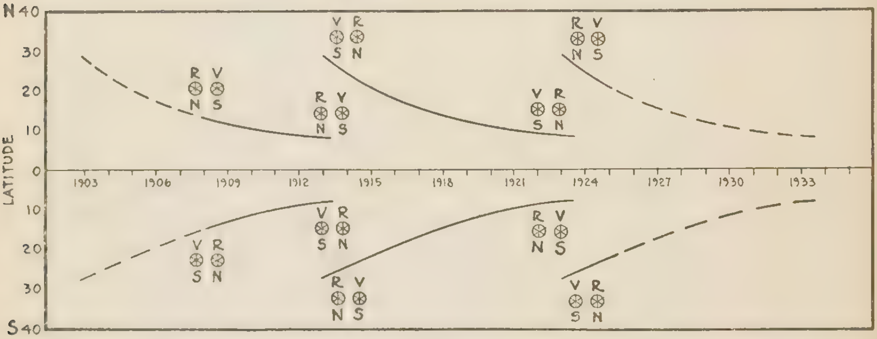

FIG. 18.—The law of sun-spot polarity. The curves represent the approximate variation in mean latitude and the corresponding magnetic polarities of spot groups observed at Mount Wilson from June 1908 to January 1925. The preceding spot is shown on the right.

It can hardly be doubted that this law will apply in future cycles, involving a complete reversal of polarities at each successive minimum. Thus while the 11½-year interval correctly represents the periodic variation in the number or total area of sun-spots, the full sun-spot period, corresponding to the interval between the successive appearances in high latitudes of spots of the same magnetic polarity, is twice as long.

This 23-year interval may be called the magnetic sun-spot period, to distinguish it clearly from the familiar 11½-year frequency period. The sun-spot numbers or areas might be expected, however, to show some evidence of a 23-year period, and this was actually detected by Professor Turner in 1913 from a careful analysis of the

Wolf numbers. In the *Monthly Notices* for November, 1913, he remarks: "Now in the first place we find that there is not a satisfactorily uniform period of 11½-years, but rather a double period of 23 years, the halves of which are not quite symmetrical." In a recent paper,[1] describing a harmonic analysis of the Greenwich north and south mean latitudes and the logarithms of the north and south spotted areas, he confirms the earlier result and adds the following important conclusions:

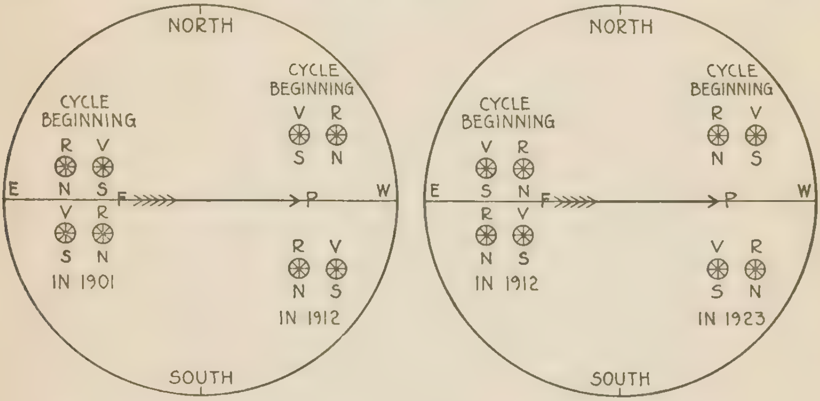

FIG. 19.—Sun-spot zones during the minimum of solar activity. Two zones in each hemisphere, in which the spots are of opposite magnetic polarity, exist for about two years at the time of each sun-spot minimum.

The "even" cycles 1888–99 and 1912–23 differ from the "odd" cycles 1876–87 and 1900–11 as follows:

a) The spots are in the mean 1° further from the equator in both hemispheres, and the spotted area larger in the ratio of 143 to 126.

b) The phases of the variation are earlier by about 5.2 months, both as regards latitude and area; the ranges are also slightly greater.

c) The latitudes indicate a mean period of 11.35 years and the areas a mean period of 11.65 years, the mean being closely 11.50 years, for the 48 years analyzed.

It is to be hoped that solar investigators will look for other possible differences in the behavior of the spots of successive 11½-year cycles.

MOUNT WILSON OBSERVATORY
June 1925

---

[1] *Monthly Notices*, **85**, 467, 1925.

Contributions from the Mount Wilson Observatory, No. 301
Reprinted from the *Astrophysical Journal*, Vol. LXII, pp. 320–374, 1925

MEAN DISTRIBUTION OF STARS ACCORDING TO APPARENT MAGNITUDE AND GALACTIC LATITUDE

By FREDERICK H. SEARES, P. J. VAN RHIJN, MARY C. JOYNER, and MYRTLE L. RICHMOND

ABSTRACT

Mean distribution of stars according to magnitude and galactic latitude.—The distribution has been determined from (*a*) *Mount Wilson Catalogue of Selected Areas*, covering $m=13.5$ to 18.5; (*b*) 33 zones of the *Astrographic Catalogue*, $m=9.0$ to 13.5; and (*c*) Tables II and IV, *Groningen Publication* No. 27, corrected for scale error, $m=4.0$ to 9.0. Systematic deviations in longitude and between northern and southern galactic hemispheres have been disregarded. The values of $\log N_m$ (N_m=number of stars per square degree brighter than m), extrapolated to $m=21.0$, are in Tables XVII and XVIII. In general, the results refer to a grouping according to photographic magnitude, international scale. The means for latitudes 0°–90°, however, have been transformed into corresponding means for a grouping according to visual magnitude.

Total number of stars and galactic concentration.—To the twenty-first photographic magnitude the total number of stars is 890,000,000, or to the twentieth visual magnitude, 1,000,000,000. The values of dN_m/dm (Table XXII) from $m=12$ or 13 to $m=21$ can be represented by quadratic exponentials in m (Table XXIII). The assumption that these formulae also apply to the luminous stars beyond observational reach leads to 3×10^{10} as the total number of stars in the galactic system, 95 per cent of which are within 20° of the galactic plane. For the whole system, the ratio of N_m for latitudes 0° and 90° (galactic concentration) is more than 700. All results depending on the unrestricted summation of the quadratic exponentials are, however, very uncertain. Within the interval covered by the adopted distribution table, $m=4.0$ to 21.0, the galactic concentration increases from 3.4 to 44 (Table XXV).

Mount Wilson Catalogue.—The *Catalogue* gives magnitudes for about 70,000 individual stars in Selected Areas 1–139, declinations +90° to −15°. Photographs with the 60-inch reflector, exposures 2^m and 15^m, measured at Mount Wilson, determine the scales and zero-points, and give magnitudes of 65,683 stars in fields 23′ in diameter. Plates of 60^m exposure, measured at Groningen, give the magnitudes of 44,910 stars in fields $15'\times15'$ or $20'\times20'$. The two series of measures were counted separately (Tables I*a*, I*b*), the counts being completed to a uniform limiting magnitude of 18.5. Cumulative sums, reduced to unit area, were formed for 28 latitude groups. Means and differences for Mount Wilson and Groningen counts are in Tables VII and VIII; smoothed values—the final result from the *Catalogue*—in Table IX.

Reduction of van Rhijn's distribution table to international scale.—For $m>10$, Tables II and IV of *Groningen Publication* No. 27 depend on 65 Selected Areas in the *Harvard-Groningen Durchmusterung;* for $m<6$, they are based on the visual magnitudes of *Harvard Annals*, 50, corrected for color. The corresponding scale corrections from *Contributions* Nos. 288 and 289 are in Table XI, the interval $m=6$ to 10 being bridged by interpolation.

Astrographic zones.—The published counts for 33 zones, mostly by Turner, were reduced to the international scale through the intermediary of *Groningen Publication* No. 27, corrected as above. Mean densities for 3–5 limiting magnitudes and latitudes 0°, 10°, 20° . . . ., are given for each zone in Table XV; condensed means, in Table

XVI. The latter, together with Table IX from the *Mount Wilson Catalogue,* is the basis of the adopted distribution (Table XVII) for $m>9.0$.

Scale correction to Groningen Publication No. 18.—Table XX gives a mean scale correction for Kapteyn's distribution table, derived by comparison with $\log N_m$ in Table XVIII, 0°–90°, for a grouping according to visual magnitude. The correction seems to vary with the latitude.

The completion of the *Mount Wilson Catalogue of Selected Areas* and of certain preliminary investigations has made it possible to redetermine the distribution of stars with respect to apparent magnitude and galactic latitude. Counts of stars in this *Catalogue* cover the interval $m=13.5$ to 18.5, international photographic scale. The distribution between $m=9.0$ and 13.5 has been determined from 33 zones of the *Astrographic Catalogue* published by Turner.[1] These have been reduced to the international system through the intermediary of van Rhijn's Table IV, *Groningen Publication* No. 27, corrected for scale error. The revised distribution for $m<9.0$ is that of van Rhijn's Table IV, extended to $m=4.0$ by Table II of his paper and reduced to the international system. By what seems a permissible extrapolation, the results thus found have been extended to the twenty-first magnitude. The adopted values for the mean distribution are given, in the usual form, in Tables XVII and XVIII.

I. THE "MOUNT WILSON CATALOGUE"

Pending the appearance of the *Mount Wilson Catalogue,* much information relating to the observations and reductions and to the precision and consistency of the results may be found in the *Third Report on the Progress and Plan of Selected Areas.*[2] Certain details, however, are necessary for an understanding of the present discussion.

The *Catalogue* gives the photographic magnitudes of stars in Selected Areas 1–139, declinations +90° to −15°. The photographs were made with the 60-inch reflector, in three series: (*a*) exposures of 2 minutes and 15 minutes, with the full aperture and with diaphragms and a wire-gauze screen; (*b*) exposures on the same plate of 60 minutes and 5 minutes, both with full aperture; (*c*) comparison exposures of 2 minutes, all with the full aperture, connecting each area with the adjacent areas of the same zone, and six areas in each zone with the North Pole.

---

[1] References are given in Table XIII.

[2] Groningen, 1923. See especially Second Appendix.

Series (*a*) and (*c*) were measured and reduced at Mount Wilson, the diaphragm exposures being used to determine the scale in each area, while the comparison exposures served to reduce the results to the international zero-point. The fields are circular, 23′ in diameter, with the bright central star at the center of the plate. The results include magnitudes for 65,683 stars.

Series (*b*) was measured and reduced at Groningen with the aid of standard stars supplied from Mount Wilson, the secondary exposure of 5 minutes being used to extend the scale to the faint stars shown by the principal exposure of 60 minutes. To galactic latitude 40° the fields measured are 15′×15′; in higher latitudes they are 20′×20′. The centers are the even minutes of right ascension and the 10′ multiples of declination nearest to the positions of the central stars for 1900. Magnitudes were derived for 44,910 stars. The fields measured at Mount Wilson and Groningen thus overlap but do not coincide. Their respective areas are:

	Sq. Deg.
Mount Wilson	0.1154
Groningen, 0°–39°	0.0625
Groningen, 40°–90°	0.1111

The total number of individual stars is about 70,000.

The results agree well with the international scale.[1] It will be seen later that counts of the Groningen and Mount Wilson magnitudes are in excellent agreement, which establishes the identity of both scale and zero-point for the two series of measures, while it has already been shown[2] that the Mount Wilson magnitudes are on the international scale, at least to $m=16$. Since the scales in the individual areas were established by methods used in deriving the standard magnitudes at the Pole, which are on the international system, it is reasonable to suppose that the accordance with this system extends to the limiting magnitude of the plates.

For stars occurring in both series of measures, the *Catalogue* gives the weighted mean magnitude; but in the initial stages of the

---

[1] *Transactions of the International Astronomical Union*, **1**, 69, 1922.

[2] *Mt. Wilson Contr.*, No. 289; *Astrophysical Journal*, 61, 305, 1925.

TABLE I*a*

MOUNT WILSON COUNTS OF STARS IN SELECTED AREAS

Area	13.0	13		14		15		16		17		18		19		Total	Limit Com-plete
1	4	0	1	4	4	5	20	19	19	52	9	...	...	..	..	137	17.5
2	9	1	7	5	16	17	59	61	78	60	54	3	...	..	..	370	17.0
3	7	4	5	10	16	25	35	39	62	83	93	16	...	..	..	395	17.5
4	7	3	3	10	8	14	21	13	19	35	5	...	...	..	..	138	17.5
5	6	4	4	2	5	7	6	14	18	24	...	...	...	..	..	90	17.5
6	6	2	0	5	5	11	20	12	18	37	8	...	...	..	..	124	17.5
7	4	2	4	8	9	20	26	38	57	43	...	...	...	..	..	211	17.0
8	16	9	11	22	25	38	54	84	153	156	197	95	5	..	..	865	18.0
9	11	4	8	6	5	19	20	31	61	78	96	174	112	2	..	627	18.5
10	9	3	3	7	11	22	20	30	75	75	117	222	26	2	..	622	18.5
11	9	3	5	5	6	20	13	18	36	32	38	5	...	..	..	190	17.5
12	4	0	3	4	5	7	14	3	13	18	9	...	...	..	..	80	17.5
13	4	0	2	0	4	8	7	9	12	3	13	8	1	..	..	71	18.0
14	2	3	1	4	5	6	7	4	14	30	1	...	...	..	..	77	17.5
15	8	1	2	5	5	5	14	11	15	24	3	...	...	..	..	93	17.5
16	6	5	2	6	7	12	20	27	22	31	22	14	5	..	..	179	17.5
17	9	4	7	9	17	35	21	54	99	70	90	107	4	1	..	527	18.0
18	14	11	8	22	25	36	62	100	144	264	311	302	237	51	..	1587	18.0
19	20	11	17	16	24	39	45	57	113	102	170	258	20	..	..	892	18.5
20	13	11	9	4	13	34	36	42	74	70	81	89	267	16	..	759	18.0
21	17	4	4	13	17	33	34	30	132	66	127	241	48	2	..	768	18.5
22	10	10	8	19	19	29	46	58	81	136	128	132	153	17	1	847	18.5
23	10	5	7	16	15	22	29	53	129	141	122	365	200	17	..	1131	18.5
24	10	4	4	14	16	34	51	61	91	114	100	179	59	..	..	737	18.5
25	6	4	9	11	17	40	40	58	84	113	113	157	129	7	3	791	18.5

26	8	12	11	7	17	22	28	33	75	34	132	127	12	..	..	518	18.0
27	9	2	3	11	10	12	15	17	30	42	24	31	38	7	..	251	17.5
28	11	3	1	4	8	5	8	9	21	15	32	41	4	..	..	162	18.0
29	7	2	1	1	7	8	6	12	8	8	13	8	...	..	..	81	18.0
30	6	1	1	3	4	6	4	7	8	10	13	1	1	..	..	65	18.0
31	5	2	0	5	0	8	5	6	10	14	10	16	1	..	..	82	17.5
32	4	1	4	2	3	0	2	11	11	7	17	6	...	..	..	68	18.0
33	5	3	1	3	2	5	4	7	19	19	1	...	...	..	..	69	17.0
34	6	1	1	1	4	11	8	6	13	24	4	...	...	..	..	79	17.5
35	3	7	5	7	3	5	8	11	26	49	3	...	...	..	..	127	17.5
36	2	5	3	5	17	5	11	22	18	15	34	17	1	..	..	155	18.0
37	10	5	7	7	11	23	20	33	48	42	89	25	5	..	..	325	18.0
38	21	8	14	12	20	30	43	98	80	93	168	16	...	..	..	603	18.0
39	20	6	13	26	48	66	105	204	313	281	556	56	...	..	..	1694	18.0
40	18	6	14	17	23	60	58	66	219	239	259	213	47	2	..	1241	17.5
41	19	6	16	23	46	83	63	208	285	210	453	265	87	..	..	1764	18.0
42	10	4	6	20	36	30	54	151	88	110	265	238	20	..	..	1032	18.0
43	12	5	9	18	20	24	33	61	90	46	136	233	16	..	..	703	18.5
44	11	1	5	7	9	19	8	15	36	28	55	30	...	..	..	224	18.0
45	9	2	6	3	12	9	19	12	25	45	38	34	3	..	..	217	17.5
46	6	3	3	5	10	12	16	9	24	39	31	38	50	7	..	253	18.5
47	1	1	0	0	2	1	5	3	9	13	39	11	...	..	..	85	18.0
48	4	2	4	11	14	26	32	48	63	126	90	229	74	..	..	723	18.5
49	12	7	14	14	28	27	47	80	144	124	458	392	16	..	..	1363	18.0
50	16	10	14	19	29	29	79	81	127	176	172	219	200	42	4	1217	18.5
51	6	7	8	12	19	21	24	40	56	55	88	10	...	..	..	346	18.0
52	4	1	3	6	3	9	7	29	24	8	42	34	14	..	..	184	18.0
53	1	3	0	5	4	8	5	7	13	18	34	6	...	..	..	104	18.0
54	4	0	3	2	4	3	3	6	4	5	16	17	17	4	..	88	18.0
55	5	1	2	1	1	4	4	5	8	4	11	1	...	..	..	47	18.0

TABLE Ia—*Continued*

Area	13.0	13		14		15		16		17		18		19		Total	Limit Complete
56	4	1	4	2	1	6	2	8	13	12	17	1	...	..	..	71	18.0
57	2	2	3	4	5	4	4	5	3	11	10	4	3	23	12	95	18.0
58	6	1	2	5	7	3	4	7	7	12	30	13	5	..	..	102	18.0
59	3	2	3	7	5	0	8	20	11	19	50	18	1	..	..	147	18.0
60	7	2	2	2	10	6	14	20	20	18	25	7	1	..	..	134	18.0
61	11	3	6	7	15	9	25	39	30	31	53	54	16	1	1	301	18.0
62	17	11	3	12	20	20	24	87	57	100	222	118	24	11	..	726	18.0
63	17	12	21	21	66	84	71	135	380	251	217	251	154	49	..	1729	18.5
64	32	31	26	42	71	77	137	314	307	459	884	446	90	2	..	2918	18.0
65	15	9	12	20	24	47	75	98	215	241	257	526	146	1	..	1686	18.5
66	12	4	8	13	27	22	54	36	66	110	64	124	60	..	..	600	17.5
67	6	5	3	8	7	15	20	31	23	53	37	50	24	3	..	285	18.5
68	3	5	10	1	5	9	13	2	8	27	21	11	14	8	9	146	18.0
69	4	2	0	3	7	5	7	7	10	12	15	37	22	..	..	131	18.5
70	3	2	0	2	2	5	12	6	12	18	12	22	10	1	..	107	17.5
71	7	2	0	1	4	11	10	11	12	21	23	17	...	..	..	119	18.0
72	1	1	1	4	2	5	10	9	21	51	31	7	...	..	..	143	17.5
73	2	5	3	11	25	9	31	58	58	65	176	38	...	..	..	481	18.0
74	11	2	11	11	17	31	33	52	150	100	109	219	236	3	..	985	18.5
75	11	7	17	15	26	44	48	87	116	60	81	8	1	..	..	521	18.0
76	5	6	2	6	12	16	13	16	41	15	35	25	2	..	..	194	18.0
77	5	5	5	5	3	8	16	8	11	13	33	3	...	..	..	115	18.0
78	6	0	5	1	6	1	4	6	11	11	15	3	...	..	..	69	18.0
79	5	1	1	3	4	1	12	7	8	10	2	...	...	..	..	54	17.5
80	3	3	0	3	4	1	4	14	4	8	17	...	...	..	..	61	18.0
81	2	3	0	2	5	2	10	6	6	14	15	1	...	..	..	66	17.5
82	2	2	0	1	4	1	2	21	5	18	37	...	...	..	..	93	18.0
83	6	3	3	1	8	7	9	17	15	18	42	2	...	..	..	131	18.0
84	8	4	6	8	11	8	24	39	79	2	...	...	...	..	..	189	17.0
85	8	9	4	9	14	13	35	33	95	88	136	53	...	..	..	497	18.0

86	12	10	21	14	24	36	42	58	179	170	229	288	87	24	..	1194	18.5
87	10	3	10	12	9	27	46	66	88	292	244	432	405	25	1	1670	18.5
88	20	11	25	26	50	70	114	110	230	363	361	531	401	2	..	2314	18.5
89	10	6	8	4	17	19	28	77	63	69	162	165	31	..	..	659	18.0
90	8	2	4	6	6	17	14	14	34	35	36	38	24	43	18	299	18.0
91	4	0	1	5	7	7	7	21	21	15	28	84	13	..	..	213	18.5
92	4	2	4	1	2	7	8	10	4	7	13	14	13	9	..	98	18.5
93	9	1	1	6	5	5	6	4	6	8	11	26	4	..	..	92	18.5
94	10	2	1	3	3	2	8	12	11	11	13	31	9	1	..	117	18.5
95	2	0	1	1	3	7	10	2	20	12	16	26	1	..	..	101	18.5
96	7	2	6	6	9	13	24	23	42	30	25	47	12	1	..	247	18.5
97	6	2	5	3	8	14	20	36	54	63	78	98	12	1	..	400	18.5
98	38	8	13	34	56	40	116	151	189	559	155	59	17	..	..	1435	17.5
99	12	15	7	32	27	37	72	139	74	144	172	15	...	..	..	746	17.5
100	12	3	6	11	14	17	30	29	33	63	3	...	...	..	..	221	17.5
101	5	3	5	4	5	11	6	12	12	23	12	38	22	..	..	158	18.5
102	4	2	4	4	9	4	11	22	6	12	43	35	...	..	..	156	18.0
103	4	2	1	4	6	7	5	6	22	11	15	12	12	2	..	109	18.0
104	7	0	1	4	6	4	8	11	18	15	22	11	8	..	..	115	18.0
105	6	0	4	7	5	8	5	9	21	18	26	31	13	1	..	154	18.0
106	4	0	1	4	12	6	19	14	20	20	10	37	14	..	..	161	17.5
107	7	5	3	3	3	14	6	7	27	56	54	21	4	..	..	210	18.0
108	7	2	3	6	10	22	23	64	84	65	100	69	...	..	..	455	18.0
109	6	3	13	4	11	36	43	59	124	233	162	273	217	22	..	1206	18.5
110	7	1	1	2	2	6	4	4	20	14	16	59	11	..	..	147	18.5
111	4	5	10	7	19	43	73	79	131	360	361	383	279	20	..	1774	18.5
112	8	5	9	12	20	34	37	27	99	85	170	183	4	..	..	693	18.0
113	9	3	2	4	17	15	6	19	35	21	27	87	43	7	..	295	18.5
114	3	3	4	3	10	11	8	11	21	41	44	10	...	..	..	169	17.5
115	5	3	2	2	2	6	6	9	12	9	15	25	16	..	..	112	18.5

TABLE I*a*—*Continued*

Area	13.0	13		14		15		16		17		18		19		Total	Limit Complete
116	6	1	1	2	3	4	2	3	5	9	7	6	17	7	8	81	18.0
117	1	2	3	1	5	2	2	7	16	5	12	23	1	..	..	80	18.5
118	4	1	2	0	3	3	6	8	8	3	41	4	...	..	..	83	18.0
119	3	4	6	2	5	4	6	7	12	10	11	10	9	..	..	89	18.0
120	6	3	1	5	5	6	6	13	29	22	37	11	...	..	..	144	18.0
121	2	5	5	3	14	11	17	28	23	34	36	41	14	..	..	233	17.5
122	8	6	6	14	18	23	34	81	69	109	188	36	...	..	..	592	18.0
123	36	22	14	47	81	76	111	252	232	288	399	134	20	..	..	1712	18.0
124	18	4	20	21	29	53	43	173	103	104	270	21	1	..	..	860	18.0
125	13	6	7	5	21	22	22	47	27	64	56	9	...	..	..	299	17.5
126	6	3	3	6	8	8	10	15	31	25	43	40	3	..	..	201	18.0
127	6	2	2	5	8	10	9	17	15	45	27	1	...	..	..	147	17.5
128	7	1	4	4	2	9	6	19	21	14	43	10	...	..	..	140	18.0
129	5	3	4	6	9	10	4	14	18	28	26	26	5	..	..	158	17.5
130	6	2	2	4	7	11	7	14	39	27	53	34	6	..	..	212	18.0
131	9	4	1	2	7	16	16	34	37	46	25	12	1	..	..	210	17.5
132	6	3	2	6	5	6	16	37	67	50	89	73	6	..	..	366	18.0
133	5	3	6	8	14	17	35	95	167	233	293	106	19	4	..	1005	18.0
134	35	11	22	24	31	70	95	171	132	172	314	49	...	..	..	1126	18.0
135	15	13	11	27	49	54	135	203	259	648	705	...	...	..	..	2119	17.5
136	10	6	5	10	20	29	28	65	66	159	180	3	...	..	..	581	17.5
137	6	4	4	6	5	9	13	20	27	37	59	52	...	..	..	242	18.0
138	4	4	3	3	2	10	7	11	19	17	15	25	7	..	..	127	18.5
139	3	1	3	3	1	6	7	6	9	15	16	9	2	1	..	82	18.0
Sums	1170	588	780	1162	1859	2593	3617	5867	8439	10,612	13,424	10,602	4464	449	57	65,683	......

TABLE I*b*

GRONINGEN COUNTS OF STARS IN SELECTED AREAS

Area	13.0	13		14		15		16		17		18		19		Total	Limit Complete
1	4	0	1	2	2	3	9	8	12	33	34	8	...	..	..	116	17.5
2	3	0	2	1	10	10	40	26	37	46	96	34	52	3	..	360	18.0
3	4	4	4	4	9	10	16	15	39	40	63	43	5	..	..	256	18.0
4	4	1	2	4	5	7	11	10	12	15	16	...	...	..	..	87	17.5
5	6	5	4	2	3	7	6	13	19	32	22	2	...	..	..	121	17.5
6	2	2	0	3	5	4	11	10	7	24	11	12	...	..	..	91	17.5
7	3	1	2	4	6	10	15	20	32	33	24	66	15	..	..	231	17.0
8	8	3	5	10	15	21	25	38	63	71	129	157	130	..	..	675	18.5
9	4	3	4	1	3	13	11	16	36	51	61	86	58	..	..	347	18.5
10	6	3	1	3	7	7	10	18	38	54	37	28	...	..	..	212	17.5
11	4	2	2	2	3	11	10	13	20	20	19	23	18	30	1	178	18.5
12	5	0	2	5	6	6	12	5	9	12	10	7	10	..	..	89	17.5
13	4	0	2	0	3	6	7	8	10	12	41	7	...	..	..	100	18.0
14	1	3	1	4	4	7	6	4	12	33	15	12	...	..	..	102	17.5
15	8	0	2	4	6	7	16	10	15	41	24	18	...	..	..	151	17.5
16	3	4	2	4	4	7	11	16	14	20	15	11	1	..	..	112	17.5
17	6	4	2	2	11	13	9	20	41	54	46	71	13	..	..	292	18.5
18	9	8	3	10	14	15	33	60	84	135	194	148	100	3	..	816	18.0
19	11	8	10	10	10	26	28	27	61	66	77	90	23	..	..	447	18.0
20	8	8	4	1	7	19	25	35	32	36	49	32	50	6	..	312	18.0
21	7	3	3	6	11	18	15	17	75	39	70	80	4	..	..	348	18.0
22	6	6	3	10	11	17	22	30	53	90	74	71	50	5	..	448	17.5
23	6	1	3	9	8	14	15	34	62	86	65	90	49	3	..	445	18.5
24	6	3	2	8	6	15	36	31	45	88	55	139	47	..	..	481	18.5
25	3	1	3	3	11	26	25	31	42	45	64	80	55	..	..	389	18.0

TABLE I*b*—*Continued*

Area	13.0	13		14		15		16		17		18		19		Total	Limit Complete
26	4	8	4	3	9	10	12	20	35	26	39	91	24	30	..	315	18.5
27	7	0	2	6	6	5	8	10	17	21	16	21	27	2	..	148	18.5
28	6	3	0	3	5	2	3	4	19	4	9	15	6	..	..	79	18.5
29	8	1	1	2	5	8	7	11	6	12	18	7	...	..	..	86	18.0
30	5	1	1	4	3	5	4	7	8	6	17	3	...	..	..	64	18.0
31	6	2	0	4	1	8	3	6	10	13	16	13	...	..	..	82	18.0
32	4	1	2	3	2	1	4	12	11	6	13	12	1	..	..	72	18.0
33	5	3	1	3	1	5	3	8	19	28	11	...	...	..	..	87	17.5
34	7	1	1	1	4	10	6	9	15	24	6	1	...	..	..	85	17.5
35	4	8	3	7	3	4	8	11	27	55	34	...	...	..	..	164	17.5
36	1	4	3	2	9	2	5	11	12	6	23	19	6	..	..	103	18.0
37	5	5	5	5	6	13	13	21	20	32	46	39	44	..	..	254	18.0
38	12	5	7	8	9	16	24	39	50	71	77	31	1	..	..	350	17.5
39	10	3	5	13	28	37	54	95	210	131	341	154	...	..	..	1081	18.0
40	9	3	8	7	12	27	38	39	97	147	170	201	199	..	..	957	18.0
41	10	2	11	10	17	41	67	77	102	160	307	191	62	..	..	1057	18.0
42	8	3	3	12	13	13	32	43	51	127	91	58	3	..	..	457	17.5
43	3	6	7	8	12	19	14	25	29	66	61	40	13	..	..	303	18.0
44	7	1	1	7	5	11	5	12	9	16	29	9	8	..	..	120	18.0
45	5	2	4	4	3	8	7	12	7	24	13	21	45	..	..	155	19.0
46	4	1	2	2	2	8	8	12	14	14	17	14	27	30	7	162	19.0
47	1	0	0	0	2	0	3	3	3	7	9	26	21	..	..	75	18.5
48	4	0	5	3	8	8	19	23	40	54	56	125	131	12	..	488	18.5
49	7	3	8	11	13	14	29	41	68	84	172	308	106	131	..	995	18.5
50	7	2	6	15	15	13	31	73	71	106	79	116	167	18	..	719	18.5
51	3	5	4	4	17	13	9	23	29	24	31	46	...	..	..	208	18.5
52	3	0	0	6	3	3	8	12	6	6	17	13	15	..	..	92	18.5
53	2	3	0	6	4	4	10	11	8	18	15	31	26	11	..	149	18.5
54	2	1	3	2	7	1	5	5	1	8	9	18	23	20	1	106	19.0
55	4	1	2	1	1	5	3	6	3	8	9	6	...	..	..	49	18.0

56	4	0	4	1	3	1	10	7	9	9	12	33	...	..	..	93	18.5
57	2	2	3	5	8	2	4	3	8	4	11	8	10	22	8	100	19.0
58	5	1	1	5	7	3	2	3	9	16	23	22	13	1	..	111	18.0
59	3	1	3	6	5	5	7	11	8	20	55	53	2	..	..	179	18.0
60	7	2	2	2	8	7	13	19	19	26	28	13	...	..	..	146	17.5
61	5	2	5	5	6	5	17	8	15	35	18	27	6	..	..	154	18.5
62	11	6	3	5	11	8	19	34	46	34	117	59	11	..	..	364	18.0
63	8	9	10	18	26	49	70	64	126	113	264	139	134	..	..	1030	18.0
64	20	19	8	27	41	43	91	149	160	241	404	347	174	..	..	1724	18.0
65	12	2	5	14	12	25	49	41	134	126	185	297	148	106	..	1156	18.5
66	6	1	1	5	14	22	23	16	26	26	101	73	33	..	..	347	18.5
67	5	2	1	5	3	9	12	16	10	25	22	30	29	30	4	203	18.5
68	3	2	9	1	5	9	10	3	13	23	26	18	13	7	2	144	18.0
69	4	2	1	2	6	6	9	4	10	11	17	27	14	1	..	114	18.5
70	3	0	0	2	2	4	11	6	13	17	17	23	4	..	..	102	18.0
71	6	1	0	1	2	5	3	6	10	8	16	21	5	..	..	84	18.5
72	1	1	0	3	0	3	5	5	12	20	86	5	...	..	..	141	18.0
73	1	1	2	9	12	6	19	31	30	48	114	102	3	..	..	378	18.0
74	6	1	8	7	10	19	17	25	96	47	68	98	132	5	..	539	18.5
75	8	5	9	8	13	23	28	44	53	42	80	47	53	20	..	433	18.0
76	4	5	2	4	7	9	10	5	29	13	29	43	27	26	..	213	18.5
77	3	2	4	3	1	4	9	7	3	7	27	17	...	.	..	87	18.5
78	6	0	3	1	6	2	4	6	12	13	28	6	...	..	..	87	18.0
79	5	1	1	3	5	2	9	6	11	8	21	12	21	2	..	107	18.0
80	3	3	1	2	3	1	7	11	5	10	20	16	27	2	..	111	18.0
81	3	3	1	3	4	3	8	5	8	16	17	13	16	35	10	145	18.0
82	2	2	0	1	3	3	1	17	7	17	44	40	6	..	..	143	18.0
83	5	3	3	1	7	5	9	14	15	18	38	29	21	..	..	168	18.0
84	8	4	4	8	11	9	26	34	36	57	53	70	21	..	..	341	18.5
85	4	4	0	6	7	7	18	19	51	63	72	18	...	..	..	269	17.5

TABLE I*b*—*Continued*

Area	13.0	13		14		15		16		17		18		19		Total	Limit Complete
86	4	4	13	9	15	25	20	29	89	109	121	156	36	..	..	630	18.5
87	5	1	8	9	3	19	28	37	48	152	190	255	213	..	..	968	18.5
88	10	9	13	11	23	40	53	62	117	176	218	343	418	66	..	1559	18.5
89	8	0	4	1	7	11	20	34	43	33	73	81	36	2	..	353	18.5
90	6	2	2	6	2	10	6	10	13	19	21	22	20	11	4	154	18.5
91	5	0	1	4	8	6	9	16	23	19	31	55	12	..	..	189	18.5
92	5	2	3	1	3	8	10	11	1	13	35	28	38	16	..	174	18.5
93	10	1	3	6	5	5	3	7	6	11	20	23	3	..	..	103	18.0
94	10	2	1	3	3	1	7	9	9	9	13	15	7	..	..	89	18.0
95	1	0	0	1	3	5	5	1	7	4	8	13	...	..	..	48	18.5
96	3	0	2	4	4	9	14	7	22	22	18	34	26	16	24	205	18.5
97	5	1	2	1	4	4	10	20	24	30	33	68	126	18	..	346	18.5
98	21	5	8	20	36	22	56	96	115	281	222	22	...	..	..	904	17.5
99	6	9	4	24	16	20	31	71	44	79	82	13	...	..	..	399	17.5
100	10	2	3	6	8	8	14	11	15	39	4	...	...	..	..	120	17.5
101	4	3	6	4	4	10	6	12	10	19	13	31	41	52	24	239	19.0
102	6	2	4	4	5	4	9	18	10	13	34	32	...	..	..	141	18.0
103	4	2	0	3	6	7	5	6	22	12	13	31	28	..	..	139	18.5
104	6	0	0	4	6	4	9	12	17	19	26	8	...	..	..	111	18.0
105	6	0	4	6	4	7	5	12	17	20	29	40	11	..	..	161	18.5
106	4	0	1	1	11	7	17	13	20	22	11	7	...	..	..	114	17.5
107	7	6	4	3	2	15	5	8	21	54	57	13	...	..	..	195	18.0
108	3	1	1	5	6	17	10	42	45	53	68	62	...	..	..	313	18.0
109	2	2	7	2	5	19	25	31	62	122	103	143	23	..	..	546	18.5
110	6	1	1	1	0	4	4	4	6	7	7	30	14	19	3	107	18.5
111	2	2	7	4	15	24	37	52	70	195	245	196	226	17	..	1092	18.0
112	5	3	6	11	10	18	21	12	40	57	75	72	3	..	..	333	18.0
113	3	2	0	1	8	9	3	8	12	16	22	28	18	..	..	130	18.5
114	2	3	4	4	8	10	7	10	22	24	64	43	8	..	..	209	18.0
115	7	2	2	2	2	6	5	10	12	5	21	23	18	2	..	117	18.5

116	4	1	1	3	3	5	3	3	4	6	6	12	15	7	1	74	19.0
117	1	2	4	1	5	2	4	5	15	10	17	24	2	..	..	92	18.5
118	5	1	1	0	4	4	7	6	8	22	42	7	...	..	..	107	18.0
119	2	4	8	2	5	2	7	5	10	14	13	7	1	..	..	80	17.5
120	5	2	2	3	5	6	8	11	30	21	40	34	4	..	..	171	18.0
121	2	3	3	2	9	4	7	15	11	20	26	31	12	..	..	145	18.0
122	6	3	5	7	11	12	23	44	48	61	138	71	...	..	..	429	18.0
123	24	14	8	28	44	43	58	127	167	174	256	329	16	..	..	1288	18.5
124	10	4	17	15	17	26	26	100	68	69	94	...	...	..	..	446	18.0
125	11	4	2	3	12	14	12	22	27	28	41	30	2	..	..	208	18.0
126	4	2	1	2	8	4	5	7	18	15	15	25	12	2	..	120	18.5
127	7	1	2	6	6	10	7	17	17	38	27	1	...	..	..	139	17.5
128	7	2	4	4	3	11	4	16	21	18	43	12	...	..	..	145	18.0
129	4	2	4	3	10	8	5	13	18	27	25	39	2	..	..	160	18.5
130	5	3	2	5	7	12	7	17	35	25	48	35	2	..	..	203	18.0
131	5	3	0	2	3	5	10	16	19	22	53	39	36	1	..	214	18.0
132	4	3	1	3	3	5	9	23	31	33	54	39	...	..	..	208	18.0
133	1	1	4	3	11	13	19	55	105	133	215	209	418	118	..	1305	19.0
134	24	6	16	15	17	42	57	99	101	117	221	169	...	..	..	884	18.0
135	9	4	7	18	32	31	70	140	176	423	819	300	...	..	..	2029	18.0
136	6	2	3	8	11	18	22	44	33	100	116	...	...	..	..	363	17.5
137	5	0	3	4	4	6	12	17	25	23	35	39	17	..	..	190	18.0
138	5	3	5	4	4	8	9	12	26	28	30	29	1	..	..	164	17.5
139	3	1	3	2	1	6	4	5	10	13	18	11	...	..	..	77	18.0
Sums	792	376	482	741	1120	1563	2235	3305	4836	6667	9344	8029	4423	908	89	44910	......

following statistical discussion, it is both desirable and necessary to treat the Mount Wilson and Groningen results separately. The counts which are the basis of the discussion are given for each half-magnitude interval below $m=13.0$ in Tables I*a* and I*b*, respectively. The numbers of stars brighter than $m=13.0$ are listed in the second column; and in the last column but one, the total counted in each area. Thus for Area 1, the first line of Table I*a* indicates that the Mount Wilson counts in an area of 0.115 square degrees show a total of 4 stars brighter than 13.0; 0 stars in the interval 13.00–13.49; 1 in the interval 13.50–13.99, etc.; and a total of 137 for the area.

The numbers in the last columns of Tables I*a* and I*b* are the magnitude limits to which the counts are assumed to be complete. For a reflector having a focal ratio of 5 to 1, the limiting magnitude falls off rapidly with increasing distance from the optical axis. For the field used the maximum loss is about 0.5 mag., and allowance must be made for at least this amount in assigning the limit to which the counts are complete. For safety the limits have been rather conservatively fixed.

It should be explained that Table I*a* includes about 3800 faint stars which do not appear in the *Catalogue* because their magnitudes depend on a single plate. Series (*a*) includes two photographs of each area with two equal exposures of 15 minutes on each plate, but in the case of faint stars the magnitude for one of the plates is often missing. Defective and superposed images account for some of these cases, but difference in limiting magnitude is the usual explanation. Such stars, although retained for the statistical discussion, have been omitted from the *Catalogue*, unless measured at Groningen on plates of series (*b*). Everything that could be seen on the Mount Wilson photographs has been measured, and the relatively large error of measurement near the limiting magnitude explains the omissions from the *Catalogue*. The statistical value of the data is, however, little affected. All the Groningen magnitudes, on the other hand, depend on a single plate, but here there is less danger of error, for the measures could not be pushed so close to the limiting magnitude as in the case of the Mount Wilson plates where the multiple images guard against confusion with defects in the film.

2. DISCUSSION OF THE MOUNT WILSON COUNTS

The data in Tables I*a* and I*b* lead to the values of log N_m for different galactic latitudes given in Table VII, where N_m is the mean number of stars per square degree brighter than m derived from the two series of counts. These results, which are the basis for the mean distribution for $m > 13.5$, can be reproduced from the original counts by following the steps now to be described.

Formation of latitude groups.—Since the fields measured are small, the counts are much affected by local irregularities of distribution. These are partially eliminated by combining the 139 areas into 28 groups, arranged according to galactic latitude as shown in Table II, each line of which gives in succession the mean latitude of the group, the serial numbers of the areas, and their respective latitudes. Southern latitudes are indicated by italic figures, although in the present discussion any possible systematic difference between the two galactic hemispheres is ignored. For the completion of the counts to a uniform limiting magnitude, the data were further condensed into seven groups indicated by the divisions of Table II.

Completion of the counts.—For the discussion it is important that the counts for all areas should be complete to the same limiting magnitude. The frequencies of the limits of completeness given in the last columns of Tables I*a* and I*b* are shown in Table III. For a considerable percentage of cases, the data are complete to magnitude 18.5; for the others, the distribution is such that the counts can be extended to this limit with little uncertainty.

The procedure was as follows: The original counts in Tables I*a* and I*b* were tabulated in subgroups according to the latitude and magnitude limits shown in Table III. Thus for Mount Wilson, group I, the tabulation included three subgroups: two areas complete to 17.5, eight complete to 18.0, and nine complete to 18.5. The logarithms of the sums of the numbers of stars in each half-magnitude interval were plotted for each subgroup. The ordinates of the resulting curves (log S curves) were tabulated for each half-magnitude and differenced, the individual first differences thus having the form

$$\log R = \log \left(\frac{\text{No. stars } m \text{ to } m+0.5}{\text{No. stars } m-0.5 \text{ to } m} \right)$$

where, briefly, R is the ratio of the numbers of stars in adjacent half-magnitude intervals. Each subgroup thus gives a sequence of values of log R, terminating at $m = 17.0$, 17.5, or 18.0, and, for a few scattering areas, at 16.5. Means were formed for corresponding intervals, Mount Wilson and Groningen results and each of groups I–VII being treated separately. Finally, the Mount Wilson and Groningen means, the agreement of which affords a useful check, were themselves combined to form for each latitude group a single mean sequence of values of log R. The values actually required for the completion of the counts are given in Table IV.

TABLE II

Grouping of Areas according to Galactic Latitude

Group	Mean Lat.	Serial Numbers of Areas					Galactic Latitudes				
I.	0°	24,	40,	123,	134,	...	0°,	0°,	0°,	0°,	..
	1	19,	64,	74,	87,	98	*1*,†	*1*,	1,	1,	1
	3	(110),	9,	49,	8,	18	1,	2,	*2*,	*3*,	6
	8	23,	25,	41,	39,	50	*7*,	8,	*8*,	9,	10
II.	11	63,	97,	111,	48,	65	10,	*11*,	*11*,	*12*,	*12*
	12	73,	88,	124,	133,	2	*12*,	*12*,	12,	12,	13
	13	10,	22,	42,	122,	135	13,	*13*,	*13*,	*13*,	*13*
	15	75,	109,	86,	99,	43	14,	14,	15,	15,	*16*
III.	18	3,	21,	20,	26,	38	17,	*17*,	*18*,	18,	18
	20	17,	7,	66,	47,	51	19,	20,	*20*,	*21*,	22
	24	62,	89,	72,	125,	132	23,	*23*,	*24*,	24,	24
	26	96,	112,	11,	121,	136	*25*,	*25*,	26,	*26*,	*26*
IV.	27	46,	76,	85,	1,	27	*27*,	27,	27,	28,	28
	29	37,	67,	100,	108,	4	28,	*28*,	28,	28,	32
	33	44,	45,	16,	52,	61	*32*,	*32*,	33,	34,	34
	35	71,	90,	131,	126,	6	*34*,	*34*,	34,	35,	36
V.	39	95,	113,	28,	36,	77	*38*,	*38*,	39,	39,	39
	40	137,*	84,	120,	12,	101	*39*,*	40,	*40*,	41,	41
	42	107,	5,	70,	127,	91	41,	42,	*42*,	42,	*43*
	46	130,	53,	68,	69,	128	43,	47,	*47*,	*47*,	47
VI.	48	129,	15,	60,	29,	35	47,	48,	48,	49,	49
	51	94,	114,	106,	102,	13	*49*,	*49*,	51,	52,	53
	54	138,	78,	83,	119,	14	*53*,	54,	54,	*54*,	57
	59	93,	115,	34,	59,	30	*58*,	*58*,	59,	59,	60
VII.	61	54,	103,	105,	92,	104	60,	60,	60,	*62*,	62
	66	118,	82,	139,	79,	31	*65*,	66,	*66*,	67,	68
	73	33,	32,	58,	55,	80	68,	72,	73,	74,	76
	79	81,	116,	117,	56,	57	76,	*76*,	*76*,	80,	85

* Areas of Groningen fields 15′×15′ for latitudes less than 40°; 20′×20′ for higher latitudes.

† Italic figures indicate negative latitudes. The position used for the galactic pole is $\alpha = 12^h\,41^m\,20^s$, $\delta = +27°\,21'$ (1875).

The values of log *R*, being first differences of the ordinates of the log *S* curves, can be used to extend the curves terminating at 17.0, 17.5, and 18.0 to the uniform limit of 18.5. Thus again for Mount Wilson, group I, the last ordinate of the log *S* curve for the eight areas complete to 18.0 is 3.53, which is the logarithm of the total number of stars in these areas having magnitudes between 17.5 and 18.0. Applying now log $R=0.13$, from Table IV, we find for the interval 18.0–18.5, log $S=3.66$. The total number of stars in the eight areas having magnitudes in this interval is therefore 4570, which is the "completed" total for this particular subgroup of areas. These stars are now to be distributed among the individual areas

TABLE III

FREQUENCIES OF LIMITS TO WHICH ORIGINAL COUNTS ARE COMPLETE

Group	Gal. Latitude	Mount Wilson				Groningen				
		17.0	17.5	18.0	18.5	17.0	17.5	18.0	18.5	19.0
I.	0°–10°	0	2	8	9	0	1	8	10	0
II.	10–16	1	2	6	11	0	4	9	6	1
III.	17–26	1	7	10	2	1	2	9	8	0
IV.	27–36	0	8	10	2	0	6	4	8	2
V.	38–47	1	4	10	5	0	3	8	8	1
VI.	47–60	0	7	9	4	0	8	10	2	0
VII.	60–85	1	3	14	2	0	1	11	5	3
Totals.	. . . .	4	33	67	35	1	25	59	47	7

TABLE IV

VALUES OF LOG *R* USED TO COMPLETE COUNTS

Group	*m*		
	17.0	17.5	18.0
I.	0.151	0.141	0.130
II.	.160	.149	.138
III.	.138	.130	.120
IV.	.122	.111	.105
V.	.116	.107	.096
VI.	.109	.100	.092
VII.	0.108	0.100	0.093

in accordance with the totals counted in each area to the "observed" limit of completeness, namely, 18.0. The details are as follows:

S.A. No.	123	134	64	49	8	18	41	39	Total
$N_{18.0}$	1558	1077	2380	955	765	997	1412	1638	10782
Fraction	0.145	0.100	0.220	0.089	0.071	0.092	0.131	0.152	1.000
$N_{18.0-18.5}$	663	457	1005	407	324	420	599	695	4570

The numbers counted in each area to 18.0, as found from Table I*a*, are given in the second line, while their fractional distribution among the total of 10,782 appears in the third line. The numbers in the last line give the corresponding distribution of the 4570 stars in the interval 18.0–18.5. These are the completed counts for the individual areas, and together with similar results for other areas are collected in Table V.

Systematic correction for central stars.—The original counts require a correction arising from the fact that each field is centered on a bright star, usually of the eighth or ninth magnitude. The areas measured are, however, so small that a random choice of fields would by no means always include a star of this order of brightness. For example, suppose all the central stars were between magnitudes 8.5 and 9.0, and that all the fields were exactly $\frac{1}{9}$ square degree. Counts of the central stars alone, on the assumption that the fields were representative, would then give 9 stars per square degree between 8.5 and 9.0, whereas the actual number for all latitudes averages less than a single star. The counts for the interval in question and all the cumulative sums to lower limits of magnitude would be too large by about 8 stars per square degree. The percentage error for faint magnitudes, especially in rich regions, is small, but this is by no means the case in general. Thus to $m=15.0$, in latitude 70°, the average total number of stars per square degree is about 100, and the systematic error would accordingly be 8 per cent.

The required corrections have been calculated for each area on the basis of the adopted mean magnitude of the central star and the distribution table of van Rhijn, *Groningen Publication* No. 27, corrected for scale, which, for the region of brightness involved, is practically identical with Table XVII, the final result of the present discussion. The corrections, referred to an area of 1 square degree, are in the last two columns of Table V. The magnitudes of the

TABLE V

Completed Counts and Corrections for Central Stars

S.A.	M.W.		Gr.		Mag. Cent. Star	Gal. Lat.	Corr. for Cent. Star	
	17.5–18.0	18.0–18.5	17.5–18.0	18.0–18.5			M.W.	Gr.
1	48	62	23	30	7.27	+28°	8.5	15.9
2*	195	275	....	118	9.95	+13	6.4	13.8
3	111	146	....	75	8.51	+17	8.0	15.3
4	50	64	22	29	9.94	+32	7.4	14.7
5	31	38	28	36	9.35	+42	8.0	8.4
6	43	56	21	28	10.49	+36	6.9	14.2
7*	102	135	58	76	10.23	+20	5.9	13.2
8	....	324	....	....	8.84	− 3	7.6	14.9
9	....	....	....	....	7.63	+ 2	8.3	15.6
10	....	....	70	99	8.89	+13	7.8	15.2
11	57	76	....	....	8.30	+26	8.3	15.7
12	24	30	18	23	8.64	+41	8.2	8.6
13	....	16	....	25	7.83	+53	8.5	8.9
14	24	29	22	27	10.50	+57	6.6	6.9
15	28	35	32	40	9.98	+48	7.7	8.0
16	51	66	27	34	9.16	+33	7.9	15.2
17	....	161	....	....	9.05	+19	7.6	14.9
18	....	420	....	225	10.08	+ 6	4.1	11.4
19	....	....	....	133	9.36	− 1	6.8	14.2
20	....	150	....	81	8.97	−18	8.0	15.3
21	....	....	....	95	10.03	−17	5.6	13.0
22	....	....	119	168	8.77	−13	7.8	15.2
23	....	....	....	....	8.83	− 7	7.7	15.0
24	....	....	....	....	10.28	0	3.8	11.2
25	....	....	....	101	9.29	+ 8	7.1	14.4
26	....	147	....	....	10.47	+18	5.7	13.0
27	56	72	....	....	10.40	+28	6.4	13.7
28	....	37	....	....	10.59	+39	5.9	13.3
29	....	19	....	21	8.78	+49	8.3	8.6
30	....	16	....	16	10.4†	+60	7.4	7.7
31	16	19	....	20	9.49	+68	8.2	8.5
32	....	18	....	17	9.71	+72	7.9	8.3
33*	18	22	26	32	9.40	+68	8.2	8.5
34	24	29	23	28	9.63	+59	7.8	8.1
35	39	48	39	47	10.85	+49	6.3	6.6
36	....	43	....	23	9.34	+39	8.0	15.3
37	....	98	....	48	10.58	+28	5.0	12.3
38	....	228	92	122	9.71	+18	6.8	14.1
39	....	695	....	370	9.16	+ 9	7.2	14.5
40	297	401	....	223	9.84	0	5.6	12.9
41	....	599	....	321	10.06	− 8	4.4	11.7
42	....	338	146	206	8.3†	−13	8.2	15.5
43	....	....	....	110	10.10	−16	5.5	12.8
44	....	64	....	29	8.96	−32	8.2	15.5
45	53	68	....	....	9.00	−32	7.9	15.2

* Completed counts for 17.0–17.5:

S.A.	M.W.	Gr.
2	141	..
7	76	43
33	14	..
84	63	..

† Combined brightness of components.

TABLE V—*Continued*

S.A.	M.W.		Gr.		Mag. Cent. Star	Gal. Lat.	Corr. for Cent. Star	
	17.5–18.0	18.0–18.5	17.5–18.0	18.0–18.5			M.W.	Gr.
46....	....	....	....	....	9.51	−27°	7.2	14.6
47....	....	28	....	....	7.46	−21	8.5	15.9
48....	....	....	....	....	(6.9)‡	−12	....	....
49....	....	407	....	....	9.90	− 2	5.8	13.2
50....	....	....	....	....	8.55	+10	7.8	15.1
51....	....	130	....	....	10.71	+22	4.6	12.0
52....	....	46	....	....	8.53	+34	8.2	15.5
53....	....	31	....	....	9.61	+47	7.6	8.0
54....	....	14	....	....	10.23	+60	7.4	7.7
55....	....	13	....	12	10.08	+74	7.5	7.9
56....	....	20	....	....	10.13	+80	7.6	8.0
57....	....	15	....	....	9.01	+85	8.2	8.6
58....	....	24	....	21	9.72	+73	8.0	8.3
59....	....	33	....	33	9.42	+59	8.1	8.5
60....	....	32	31	38	9.50	+48	7.7	8.0
61....	....	76	....	....	9.56	+34	7.4	14.7
62....	....	222	....	106	8.36	+23	8.3	15.6
63....	....	....	....	328	9.61	+10	6.2	13.6
64....	....	1005	....	479	8.31	− 1	8.0	15.3
65....	....	....	....	....	9.45	−12	7.3	14.7
66....	130	180	....	....	10.10	−20	5.9	13.2
67....	....	....	....	....	9.67	−28	7.3	14.6
68....	....	33	....	31	9.08	−47	8.0	8.4
69....	....	....	....	....	8.22	−47	8.4	8.8
70....	21	26	....	23	8.20	−42	8.4	8.8
71....	....	34	....	....	9.74	−34	7.4	14.7
72....	41	54	....	49	6.89	−24	8.6	15.9
73....	....	193	....	118	8.34	−12	8.1	15.5
74....	....	....	....	....	8.89	+ 1	7.6	14.9
75....	....	223	....	136	9.62	+14	6.5	13.9
76....	....	55	....	....	9.57	+27	7.2	14.6
77....	....	35	....	....	8.66	+39	8.2	15.6
78....	....	17	....	22	9.58	+54	7.8	8.1
79....	15	18	....	21	9.60	+67	7.9	8.2
80....	....	18	....	19	8.53	+76	8.4	8.7
81....	14	17	....	20	10.29	+76	7.6	7.9
82....	....	27	....	28	9.74	+66	7.9	8.3
83....	....	33	....	31	9.25	+54	8.1	8.4
84*...	79	100	....	....	8.82	+40	8.2	8.6
85....	....	148	56	72	9.37	+27	7.6	15.1
86....	....	....	....	....	10.49	+15	5.4	12.7
87....	....	....	....	....	9.66	+ 1	5.6	13.0
88....	....	....	....	....	8.82	−12	7.8	15.2
89....	....	180	....	....	8.70	−23	8.0	15.4
90....	....	58	....	....	9.04	−34	7.9	15.2
91....	....	....	....	....	8.86	−43	8.2	8.6
92....	....	....	....	....	9.24	−62	8.1	8.5
93....	....	....	....	21	10.10	−58	7.3	7.7
94....	....	....	....	18	10.58	−49	6.3	6.6
95....	....	....	....	....	9.34	−38	8.0	15.3
96....	....	....	....	....	9.46	−25	7.8	15.1

‡ Approximate magnitude. Too bright for measurement.

TABLE V—*Continued*

S.A.	M.W.		Gr.		Mag. Cent. Star	Gal. Lat.	Corr. for Cent. Star	
	17.5–18.0	18.0–18.5	17.5–18.0	18.0–18.5			M.W.	Gr.
97	....	....	....	....	6.81	−11°	8.6	15.8
98	497	670	269	363	7.92	+ 1	8.3	15.6
99	358	505	146	206	9.81	+15	6.6	13.9
100	81	105	36	47	9.27	+28	7.8	15.1
101	....	....	....	....	9.42	+41	8.0	8.3
102	....	31	....	29	9.12	+52	8.1	8.4
103	....	24	....	....	8.94	+60	8.3	8.7
104	....	28	....	29	10.89	+62	6.8	7.1
105	....	31	....	....	9.74	+60	7.8	8.2
106	31	39	28	35	10.65	+51	6.5	6.8
107	....	58	....	54	8.04	+41	8.4	8.8
108	....	128	....	70	9.37	+28	7.8	15.1
109	....	....	....	....	9.08	+14	7.4	14.8
110	....	....	....	....	10.31	+ 1	4.0	11.3
111	....	....	....	283	(7.0)‡	−11	....	....
112	....	195	....	93	9.56	−25	7.2	14.5
113	....	....	....	....	9.33	−38	8.0	15.3
114	36	44	....	42	9.64	−49	7.7	8.1
115	....	....	....	....	9.66	−58	7.8	8.2
116	....	12	....	....	10.28	−76	7.6	7.9
117	....	....	....	....	10.21	−76	7.6	7.9
118	....	23	....	29	8.96	−65	8.4	8.7
119	....	18	17	21	9.13	−54	8.1	8.4
120	....	42	....	40	10.22	−40	6.9	7.2
121	56	73	....	37	8.41	−26	8.3	15.7
122	....	242	....	155	9.02	−13	7.4	14.7
123	....	663	....	....	8.05	0	8.0	15.3
124	....	365	....	193	10.55	+12	2.9	10.2
125	91	120	....	63	9.28	+24	7.7	15.0
126	....	52	....	....	(7.4)‡	+35	....	....
127	41	50	33	41	9.31	+42	8.0	8.4
128	....	41	....	40	9.38	+47	8.1	8.4
129	32	39	....	....	9.30	+47	8.1	8.4
130	....	54	....	50	9.04	+43	8.1	8.4
131	64	82	....	39	8.86	+34	8.2	15.5
132	....	112	....	61	8.10	+24	8.3	15.6
133	....	381	....	....	10.26	+12	5.1	12.4
134	....	457	....	285	7.79	0	8.3	15.6
135	905	1277	....	749	9.42	−13	7.4	14.7
136	155	204	94	124	8.62	−26	8.1	15.4
137	....	60	....	71	9.06	−39	8.0	15.3
138	....	....	31	38	9.95	−53	7.8	8.1
139	....	20	....	19	9.99	−66	7.9	8.3

central stars and the galactic latitudes of the areas appear in the two columns immediately preceding. In a few cases the central stars are doubles; for these the combined magnitude of the components, counted as a single star, has been used. In two or three instances the central star is too bright for measurement, and has not been counted.

As an illustration, the calculation of the corrections for S.A. 1 follows: The magnitude of the central star falls in the interval 7.0–7.5; the latitude is 28°. From Table XVII,[1] $\log N_{7.5}=9.484$, $\log N_{7.0}=9.261$. The average number of stars per square degree in the interval is therefore 0.123. The reciprocals of the areas, in square degrees, of the Mount Wilson and Groningen fields are 8.666 and 16. Reduced to unit area, the counts will therefore be in excess by 8.5 and 15.9 stars, respectively. These numbers accordingly appear in Table V as corrections.

Collection of data for 28 latitude groups.—The derivation of Table VII will now be understood from the following details relating to the first latitude group, which, as shown by Table II, includes Areas 24, 40, 123, and 134. The sums of the counts for these areas, formed from the data in Tables I*a* and I*b* and the completed counts in Table V, are given in the first two lines of Table VI.[2] Below $m=13.0$ the sums refer to half-magnitude intervals for which the column heading is the lower limit. The cumulative sums are in the third and fourth lines, and their logarithms, reduced to an area of 1 square degree, in the fifth and sixth lines. The constants for reduction of the logarithms to unit area are

$$\log(8.666/4)=0.336\ (MW);\quad \log(16/4)=0.602\ (Gr).$$

The corrections for the central stars are most easily applied with the aid of subtraction logarithms. The total excess for the four areas, from the last two columns of Table V, is 25.7 for Mount Wilson and 55.0 for Groningen. The logarithms of the corrections are, therefore,

$$\log(25.7/4)=0.808\ (MW)\text{ and }\log(55.0/4)=1.138\ (Gr).$$

Combined with the fifth and sixth lines, these give the corrected values of $\log N_m$, which are the final results from the Mount Wilson and Groningen counts. The means of the corrected logarithms[3] appear in the first line of Table VII, and their differences *MW−Gr* in the first line of Table VIII.

---

[1] For convenience, this table is used for the illustration instead of van Rhijn's.

[2] In combining the Groningen counts for the group at 40° an obvious modification is necessary to take account of the change in the area of the fields at latitude 40°.

[3] Strictly speaking, the logarithms of the mean of the numbers should be used; but the numbers are so nearly alike that the difference, even when appreciable, is unimportant. The distinction is that between the arithmetical and geometrical means.

The counts for one area (No. 110) have been omitted altogether. The region is in Serpens, between the two branches of the Milky Way, and so heavily obscured that its inclusion would have affected the mean density seriously.

TABLE VI

Details for First Latitude Group Tables VII and VIII

		13.0	13.5	14.0	14.5	15.0	15.5	16.0	16.5	17.0	17.5	18.0	18.5
Counts	M. W.	99	43	54	102	151	240	315	550	674	813	1110	1700
	Gr.	63	26	34	58	79	127	189	296	410	526	702	976
Cum. sums	M. W.	99	142	196	298	449	689	1004	1554	2228	3041	4151	5851
	Gr.	63	89	123	181	260	387	576	872	1282	1808	2510	3486
Log N_m	M. W.	2.332	2.488	2.628	2.810	2.988	3.174	3.338	3.527	3.684	3.819	3.954	4.103
	Gr.	2.401	2.551	2.692	2.860	3.017	3.190	3.362	3.543	3.710	3.859	4.002	4.144
Corr. log N_m	M. W.	2.319	2.479	2.621	2.806	2.985	3.172	3.337	3.526	3.683	3.819	3.954	4.103
	Gr.	2.377	2.534	2.680	2.852	3.011	3.186	3.359	3.541	3.709	3.858	4.001	4.144
Mean table VII		2.348	2.506	2.650	2.829	2.998	3.179	3.348	3.534	3.696	3.838	3.978	4.124
Diff. table VIII		−0.058	−0.055	−0.059	−0.046	−0.026	−0.014	−0.022	−0.015	−0.026	−0.039	−0.047	−0.041

The differences in Table VIII afford a useful check. If the fields and the observed magnitudes for the two series of counts were the same, these differences would be zero. Actually, neither of the conditions specified is wholly satisfied, and appreciable systematic differences are to be expected, especially for small groups of four or five areas; but, as a whole, the two series should agree closely, as in fact they do, except for a small but persistent systematic difference. The mean differences for latitudes 0°–20°, 24°–42°, 46°–79°,

TABLE VII

MEAN OBSERVED LOG N_m

Lat.	13.0	13.5	14.0	14.5	15.0	15.5	16.0	16.5	17.0	17.5	18.0	18.5
0°	2.348	2.506	2.650	2.829	2.998	3.179	3.348	3.534	3.696	3.838	3.978	4.124
1	2.269	2.460	2.626	2.805	2.978	3.128	3.306	3.493	3.664	3.856	4.019	4.171
3	2.016	2.234	2.408	2.590	2.756	2.916	3.086	3.268	3.462	3.628	3.814	3.978
8	2.034	2.172	2.388	2.610	2.825	3.036	3.222	3.430	3.632	3.772	3.930	4.076
11	1.917	2.118	2.348	2.532	2.747	2.964	3.162	3.325	3.542	3.716	3.866	4.015
12	1.882	2.085	2.372	2.556	2.773	2.949	3.141	3.352	3.528	3.692	3.858	4.013
13	1.951	2.179	2.324	2.564	2.778	2.937	3.136	3.354	3.524	3.738	3.948	4.114
15	1.855	2.172	2.433	2.628	2.790	2.972	3.125	3.302	3.470	3.622	3.767	3.922
18	2.011	2.258	2.404	2.517	2.674	2.854	3.006	3.154	3.335	3.447	3.584	3.730
20	1.681	1.909	2.074	2.251	2.510	2.700	2.850	2.994	3.160	3.295	3.440	3.576
24	1.924	2.114	2.217	2.334	2.512	2.656	2.808	3.024	3.180	3.310	3.500	3.636
26	1.712	1.933	2.138	2.326	2.520	2.716	2.869	3.012	3.164	3.323	3.459	3.590
27	1.726	1.938	2.038	2.234	2.404	2.550	2.720	2.840	3.030	3.178	3.300	3.417
29	1.838	2.008	2.147	2.336	2.484	2.672	2.822	2.988	3.119	3.256	3.384	3.500
33	1.784	1.932	2.092	2.278	2.422	2.566	2.710	2.854	2.962	3.080	3.201	3.314
35	1.763	1.930	1.986	2.134	2.288	2.468	2.614	2.751	2.895	3.029	3.162	3.282
39	1.552	1.830	1.950	2.086	2.312	2.439	2.555	2.663	2.804	2.882	3.012	3.139
40	1.654	1.816	1.996	2.166	2.308	2.442	2.598	2.744	2.909	3.036	3.158	3.274
42	1.594	1.788	1.902	2.042	2.178	2.353	2.470	2.607	2.756	2.930	3.062	3.194
46	1.460	1.707	1.899	2.042	2.189	2.359	2.474	2.586	2.734	2.854	2.996	3.121
48	1.663	1.850	1.972	2.108	2.270	2.392	2.519	2.650	2.778	2.931	3.042	3.152
51	1.574	1.698	1.851	1.973	2.187	2.314	2.468	2.606	2.724	2.830	2.980	3.090
54	1.438	1.710	1.928	2.022	2.179	2.295	2.410	2.522	2.665	2.800	2.927	3.032
59	1.662	1.766	1.870	2.032	2.153	2.288	2.388	2.512	2.614	2.726	2.876	2.988
61	1.538	1.628	1.798	1.966	2.134	2.268	2.382	2.504	2.634	2.736	2.859	2.978
66	1.432	1.596	1.692	1.836	1.962	2.109	2.250	2.408	2.521	2.652	2.835	2.946
73	1.486	1.668	1.782	1.932	2.052	2.138	2.231	2.388	2.518	2.632	2.772	2.883
79	1.248	1.514	1.732	1.876	2.050	2.144	2.262	2.360	2.485	2.591	2.698	2.820

TABLE VII*a*

Deviation of Table VII from Adopted Mean Distribution of Table XVII

Lat.	13.0	13.5	14.0	14.5	15.0	15.5	16.0	16.5	17.0	17.5	18.0	18.5
0°	+0.185	+0.138	+0.081	+0.063	+0.039	+0.032	+0.018	+0.027	+0.017	−0.008	−0.030	−0.041
1	+ .115	+ .102	+ .067	+ .049	+ .029	− .010	− .015	− .006	− .007	+ .018	+ .019	+ .014
3	− .119	− .105	− .131	− .146	− .174	− .203	− .217	− .214	− .193	− .195	− .171	− .163
8	− .033	− .097	− .079	− .053	− .030	− .008	− .007	+ .022	+ .050	+ .022	+ .018	+ .008
11	− .100	− .098	− .065	− .075	− .050	− .020	− .005	− .019	+ .025	+ .032	+ .021	+ .016
12	− .117	− .113	− .022	− .031	− .003	− .012	− .002	+ .033	+ .038	+ .036	+ .043	+ .044
13	− .031	.000	− .050	− .002	+ .024	− .002	+ .018	+ .061	+ .061	+ .111	+ .162	+ .176
15	− .091	+ .030	+ .098	+ .103	+ .079	+ .079	+ .055	+ .060	+ .061	+ .051	+ .040	+ .045
18	+ .112	+ .166	+ .123	+ .051	+ .028	+ .032	+ .013	− .005	+ .015	− .029	− .042	− .041
20	− .187	− .150	− .171	− .175	− .092	− .074	− .091	− .109	− .100	− .117	− .119	− .125
24	+ .111	+ .113	+ .034	− .025	− .018	− .040	− .050	+ .011	+ .017	+ .003	+ .055	+ .058
26	− .074	− .040	− .015	− .001	+ .023	+ .055	+ .050	+ .040	+ .046	+ .064	+ .066	+ .068
27	− .048	− .021	− .101	− .079	− .077	− .094	− .082	− .113	− .068	− .059	− .069	− .079
29	+ .089	+ .076	+ .036	+ .052	+ .034	+ .061	+ .055	+ .073	+ .062	+ .064	+ .062	+ .055
33	+ .083	+ .050	+ .033	+ .049	+ .029	+ .015	+ .008	+ .008	− .022	− .036	− .041	− .047
35	+ .085	+ .072	− .047	− .068	− .077	− .053	− .056	− .062	− .055	− .051	− .042	− .039
39	− .082	+ .018	− .035	− .066	.000	− .027	− .057	− .090	− .083	− .132	− .123	− .110
40	+ .031	+ .015	+ .023	+ .027	+ .009	− .010	.000	+ .006	+ .038	+ .038	+ .040	+ .043
42	− .012	+ .005	− .052	− .076	− .099	− .076	− .103	− .105	− .088	− .040	− .027	− .008
46	− .112	− .039	− .016	− .035	− .044	− .023	− .050	− .075	− .057	− .061	− .036	− .022
48	+ .108	+ .122	+ .077	+ .051	+ .059	+ .034	+ .019	+ .015	+ .014	+ .044	+ .038	+ .038
51	+ .044	− .003	− .016	− .053	+ .008	− .011	+ .003	+ .007	− .002	− .018	+ .016	+ .016
54	− .067	+ .035	+ .088	+ .024	+ .029	.000	− .024	− .045	− .030	− .016	− .004	− .008
59	+ .198	+ .134	+ .076	+ .082	+ .052	+ .043	+ .005	− .003	− .028	− .036	.000	+ .004
61	+ .088	+ .012	+ .020	+ .032	+ .051	+ .041	+ .018	+ .008	+ .012	− .006	+ .004	+ .015
66	+ .013	+ .013	− .051	− .061	− .082	− .077	− .071	− .043	− .054	− .042	+ .028	+ .031
73	+ .105	+ .124	+ .081	+ .079	+ .054	+ .001	− .040	− .010	− .003	− .007	+ .021	+ .025
79	−0.108	−0.003	+0.058	+0.052	+0.082	+0.038	+0.024	−0.006	−0.003	−0.014	−0.018	−0.001

TABLE VIII

DIFFERENCES, *MW*−*Gr*, IN OBSERVED LOG N_m

Lat.	13.0	13.5	14.0	14.5	15.0	15.5	16.0	16.5	17.0	17.5	18.0	18.5
0°	−0.058	−0.055	−0.059	−0.046	−0.026	−0.014	−0.022	−0.015	−0.026	−0.039	−0.047	−0.041
1	−.004	−.023	−.016	−.034	−.029	−.033	−.033	−.016	−.018	−.004	.000	+.006
3	+.043	+.024	+.030	+.032	+.023	+.019	+.016	+.015	+.021	+.013	+.014	.000
8	+.061	+.118	+.094	+.061	+.048	+.029	+.001	+.009	+.013	+.003	−.012	+.003
11	−.078	−.025	−.021	−.040	−.008	+.003	−.035	−.014	+.017	+.024	−.029	−.060
12	+.119	+.052	−.002	−.003	−.002	−.010	−.010	−.009	−.012	−.002	−.007	−.010
13	−.070	−.036	−.030	−.028	−.022	−.006	−.003	+.002	−.021	−.056	−.100	−.088
15	+.154	+.035	.000	−.019	−.019	−.027	−.008	+.008	+.024	−.006	.000	+.013
18	+.042	−.028	−.014	+.002	+.001	+.011	+.012	+.014	+.008	−.006	+.004	+.011
20	+.018	−.010	+.058	+.100	+.012	−.005	+.020	+.029	+.043	+.048	+.032	+.043
24	−.119	−.071	−.044	−.022	−.005	−.010	−.030	+.009	−.022	+.005	−.015	−.007
26	+.048	+.052	+.036	−.026	−.015	−.015	−.028	−.025	.000	−.024	−.008	−.001
27	−.088	−.040	−.032	−.028	−.002	−.003	−.001	−.006	−.017	−.027	−.004	+.010
29	−.039	−.043	−.032	−.035	−.029	−.033	−.019	−.024	−.006	−.025	−.018	−.006
33	+.034	−.016	−.011	−.083	−.039	−.038	−.041	−.017	+.021	−.011	+.022	+.049
35	−.026	−.066	−.038	−.059	−.069	−.016	−.002	−.008	+.004	+.004	−.010	+.005
39	+.155	+.034	+.019	+.017	+.009	+.006	+.014	+.016	+.020	+.025	+.002	+.030
40	−.054	+.016	+.005	−.003	−.013	−.016	−.036	−.037	−.002	+.004	+.013	+.019
42	−.054	−.028	−.035	−.029	−.004	−.006	−.003	+.002	−.003	−.009	−.005	+.015
46	−.015	−.002	−.006	−.016	−.016	−.016	−.021	−.024	−.015	−.013	.000	+.006
48	−.032	−.005	+.009	+.021	+.017	+.009	−.004	.000	−.001	−.036	−.038	−.040
51	−.035	−.031	−.026	−.008	+.028	+.028	+.031	+.037	+.023	+.022	−.025	−.015
54	+.039	+.028	−.007	−.016	−.016	.000	−.010	−.003	−.012	−.037	−.058	−.061
59	−.066	−.029	−.047	−.037	−.026	−.036	−.010	−.007	−.007	−.004	−.031	−.020
61	+.029	+.003	+.033	+.035	+.001	+.004	−.016	−.026	−.004	−.028	−.046	−.069
66	−.072	−.056	−.032	−.004	−.025	−.046	−.003	+.017	−.004	−.029	−.042	−.045
73	+.035	+.017	+.035	+.019	+.031	+.012	+.002	+.009	+.007	−.039	−.030	−.034
79	+0.027	+0.032	−0.015	−0.036	−0.057	−0.021	−0.057	−0.030	−0.028	−0.014	−0.019	−0.029
0°–20°	+0.023	+0.005	+0.004	+0.002	−0.002	−0.003	−0.006	+0.002	+0.005	−0.002	−0.014	−0.012
24–42	−.016	−.018	−.015	−.030	−.019	−.015	−.016	−.010	−.001	−.006	−.003	+.013
46–79	−.010	−.005	−.006	−.005	−.007	−.007	−.010	−.003	−.005	−.020	−.032	−.034
0–79	0.000	−0.005	−0.005	−0.010	−0.009	−0.008	−0.011	−0.003	0.000	−0.009	−0.016	−0.011

and 0°–79°, given in the last four lines of Table VIII, show no progression either in latitude or in magnitude. The mean, Mount Wilson *minus* Groningen, for all latitudes and magnitudes is -0.007. Interpreted as a difference in zero-points, this corresponds to 0.02 mag.; as an error in the areas of the fields, it corresponds to a systematic difference of about $10''$ in the diameters of the fields of one series relative to those of the other.

Provisional mean distribution from the "Mount Wilson Catalogue."—The combined Mount Wilson and Groningen counts in Table VII, although mean values for five widely separated regions, are still much affected by local irregularities of distribution, which, in the case of small fields, are frequently a large percentage of the total star density. A further step toward the mean distribution was made by plotting the data in each column of Table VII against the corresponding latitude. The resulting curves represent the variation in log N_m with galactic latitude for each half-magnitude value of m from 13.0 to 18.5. These are reproduced in Figure 1, which shows the character and general order of the irregularities in the data of Table VII. The deviations for any given group of areas are naturally much alike for all the curves. A conspicuous case is the group for 3°. Special examination shows that all the fields are more or less obscured, which accounts for the persistently low density evident for all magnitudes. The fluctuations from group to group for any given magnitude are, however, accidental, and of such a character that the variation in log N_m with latitude is well defined. Thus, inspection of Figure 1 shows that a separate plotting of the data for alternate latitude groups in Table VII would have led to curves practically identical with those found from all the groups. The irregularities affecting the individual groups are still better shown by Table VII*a*, which gives the deviations from the adopted mean distribution in Table XVII.

To eliminate errors in the spacing of the curves of Figure 1 their ordinates were tabulated with values of m as argument for each 10° of latitude and adjusted until the first differences became regular. The smoothed ordinates for the interval $m=13.5$ to 18.5 are in Table IX, which represents the provisional mean distribution derived from the *Mount Wilson Catalogue.*

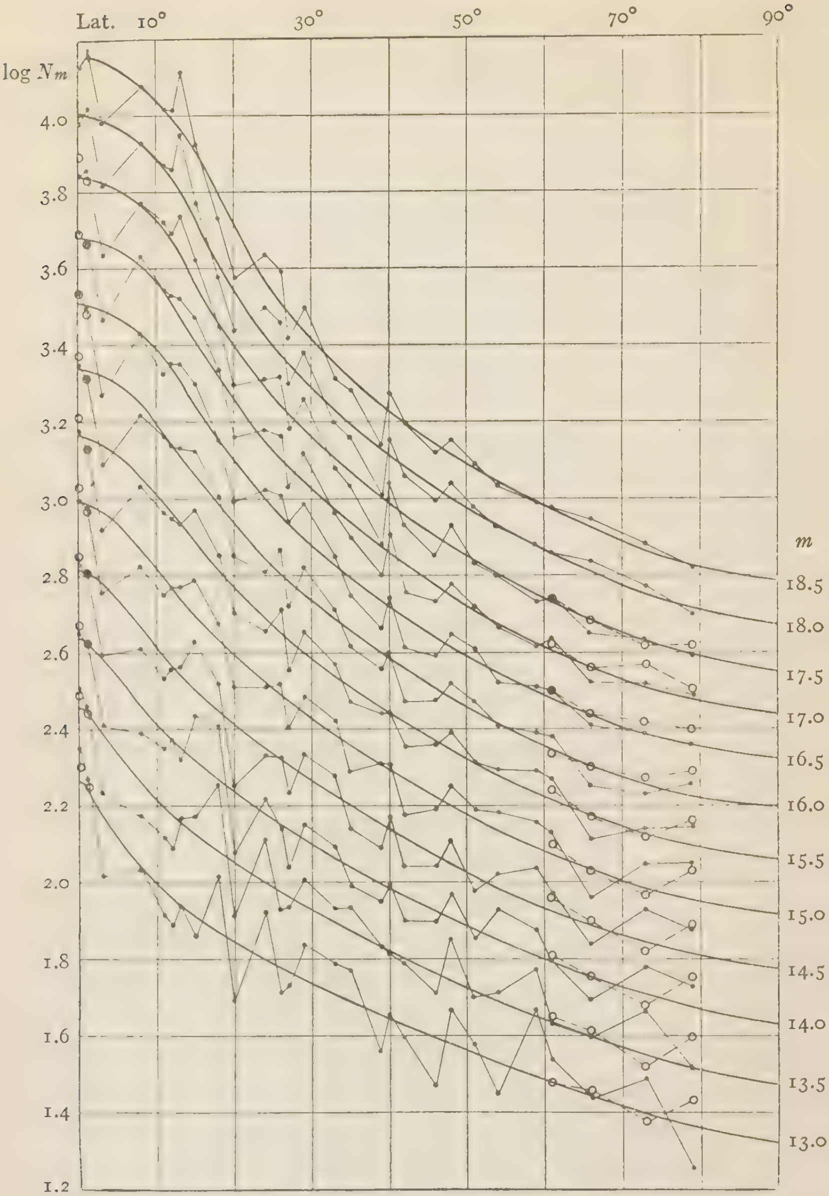

FIG. 1.—Observed values of log N_m for different galactic latitudes and magnitudes. Points are from Table VII, based on the *Mount Wilson Catalogue of Selected Areas;* circles represent counts from the *Harvard-Groningen Durchmusterung.* The curves are the basis of Table IX.

Local irregularities have now been rather thoroughly eliminated. Any residual effect will, however, be systematic, and is most likely to appear in the brighter magnitudes and in low galactic latitudes. The number of stars counted to the brighter limits of magnitude is small, even in the Milky Way; and in low latitudes the distribution in galactic longitude is not representative. Thus for latitudes less than 13° no counts whatever are available for stars fainter than $m=13$ between longitudes 190° and 350°. This is an unavoidable defect in the data. The order of the uncertainty will appear later when the results are combined with those from the astrographic zones.

TABLE IX

SMOOTHED VALUES OF LOG N_m FROM TABLE VII

m	0°	10°	20°	30°	40°	50°	60°	70°	80°	90°
13.5	2.445	2.210	2.047	1.924	1.817	1.716	1.632	1.562	1.504	1.469
14.0	2.629	2.414	2.233	2.097	1.981	1.874	1.786	1.713	1.656	1.624
14.5	2.811	2.615	2.415	2.266	2.140	2.026	1.935	1.861	1.805	1.774
15.0	2.990	2.813	2.594	2.429	2.295	2.174	2.080	2.003	1.948	1.919
15.5	3.166	3.007	2.768	2.586	2.444	2.318	2.220	2.142	2.087	2.058
16.0	3.340	3.197	2.937	2.740	2.587	2.458	2.356	2.275	2.220	2.193
16.5	3.510	3.381	3.101	2.887	2.727	2.593	2.488	2.405	2.349	2.322
17.0	3.677	3.557	3.260	3.027	2.861	2.724	2.616	2.531	2.474	2.447
17.5	3.841	3.727	3.413	3.161	2.990	2.852	2.741	2.655	2.594	2.567
18.0	4.001	3.890	3.559	3.289	3.114	2.975	2.863	2.775	2.710	2.682
18.5	4.156	4.045	3.699	3.410	3.232	3.093	2.980	2.891	2.822	2.792

Comparison with the "Harvard-Groningen Durchmusterung."—The *Harvard-Groningen Durchmusterung* of the Selected Areas gives the magnitudes of about a quarter of a million stars brighter than the sixteenth magnitude in the 206 Selected Areas between the North and South poles. The fields are 40′×40′, 60′×60′, and 80′×80′, according to the galactic latitude, and hence, on the average, some ten times the area of the fields of the *Mount Wilson Catalogue*. When the scale corrections for the areas south of declination −15° are better known, the *Durchmusterung* will be especially useful in deriving the distribution in the southern sky. Scale corrections for the areas north of −15° are already available,[1] and this part of the *Durchmusterung* might have been utilized in the present discussion. In fact, it has been used to some extent in extrapolating the curves of Figure 1 to 90°, but chiefly in a comparison of results for the 29 areas in the first two and the last four latitude groups of Table VII. The relatively large fields of the *Durchmusterung* undoubtedly would have smoothed out some of the irregularities appearing in Figure 1; but the comparison shows that the mean distribution defined by the curves themselves would have been little affected. Figure 1, in which circles indicate data from the *Durchmusterung*, also shows the agreement.

---

[1] Seares, Joyner, and Richmond, *Mt. Wilson Contr.*, No. 289; *Astrophysical Journal*, **61**, 303, 1925.

The stars in the 29 areas were counted for half-magnitude intervals in the usual manner and summed to $m=15.5$ or 16.0, according to the limiting magnitude. Curves derived by plotting the logarithms of the cumulative sums against magnitude were then corrected graphically for scale error by means of Table III, *Contribution* No. 289, and extrapolated to $m=17.5$. The ordinates read from these curves, reduced to an area of 1 square degree, gave values of N_m for each area which were then grouped into means according to Table II. Finally, the logarithms of the mean values of N_m were compared with the corresponding values of log N_m in the first two and the last four lines of Table VII, with the results shown in Table X. In view of the difference in the areas counted, the agreement is satisfactory. Even the large systematic differences for the group at 73° represent irregularities of only a few stars in the counts from the *Mount Wilson Catalogue*. The mean differences for the six groups are small, and show that the adopted distribution would have been little affected by including counts from the *Durchmusterung*.

TABLE X

COMPARISON OF LOG N_m FOR *Mount Wilson Catalogue* AND *Harvard-Groningen Durchmusterung*. (*Cat.*−*DM.*)

Group	13.0	13.5	14.0	14.5	15.0	15.5	16.0	16.5	17.0	17.5
0°	+0.05	+0.02	−0.02	−0.02	−0.03	−0.03	−0.02	0.00	0.00	−0.05
1	+ .02	+ .02	.00	+ .01	+ .01	− .02	− .01	+ .01	+ .01	+ .03
61	+ .06	− .02	− .01	+ .01	+ .03	+ .03	+ .01	.00	+ .01	.00
66	− .02	− .02	− .06	− .06	− .07	− .06	− .06	− .03	− .04	− .02
73	+ .11	+ .15	+ .11	+ .11	+ .08	+ .02	− .04	− .03	− .05	− .09
79	−0.18	−0.08	−0.02	−0.01	+0.02	−0.02	−0.02	−0.04	−0.02	−0.03
Mean	+0.01	+0.01	0.00	+0.01	+0.01	−0.01	−0.02	−0.02	−0.02	−0.03

An important result of the comparison is that the differences in the last three columns of Table X, all of which depend on an extrapolation of the *Durchmusterung* counts, are comparable with those in the other columns. The possibility of such an extrapolation is used later to extend the mean distribution table to the twenty-first magnitude.

3. CORRECTION OF VAN RHIJN'S DISTRIBUTION TABLE FOR SCALE ERROR

Table IV of *Groningen Publication* No. 27 plays an important part in the determination of the distribution of stars brighter than $m=13.5$. For the stars fainter than $m=10$ this table is based on 65 northern Selected Areas of the *Harvard-Groningen Durchmusterung*.

TABLE XI

REDUCTION OF TABLES II AND IV, *Groningen Publication* No. 27, TO INTERNATIONAL SCALE

Gr. 27 Mag.	Scale Corr.	Corr. Mag.
4.0	−0.08	3.92
4.5	− .08	4.42
5.0	− .07	4.93
5.5	− .05	5.45
6.0	.00	6.00
6.5	+ .05	6.55
7.0	+ .10	7.10
7.5	+ .15	7.65
8.0	+ .20	8.20
8.5	+ .25	8.75
9.0	+ .29	9.29
9.5	+ .33	9.83
10.0	+0.38	10.38
10.5	+0.39	10.89
11.0	.40	11.40
11.5	.40	11.90
12.0	.40	12.40
12.5	.40	12.90
13.0	.38	13.38
13.5	.36	13.86
14.0	.33	14.33
14.5	.30	14.80
15.0	.27	15.27
15.5	.22	15.72
16.0	+0.16	16.16

For stars brighter than $m=5.5$ it depends on counts from *Harvard Annals*, **50**, reduced to the photographic scale by correction for color-index. The *Göttingen Aktinometrie* was used to cover the interval $m=5.5$ to 7.0, and Greenwich astrographic magnitudes from $m=6.5$ to 8.5 (latitudes 10° to 50° only). The remaining interval in the scale of brightness was bridged by interpolation.

Below $m=10$ the scale correction to the magnitudes of van Rhijn's table is that given in the first column of Table IV, *Contribution* No. 289, while for $m<6$ it is that of the Harvard visual scale, given in Table II, *Contribution* No. 288,[1] modified by a small color equation which may be neglected here. The Greenwich astrographic magnitudes are on the Harvard photographic scale, for which the reduction to the international system, in the region in question, is similar to that for the Harvard visual scale. The *Aktinometrie* has little influence on the scale error of van Rhijn's table, and may be disregarded.

---

[1] *Astrophysical Journal*, **61**, 284, 1925.

For practical purposes we may adopt the corrections specified for $m<6$ and >10, and cover the interval $m=6$ to 10 by interpolation. The results, smoothed by 0.01 or 0.02 mag., are in the second column of Table XI. The corrected arguments for van Rhijn's table are in the last column of this table.

TABLE XII

TABLE XVII MINUS *Groningen Publication* NO. 27, TABLE IV, CORRECTED FOR SCALE

m	0°	10°	20°	30°	40°	50°	60°	70°	80°	90°
9	+0.03	+0.02	−0.01	−0.01	−0.02	+0.01	+0.01	+0.01	+0.01	0.00
10	.06	.03	.01	− .03	− .03	.00	.01	.01	+ .01	.00
11	.06	.02	.03	− .03	− .03	.00	.00	.00	− .01	.00
12	.07	.00	.05	− .03	− .03	.01	.00	.00	− .01	.00
13	.09	.00	.05	− .02	− .01	.04	.03	.00	− .02	− .03
14	.13	.02	.03	+ .01	+ .04	.08	.03	.02	.00	.00
15	.15	.05	.01	+ .04	+ .06	.07	.05	.02	.00	.00
16	+0.17	+0.07	−0.03	+0.02	+0.04	+0.05	+0.02	+0.01	−0.01	−0.01

Van Rhijn's table thus corrected was compared with the provisional mean distribution for the interval $m=13.5$–18.5, derived from the *Mount Wilson Catalogue* and given in Table IX. No serious systematic differences were found outside the Milky Way, from which it was inferred that the corrected table must also be near the truth for the interval $m=9.0$ to 13.5, covered by the astrographic zones. This inference was afterward justified by a comparison with the adopted distribution given in Table XVII, the details of which, in Table XII, are inserted at this point.

4. COUNTS FROM THE "ASTROGRAPHIC CATALOGUE"

Ten zones of the *Astrographic Catalogue*[1] were used in 1917 to determine the galactic concentration in the interval $m=8.5$ to 12.5. The values of $\log N_m$ were necessarily referred to the magnitude scale used by Kapteyn, which even then was known to be seriously in error. Although the results confirmed the rapid increase in concentration with magnitude found by Kapteyn in *Groningen Publication*

---

[1] Seares, *Mt. Wilson Contr.*, No. 135; *Astrophysical Journal*, **46**, 117, 1917.

No. 18, the absolute values of the density were approximate. With a reliable scale available, the method used in *Contribution* No. 135 can now be applied very effectively to the abundant material from the *Astrographic Catalogue* for a determination of the mean distribution of stars in the interval $m=9.0$ to 13.5.

Thanks largely to Professor Turner, counts for 33 zones including about 1,400,000 stars[1] are now available. The declinations of the zones, the observatories concerned, and references to the volumes of the *Monthly Notices* giving the results are collected in Table XIII. The counts are referred to the arbitrary scales of magnitude or diameter of images used in preparing the zones for publication. In using the material it is necessary to assume that a given scale reading[2] always corresponds to the same magnitude on the international scale. For various reasons this is by no means always the case. Differences in exposure time; in observing conditions, both accidental and seasonal; in the sensitiveness of the plates; and variations in the measures themselves arising from subjective factors all tend to invalidate the assumption; but the material is now so extensive that in the mean these factors operate largely as accidental disturbances.

The published counts, usually the numbers of stars in each hour of right ascension in successive intervals of scale reading, have been treated just as in *Contribution* No. 135, except that the exact area of an astrographic plate, instead of the approximation of 4 square degrees, has been used. Some of the original curves have been revised, and data for additional limiting magnitudes have been introduced in a few cases. Logarithms of the cumulative sums for an area of 1 square degree were plotted against galactic latitude for four or five limiting values of the scale reading, and smoothed values of log N_m for latitudes 0°, 10°, 20°, ... were read from the resulting curves. Known regions of obscuration, such as that in Taurus, were disregarded in drawing the curves.

---

[1] The totals actually counted in the zones used, as listed in Table XIII, sum up to about 1,810,000. Allowance for overlapping zones reduces the number to that mentioned.

[2] This term is used to designate the values of the brightness of the stars as given in the zones, irrespective of whether they represent readings with a comparison scale, diameters of images, or estimates of magnitude.

TABLE XIII

Data for Astrographic Zones

Zone	Observatory	Reference *Monthly Notices*	No. Stars Counted	No. Plates per Hour
+64°	Vatican	75,601	88,782	10
+62	Vatican			
+60	Vatican			
+31	Oxford	85,471	69,332	7,6,7
+30	Oxford	85,471	83,747	7,7,6
+29	Oxford	85,471	68,062	7,6,7
+28	Oxford	75,465	70,141	7,7,6
+27	Oxford	85,471	62,411	7,8
+26	Oxford	85,471	73,764	8,7
+25	Oxford	85,471	76,402	7,8
+24	Paris	83,385	....	....
+23	Paris	83,385	70,538	7,8
+22	Paris	83,385	72,285	8,7
+17	Bordeaux	72,464	49,747	7,8
+16	Bordeaux	79,136	40,183	8,7
+15	Bordeaux	79,136	36,746	7,8
+14	Bordeaux	79,136	53,784	8,7
+ 9	Toulouse	76,149	35,700	See note
− 1	Algiers	72,700	41,322	7,8
− 3	San Fernando	83,385	56,117	7,8
− 4	San Fernando	84,735	41,441	8,7
− 5	San Fernando	83,385	46,279	7,8
− 6	San Fernando	84,735	39,466	8,7
−15	Tacubaya	78,54	63,945	7,8
−16	Tacubaya	79,565	63,106	8,7
−17	Hyderabad	77,432	63,000	See note
−18	Hyderabad	78,367	61,379	See note
−19	Hyderabad	80,623	58,500	See note
−25	Cordoba	78,54	68,764	7,8
−27	Cordoba	81,525	54,584	7,8
−29	Cordoba	81,525	49,552	7,6,7
−31	Cordoba	81,525	61,162	7,6,7
−32	Perth	75,143	59,629	See note
−34	Perth	78,578	63,050	See note
−36	Perth	80,620	68,535	See note
−38	Perth	78,578	68,453	6
−41	Cape	75,57	71,433	6
−42	Cape	79,565	84,217	6
−43	Cape	79,565	73,781	6
−65	Melbourne	77,35	33,813	3,4,3

NOTES TO TABLE XIII

+62°: The counts are means for zones +60°, +62°, and +64°, extending from +59° to +65°. Unit=0.1 star per plate. Since in the three zones together there are 10 plates per hour, the counts are also numbers of stars per hour.

+28°: Counts for +28° only of the Oxford zones were available when the reductions were made. For completeness, references are given for the other zones, which have recently appeared. The abnormally low densities in the obscured region, 3^h–5^h, +28°, have been disregarded in deriving the means given in Table XV.

NOTES TO TABLE XIII—*Continued*

+24°: Detailed counts have not been published.

+23°, +22°: Obscured region (see +28°) disregarded. For 6, 8, 18, and 22^h the published values under the heading "All" do not agree with the sums of the numbers in the successive intervals of scale reading. The individual numbers are assumed to be correct.

+17° to +14°: All the Bordeaux zones show abnormally low densities in the region of 4^h.

+9°: The scale for 0^h–6^h differs from that for 7^h–23^h, the densities for the first quadrant being relatively low. See comment by Turner, *loc. cit.* Total number of plates is 180; an average of 7.5 per hour has been used for the reduction.

−1°: The sign of the declination, wrongly given with the original counts, was later corrected (cf. *M.N.*, 84, 738). The densities from 12^h to 18^h, galactic latitudes +60° to +3°, are nearly constant. Since the San Fernando zones, −3° to −6°, show a similar phenomenon, the abnormality is probably real.

−3° to −6°: See preceding note.

−15°: Density from 12^h to 17^h, galactic latitude +46° to +8°, nearly constant. The published total, *loc. cit.*, for scale reading 10.5 should be 13377. The values of N' are correspondingly affected.

−16°: Density from 0^h to 4^h, galactic latitude −78° to −36°, nearly constant.

−17°: Data published by Pocock. The number of plates is 8 and 7 per hour, but the counts have been reduced to a total of 10 per hour. The number of stars given is approximate.

−18°: Data published by Pocock. Cumulative sums, reduced to a total of 10 plates per hour, calculated from Table I of Pocock's paper.

−19°: Data published by Bhaskaran. Number of plates, 7 and 8; counts reduced to 10 plates per hour. Number of stars approximate.

−32° to −36°: Number of plates, 6 and 7; counts reduced to 10 per hour. Totals counted approximate.

−41° to −43°: The density for all three zones at 12^h, galactic latitude +20°, is conspicuously low as compared with that at 18^h, latitude −16°.

−65°: The systematic difference in scale readings discussed by Turner, *loc. cit.*, affects all hours of right ascension, and is therefore probably well eliminated from the mean densities in Table XV.

As an illustration, the mean values of log N_m thus found for the Vatican zones, +62°, are given in Table XIV under the scale readings 40, 30, ... 0. Each of these, in conjunction with van Rhijn's Table IV, corrected as in the preceding section, determines a value of the limiting magnitude corresponding to the scale reading at the head of the column. The differences in Table XII show, however, that magnitudes interpolated for latitude 0° cannot safely be used. These were accordingly rejected in forming the mean limiting magnitudes. As a matter of convenience, the graphical equivalent of van Rhijn's table given in Figure 2, *Groningen Publication* No. 27, was used for the interpolation, the correction for scale being applied to the mean of the resulting magnitudes. Thus for the Vatican zones the mean magnitude for each scale reading, the scale correction from Table XI, and the corrected magnitude are in the last three lines of Table XIV.

The residuals for the individual values of the magnitude are in the right half of the table. In view of the numerous possible sources of error, these are smaller than might have been expected. Since the part of van Rhijn's table used shows no serious systematic error (see Table XII), large progressive changes in the residuals, like those for scale reading 40, must originate in the astrographic counts. Whether these represent systematic errors in scale reading or real deviations from the assumed symmetrical mean distribution of the stars cannot be decided at present.

TABLE XIV

MEAN LOG N_m, LIMITING MAGNITUDE, AND RESIDUALS IN m FOR VATICAN ZONES

GAL. LAT.	SCALE READING					SCALE READING				
	40	30	20	10	0	40	30	20	10	0
0°........	0.56	0.98	1.40	1.89	2.15	......	......	......	......	......
10........	0.42	.87	1.28	1.77	2.03	−0.34	−0.21	−0.07	−0.01	−0.02
20........	0.21	.70	1.17	1.67	1.90	− .15	− .04	− .06	− .03	.00
30........	0.01	.55	1.03	1.53	1.74	+ .08	+ .08	.00	− .06	+ .05
40........	9.90	.47	0.93	1.39	1.60	+ .13	+ .06	+ .01	.00	+ .02
50........	9.83	.40	0.83	1.27	1.51	+ .16	+ .04	+ .03	+ .02	− .03
60........	9.78	0.34	0.75	1.19	1.44	+0.15	+0.05	+0.07	+0.06	−0.03
Mean mag.	8.56	9.69	10.71	11.92	12.57	......	......	......	......	......
Sc. corr....	+0.25	+0.35	+0.39	+0.40	+0.40	......	......	......	......	......
Int. mag...	8.81	10.04	11.10	12.32	12.97	......	......	......	......	......

The other zones listed in Table XIII were treated in precisely the same manner. The results for all the zones are collected in Table XV in order of limiting magnitude. Thus opposite magnitudes 8.81, 10.04, etc., in the first column stand the values of log N_m for different galactic latitudes given in the successive columns of Table XIV. To simplify the combination of these data, missing values of the density for high latitudes have been supplied by extrapolation. These are inclosed in parentheses.

It should be noted that the variation of density for any magnitude in Table XV depends solely on the counts from the astrographic zones. Van Rhijn's table has been used only to determine the mean limiting magnitudes, and these are little affected by residual errors in his corrected table. Thus a redetermination of the limits by comparing all the densities in Table XV with the adopted distribution in Table XVII gives a maximum difference of 0.09 and a mean of ±0.027 mag. The revised limiting magnitudes, it may be remarked, provide a mean calibration of the provisional scales of the astrographic zones which may be used until a more detailed reduction to the international scale is available. These results will be collected in a later *Contribution*.

The 128 sequences of log N_m in Table XV were combined into the 11 means given in Table XVI.[1] The division lines in Table XV show the zones contributing to each mean; the place of observation can be identified by means of Table XIII. In general, each mean sequence depends on data from widely separated parts of the sky, based on measures made at several different observatories. Systematic errors affecting the counts of individual zones and deviations from the mean distribution have therefore little influence on Table XVI, which is the final form for the data from the astrographic zones. Residual errors are still further reduced by the smoothing process involved in the combination with data from other sources to form the mean distribution table.

5. THE MEAN DISTRIBUTION TABLE

Tables IX and XVI, based on the *Mount Wilson Catalogue* and the astrographic zones, determine the distribution for stars fainter than $m=9.0$. As already stated, the data to be used for stars brighter than $m=9.0$ are those of van Rhijn, reduced to the international scale. For the interval $m=7.0$ to 9.0, the densities can be taken directly from Table IV, *Groningen Publication* No. 27; for still brighter stars, Table II of van Rhijn's paper must be used. The corresponding magnitudes are in both cases the corrected arguments in the third column of Table XI.

---

[1] Here again, as a matter of convenience, the geometrical mean has been used for N_m, whereas, strictly speaking, the arithmetical mean is required.

TABLE XV

Log N_m from Astrographic Zones

m	Zone	0°	10°	20°	30°	40°	50°	60°	70°	80°	90°
8.62	−27°	0.28	0.23	0.13	9.95	9.85	9.79	9.74	9.72	9.71	9.70
8.66	+16	0.19	0.12	0.02	9.92	9.89	9.86	9.83	9.80	9.78	(9.77)
8.74	−25	0.26	0.21	0.13	0.03	9.94	9.88	9.83	9.78	9.75	9.73
8.81	+62	0.56	0.42	0.21	0.01	9.90	9.83	9.78	(9.75)	(9.73)	(9.72)
8.84	−34	0.58	0.44	0.25	0.12	9.99	9.89	9.83	9.77	9.72	9.68
8.92	+ 9	0.66	0.53	0.28	0.09	9.95	9.86	9.82	9.78	(9.76)	(9.75)
9.15	−31	0.68	0.53	0.28	0.08	0.01	9.99	9.98	9.98	9.98	9.98
9.20	+23	0.41	0.34	0.25	0.17	0.11	0.08	0.05	0.03	0.00	9.98
9.21	− 1	0.52	0.45	0.34	0.23	0.13	0.04	9.98	(9.95)	(9.93)	(9.92)
9.25	−29	0.66	0.55	0.38	0.27	0.18	0.08	0.00	9.94	9.91	9.89
9.26	+22	0.44	0.37	0.28	0.20	0.14	0.10	0.07	0.05	0.03	0.01
9.32	−38	0.63	0.51	0.33	0.18	0.14	0.11	0.08	0.05	0.04	(0.04)
9.38	−36	0.64	0.49	0.33	0.21	0.16	0.13	0.12	0.11	0.10	(0.10)
9.39	−19	0.44	0.40	0.35	0.28	0.21	0.16	0.13	0.10	0.09	(0.09)
9.49	−42	0.63	0.57	0.49	0.39	0.27	0.17	0.11	0.06	0.04	(0.03)
9.53	−17	0.62	0.55	0.44	0.32	0.25	0.20	0.17	0.14	0.13	(0.12)
9.57	−18	0.58	0.47	0.37	0.33	0.28	0.26	0.23	0.20	0.18	(0.18)
9.57	−43	0.71	0.63	0.52	0.39	0.28	0.20	0.16	0.12	0.09	(0.08)
9.66	+15	0.73	0.62	0.51	0.41	0.33	0.26	0.21	0.16	0.13	(0.12)
9.94	−16	0.68	0.63	0.53	0.47	0.42	0.40	0.39	0.37	0.36	(0.36)
9.95	−25	0.94	0.83	0.68	0.55	0.45	0.38	0.30	0.26	0.23	0.21
9.99	+14	0.89	0.82	0.66	0.53	0.45	0.39	0.34	0.30	0.27	(0.26)
10.00	− 4	0.78	0.73	0.65	0.58	0.49	0.39	0.35	0.33	(0.32)	(0.32)
10.02	− 5	0.77	0.73	0.65	0.58	0.48	0.40	0.37	0.35	(0.34)	(0.33)
10.03	−15	0.80	0.73	0.65	0.55	0.48	0.43	0.40	0.37	(0.36)	(0.36)
10.04	+62	0.98	0.87	0.70	0.55	0.47	0.40	0.34	(0.31)	(0.29)	(0.29)
10.04	− 6	0.82	0.77	0.68	0.55	0.46	0.43	0.40	0.37	(0.36)	(0.35)
10.04	−27	0.97	0.90	0.73	0.53	0.44	0.38	0.33	0.31	0.30	0.29
10.04	−38	0.95	0.80	0.64	0.50	0.45	0.42	0.40	0.38	0.36	(0.36)
10.05	+28	0.83	0.78	0.67	0.54	0.47	0.42	0.39	0.38	(0.38)	(0.38)
10.06	+16	0.85	0.77	0.64	0.53	0.48	0.44	0.40	0.37	0.34	(0.33)
10.12	−34	1.08	0.93	0.77	0.62	0.51	0.42	0.37	0.33	0.29	0.25
10.16	− 3	0.88	0.83	0.74	0.63	0.55	0.46	0.41	0.37	(0.36)	(0.35)
10.19	−19	0.87	0.80	0.71	0.61	0.54	0.49	0.45	0.43	0.42	(0.42)
10.28	+ 9	1.20	1.07	0.82	0.65	0.52	0.46	0.42	0.39	(0.37)	(0.36)
10.35	−32	1.08	0.98	0.83	0.67	0.53	0.48	0.47	0.47	0.47	(0.47)
10.38	+22	0.96	0.88	0.76	0.68	0.59	0.55	0.53	0.51	0.47	0.44
10.45	+23	0.93	0.86	0.78	0.68	0.64	0.61	0.57	0.53	0.50	0.48
10.58	−31	1.29	1.07	0.87	0.73	0.64	0.58	0.57	0.55	0.54	0.53
10.62	−36	1.18	1.07	0.85	0.72	0.68	0.65	0.63	0.61	0.59	(0.59)
10.70	−29	1.33	1.19	0.99	0.88	0.78	0.70	0.61	0.53	0.48	0.45
10.75	−41	1.15	1.05	0.91	0.80	0.74	0.70	0.67	0.66	0.65	(0.64)
10.76	+17	1.07	1.03	0.96	0.87	0.79	0.72	0.67	0.63	0.59	(0.57)
11.00	−65	1.43	1.32	1.11	0.96	0.83	0.76	0.71	(0.68)	(0.67)	(0.67)
11.10	+62	1.40	1.28	1.17	1.03	0.93	0.83	0.75	(0.72)	(0.70)	(0.69)
11.23	+15	1.43	1.31	1.17	1.04	0.97	0.92	0.85	0.79	0.74	(0.72)
11.27	−15	1.37	1.28	1.18	1.06	0.97	0.91	0.88	0.86	(0.85)	(0.84)
11.29	−16	1.33	1.25	1.13	1.03	0.97	0.92	0.89	0.88	0.87	(0.87)
11.33	− 6	1.43	1.32	1.18	1.08	1.01	0.96	0.91	0.86	(0.84)	(0.83)
11.33	−25	1.54	1.45	1.29	1.13	0.99	0.92	0.85	0.80	0.77	0.73
11.33	−38	1.50	1.32	1.15	1.05	1.00	0.95	0.90	0.87	0.85	(0.84)
11.35	−19	1.30	1.24	1.15	1.07	1.01	0.97	0.93	0.90	0.87	(0.86)
11.38	+ 9	1.63	1.47	1.29	1.12	1.01	0.93	0.87	0.82	(0.79)	(0.77)
11.38	−27	1.56	1.46	1.25	1.04	0.97	0.92	0.90	0.87	0.84	0.83
11.38	−34	1.63	1.46	1.27	1.15	1.05	0.96	0.88	0.82	0.76	0.72
11.39	− 1	1.56	1.46	1.29	1.14	1.01	0.92	0.85	(0.81)	(0.79)	(0.79)
11.41	− 5	1.39	1.33	1.23	1.14	1.07	0.99	0.93	0.88	(0.85)	(0.84)
11.43	+14	1.62	1.49	1.32	1.14	1.04	0.97	0.90	0.83	0.77	(0.73)
11.43	− 4	1.42	1.33	1.23	1.15	1.07	0.99	0.94	0.92	(0.91)	(0.90)
11.46	+16	1.51	1.38	1.23	1.12	1.05	1.00	0.95	0.91	0.88	(0.86)
11.48	−18	1.28	1.21	1.13	1.09	1.06	1.03	1.01	0.99	0.97	(0.97)
11.62	− 3	1.47	1.43	1.33	1.20	1.13	1.05	1.01	0.98	(0.97)	(0.96)
11.66	−41	1.65	1.52	1.38	1.23	1.10	1.03	0.99	0.97	0.95	(0.94)
11.71	+22	1.52	1.43	1.33	1.22	1.13	1.07	1.04	1.01	0.99	0.97
11.74	+23	1.47	1.44	1.37	1.29	1.19	1.12	1.04	0.99	0.95	0.93
11.76	−36	1.66	1.48	1.32	1.21	1.14	1.11	1.08	1.05	1.03	(1.02)
11.76	−43	1.66	1.58	1.47	1.34	1.20	1.06	0.99	0.93	0.90	(0.89)
11.80	−42	1.68	1.62	1.50	1.37	1.22	1.10	1.00	0.94	0.88	(0.86)
11.88	−32	1.83	1.67	1.50	1.31	1.17	1.08	1.04	1.03	1.03	(1.03)

TABLE XV—*Continued*

m	Zone	0°	10°	20°	30°	40°	50°	60°	70°	80°	90°
12.15	+15°	1.80	1.69	1.54	1.42	1.33	1.24	1.18	1.13	1.08	(1.05)
12.16	−17	1.76	1.63	1.48	1.38	1.31	1.25	1.20	1.17	1.16	(1.15)
12.18	−18	1.69	1.51	1.36	1.33	1.32	1.31	1.28	1.25	1.23	(1.22)
12.19	−19	1.73	1.63	1.47	1.39	1.32	1.26	1.23	1.20	1.17	(1.16)
12.24	+16	1.84	1.72	1.57	1.43	1.33	1.27	1.22	1.18	1.15	(1.13)
12.28	− 6	1.83	1.69	1.53	1.43	1.37	1.32	1.27	1.23	(1.21)	(1.20)
12.32	+62	1.89	1.77	1.67	1.53	1.39	1.27	1.19	(1.14)	(1.11)	(1.10)
12.35	+17	1.80	1.73	1.63	1.48	1.38	1.30	1.25	1.20	1.17	(1.16)
12.43	+28	1.88	1.81	1.63	1.45	1.38	1.35	1.31	1.30	(1.29)	(1.29)
12.43	+14	2.06	1.92	1.69	1.51	1.40	1.33	1.26	1.19	1.13	(1.10)
12.45	−16	1.97	1.83	1.65	1.49	1.37	1.30	1.28	1.27	1.26	(1.26)
12.45	−43	1.97	1.89	1.76	1.60	1.45	1.31	1.21	1.15	1.11	(1.10)
12.47	−15	1.89	1.78	1.64	1.53	1.43	1.36	1.31	1.28	(1.26)	(1.25)
12.48	−29	1.98	1.83	1.68	1.56	1.46	1.37	1.27	1.21	1.18	1.15
12.49	−42	1.95	1.86	1.76	1.63	1.49	1.35	1.25	1.17	1.10	(1.09)
12.51	− 5	1.87	1.76	1.63	1.53	1.44	1.39	1.35	1.32	(1.31)	(1.30)
12.51	−31	2.08	1.89	1.69	1.53	1.39	1.33	1.29	1.27	1.24	1.23
12.51	−34	2.09	1.91	1.69	1.56	1.47	1.38	1.29	1.23	1.17	1.14
12.55	+ 9	2.06	1.94	1.75	1.60	1.47	1.35	1.25	1.20	(1.17)	(1.16)
12.59	− 4	1.96	1.83	1.65	1.53	1.45	1.42	1.38	1.36	(1.35)	(1.34)
12.66	+15	1.99	1.90	1.74	1.63	1.51	1.42	1.34	1.28	1.24	(1.22)
12.74	− 3	1.99	1.90	1.75	1.62	1.53	1.45	1.39	1.36	(1.35)	(1.34)
12.75	+16	2.08	1.95	1.76	1.63	1.52	1.45	1.39	1.34	1.30	(1.28)
12.76	−36	2.00	1.83	1.68	1.58	1.53	1.48	1.44	1.40	1.37	(1.36)
12.79	+22	2.02	1.92	1.77	1.63	1.52	1.45	1.41	1.37	1.33	1.31
12.79	−27	2.13	2.02	1.79	1.63	1.52	1.42	1.38	1.35	1.33	1.32
12.82	+23	1.95	1.90	1.82	1.73	1.59	1.46	1.39	1.34	1.31	1.28
12.84	−18	1.94	1.80	1.64	1.59	1.56	1.53	1.49	1.46	1.43	(1.42)
12.85	−41	2.15	2.03	1.86	1.70	1.55	1.42	1.37	1.36	1.35	(1.35)
12.87	− 6	2.11	1.96	1.78	1.67	1.58	1.50	1.44	1.41	(1.39)	(1.38)
12.88	−25	2.06	1.99	1.83	1.68	1.59	1.51	1.43	1.37	1.33	1.31
12.89	−38	2.08	1.96	1.80	1.65	1.55	1.49	1.45	1.41	1.38	(1.37)
12.92	+14	2.33	2.15	1.91	1.70	1.57	1.48	1.41	1.34	1.29	(1.27)
12.94	− 1	2.24	2.12	1.92	1.72	1.57	1.45	1.38	(1.34)	(1.32)	(1.31)
12.96	−29	2.19	2.06	1.88	1.73	1.62	1.52	1.43	1.38	1.34	1.32
12.97	+62	2.15	2.03	1.90	1.74	1.60	1.51	1.44	(1.39)	(1.36)	(1.35)
13.02	−65	2.26	2.16	1.98	1.76	1.58	1.46	1.40	(1.37)	(1.35)	(1.34)
13.03	−27	2.23	2.13	1.88	1.70	1.58	1.51	1.46	1.43	1.41	1.39
13.04	− 4	2.18	2.03	1.84	1.72	1.59	1.54	1.52	1.49	(1.48)	(1.47)
13.06	− 5	2.18	2.08	1.90	1.76	1.63	1.53	1.47	1.42	(1.39)	(1.38)
13.11	−32	2.32	2.15	1.94	1.76	1.62	1.51	1.46	1.44	1.43	(1.43)
13.18	+17	2.17	2.08	1.93	1.78	1.64	1.58	1.53	1.49	1.47	(1.46)
13.19	−34	2.39	2.18	1.94	1.83	1.71	1.60	1.52	1.45	1.38	1.34
13.21	−31	2.28	2.18	2.02	1.81	1.64	1.54	1.49	1.47	1.45	1.43
13.23	−16	2.43	2.18	1.96	1.78	1.64	1.58	1.53	1.50	1.47	(1.45)
13.25	+23	2.33	2.24	2.08	1.91	1.73	1.56	1.47	1.42	1.39	1.38
13.27	− 3	2.24	2.14	1.98	1.81	1.69	1.62	1.55	1.50	(1.47)	(1.46)
13.27	−15	2.28	2.17	1.99	1.83	1.70	1.59	1.53	1.49	(1.47)	(1.46)
13.30	−19	2.23	2.12	1.93	1.78	1.70	1.63	1.58	1.54	1.52	(1.51)
13.34	+22	2.33	2.22	2.03	1.90	1.75	1.64	1.55	1.48	1.43	1.40
13.36	−25	2.21	2.12	1.97	1.84	1.74	1.65	1.59	1.53	1.50	1.46
13.38	−17	2.29	2.12	1.93	1.82	1.73	1.66	1.60	1.55	1.53	(1.52)
13.38	−18	2.27	2.06	1.87	1.80	1.74	1.70	1.64	1.59	1.56	(1.55)
13.48	−41	2.40	2.26	2.08	1.90	1.75	1.65	1.58	1.55	1.53	(1.53)
13.53	−36	2.38	2.15	1.99	1.85	1.77	1.72	1.68	1.64	1.61	(1.59)
13.54	−43	2.38	2.28	2.15	2.00	1.83	1.67	1.56	1.51	1.46	(1.44)
13.56	−38	2.37	2.20	2.04	1.90	1.80	1.71	1.65	1.60	1.57	(1.57)
13.57	−42	2.36	2.29	2.18	2.02	1.85	1.69	1.59	1.49	1.45	(1.44)
13.68	+28	2.38	2.29	2.10	1.88	1.80	1.75	1.71	1.69	(1.68)	(1.68)

Together, all these data define log N_m as a function of m from 4.0 to 18.5 for each of the latitudes 0°, 10°, ... 90°. The smooth curves obtained by plotting the densities on a large-scale diagram (Fig. 2) eliminate the remaining accidental irregularities from magnitude to magnitude for each latitude, and the slight systematic differences between the data drawn from the three sources. The latter are appreciable in latitude 0°, $m = 13.5$ to 15.5, where the densities from the *Mount Wilson Catalogue* are clearly too large (Fig. 2 and Table VII*a*), and in latitudes 80° and 90° in the interval covered by the astrographic zones (Fig. 2). In neither case is the difference surprising. The Selected Areas in and near the Milky Way are few in number, badly distributed in longitude, and show large fluctuations in density. The astrographic counts in this region are far more reliable and really determine, by extrapolation, the 0° curve to $m = 15.5$. In high latitudes, on the other hand, Table XV shows that the densities from the astrographic zones are nearly all extrapolated. The small systematic error, now revealed in the extrapolation, has been corrected in drawing the curves.

TABLE XVI

MEAN LOG N_m FROM ASTROGRAPHIC ZONES

Mean m	0°	10°	20°	30°	40°	50°	60°	70°	80°	90°	No. Zones
8.91	0.46	0.36	0.21	0.07	9.97	9.91	9.87	9.84	9.82	9.80	9
9.44	0.61	0.52	0.40	0.30	0.22	0.17	0.13	0.09	0.07	0.07	10
10.02	0.86	0.78	0.66	0.54	0.46	0.41	0.37	0.34	0.33	0.32	12
10.44	1.08	0.98	0.83	0.71	0.63	0.57	0.53	0.50	0.48	0.46	12
11.29	1.47	1.36	1.20	1.07	0.98	0.91	0.86	0.82	0.79	0.78	13
11.63	1.55	1.45	1.33	1.22	1.12	1.05	0.99	0.96	0.93	0.92	13
12.30	1.85	1.74	1.58	1.45	1.36	1.28	1.24	1.20	1.17	1.16	12
12.58	2.00	1.86	1.70	1.58	1.47	1.40	1.33	1.28	1.25	1.24	12
12.88	2.11	2.00	1.82	1.68	1.57	1.48	1.42	1.38	1.35	1.33	12
13.16	2.27	2.14	1.95	1.79	1.65	1.55	1.49	1.46	1.43	1.42	12
13.47	2.33	2.19	2.02	1.88	1.77	1.68	1.61	1.56	1.53	1.52	11

To eliminate any irregularity in the spacing of the curves (log N_m against m for each latitude), ordinates were plotted against galactic latitude for each half-magnitude, 4.0, 4.5, etc. The ordinates of the new series of curves thus formed (log N_m against latitude for each m) extrapolated to $m = 21.0$, are in Table XVII, which is adopted as representing the mean distribution for the whole sky.

At the end of section 2 it was shown that counts from the *Harvard-Groningen Durchmusterung* for single Selected Areas could be extrapolated from 15.5 or 16.0 to 17.5 without serious error. In

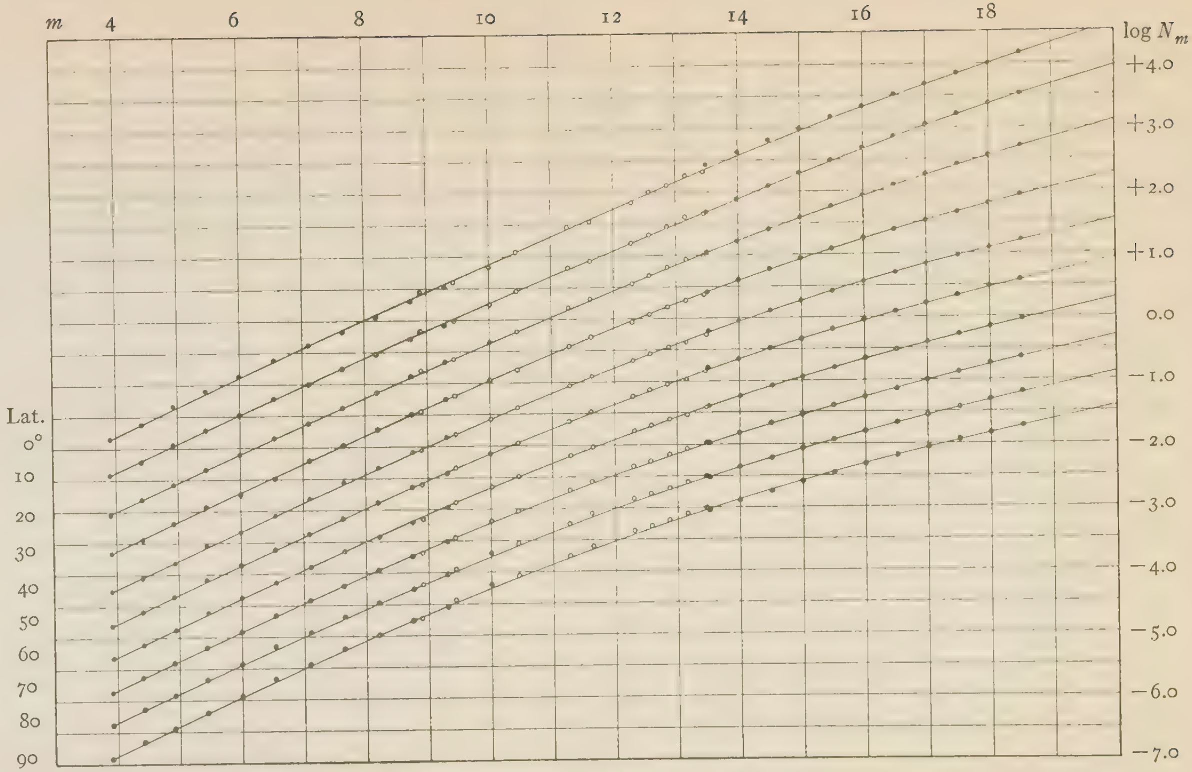

FIG. 2.—Mean values of log N_m from *Groningen Publication*, No. 27 ($m=4$ to 9), from 33 *Astrographic Zones* ($m=9$ to 13.5), and from the *Mount Wilson Catalogue* ($m=13.5$ to 18.5). The curves are the basis of the adopted distribution in Table XVII. The ordinates refer to latitudes 0°. To find log N_m for other latitudes add 0.05×Lat. to the printed ordinate.

extrapolating the final results from $m=18.5$ to 21.0 we are dealing with mean densities based upon a large amount of material. This greatly reduces the danger of systematic error, which is further controlled by the condition that the extrapolated densities must vary smoothly with the galactic latitude. The method used was graphical (see Fig. 2), followed by a numerical smoothing of the differences in $\log N_m$. The greatest danger lies, not in the extrapolation itself, but rather in the magnitude scale in the interval $m=16.5$ to 18.5. A systematic divergence in scale in this region would of course be carried downward by the extrapolation with steadily increasing effect. Unfortunately, we have no control on the extrapolated result, but it is, at least, an approximation for the distribution of the very faint stars.

6. MEAN VALUES OF LOG N_m

The determination of mean values of $\log N_m$ for wide zones of latitude and for the whole sky requires a summation of the values in Table XVII with respect to galactic latitude. To represent the values of N_m for a given magnitude, Kapteyn has used the formula

$$N_m=A+\frac{B}{1+h\sin^2 b}\,, \tag{1}$$

which is easily integrated with respect to the latitude b; but for the faint magnitudes, at least, the variation in N_m is so large that the interval 0°–90° must be divided into three parts in order to obtain satisfactory results. It is therefore simpler to integrate numerically. This has been done for $m=4, 5, \ldots 21$ for the intervals 0°–20°, 20°–40°, and 40°–90°, the results being combined to cover the interval 0°–90°. The mean values of $\log N_m$ are in the second to the fifth columns of Table XVIII, data for $m=4.5$, 5.5, etc., being supplied by interpolation. The last value in the fifth column corresponds to a total, for the whole sky, of 890,000,000 stars to the twenty-first photographic magnitude.

7. MEAN VALUES OF LOG N_m FOR STARS GROUPED ACCORDING TO VISUAL MAGNITUDE

The distribution of stars grouped according to visual magnitude differs appreciably from that given in Table XVII. Detailed results

TABLE XVII

MEAN DISTRIBUTION OF STARS*

m	0°	5°	10°	15°	20°	25°	30°
4.0	8.193	8.168	8.117	8.054	7.989	7.930	7.870
	230	230	230	230	230	230	231
4.5	8.423	8.398	8.347	8.284	8.219	8.160	8.101
	229	229	229	229	229	229	230
5.0	8.652	8.627	8.576	8.513	8.448	8.389	8.331
	228	228	228	228	228	228	229
5.5	8.880	8.855	8.804	8.741	8.676	8.617	8.560
	227	227	226	226	226	227	228
6.0	9.107	9.082	9.030	8.967	8.902	8.844	8.788
	226	226	225	225	225	226	226
6.5	9.333	9.308	9.255	9.192	9.127	9.070	9.014
	225	225	224	224	223	224	225
7.0	9.558	9.533	9.479	9.416	9.350	9.294	9.239
	224	223	222	222	221	222	223
7.5	9.782	9.756	9.701	9.638	9.571	9.516	9.462
	223	222	220	219	219	220	221
8.0	0.005	9.978	9.921	9.857	9.790	9.736	9.683
	222	220	219	218	217	217	218
8.5	0.227	0.198	0.140	0.075	0.007	9.953	9.901
	221	219	217	216	215	215	216
9.0	0.448	0.417	0.357	0.291	0.222	0.168	0.117
	220	218	216	214	213	213	214
9.5	0.668	0.635	0.573	0.505	0.435	0.381	0.331
	219	217	215	212	211	211	212
10.0	0.887	0.852	0.788	0.717	0.646	0.592	0.543
	217	215	213	210	209	209	209
10.5	1.104	1.067	1.001	0.927	0.855	0.801	0.752
	215	213	211	208	208	206	205
11.0	1.319	1.280	1.212	1.135	1.063	1.007	0.957
	214	212	209	206	206	203	201
11.5	1.533	1.492	1.421	1.341	1.269	1.210	1.158
	212	210	207	204	204	200	197
12.0	1.745	1.702	1.628	1.545	1.473	1.410	1.355
	210	208	205	202	200	197	193
12.5	1.955	1.910	1.833	1.747	1.673	1.607	1.548
	208	206	202	199	195	192	188
13.0	2.163	2.116	2.035	1.946	1.868	1.799	1.736
	205	203	200	196	191	187	183
13.5	2.368	2.319	2.235	2.142	2.059	1.986	1.919
	201	200	198	193	186	181	178
14.0	2.569	2.519	2.433	2.335	2.245	2.167	2.097
	197	197	195	190	181	175	172
14.5	2.766	2.716	2.628	2.525	2.426	2.342	2.269
	193	194	191	186	176	170	166
15.0	2.959	2.910	2.819	2.711	2.602	2.512	2.435
	188	190	188	182	172	165	160
15.5	3.147	3.100	3.007	2.893	2.774	2.677	2.595
	183	185	184	177	167	160	154
16.0	3.330	3.285	3.191	3.070	2.941	2.837	2.749
	177	180	179	172	162	154	147
16.5	3.507	3.465	3.370	3.242	3.103	2.991	2.896
	172	174	174	167	157	148	140
17.0	3.679	3.639	3.544	3.409	3.260	3.139	3.036
	167	168	168	162	152	142	134
17.5	3.846	3.807	3.712	3.571	3.412	3.281	3.170
	162	162	162	156	147	136	128
18.0	4.008	3.969	3.874	3.727	3.559	3.417	3.298
	157	156	156	150	142	130	122
18.5	4.165	4.125	4.030	3.877	3.701	3.547	3.420
	152	150	150	144	137	124	116
19.0	4.317	4.275	4.180	4.021	3.838	3.671	3.536
	146	144	144	138	131	118	110
19.5	4.463	4.419	4.324	4.159	3.969	3.789	3.646
	140	138	138	132	125	112	104
20.0	4.603	4.557	4.462	4.291	4.094	3.901	3.750
	135	132	131	126	119	106	98
20.5	4.738	4.689	4.593	4.417	4.213	4.007	3.848
	129	126	124	120	113	100	91
21.0	4.867	4.815	4.717	4.537	4.326	4.107	3.939

---

* The table gives log N_m; N_m=number of stars per square degree brighter than m, international photographic scale. Pole of Milky Way: α $12^h41^m20^s$, $\delta+27°21'$ (1875).

TABLE XVII—*Continued*

m	30°	40°	50°	60°	70°	80°	90°
4.0	7.870	7.784	7.744	7.711	7.689	7.668	7.655
	231	230	229	229	231	230	230
4.5	8.101	8.014	7.973	7.940	7.920	7.898	7.885
	230	229	228	229	230	230	230
5.0	8.331	8.243	8.201	8.169	8.150	8.128	8.115
	229	228	227	228	228	228	229
5.5	8.560	8.471	8.428	8.397	8.378	8.356	8.344
	228	227	226	227	226	225	226
6.0	8.788	8.698	8.654	8.624	8.604	8.581	8.570
	226	226	225	225	224	223	223
6.5	9.014	8.924	8.879	8.849	8.828	8.804	8.793
	225	225	224	223	221	220	220
7.0	9.239	9.149	9.103	9.072	9.049	9.024	9.013
	223	223	222	221	218	218	217
7.5	9.462	9.372	9.325	9.293	9.267	9.242	9.230
	221	221	220	219	215	215	214
8.0	9.683	9.593	9.545	9.512	9.482	9.457	9.444
	218	219	218	216	212	212	210
8.5	9.901	9.812	9.763	9.728	9.694	9.669	9.654
	216	217	215	212	208	207	205
9.0	0.117	0.029	9.978	9.940	9.902	9.876	9.859
	214	214	211	207	204	202	201
9.5	0.331	0.243	0.189	0.147	0.106	0.078	0.060
	212	210	206	202	199	197	197
10.0	0.543	0.453	0.395	0.349	0.305	0.275	0.257
	209	206	202	197	195	192	192
10.5	0.752	0.659	0.597	0.546	0.500	0.467	0.449
	205	202	198	192	190	187	187
11.0	0.957	0.861	0.795	0.738	0.690	0.654	0.636
	201	198	194	187	184	182	182
11.5	1.158	1.059	0.989	0.925	0.874	0.836	0.818
	197	193	189	182	179	177	177
12.0	1.355	1.252	1.178	1.107	1.053	1.013	0.995
	193	188	183	177	173	172	171
12.5	1.548	1.440	1.361	1.284	1.226	1.185	1.166
	188	183	177	172	168	167	165
13.0	1.736	1.623	1.538	1.456	1.394	1.352	1.331
	183	178	172	167	163	161	160
13.5	1.919	1.801	1.710	1.623	1.557	1.513	1.491
	178	172	166	162	158	156	155
14.0	2.097	1.973	1.876	1.785	1.715	1.669	1.646
	172	166	160	156	152	150	150
14.5	2.269	2.139	2.036	1.941	1.867	1.819	1.796
	166	160	153	150	146	144	144
15.0	2.435	2.299	2.189	2.091	2.013	1.963	1.940
	160	153	146	144	140	138	138
15.5	2.595	2.452	2.335	2.235	2.153	2.101	2.078
	154	146	140	138	134	132	133
16.0	2.749	2.598	2.475	2.373	2.287	2.233	2.211
	147	140	134	132	128	127	127
16.5	2.896	2.738	2.609	2.505	2.415	2.360	2.338
	140	133	128	126	123	122	121
17.0	3.036	2.871	2.737	2.631	2.538	2.482	2.459
	134	127	122	120	118	117	115
17.5	3.170	2.998	2.859	2.751	2.656	2.599	2.574
	128	120	116	114	113	111	109
18.0	3.298	3.118	2.975	2.865	2.769	2.710	2.683
	122	113	110	108	107	105	104
18.5	3.420	3.231	3.085	2.973	2.876	2.815	2.787
	116	107	104	102	102	100	99
19.0	3.536	3.338	3.189	3.075	2.978	2.915	2.886
	110	100	98	96	96	94	93
19.5	3.646	3.438	3.287	3.171	3.074	3.009	2.979
	104	94	92	90	90	88	87
20.0	3.750	3.532	3.379	3.261	3.164	3.097	3.066
	98	87	86	84	84	82	81
20.5	3.848	3.619	3.465	3.345	3.248	3.179	3.147
	91	81	80	78	78	76	75
21.0	3.939	3.700	3.545	3.423	3.326	3.255	3.222

for such a grouping cannot be given at present because of lack of knowledge of the variation of average color-index with galactic latitude and longitude. The relation of mean color to magnitude for all latitudes together, however, was determined in *Contribution* No.

TABLE XVIII

MEAN VALUES OF LOG N_m

m	PHOTOGRAPHIC GROUPING				VISUAL 0°–90°
	0°–20°	20°–40°	40°–90°	0°–90°	
4.0	8.116	7.884	7.726	7.938	8.112
4.5	8.347	8.114	7.956	8.168	8.354
5.0	8.576	8.344	8.186	8.398	8.595
5.5	8.804	8.573	8.414	8.626	8.834
6.0	9.030	8.800	8.640	8.853	9.071
6.5	9.255	9.026	8.865	9.078	9.306
7.0	9.478	9.250	9.088	9.301	9.539
7.5	9.700	9.473	9.309	9.523	9.771
8.0	9.920	9.694	9.528	9.743	0.001
8.5	0.140	9.912	9.743	9.961	0.228
9.0	0.358	0.128	9.955	0.178	0.453
9.5	0.575	0.341	0.163	0.392	0.675
10.0	0.791	0.551	0.367	0.604	0.895
10.5	1.005	0.759	0.567	0.814	1.111
11.0	1.217	0.964	0.763	1.020	1.324
11.5	1.427	1.166	0.954	1.224	1.534
12.0	1.634	1.364	1.141	1.425	1.740
12.5	1.839	1.558	1.322	1.623	1.943
13.0	2.042	1.748	1.498	1.818	2.141
13.5	2.242	1.933	1.667	2.009	2.335
14.0	2.439	2.113	1.831	2.196	2.525
14.5	2.633	2.287	1.989	2.379	2.710
15.0	2.823	2.454	2.140	2.559	2.891
15.5	3.009	2.616	2.286	2.734	3.066
16.0	3.190	2.772	2.427	2.905	3.235
16.5	3.366	2.922	2.561	3.071	3.399
17.0	3.537	3.067	2.689	3.232	3.557
17.5	3.703	3.205	2.811	3.388	3.709
18.0	3.864	3.338	2.927	3.539	3.856
18.5	4.019	3.465	3.037	3.684	3.997
19.0	4.169	3.586	3.141	3.824	4.132
19.5	4.313	3.701	3.239	3.959	4.261
20.0	4.450	3.810	3.330	4.089	4.385
20.5	4.581	3.913	3.415	4.214	....
21.0	4.707	4.011	3.495	4.334	....

287,[1] where it was found that the correction $-0.16-0.050m$, applied to the argument, transforms a grouping according to photographic magnitude into one according to visual magnitude.

The use of this correction in connection with $\log N_m$ for 0°–90° in the fifth column of Table XVIII gives the corresponding mean densities on the basis of a grouping according to visual magnitude. Interpolation of $\log N_m$ for corrected magnitudes 4.0, 4.5 . . . . gives at once the results in the sixth column of Table XVIII. The value for the twentieth visual magnitude corresponds to a total of 1,000,000,000 stars for the whole sky.

TABLE XIX

COMPARISON WITH *Draper Catalogue*

Vis. Mag.	*D.C.* Log N_m	Scale Corr.	Color Equation	Corr. Mag.	Table XVIII Log N_m	*D.C. minus* Table XVIII
6.25	9.204	0.00	−0.07	6.18	9.156	+0.048
6.75	9.434	+ .04	.09	6.70	9.399	+ .035
7.25	9.672	.08	.09	7.24	9.650	+ .022
7.75	9.891	.12	.10	7.77	9.895	− .004
8.25	0.152	.16	.10	8.31	0.142	+ .010
8.75	0.379	.21	.11	8.85	0.386	− .007
9.25	0.550	+0.26	−0.12	9.39	0.626	−0.076

Comparison with the "Draper Catalogue."—These results can be partially checked by comparison with Shapley's counts of stars in the *Draper Catalogue* given in *Harvard Circular* No. 226, Table II. The totals in the last line of this table, reduced to an area of 1 square degree, give the values of $\log N_m$ in the second column of Table XIX. These correspond to magnitudes on the Harvard scale shown in the first column. The scale correction and color equation necessary for reduction to the international system given in the third and fourth columns are taken from Table II and from data under (2) of *Contribution* No. 288. The corrected magnitudes and the corresponding densities interpolated from Table XVIII are in the fifth and sixth columns of Table XIX.

In view of the indirect method of comparison, the agreement shown by the differences in the last column is all that can be expected. The first two or three values are large because of the partial neglect of the color equation in reducing van Rhijn's table to the international system, which affects the magnitudes near $m=6$ by 0.03 or 0.04 mag. The comparison in Table XIX is not altogether consistent in that the *Draper Catalogue* has been corrected for color. Here, however, the grouping is according to visual magnitude, and the relatively large mean color-index of stars grouped in this manner leads to a color equation which cannot be neglected. The last difference in Table XIX is merely an indication that the counts from the *Draper Catalogue* are not complete to the limit in question.

---

[1] *Astrophysical Journal*, **61**, 114, 1925.

TABLE XX

Scale Correction for Kapteyn's Distribution Table, *G.P.* No. 18

Mag.	Corr.	Mag.	Corr.	Mag.	Corr.
4	−0.17	9	+0.17	14	+0.64
5	− .09	10	.24	15	0.82
6	− .03	11	.31	16	1.07
7	+ .04	12	.39	17	1.41
8	+0.11	13	+0.50	18	+1.88

TABLE XXI

Comparison of Mean Color-Indices

Pg. Mag.	Source	Galactic Latitude					
		0°	10°	30°	50°	70°	90°
7.............	a*	+0.37	+0.42	+0.54	+0.65	+0.72	+0.76
	b†	0.35	0.43	0.55	0.64	0.68	0.69
14.............	a	0.89	0.91	0.75	0.81	0.93	1.02
	b	0.56	0.68	0.84	....	....	....
17.............	a	+1.09	+1.02	+0.97	+0.87	+0.66	+0.56

* *a* from distribution tables for stars grouped according to photographic and visual magnitudes.

† *b* from *Contribution* No. 287, data groups (1) and (2), and Table X.

Scale correction to "Groningen Publication" No. 18.—The comparison of the values of log N_m in the sixth column of Table XVIII with those in the last column of Kapteyn's distribution table in *Groningen Publication* No. 18 leads to the scale correction for Kapteyn's table given in Table XX. It should be emphasized that this correction is an average for all galactic latitudes.

Were the correction independent of latitude, the comparison of Kapteyn's table, reduced to the international system by means of this correction, with Table XVII would throw much light on the variation of mean color-index with galactic latitude. Thus in Table XVII, log N_m corresponds to photographic magnitude m_p. With these values of the density as argument, interpolate the corresponding visual magnitude m_v from Kapteyn's corrected table. The color effect would then be $C=m_p-m_v$, which, by *Contribution* No. 287, is sensibly equal to $\frac{1}{2}(C_v+C_p)$, where C_v and C_p are mean color-indices for groupings of stars according to photographic and visual magnitudes, respectively. Table XXI shows, under a, values of C found in this manner. For comparison, means of C_v and C_p from *Contribution* No. 287 are given under b. The agreement for $m=7$ is excellent, except at 90° latitude; but for $m=14$ the values a increase too slowly, while at $m=17$ the effect of color calculated as above diminishes with increasing latitude, instead of increasing, as is known to be the case. The inference is that Kapteyn's distribution table is not homogeneous in the matter of scale, the correction varying with the latitude.

8. THE DERIVATIVES OF N_m

The values of dN_m/dm, which are of much importance in statistical discussions, have been calculated from the data in Table XVII by

$$\frac{dN_m}{dm}=\frac{N_m}{\text{Mod.}}\,\frac{d(\log N_m)}{dm}\,, \tag{2}$$

where, with sufficient accuracy,

$$\frac{d(\log N_m)}{dm}=\log N_{m+\frac{1}{2}}-\log N_{m-\frac{1}{2}}\,. \tag{3}$$

The results for selected latitudes and intervals of latitude are given in logarithmic form in Table XXII. It is customary to attempt to represent the values of dN_m/dm by quadratic exponentials in m, or the logarithms of the derivatives by ordinary quadratics in m having the form

$$\log\left(\frac{dN_m}{dm}\right)=a+bm+cm^2\,. \tag{4}$$

Table XXII shows that this will not be possible for the entire range in *m*, because the second differences are not constant for $m < 12$ or 13. Below this limit, however, the quadratic relation is applicable. The values of the coefficients *a*, *b*, and *c* are to be found at the bottom of Table XXII, and the corresponding representation, in the sense Table XXII *minus* formula (4) in Table XXIII.

TABLE XXII

VALUES OF LOG $\left(\frac{dN_m}{dm}\right)$

m	PHOTOGRAPHIC GROUPING								VISUAL 0°–90°
	0°	30°	60°	90°	0°–20°	20°–40°	40°–90°	0°–90°	
4.0	8.219	7.898	7.734	7.680	8.143	7.911	7.753	7.965	8.159
4.5	8.447	8.127	7.963	7.910	8.371	8.139	7.981	8.193	8.400
5.0	8.674	8.355	8.191	8.139	8.598	8.367	8.208	8.420	8.638
5.5	8.900	8.582	8.417	8.364	8.823	8.593	8.433	8.646	8.874
6.0	9.125	8.807	8.641	8.584	9.046	8.818	8.656	8.870	9.107
6.5	9.349	9.030	8.863	8.802	9.268	9.041	8.878	9.092	9.339
7.0	9.572	9.252	9.082	9.016	9.489	9.262	9.098	9.312	9.569
7.5	9.794	9.471	9.299	9.227	9.708	9.482	9.315	9.531	9.797
8.0	0.016	9.688	9.512	9.433	9.926	9.699	9.528	9.748	0.023
8.5	0.236	9.901	9.721	9.634	0.143	9.912	9.736	9.963	0.246
9.0	0.455	0.113	9.924	9.830	0.359	0.123	9.940	0.175	0.466
9.5	0.673	0.323	0.121	0.022	0.574	0.330	0.140	0.384	0.683
10.0	0.889	0.529	0.312	0.209	0.787	0.534	0.336	0.591	0.897
10.5	1.102	0.731	0.498	0.390	0.997	0.736	0.527	0.795	1.106
11.0	1.314	0.928	0.679	0.565	1.204	0.935	0.713	0.995	1.312
11.5	1.525	1.120	0.854	0.735	1.409	1.130	0.894	1.193	1.515
12.0	1.733	1.308	1.024	0.898	1.611	1.320	1.069	1.388	1.714
12.5	1.938	1.491	1.189	1.054	1.812	1.505	1.237	1.580	1.908
13.0	2.141	1.668	1.348	1.205	2.010	1.684	1.398	1.767	2.097
13.5	2.339	1.839	1.502	1.351	2.204	1.857	1.552	1.949	2.281
14.0	2.532	2.003	1.649	1.491	2.394	2.023	1.700	2.127	2.461
14.5	2.720	2.160	1.789	1.625	2.579	2.182	1.841	2.301	2.636
15.0	2.902	2.310	1.922	1.752	2.760	2.334	1.976	2.471	2.805
15.5	3.078	2.453	2.048	1.873	2.936	2.480	2.105	2.636	2.966
16.0	3.248	2.589	2.167	1.988	3.105	2.620	2.227	2.795	3.120
16.5	3.412	2.716	2.279	2.095	3.269	2.754	2.342	2.948	3.269
17.0	3.571	2.836	2.384	2.194	3.427	2.881	2.440	3.095	3.411
17.5	3.725	2.950	2.482	2.287	3.580	3.001	2.549	3.237	3.547
18.0	3.874	3.058	2.573	2.374	3.726	3.115	2.643	3.373	3.677
18.5	4.017	3.159	2.657	2.456	3.865	3.222	2.730	3.502	3.800
19.0	4.153	3.253	2.734	2.531	3.998	3.321	2.808	3.626	3.916
19.5	4.282	3.339	2.803	2.597	4.124	3.413	2.878	3.744	4.026
20.0	4.405	3.417	2.864	2.654	4.242	3.498	2.940	3.857	4.131
20.5	4.522	3.487	2.917	2.702	4.353	3.576	2.995	3.965	....
21.0	4.631	3.547	2.961	2.743	4.458	3.647	3.042	4.067	....
a	−5.055	−5.244	−5.179	−5.131	−5.520	−5.185	−5.303	−5.134	−5.010
b	+0.703	+0.715	+0.688	+0.669	+0.744	+0.704	+0.706	+0.6796	+0.7130
c	−0.0115	−0.0141	−0.0143	−0.0140	−0.0128	−0.0135	−0.0147	−0.0115	−0.0128
m_0	30.6	25.4	24.0	23.9	29.1	26.1	24.0	29.6	27.8

The failure of the quadratic formula for the brighter stars is not unexpected, for the following reason. We have the general relation

$$\frac{dN_m}{dm}\,dm = KdM\int_0^\infty \phi(M)\Delta(\rho)\rho^2 d\rho \tag{5}$$

where K is a constant, $\phi(M)$ the luminosity function, and $\Delta(\rho)$ the density function. Table III of *Contribution* No. 271[1] shows that practically all the stars brighter than $m=12$ or 13 have absolute magnitudes brighter than $M=8$. Further, in *Contribution* No. 273[2] it is shown that the luminosities of all such stars can still be represented approximately by a quadratic exponential in M. If now it were possible to represent the derivative in the left-hand member of (5) by a quadratic exponential in m, we should have for $\Delta(\rho)$, according to Schwarzschild's theorem, a quadratic exponential in $\log \rho$, which is impossible, since the space density of stars is not zero for $\rho=0$. Hence, for the bright stars, at least, the assumption of a quadratic exponential for dN_m/dm is not justified.

TABLE XXIII

REPRESENTATION OF LOG $\left(\frac{dN_m}{dm}\right)$ BY QUADRATIC FORMULAE

(Table XXII *minus* Eq. (4); unit=0.001)

m	PHOTOGRAPHIC GROUPING								VIS. GR. 0°–90°
	0°	30°	60°	90°	0°–20°	20°–40°	40°–90°	0°–90°	
11	+28	+13	+20	+31	+89	+10	+29	+45	+28
12	+ 8	+ 2	+ 6	+17	+46	+ 1	+17	+23	+11
13	+ 1	0	0	+ 5	+21	− 1	+ 7	+10	+ 1
14	− 1	+ 1	− 1	0	+ 7	− 2	0	+ 1	− 2
15	0	+ 1	− 1	− 2	0	− 3	− 3	− 1	0
16	− 1	+ 3	− 1	− 1	− 2	− 3	− 3	− 1	− 1
17	− 1	0	0	− 2	− 2	0	− 2	0	− 1
18	+ 1	0	+ 1	− 1	+ 1	− 2	+ 1	0	0
19	+ 3	+ 2	+ 3	+ 5	+ 3	+ 4	+ 4	0	0
20	0	+ 1	+ 3	+ 5	+ 2	+ 3	+ 3	− 1	+ 1
21	− 5	− 6	− 2	− 1	− 1	+ 2	+ 2	+ 1	....

In view of the probable complexity of the analytic form of the luminosity and density functions, it is, in fact, surprising to find that a simple expression for dN_m/dm or its logarithm is applicable at all. That such is the case for the faint stars probably means that the variation of $\Delta(\rho)$ is relatively simple for large values of ρ, so that the quadratic exponential in log ρ applies to a great range in distance, and further that the deviations of the luminosity function from a Gaussian curve do not seriously affect the values of N_m calculated by (5) until a very low limit for m is reached.

---

[1] *Astrophysical Journal*, 59, 11, 1924.

[2] *Ibid.*, 59, 310, 1924.

9. TOTAL NUMBER OF STARS AND GALACTIC CONCENTRATION

The total of 890,000,000 stars to the twenty-first photographic magnitude, or a round billion to the twentieth visual magnitude, has already been given. The run in the differences in Tables XVII and XXII reflects what has long been accepted as a demonstrated fact, namely, that the total in the system is finite. Attempts to evaluate this total presuppose that the relation between N_m and m defined by the stars within observational reach applies also to the invisible luminous stars. The preceding section suggests how precarious such an assumption must be, but in the absence of any other method of procedure, we make the assumption tentatively, and write for the total in the system

TABLE XXIV

COMPARISON OF LOG N_m FOR 0°–90° WITH RESULTS FROM EQ. (6)

m	Cal. Log N_m	Table XVII —Cal.	m	Cal. Log N_m	Table XVII —Cal.
12	1.472	−0.045	17	3.232	0.000
13	1.827	− .009	18	3.539	.000
14	2.196	.000	19	3.824	.000
15	2.558	+ .001	20	4.090	+ .001
16	2.905	0.000	21	4.334	0.000

$$N=41,253\int_{-\infty}^{+\infty} e^{\frac{1}{\text{Mod.}}(a+bm+cm^2)}dm\ . \tag{6}$$

The fact that (4) does not hold for $m<12$ or 13 can be disregarded, since the number of stars brighter than this limit is an insignificant percentage of the total. The limiting magnitude, m_0, above which, in accordance with the assumed validity of (6), one-half of the stars are found, is equal to $-b/2c$. Its values for different galactic latitudes are given in the last line of Table XXII.

The formulae for the evaluation of (6) are well known.[1] As a preliminary, they may be used to test the accuracy of the results for log (dN_m/dm), 0°–90°, in the ninth column of Table XXII by integrating (6) to the upper limits $m=12, 13, \ldots 21$ (without the numerical factor, however) and comparing the resulting values of log N_m with those in Table XVII. Below $m=13$ the differences, which are shown in the last column of Table XXIV, are insignificant.

Integrating, now to $m=+\infty$, we find

$$N=3.66\times 10^{10}\,. \tag{7}$$

The total can also be found from the data for a grouping according to visual magnitude given in the last column of Table XXII. The result is

$$N=3.53\times 10^{10}\,. \tag{8}$$

Further, the zones 0°–20°, 20°–40°, and 40°–90° can be treated separately, the numbers for the zone totals being summed to obtain the total for the system. This gives:

$$\left.\begin{array}{ll} 0^\circ\text{–}20^\circ & N_1=2.84\times 10^{10} \\ 20\text{–}40 & N_2=0.12\times 10^{10} \\ 40\text{–}90 & N_3=0.02\times 10^{10} \\ \hline 0\text{–}90 & N\;=2.98\times 10^{10} \end{array}\right\} \tag{9}$$

Results (7), (8), and (9) agree within the uncertainty of the calculation. That under (9) is perhaps the most reliable, and we adopt simply

$$N=3\times 10^{10} \tag{10}$$

as the total number of the stars in the system on the basis of the assumed validity of equation (4).

Finally, by omitting the numerical factor in (6) and applying the formula to the data in the second and fifth columns of Table

---

[1] See, for example, van Rhijn, *Groningen Publication* No. 27, p. 23.

XXII, we find the numbers of stars per square degree to the limit of the system in latitudes 0° and 90°. The results are

$$N_0 = 5{,}320{,}000; \quad N_{90} = 7160. \tag{11}$$

The corresponding totals to $m = 21$ from Table XVII are

$$N_0 = 73{,}600; \quad N_{90} = 1670. \tag{12}$$

The totals for the three zones under (9) are remarkable in that they assign 95 per cent of all the stars to a region within 20° of the galactic plane, and less than 1 per cent to that third of the sky between 40° and 90° of galactic latitude. The numbers (11) and (12), however, well illustrate the hazardous character of the extrapolation involved in the unrestricted summation of equation (6), for even in the direction of the poles of the Milky Way, less than a fourth of the estimated total number of stars is within reach of observation, while in the Milky Way the fraction is only one-seventieth. Future revisions and extensions of the observational data may therefore produce large changes in these rather speculative results.

TABLE XXV

GALACTIC CONCENTRATION; RATIO OF N_m FOR 0° AND 90°

m	Ratio	m	Ratio	m	Ratio
4	3.4	10	4.3	16	13.2
5	3.4	11	4.8	17	16.6
6	3.4	12	5.6	18	21.1
7	3.5	13	6.8	19	27.0
8	3.6	14	8.4	20	34.4
9	3.9	15	10.4	21	44.2

The ratio of the numbers (11), which is over 700, emphasizes the enormous galactic concentration for the stars as a whole already suggested in connection with (9). For the interval of brightness covered by the final distribution table, the values of the concentration (ratios of N_m for 0° and 90°) are as given in Table XXV.

10. TOTAL AMOUNT OF STARLIGHT

The total amount of starlight in terms of the light of a star of magnitude 1.0 is easily obtained by a numerical integration based on the data in the last two columns of Table XXII. Any value of dN_m/dm is sensibly equal to the number of stars in the interval $m-\frac{1}{2}$ to $m+\frac{1}{2}$; and the addition of 0.4 $(1-m)$ to log (dN_m/dm) gives the logarithm of the amount of light contributed by the stars in that interval. For $m>13$, equation (6), with the factor $e^{\frac{0.4}{\text{Mod.}}(1-m)}$ inserted under the integral, can also be used for the calculation. The results per square degree for the successive intervals $m-\frac{1}{2}$ to $m+\frac{1}{2}$ are given in Table XXVI. The amount contributed by the brightest stars is so small that the extrapolation of log (dN_m/dm) upward to $m=0$ introduces only a small uncertainty.

TABLE XXVI

AVERAGE LIGHT OF STARS PER SQUARE DEGREE

(Interval $=m-\frac{1}{2}$ to $m+\frac{1}{2}$; unit = a star of mag. 1.0, int. scale)

m	Photo.	Visual	m	Photo.	Visual
0	0.00033	0.00038	12	0.00098	0.00204
1	38	050	13	93	200
2	44	062	14	85	182
3	51	075	15	74	160
4	58	091	16	62	132
5	66	110	17	50	102
6	74	129	18	37	076
7	81	148	19	27	052
8	89	166	20	18	034
9	94	186	21	12	021
10	98	200	21.5–∞	0.00016	0.00025
11	0.00099	0.00204			
			Total	0.01397	0.02647

The totals for the whole sky are:

$$\left.\begin{aligned}\text{Vis. light} &= 1092 \text{ stars of vis. mag. } 1.0 \text{ int. scale}\\ \text{Pg. light} &= 577 \text{ stars of pg. mag. } 1.0 \text{ int. scale}\end{aligned}\right\} \qquad (13)$$

The first of these values may be compared with results of direct measures of the visual brightness of the sky:

$$\left.\begin{aligned}\text{Van Rhijn}^{1}\text{—}1440 \text{ stars of vis. mag. } 1.0 \text{ Harv. scale}\\ \text{Yntema}^{2}\text{—}1350 \text{ stars of vis. mag. } 1.0 \text{ Harv. scale}\end{aligned}\right\} \qquad (14)$$

---

[1] *Groningen Publication* No. 31, 1921.

[2] *Ibid.*, No. 22, 1909.

The best indication as to the relation between the units in which the results are expressed is that[1]

$$\text{Harv. mag. } 1.0 = 0.92 \text{ int. scale.} \tag{15}$$

Allowance for color equation would reduce the value on the right probably by 0.03 or 0.04 mag., so that altogether the discrepancy between (13) and (14) is even larger than appears on the surface.

It is difficult, at present, to say anything conclusive as to the origin of this difference. Table XXVI shows that the stars fainter than the twentieth visual magnitude, which according to the estimate in the preceding section comprise 97 per cent of all the luminous stars, contribute only about 3 per cent of the total amount of starlight. Whatever the uncertainty in number of stars in the system as calculated by (6), it is not likely, therefore, to affect seriously the calculated total of starlight. Since, further, as shown by Table XXVI, the maximum amount of light is contributed by the stars of the eleventh and twelfth magnitudes, it is improbable that the discordance lies wholly in the residual errors in the magnitude scale. The assumption of a constant scale error, which is equivalent to throwing the whole difference into the units, would require the substitution of

$$\text{Harv. mag. } 1.0 = 1.25 \text{ int. scale} \tag{16}$$

for the probable relation (15), in order to reconcile the results of van Rhijn's measures with those found here.

Mount Wilson Observatory
August 1925

---

[1] *Mt. Wilson Contr.*, No. 288; *Astrophysical Journal*, **61**, 284, 1925.

Contributions from the Mount Wilson Observatory, No. 302
Reprinted from the *Astrophysical Journal*, Vol. LXII, pp. 387–408, 1925

ON THE STRUCTURE AND ORIGIN OF SOLAR MAGNETIC FIELDS

By SVEIN ROSSELAND[1]

ABSTRACT

Discussion of solar magnetism on the basis of ordinary electrodynamics and electron theory.—The *first section* of the investigation *discusses the observations* of the general magnetic field. It is pointed out that the current picture of the general magnetic field as being similar to that of an elementary magnet in each level, while the field-strength varies rapidly from level to level, is irreconcilable with ordinary magnetic theory. An alternative, not suffering from this disadvantage, is discussed. The *second section considers the origin* of the magnetic fields. It is shown that the motion of an ionized gas must, in general, be accompanied by an electric current, *even if, macroscopically, the gas is electrically neutral.* This effect, as well as others, appears to be much too small to account for the large values of the field found by observation. If the solar substance emits long-range β- or α-particles, the situation would be more favorable for an explanation, although we should have to contemplate very extreme conditions in order to explain solar magnetism in this way.

Through the extensive work of Hale and his collaborators at the Mount Wilson Observatory it has become an established fact that sun-spots are the seat of intense magnetic fields the strength of which may amount to several thousand gausses. The magnetic field in a spot is generally centrally symmetrical around an axis perpendicular to the sun's surface, and coinciding with the center of the spot. Judged from an investigation by Hale, Ellerman, Nicholson, and Joy,[2] the detailed structure of the field does not seem to deviate much from that of a single magnetic pole, or from the field corresponding to the superposition of a small number of such poles with parallel axes. This would mean, in general, that the electric current generating the field must circulate in approximately circular paths with the spot as a center. A complete investigation of the spatial distribution of magnetic intensity might give important information about the localization of this current; but, for the moment, observation does not appear to permit more definite conclusions on this point.

---

[1] Fellow of the International Educational Board 1924–26.

[2] *Mt. Wilson Contr.*, No. 165; *Astrophysical Journal*, **49**, 153, 1919

In addition to these local fields, the sun possesses also a general field, symmetrical around an axis which is but slightly inclined to the main axis of the sun's rotation. The strength of this latter field appears to average about 40 gausses just above the photosphere and to decrease so rapidly with increasing height as to be less than 10 gausses at a distance of 500 km above the photosphere.[1] Although the available observations are scarcely accurate enough to warrant definite conclusions to be drawn about the detailed distribution of the general field over the solar surface, we shall discuss this question a little more closely in the following section.

Constitution of the general magnetic field of the sun.—The observations on the general magnetic field of the sun are based on measurements of the Zeeman effect of solar lines. Because of the feeble intensity of the field and the width of the lines, it has in no case been possible to observe separately the magnetic components into which a single line is split up in the presence of the field. Under the particular observational conditions at hand, however, the superposed intensity of all components will not have its maximum at the same place as the line without the field, but will be displaced by small amounts proportional to the component of the magnetic force in the line of sight.[2] Under strictly stationary conditions it would thus be impossible by such observations to determine all components of the magnetic field. In the case of the sun, however, the determination of all components is possible, in principle, because the earth is moving around the sun, and the sun rotating around an axis which makes a finite angle with the perpendicular to the plane of the ecliptic. It can scarcely be doubted, however, that the observations do not determine all components with the same precision, as the magnetic field is found to be axially symmetrical, with its axis only very little inclined to the axis of rotation of the sun, while this latter is but little inclined relative to the axis of the ecliptic. In the limit, when all three axes are parallel, the component of the magnetic field which is parallel to the axis of symmetry would practically escape observation, and it follows that for small values of the inclinations the determination of this component becomes especially difficult. This difficulty can be removed very simply by the application of general magnetic theory.

---

[1] G. E. Hale, F. H. Seares, A. van Maanen, and F. Ellerman, *Mt. Wilson Contr.*, No. 148; *Astrophysical Journal*, **47**, 206, 1918.

[2] Cf. F. H. Seares, *Mt. Wilson Contr.*, No. 72; *Astrophysical Journal*, **38**, 99, 1913.

Denoting the magnetic field-strength by H (considered as a vector) this theory requires that

$$\operatorname{div} H = 0 \tag{1}$$

under all conditions, provided a small correction for the possibly finite value of the magnetic susceptibility of the substance in question may be neglected. Under stationary conditions the equation

$$\operatorname{curl} H = 4\pi I \tag{2}$$

is also valid, I being the electric current-density. Assume the current generating the magnetic field to be situated within a finite portion of space in the vicinity of the origin of co-ordinates, a condition which corresponds to the case of the sun. When the x- and y-components of the field are known, we obtain the z-component from (1) in the form

$$H_z = \int_z^\infty (\partial H_x/\partial x + \partial H_y/\partial y)dz + a\ , \tag{3}$$

where a is an arbitrary function of x and y. The magnetic force must, however, be zero at an infinite distance from the system, and we are therefore compelled to put $a = 0$ everywhere. The component parallel to the axis of symmetry is therefore given uniquely as soon as the component perpendicular to this axis is known. On the other hand, when the observations are extended to all three components, the foregoing considerations should afford a useful check on the interpretation of the observations. Thus the measurements of the solar magnetic field are reported to be compatible with the view that this field, measured in a particular level, is similar to that of an elementary magnet situated at the sun's center with its axis directed nearly parallel to the sun's axis of rotation. Ascending from lower to higher levels, the field intensity decreases very rapidly.[1] The components of the magnetic force would then be given by the expressions

$$H_x = xzA_r\ ; \qquad H_y = yzA_r \tag{4}$$

$$H_z = -(x^2+y^2-2z^2)A_r/3\ ; \qquad r^2 = x^2+y^2+z^2\ , \tag{5}$$

---

[1] Cf. G. E. Hale, F. H. Seares, A. van Maanen, and F. Ellerman, *Mt. Wilson Contr.*, No. 148; *Astrophysical Journal*, 47, 206, 1918.

where A_r is a function of r which decreases very rapidly with increasing height above the photosphere. By (1), (4), and (5) we obtain

$$\operatorname{div} H = 2z/3r^4 \frac{\partial}{\partial r}(r^5 A_r) \, . \tag{6}$$

This expression vanishes only for $r^5 A_r = \text{constant}$, corresponding to the case of an elementary magnet, which in turn would correspond only to an insensible change in the magnetic field from level to level in the solar atmosphere. The requirements of equation (1) thus necessitate a reinterpretation of the observational results; either the conclusion that the magnetic field-strength decreases rapidly with increasing height in the atmosphere must be given up, or the similarity of the field in a particular level to that of an elementary magnet must be doubted.

There seems to be a way to escape from this dilemma without violating the results of observations. On account of the small inclination of the axis of symmetry to the axis of the ecliptic, the observations are essentially concerned with the x- and y-components only, while the z-component enters the problem in terms having coefficients so small that it probably does not influence the result materially. The component H_z is thus practically outside of direct observational control, and we are at liberty to adjust its value in such a manner that equation (1) is satisfied. In this way we obtain for H_z, on using (3) and (4), the expression

$$H_z = -(x^2+y^2)A_r + 2\int_z^\infty A_r z dz \, . \tag{7}$$

If h denotes a certain length which is a function of r and z and of the order of magnitude of the height of the solar atmosphere, equation (7) may be written in the form

$$H_z = -(x^2+y^2-h^2)A_r \, . \tag{8}$$

Except for a region close to the poles, h^2 must be negligibly small compared to x^2+y^2. A comparison between (4) and (7) shows, therefore, that at the magnetic equator the corrected field-strength is about three times as large as that given by (5), and that the lines of force run nearly parallel to the solar surface within the whole region covered by observation.

If the measurements of the magnetic field of the sun in different levels could be made with great precision, it would be possible, by application of equation (2), to decide whether the solar atmosphere is the seat of electric currents or not. This analysis, applied to the magnetic field of the earth, leads, as is well known, to the result that the currents generating this field are localized, primarily, in the earth's interior. In the case of the sun conditions seem to differ essentially from those on the earth; and if the strong decrease of magnetic field-strength with increasing height in the solar atmosphere be accepted as an observational fact, strong electric currents must necessarily exist in the atmosphere. Assume, as an illustration, the general magnetic field to have the constitution determined by (4) and (8). By (2), we then obtain the following expressions for the rectangular components of the current density

$$I_x = -I_0 y/r\ ; \quad I_y = I_0 x/r\ ; \quad I_z = 0\ ; \quad 4\pi I_0 = r^2 \partial A_r/\partial r + rA_r\,. \tag{9}$$

The current thus flows along the magnetic parallels, the current density being given by

$$I = I_0 \cos\theta\,, \tag{10}$$

where θ is the magnetic latitude of the point in question. The conditions are thus as though the current were produced by uniform rotation of a spherically symmetrical distribution of electricity in the atmosphere. The dominating term in the expression of I_0 is negative, and it follows that the electron current flows in the direction of rotation of the sun. The magnetic field due to a uniformly charged rotating sphere corresponds to that of an elementary magnet outside the charged surface, and is constant in strength and direction (parallel to the axis of rotation) inside the surface. The field given by (4) and (6) is, however, essentially different from the field in the electric layer of a uniformly charged, rotating sphere; and the foregoing results would mean, if taken literally, that the solar field is largely generated by electric currents which are localized below the reversing layer. The precision of the observational results is, however, scarcely great enough for conclusions of this kind to be warranted for the moment.

Origin of electric currents producing solar magnetism.—Apart from such minor uncertainties as are discussed in the preceding section, the existence and general character of the solar magnetic fields are established beyond doubt. The origin of the fields, on the other hand, appears to remain essentially in the dark, and in this section we shall take up a general discussion of this question, on the basis of ordinary electromagnetic theory as applied to free electric charges. The result of the investigation turns out to be essentially negative, but it is hoped that a detailed discussion of the difficulties may serve a useful purpose.

A stationary magnetic field is, according to ordinary electromagnetic theory, always connected with a system of steady electric currents, and when the current-density is known throughout all space it is a simple process of integration to obtain the corresponding magnetic field. The possible kinds of steady electric currents are conveniently subdivided into three different classes: intermolecular, convectional, and galvanic. Solar magnetism might be assumed to be produced by currents belonging to any of these classes. It appears, however, that the first two hypotheses may be eliminated. In fact, from known values of the atomic magnetic moments of different substances, combined with a liberal estimate of the gas density in the solar photosphere, it can be concluded that it is virtually impossible to account for magnetism in sun-spots by assuming the atoms of the solar gases to be paramagnetic and to be all arranged parallel to a given direction. Moreover, this hypothesis ignores the fact that the systematic arrangement of the atoms would, in absence of other causes, have to be brought about by rotation as in the well-known experiments of S. J. and L. J. Barnett; but the rotational velocity of the sun as a whole, as well as that presumable for the gases in the spots, is so small that any perceptible effect of the kind anticipated must be regarded as definitely excluded. The same argument may be raised against the hypothesis that solar magnetism is generated by convection currents. Assume, for instance, the sun's general field to be generated by rotation of a uniform volume charge. This charge would correspond to an electric field intensity at the sun's surface of the order 10^6 volts per centimeter, and if this field were for a moment conceived as existing, the solar atmosphere would emit surplus ions with a rapidity which can be characterized best as an explosion. We are therefore forced to admit that solar magnetism must somehow owe its origin to galvanic currents, i.e., to a real interdiffusion of free electrons through the mass of positive ions.

For a closer discussion of this point it is convenient to consider the question from the point of view of diffusion theory, using for this purpose not the complicated, exact methods of Chapman and Enskog, but a short-cut method which more directly reveals the underlying physical phenomena. Consider a gaseous mixture of free electrons and positive ions moving in any manner. We shall write the hydrodynamical equation for the motion of the electrons parallel to the x-axis in the form

$$n_e m_e du_e/dt = -\partial P_e/\partial x - n_e \partial \phi_e/\partial x - \Gamma_x^e \,, \tag{11}$$

the equations for the motion along the other axes being of exactly the same form. In the foregoing equation m_e denotes the mass of an electron, n_e the number of electrons per unit volume, u_e the component of the arithmetical mean velocity of the individual electrons at the point x, y, z, at the time t, while the y- and z-components will be denoted by v_e and w_e; p_e is the hydrostatic electron pressure which is given by $n_e kT$ where k is Boltzmann's constant, and T the temperature of the gas; ϕ_e is the potential of the external force acting on a single electron, while Γ_x^e is the x-component of the aggregate frictional resistance experienced by the electrons in unit volume. The equations of motion for the atoms will be of exactly similar form, and will be distinguished by an index a. Each frictional term is conveniently subdivided into two different parts, Γ_{x1}^e and Γ_{x2}^e, each of which proceeds from a specific source. Thus Γ_{x1}^e will be assumed to correspond to the viscosity which according to ordinary gas theory corresponds to a homogeneous gas, the expression of which is

$$\Gamma_{xx}^e = \partial \Gamma_{xx}^e/\partial x + \partial \Gamma_{xy}^e/\partial y + \partial \Gamma_{xz}^e/\partial z \,,$$

where

$$\Gamma^e_{xx} = -2\kappa_e \frac{\partial u_e}{\partial x} + \tfrac{2}{3}\kappa_e \left(\frac{\partial u_e}{\partial x} + \frac{\partial v_e}{\partial y} + \frac{\partial w_e}{\partial z} \right) ; \quad \Gamma^e_{xy} = -\kappa_e \left(\frac{\partial v_e}{\partial x} + \frac{\partial u_e}{\partial y} \right) ; \qquad (12)$$
$$\Gamma^e_{xz} = -\kappa_e \left(\frac{\partial w_e}{\partial x} + \frac{\partial u_e}{\partial z} \right) ,$$

and where κ_e is a special coefficient of viscosity which will be considered more closely later on. The second term Γ^e_{x2} refers to the additional interaction between electrons and atoms, which is due to the fact that the mean motions of the two different kinds of particles are in general not identical. It is easy to see that Γ^e_{x2} must depend essentially on the difference in mean velocity of electrons and atoms, as it must disappear when these velocities are equal. It can, moreover, be shown that to a high degree of approximation Γ^e_{x2} will be proportional to a certain linear average value of the x-component of the relative velocity only.[1] The average in question will only in special cases be identical with an ordinary arithmetical average, but for the present purpose this distinction will be neglected by writing

$$\Gamma^e_{x2} = \beta_e (u_e - u_a) , \qquad (13)$$

where β_e is an additional coefficient of viscosity.

In an ordinary gas consisting of atoms which are electrically neutral, it offers no difficulty to derive approximate expressions for the coefficients κ and β. In fact, by ordinary gas theory, κ is given by

$$\kappa = \tfrac{1}{3}\, nm\lambda c , \qquad (14)$$

where c is the mean thermal velocity of an atom and λ its mean free path defined in such a way that an atom moving a distance λ will, on an average, lose completely its momentum parallel to a fixed direction. In applications to the present problem, λ will signify the mean free path, defined in the foregoing manner, for an atom threading its way through a mixture of two gases. By similar considerations we obtain

$$\beta_1 = n_1 m_1 c_1 / \lambda_{12} , \qquad (15)$$

---

[1] Cf. N. Bohr, *Studier over Metallernes Elektronteori*, pp. 20 and 21, Copenhagen, 1911.

where λ_{12} denotes the mean free path of an atom of the first kind relative to atoms of the second kind only, but otherwise it is defined in the same manner as λ.

In a gas consisting of free electrons and positive ions these considerations do not give the total friction. In fact, due to the slow decrease of the force with increasing distance between two particles as calculated from the inverse square law, it is not certain that the kinetic theory of the gas mixture can be founded on the hypothesis of random distribution of electrons relative to atoms, as is tacitly done above. Broadly speaking, the conditions may be described as follows: On following an individual particle in its Brownian movement through the gas we shall find that it constantly attracts particles of the opposite sign and repels particles of the same sign, as a consequence of which it will, on an average, be attended by a small atmosphere of particles of the opposite sign. This atmosphere will only in exceptional cases be spherically symmetrical, and it will, therefore, in general exert an attraction on the specified particle, thus contributing to the internal viscosity in a manner not covered by the two terms discussed above. The additional terms introduced in this way will, as regards the form, be expected to duplicate Γ^e_{x1} and Γ^e_{x2} plus a hydrostatic term, but the values of the coefficients involved may be essentially different from those given above. The analytical discussion of this electrical viscosity is given in the appendix, and it appears that its effect is negligible for the problem at hand, as will be shown presently.

In the current applications of statistical principles to electron theory, it is customary to neglect all frictional terms except the one given by (13), and a discussion of the equations of motion (11) leads then in a very simple manner to the ordinary results of the classical electron theory of metals as regards electric conductivity and thermoelectric phenomena. Thus in the presence of an electric field, electrons and positive ions will be set moving in opposite directions, and this case is taken care of by the presence of the term in (11) which gives the external force on the particles. By using (15), the expression for the electric conductivity of a metallic conductor given by Lorentz follows immediately, apart from a numerical factor of the order unity. For the problem in hand, a further consideration of this case is of little interest, since an external field of force which will keep electrons running continually in a closed circuit in the sun against the resistance offered by the atoms is unknown to us.

It will further be seen from (11) that an electric current may be produced by variations in pressure, a fact which is shown experimentally by the thermoelectric phenomena. Assume for a moment that an insulated metallic rod, as regards conduction of electricity, can be considered as consisting of fixed positive atoms between which electrons are free to move, being hampered in their motion by collisions with the metallic atoms only. If the rod is at a uniform temperature T and no external forces are acting, the electron pressure $p_e = n_e kT$ is a constant throughout the rod, except quite close to the surface where special forces must act to keep the electrons from escaping from the rod. Special consideration of the surface conditions are, however, unnecessary for the present purpose. Assume now that one end of the rod is cooled while the temperature of the other end is kept constant. Due to the decrease in p_e at the cold end of the rod, electrons will begin to flow from the warmer to the colder regions, and a thermocurrent is brought into play which will tend to separate positive and negative charges, the former being assumed to be fixed. Finally, a state of equilibrium is attained in which the diffusion of the electrons enforced by the temperature gradient is exactly counterbalanced by diffusion in the opposite direction enforced by an electric potential gradient $\partial\psi/\partial x$, etc., which from (11) is seen to be given by

$$\partial\psi/\partial x = -\frac{1}{n_e e}\partial p_e/\partial x\,, \text{ etc.}\,, \qquad (16)$$

at any point inside the rod that is not so close to the surface that the neglected surface conditions play an essential part.

It was once an idea of Hale's[1] that similar processes might take place in sun-spots. Hale assumed that the primary phenomenon in the formation of a spot was a very strong and local lowering of temperature, which in turn would be expected to generate a radial electric current according to the principles considered above. If the spot was also a local hydrodynamic vortex, the stream lines of this current would, by hypothesis, be deformed into spirals, and the transverse component of the current thus produced would then give rise to an axially symmetrical magnetic field.

---

[1] G. E. Hale, *Mt. Wilson Contr.*, No. 71, p. 69; *Astrophysical Journal*, 38, 97, 1913.

There can scarcely be any doubt that thermoelectric phenomena of this kind must occur when a sun-spot is formed, and it may be shown that the difference between a gas and a solid metal does not change the conditions seriously. The essential difficulty in this theory seems to lie in the hypothesis that a radial current of the foregoing type would acquire a transverse component by rotation of the gases. In fact, superposing a rotation on the radial motion of the gases does not introduce any agency causing relative motion of electrons and atoms in a transverse direction, as the pressure gradient must be directed radially, irrespective of the spiral motion of the gases. The underlying conditions are, perhaps, best elucidated from the point of view of the circulation theorem as formulated by Bjerknes.[1] Suppose a certain closed curve to be drawn in the medium and to move as if it consisted of molecules belonging to the medium. The circulation, C, of such a curve is defined as the instantaneous line integral of the velocity of the medium taken around the given curve.

$$C=\int(udx+vdy+wdz)\,. \tag{17}$$

By forming the circulation of free electrons, C_e, and of positive atoms, C_a, separately, for a circular path with the spot as a center and situated in a plane perpendicular to the axis of the spot, it is clear that $n_e e(C_e-C_a)$, divided by the length of the curve, will be proportional to the current density at the requisite distance from the center of the spot. The circulation theorem now states that the variation in C per unit time, which is due to the particular distribution of pressure and density present, is, in ordinary vector notation, given by

$$dC/dt=\int\int[\nabla\alpha\nabla p]_n d\sigma\,, \tag{18}$$

the integral being extended to any surface bounded by the curve in question, α being the specific volume. If the vortex possesses circular symmetry, the curve will be situated completely on a surface of constant pressure as well as of constant density, and the foregoing integral will be identically zero. The distribution of pressure and density in the vortex will therefore have no influence on the circulation of such a curve, and hence it will have no tendency to impress a systematic horizontal motion on electrons and atoms, taken separately. On the other hand, the maximum circulation impressed, according to (18), will be for a curve in a vertical plane through the axis of the spot, thus leading to a congestion of electricity at the axis. The free charges produced in this way must very soon react on the current, just as in the example with the insulated rod, and a steady state must soon be reached in which the variation in electronic pressure is balanced by an electric field. All things considered, it does not seem likely that the magnetic fields in sun-spots originate by thermocurrents of the foregoing type, and we must look for some other cause, both for the problem of magnetism in spots, as well as for the general magnetic field, which latter under no circumstances can be related to phenomena of the foregoing sort.

---

[1] Cf. *Dynamics of the Circular Vortex*, p. 9; *Geofysiske Publikationer*, **5**, No. 4, Oslo, 1921.

Turning to the discussion of the electric currents produced by the forces of internal viscosity, it will be apparent that these forces are of such a kind as to set up currents without producing space charges (as was the case with thermo-currents), and therefore will last as long as the motion lasts that brings viscosity into play. To bring out this point clearly, consider the case of a straight circular vortex. This case will correspond to the motion of the sun as a whole, as well as to a symmetrical spot on the solar surface. The motion will be assumed to be quasi-stationary. Choosing the axis of rotation as a z-axis, and simplifying equation (1) according to the foregoing assumptions, we arrive at the following expression for the current density:

$$I=-\frac{n_e e}{\beta}\left\{\kappa\frac{\partial}{\partial r}\left(2w+r\frac{\partial w}{\partial r}\right)+r\frac{\partial\kappa}{\partial r}\frac{\partial w}{\partial r}+r\frac{\partial}{\partial z}\left(\kappa\frac{\partial w}{\partial z}\right)\right\}\ ;\quad r^2=x^2+y^2\ , \tag{19}$$

where we have put

$$\kappa=\kappa_e/n_e m_e-\kappa_a/n_a m_a\ ;\qquad \beta=\beta_e/n_e m_e+\beta_a/n_a m_a\ , \tag{20}$$

and where ω is the angular velocity of the vortex at the point r, z. When the vortex rotates like a rigid body, ω is constant, and by (19) I becomes zero, as it should be. It is essential to note that in the general case the direction of the current is not determined by the direction of rotation of the vortex, and that the vortex will, in the general case, consist of a system of annular current tubes, the sign of the current changing when passing from a specified tube to an adjacent one. Without detailed analysis it will be seen that the electric currents produced by internal viscosity are qualitatively of the type which appear to underlie the phenomena of solar magnetism. As regards the sun-spots, the hypothesis requires the existence of circulating motion of some kind around a spot, an assumption which seems to be compatible with observational results. To explain the existence of the general magnetic field in the same manner, it is necessary to postulate the existence of a universal wind system, extending over most of the surface or interior of the sun, since, as remarked above, the uniform rotation can produce no effect at all. The sun, however, does not rotate like a rigid body, as the angular velocity increases on passing from pole to equator, and the foregoing hypothesis would thus require the existence of a causal connection between the general magnetic field and the non-uniform rotation of the sun.

The foregoing hypothesis seems to work well qualitatively, but very serious objections against it appear when attempting to develop a quantitative theory on this basis. It is for this purpose sufficient to consider a straight and infinitely long vortex of uniform composition, taking κ and β as constants and ω to be of the form $G(r)z^2/z_0^2$, where z_0 is a certain constant with dimensions of a length. The transverse dimensions of the vortex will be assumed to be finite. On these assumptions the magnetic force inside the vortex will be a function of r only, which is zero at an infinite distance from the axis. Calculating the line integral of the magnetic force along a contour consisting of two coplanar straight lines perpendicular to and in the plane of the vortex axis, and two lines parallel to this axis, we find, on using (2), that the magnetic field-strength at a distance r from the axis is given by

$$H=4\pi\int_r^\infty I\,dr\,, \qquad (21)$$

which, by (19) and by our assumption concerning the form of ω, becomes

$$H=\gamma\left\{\left(2\omega_r+r\frac{\partial\omega_r}{\partial r}\right)+\frac{2}{z_0^2}\int_r^{\infty}G(r)rdr\right\}\;;\quad\gamma=4\pi n_e e\kappa/\beta\,. \tag{22}$$

The first term of this expression depends only on the state of the vortex at the point under consideration, while the last term depends on the constitution of the vortex in the entire region external to this point. Suppose it is possible to define properly a certain mean radius, R, of the vortex, and a certain mean value, G_r, of G by the equation

$$\int_r^{\infty}2G(r)rdr=G_r(R^2-r^2)\,. \tag{23}$$

Equation (22) then transforms into

$$H=\gamma\{2\omega_r+r\partial\omega_r/\partial r+G_r(R^2-r^2)/z_0^2\}\,. \tag{24}$$

The constitution of solar matter enters the problem through the single coefficient γ. Since the electronic mass is very much smaller than the mass of an atom, the terms involving m_a may be neglected in the expression of γ. Thus for the case in which the effects of ionic forces are neglected and κ and β are assumed to be given by the expressions (14) and (15), we obtain, approximately,

$$\gamma_c=\tfrac{1}{3}en_e\lambda_e\lambda_{ea}\,. \tag{25}$$

For the case of the "electric" viscosity discussed in the appendix, the value of γ is, as regards order of magnitude,

$$\gamma_e=n_e e\left(\frac{1}{\kappa}\right)^2, \tag{26}$$

and the only essential difference between the two cases is seen to consist in replacing the mean free path by the mean thickness $1/\kappa$ of the electric layer around an ion.

An upper limit to the mean free paths λ_e and λ_{ea} may be obtained in the following way. Consider a region so far down in the photosphere that the atoms may be assumed to be all ionized, with N free electrons per atom. An electron moving with a velocity v and colliding with such an atom, considered to be at rest, will be deflected through an angle θ which is given by

$$\tan \theta/2 = Ne^2/pmv^2 \, , \tag{27}$$

where p is the distance from the atom to the direction of the initial path of the electron. Consider all collisions for which $\theta > \pi/2$ and for which, accordingly, $p < p_m = Ne^2/mv^2$. The number of such collisions suffered per second by an electron of the type in question is $\pi P_m^2 n_a v$ corresponding to a mean free path

$$\lambda = m^2 v^4 / \pi n_a N^2 e^4 \tag{28}$$

approximately. In addition to collisions of the foregoing type, the electron will also suffer collisions in which $\theta < \pi/2$ and which, of course, will change the momentum of the electron to some extent. An upper limit to λ_{ea}, as well as to λ_e, is thus given by the above expression alone, provided it is averaged over all velocities. For the case of thermal equilibrium the mean value of $(mv^2)^2$ is $15k^2T^2$, and the upper limit to γ_c is accordingly

$$\gamma_c = \frac{n_e e}{3} \left(\frac{15 k^2 T^2}{\pi n_a N^2 e^4} \right)^2 . \tag{29}$$

Introducing the expression of κ (eq. 37 in appendix), we find

$$\gamma_e = kT/4\pi e(N+1) \, . \tag{30}$$

It appears that for all cases of interest for the present problem, γ_e must be very small compared to γ_c. In order that $\gamma_e = \gamma_c$ in the sun's photosphere ($T = 6000^\circ$, $N \rightarrow 1$), the number n_a would have to be of the order 10^{22}, a figure much larger than can be admitted on spectroscopic grounds, as well as on the basis of the known value of the sun's mean density. It seems, therefore, safe to conclude that the electrical viscosity is immaterial to this problem.

It is now frequently assumed that the pressure in the sun's reversing layer is as small as 10^{-4} atmosphere, which for $T = 6000^\circ$, $N = 1$, would correspond to $n_a = 10^{13}$. The corresponding value of γ_c is about 10^6 c.g.s., and a sensibly larger value is hardly permissible.

The terms in the parenthesis of (24) have dimensions of angular velocities, and, in order of magnitude, neither of them can be expected to be greatly in excess of the angular velocity of the vortex itself at the point in question. Remembering that the magnetic field in sun-spots often attains values of several thousand gausses, and adopting the above value of γ_c, we find that this theory would require a spot to revolve with an angular velocity of several million revolutions per second. This figure, which in itself seems prohibitive enough, is only a lower limit. It is easy to convince one's self that the case is exactly the same for the general magnetic field.

This result would seem to require careful consideration, for the foregoing discussion apparently covers all available possibilities. In fact, the deductions have been based partly on the ordinary electron theory—including the validity of Coulomb's law as applied to collisions between electrified particles—and partly on the assumption that the free electrons considered are in temperature equilibrium with the solar substance. Coulomb's law may, for the collisions in question, be in error by minor amounts, but discrepancies such as would remove the difficulties are entirely out of question. Within the frame of ordinary electromagnetic theory there appears thus to be only a single possibility left for escape, viz., to assume that the electrons which are answerable for the magnetic fields are not in temperature equilibrium with the solar gases, and are capable of describing excessively long free paths; in short, that they are β-particles. Measurements of the mean range of homogeneous β-particles have been made by Varder.[1] In these experiments the velocities of the particles were about 0.85 of the velocity of light, and the mean range found corresponded roughly to the formula

$$\lambda = (2 n_a m_a)^{-1} \text{ c.g.s.} \tag{31}$$

For atomic weight 60 and $n_a = 10^{13}$, the value of λ is 5000 km. The range of such a particle is therefore enormous as compared with the mean free path of an ordinary electron, which under the same conditions and a temperature of 6000° would be of the order of 10 cm. Proceeding in a manner analogous to the derivation of the coefficient of viscosity in gas theory, we find that the electric current density due to emission of β-particles in a moving medium is given by an expression which is practically identical with that used for the conduction by free electrons, (19), provided the average range of a β-particle is substituted for the mean free path of an electron, and, further, that the problem is still characterized by a constant γ. Denoting the number of β-particles emitted from the solar substance per unit time and volume by Qn_a, and remembering that the mean time required by a particle with a velocity v to complete a range λ is λ/v, we obtain $n_e = Qn_a\lambda/v$, and, finally, as regards order of magnitude,

---

[1] *Philosophical Magazine*, **29**, 725, 1915.

$$\gamma_e = \lambda^3 Qn_a e/3v \,. \tag{32}$$

By combination of (32), (31), and (24) it is now possible to estimate the upper limit Q^{-1} of the mean life-period of the hypothetical element in question. We arrive in this way at the result that Q^{-1} cannot possibly be longer than a few years. This estimate might be increased, provided the particles in question were emitted with larger initial velocities than assumed above. On the other hand, the theory involves several unwarranted approximations which, when removed, would reduce the foregoing limit very seriously. The most important of these approximations is perhaps the implicit assumption that the particles travel in straight lines. In fact, due to the action of the magnetic field, the path of such a particle will be very strongly curved, and in just such a way as to reduce the intensity of the field. The effective range to be introduced in (32) is therefore considerably smaller than the experimental value used above. In short, it does not seem likely that the foregoing estimate of Q^{-1} can be appreciably enlarged.[1] The conclusion follows that Q^{-1} is of an entirely different order of magnitude from the life-period of a star, and that therefore the radioactivity in question, if existing, must differ essentially in nature from radioactivity as it manifests itself in terrestrial experiments. When we consider the balance of energy in a star, difficulties still more serious arise. In fact, the energy of a fast-moving β-particle is enormous as compared with the energy residing in a quantum of radiation of visible light; and, relatively speaking, a very small number of such particles emitted per second, so far within the sun as to be absorbed, would be sufficient to account for the total solar radiation. As far as may be judged from the foregoing simple theory, it seems that the emission of β-particles of median velocities necessary to explain the general magnetic field would require a much larger emission of energy than is compatible with the known luminosity of the sun.

---

[1] Note added in proof. In expression (32) the secondary ionization produced by the primary particles is neglected. This ionization, however, is considerable, each primary particle producing some millions of ions. The ranges of secondary particles are known to be relatively small, and it does not seem probable that a correction in this sense will essentially alter the conclusions in the text.

A way out of this difficulty, on the foregoing lines, is only attainable by assuming the β-particles in question to be very much more penetrating than any rays observed in terrestrial experiments, as theory would indicate that the range of such particles is proportional to the energy of expulsion,[1] while the magnetic field-strength, according to the above theory, would be proportional to the square of the range. By increasing the range indefinitely and keeping the magnetic field-strength constant, it is thus possible to reduce the total energy emitted below any assigned limit.

A further enlargement of the question does not seem profitable at present. We have discussed in this paper the general problem of accounting for solar magnetism on the basis of ordinary physical theory. Although it is possible to construct a theory which qualitatively meets observational requirements, the quantitative discussion does not lead to conclusions which stand in any immediate relation to observational results. The question whether the sun can be assumed to emit extremely penetrating corpuscular radiation should be carefully looked into. On the other hand, we have no a priori reason for expecting ordinary magnetic theory to apply to cosmical phenomena in all details. Whether one view or the other is taken, it seems rather certain that solar magnetism cannot be accounted for on the basis of physical facts with which we are completely familiar from ordinary terrestrial physics.

APPENDIX

Electrical stresses in an ionized gas.—Since electrical viscosity is due to the systematic distribution of particles of opposite sign in a moving gas, we shall follow, in deriving a first-order expression for the coefficient, a method first used by Debye and Hückel in the theory of electrolytes.[1] Consider an ionized gas consisting of free electrons and positive ions of r different kinds, the charge on an ion of the ith kind being $N_i e$, where $-e$ is the charge on an electron. The mean value of the electric potential at a point x, y, z, relative to a co-ordinate system which is fixed with respect to a particular ion, we denote by ψ and assume that it is, to a first approximation, given by Poisson's equation

---

[1] Cf. N. Bohr, *Philosophical Magazine*, **30**, 594, 1915.

$$\nabla^2\psi = -4\pi e \sum_{1}^{r} n_i N_i \,, \tag{33}$$

where n_i is the mean number of ions of the ith kind per unit volume at the point x, y, z, and where the free electrons are regarded as a particular kind of ions. In a state of equilibrium, the numbers n_i will be determined by the competing action of the electric forces, the motion of the gas, and ordinary spontaneous diffusion. Let V be the mean value of the vectorial velocity of all particles in the vicinity of the point in question. The mean velocity of each specified particle will differ from V by small amounts. Thus spontaneous diffusion introduces an additional mass motion with a velocity

$$V_d^i = -\nabla n_i D_i / n_i \,,$$

relative to the other gases, where D_i is the coefficient of diffusion of the ions of the ith kind. The electric forces will, on the other hand, induce a forced diffusion with a mean velocity

$$V_f^i = -\alpha_i N_i e \nabla\psi \,,$$

where α_i is the mobility of the i-ions. The total velocity of these ions is thus

$$V^i = V + V_d^i + V_f^i \,.$$

By the equation of continuity,

$$\partial(n_i V^i)/\partial t + \text{div}\,(n_i V^i) = 0 \,,$$

---

[1] Cf. *Physikalische Zeitschrift*, 24, 1, 1923.

we have that n_i, under stationary conditions, is determined by the equation

$$\operatorname{div}\left(-D_i\nabla n_i-a_iN_ien_i\nabla\psi+n_iV\right)=0\,. \tag{34}$$

If V is zero, this equation has the solution

$$n_i=n_i^\circ e^{-a_iN_ie\psi/D_i}\,, \tag{35}$$

where n_i° is the value of n_i at a point where ψ is zero. Since this expression must coincide with the Boltzmann-Maxwell distribution law, it is necessary, as was first pointed out by Einstein, that

$$D_i/a_i=kT\,, \tag{36}$$

where k is Boltzmann's constant and T the absolute temperature.

We wish ultimately to determine ψ; and three simple cases will be considered.

1. $V=0$.—The n's are then given by (35). Introducing these expressions in (33) and expanding the exponentials to the first order, we obtain

$$\nabla^2\psi=\kappa^2\psi\,;\qquad \kappa^2=4\pi e^2\Sigma n_i^\circ N_i^2/kT \tag{37}$$

the solution of which, for an electric point charge N_ie at the origin, is

$$\psi=N_ie\,e^{-\kappa r}\,;\qquad r^2=x^2+y^2+z^2\,. \tag{38}$$

2. $V=const.$—The specified ion is then moving relative to the gas with a velocity $-V$. By (33) and (34)

$$\nabla^4\psi-\left(\frac{4\pi e^2}{kT}\Sigma n_iN_i\right)\nabla^2\psi=-4\pi e\Sigma\frac{N_i}{D_i}(\nabla n_iV)+\frac{4\pi e^2}{kT}\Sigma N_i(\nabla n_i\nabla\psi)\,. \tag{39}$$

To reduce this equation to a first approximation, we must assume $n_i=n_i^\circ=$ constant in the left-hand term and neglect the last term on the right. The term in V we consider as a small correction and therefore we suppose n_i here to be given by (35) expanded to the first order, and the value of ψ involved to be given by (38). By taking the direction of V as the axis of x, equation (39) reduces to the final form

$$\nabla^2(\nabla^2-\kappa^2)\psi=N_iV\sigma\frac{x}{r}\frac{\partial}{\partial r}(e^{-\kappa r}/r)\,; \qquad \sigma=\frac{4\pi e^2}{kT}\Sigma n_i^\circ N_i^2/D_i\,. \tag{40}$$

This equation has the intermediate solution

$$\nabla^2\psi=\kappa^2N_ie\;e^{-\kappa r}/r+N_iV\sigma\times e^{-\kappa r}/2r\,, \tag{41}$$

which gives finally

$$\psi=N_ie\;e^{-\kappa r}/r+\{1-2e^{\kappa r}/\kappa^2r^2-2e^{\kappa r}\frac{d}{dr}(e^{-\kappa r}/r\kappa^2)\}N_iV\sigma\times e^{-\kappa r}/2r\kappa^2\,. \tag{42}$$

3. *V_x=linear function of z; $V_y=V_z=0$.*—We introduce a new co-ordinate system with axes parallel to the original axes, but moving with a velocity equal to the velocity of the fluid at the point in question. This problem leads to an equation of the form (40). All we need for the present is an intermediate solution corresponding to (41), and this is found to be

$$\nabla^2\psi=\kappa^2N_ie\;e^{-\kappa r}/r+N_i\frac{\partial V_x}{\partial z}\frac{\sigma x}{4}e^{-\kappa r}/r\,, \tag{43}$$

where $\partial V/\partial z$ has been regarded as a constant.

We are now prepared for the discussion of the electrical stresses in the moving gas. Consider the momentum parallel to the x-axis transferred per unit area by electrical forces from the upper to the lower side of a plane parallel to the xy-plane. We specify a certain particle, fixed at a distance ζ below the given plane. The particle will be attracted or repelled by the particles above the plane with a mean resultant force the x-component of which we shall denote by f_x^i and calculate by means of expression (43). Introducing a co-ordinate system with axes parallel to the original ones and with origin in the particle, we find for f_x^i the expression

$$f_x^i=N_ie/4\pi\int\frac{\nabla^2\psi x}{r^3}dxdydz\,, \tag{44}$$

where the integration is to be extended to the whole gas above the given plane. The value of $\nabla^2\psi$, however, will decrease so rapidly with increasing distance from the particle that only a very thin layer of gas just above the plane will contribute appreciably to the integral in question. The first term on the right-hand side of (43) is symmetrical with respect to positive and negative directions of x, and will therefore contribute nothing to the x-component of the force. The second term, on the other hand, corresponds to a distribution of electricity of opposite sign for the two directions, and will therefore in general determine a value of f_x^i different from zero. Performing the integration, we obtain

$$f_x^i = \pi N_i^2 e\sigma\phi(x\zeta)\frac{\partial V_x}{\partial z}/16\kappa^2 \; ; \quad \phi(x) = \frac{1}{\pi}\int_x^\infty e^{-u}(1 - x^2/u^2)^2\, u\, du \, . \tag{45}$$

Multiplying f_x^i by n_i° and integrating from $\zeta = 0$ to $\zeta = \infty$, we obtain as an expression for the total momentum parallel to the x-axis transferred per unit time and area through the plane in question, and to particles of the ith kind only,

$$-\Gamma_{xz}^i = \alpha\pi e\sigma n_i^\circ N_i^2 \frac{\partial V_x}{\partial z}/8\kappa^3 \; ; \qquad \alpha = \int_0^\infty \phi(x)dx \, , \tag{46}$$

where α is a pure number of order unity. The coefficient of electric viscosity is, therefore, as regards first-order quantities, given by

$$\kappa_i^e = n_i^\circ N_i^2 \alpha\pi e\sigma/8\kappa^3 \, . \tag{47}$$

The additional resistance experienced by an electric particle moving with a velocity V through an ionized gas is simply obtained from (42). The first term in ψ is symmetrical and will give rise to no forces on the particle. Expanding the second term to first-order quantities, close to the origin, we find that the particle is acted upon by a force which is directed opposite to the velocity and equal to

$$\beta_i^e V = 4\kappa^2\kappa_i^e V/\pi\alpha \, . \tag{48}$$

The hydrostatic electric pressure might be calculated in an analogous manner, but has no interest for the present purpose.[1]

MOUNT WILSON OBSERVATORY
July 1925

---

[1] *Monthly Notices*, 84, 723, 1924.

PLATE XVII

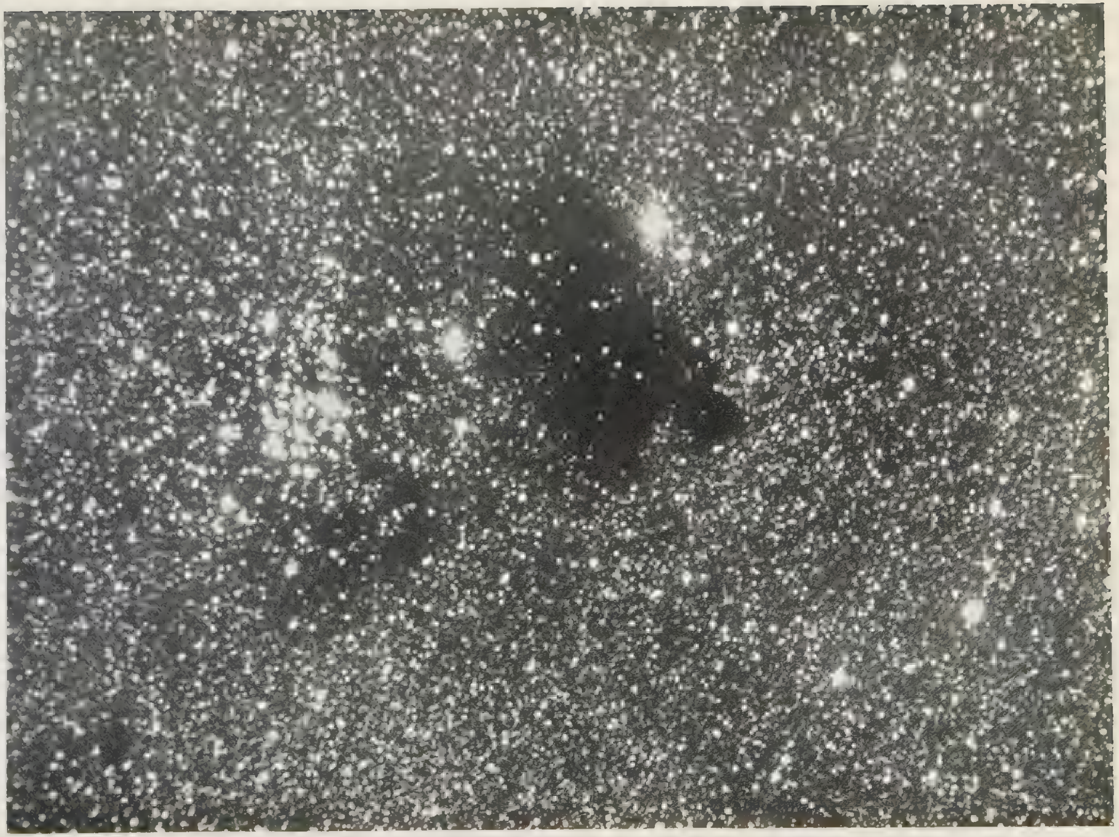

Negative Δ 240

THE DARK NEBULA BARNARD 86

Photographed with the 100-inch Hooker telescope, 1925, July 19
Exposure, 2^h30^m
Scale: 1 mm = 8″.6 (1.84 times that of original negative)

Contributions from the Mount Wilson Observatory, No. 303.
Preprinted from the *Astrophysical Journal*

PHOTOGRAPHIC STUDIES OF NEBULAE

FOURTH PAPER

By JOHN CHARLES DUNCAN

ABSTRACT

Studies of the form and structure of diffuse nebulae, both luminous and obscure, from photographs made with the 100-inch and 60-inch reflectors. *Halftone reproductions* are given of photographs with the Hooker telescope of the dark nebula Barnard 86 and of uncatalogued nebulosities near α and γ Cygni. The nebulosity between α Cygni and the America nebula is found to possess a number of interesting features. Two *nebulous stars* are found in the neighborhood of γ Cygni. The *spectra* of one of these and of H.D. 195255 situated at the edge of a dark marking in the nebula east of γ Cygni are of late B type. The spectrum of H.D. 199178, situated on the line dividing a bright nebula from a dark one, is of type G5, and its *spectroscopic parallax,* determined by Mr. Adams, is $0''.015$.

The study of the forms of the nebulae has been continued, mainly with the 100-inch Hooker telescope, at intervals since the publication of the last paper[1] of this series. Special attention has been given to the diffuse nebulae, both luminous and obscure, in the constellations of Sagittarius and Cygnus.

The Dark Nebula Barnard 86 Sagittarii

$\alpha = 17^h58^m.2, \quad \delta = -27^\circ 52'$ (1925)

Negative Δ 180, Hooker telescope, 1921, June 6. Seed 30 plate, exposure 2^h. Seeing poor, images large and elongated by atmospheric dispersion. Illustrated in Hale's *The Depths of the Universe,* page 47

Δ 249, Hooker telescope, 1925, July 19. Eastman Speedway plate, exposure 2^h30^m. Seeing fair, images elongated. Illustrated in Plate XVII

Discovered in 1883 with a 5-inch refractor by Barnard, who describes it as "like a drop of ink on the bright sky,"[2] this object is probably the most striking in its visual appearance of all the dark nebulae. Especially so is the pocket at the south-preceding end, the edge of which is very sharp and which contains only two tiny stars, both of them too faint to be detected visually. The eastern border of the dark body is much less clearly defined than the western. About 10′

---

[1] *Mt. Wilson Contr.,* No. 256; *Astrophysical Journal,* **57,** 137, 1923.

[2] *Publications of the Lick Observatory,* **11,** Plate 50, 1913.

east of the center of the dark nebula is the bright open cluster N.G.C. 6520, and south of this, as shown in the illustration, is a dark marking that is less pronounced than the main nebula, and is not noticeable visually. The brightest star in the immediate neighborhood is H.D. 164562, visual magnitude 6.68, spectrum Ko, situated on the north-preceding border of Barnard 86. It is of a deep orange-red color that is very striking when seen in the great reflector. In the bright star-cluster also are a number of orange-colored stars. The background against which the dark nebula is seen seems to be composed of faint stars, and there is no evidence on the negatives of any bright nebulosity.

At the latitude of Mount Wilson ($+34^\circ 13'$), objects having so great a south declination as this are always so near the horizon that the star-images, drawn out into short spectra by atmospheric dispersion, appear elongated on all plates made with the Hooker telescope.

A photograph made by H. D. Curtis with the Crossley reflector is reproduced in *Publications of the Lick Observatory*, **13**, Plate VII, 1918.

Portion of the Faint Nebulosity Preceding the North America Nebula (N.G.C. 7000 Cygni)

$\alpha = 20^h 49^m.7, \quad \delta = +44^\circ 7'$ (1925)

Negative Δ 248, Hooker telescope, 1925, July 18. Aperture 84 inches. Eastman 40 plate, exposure $3^h 30^m$

Δ 252, Hooker telescope, 1925, July 20. Eastman Speedway plate, exposure $4^h 45^m$. Illustrated in Plate XVIII

The existence of faint nebulosity west of the America nebula is shown on the small-scale photographs of Barnard and Wolf and on plates taken with the 10-inch Cooke lens at Mount Wilson, but these photographs disclose only a little of the interesting detail. The subject of the present study is the brightest portion of this nebulosity, which is situated nearly halfway between α Cygni and the "isthmus" of N.G.C. 7000. It is shown on the Cooke plate reproduced in my third paper,[1] 30 mm from the right border and 64 mm from the bottom of the illustration.

The character of the nebulosity is much the same as that of the

---

[1] *Mt. Wilson Contr.*, No. 256, Plate X; *Astrophysical Journal*, **57**, Plate XIV, 1923.

PLATE XVIII

N

E

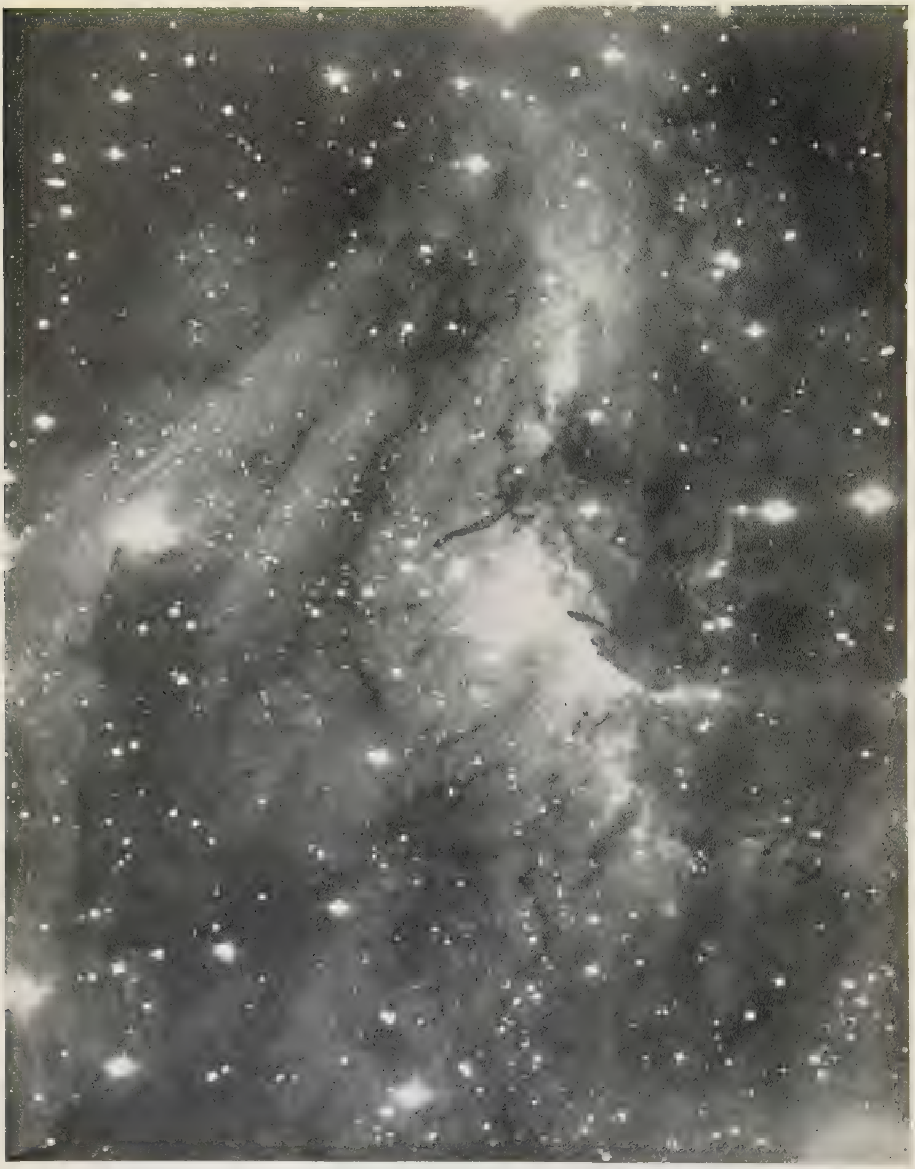

W

Negative Δ 252

Nebulosity Preceding the America Nebula in Cygnus

Photographed with the 100-inch Hooker telescope, 1925, July 20
Exposure, 4^h45^m
Scale: 1 mm = $14''.2$ (1.11 times that of original negative)

southern part of the America nebula proper, consisting of luminous nebulosity in streaks and filaments with numerous dark markings. It is well shown in Plate XVIII, which is a good reproduction. The brightest star in the illustration is H.D. 199178, visual magnitude 7.56, situated 19 mm from the left edge and 69 mm from the top. In the lower right corner is the glow of light from 56 Cygni, magnitude 5.5. The following features are perhaps especially worthy of notice:

1. The slender dark marking, $2'.5$ long, with a faintly luminous core and with a faint star near the end, which extends into the bright nebula eastward from a dark gulf just about the middle of Plate XVIII.

2. A similar, but shorter, dark indentation in the brightest part of the nebula, about $4'$ south of the first. Below this are two still smaller dark bays.

3. The long, parallel streaks of luminous nebulosity extending in a SE.-NW. direction across the upper left quarter of the plate.

4. The patch of faint stars extending westward from H.D. 199178.

5. The well-marked line of division between the bright and dark nebulosity that extends southward from the above-mentioned star.

6. The irregularly curved, bright filaments at the south end of the brightest part of the nebula.

The form of the luminous nebulosity has been likened to that of a pelican, the body of the bird being in the brightest part, the head rising nearly to the top of the plate, and the long, open beak extending nearly to the left edge.

Three spectrograms of the star H.D. 199178 are among those made with the spectrograph of the 60-inch telescope. The type is G5, as given in the *Henry Draper Catalogue*, but with unusually diffuse lines. Mr. Adams has kindly told me the result of his determination of the absolute magnitude of the star from these spectrograms, which is 3.5. With the apparent visual magnitude of 7.56 given in the *Henry Draper Catalogue*, this indicates a parallax of about $0''.015$, corresponding to a distance of 220 light-years. Whether or not this star is associated with the nebula is of course doubtful, but its location at an abrupt turn in the edge of the luminous nebulosity is suggestive.

Faint Nebula Following γ Cygni

$\alpha = 20^h 25^m.5, \quad \delta = +39°46' \ (1925)$

Negative Δ 273, 60-inch telescope, 1925, August 20. Eastman Speedway plate, exposure 2^h

Δ 278, Hooker telescope, 1925, August 22. Eastman Speedway plate, exposure 4^h. Illustrated in Plate XIX

This nebula follows γ Cygni by 6 minutes of time. It is shown 53 mm from the left edge and 82 mm from the bottom of the reproduction of Barnard's photograph made in 1894 with the Willard lens.[1] As shown in Plate XIX, it consists of a mottling of luminous and obscure nebulosities, a conspicuous feature being the large dark marking that extends southwestward from the prominent star, which is 43 mm from the left edge and 37 mm from the bottom of the plate. This star is B.D. +39°4206 = H.D. 195255, visual magnitude 8.80. Somewhat separated from the main mass of nebulosity, 15 mm from the right edge and 43 mm from the top of Plate XIX, is a nebulous star of the tenth magnitude, the nebulous character of which I believe has never before been recorded. Although not prominent on the photograph, the most conspicuous object seen by the eye in this field is the star 39 mm from the left edge and 44 mm from the bottom of the illustration, which in the field of the great reflector shone out startlingly with a deep red light. It was later identified as the variable star RW Cygni.

On September 1, 1925, I secured a spectrogram of the nebulous star above referred to, and one of H.D. 195255, with the Cassegrain spectrograph of the Hooker telescope, using the rapid camera of 10 inches focal length. Both spectra are of late B type. Mr. Joy, who examined them carefully, considers the brighter star to be of type B9 and the nebulous star to be somewhat earlier, perhaps B8.

Faint Nebula North-Preceding γ Cygni

$\alpha = 20^h 14^m.1, \quad \delta = +41°38' \ (1925)$

Negative Δ 281, Hooker telescope, 1925, August 23. Eastman Speedway plate, exposure 4^h. Images elongated. Illustrated in Plate XX

This nebula is 1°.6 north of γ Cygni, and precedes that star by 5 minutes of time. It is shown 81 mm from the right edge and 94 mm

---

[1] *Publications of the Lick Observatory*, **11**, Plate 76, 1913.

PLATE XIX

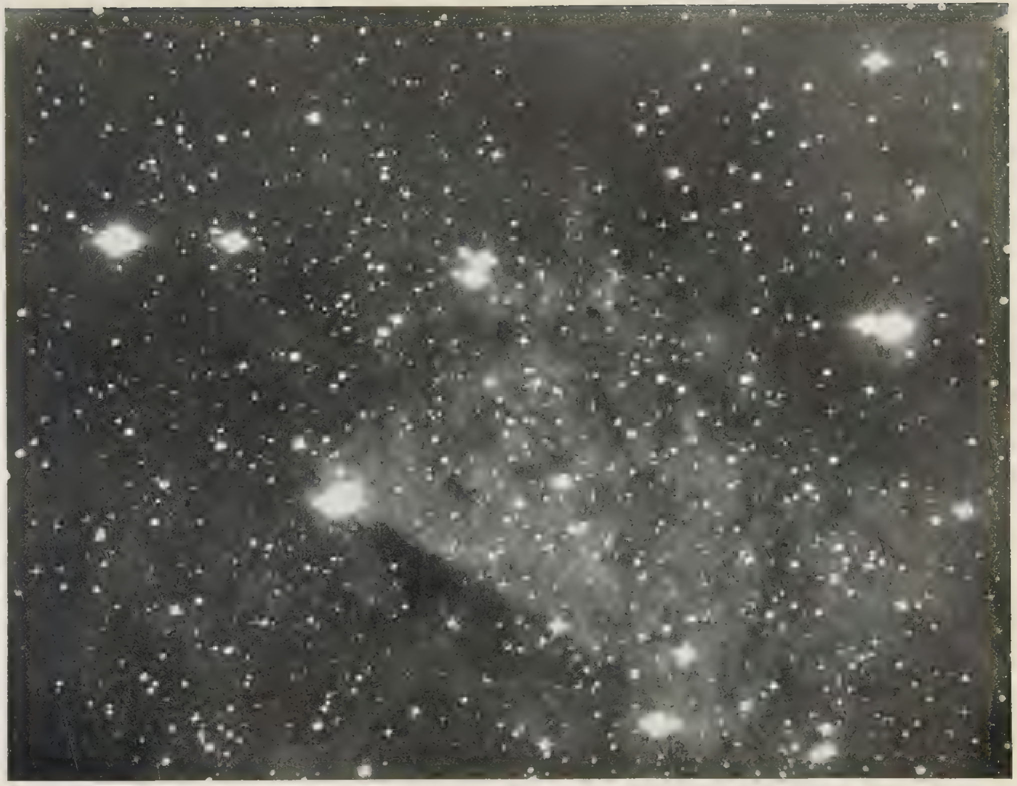

Negative Δ 278

Nebulosity Following γ Cygni

Photographed with the 100-inch Hooker telescope, 1925, August 22
Exposure, 4^h
Scale: 1 mm = $15''.8$ (same as that of original negative)

PLATE XX

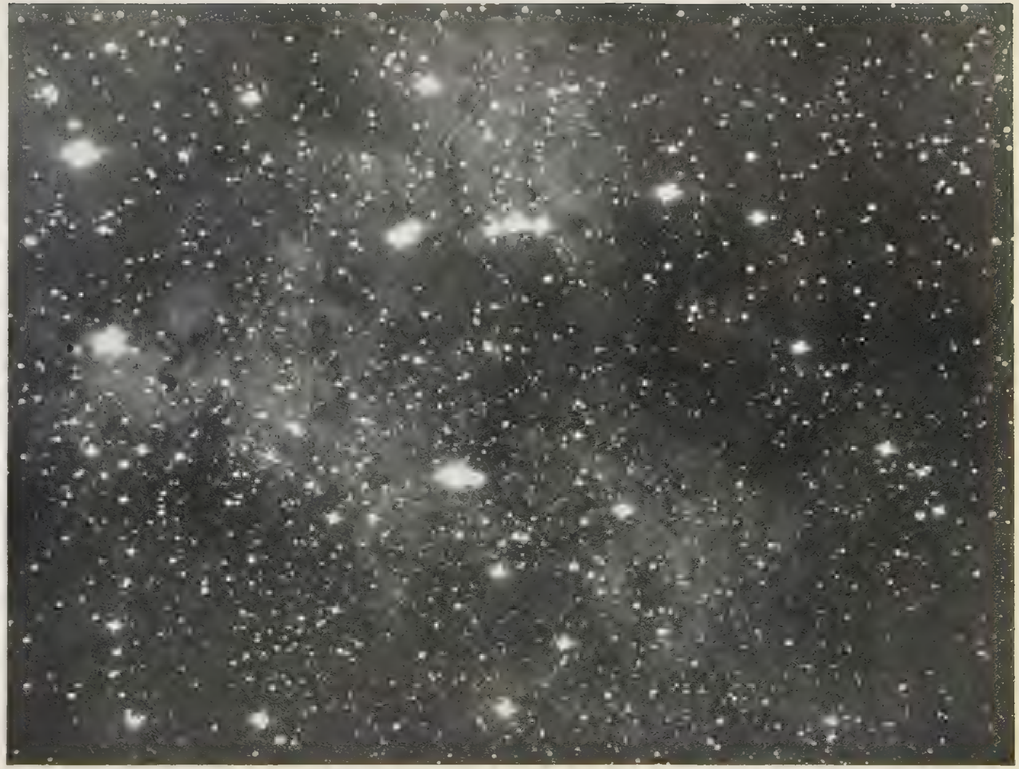

Negative Δ 281

NEBULOSITY NORTH—PRECEDING γ CYGNI

Photographed with the 100-inch Hooker telescope, 1925, August 23
Exposure, 4^h
Scale: 1 mm = $15''.7$ (1.02 times that of original negative)

from the top of the reproduction of Barnard's photograph of 1894.[1] It is quite similar in general appearance to the nebula shown in Plate XIX. A nebulous star appears 14 mm from the left edge and 45 mm from the top of Plate XX. This is considerably fainter than the one on Plate XIX, and a spectrogram has not yet been made. The brightest star appearing on Plate XX is B.D. +41°3693, magnitude 8.6, which is 10 mm from the left edge and 20 mm from the top.

MOUNT WILSON OBSERVATORY
AND WHITIN OBSERVATORY
September 1925

---

[1] *Loc. cit.*

END OF VOLUME XIII

INDEX TO VOLUME XIII

Nos. 283 to 303

AUTHORS

PAGE

BURWELL, CORA G. *See* Merrill, Paul W.

DUNCAN, JOHN CHARLES—
  Photographic Studies of Nebulae. Fourth Paper 461

HALE, GEORGE E., AND SETH B. NICHOLSON—
  The Law of Sun-Spot Polarity 351

HUMASON, MILTON L. *See* Merrill, Paul W.

JOYNER, MARY C. *See* Seares, Frederick H.

KING, ARTHUR S.—
  Electric Furnace Spectra of Vanadium and Chromium in the Ultra-Violet 1
  Spectroscopic Phenomena of the High-Current Arc 299

MERRILL, PAUL W.—
  Two Stellar Spectra of the P Cygni Type 261

MERRILL, PAUL W., MILTON L. HUMASON, AND CORA G. BURWELL—
  Discovery and Observations of Stars of Class Be 231

NICHOLSON, SETH B. *See* Hale, George E.; Pettit, Edison

PETTIT, EDISON, AND SETH B. NICHOLSON—
  Radiation Measurements of the Solar Corona, January 24, 1925 . 327

RICHMOND, MYRTLE L. *See* Seares, Frederick H.

ROSSELAND, SVEIN—
  On the Structure and Origin of Solar Magnetic Fields . . . 439
  The Theory of the Stellar Absorption Coefficient 267

RUSSELL, HENRY NORRIS—
  A List of Ultimate and Penultimate Lines of Astrophysical Interest 47

SANFORD, ROSCOE F.—
  The Orbits of Four Spectroscopic Binaries 181

SEARES, FREDERICK H.—
  Mean Color-Index of Stars of Different Apparent Magnitudes . 109
  Note on the Distribution and Number of Nebulae 287
  Some Relations between Magnitude Scales 125

SEARES, FREDERICK H., MARY C. JOYNER, AND MYRTLE L. RICHMOND—
  Reduction of the Harvard-Groningen *Durchmusterung* to the International System of Magnitude and Color 145

PAGE

SEARES, FREDERICK H., P. J. VAN RHIJN, MARY C. JOYNER, AND MYRTLE L. RICHMOND—
Mean Distribution of Stars according to Apparent Magnitude and Galactic Latitude 383

SMITH, SINCLAIR—
Study of Electrically Exploded Wires 29

STRÖMBERG, GUSTAF—
Analysis of Radial Velocities of Globular Clusters and Non-Galactic Nebulae 195
Asymmetry in Stellar Motions as Determined from Radial Velocities 205

VAN MAANEN, ADRIAAN—
Investigations on Proper Motion. Eleventh Paper: The Proper Motion of Messier 13 and Its Internal Motion 21
Photographic Determination of Stellar Parallaxes with the 60- and 100-Inch Reflectors. Eighth Series 163

VAN RHIJN, P. J. *See* Seares, Frederick H.

SUBJECTS

Absorption coefficient, stellar, theory, 267
Arc, high-current, spectroscopic phenomena, 299
Asymmetry in stellar motions, 205
Binaries, spectroscopic, orbits of B 1131, H.D. 101206, B.D.+55°2215, βGC 9818S, 181
Chromium spectrum, electric furnace, in ultra-violet, 1
Clusters, globular, analysis of radial velocities, 195
———, proper motion and internal motion of Messier 13, 21
Color, stellar, reduction of Harvard-Groningen *Durchmusterung* to international system, 145
Color-index, mean, of stars of different apparent magnitudes, 109
Corona, solar, radiation measurements, 327
Eclipses, solar, radiation measurements of corona, 327
Electric furnace spectra of vanadium and chromium in ultra-violet, 1
Harvard-Groningen *Durchmusterung*, reduction to international system of magnitude and color, 145
Lines, spectral, ultimate and penultimate, of astrophysical interest, 47
Magnetic fields, solar, structure and origin, 439
Magnitude scales, relations between, 125
Magnitudes, apparent, of stars, and their mean distribution, 383
———, stellar, reduction of Harvard-Groningen *Durchmusterung* to international system, 145
Nebulae, distribution and number, 287
———, non-galactic, analysis of radial velocities, 195
———, photographic studies, 461
Parallaxes, stellar, determination with 60- and 100-inch reflectors, 163
Proper motion of Messier 13, 21
Spectra, of electrically exploded wires, 29
———, stellar, of P Cygni type, 261
Spectroscopic binaries, orbits of Boss 1131, H.D. 101206, B.D.+55°2215, βGC 9818S, 181
Spectroscopic phenomena of high-current arc, 299
Spectrum, chromium, in ultra-violet, 1
———, vanadium, in ultra-violet, 1
Star clusters, proper motion of Messier 13, 21
Stars, asymmetry in motions as determined from radial velocities, 205
———, mean distribution according to apparent magnitude and galactic latitude, 383
———, of class Be, discovery and observations, 231

Stars, of different apparent magnitudes, mean color-index, 109
———, parallaxes, determination with 60- and 100-inch reflectors, 163
———, relations between magnitude scales, 125
———, spectra, of P Cygni type, 261
———, theory of absorption coefficient, 267
Sun, structure and origin of solar magnetic fields, 439
Sun-spot polarity, law, 351
Vanadium spectrum, electric furnace, in ultra-violet, 1
Velocities, radial, of globular clusters and non-galactic nebulae, 195
Wires, electrically exploded, spectra, 29

522 19 C28 V13

MOUNT WILSON OBSERVATORY CONTRIBUTION

INSERT BOOK
MASTER CARD
FACE UP IN
FRONT SLOT
OF S.R PUNCH

1885

UNIVERSITY OF ARIZONA
LIBRARY

MASTER CARD

GLOBE 901144-C